VOL. 513 JULY 27, 1990
COMPLETE IN ONE ISSUE

NAL OF HROMATOGRAPHY

RNATIONAL JOURNAL ON CHROMATOGRAPHY, ELECTROPHORESIS AND RELATED METHODS

ELSEVIER

JOURNAL OF CHROMATOGRAPHY

Scope. The *Journal of Chromatography* publishes papers on all aspects of chromatography, electrophoresis and related methods. Contributions consist mainly of research papers dealing with chromatographic theory, instrumental development and their applications. The section *Biomedical Applications*, which is under separate editorship, deals with the following aspects: developments in and applications of chromatographic and electrophoretic techniques related to clinical diagnosis or alterations during medical treatment; screening and profiling of body fluids or tissues with special reference to metabolic disorders; results from basic medical research with direct consequences in clinical practice; drug level monitoring and pharmacokinetic studies; clinical toxicology; analytical studies in occupational medicine.

Submission of Papers. Papers in English, French and German may be submitted, in three copies. Manuscripts should be submitted to: The Editor of *Journal of Chromatography*, P.O. Box 681, 1000 AR Amsterdam, The Netherlands, or to: The Editor of *Journal of Chromatography, Biomedical Applications*, P.O. Box 681, 1000 AR Amsterdam, The Netherlands. Review articles are invited or proposed by letter to the Editors. An outline of the proposed review should first be forwarded to the Editors for preliminary discussion prior to preparation. Submission of an article is understood to imply that the article is original and unpublished and is not being considered for publication elsewhere. For copyright regulations, see below.

Subscription Orders. Subscription orders should be sent to: Elsevier Science Publishers B.V., P.O. Box 211, 1000 AE Amsterdam, The Netherlands, Tel. 5803 911, Telex 18582 ESPA NL. The *Journal of Chromatography* and the *Biomedical Applications* section can be subscribed to separately.

Publication. The *Journal of Chromatography* (incl. *Biomedical Applications*) has 37 volumes in 1990. The subscription prices for 1990 are:

J. Chromatogr. (incl. *Cum. Indexes, Vols. 451–500*) + *Biomed. Appl.* (Vols. 498–534):
Dfl. 6734.00 plus Dfl. 1036.00 (p.p.h.) (total *ca.* US$ 3885.00)

J. Chromatogr. (incl. *Cum. Indexes, Vols. 451–500*) only (Vols. 498–524):
Dfl. 5616.00 plus Dfl. 756.00 (p.p.h.) (total *ca.* US$ 3186.00)

Biomed. Appl. only (Vols. 525–534):
Dfl. 2080.00 plus Dfl. 280.00 (p.p.h.) (total *ca.* US$ 1180.00).

Our p.p.h. (postage, package and handling) charge includes surface delivery of all issues, except to subscribers in Argentina, Australia, Brasil, Canada, China, Hong Kong, India, Israel, Malaysia, Mexico, New Zealand, Pakistan, Singapore, South Africa, South Korea, Taiwan, Thailand and the U.S.A. who receive all issues by air delivery (S.A.L. — Surface Air Lifted) at no extra cost. For Japan, air delivery requires 50% additional charge; for all other countries airmail and S.A.L. charges are available upon request. Back volumes of the *Journal of Chromatography* (Vols. 1–497) are available at Dfl. 195.00 (plus postage). Claims for missing issues will be honoured, free of charge, within three months after publication of the issue. Customers in the U.S.A. and Canada wishing information on this and other Elsevier journals, please contact Journal Information Center, Elsevier Science Publishing Co. Inc., 655 Avenue of the Americas, New York, NY 10010. Tel. (212) 633-3750.

Abstracts/Contents Lists published in Analytical Abstracts, ASCA, Biochemical Abstracts, Biological Abstracts, Chemical Abstracts, Chemical Titles, Chromatography Abstracts, Clinical Chemistry Lookout, Current Contents/Life Sciences, Current Contents/Physical, Chemical & Earth Sciences, Deep-Sea Research/Part B: Oceanographic Literature Review, Excerpta Medica, Index Medicus, Mass Spectrometry Bulletin, PASCAL-CNRS, Pharmaceutical Abstracts, Referativnyi Zhurnal, Science Citation Index and Trends in Biotechnology.

See inside back cover for Publication Schedule, Information for Authors and information on Advertisements.

0021-9673/90/$03.50

This issue is printed on acid-free paper.

Printed in The Netherlands

CONTENTS

(Abstracts/Contents Lists published in Analytical Abstracts, ASCA, Biochemical Abstracts, Biological Abstracts, Chemical Abstracts, Chemical Titles, Current Contents/Life Sciences, Current Contents/Physical, Chemical & Earth Sciences, Deep-Sea Research/Part B: Oceanographic Literature Review, Excerpta Medica, Chromatography Abstracts, Index Medicus, Mass Spectrometry Bulletin, PASCAL-CNRS, Referativnyi Zhurnal and Science Citation Index)

(Continued overleaf)

(Continued overleaf)

In articles with more than one author, the name of the author to whom correspondence should be addressed is indicated in the article heading by a 6-pointed asterisk (*)

JOURNAL OF CHROMATOGRAPHY

VOL. 513 (1990)

JOURNAL *of* CHROMATOGRAPHY

INTERNATIONAL JOURNAL ON CHROMATOGRAPHY,
ELECTROPHORESIS AND RELATED METHODS

ELSEVIER
AMSTERDAM — OXFORD — NEW YORK — TOKYO

J. Chromatogr., Vol. 513 (1990)

0021-9673/90/$03.50

Printed in The Netherlands

Journal of Chromatography, 513 (1990) 1–11
Elsevier Science Publishers B.V., Amsterdam

CHROM. 22 495

Use of a gamma energy distribution to model the gas chromatographic temperature dependence of solute retention on aryl-siloxane chemically modified porous carbon

R. K. GILPIN*, M. JARONIEC[a] and M. B. MARTIN-HOPKINS
Department of Chemistry, Kent State University, Kent, OH 44242 (U.S.A.)
(First received January 24th, 1990; revised manuscript received April 2nd, 1990)

ABSTRACT

A new equation is derived for the corrected specific retention volume of an infinitely dilute solute on an energetically heterogeneous surface. The equation, which is based on a gamma-type distribution for the adsorption energy, is used to model the temperature dependence of the specific retention volume for benzene chromatographed on four different chemically modified porous carbon adsorbents. Biphasic behavior in plots of the ln $V_{s,t}$ *vs.* $1/T$ are interpreted in terms of differing energetic heterogeneities of the modified carbons.

INTRODUCTION

Since it is well-known that surface heterogeneity, especially under dilute conditions, substantially influences the adsorption process[1], gas–solid chromatography (GSC), which permits measurements to be made at low concentrations[2], is an attractive technique for studying surface and structural differences of adsorbents and catalysts[3]. Although many investigators[4–8] have used both temperature- and concentration-dependent retention measurements to characterize surface heterogeneity, further theoretical and experimental studies via GSC are important in order to develop additional numerical models which may be used to describe surface and structural heterogeneities of solids.

In the current paper a simple equation is derived using a gamma-type distribution to describe the surface adsorption energy heterogeneity. Additionally this relationship has been used to model the temperature dependence of retention data for benzene chromatographed on four different chemically modified porous carbons. It has been shown that this simple equation can be used to explain two linear segments of the temperature-dependent retention curves which have different slopes and occur in the temperature range from 363 K to 458 K.

[a] Permanent address: Chemistry Faculty, M. Curie-Sklodowska University, 20031 Lublin, Poland.

0021-9673/90/$03.50

THEORY

For an infinitely dilute solute in the gas (mobile) phase the corrected specific retention volume, V_s, at a column temperature T (K) is equal to the distribution constant K_c (refs. 9 and 10):

$$V_s = K_c \equiv c_s/c_g \tag{1}$$

where c_g expressed in mol/ml is the equilibrium solute concentration in the mobile (gas) phase and c_s expressed in mol/m^2 is the equilibrium solute concentration on the stationary (surface) phase. Using c_s^0 to denote the maximum solute concentration on the surface and $\theta = c_s/c_s^0$ to describe relative coverage eqn. 1 may be rewritten such that:

$$V_s = c_s^0 K \tag{2}$$

where $K = \theta/c_g$. The distribution constant K also may be expressed as follows[5]:

$$K = \alpha \exp(\varepsilon/RT) \tag{3}$$

where ε is the adsorption energy of a solute, R is the universal gas constant, and α is the temperature-dependent entropy factor[11].

For a heterogeneous surface containing L types of adsorption sites the total specific retention volume, $V_{s,t}$, of a solute is the sum of the specific retention volumes, $V_{s,l}$, arising from all types of adsorption sites. This relationship is given in eqn. 4

$$V_{s,t} = \sum_{l=1}^{L} V_{s,l} \tag{4}$$

where $V_{s,l}$ denotes the individual specific retention volumes for the 1, 2, ..., L (lth) type of adsorption sites. Taking into account eqns. 2 and 3, $V_{s,l}$ may be expressed as follows:

$$V_{s,l} = \alpha c_{s,l}^0 \exp(\varepsilon_l/RT) \tag{5}$$

where $c_{s,l}^0$ and ε_l denote respectively the maximum solute concentration and adsorption energy. In developing eqn. 5 it is assumed that the entropy factor, α, is independent of the type of adsorption sites. This assumption has been commonly used in developing other gas adsorption models for energetically heterogenous solids[1].

Eqn. 4 may be rewritten to the following:

$$V_{s,t} = \alpha c_{s,t}^0 \sum_{l=1}^{L} f_l \exp(\varepsilon_l/RT) \tag{6}$$

where

$$f_l = c_{s,l}^0/c_{s,t}^0 \tag{7}$$

and

$$c^0_{s,t} = \sum_{l=1}^{L} c^0_{s,l} \tag{8}$$

In the above relationship f_l is the fraction of adsorption sites of the lth type and $c^0_{s,t}$ is the maximum solute concentration for the total surface.

In cases where a large number of different types of adsorption sites exist ($L \to \infty$), the summation used in eqn. 6 to define a finite number may be replaced by an integration. After doing this eqn. 9 is obtained

$$V_{s,t} = \alpha c^0_{s,t} \int_{\triangle} \exp(\varepsilon/RT) F(\varepsilon) d\varepsilon \tag{9}$$

where the distribution function of the adsorption energy $F(\varepsilon)$ satisfies the following normalization condition:

$$\int_{\triangle} F(\varepsilon) d\varepsilon = 1 \tag{10}$$

over an the integration region $\triangle$.

Eqn. 9 describes the total specific retention volume $V_{s,t}$ of a infinitely dilute solute chromatographed on an energetically heterogeneous surface with a distribution of adsorption sites. Although this equation may be integrated for different assumed distributions of the adsorption energy, it has been shown elsewhere[1,12] that a gamma-type function is a good mathematical model for describing the behaviour of many heterogeneous surfaces. This function for $\varepsilon > \varepsilon_m$ is given in eqn. 11

$$F(\varepsilon) = [\rho^\gamma/\Gamma(\gamma)] (\varepsilon - \varepsilon_m)^{\gamma-1} \exp[-\rho(\varepsilon - \varepsilon_m)] \tag{11}$$

where ε_m is the minimum adsorption energy, γ and ρ are parameters greater than zero, and Γ is the gamma special function. For $0 \leqslant \gamma \leqslant 1$ the gamma distribution is an exponentially decreasing relationship and for $\gamma > 1$ it is an asymmetrical single-peak with a maximum at:

$$\varepsilon_0 = \varepsilon_m + (\gamma - 1)/\rho \tag{12}$$

The parameters ρ and γ are associated with the average adsorption energy ε[5], where $\varepsilon^* = \gamma/\rho$ (eqn. 13) and its dispersion σ (eqn. 14).

$$\bar{\varepsilon} = \varepsilon_m + \varepsilon^* \tag{13}$$

and

$$\sigma = \gamma^{1/2}/\rho \tag{14}$$

The quantities $\bar{\varepsilon}$ and σ in eqns. 13 and 14 have a clear physical meaning; $\bar{\varepsilon}$ denotes the average adsorption energy, whereas σ denotes the dispersion in the energy distribution function $F(\varepsilon)$. $\bar{\varepsilon}$ provides information about position of the distribution function $F(\varepsilon)$ on the energy axis, whereas, σ reflects its width (*i.e.*, energy range). Also, a comparison of $\bar{\varepsilon}$ with ε_0 provides information about the asymmetry of $F(\varepsilon)$. For $\varepsilon_0 = \bar{\varepsilon}$ the function $F(\varepsilon)$ is symmetrical, whereas for $\bar{\varepsilon} > \varepsilon_0$ it is asymmetrical in the direction of high values of ε, and for $\bar{\varepsilon} < \varepsilon_0$ it is asymmetrical in the opposite direction.

Presented in Fig. 1 for illustrative purposes are a series of $F(\varepsilon)$ curves generated for the case where $\varepsilon^* = 2.1$ kJ/mol. Larger values of σ and ε^* are obtained for more heterogeneous surfaces and the energy distribution function $F(\varepsilon)$ is skewed in the high-energy direction.

Substitution of eqn. 11 into eqn. 9 gives:

$$V_{s,t} = [\alpha c^0_{s,t} \rho^\gamma / \Gamma(\gamma)] \int_{\varepsilon_m}^{\infty} (\varepsilon - \varepsilon_m)^{\gamma - 1} \exp(\varepsilon / RT) \exp[-\rho(\varepsilon - \varepsilon_m)] d\varepsilon \tag{15}$$

Because the gamma distribution, $F(\varepsilon)$, approaches zero as ε goes to infinity, the upper integration limit in eqn. 15 is set at ∞. Introducing the new variable $E = \varepsilon - \varepsilon_m$ into eqn. 15:

$$V_{s,t} = [\alpha c^0_{s,t} \rho^\gamma \exp(\varepsilon_m / RT) / \Gamma(\gamma)] \int_0^{\infty} E^{\gamma - 1} \exp[-(\rho - 1/RT)E] dE \tag{16}$$

After integration:

$$V_{s,t} = \alpha c^0_{s,t} (1 - 1/\rho RT)^{-\gamma} \exp(\varepsilon_m / RT) \tag{17}$$

or

$$V_{s,t} = V_{s,m} (1 - 1/\rho RT)^{-\gamma} \tag{18}$$

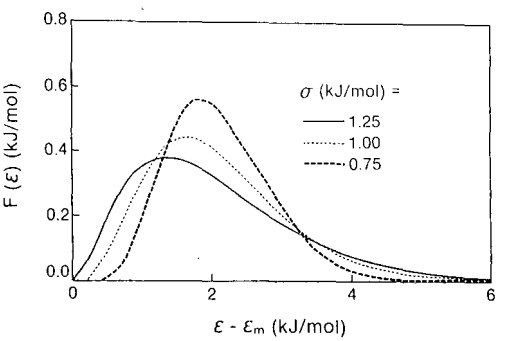

Fig. 1. Adsorption energy distributions calculated according to eqn. 11 for $\varepsilon^* = 2.1$ kJ/mol and different values of σ.

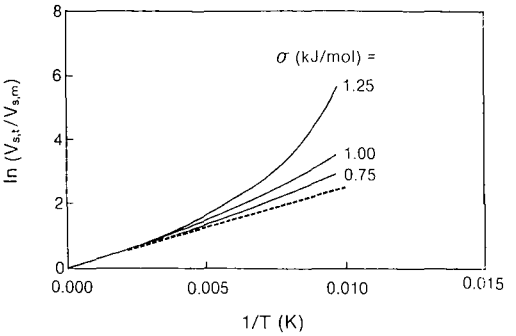

Fig. 2. Dependences of the logarithm of the relative retention volume $V_{s,t}/V_{s,m}$ against reciprocal of temperature associated with the adsorption energy distributions shown in Fig. 1. The dashed line represents the high temperature limit of eqn. 20, which is given by eqn. 21. $\varepsilon^* = 2.1$ kJ/mol.

where

$$V_{s,m} = \alpha c^0_{s,t} \exp(\varepsilon_m/RT) \tag{19}$$

$V_{s,m}$ in eqns. 18 and 19 is the specific retention volume associated with the adsorption site with minimum energy, ε_m. Thus the influence of an adsorbent's heterogeneity on $V_{s,t}$ is described by the expression $(1 - 1/\rho RT)^{-\gamma}$. This relationship is illustrated in Fig. 2 where $\ln(V_{s,t}/V_{s,m})$ is plotted against the reciprocal of temperature according to the following equation:

$$\ln(V_{s,t}/V_{s,m}) = -\gamma \ln(1 - 1/\rho RT) \tag{20}$$

For small values of $1/\rho RT$ eqn. 20 may be approximated as follows:

$$\ln(V_{s,t}/V_{s,m}) = \gamma/\rho RT = \varepsilon^*/RT \tag{21}$$

For $\varepsilon^* = 2.1$ kJ/mol. The dotted line in Fig. 2 represents linear fits according to eqn. 21, whereas the solid lines were calculated according to eqn. 20 for the values of the energy distributions function shown in Fig. 1 (*i.e.*, $\sigma = 0.75$, 1.00 and 1.25 kJ/mol). From Fig. 2 it can be seen that at lower temperatures an adsorbent's heterogeneity influences strongly the temperature dependence of the specific retention volume (*i.e.*, a significant deviation of the solid curves from the dotted straight line). However, this deviation decreases when the surface heterogeneity, σ, decreases. At higher temperatures where the solid curves and the dotted line is nearly superimposable changes in σ do not influence significantly the temperature-dependence of $V_{s,t}$. A characteristic feature of each of the curves in the higher temperature region is linearity with a slope equal to ε^*/R. Thus, the adsorbent's heterogeneity is reflected in the parameters γ and ρ, which influence the slope, ε^*/R, of the linear temperature dependence of $V_{s,t}$ shown in Fig. 2.

If eqn. 17 is rewritten in logarithmic form, we obtain

$$\ln V_{s,t} = \ln(\alpha c^0_{s,t}) + \varepsilon_m/RT - \gamma \ln(1 - 1/\rho RT) \tag{22}$$

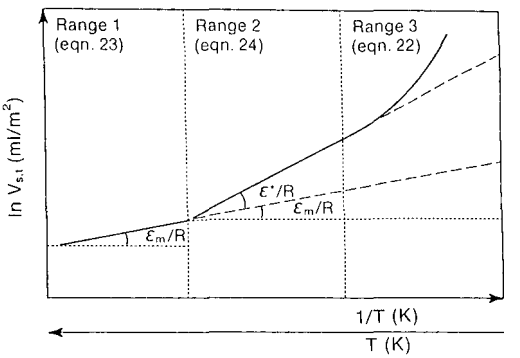

Fig. 3. A schematic representation of the dependence of the logarithm of the specific retention volume on reciprocal of temperature of a heterogeneous solid.

The first term in the above expression is related to the entropy effect in GSC, the second term provides information about the minimum adsorption energy, and the third term describes the effect of adsorbent heterogeneity on the specific retention volume. The temperature dependence of the first term in comparison to the other terms is negligible[11].

At higher temperatures $1/\rho RT$ is nearly zero and the third term in eqn. 22 may be neglected. Under these conditions eqn. 22 is reduced to a linear relationship (eqn. 23) with a slope of ε_m/R.

$$\ln V_{s,t} = \ln(\alpha c^0_{s,t}) + \varepsilon_m/RT \tag{23}$$

For the intermediate temperatures the third term of eqn. 22 can be approximated by eqn. 21 and a new linear expression is obtained (eqn. 24).

$$\ln V_{s,t} = \ln(\alpha c^0_{s,t}) + \varepsilon_m/RT + \varepsilon^*/RT = \ln(\alpha c^0_{s,t}) + \bar{\varepsilon}/RT \tag{24}$$

in which the third term can be approximated by ε^*/RT. In this second temperature range a higher value for the slope is obtained compared to that at higher temperatures.

The above conditions are illustrated schematically in Fig. 3. Range 1 corresponds to higher temperatures where $1/\rho RT$ is assumed to be zero (eqn. 23). Range 2 corresponds to intermediate temperatures where $1/\rho RT$ is small but non-negligible (eqn. 24) and range 3 corresponds to lower temperatures where all terms in eqn. 22 must be considered. In this latter region $\ln V_{s,t}$ *vs.* $1/T$ deviates significantly from linearity. The degree of deviation depends strongly on the adsorbent heterogeneity (*i.e.*, the σ value as illustrated in Fig. 2).

Thus, in summary, eqn. 22 can be utilized to model retention behavior over a broad range of temperatures. Mathematical analysis of this expression shows that at higher and intermediate temperatures simplified versions (respectively, eqns. 23 and 24) can be used to describe the linear behavior of $\ln V_{s,t}$ *vs.* $1/T$. At higher temperatures (range 1) little information is provided about adsorbent heterogeneity, only an estimate of the minimum adsorption energy, ε_m. However, the increase in the slope of

the linear plot of ln $V_{s,t}$ *vs.* $1/T$ observed for intermediate temperatures (range 2) is related to the adsorbent's heterogeneity. This increase is equal to:

$$\varepsilon^*/R = \bar{\varepsilon}/R - \varepsilon_m/R \tag{25}$$

The first and second terms of eqns. 25 are respectively the slopes from the linear fits of range 2 and range 1. It can be seen from eqn. 13 that ε^* depends on the parameters γ and ρ, which characterize the gamma energy distribution function $F(\varepsilon)$ (eqn. 11). Fig. 2 shows that range 2 is expected to be wider for more heterogeneous cases. A further characteristic of range 2 is an independence of the slope on the dispersion, σ. Thus, range 2 provides an estimate of ε^*, a measure of the adsorbent heterogeneity.

A more complete picture of the surface heterogeneity can be obtained by studying $V_{s,t}$ over a wide range of temperatures, which include experimental measurements in ranges 1, 2 and 3. Fig. 2 also illustrates that the deviations from linearity in the curves is a measure of the dispersion, σ. If the deviation is large, then σ is also large. Thus, range 3 provides information about the dispersion, σ, of the energy distribution function.

EXPERIMENTAL

Chemically modified porous carbons

Porous chromatographic grade carbon (Carbopack B) from Supelco (Bellefonte Park, PA, U.S.A.) with an approximate surface area of 100 m^2/g was used to prepare four types of chemically modified adsorbents. This was carried out by first reacting the Carbopack B with 3-aminopropyltriethoxysilane (AS) in the presence of a primary amine. Subsequently, the AS-carbon was modified further by treatment with one of four different arylacid chlorides, 3,5-dinitrobenzoyl chloride (DNBA), 4-nitrobenzoyl chloride (PNBA), 4-methylbenzoyl chloride (PMBA), and benzoyl chloride (BA). More exact details concerning preparation of the chemically modified porous carbons are given elsewhere[13].

A schematic representation of the attached functional groups on the carbon is shown in Fig. 4. The four chemically modified porous carbons are referred to throughout the remainder of the text as: AS-DNBA, AS-PNBA, AS-PMBA and AS-BA. All solvents used in preparation of these materials were reagent grade. The 3-aminopropyltriethoxysilane was obtained from Petrarch Systems (Levittown, PA, U.S.A.) and DNBA, PNBA, PMBA and BA were from Aldrich (Milwaukee, WI, U.S.A.).

Chromatographic measurements

Since the surface properties of porous carbons are frequently characterized using benzene as a test adsorbate[14], benzene also was used in the current study as a test solute. Before making retention measurements, each of the modified carbons, about 0.15 g, was dry packed into a stainless-steel column, 10 cm × 3.2 mm I.D. Pressure drop and void volume measurements were made as described elsewhere[13].

All gas chromatographic measurements were carried out using a Shimadzu model Mini-2 gas chromatograph with a flame ionization detector using nitrogen as the carrier gas. Retention times were recorded by a Hewlett-Packard Model 3393A

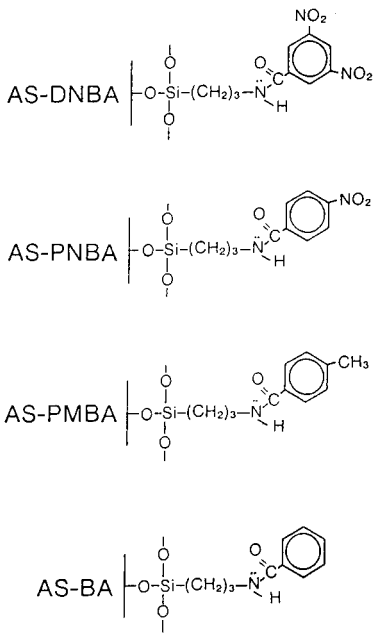

Fig. 4. Surfaces of modified porous carbon prepared by attachment of different benzamide ligands.

integrator. Each retention measurement represents the average of at least two injections and each column was studied twice to determine reproducibility of the measurements.

RESULTS AND DISCUSSION

Shown in Fig. 5 are plots of ln $V_{s,t}$ *vs.* $1/T$ for benzene chromatographed on columns packed with the AS-DNBA, AS-PNBA, AS-PMBA and AS-BA carbons. Over the temperature range studied, 363–458 K, the experimental dependence of ln $V_{s,t}$ *vs.* $1/T$ are approximated by two linear segments, with intersection points from about 398 K for AS-PNBA and AS-BA, and about 423 K for AS-DNBA and AS-PMBA. If it assumed that the linear segments in Fig. 5 at the higher temperatures (low values of $1/T$) correspond to range 1 in Fig. 3 and at lower temperatures (higher values of $1/T$) are related to range 2 in Fig. 3, then these data may be interpreted in terms of eqns. 23 and 24, respectively. Summarized in Table I are calculated values of ε_m and ε^*, studied. The highest value of ε_m was obtained for the AS-PNBA adsorbent and decreased in the order: AS-PNBA > AS-BA > AS-DNBA > AS-PMBA.

All four of the materials studied were prepared via chemical modification of the same porous carbon which consists of twisted aromatic sheets with a number of different types to exposed oxygen groups[15]. During chemical modification a portion of the surface oxygen groups were silanized and then modified by attaching selected benzamide groups: PNBA, BA, DNBA or PMBA. Thus, each of the modified carbons possesses a similar set of unmodified groups or patches plus a selected type of

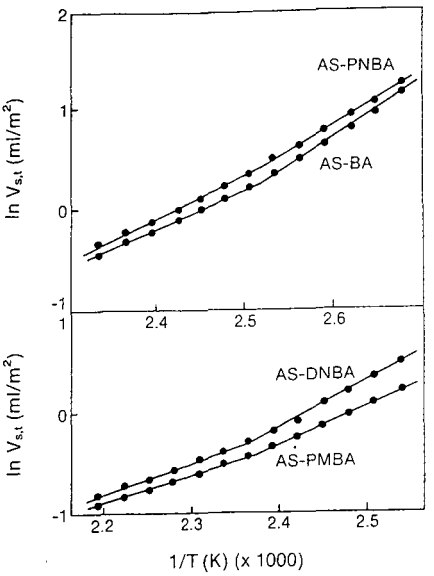

Fig. 5. Experimental dependences ln $V_{s,t}$ *vs.* $1/T$ for benzene on four modified porous carbons. The solid lines show linear segments of these depencences.

arylamide group. If the minimum adsorption energy, ε_m, represented the interaction of benzene with the unreacted patches, the values of ε_m should have been identical for all of the modified carbons. This was found not to be the case as seen by the data in Table I. Rather, since the values of ε_m were dependent on surface modification, it seems reasonable to infer that they reflect the interaction energy between benzene and the various bonded aryl-ligands. Based on this premise, the strongest interaction was observed for benzene with the PNBA ligand, whereas, the weakest was observed for benzene with the PNBA ligand. The interactions between benzene and the BA and

TABLE I

ADSORPTION ENERGY PARAMETERS EVALUATED FROM TWO LINEAR SEGMENTS OF THE EXPERIMENTAL DEPENDENCE LN $V_{s,t}$ *VS.* $1/T$ FOR BENZENE CHROMATOGRAPHED ON FOUR SAMPLES OF MODIFIED POROUS CARBONS

For AS-PNBA and AS-BA the linear segments were drawn at the 363–388 and 408–423 K temperature ranges, whereas for AS-DNBA and AS-PMBA these linear segments were drawn at the 388–413 and 433–458 K temperature ranges.

Modified carbon	*Minimum adsorption energy, ε_m (kJ/mol)*	*Additional average energy generated by surface heterogeneity, ε^* (kJ/mol)*
AS-PNBA	32.6 ± 0.8	5.9 ± 3.8
AS-BA	28.0 ± 0.8	13.0 ± 5.0
AS-DNBA	27.6 ± 1.3	10.5 ± 1.3
AS-PMBA	22.6 ± 1.7	8.4 ± 2.5

DNBA ligands were intermediate. In the case of the simple aromatic and mono substituted aromatic ligands the order of ε_m is consistent with simple ring inductive effects, where the pi-electron density for the ring decreases in the order of PMBA > BA > PNBA.

The second quantity reported in Table I is ε^*. The values of ε^* were calculated according to eqn. 21 from the linear fits of the ln $V_{s,t}$ *vs.* $1/T$ plots associated with temperatures below 400 K. Based on theoretical considerations discussed earlier, ε^* should reflect differences in surface heterogeneities between the modified adsorbents. For a heterogeneous surface with a distribution of sites with energy higher than the minimum adsorption energy, ε_m the value of the ith adsorption site is ε_i and the value $\varepsilon_{im} \equiv \varepsilon_i - \varepsilon_m \geqslant 0$ for all adsorption sites. The average value over all values ε_{im} is defined as ε^*. Thus, smaller values of ε^* indicate that the adsorption energies of all sites do not differ greatly and that they are close to ε_m. Under these conditions the adsorbent's surface is nearly homogeneous with respect to the adsorption energies of all sites. High values of ε^* indicate the presence of sites with a greater distribution of adsorption energies compared to ε_m.

Analysis of the calculated values of ε^* summarized in Table I indicate that the heterogeneity of the modified carbons decrease in the order: AS-BA > AS-DNBA > AS-PMBA > AS-PNBA. Based on the above arguments, the minimum adsorption energy is mainly due to the benzene-ligand interaction; whereas the primary groups on the (unmodified) carbon surface aromatic sheets are main sources of surface heterogeneity. If these arguments are true, then the modified carbons with the smallest concentrations of bonded ligands should be more heterogeneous (higher values of ε^*) than those with the higher concentrations of the bonded ligands. As reported elsewhere chemical cleavage, extraction and high-performance liquid chromatographic analyses have shown that the ligand concentration on the modified carbons were[13]: 2.1 $\pm$ 0.8 molecules/1000Å^2 for AS-BA, 2.7 $\pm$ 0.3 molecules/1000Å^2 for AS-DNBA, 3.3 $\pm$ 0.4 molecules/1000Å^2 for AS-PMBA and 5.3 $\pm$ 0.3 molecules/1000Å^2 for AS-PNBA. A comparison of this order coincides with that obtained for the values of ε^*. The smallest value of ε^* was obtained for the AS-PNBA sample, which contained a highest concentration of the bonded ligands in comparison to the modified adsorbent indicating that it was less heterogeneous than other materials. The AS-BA and AS-DNBA modified carbons were more heterogeneous than the AS-PMBA and AS-PNBA carbons.

The sequence of the ln $V_{s,t}$ *vs.* $1/T$ plots shown in Fig. 5 is determined by the slope and expression ln $(\alpha c^0_{s,t})$, which depends on the entropy parameter α, and on the maximum solute concentration $c^0_{s,t}$ of benzene on the modified carbon surface. It is difficult to estimate, how these quantities contribute to the value of ln $(\alpha c^0_{s,t})$. Because the bonded ligands have a complex chemical structure, the entropy effects arising from the different solute–ligand structures may be significant. Further theoretical and experimental studies are needed to provide a clear interpretation of the entropy effects in these complex chromatographic systems.

ACKNOWLEDGEMENT

Support from DARPA-ONR Contract N00014-86-K-0766 is acknowledged.

REFERENCES

1 M. Jaroniec and R. Madey, *Physical Adsorption on Heterogeneous Solids*, Elsevier, Amsterdam, 1988.
2 A. V. Kiselev and Y. I. Yashin, *Gas Adsorption Chromatography*, Plenum Press, New York, 1969.
3 T. Paryjczak, *Gas Chromatography in Adsorption and Catalysis*, Wiley, Chichester, 1986.
4 A. Waksmundzki, W. Rudzinski, Z. Suprynowicz, R. Leboda and M. Lason, *J. Chromatogr.*, 92 (1974) 9, 25.
5 Z. Suprynowicz, M. Jaroniec and J. Gawdzik, *Chromatographia*, 9 (1976) 161.
6 R. Leboda and S. Sokolowski, *J. Colloid Interface Sci.*, 61 (1977) 365.
7 S. P. Boudreau and W. T. Cooper, *Anal. Chem.*, 59 (1987) 353.
8 W. Rudzinski, A. Waksmundzki, Z. Suprynowicz and J. Rayss, *J. Chromatogr.*, 72 (1972) 221.
9 J. R. Conder and C. L. Young, *Physicochemical Measurements by Gas Chromatography*, Wiley, Chichester, 1979.
10 D. T. Sawyer and D. J. Brookman, *Anal. Chem.*, 40 (1968) 1847.
11 J. Gawdzik, Z. Suprynowicz and M. Jaroniec, *J. Chromatogr.*, 121 (1976) 185.
12 S. Sircar, *J. Chem. Soc., Faraday Trans. I*, 80 (1984) 1101.
13 M. B. Martin-Hopkins, *Ph.D. Thesis*, Kent State University, Kent, OH, 1989.
14 M. M. Dubinin, *Prog. Surf. Membr. Sci.*, 9 (1975) 1.
15 R. C. Bansal, J. B. Donnet and F. Stoeckli, *Active Carbon*, Marcel Dekker, 1988.

Journal of Chromatography, 513 (1990) 13–19
Elsevier Science Publishers B.V., Amsterdam

CHROM. 22 449

Computer-assisted optimization of two-factor selectivity in gas chromatography using an advanced simplex method

QIN-SUN WANG*, CHANG-SHOU ZHU and BING-WEN YAN
National Laboratory of Elemento-Organic Chemistry, Nankai University, Tianjin 300071 (China)
(First received November 10th, 1989; revised manuscript received March 13th, 1990)

ABSTRACT

A computer-assisted simplex method is presented for the optimization of two-factor (carrier gas flow-rate and column temperature) selectivity for the optimum separation of ten compounds in gas chromatography. A two-factor selectivity rectangle concept was used. The method is based on a special polynomial estimated from nine preliminary experimental runs, using the resolution as the selection criterion, with connection to a general simplex method for optimization selection using a microcomputer. Excellent agreement was obtained between predicted data and experimental results, and more than half the number of experiments required in the general simplex method can be omitted.

INTRODUCTION

Studies of systematic strategies for the optimization of gas chromatography (GC) have demostrated the great potential of this approach for improving separations. The sequential simplex method[1,2], response surface method[3], window diagrams[4–7] and computer-simulation techniques[8–10] have been suggested as methods for the optimization of stationary phase loading, column temperature and carrier gas flow-rate selectivity in GC. In most of the previously published papers only one factor was optimized in GC, apart from the simplex method. With optimization of a single factor often the results are not as good as might be expected from a optimum separation. Sometimes a multi-factor optimization can give a completely optimized separation. However, with the sequential simplex method a larger number of experiments are required and local optima may be found, which are distinct disadvantages.

In this paper, a computer-assisted simplex method is presented for the optimization of two-factor (carrier gas flow-rate and column temperature) selectivity for the optimum separation of a mixture of ten compounds in GC. The principle of method is based a special polynomial between the capacity factor, k', and two factors which are estimated from nine preliminary experiments according to the full factorial design, followed by the general simplex method. Excellent agreement was obtained

0021-9673/90/$03.50

between predicted and experimental results and, compared with the original simplex method, more than half the number of experiments can be omitted. For the optimization the computer program SDO-G (simplex difactor optimization for GC) was developed.

EXPERIMENTAL

Materials

The sample contained equal volumes of ten compounds diluted 1:100 in acetone: isoamyl acetate, dodecane, chlorobenzene, 1,3,5-trimethylbenzene,*o*-chlorotoluene, bromobenzene, *m*-dichlorobenzene, *o*-dichlorobenzene, diethyl malonate and 1,4-butyrolactone. These components were eluted in the above order under every set of experimental conditions.

Stainless-steel columns (1 m × 2 mm I.D.) packed with 10% polyethylene glycol 20000 on Chromosorb (80–100 mesh) were used.

Apparatus

All computer studies were carried out on a Model IBM-XT personal computer system with an HP-7470A graphics plotter (Hewlett-Packard, Palo, Alto, CA, U.S.A.). The SDO-G program was written in True BASIC language. An HP-5890A gas chromatograph equipped with flame ionization detectors was employed. The carrier gas was nitrogen. A 10-μl syringe was used for all sample injections.

Chromatography

During the chromatographic runs, all experimental variables except those being investigated were carefully maintained at fixed values. Those variables held constant included the detector air and hydrogen flow-rates, the detector and injection port temperatures (235 and 240°C, respectively) and the sample size (2 μl). The effects of carrier gas flow-rate and column oven temperature were assessed using a full 3^2 factorial design. The flow-rate levels in the design were 10, 20 and 30 ml/min and the temperature levels were 150, 165 and 180°C. The retention time of acetone was employed as t_0.

RESULTS AND DISCUSSION

The principle of the computer-assisted simplex method is based a special polynomial between capacity factor and the two factors considered. In order to investigate the effect of two variables (carrier gas flow-rate and column temperature) in GC and their possible interaction, a full factorial design (Fig. 1) was adopted as the optimization strategy. Nine preliminary experiments were carried out and the capacity factor values were measured. These values were then substituted into the following equation, in order to establish the values of the constants:

$$k' = b_0 + b_1 \log X_1 + b_2 \log X_2 + b_{11} (\log X_1)^2 + b_{22} (\log X_2)^2 + b_{12} \log X_1 \log X_2 \quad (1)$$

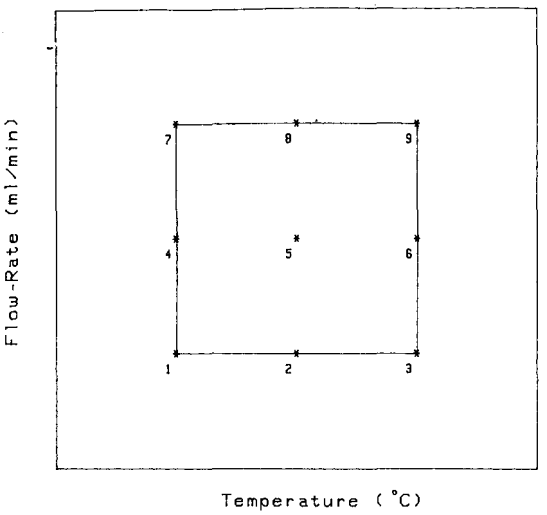

Fig. 1. Full factorial design for two-factor effects.

where X_1 is the carrier gas flow-rate, X_2 is the column temperature and b_0, b_1, b_2, b_{11}, b_{22} and b_{12} are constants characteristic of a given compound. Eqn. 1 means that if X_1 and X_2 are known the capacity factor can be determined for the chromatographic conditions applied.

As the SDO-G method considers only two factors, only three initial experiments were required, which can be selected from the nine preliminary experiments to perform the simplex process and obtain the maximum resolution (R_s). The analysis time can be controlled to limit the k' value.

Resolution is used as a criterion of separation, which can be affected by three independent factors:

$$R_s = \frac{1}{4}\left(\frac{\alpha - 1}{\alpha}\right)\sqrt{N}\left(\frac{k'}{1 + k'}\right) \tag{2}$$

where α is the selectivity factor for two peaks and N is the column plate number.

Note that the predicted k' values are used to arrange the solutes in order, then calculate R_s only of adjacent pairs not of all pairs of peaks; the result is satisfactory if the peaks do not all have the same relative order of retention in the experimental runs. Minimal resolution was selected in every simplex iterative proceeding. The result selects the highest resolution for the worst separated pair of peaks as a criterion of separation. All the other pairs of peaks give larger resolution values.

The SDO-G method can be used to carry out this optimization procedure. The above series of ten compounds were applied for the two-factor (carrier gas flow-rate and column temperature) optimization in GC. Table I gives the experimental k' values and Table II the b_i coefficients. The experimental boundary conditions are carrier gas flow-rate = 10–30 ml/min, column temperature = 150–180°C and analysis time

TABLE I

k' VALUES OF TEN COMPOUNDS MEASURED BY GC USING DIFFERENT CARRIER GAS FLOW-RATES AND COLUMN TEMPERATURES

Chromatography[a]			*Compound No.*[b]									
No.	*F (ml/min)*	*T (°C)*	*1*	*2*	*3*	*4*	*5*	*6*	*7*	*8*	*9*	*10*
1	10	150	2.258	2.725	3.358	3.667	4.625	5.358	6.792	8.917	10.790	15.367
2	10	165	1.941	2.291	2.789	2.981	3.663	4.258	5.519	6.681	7.424	10.752
3	10	180	1.725	1.963	2.637	2.486	3.018	3.376	4.009	5.037	5.300	7.743
4	20	150	2.181	2.663	3.265	3.554	4.470	5.229	6.578	8.711	10.520	14.879
5	20	165	1.895	2.263	2.763	2.974	3.645	4.184	5.118	6.592	7.434	10.671
6	20	180	1.662	1.883	2.247	2.389	2.857	3.234	3.818	4.779	5.117	7.415
7	30	150	2.138	2.615	3.185	3.492	4.385	5.108	6.400	8.492	10.260	14.538
8	30	165	1.869	2.180	2.705	2.869	3.541	4.049	4.951	6.377	7.180	10.311
9	30	180	1.672	1.914	2.276	2.396	2.914	3.276	3.914	4.879	5.207	7.586

[a] F = carrier gas flow-rate; T = column temperature.

[b] Compounds: 1 = isoamyl acetate; 2 = dodecane; 3 = chlorobenzene; 4 = 1,3,5-trimethylbenzene; 5 = *o*-chlorotoluene; 6 = bromobenzene; 7 = *m*-dichlorobenzene; 8 = *o*-dichlorobenzene; 9 = diethyl malonate; 10 = 1,4-butyrolactone.

TABLE II

VALUES OF THE COEFFICIENTS b_0, b_1,b_2, b_{11},b_{22} AND b_{12} OF THE TEN COMPOUNDS AND CORRELATION COEFFICIENT, r

Compound No.[a]	b_0	b_1	b_2	b_{11}	b_{22}	b_{12}	r
1	103.287	−82.565	−4.336	16.719	0.198	1.658	0.9994
2	128.070	−102.217	−3.157	20.555	−0.002	1.342	0.9983
3	187.891	−161.529	10.163	35.532	0.749	−5.618	0.9887
4	134.894	−101.818	−4.607	19.108	−0.131	2.107	0.9990
5	244.225	−192.618	−8.125	38.090	0.251	3.238	0.9987
6	243.506	−186.804	−7.952	35.651	−0.048	3.466	0.9993
7	461.392	−368.403	−16.474	73.472	0.047	7.161	0.9991
8	651.345	−525.547	−13.987	106.016	−0.042	6.078	0.9994
9	1437.433	−1210.240	−22.895	254.893	−0.654	10.788	0.9996
10	1863.054	−1557.112	−37.881	325.710	−0.021	16.666	0.9996

[a] See Table I.

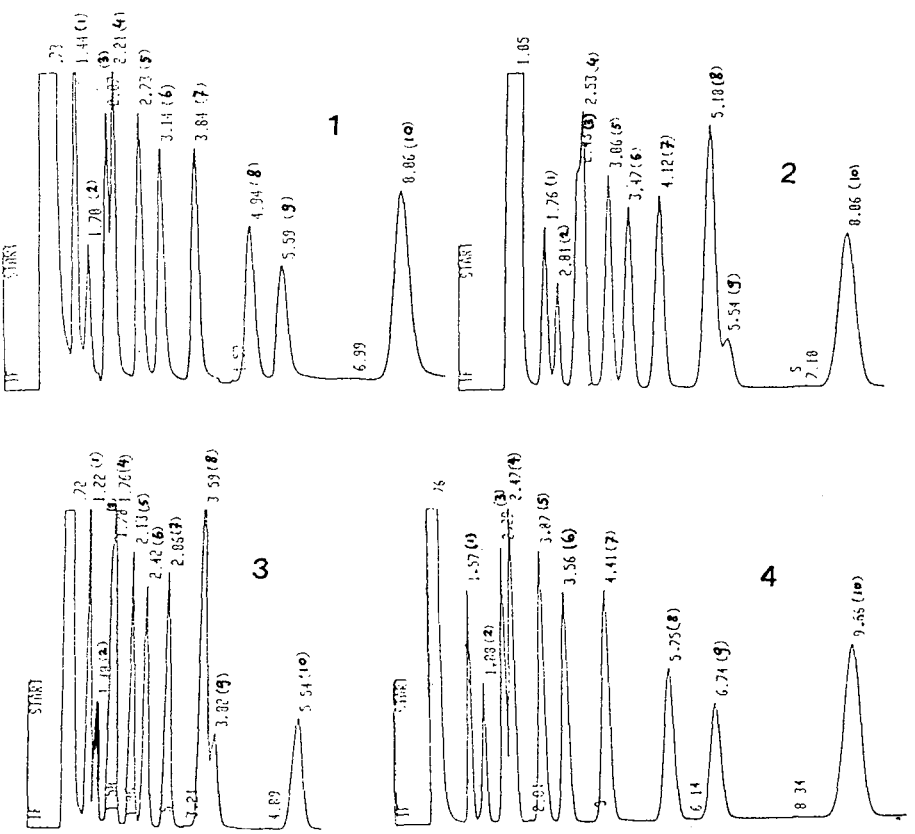

Fig. 2. Experimental chromatograms obtained under the following conditons: (1) T = 165°C, F = 20 ml/min. (2) T = 180°C, F = 10 ml/min. (3) T = 180°C, F = 20 ml/min. (4) T = 157.7°C, F = 19.4 ml/min. Numbers at the peaks indicate retention times in min, and (in parentheses) compound Nos. (as in Table I).

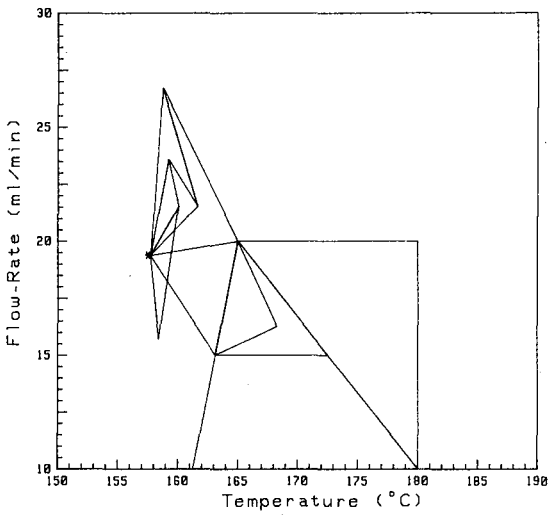

Fig. 3. Simplex optimization using SDO-G.

TABLE III

RESULTS OF THE COMPUTER-ASSISTED SIMPLEX PROCESS

No.	*Temperature (°C)*	*Flow-rate (ml/min)*	*Resolution, R_s*
1	165.00	20.0	0.9809
2	180.00	10.0	0.4601
3	180.00	20.0	0.4181
4	161.25	10.0	0.7195
5	172.50	15.0	0.5395
6	150.00	22.5	0.0000
7	171.56	12.5	0.4068
8	165.00	20.0	0.9809
9	172.50	15.0	0.5395
10	163.13	15.0	0.9418
11	163.13	15.0	0.9418
12	151.41	21.3	0.0000
13	168.28	16.3	0.7889
14	164.06	17.5	0.9750
15	157.73	19.4	1.1454
16	151.41	21.3	0.0000
17	164.06	17.5	0.9750
18	158.73	26.7	1.0399
19	161.37	19.7	1.0702
20	150.00	27.6	0.0000
21	161.62	21.5	1.0636
22	158.23	23.0	1.1049
23	161.09	11.0	0.8171
24	159.20	23.6	1.0855
25	159.68	20.4	1.1051
26	153.75	21.4	0.0000
27	160.04	21.5	1.0931
28	158.47	21.5	1.1192
29	158.42	15.7	1.1105
30	158.89	20.4	1.1197
31	155.13	11.6	0.0000
32	159.06	19.5	1.1196
33	158.08	17.5	1.1378

control $k' = 13$. Three initial experiments were required, which can be selected repeatedly from the nine preliminary experiments to perform the simplex process and obtain the maximum R_s. The initial experimental condition are (1) $T = 165°C$, $F = 20$ ml/min, (2) $T = 180°C$, $F = 10$ ml/min and (3) $T = 180°C$, $F = 20$ ml/min (T = column temperature, F = carrier gas flow-rate).

The chromatograms of three initial experiments are shown in Fig. 2 and results for SDO-G are given in Fig. 3 and Table III. Thirty-three iterative processes were performed by the computer; processes 6, 12, 20, 26 and 31 attempted to cross boundaries and were assigned an R_s of zero. The maximum R_s (1.12) is the highest resolution for the worst separated pair of peaks. The optimum conditions are a carrier gas flow-rate of 19.4 ml/min and a column temperature of 157.7°C. The same result was obtained from the general sequental simplex method. Fig. 2 shows the chromatogram of the ten compounds using these conditions. Excellent agreement was obtained between the predicted and experimental results.

Comparing experiments with the SDO-G method and the general sequential simplex method, ten and about thirty-three experiments (Table III), respectively, were required. In addition, SDO-G can select repeatedly the initial simplex experiments from the nine preliminary experiments without any additional experiment and the result gives the maximum R_s. Therefore the SDO-G method has distinct advantages over the general sequental simplex method for two-factor optimization in GC.

ACKNOWLEDGEMENTS

We thank Ms. Xiang-Hua Kong for her help with the computer programming.

REFERENCES

1 S. L. Morgan and S. N. Deming, *J. Chromatogr.*, 112 (1975) 267.
2 E V. Dose, *Anal. Chem.*, 59 (1987) 2420.
3 S. L. Morgan and C. A. Jacques, *J. Chromatogr. Sci.*, 16 (1978) 500.
4 D. F. Ingraham, C. F. Shoemaker and W. Jennings, *J. Chromatogr.*, 239 (1982) 35.
5 G. Castello and T. C. Gerbino, *J. Chromatogr.*, 366 (1986) 59.
6 W. Czelakowski, P. Kusz and A. Andrysiak, *Chromatographia*, 22 (1986) 278.
7 Q.-S. Wang and D.-M. Chen, *Chin. J. Chromatogr.*, 3 (1987) 171.
8 B.-S. Lin, H.-C. Li and P.-C. Lu, *Chin. J. Chromatogr.*, 4 (1986) 193.
9 H.-Y. Wang, *Master's Thesis*, Nankai University, Tianjin, 1988.
10 M.-G. Xie, C.-F. Zhou, X.-H. Yang and G.-Y. Ding, *Chromatographia*, 28 (1989) 274.

Journal of Chromatography, 513 (1990) 21–29
Elsevier Science Publishers B.V., Amsterdam

CHROM. 22 508

Flame infrared emission–flame ionization detector for gas chromatography

M. KEITH HUDSON*
Department of Electronics and Instrumentation, University of Arkansas at Little Rock, 2801 S. University, Little Rock, AR 72204 (U.S.A.)
and
TIM FAU, KATHY UNDERHILL and STEVE APPLEQUIST
Department of Chemistry, Southwest Missouri State University, Springfield, MO 65804 (U.S.A.)
(First received November 29th, 1989; revised manuscript received March 30th, 1990)

ABSTRACT

The utility of combining flame infrared emission detection (FIRE) and flame ionization detection (FID) into one system is discussed. An improved flame infrared detector using the 4.3 μm CO_2 emission band was constructed and fitted with electrodes to monitor the ionization in the hydrogen–air flame. The resulting system was found to provide the superior quantitation of moles carbon of FIRE and the greater sensitivity of FID. The system was successfully applied to the determination of carbon dioxide, carbon monoxide and hydrocarbons in gas mixtures.

INTRODUCTION

For the past several decades, flame ionization detection (FID) has held the distinction of being the most popular universal detection system available for use in gas chromatography (GC)[1]. There are, however, a number of limitations to this method of detection. For example, FID exhibits greater response to compounds containing acetylenic groups, while showing less response for alcohols and chlorinated compounds. Also, FID does not respond at all to carbon monoxide and carbon dioxide. Furthermore, other compounds, such as carbon disulfide, exhibit very little response.

Thermal conductivity detection (TCD) also has been used extensively in GC and gas analysis[1]. TCD has the advantage of responding not only to compounds containing carbon, but also the fixed gases. The major disadvantage of TCD is the lack of sensitivity. Additionally, the TCD response varies directly with the heat capacity and not number of moles carbon. As with FID, there is a structure factor present, requiring that standards be run before comparison of chromatographic peaks.

To enable the sensitive analysis of mixtures of gases, several methods have been used. These include the sequential connection of TCD and FID[2], the use of several columns with back-flushing of certain gases[3], and the addition of a methanation

0021-9673/90/$03.50

chamber to an FID-equipped gas chromatograph[4]. All of these methods complicate the analysis, adding more complexity and, therefore, more possible variables.

Recently, Hudson and Busch[5] introduced infrared emission from a flame as the basis for detecting organic compounds, initially in liquid chromatography and later in GC[6]. This detection method used a hydrogen–air flame to first combust compounds and then to vibrationally excite the carbon dioxide product while monitoring the resulting band at 4.3 μm with a filter photometer system. The flame infrared emission detection (FIRE) system for GC was developed, exhibiting good sensitivity and wide linear range. Additionally, FIRE gave sensitive response to carbon dioxide, carbon monoxide and carbon disulfide.

This paper reports on work done to combine the concepts of flame ionization and flame infrared emission into one gas chromatographic detector. Also, modifications were made in the infrared flame photometer system design of the combined FIRE–FID system resulting in improved response and sensitivity in the FIRE mode. These modifications are discussed also.

EXPERIMENTAL

Instrumentation

A Shimadzu (Kyoto, Japan) Model GC-8A gas chromatograph equipped with temperature programming and dual flame ionization detectors was used for the study. A small covered port in the side of the oven wall was used to bring column effluent out to the hydrogen–air burner via a stainless-steel tube of 1.5 mm I.D. A specially designed burner, as reported previously[6], was used to combust the eluted components. The previously described IR radiometer was modified with a field of view limiter made by drilling a hole of 2.4 mm I.D. through a 12.7 mm aluminum plate. This plate was mounted directly in front of and centered on the PbSe (P-2038-SPECIAL, Hamamatsu, San Jose, CA, U.S.A.) IR sensor. The PbSe sensor included an integral narrow bandpass filter centered on 4.45 μm. A special 600-Hz chopper was designed which allowed closer positioning of the PbSe sensor to the burner and flame. Shields of sheet aluminum painted flat black limited the viewed detector background and minimized air drafts. The PbSe sensor and its associated preamplifier were powered from a 24-V battery. The amplified signal was processed with an Ithaco Model 3921 lock-in-amplifier and recorded on a Shimadzu Model C-R6A Chromatopac chromatographic integrator.

The flame ionization detector used Plexiglass-supported high-voltage electrodes from a Beckman (Fullerton, CA, U.S.A.) GC4 chromatograph modified to fit the FIRE hydrogen–air burner. The 1 × 3 cm electrodes were positioned vertically and placed 7 mm apart, centered over the flame. Various heights were tried. The bottom limit (3.5 mm above the burner head) was found to be the minimum safe electrical working distance from the burner. Fig. 1 shows a close-up view of the electrodes and burner assembly and their mounting relative to the chopper–IR sensor used with the FIRE. A sodium chloride window was cemented to the Plexiglass electrode supports for some of the experiments. A Hewlett-Packard (Avondale, PA, U.S.A.) Model 6209B d.c. power supply supplied 300 V d.c. Current was monitored on a Keithley (Cleveland, OH, U.S.A.) Model 610BR electrometer. A Varian (Palo Alto, CA, U.S.A.) Aerograph recorder was used to record the signal monitored as a chromatogram.

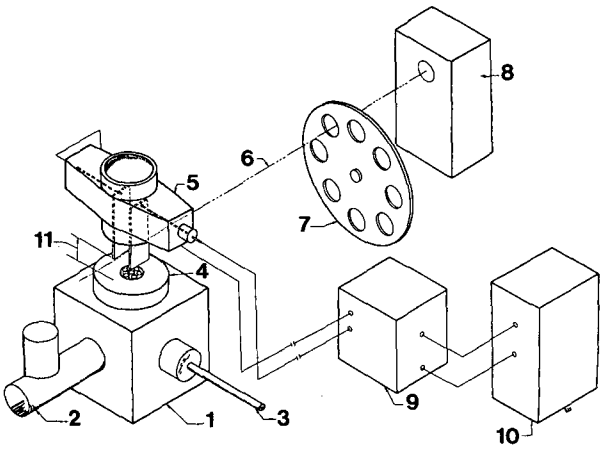

Fig. 1. Isometric close-up of FIRE–FID system. 1 = Burner body; 2 = fuel gas inlets; 3 = effluent capillary; 4 = burner head; 5 = electrode assembly; 6 = optical path; 7 = chopper; 8 = PbSe detector; 9 = electrometer; 10 = recorder; 11 = electrode height.

All flame or carrier gas flows were monitored using flow meters with integral metering valves (Cole-Parmer, Chicago, IL, U.S.A.). Hydrogen and helium were obtained locally. The air used was compressed, dried and filtered on site. Copper tubing (1/8 in.) was used in construction of all columns. Helium was used as the carrier gas in all experiments.

Reagents

A total of 21 different liquid organic compounds were analyzed, as specified in Table I. All compounds were reagent grade or the best possible grade.

Gas samples were obtained from Aldrich (Milwaukee, WI, U.S.A.), Matheson (Secaucus, NJ, U.S.A.) and Airco.

Procedure

An injection of 1 μl of the pure liquid was made to measure detector response per mole carbon in the compound. In the response studies, the oven temperature was elevated above the boiling point of sample compounds to minimize sample interactions with the column stationary phase. Detector response studies with respect to moles carbon were performed only for the modified FIRE system. Ratioed pentane–hexane solutions were injected to study detection limits. The column oven temperature was held above the boiling point of pentane but below that of hexane to effectively separate pentane from the hexane solvent and allow the pentane to travel through the column with minimal stationary phase effects. A 10% OV-101 on Chromosorb W AW 80–100 mesh column was used for all liquid samples, with a carrier flow-rate of 35 ml/min. Detection limits for both the FIRE and FID systems were evaluated in this manner.

All gaseous compounds were collected over water at 23°C. Mixtures of gases were collected initially into a 500-ml graduated cylinder to allow measurement of gas volumes, and then transferred into 250-ml flasks, equipped with Subaseal (Aldrich)

rubber septa to allow gas-tight syringe (0.5 ml Hamilton) sample removal. Pure gaseous samples were directly collected in 250-ml flasks.

Up to 0.5 ml of gaseous sample was injected onto the column (3 m Porapak R, 80–100 mesh, 23°C) to establish calibration curves. Carrier flow for all calibration curves was 25 ml/min. For gas mixtures where separation of carbon monoxide and methane was desired, the Porapak R column was run at sub-ambient temperature for 1.5 min to allow carbon monoxide and methane to elute. Subambient temperatures were achieved by placing a container of dry ice on the floor of the oven chamber with the oven circulator fan running. This allowed the circulated chamber air to reach a lower temperature of approximately −30°C. The column also reached this temperature after approximately 30 min. The oven was then raised to 200°C at a rate of 32°C/min. The column was maintained at this final temperature for approximately 4, min, allowing butane to completely elute. If separation of carbon monoxide and methane was not necessary, a temperature of 25°C was used at the start of the temperature program. An initial carrier flow-rate of 25 ml/min was used in all the gas mixture studies. As the eluted compounds combusted in the hydrogen–air flame, two chromatograms were recorded simultaneously, one from FIRE and one from FID.

RESULTS AND DISCUSSION

FIRE modification

The flame infrared emission detector used in this study was similar to units previously reported by Hudson and Busch[5,6]. Modifications were made in four areas: chopping rate, detector field of view, infrared filter type and the addition of an infrared window.

The chopper design used a 3000 rpm electric motor with a 12-hole chopper blade which resulted in a 600-Hz chopping rate. Comparing this rate with the previously reported rate of 90 Hz, an improvement in flicker, or $1/f$, noise is expected. In fact, at the rate of 600 Hz, flicker noise should be insignificant.

The detector utilized an aperture for field of view limiting, therefore, the PbSe device "saw" only the analytical flame and the area directly behind the flame. The field of view limiter restricted the amount of background radiation incident on the detector. This resulted in an overall decrease in baseline level and greatly decreased the effect of activity present in the laboratory, practically eliminating that source of noise.

Previously reported detectors used a high pass filter with a cut-off of 3.5 μm and a PbSe device with a cut-off above 5.0 μm. This resulted in a bandwidth of at least 1.5 μm which is much wider than the 4.3-μm carbon dioxide emission band. A different PbSe device was selected in this study which included an integral infrared filter with a center wavelength of 4.45 μm ($\pm$ 0.1 μm) and a bandwidth of 0.65 μm at 50% transmittance. This detector–filter combination gave a decrease in overall signal but since the noise level decrease was greater, the signal-to-noise ratio was increased. A further decrease in bandpass should result in even better signal-to-noise ratios.

An infrared window was placed between the burner flame and the chopper–detector assembly to eliminate the effect of air drafts caused by the chopper blade. As with the other modifications, the window resulted in a decrease in signal which was compensated for by a corresponding decrease in noise level.

Overall, the combination of these improvements gave a substantial increase in

signal-to-noise ratio, compared to FIRE units previously reported[6,7]. Injections of a pentane in hexane solution were used to ascertain the exact signal-to-noise ratio of the modifications. Using the criteria of detection limit equal to twice the noise, a detection limit for pentane of 0.002 μl was found which corresponds to about 1.5 μg of pentane.

Initially, it was thought that the use of a smaller hydrogen–air flame would result in better sensitivity and greater signal-to-noise ratio. Burners were constructed using smaller capillary tubes for flame support. These burners would not maintain the hydrogen–air flame. Therefore, the 1.5 mm capillary tubes were used and flame gas flow-rates were decreased. Flow-rates of 130 ml/min hydrogen and 340 ml/min air were found to be optimum for signal-to-noise ratio and stabilization of the FIRE chromatographic baseline. It can be noted that these flow-rates, while lower, give the same flame stoichiometry as previously reported[6].

When the FIRE hydrogen–air flame is functioning at high efficiency, all organic compounds are expected to completely combust, giving a proportionate number of moles of carbon dioxide. Ideally, the signal monitored from the 4.3-μm carbon dioxide emission should be directly proportional to the number of moles carbon in the sample. Earlier work had roughly indicated this trend, but the data showed anomalous behavior for certain compounds. Table I shows the results of the injection of 1 μl of a variety of organic compounds, listing peak areas and signal per mole carbon. Signals

TABLE I

SIGNAL PER MOLE CARBON

Compound	*Peak area*	*Signal per mole carbon (× 10^9)*
Pentane	111 787	2.58
Hexane	123 995	2.70
Heptane	117 641	2.46
Octane	114 119	2.32
Cyclohexane	138 027	2.49
Methyl cyclohexane	132 364	2.41
Cyclooctane	124 914	2.10
Benzene	172 746	2.56
Toluene	152 118	2.31
Methanol	58 826	2.52
Ethanol	79 223	2.31
1-Propanol	90 152	2.25
2-Propanol	97 397	2.48
1-Butanol	91 506	2.09
t-Butanol	107 929	2.54
Carbon tetrachloride	22 521	2.17
Dichloromethane	32 982	2.11
Chloroform	28 678	2.31
Tetrachloroethane	36 824	2.01
2-Butanone	110 019	2.46
Butyl acetate	99 851	2.19
Mean value		2.35
Standard deviation ($n-1$)		0.19

per mole carbon were calculated from the injected volume, density of the compound, formula weight of the compound and the number of moles carbon contained in the compound. As shown in Table I, an average signal per mole carbon for all compounds injected of $2.35 \cdot 10^9$ was found, with a standard deviation of 0.19.

The discrepancies found in comparing the data presented in Table I and the reported responses in the literature[6,7] can be explained in view of the instrument modifications. The use of the aperture limiter and the narrow bandpass filter each contribute to this difference. Some compounds may favor multiple emission from each carbon dioxide. By limiting the view of the detector to one area of the flame zone, any secondary emission by excited carbon dioxide may occur outside the view of the detector. Secondly, and most importantly, some compounds combust not only to carbon dioxide, but give other products in small amounts. For example, aromatic compounds are known to burn with a sooty flame characteristic of carbon particle formation. Using the detector–filter combination of Hudson and Busch, the wide bandpass would allow blackbody radiation from carbon particles to be monitored. The described system would limit greatly that effect.

The signal observed suggested that all compounds were combusted with about the same degree of efficiency, if not 100% then a constant percentage. This response suggests that FIRE may be used for standardless analysis, that is, where no standards are available. The advantages of this type response are obvious when compared to either TCD or FID, each of which must have standards for each component for accurate quantitation.

FID design and performance

Best FID response was found with the Keithley electrometer set on the 10^{-10} A scale. The scale multiplier could then be used to select the overall sensitivity.

The FID section of the combination detector gave response to various compounds as expected[1–3]. The FID sensitivity easily exceeded that of FIRE for compounds which both systems responded to. As a basis for comparison, the detection limit of the FID unit for the same pentane in hexane solutions as used in the FIRE studies was evaluated. Using a carrier flow-rate of 25 ml/min, a detection limit of 0.000006 μl was found by averaging the signal for 5 injections of 0.1 μl of a 1 part pentane in 5000 parts pentane in hexane solution, giving a signal-to-noise ratio of 10. The amount that would give a signal-to-noise ratio of 2 was then calculated. This corresponded to about 4.5 ng pentane, which when compared with modern, commercially available units was not as sensitive. This can be explained by examining several factors. First, the specialized burner was optimized for FIRE. This burner is a premixed hydrogen–air system, as opposed to the non-premixed type found in most, if not all, FID units. Studies have shown that the non-premixed burner supports greater ionization in the flame[1], hence greater FID signal. Secondly, the electrode assembly was chosen to not interfere with FIRE. This unit used two flat electrodes on opposite sides of the flame. Most modern FID units utilize the actual flame jet as the positive electrode, with the negative electrode typically of cylindrical shape and surrounding the flame which has been found to give better response. Another factor affecting the detection limit was the nature and origin of the limiting noise. As previously noted, this unit was not fully shielded, either from the surroundings or from the FIRE components. The slight vibrations from the chopper assembly seemed to be

the source of the limiting noise on FID since FID had less noise without the FIRE components active. Since the purpose of this work was to investigate the combination detector, all detection limits are stated for both detection modes active.

One effect not expected with FID was noted. With the configuration used in this study, a decrease in carrier flow-rate resulted in decreased sensitivity. This phenomena may be due to the physical configuration of the FID system constructed for this study. However, the authors have not evaluated this further.

Concomitant operation of FIRE–FID confirmed no significant interference observed in either the FIRE or FID chromatograms. The parallel, flat electrodes could be positioned out of the field of view of the FIRE system. While this was not optimum for FID, it did control any blackbody background problems that a more typical cylindrical FID electrode may have introduced to FIRE. The configuration of the Plexiglass electrode mounts and IR window isolated the flame from the chopper air drafts. A schematic representation of the overall FIRE–FID system is shown in Fig. 2.

Analysis of gas mixtures.

The FIRE–FID detector was used to analyze gaseous mixtures of carbon monoxide, carbon dioxide and hydrocarbons. Ratioed synthetic samples were made of the gases and injected. Sample 1 contained 57% methane, 20% carbon monoxide, 20% carbon dioxide, 1% ethane, 1% propane and 1% butane (v/v). Sample 2 consisted of 49% carbon monoxide, 49% carbon dioxide, 1% methane and 1% ethane (v/v).

Chromatograms of samples 1 and 2 are shown in Figs. 3 and 4, respectively. Both chromatograms showed that carbon monoxide and carbon dioxide are detected only with the FIRE unit. All the hydrocarbons are detected by both units, when present in sufficient concentration. Fig. 3 graphically illustrates this, as peaks 1 and 3 are due to carbon monoxide and carbon dioxide, respectively, and are present only in the FIRE chromatogram. The FIRE detector responds to these gases with the same response per mole carbon seen for all carbon containing species. Peaks 2, 4, 5 and 6 are for the hydrocarbon gases, and these are seen in both the FIRE and FID modes.

Fig. 4 is the isothermal chromatogram for the separation of four gases, In this case, carbon monoxide and methane are not separated completely on the column. However, this chromatogram illustrates one advantage of the FIRE–FID combina-

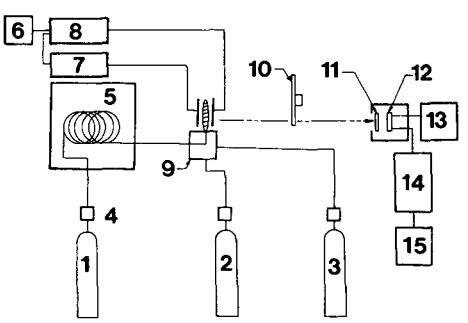

Fig. 2. Schematic diagram of FIRE–FID apparatus. 1 = Carrier gas; 2 = air; 3 = hydrogen; 4 = flow meters; 5 = chromatograph; 6 = FID recorder; 7 = 300 V power supply; 8 = electrometer; 9 = burner assembly; 10 = chopper; 11 = IR filter; 12 = PbSe device; 13 = 24 V power supply; 14 = lock-in-amplifier; 15 = FIRE recorder.

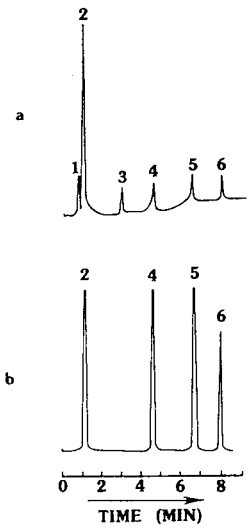

Fig. 3. Dual FIRE–FID chromatogram for gas mixture sample 1 (see text). (a) FIRE mode; (b) FID mode. Peaks: 1 = carbon monoxide; 2 = methane; 3 = carbon dioxide; 4 = ethane; 5 = propane; 6 = butane.

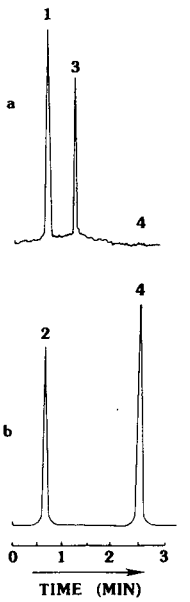

Fig. 4. Dual FIRE–FID chromatogram for gas mixture sample 2 (see text). (a) FIRE mode, (b) FID mode. Peaks: 1 = carbon monoxide; 2 = methane; 3 = carbon dioxide; 4 = ethane.

tion unit in that peak 1, in the FIRE mode, represents predominantly carbon monoxide. Peak 2, in the FID mode, represents methane present in small amounts in the sample. While the two components are not separated on the column, they are separately detected, allowing individual analysis. Peak 3 is due to the carbon dioxide in the sample, and is seen only in the FIRE mode. Peak 4 is due to ethane and is seen only in the FID mode, at this concentration.

In addition, only a fraction of the expected response for the hydrocarbon gases using the FID was observed due to the decrease in carrier flow-rate seen with the Porapak R column upon increasing column temperature. As the carrier flow-rate is decreased, the response drops off with this FID configuration. This effect was noted also in the detection limit studies on pentane.

CONCLUSIONS

FIRE can be applied generally to all carbon containing species. The superior quantitation of carbon seen with FIRE compared to other methods is a definite advantage. FIRE is more sensitive than TCD and, while not as sensitive as FID, offers an attractive alternative for those samples not requiring the extreme sensitivity found using FID.

However, the combination detector described in this work allows the analyst the advantages of both types of detection in the dual mode. If a particular compound is present in sufficient amounts to be detected by FIRE, the superior quantitation of that

method is seen. For compounds present in small amounts, FID may be used. This synergistic approach has two obvious strengths. Compounds that are not detected by one method may be detected by the other, such as the carbon monoxide and carbon dioxide used in this study. FIRE is more sensitive for both these gases than either TCD alone or in combination with FID. Also, it is not always necessary to separate certain compounds to analyze them, thereby potentially eliminating hours of laborious methods development. At this time, no compounds have been encountered that FID exhibits a response to that FIRE does not. The reverse situation is true for the compounds mentioned above and is indicated for some other classes of compounds, such as the halogenated hydrocarbons.

Additional work is being undertaken to study the process of combustion in the hydrogen–air flame. Basic insights gained in such a study should reveal additional information useful in the design and implementation of the FIRE and FIRE–FID systems.

ACKNOWLEDGEMENTS

The authors express their appreciation to Joe Shipman, Mike Murphy and Robert Holmes of the SMSU Temple Hall Support Services for help in fabrication and assembly of circuits and apparatus used in this study. We also express our appreciation to Jim Riley of the Drury College Physics Department for the generous loan of the Keithley Electrometer. Finally, the authors are indebted to Rex Whitfield and Mike Dugan for their graphics skills in preparing the figures in this paper.

This work was supported in part by Southwest Missouri State University Faculty Research Grant 15221-890-7 and a grant from Research Corporation, Tuscon, AZ, U.S.A. Portions of this paper were presented at the *1988 Missouri Academy of Science Annual Meeting, Kirksville, MO, April 30, 1988,* (paper No. 53), *23rd American Chemical Society Midwest Regional Meeting, Iowa City, IA, November 17, 1988,* (paper No. 218) and the *16th Annual Federation of Analytical Chemistry and Spectroscopy Societies Meeting, Chicago, IL, October 4, 1989* (paper No. 531).

REFERENCES

1 D. J. David, *Gas Chromatography Detectors,* Wiley, New York, 1974.
2 J. S. Stufkens and H. J. Bogard, *Anal. Chem.*, 47 (1975) 383.
3 M. Shykles, *Anal. Chem.*, 47 (1978) 949.
4 H. H. Willard, L. L. Merritt, J. A. Dean and F. A. Settle, *Instrumental Methods of Analysis,* Wadsworth, Belmont, CA, 7th ed., 1988, p. 555.
5 M. K. Hudson and K. W. Busch, *Anal. Chem.*, 59 (1987) 2603.
6 M. K. Hudson and K. W. Busch, *Anal. Chem.*, 60 (1988) 2110.
7 M. K. Hudson, *Ph.D. Thesis,* Baylor University, Waco, TX, December 1987.

Journal of Chromatography, 513 (1990) 31–37
Elsevier Science Publishers B.V., Amsterdam

CHROM. 22 394

Use of M-series retention index standards in the identification of trichothecenes by electron impact mass spectrometry

R. KOSTIAINEN* and S. NOKELAINEN
Food and Environmental Laboratory of Helsinki, Helsinginkatu 24, Helsinki 53 (Finland)
(First received December 5th, 1989; revised manuscript received February 26th, 1990)

ABSTRACT

A method for the reliable identification of a series of trichothecenes as their trifluoroacetate esters in porridge flake samples is described. The esters were separated by gas chromatography and identified from their retention times relative to *n*-alkylbis(trifluoromethyl)phosphine sulphide (M-series) retention index standards and their electron impact mass spectra. The relative retention times offer an independent identification method by which the reliability of the identification can be improved. The mass spectra and the relative retention times were obtained from the same gas chromatographic–mass spectrometric run. Detection limits were of the order to 0.005–0.05 mg/kg. All the flake samples including oats (ten of fourteen samples studied) contained deoxynivalenol (0.01–0.2 mg/kg) and one oat flake sample contained HT-2 toxin (0.008 mg/kg). The other trichothecenes monitored were not found.

INTRODUCTION

Trichothecenes are a significant contamination problem in foods and feeds[1–5]. They are naturally produced by a variety of fungi, which can be formed rapidly in grain and feed during harvest, transport and storage. Because of the extreme toxicity[3,6] and natural occurrence of trichothecenes, several identification methods have been developed. Gas chromatography (GC) is often used[7–11], but the specificity is limited[8,11]. Tandem mass spectrometry (MS–MS) seems to be the most specific and sensitive method for trichothecenes in complex matrices[12–20], but needs expensive and sophisticated instrumentation. GC–MS is a very common method in the routine analysis of trichothecenes[21–23], but the specificity with complex matrices may be insufficient, leading to reduced reliability of the identification. The use of retention indices in GC–MS offers, in addition to MS data, an independent identification method by which the reliability of the identification can be improved. The detection result is accepted only if the relative abundances of the monitored ions in the mass

0021-9673/90/$03.50

spectrum do not vary by more than an allowed amount and if the monitored compounds are found inside a certain allowed retention index "window".

Retention indices have been widely used in GC[24–27] but very seldom in GC–MS[28,29]. This paper describes the use of *n*-alkylbis(trifluoromethyl)phosphine sulphides (M-series) as retention index standards in the identification of some trichothecenes (Table I) in porridge flakes by GC–electron impact (EI) MS. The M-series standards were prepared for use as universal retention index standards detectable with all common detectors used in GC[24]. However, the standards are also well suited to MS.

EXPERIMENTAL

Chemicals

All the trichothecenes (Table I) and trifluoroacetic anhydride (TFAA) were obtained from Sigma. 4-Dimethylaminopyridine (4-DMAP) was obtained from Aldrich. The retention index standard solution ($2.5 \cdot 10^{-4}$ *M*) including even-number standards M_6–M_{20} (Table I) was obtained from HNU-Nordion.

Sample clean-up

About 100 g of porridge flakes were mixed, an aliquot (10 g) of flake was

TABLE I

THE TRICHOTHECENES STUDIED

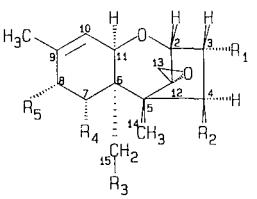

Trichothecene	R_1	R_2	R_3	R_4	R_5
T-2 toxin (T-2)	OH	OAc[a]	OAc	H	$OCOCH_2CH(CH_3)_2$
Iso-T-2 toxin (Iso-T-2)	OAc	OH	OAc	H	$OCOCH_2CH(CH_3)_2$
HT-2 toxin (HT-2)	OH	OH	OAc	H	$OCOCH_2CH(CH_3)_2$
Triacetoxyscirpenol (TAS)	OAc	OAc	OAc	H	H
Diacetoxyscirpenol (DAS)	OH	OAc	OAc	H	H
Monoacetoxyscirpenol (MAS)	OH	OH	OAc	H	H
Deoxynivalenol (DON)	OH	H	OH	OH	=O

Compounds in M-series:

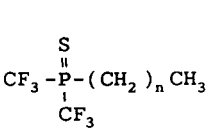

n = 5,7,9,11,13,15,17,19

[a] OAc = CH_3COO.

removed and 0.01 mg of Iso-T-2 was added as an internal standard. Methanol–water (95:5) (170 ml) was added and the sample was ground in a homogenizer for about 5 min. Otherwise the sample clean-up was performed according to the method described previously[17].

Derivatization

After clean-up the sample was evaporated to dryness with nitrogen and to the residue were added 100 μl of toluene–acetonitrile (9:1) containing 4-DMAP (2 mg/ml). Sodium hydrogencarbonate (10 mg) and 50 μl of TFAA were added and derivatization was carried out at 333 K for 20 min. After cooling, the reaction mixture was evaporated to dryness with nitrogen and 200 μl of toluene and 0.5 ml of water were added to the residue. The sample was mixed for 4 min and allowed to stand until the layers had separated. The toluene phase was transferred into a 2.5-ml vial containing anhydrous sodium sulphate. The toluene extraction was repeated twice and the final volume in the vial was adjusted to 1 ml with toluene.

Gas chromatography–mass spectrometry

All the mass spectra were obtained with an HP 5970 quadrupole mass spectrometer interfaced by direct coupling with an HP 5890 gas chromatograph. The mass spectrometer was operated in the electron impact mode (70 eV). The ion source temperature was 493 K. A 2-μl volume of the sample together with 1 μl of M-series retention index standard solution ($2.5 \cdot 10^{-4}$ *M*) were injected into the gas chromatograph using splitless (1 min) injection. The injector temperature was 533 K and the carrier gas (helium) flow-rate was about 1.5 ml/min. An HP-5 (5% phenylmethylsilicone) capillary column (25 m × 0.2 mm I.D.; 0.33 μm film thickness) was used. The interface temperature was 543 K. The temperature programme was 333 K (held for 1 min) to 473 K at 20 K/min and from 473 to 553 K at 10 K/min, the final temperature being held for 10 min.

The mass spectra were recorded by using the scan range 50–700 u. The linearity studies, determination of detection limits and the analysis of porridge flake samples were done by using multi-grouping and selected ion monitoring (Table II), in which only the most intense and characteristic ions were monitored.

TABLE II

RUN PROGRAMME FOR THE TRICHOTHECENES AND M-SERIES COMPOUNDS (*m/z* 147)

Compound	*Monitored ions*[a] *(m/z)*	*Start time (min)*
$DON(TFA)_3$	584*,259,231,147	10.00
$MAS(TFA)_2$	456*,343,329,147	13.00
DAS(TFA)	402*,359,329,147	15.00
$HT\text{-}2(TFA)_2$	472,455*454,147	16.25
TAS	348*,320,275,147	17.50
T-2(TFA)	401*,329,327,147	19.00
Iso-T-2(TFA)	460*,400,357,147	19.85

[a] Asterisks indicate ions used in quantification.

TABLE III

SELECTED ION MASS SPECTRA OF STUDIED TRICHOTHECENES

Compound	*MW*	*m/z (relative abundance, %)*
$DON(TFA)_3$	584	231(100, 259(87), 584(80)
$MAS(TFA)_2$	516	329(29), 343(21), 456(100)
DAS(TFA)	462	329(63), 359(20), 402(100)
$HT\text{-}2(TFA)_2$	616	454(50), 455(100), 472(39)
TAS	426	275(48), 320(63), 348(100)
T-2(TFA)	562	327(100), 329(52), 401(91)
Iso-T-2(TFA)	562	357(100), 400(63), 460(71)

The TFA derivatives of five barley samples containing increasing amounts (0.01, 0.03, 0.06, 0.09 and 0.2 mg/kg) of trichothecenes DON, MAS, DAS, HT-2, TAS and T-2 (Table I) and 1 mg/kg of Iso-T-2 as an internal standard were prepared for linearity studies. Each sample was analysed twice. The peak areas of the ion currents were used in the linear regression. The calibration graphs were evaluated as the ratio of the ion of *m/z* 460 of Iso-T-2 (TFA) to that of the most characteristic and if possible most abundant ion of the TFA ester (asterisks in Table II indicate the ions used in quantification). The detection limits were evaluated at a signal-to-noise ratio of 5:1.

RESULTS AND DISCUSSION

The TFA esters of the trichothecenes were identified on the basis of the selected ion mass spectra and relative retention times. Selected ion monitoring was used to increase the sensitivity. The ions of the TFA esters monitored were chosen so that the chemical noise from the matrix would be at a minimum and the maximum signal-to-noise ratio would be achieved. Ions with high mass values often meet these requirements. The selected ion mass spectra are presented in Table III. The mass spectra of the TFA esters and their partial fragmentation pathways are presented elsewhere[23].

Selective ion monitoring together with retention time information is in most instances sufficient for a reliable identification. However, the retention times are very dependent on the GC conditions, *e.g.*, on the condition of the column, the stability of the temperature programme and the carrier gas flow-rate. More reliable results can be obtained by using relative retention times, which are much less dependent on the conditions than the actual retention times. The retention index series used in this study (M-series) (Table I) was prepared mainly for GC detectors[24], but is also well suited to GC–EI-MS analysis. All compounds in the M-series produced two characteristic and common ions, *viz.*, *m/z* 147 ($C_2H_3SPF_3$) and *m/z* 229 ($C_4H_4SPF_6$), which can be selected for monitoring together with characteristic ions of the analyte. The elemental compositions of the ions of *m/z* 147 and 229 were confirmed by high-resolution mass spectrometry (resolution, $R = 10\ 000$). Fig. 1 presents an example of the identification of the trichothecenes as their TFA esters in a standard solution and in an oat flake sample.

The relative retention times (*RRT*) of the TFA esters were calculated with the equation

$$RRT = 100M_n + 100(M_{n+i} - M_n) \cdot \frac{T_x - T_n}{T_{n+i} - T_n} \quad (1)$$

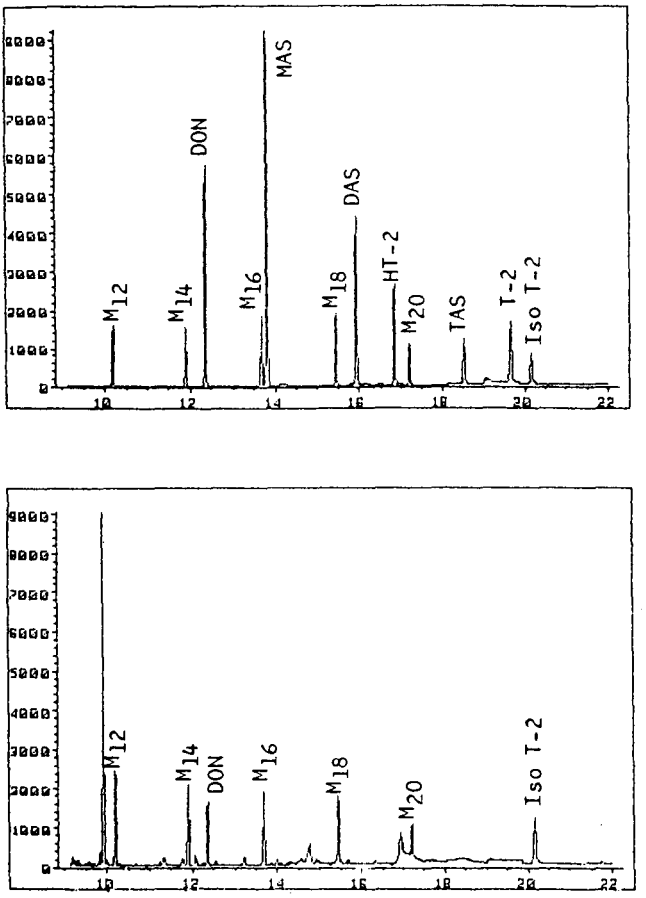

Fig. 1. Selected ion current chromatograms recorded (a) from a TFA-derivatized standard sample and (b) from a TFA-derivatized oat flake sample. x-Axis and y-axis represent retention time (in minutes) and intensity, respectively. The monitored ions are presented in Table II.

where M_n and M_{n+i} are carbon numbers in the alkyl chain of the compounds eluted one on each side of the monitored trichothecene, T_x is the retention time of the monitored trichothecene and T_n and T_{n+i} are the retention times of the compounds of M_n and M_{n+i}. The relative retention times for the compounds eluted after the last M-series compound (M_{20}) (TAS, T-2 and Iso-T-2) are obtained by using calculated values for M_{22} and M_{24} [$T_{22} = T_{20} + (T_{20} - T_{18})$; $T_{24} = T_{20} + 2(T_{20} - T_{18})$].

The relative retention times of the TFA esters were measured using pure compounds and are presented together with standard deviations ($n = 6$) in Table IV. The relative retention times are more accurate for compounds eluted between the standards than for those eluted after the last standard, M_{20}. Standard M_{24} is not commercially available. However, accurate enough results are obtained for TAS, T-2 and Iso-T-2 with the calculated retention times of M_{22} and M_{24}. The relative retention times were measured six times and the measurements were made every second week, but no systematic changes in the results were observed.

TABLE IV

RELATIVE RETENTION TIMES (RRT), DETECTION LIMITS AND LINEAR REGRESSION OF THE QUANTIFICATION

The concentrations of the studied trichothecenes in the spiked barley samples were 0.01, 0.03, 0.06, 0.09 and 0.2 mg/kg; Iso-T-2 was used as an internal standard (1 mg/kg).

Compound	*RRT (±S.D.) (n = 6)*	*r*[a]	*Slope*	*Intercept (mg/kg)*	*Detection limit (pg)*
$DON(TFA)_3$	1451.89 ± 0.12	0.9926	2.0342	0.00377	10
$MAS(TFA)_2$	1614.61 ± 0.18	0.9963	0.5102	−0.00009	5
DAS(TFA)	1855.94 ± 0.27	0.9991	0.8357	0.00383	15
$HT\text{-}2(TFA)_2$	1958.03 ± 0.16	0.9985	1.5168	0.00502	10
TAS	2152.99 ± 0.86	0.9997	3.0450	0.00213	40
T-2(TFA)	2283.67 ± 1.26	0.9991	2.0282	0.00438	30
Iso-T-2(TFA)	2341.25 ± 1.63				

[a] Correlation coefficient

The identification of a trichothecene was accepted if the relative abundance of the monitored ion of the TFA ester did not vary more than ±10% and the relative retention time by more than ±2 units. If the relative retention time of the analyte peak was within the acceptable values but the relative abundance of the monitored ion showed intergerence by the matrix, the ion was changed to one not subject to interference and the run was repeated. In all instances where the relative retention times varied by more than 2 units the relative abundances of the monitored ions also varied by more than ±10%.

The studied trichothecenes were quantified by using Iso-T-2, which does not occur naturally, as an internal standard. The correlation coefficients showed good linearity between concentration levels of 0.02 and 0.2 mg/mg. The detection limits were between 0.005 and 0.05 mg/kg with the porridge flake samples and between 5 and 40 pg with standards (Table IV).

Fourteen porridge flake samples were analysed by the method described above. Eight of the samples were prepared from oats, three from a mixture of four corns (oats, rye, barley and wheat), two from rye, one from barley and one from wheat. DON was found at levels 0.01 and 0.2 mg/kg in all of the samples containing oats. One rye sample contained 0.005 mg/kg of DON and one oat sample contained 0.008 mg/kg of HT-2.

CONCLUSIONS

The use of relative retention times in GC–MS offers, in addition to the MS data, an independent identification method, by which the reliability of the identification can be improved. The MS and relative retention time data are obtained from the same GC run. In an analytical problem in which unknown peaks detected by GC detectors are to be identified by GC–MS, it might be difficult to find the unknown peak by GC–MS owing to the response differences. In this event the use of relative retention times helps to establish the peak of interest.

ACKNOWLEDGEMENTS

Financial support from the Magnus Ehrnrooth and Oskar Öfland Foundations is gratefully acknowledged.

REFERENCES

1 Y. Ueno, in K. Miller (Editor), *Toxicological Aspects of Food*, Elsevier Applied Science, Barking, 1987, p. 150.
2 Y. Ueno, in P. Krogh (Editor) *Mycotoxins in Food*, Academic Press, London, 1988, pp. 123–147 and 217–249.
3 Y. Ueno (Editor), *Trichothecenes —Chemical, Biological and Toxicological Aspects, (Developments in Food Science*, Vol. 4), Kodansha, Tokyo, and Elsevier, Amsterdam, 1983, p. 195.
4 E. Karppanen, A. Rizzo, S. Berg, E. Lindfors and R. Aho, *J. Agric. Sci. Finl.*, 57 (1985) 195.
5 H. Petterson, K. H. Kiessling and K. Sandholm, *Swed. J. Agric. Res.*, 16 (1986) 179.
6 K. C. Erlich and K. W. Daigle, *Biochim. Biophys. Acta*, 923 (1987) 206.
7 C. E. Kientz and A. Verweij, *J. Chromatogr.*, 355 (1986) 229.
8 A. F. Rizzo, L. Saari and E. Lindfors, *J. Chromatogr.*, 368 (1986) 381.
9 H. D. Rood, Jr., W. B. Buck and S. P. Swanson, *J. Agric. Food Chem.*, 36 (1988) 74.
10 H. D. Rood, Jr., W. B. Buck and S. P. Swanson, *J. Assoc. Off. Anal. Chem.*, (1988) 493.
11 R. M. Black, R. J. Clarke and R. W. Read, *J. Chromatogr.*, 388 (1987) 365.
12 T. Krishnamurthy and E. W. Saver, *Anal. Chem.*, 59 (1987) 1272.
13 T. Krishnamurthy and E. W. Saver, *Biomed. Environ. Mass Spctrom.*, 15 (1988) 13.
14 H. T. Kalinoski, H. R. Udseth and B. W. Wright, *J. Chromatogr. Sci.*, 23 (1985) 192.
15 R. Kostiainen, T. Kotiaho and A. Hesso, in M. Rautio (Editor), *Systematic Identification of Mycotoxins: B5: Selected Trichothecenes, Aflatoxins and Related Mycotoxins, Mass Spectrometric Analysis*, Ministry for Foreign Affairs of Finland, Helsinki, 1986, p. 53.
16 R. Kostiainen and A. Hesso, *Biomed. Environ. Mass Spectrom.*, 15 (1988) 279.
17 R. Kostiainen and A. Rizzo, *Anal. Chim. Acta*, 204 (1988) 233.
18 R. Kostiainen, *Biomed. Environ. Mass Spectrom.*, 16 (1988) 197.
19 R. Kostiainen, *Biomed. Environ. Mass Spectrom.*, 18 (1988) 116.
20 R. Kostiainen, A. Rizzo and A. Hesso, *Arch. Environ. Contam. Toxicol.*, 18 (1989) 356.
21 R. T. Rosen and J. D. Rosen, *Biomed. Mass Spectrom.*, 9 (1982) 443.
22 J. D. Rosen, R. T. Rosen and T. G. Hartman, *J. Chromatogr.*, 355 (1986) 241
23 C. J. Mirocha, S. V. Pathre, R. J. Pawlosky, R. J. Pawlosky and D. W. Hewetson, in R. J. Cole (Editor), *Modern Methods in the Analysis and Structural Eludiation of Mycotoxins*, Academic Press, Orlando, FL, 1986, p. 353.
24 A. Manninen, M.-L. Kuittinen and L. Julin, *J. Chromatogr.*, 394 (1987) 465.
25 E. Kovats, *Helv. Chim. Acta*, 41 (1958) 1915.
26 M. V. Budahegyi, E. R. Lombosi, T. S. Lombosi, S. Y. Meszaros, S. Nyiredy, G. Tarjan, I. Timai and J. M. Takacs, *J. Chromatogr.*, 271 (1983) 213 and 226.
27 J. Enqvist, M. Kokko, M. Pajarinen, K. Himberg and U.-M. Lakkisto, in M. Rautio (Editor), *Air Monitoring as a Means for Verification of Chemicals Disarmament, Report C.2, Development and Evaluation of Basic Techniques, Part I, Mass Spectrometric Analysis*, Ministry for Foreign Affairs of Finland, Helsinki, 1986, p. 207.
28 H. Nau and K. Biemann, *Anal. Lett.*, 6 (1973) 1071.
29 R. Kostiainen and A. Hesso, in M. Rautio (Editor), *Air Monitoring as a Means for Verification of Chemical Disarmament, Report C.2, Development and Evaluation of Basic Techniques, Part I, Mass Spectrometric Analysis*, Ministry for Foreign Affairs of Finland, Helsinki, 1986, p. 129.

Journal of Chromatography, 513 (1990) 39–45
Elsevier Science Publishers B.V., Amsterdam

CHROM. 22 469

Determination of biogenic and anthropogenic volatile halocarbons in sea water by liquid–liquid extraction and capillary gas chromatography

KATARINA ABRAHAMSSON* and SILKE KLICK
Department of Analytical and Marine Chemistry, Chalmers University of Technology and University of Göteborg, S-412 96 Göteborg (Sweden)
(First received December 20th, 1989; revised manuscript received March 28th, 1990)

ABSTRACT

A method is presented for the determination of fifteen biogenic and anthropogenic halogenated hydrocarbons, including brominated and iodated compounds, in sea water at concentrations below the nanograms per litre range. The method includes liquid–liquid extraction of the sea water with pentane, gas chromatographic separation and electron-capture detection. The separation was performed on two coupled fused-silica columns of different polarity and film thickness. In this way trichloroethene, bromodichloromethane and dibromomethane could be separated.

INTRODUCTION

The determination of anthropogenic halocarbons in environmental samples has become a standard procedure for many laboratories during the last 15 years, since they are regarded as indicators of pollution impact. Common methods usually include some kind of preconcentration step, either by a dynamic headspace technique combined with solid-phase adsorption or cold trapping[1,2], or by liquid–liquid extraction with organic solvents[3,4]. A typical procedure involves separation of the halocarbons by capillary gas chromatography on a non-polar silicone stationary phase and electron-capture detection (ECD). For sea-water samples with concentrations of volatile halocarbons in the lower nanograms per litre range, preconcentration is essential. Additionally, when dealing with sea water special problems are encountered, as a number of volatile halocarbons produced by marine organisms can be present in the sample and interfere with the determination of anthropogenic halocarbons[5–7]. Hence standard methods available for the determination of halocarbons in drinking water, waste water, etc., are often unsuitable for sea water, owing to differences as regards detection limits, separation properties, choice of standard mixtures, etc.

Liquid–liquid extraction with pentane has frequently been used for the determination of halocarbons in sea water[4,7–9]. The method produces reliable results in

0021-9673/90/$03.50

terms of precision, detection limits and contamination risks[3,8]. The technique is simple regarding instrumental set-up and the total analysis time is short.

Non-polar methyl or methylphenyl silicone phases, such as DB-1 or DB-5, are commercially available as bonded, cross-linked phases on fused-silica capillary columns. These columns, which provide a greater separation efficiency than packed columns, have frequently been used for the analysis of halogenated organic compounds[7,10–13], although their ability to separate halocarbons is limited[14,15]. For instance, the separation of trichloroethene, bromodichloromethane and dibromomethane from each other cannot be obtained on these stationary phases, and this problem also limits their use in sea-water analysis[16]. Mehran *et al.*[14] coupled two segments of capillary columns coated with two stationary phases of different polarity, 100% methylpolysiloxane (DB-1) and 14% cyanopropylphenylmethylpolysiloxane (DB-1701), and achieved the separation of eighteen mainly anthropogenic volatile halocarbons. Class *et al.*[17] used a similar combination of stationary phases (5% phenylmethylpolysiloxane, DB-5, and BP-10, equivalent to DB-1701) for the separation of halogenated trace compounds in marine air. A 6% cyanopropylpolymethylsiloxane-coated capillary column, DB-1301, has recently been introduced in the analysis of volatile priority pollutants by Mehran *et al.*[18], which seems to provide a new approach to the separation problems with halogenated compounds. The use of PLOT columns in the separation of volatile halocarbons has also been shown to be an attractive alternative to the widely used WCOT columns[19].

Our aim was to develop a method to determine biogenic and anthropogenic halocarbons in sea water. This required the separation of a number of substances which can be expected in sea water, including brominated and iodated compounds. The analytical procedure should be as simple and fast as possible, in order to allow the investigation of a large number of samples within a short time, both in the laboratory and under more primitive circumstances on-board ship. The standard substances were chosen according to results from algal extracts[5,6], sea water[7,8] and ambient air in marine environments[17,20,21].

EXPERIMENTAL

The following substances were evaluated and they were all pure (>98%; CH_2ClI >97%): $CHCl_3$ (Merck), CH_3CCl_3 (Fluka), (Merck), CH_3CHICH_3 (Fluka), $CHCl=CCl_2$ (Mallinckrodt), CH_2Br_2 (Merck), $CHBrCl_2$ (Fluka), $CH_3CH_2CH_2I$ (Fluka), CH_2ClI (Fluka), $CH_3CHICH_2CH_3$ (Fluka), $CHBr_2Cl$ (Fluka), $CCl_2=CCl_2$ (Merck), $CH_3CH_2CH_2CH_2I$ (Fluka), $CHBr_3$ (Merck) and CH_2I_2 (Fluka). Standard stock solutions were prepared in acetone (Merck).

The determinations were made with a Carlo Erba 4160 gas chromatograph equipped with a ^{63}Ni electron-capture detector (275°C). Sea water (100 ml) was extracted for 5 min directly in sampling bottles with 1 ml of distilled pentane, containing $CBrCl_3$ (Fluka) as internal standard, as this substance has never been found in natural sea water[3]. A 15-μl volume of the pentane phase was injected onto the column using an automatically driven liquid chromatography injection valve (Valco) with a 15-μl sample loop. Two fused-silica capillary columns were connected with a press-fit connector (Mikro Kemi), a 30 m × 0.32 mm I.D. DB-5 column of film thickness 1 μm (J&W Scientific) and a 25 m × 0.32 mm I.D. DB-1701 column of film thickness 0.1

μm (Nordion) in front of the DB-5 column. The hydrogen carrier gas flow-rate was 1.8 ml/min and the make-up gas (nitrogen) flow-rate was 30 ml/min.

During the separation the oven was held at an initial temperature of 40°C for 2 min and then raised to 100°C at 10°C/min. The chromatographic peaks were integrated using a Jones Model JCL 6000 chromatography system or a C-R5A Shimadzu integrator.

RESULTS AND DISCUSSION

Separation

With the combination of two columns of different polarity and different film thickness, separation was achieved for all fifteen substances studied (Fig. 1). The DB-1701 column caused a preseparation which made it possible to separate even trichloroethene, bromodichloromethane and dibromomethane. This separation could not be obtained if the DB-5 column was used separately. Large on-column injections for the determination of volatile halocarbons at extremely low concentrations have been described by Fogelqvist and Larsson[22]. With the arrangement described in this method, at least 15 μl of the pentane phase could be injected onto the column. This was not possible when using the DB-5 column only, because it resulted in peak deterioration. Hence the DB-1701 column acts both as a separation column and as a retention gap. The coupling of two columns did not result in a considerable increase in analysis time. The gas chromatographic run took 10 min and subambient cooling was not necessary. In principle, the coupled columns described here can be used in combination with a suitable purge and trap system.

Extraction efficiency

The extraction combines preconcentration with the transfer of the halocarbons to the organic solvent. The transfer of an individual compound is dependent on its

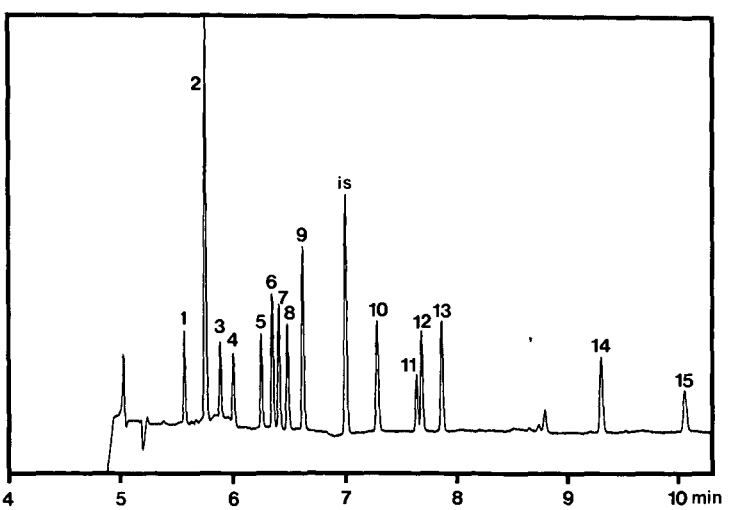

Fig. 1. Chromatogram of spiked sea water. The concentrations of the individual compounds vary between 4 and 110 ng/l. Peak integration was performed with a Jones chromatography system.

TABLE I

EXTRACTION YIELDS, PRECISION, RELATIVE RESPONSE FACTORS (R) AND DETECTION LIMITS FOR HALOCARBONS

No.	*Compound*	*Extraction yield (%)*	*Precision*[a] *(%)*	*Detection limit (ng/l)*	*R*
1	$CHCl_3$	48	9	2	0.05
2	CH_3CCl_3	80	8	0.2	0.4
3	CCl_4	84	10	0.05	1.3
4	CH_3CHICH_3	81	9	0.7	0.1
5	$CHCl=CCl_2$	75	8	0.4	0.18
6	CH_2Br_2	36	10	0.3	0.50
7	$CHBrCl_2$	52	10	0.2	0.61
8	$CH_3CH_2CH_2I$	79	7	0.2	0.28
9	CH_2ClI	41	3	0.03	1.3
10	$CH_3CHICH_2CH_3$	86	11	0.3	0.19
11	$CHBr_2Cl$	55	7	0.2	0.64
12	$CCl_2=CCl_2$	87	9	0.07	0.80
13	$CH_3CH_2CH_2CH_2I$	88	12	0.4	0.24
14	$CHBr_3$	59	5	0.2	0.22
15	CH_2I_2	55	7	0.4	0.15

[a] Relative standard deviation (n = 5).

partition coefficient and will influence the degree of preconcentration. The extraction efficiency was determined by consecutive extractions of spiked sea water for all compounds (Table I).

Precision and detection limits

The precision (relative standard devition, R.S.D.) was determined by calculating the amounts of halocarbons in spiked sea water samples (n = 5). For the low concentrations encountered in sea water, the R.S.D. is in the range 3–12% and the values for each compound are shown in Table I. The linearity down to concentrations as low as the detection limit was confirmed by correlation coefficients for the compounds of 0.996–0.999.

The detection limits, defined as a signal-to-noise ratio of 10:1 (blank signal plus nine standard deviations of the blank), were determined in natural sea water spiked with halocarbons. As can be seen from Table I, the detection limits are in the range of 30–700 pg/l, except for $CHCl_3$. The detection limit for $CHCl_3$ can be lowered if the phase ratio is increased[23]. The values given in Table I should be regarded as the limits of precise quantitative determination[24]. Depending on the chromatographic system, the integration system, the purity of the pentane and the matrix, it is possible to confirm the presence of a substance even at concentrations lower than the limits given here. The analysis of a large number of natural samples with concentrations of anthropogenic and biogenic halocarbons close to their detection limits showed good agreement with the values for detection limits and precision given in Table I.

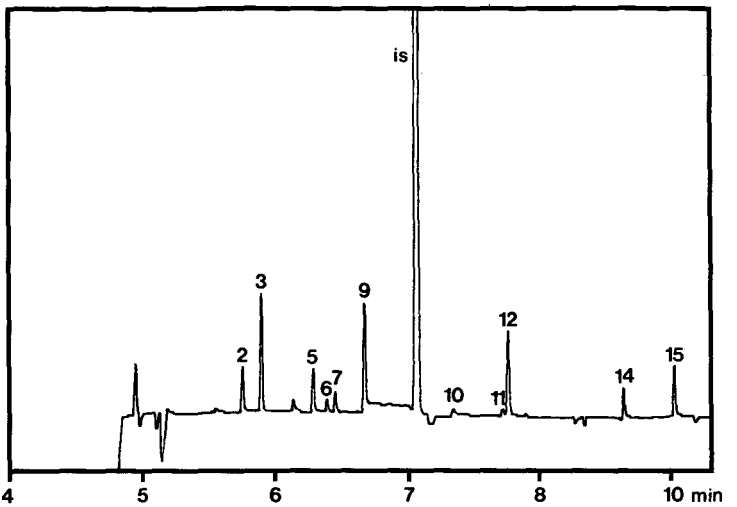

Fig. 2. Chromatogram of sea water, sampled in the central Skagerrak. 2 = CH_3CCl_3 (3.4 ng/l); 3 = CCl_4 (1.2 ng/l); 5 = $CHClCCl_2$ (7.1 ng/l); 6 = CH_2Br_2 (1.3 ng/l); 7 = $CHBrCl_2$ (1.3 ng/l); 9 = CH_2ClI (3.2 ng/l); 10 = $CH_3CHICH_2CH_3$ (0.55 ng/l); 11 = $CHBr_2Cl$ (<0.2 ng/l); 12 = $CCl_2=CCl_2$ (0.26 ng/l); 14 = $CHBr_3$ (6.5 ng/l); 15 = CH_2I_2 (19 ng/l). Peak integration was performed with a Shimadzu C-R5A integrator.

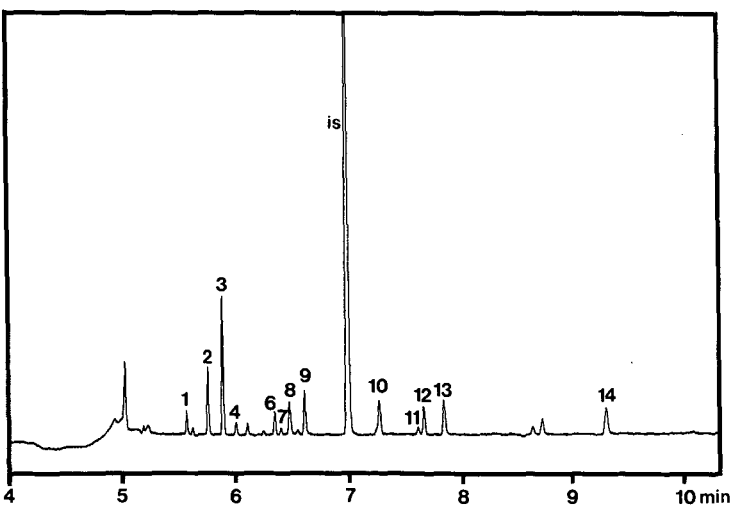

Fig. 3. Chromatogram of sea water sampled at S52°10′, W5°58′ on a cruise with R/V Polarstern, November 1989. 1 = $CHCl_3$ (9.3 ng/l); 2 = CH_3CCl_3 (1.8 ng/l); 3 = CCl_4 (1.2 ng/l); 4 = CH_3CHICH_3 (2.4 ng/l); 6 = CH_2Br_2 (1.3 ng/l); 7 = $CHBrCl_2$ (0.26 ng/l); 8 = $CH_3CH_2CH_2I$ (1.9 ng/l); 9 = CH_2ClI (1.1 ng/l); 10 = $CH_3CHICH_2CH_3$ (3.5 ng/l); 11 = $CHBr_2Cl$ (0.20 ng/l); 12 = $CCl_2=CCl_2$ (0.52 ng/l); 13 = $CH_3CH_2CH_2CH_2I$ (2.6 ng/l); 14 = $CHBr_3$ (4.5 ng/l). Peak integration was performed with a Jones chromatography system.

Application

The method described was specifically designed for the determination of biogenic and anthropogenic halocarbons at low concentrations in sea water. Emphasis was put on the separation of brominated and iodated compounds produced by marine algae and anthropogenic compounds that are detectable in almost all sea water samples. The method has been used successfully in the analysis of *ca.* 600 samples from the western coast of Sweden, from the Skagerrak and from the Antarctic. Figs. 2 and 3 show chromatograms of samples from the last two. As the iodated substances have not been determined in these areas before, it is not possible to compare the concentration levels with earlier studies. However, the values given are representative of water samples containing iodated substances in our investigations. In previous investigations on coastal waters in Sweden, no concentrations were given for dibromomethane and trichloroethene[7,9], since they could not be separated. For the other compounds the concentrations determined by us are in good agreement with these investigations.

The method described here can also be applied to the determination of volatile halocarbons in other water samples such as fresh water, drinking water and different types of waste waters.

ACKNOWLEDGEMENTS

This work was supported by a postdoctoral fellowship from the Deutsche Forschungsgemeinschaft and by the National Swedish Environmental Protection Board (SNV), which is gratefully acknowledged. We also thank Birgit Quack for valuable collaboration.

REFERENCES

1 A. J. Núnez, L. F. González and J. Janák, *J. Chromatogr.*, 300 (1984) 127–162.
2 M. E. McNally and R. L. Grob, *Am. Lab.*, 17 (1985) 20-63.
3 B. Eklund, B. Josefsson and C. Roos, *J. High Resolut. Chromatogr. Chromatogr. Commun.*, 1 (1978) 34–40.
4 E. Fogelqvist, B. Josefsson and C. Roos, *Environ. Sci. Technol.*, 16 (1982) 479–482.
5 R. E. Moore, *Acc. Chem. Res.*, 10 (1977) 40-47.
6 P. M. Gschwend, J. K. MacFarlane, K. A. Newman, *Science*, 227 (1985) 968–970.
7 K. Abrahamsson and S. Klick, *Chemosphere*, 18 (1989) 2247–2256.
8 E. Fogelqvist, *J. Geophys. Res.*, 90 (1985) 9181–9193.
9 E. Fogelqvist and M. Krysell, *Mar. Pollut. Bull.*, 17 (1986) 378-382.
10 A. R. Trussell, J. G. Moncur, F.-Y. Lieu and L. Y. C. Leong, *J. High Resolut. Chromatogr. Chromatogr. Commun.*, 4 (1981) 156–163.
11 T. Class, P. Mayer and K. Ballschmiter, *Fresenius' Z. Anal. Chem.*, 320 (1985) 707-709.
12 S. A. Vandegrift, *J. Chromatogr. Sci.*, 26 (1988) 513–516.
13 D. Dyrssen, E. Fogelqvist, M. Krysell and R. Sturm, *Tellus*, (1989) in press.
14 M. F. Mehran, W. J. Cooper and W. Jennings, *J. High Resolut. Chromatogr. Chromatogr. Commun.*, 7 (1984) 215–217.
15 R. R. Freeman and R. M. A. Lautamo, *Am. Lab.*, 18 (1986) 60–68.
16 K. Abrahamsson and S. Klick, unpublished results.
17 T. Class, R. Kohnle and K. Ballschmiter, *Chemosphere*, 15 (1986) 429–436.
18 M. F. Mehran, W. J. Cooper, R. Lautamo, R. R. Freeman and W. Jennings, *J. High Resolut. Chromatogr. Chromatogr. Commun.*, 8 (1985) 715–717.
19 J. de Zeeuw, R. C. M. de Nijs and L. T. Henrich, *J. Chromatogr. Sci.*, 25 (1987) 71–83.

20 T. Class and K. Ballschmiter, *Fresenius' Z. Anal. Chem.*, 327 (1987) 40-41.
21 G. Gassmann, B. Quack, D. G. Müller and E. Fölster, *Biologische Anstalt Helgoland, Jahresbericht*, 1988, 81–83.
22 E. Fogelqvist and M. Larsson, *J. Chromatogr.*, 279 (1983) 297–306.
23 E. Fogelqvist, *Ph.D. Thesis*, Department of Analytical and Marine Chemistry, University of Göteborg, 1984.
24 J. C. Miller and J. N. Miller, *Statistics for Analytical Chemistry*, Ellis Horwood, Chichester, 2nd ed., 1988.

Journal of Chromatography, 513 (1990) 47–54
Elsevier Science Publishers B.V., Amsterdam

CHROM. 22 518

Comparison of quarter-hourly on-line dynamic headspace analysis to purge-and-trap analysis of varying volatile organic compounds in drinking water sources

JOSEPH G. SCHNABLE, BERTRAND DUSSERT and IRWIN H. SUFFET*
Department of Chemistry and Environmental Studies Institute, Drexel University, Philadelphia PA 19104 (U.S.A.)
and
CHARLES D. HERTZ
Division of Science and Research, New Jersey Department of Environmental Protection, Trenton NJ 08625 (U.S.A.)
(First received February 29th, 1990; revised manuscript received April 24th, 1990)

ABSTRACT

On-line dynamic headspace analysis was refined for the quarter-hourly monitoring of select volatile organic compounds (VOCs) in ground and surface waters, for extended periods of time. Hourly comparisons were made to on-line purge-and-trap analysis, and to purge-and-trap analysis after sample preservation and storage. Variations in VOC concentrations of 6047% biweekly, 222% daily, 97% hourly, and 35% quarter-hourly were observable, with the 15-min cycle of the dynamic headspace analysis. The headspace analyzer had superior retention time stability, required less maintenance, and had 1/4 the analysis time as a typical purge-and-trap–gas chromatograph system used for hourly comparisons.

INTRODUCTION

The temporal monitoring of volatile organic compounds (VOCs) in water sources is important because of contamination (*i.e.* 4000 gallons of VOCs can be dissolved in a single ground water plume[1], or chemicals spilled into surface water), and the transport of contaminants. The maximum safe concentration levels for most VOCs in drinking water range from 1–5 ppb[2,a]. The speed of on-line VOC analyses is especially important at water sources with nearby contamination, or water sources near industrial or commercial operations where sudden accidental releases of VOCs to water supplies are possible.

[a] Throughout the article the American billion (10^9) is meant.

0021-9673/90/$03.50

Water sources have been monitored hourly by on-line purge-and-trap analysis[3] using a Tekmar 6000 process stream sampler (Cincinnati, OH, U.S.A.), Tekmar LSC-2 purge-and-trap–gas chromatographic (GC) system, and integrator system.

This project is the first application of quarter-hourly on-line headspace analysis for monitoring VOC concentrations in surface and ground waters, for extended periods of time[7]. A Siemens (ES Industries, Voorhees, NJ, U.S.A.) P101 dynamic headspace analyzer[4] was refined, and quality assurance was developed, for quarter-hourly analyses. Significant quarter-hourly variations in VOC concentrations in water sources, were observed with headspace analysis. The speed of headspace monitoring is a major advantage over purge-and-trap analysis for temporal monitoring.

EXPERIMENTAL

A Siemens P101 continuous on-line dynamic headspace analyzer was used to quantify VOCs quarter-hourly. The Siemens analyzer differed greatly from two traditional purge-and-trap systems which were used for hourly quality assurance comparisons.

With traditional purge-and-trap systems[5], a 5-ml grab sample is sparged with helium for 11 min. The objective of sparging is to purge the total amount of volatiles to a cool adsorbent trap. During desorption, an injection valve is turned and carrier gas flows through the trap, which is heated for 4 min to desorb VOCs to the GC apparatus.

With the Siemens headspace analyzer (Fig. 1), the sample was heated to 58°C before sparging with helium. Water continuously entered the sparger at 4 l/h, and overflowed through a headspace-free sidearm. (The headspace is the helium, volatile

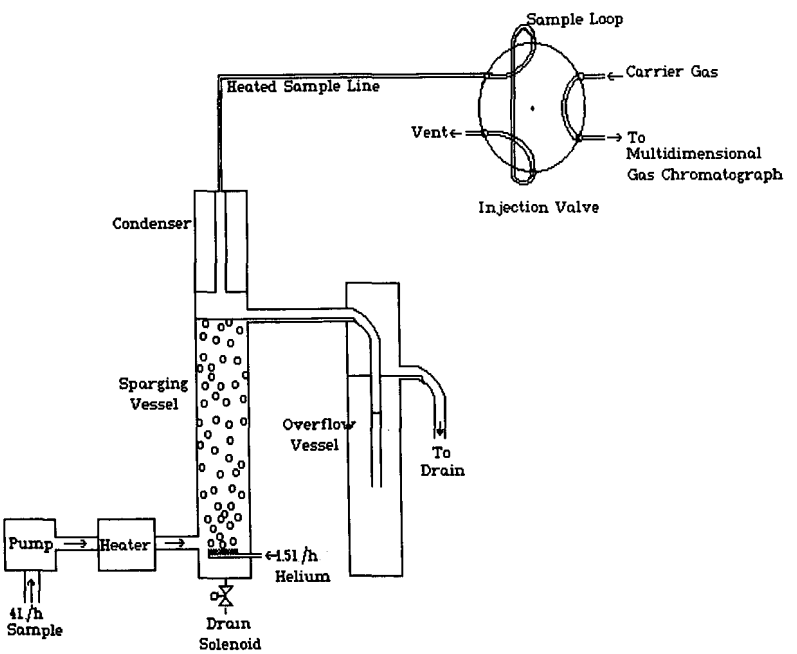

Fig. 1. Schematic diagram of the continuous headspace analyzer.

gases, and water vapor above the sample). The objective of sparging is to obtain a steady state concentration of volatiles in the headspace. Moisture is removed from the headpace by a condenser. The headspace exits through an injection valve. Once every 15 min, 10 μl of headspace are injected into the Siemens GC apparatus. Although the air–water partitioning of VOCs depends on Henry's constants, Henry's constants do not have to be known to make calibration curves on a dynamic headspace analyzer. Water entered the sparger at 4 l/h, and the overflowing sparger holds 330 ml of liquid. The headspace volume above the sparger is 80 ml. Helium purge flowed into the sparger at 1.5 l/h, and exited the sample loop at 1.5 l/h. The phase ratio (water–headspace volume ratio) was approximately 4:1, and the water–headspace flow ratio was approximately 3:1.

With the Siemens analyzer, the oven was run isothermally at 67°C, and three capillary columns with valveless column switching were available for multidimensional analysis. The primary column, a 15 m × 0.32 mm I.D., 1-μm OV-1710 capillary column, gave sufficient resolution for all compounds under study; secondary columns for multidimensional analysis were not used. Because the Siemens analyzer has no trap and runs isothermally, a 15-min analysis cycle was possible for all compounds analyzed.

On the Siemens analyzer, aqueous sample is continuously pumped into the sparging vessel, even when the sparger drains between analyses. Between analyses, the sparging vessel is drained, and influent is quickly blown down through the sparger with 70 kPa (10 p.s.i.) helium. The Siemens analyzer can be programmed to open one of fifteen different influent solenoids to analyze up to fifteen different sample streams. If the influent to the sparger is switched to a different sample stream during the beginning of the 1.2 min drain cycle, there usually is no noticeable carry over between successive 15-min samples from streams with different VOC concentrations. Influent streams were regulated to 10 p.s.i. with a pressure regulator, and solids were removed with a glass wool filter.

Quality assurance

Continuous internal standard injection was added to the Siemens analyzer for quality assurance. Dilute aqeuous fluorobenzene was pumped into the analyzer, along with the water sample, to give a 15 ppb final internal standard concentration. A Fluid Metering (Oyster Bay, NY, U.S.A.) lab pump, and lab pump junior were used for the sample and internal standard, respectively. Effluents from the sample and internal standard pumps were mixed in a 1/8 in. PTFE "T" mounted on the effluent of the internal standard pump.

The Siemens analyzer was quality assured using blanks, replicate analyses, calibration standards, other internal standards, field duplicates, lab duplicates, splits, blinds, intralaboratory comparison and interlaboratory comparison. Also, instrument maintenance was carefully evaluated.

RESULTS AND DISCUSSION

Calibration

Absolute peak areas from the injected fluorobenzene internal standard had a 5% relative standard deviation (R.S.D.). When a large homogeneous batch sample of 51

ppb tetrachloroethene (PCE) was analyzed 21 times, peak areas had 1.8% R.S.D. Duplicate analyses of other target compounds, such as chloroform, were reproducible with less than 5% R.S.D. Therefore, we decided that it would be more precise to use absolute areas of target compound peaks, without dividing by the internal standard peak areas. Internal standards peak areas were monitored, however, as additional quality assurance that the sensitivity of the Siemens analyzer did not change after thousands of injections or after being transported hundreds of kilometers to four different sites.

The EPA method detection limits[6] calculated from the Siemens analyzer, with a flame ionization detector, were: chloroform 2.8 ppb, fluorobenzene 2.0 ppb, PCE 2.3 ppb, and toluene 1.4 ppb. These compounds had similar method detection limits on a Tekmar LSC-2 purge-and-trap–Varian 3300 GC system with a flame ionization detector. Method detection limits equal the absolute standard deviation of >6 replicate determinations multiplied by the 99% t-value corresponding to the number of replicates[6]. For example, 21 Siemens analyzer determinations of a large standard had 0.89 ppb standard deviation; thus the method detection limit is 0.89 ppb $\times$ 2.53 $=$ 2.3 ppb.

Precision

The precision of the Siemens analyzer and two different purge-and-trap systems were compared by analyzing hourly tap water samples using all three systems. Fig. 2 shows the chloroform concentrations in Philadelphia tap water (treated surface water) from each hour. ▲ symbols represent chloroform concentrations determined by 15-min composite samples on the Siemens analyzer. Five min before the headspace from each composite sample was injected into the Siemens GC, two VOC bottles (with hydrochloric acid and ascorbic acid as preservatives) were filled with tap water from the same inlet. ■ symbols represent the chloroform concentrations determined from one VOC bottle which was immediately analyzed at Drexel University (intra-laboratory comparison) by a Tekmar LSC-2 purge-and-trap–Varian 3300 GC system

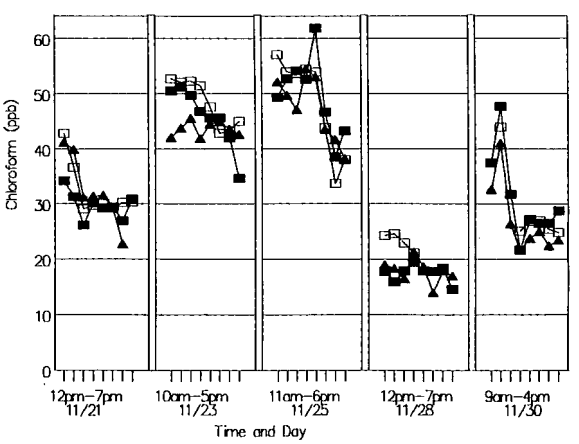

Fig. 2. System comparison plot of determinations of chloroform in Philadelphia tap water *vs.* date and hour water was sampled. ▲ = 15-min composite headspace analyses on Siemens analyzer; ■ = Grab samples analyzed immediately on Tekmar LSC-2 purge-and-trap–Varian 3300 GC system; □ = samples preserved and analyzed on purge-and-trap system at National Environmental Testing, Thorofare, NJ, U.S.A.

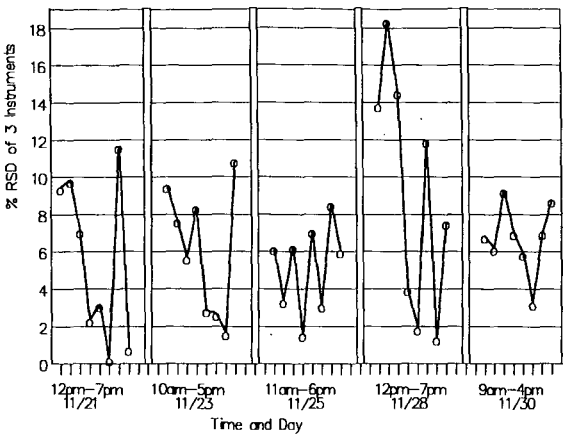

Fig. 3. System comparison plot of relative standard deviation of the determinations from 3 instruments *vs.* date and hour water was sampled.

with flame ionization detector. □ symbols represents chloroform concentrations determined from the other preserved VOC bottles, which were refrigerated and analyzed by National Environmental Testing Inc. (Thorofare, NJ, U.S.A.) by a purge-and-trap system (as interlaboratory comparison).

Fig. 3 shows that the R.S.D. of chloroform concentrations determined by the three instruments for each hour, averaged 6%, and did not exceed 18%. The Siemens analyzer and the two purge-and-trap systems had similar precision for chloroform, fluorobenzene, PCE, and toluene.

Accuracy

The accuracy of the Siemens analyzer was determined by analyzing blinds (spiked standards with expected concentrations) on the Siemens analyzer and a purge-and-trap system. Table I shows the results of analyzing chloroform blinds on the Siemens analyzer and NET's purge-and-trap system.

TABLE I

CHLOROFORM BLINDS

Expected (ppb)	*Instrument*	*Analysis Time*	*Determined (ppb)*
6.7	Siemens	on-line	9.1
6.7	Siemens	on-line	8.9
6.7	NET purge-and-trap system	within 2 weeks	7.8
13.0	Siemens	on-line	14.0
13.0	Siemens	on-line	14.0
13.0	NET purge-and-trap system	within 2 weeks	16.0
27.0	Siemens	on-line	24.0
27.0	Siemens	on-line	24.0
27.0	Siemens	on-line	28.0
27.0	NET purge-and-trap system	within 2 weeks	37.0

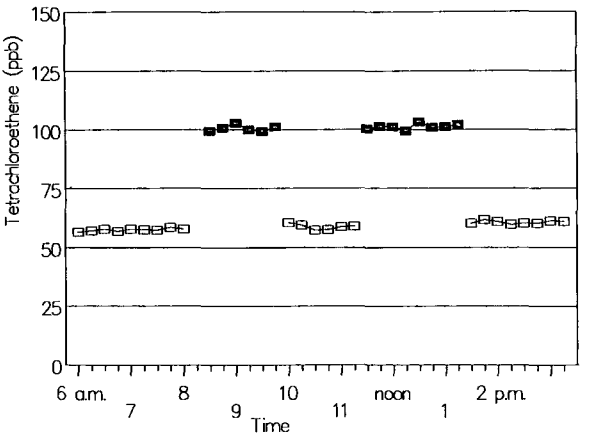

Fig. 4. Quarter-hourly headspace analyses of two adjacent wells with different tetrachloroethene concentrations, using Siemens analyzer. ■ = Raw water from well A2; □ = raw water from well A1. No memory effects were apparent when switching between samples of different concentrations.

Retention times

Retention times on the Siemens analyzer remained within ± 0.02 min per week, even with 100-fold changes in concentration. Retention times on the Tekmar LSC-2–Varian 3300 purge-and-trap system varied ± 0.30 min between a few analyses, with 100-fold changes in concentration.

Instrument variability

Before evaluating the variability of VOCs in water sources, it was determined that all compounds studied could be reproducibly determined on the Siemens analyzer with $< 5\%$ R.S.D. This was done by replicate analyses of large homogenous spiked standards (12–51 ppb concentrations).

Carry over between samples

It also was determined that the Siemens analyzer could switch between two sample streams during its drain cycle, with little carry over between successive 15-min samples from different streams. Fig. 4 shows switching between analyses of two adjacent wells, well A1 and well A2. Although the wells had different PCE concentrations, both wells had fairly constant concentrations on this day, and the analyzer did not show any carry over when switching between the two wells. Automatic switching between sample and calibration standards also worked well. The Siemens analyzer can be programmed to switch between fifteen sample streams, using solenoids.

Variability of VOCs in water sources

Fig. 5 shows quarter-hourly determinations of PCE and 1,1,1-trichloroethane in raw well water B. Quarter-hourly variations in PCE concentrations were observable, due to the speed of headspace analysis. On this day, PCE concentrations varied as much as 25% between successive 15-min analyses (between 8:30 and 8:45 a.m.), and varied as much as 97% per hour (from 8:15 to 9:15 a.m.). For this entire day, PCE

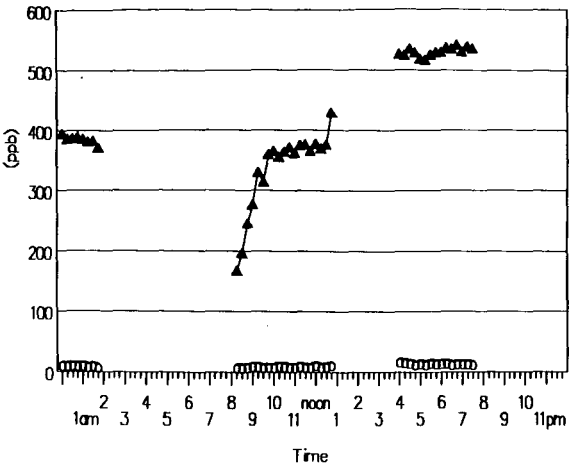

Fig. 5. Quarter-hourly headspace analyses of tetrachloroethene and 1,1,1-trichloroethane in raw well water B using Siemens analyzer (different site than Fig. 4). ▲ = tetrachloroethane; ○ = 1,1,1-trichloroethane. Tetrachloroethene concentrations varied as much as 97% per hour (between 8:15 a.m. and 9:15 a.m.) and 35% between successive 15 minute analyses (8:30 a.m. and 8:45 a.m.). 1,1,1-trichloroethane concentrations ranged from 10 to 22 ppb during this day.

concentrations varied 222% (from 168 to 541 ppb). On other days, PCE concentrations varied as much as 35% between successive 15-min analyses. Fig. 4 shows analyses of raw well water B, before it passed through granular activated carbon contactors to remove VOCs, and was chlorinated, for use as drinking water.

Fig. 6 shows minimum, average, and maximum daily PCE concentrations in raw

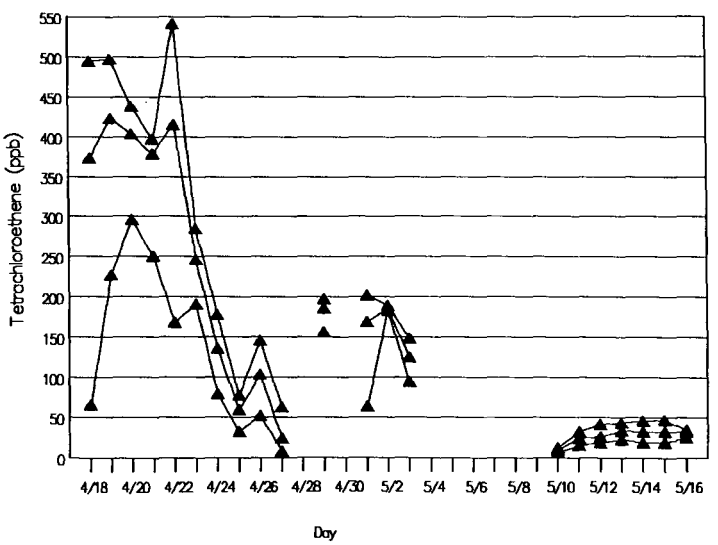

Fig. 6. Minimum, average, and maximum daily PCE concentrations in raw well water B determined by quarter-hourly headspace analyses from April 18 (4/18) to May 16 (5/16). Notice 6047% decrease in PCE concentrations between April 22 and May 10, due to dilution by rain. Analyses were not made between May 4 and 9.

well water B, determined by quarter-hourly analyses for approximately 1 month. PCE concentrations decreased 6047% in $2\frac{1}{2}$ weeks (from 541 ppb to 9 ppb), apparently due to dilution by rains. Although large variability was seen in this well, no contamination was detected in a well just 1.6 km away.

Maintenance

Maintenance required by Siemens analyzer was minimal. The sparging vessel was disassembled monthly and rinsed out with water to remove solids. A 8 m^3 (300 $foot^3$) cylinder of zero grade air was replaced once every 9 days. A 6 m^3 (200 $foot^3$) cylinder of high-purity helium was replaced every 18 days. A 6 m^3 cylinder of high-purity hydrogen would last approximately 6 months. Paper for a Hewlett-Packard 3390 integrator (added to the Siemens analyzer) would last for more than a week. Seals on the injection valve were still good after approximately 15 000 injections. The major sampling problem was the removal of solids from the water before it entered the analyzer. Large amounts of solids would appear when a well was turned on, and had to be filtered out with glass wool, which had to be replaced frequently. The traps in our Tekmar LSC-2 purge-and-trap had to be replaced every few months.

ACKNOWLEDGEMENTS

This work was supported by the New Jersey Department of Environmental Protection, Division of Science and Research, Trenton, NJ, (U.S.A.). Special thanks to Robert Lee Lippincott for helping move the Siemens analyzer to each site, and giving technical advice.

REFERENCES

1 D. M. Mackay and J. A. Cherry, *Environ. Sci. Technol.*, 23 (1989) 630.
2 New Jersey Drinking Water Quality Institute, *Maximum Contaminant Level Recommendations for Hazardous Contaminants in Drinking Water*, submitted to New Jersey Department of Environmental Protection (U.S.A.) March 26 (1987) 41.
3 G. H. Thomas, R. G. Denning, R. G. and R. G. Westendorf, *Proceedings from the American Water Works Association, Water Quality Technology Conference, St. Louis, MO, November 13–17, 1988*, American Water Works Association, Denver, CO, 1989, p. 777.
4 P. Maitoza, J. A. Valada and W. T. Madigan, *Am. Lab. (Fairfield, Conn.)*, Jan. (1989) 23.
5 *Methods For The Determination of Organic Compounds In Finished Drinking Water and Raw Source Water*, Physical and Chemical Methods Branch Environmental Monitoring and Support Laboratory, U.S. Environmental Protection Agency, Cincinnati, OH, January 1988, sections 5.2–5.3.
6 *Federal Register, Part II, Environmental Protection Agency 40 CFR Parts 141, 142, 143*, National Primary and Secondary Drinking Water Regulations, Proposed Rule, May 22, 1989.
7 J. G. Schnable, I. H. Suffet and C. D. Hertz, *Proceedings of the American Water Works Association, Water Quality Technology Conference, Philadelphia, PA, November 17, 1989*, American Water Works Association, Denver, CO, 1990, in press.

Journal of Chromatography, 513 (1990) 55–60
Elsevier Science Publishers B.V., Amsterdam

CHROM. 22 516

Determination of solanesol in tobacco by capillary gas chromatography

W. J. CHAMBERLAIN*, R. F. SEVERSON and O. T. CHORTYK
United States Department of Agriculture, Agricultural Research Service, R. B. Russell Agricultural Research Center, Tobacco Quality & Safety Research Unit, P. O. Box 5677, Athens, GA 30613 (U.S.A.)
and
V. E. SISSON
United States Department of Agriculture, Agricultural Research Service, Crops Research Laboratory, P. O. Box 1555, Oxford, NC 27565 (U.S.A.)
(First received January 30th, 1990; revised manuscript received April 24th, 1990)

ABSTRACT

A gas chromatographic (GC) method has been developed for solanesol, a long-chain (C_{45}) terpenoid alcohol of tobacco. The method separates and quantitates solanesol as its volatile trimethylsilyl derivative. After saponification of the tobacco sample with methanolic potassium hydroxide to liberate bound solanesol, total solanesol was determined on a wide-bore fused-silica SE-54 capillary column. The reproducibilities of both the extraction and GC methods were found to be excellent. As an example of application, six tobacco varieties, used in a low-solanesol tobacco breeding study, were analyzed. In these tobaccos, free solanesol content varied from 70 to 90% of the total solanesol, which ranged from 1.9 to 2.8% of dry weight.

INTRODUCTION

Solanesol [$H(CH_2–C(CH_3)=CH–CH_2)_9–OH$] is the major trisequiterpenoid (C_{45}) alcohol of tobacco. Solanesol (3,7,11,15,19,23,27,31,35-nonamethyl-2,6,10,14,18,26,30,34-hexatriacontanonaene-1-ol) was first isolated from tobacco by Rowland *et al.*[1] in 1956 and occurs both in the free and bound (esterified) form in tobacco. It is the major terpene component of the lipid fraction (hexane extractables) of tobacco and represents up to 5% of dried leaf lamina[2,3]. Solanesol has been shown to be a major precursor of the tumorigenic polynuclear aromatic hydrocarbons (PAHs) of tobacco smoke[4]. It produces more than 30% of the total PAHs that are formed on pyrolyzing the hexane-extractable fraction of tobacco[5].

Reduction of solanesol would lead to a safer smoking product, due to reduced PAH levels in cigarette smoke. Therefore, a breeding program has been undertaken to genetically develop tobacco with a lower solanesol content. In order to accomplish this goal, a rapid method to analyze thousands of tobacco samples was needed.

0021-9673/90/$03.50

Gravimetric determinations of solanesol by column chromatography[6,7] have produced low and variable results and were not suitable for routine analyses. A thin-layer chromatography–densitometry method presented difficulties, due to decomposition of solanesol[7]. A packed column gas chromatography (GC) method reported by Sheen *et al.*[8] involved a lengthy extraction procedure and hydrogenation of solanesol. Court and Hendel[9] have recently published a determination of solanesol by high-performance liquid chromatography. Consequently, it was decided to improve a GC method developed in this laboratory[10]. This method determined solanesol by GC of its trimethylsilyl (TMS) derivative, on a short, packed Dexsil 300 GC column. However, since substantial amounts of leaf solanesol may be bound as esters, an improved method for total solanesol was needed. Our previously described method for total solanesol[10] required hydrolysis of the ground tobacco in a saponification flask, followed by solvent extractions of the solanesol. Both steps were time consuming for routine analyses of large numbers of samples. In this manuscript, we describe a micro test tube hydrolysis–extraction method for ground tobacco to yield total solanesol, which was quantitated by wide-bore capillary gas chromatography on SE-54 coated columns. These GC columns have been employed for the last six years to successfully analyze over 1500 tobacco varieties and introductions in a low solanesol tobacco breeding program[11]. Recently, a similar GC method for solanesol in environmental tobacco smoke has been reported[12].

MATERIALS AND METHODS[a]

The tobaccos used in this study were grown at the Crops Research Laboratory, Oxford, NC, U.S.A., under conditions normally used for the production of flue-cured tobacco. Cured tobacco leaf lamina samples were dried over anhydrous silica in a desiccator for two days and then ground in a Wiley Mill to pass through a 20-mesh screen. All solvents were Burdick & Jackson (Muskegon, MI, U.S.A.) distilled-in-glass grade.

Solanesol purification

Crude solanesol (Hoffmann-La Roche, 80+%) was purified by repetitive recrystallizations from hexane to yield a 98+% pure compound (by GC).

Preparation of butyl triacontanoate internal standard

About 0.6 g of triacontanoic acid (Fluka, purum grade, *ca.* 98% by GC), 0.5 g *p*-toluene sulfonic acid monohydrate and 8 ml of butanol (Aldrich, 99+%, redistilled from KOH) were added to a test tube. The tube was capped and heated at 80°C for 4 h. After cooling, the mixture was transferred to a separatory funnel with hexane (50 ml) and extracted with saturated Na_2CO_3 (2 × 20 ml) and water (3 × 20 ml). The hexane fraction was dried over Na_2SO_4, filtered, and taken to dryness on a rotary evaporator. The residue was transferred with hexane to a 40-g silicic acid column. Elution with methylene chloride–hexane (1:3) yielded the C_{30} butyl ester, which was recrystallized from hexane (m.p. 65–66°C, 98%+ by GC).

---

[a] Mention of a commercial instrument or product does not constitute Agricultural Research Service endorsement.

Total solanesol determination by test tube hydrolysis methods

In method A, dried ground tobacco (50 ± 3 mg) was weighed into an 8-ml screw-cap culture test tube and 3 ml of a 1 *M* KOH in methanol–water (95:5) solution were added. The tube was sealed with a PTFE-lined cap. The solvent level was marked on the outside of the test tube and the mixture was heated at 80°C, in a heat block for 4 h, to insure complete hydrolysis of the bound solanesol. After cooling, and if necessary, methanol was added to bring solvent level to the initial volume and 3 ml of isooctane, containing the internal standard (IS, 0.5 mg of butyl triacontanoate) were added. After sonification for 15 min, 1 ml of water was added and the mixture was allowed to stand in the dark, at room temperature for two or more hours. A 250-μl aliquot of the isooctane layer was transferred to a 1-ml Reacti-vial, the solvent was removed by a stream of nitrogen at 40°C, and 100 μl of N,O-bis(trimethylsilyl)-acetamide (BSA) were added. The vial was sealed with a PTFE-lined cap and heated at 80°C for 30 min. After cooling, the sample was transferred to a micro auto-sampler vial and 1 μl was analyzed by GC.

In an alternative procedure (method B), the sample was treated as above, except that the IS was not added to the isooctane in the test tube. Instead, after standing overnight at room temperature, 250 μl of the isooctane layer (containing the saponified compounds) were added to a Reacti-vial, together with the IS (80 μg). The sample was then treated as above.

Total solanesol by saponification flask hydrolysis method

About 1 g of dried ground tobacco and 40 ml of methanolic potassium hydroxide were placed into a 250-ml saponification flask, with a 24/40 joint, and fitted with a reflux condensor. The mixture was refluxed for 2 h under nitrogen. After cooling, the mixture was filtered through fluted filter paper into a separatory funnel and the flask and filter were washed with 50 ml of a 1:1 mixture of benzene and ethanol–water (85:15). Hexane (50 ml), 25 ml of aqueous saturated KCl solution and 50 ml of water were added to the funnel and the funnel was vigorously shaken to effect solvent partitioning. The hexane layer was removed and the aqueous layer was extracted with hexane (2 × 25 ml). The hexane extracts were combined, washed with water (3 × 25 ml), reduced in volume on a rotary evaporator, and transferred to a 25-ml volumetric flask. A 300-μl aliquot was removed for GC analyses and concentrated BSA reagent was added and the sample was treated as above.

Gas chromatography

Samples were analyzed on a HP 5710A gas chromatograph, modified for capillary GC and containing an flame ionization detector[13]. The column was a 10 m × 0.53 mm I.D. fused-silica capillary column, coated with SE-54 (4 mg/ml). The detector temperature was 350°C and the injector temperature was 250°C. For total solanesol determination, the oven was heated from 220 to 300°C at 8°C/min and held 8 min at 300°C. For free solanesol determination[10], the oven temperature conditions were: hold for 2 min at 100°C, then program from 100 to 300°C at 8°C/min. The lower starting temperature was needed to allow determination of other, major leaf constituents, including malic and citric acid, fructose, glucose, sucrose and chlorogenic acid.

RESULTS AND DISCUSSION

As stated earlier, we have for a number of years routinely analyzed solanesol in cured tobacco leaf, using 45-cm packed Dexsil 300 GC columns[10]. One major disadvantage was unpredictable column life, which varied from 100 to 500 analyses per column. When wide bore (0.53 mm I.D.) glass capillary columns became available, we investigated bonded SE-54 columns as replacements for the packed columns and found that short (10 m or less) and thin-film columns lasted for 1000+ analyses and gave very reproducible results. An example of a wide-bore capillary GC separation is shown in Fig. 1.

Another problem with the packed column analyses was the cost and stability of the 1,3-dimyristin internal standard employed at that time. Consequently, we investigated a number of substitutes and found that the butyl ester of triacontanoic (C_{30}) acid was a suitable replacement.

The next step in modifying the total solanesol method was to streamline the labor-intensive flask saponification and extraction procedures. By changing the hydrolysis solvent from aqueous ethanolic KOH to methanolic KOH, we were able to hydrolyze bound solanesol and then extract the free solanesol into isooctane in the same reaction vessel, an 8-ml capped test tube. Briefly, the procedure consists of (1) methanolic KOH hydrolysis of a small sample of ground tobacco, (2) ultrasonic extraction of the hydrolysis mixture with iso-octane and addition of water to assist in phase separation, and (3) derivatization of the free solanesol with a silylating reagent (BSA) for GC analysis.

After establishing the saponification and extraction conditions, it was necessary to evaluate the reproducibility of the method. The reproducibility of the GC procedure was first examined (Table I). Two representative tobacco varieties were analyzed for solanesol by test tube method B. A sample from each tobacco was hydrolyzed and the hydrolyzate was analyzed four times to give the results in Table I. From the relative

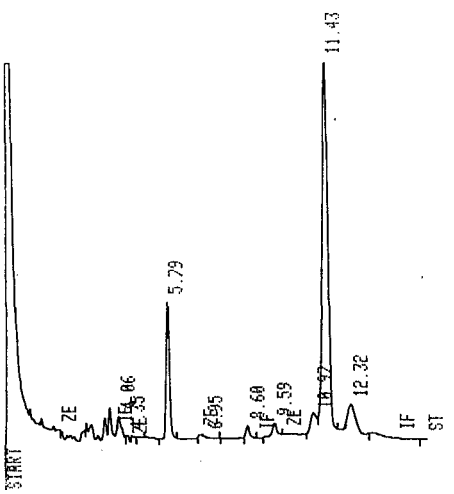

Fig. 1. Gas chromatogram for analysis of total solanesol in tobacco leaf lamina. IS at 5.79 min and solanesol at 11.43 min.

TABLE I

REPRODUCIBILITY OF GC ANALYSES FOR SOLANESOL

Tobacco[a]	*%Dry weight*				
	Run number				*Mean ± R.S.D.*
	1	*2*	*3*	*4*	
KY-14	2.75	2.77	2.83	2.81	2.78 ± .03
OX 259	2.88	2.99	2.86	2.97	2.92 ± .06

[a] See Table II.

standard deviation (R.S.D.), it was apparent that the GC part of the method yielded very reproducible and acceptable results.

In Table II, the reproducibilities of micro test tube methods A and B (for the hydrolysis and extraction of total solanesol) are compared to that of our standard saponification flask procedure. This saponification flask method contains several improvements over the previously reported[10] method. It was apparent that the more rapid test tube methods yielded data of equal validity and reproducibility compared to the original flask saponification method. Thus, the addition of internal standard to the isooctane extraction solvent (method A) or to the separated isooctane prior to GC (method B) produced identical results. Consequently, the analyses of a large number of field samples could be performed rapidly and confidently by either test tube method.

In our program to breed tobacco with a lower solanesol content, we have examined many tobacco varieties. As an example of solanesol variation and method applicability, the results for six tobaccos are shown in Table III. As each tobacco was grown in four separate field plots and samples were taken from each plot, there was

TABLE II

REPRODUCIBILITY OF METHODS FOR THE DETERMINATION OF TOTAL SOLANESOL

Tobacco[a]	*Method*	*%Dry weight*				
		Run number				*Mean ± R.S.D.*
		1	*2*	*3*	*4*	
KY-14	Saponification flask	2.86	2.76	2.82	–	2.81 ± .04
	Test tube A	2.79	2.77	2.83	2.86	2.81 ± .03
	Test tube B	2.86	2.77	2.76	2.78	2.79 ± .04
Sp G-28	Saponification flask	2.40	2.46	2.50	–	2.45 ± .04
	Test tube B	2.43	2.40	2.36	2.34	2.38 ± .04
OX 259	Test tube A	2.93	2.88	2.94	2.86	2.90 ± .03
	Test tube B	2.83	2.86	2.95	2.89	2.88 ± .04

[a] Kentucky 14 (KY-14) is a representative burley tobacco, Speight G-28 (Sp G-28) is a representative flue-cured tobacco and Oxford 259 (OX 259) is a recent flue-cured variety. Analyses data represent repetitive runs on the same sample.

TABLE III

FREE AND TOTAL SOLANESOL LEVELS OF SELECTED FLUE-CURED TOBACCOS

Values represent averages of four or more samples collected in the field.

Tobacco	*Total solanesol*[a] *% leaf (dry wt.) ± R.S.D.*	*Free solanesol*[b] *% leaf (dry wt.) ± R.S.D.*	*% Free solanesol*
Harrison Pryor	2.18 ± 0.02	1.68 ± 0.36	77
Oxford 3	1.90 ± 0.10	1.34 ± 0.23	70
Sp G-70	2.06 ± 0.08	1.83 ± 0.26	89
Coker 48	2.07 ± 0.37	2.05 ± 0.34	99
NC 95	2.81 ± 0.30	2.49 ± 0.48	89
NC 82	2.43 ± 0.20	2.31 ± 0.16	95

[a] Method A.
[b] Ref. 8.

much more variability in results between plots and this resulted in higher R.S.D., as compared to the data in Table II. The percent free solanesol (determined by the method in ref. 10) varied from 70 to 99% of the total solanesol values. Therefore free solanesol values cannot be used to calculate total solanesol in tobacco. This methodology should be applicable to analyses of other plant alcohols, such as free and bound sterols. With a pH adjustment step after saponification, free and bound fatty acids could also be determined.

REFERENCES

1 R. L. Rowland, D. H. Latimer and J. A. Giles, *J. Am. Chem. Soc.*, 78 (1956) 4680.
2 W. A. Court, J. M. Elliot and J. G. Hendel, *Tob. Sci.*, 28 (1984) 69.
3 H. R. Burton, E. Leggett and R. E. Phillips, *Beitr. Tabakforsch.*,14 (1989) 313.
4 I. Schmelz, D. Hoffmann and E. L. Wynder, *Trace Subst. Environ. Health*, 8 (1974) 281.
5 W. S. Schlotzhauer, R. F. Severson, O. T. Chortyk, R. F. Arrendale and H. C. Higman, *J. Agric. Food Chem.*, 24 (1976) 992.
6 W. B. Belinsky and R. L. Stedman, *J. Am. Oil Chem. Soc.*, 45 (1962) 532.
7 B. H. Woolen and D. H. Jones, *J. Chromatogr.*, 61 (1971) 180.
8 S. J. Sheen, D. L. Davis, D. W. Dejong and J. F. Chaplin, *J. Agric. Food Chem.*, 26 (1978) 259.
9 W. A. Court and J. G. Hendel, *Tob. Sci.*, 31 (1987) 79.
10 R. F. Severson, J. J. Ellington, P. F. Schlotzhauer, R. F. Arrendale and A. I. Schepartz, *J. Chromatogr.*, 139 (1977) 269.
11 W. J. Chamberlain, R. E. Williamson, R. F. Severson, J. L. Baker and O. T. Chortyk, presented at *42nd Tobacco Chemists' Research Conference, Lexington, KY, 1988.*
12 M. W. Ogden and K. C. Maiolo, J. H. R. C. and C. C., (1988) 341.
13 R. F. Severson, R. F. Arrendale and O. T. Chortyk, *J. High Resolut. Chromatogr. Chromatogr. Commun.*, 3 (1980) 11.

Journal of Chromatography, 513 (1990) 61–69
Elsevier Science Publishers B.V., Amsterdam

CHROM. 22 522

Gas chromatographic method for the assay of aliphatic and aromatic sulphonates as their *tert.*-butyldimethylsilyl derivatives

LAY-KEOW NG* and MICHEL HUPÉ
Laboratory & Scientific Services Directorate, Revenue Canada, Customs & Excise, Ottawa, Ontario K1A 0L5 (Canada)
(First received February 1st, 1990; revised manuscript received April 27th, 1990)

ABSTRACT

A gas–liquid chromatographic procedure is described which permits analysis of aliphatic and aromatic sulphonates as their *tert.*-butyldimethylsilyl derivatives. The *tert.*-butyldimethylsilylation of sulphonic acids in their free or sodium salt form is accomplished in a single derivatization step with N-methyl-N-(*tert.*-butyldimethylsilyl) trifluoroacetamide and *tert.*-butyldimethylchlorosilane in acetonitrile. Stability results and mass spectral analysis of all *tert.*-butyldimethylsilyl sulphonates are presented. Each derivative displays a prominent and characteristic [M—57] fragment ion in its mass spectrum.

INTRODUCTION

Organic sulphonate compounds are important industrial chemicals used as surfactants, pigments and dye intermediates etc. They constitute a significant number of samples analyzed at the Canadian Customs Laboratory for Tariff Classification purposes. In particular, it is necessary for us to determine the identity and purity of these chemicals.

Sulphonates have been investigated by various chromatographic methods. Among these methods we are particularly interested in the technique of gas chromatography (GC). Since sulphonates are compounds of low volatility, they were converted to volatile derivatives to be amenable to GC analysis. GC methods have been developed to analyze sulphonic acids as their trimethylsilyl (TMS) derivatives[1,2], methyl esters[3] and thionyl chloride derivatives[4]. Another method of analysis involves desulphonation in a reaction precolumn followed by GC analysis[5].

All the derivatization methods other than silylation involve sample work-up and are not applicable to sulphonic acids containing other polar functional groups such as hydroxy and amino groups. In general, silylation enjoys the advantage over other derivatization methods in that it is a single-step procedure and does not require

0021-9673/90/$03.50

separation of the derivatives prior to GC analysis. It is also a more versatile derivatization method. If a proper silylating reagent is employed, other polar substituents can be derivatized along with the sulphonate group.

Previous work, however, indicates that TMS derivatives suffer from instability[1] and lack of response to flame ionization detection (FID)[2]. It was also noted that the trimethylsilylation involves mainly the free acids, and very little, if any, of sulphonate salts.

This paper reports the development of a *tert.*-butyldimethyl silylation (tBDMS) method that allows derivatization of sulfonates in their free acid or sodium salt form in a single step reaction. Polar substituents such as OH, COOH and NH_2 were also derivatized by this procedure. Most of the synthesized tBDMS derivatives were found to be stable for at least 25 days at room temperature in the reaction solution. Unlike the TMS derivatives, the tBDMS-sulfonate compounds were detected by FID. All tBDMS derivatives were also subjected to GC–mass spectrometry (MS) analysis. Fragmentation patterns of these derivatives are presented.

EXPERIMENTAL

Materials

N-Methyl-N-(*tert.*-butyldimethylsilyl)trifluroacetamide(MTBSTFA), *tert.*-butyldimethylchlorosilane (tBDMCS) and acetonitrile were purchased from Pierce (Rockford, IL, U.S.A.). Benzo-15-crown-5 was obtained from Aldrich (Milwaukee, WI, U.S.A.). *n*-Tetradecane was a product of Alltech (IL, U.S.A.). Dioctyl phthalate was a commercial sample of >99% purity.

All the sulphonates used in this study are listed in Fig. 1. They were all obtained from Aldrich except compounds 8, 9 and 10 which were commercial samples.

Derivatization

The tBDMS derivatives of all the sulphonates were prepared by adding 18 mg tBDMSC1, 100 μl of MTBSTFA and 100 μl of a 2% acetonitrile solution of dioctyphthalate into a PTFE-faced Reacti-vial containing 3–4 mg of the sulphonate. Derivatization of sodium isethionate in the presence of benzo-15-crown-5 was carried out the same way except that 6 mg of the polyether was added to the reaction mixture.

The reaction mixture was stirred at 70°C for a period of 24 h. Aliquots of 1 μl were injected into GC–FID system at 1, 3, 6 and 24 h reaction time. Peak ratio of the product to the internal standard (dioctyl phthalate) was plotted against reaction time, the point at which the curve started to level off is taken as the reaction completion time. In all cases, the reaction mixtures at the end of 24 h were analyzed by GC–MS to obtain the mass spectra of the derivatives.

The stability of the phthalate internal standard in the silylation reaction mixture was tested using the same derivarization procedure described above, except 1 mg of tetradecane was used in place of the sulfonates. Peak ratio of the phthalate and *n*-alkane was found to remain constant at 70°C for 24 h and later for 25 days at room temperature, indicating that the dioctyl phthalate was stable throughout the derivatization and stability study.

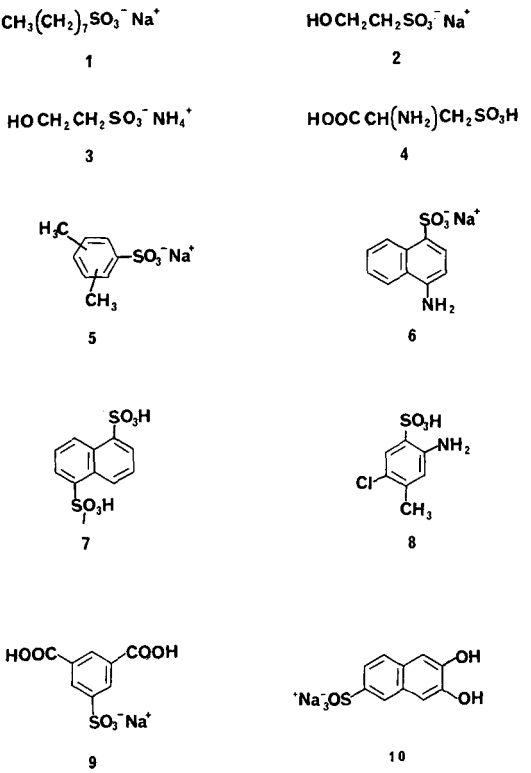

Fig. 1. Structures of sulphonates used in this study. 1 = Sodium octanesulphonate; 2 = sodium isethionate; 3 = ammonium isethionate; 4 = L-cysteic acid; 5 = sodium xylene sulphonate; 6 = sodium 4-amino-1-napthalenesulphonate; 7 = 1,5-napthalenedisulphonic acid; 8 = 2-amino-5-chlorotolenesulphonic acid; 9 = 5-(sodiosulfo)isophthalic acid; 10 = sodium 2,3-dihydroxy-6-naphthalenesulphonate.

Stability study

After 24 h at 70°C, the reaction mixture was allowed to stand at room temperature for at least 25 days. The mixture was analyzed by GC every 5 days and the peak ratio of the tBDMS derivative *vs.* the internal standard was plotted against time. A slope of zero from the plot and the absence of extraneous peaks in the chromatogram was interpreted as absence of decomposition of the derivative during the study period.

GC

A Hewlett-Packard Model 5840 A gas chromatograph equipped with a flame ionization detector was employed. The column used was a 15 m × 0.25 mm I.D., 0.25 μm thick DB5 fused-silica column. The injector temperature was 250°C and 1 μl of the reaction mixture was injected with a split ratio of 100:1 at an oven temperature of 80°C; after an initial hold time of 2 min at 80°C, the oven temperature was programmed at 10°C/min until 250°C; helium flow-rate was 1 ml/min.

GC–MS

The gas chromatograph-mass spectrometer (Finnigan Model 1020) was equipped with an electron impact source and a Nova 4 data system. The scanning rate was 1 s/scan in the range 40–650 a.m.u. The ion source temperature was held at 80°C. Electron impact (EI) spectra were obtained at 75 eV. The GC instrument (Perkin-Elmer Sigma-3B) was operated with the same column, the same oven and injector temperatures as described for GC–FID above. Helium flow-rate was 1 ml/min.

RESULTS AND DISCUSSION

Formulation of silylation cocktail

Previous work in our laboratory[6] has shown that sulfonic acids can be readily silylated by MTBSTFA in acetonitrile at 70°C. No reaction, however, was observed with various sodium salts of sulphonic acids using the same silylating reagent, even after prolonged heating. It is known that the reactivity of hexamethyldisilazane (HMDS) can be increased by the addition of a small amount of trimethylchlorosilane (TMCS), a chloride containing the same silyl group as HMDS[7]. In our laboratory, we have observed[8] that a silylation cocktail composed of a mixture of HMDS and TMCS in pyridine is able to derivatize metal salts of various carboxylic acids which fail to react with HMDS alone. Using the same reasoning, a silylation cocktail composed of MTBSTFA and tBDMCS, a chloride containing the same tBDMS silyl function as MTBSTFA, in acetonitrile were formulated as described in the Experimental section and used in this investigation.

Derivatization

As shown in Table I, among the four aliphatic sulphonates studied, sodium octanesulphonate and ammonium isethionate were completely silylated as mono- and disilylated derivatives, respectively, within the first hour.

TABLE I

DERIVATIZATION AND STABILITY RESULTS OF ALIPHATIC SULPHONATES

Compound	*Derivative*	*Degree of reaction after 1 h (%)*	*Minimum No. of days without decomposition*
1	$-SO_3$(tBDMS)	100	28
2	$-SO_3$(tBDMS) –O(tBDMS)	6[a], 75[b]	–
3	$-SO_3$(tBDMS) –O(tBDMS)	100	25
4	$-SO_3$(tBDMS) –COO(tBDMS) –NH(tBDMS)	70	Slow decomposition to yield an extraneous GC peak

[a] The degree of silylation was estimated from the GC response of the generated tBDMS derivative and that of the same derivative derived from the corresponding ammonium salt at the completion of reaction.

[b] In the presence of benzo-15-crown-5, added in equal molar amount as the substrate.

Unlike the ammonium salt, sodium isethionate was only 20% reacted after 24 h. It appears that the poor reactivity is due to a solubility problem. A macrocyclic polyether, benzo-15-crown-5, known to complex with the sodium cation and thus help to bring the anion into organic solvent[9], was added to the reaction mixture in a 1:1 molar ratio with respect to the substrate. A dramatic increase in reaction rate was observed. Sodium isethionate was 75% derivatized in the first hour. After 24 h reaction at 70°C, however, only 50% of the tBDMS derivative was detected, while no other extraneous peak was observed. We believe the complexing of sodium ion by the polyether renders the chloride ion generated from the silylation reaction more "naked". The activity of this anion is enhanced such that it is able to reverse the reaction as shown in the following equation. This postulate is presently under investigation in our laboratory.

$$\textit{tert.}\text{-butyl}(CH_3)_2SiCl + HOCH_2CH_2SO_3^- + \text{polyether-}Na^+ \rightleftarrows (tBDMS)OCH_2CH_2SO_3(tBDMS) + \text{polyether-}Na^+ + Cl^-$$

Cysteic acid, a compound containing SO_3H, NH_2 and COOH functional groups, formed a trisilylated derivative. The silylation reaction appeared to be completed in 3 h but the response of the derivative started to slide as an unidentified new peak is formed. MS analysis indicates that this peak is not the tetrasilylated derivative in which both of the hydrogens on the primary amino group are replaced by the silyl groups. Degradation of the trisilylated derivatives, however, was slow, with 15% loss in response over a period of 18 h.

TABLE II

DERIVATIZATION AND STABILITY RESULTS OF AROMATIC SULPHONATES

Compound	*Derivative*	*Degree of reaction after 1 h (%)*	*Minimum No. of days without decomposition*
5	$-SO_3$(tBDMS)	100	27
6	$-SO_3$(tBDMS)	100[a]	32
7	$-SO_3$(tBDMS) $-SO_3$(tBDMS)	84	26
8	$-SO_3$(tBDMS) -NH(tBDMS)	16[b]	34
9	-COO(tBDMS) -COO(tBDMS) $-SO_3$(tBDMS)	–[c]	–

[a] The disilyl derivative in which one of the amino proton was replaced by a tBDMS group was observed only after 24 h of reaction.

[b] Mono- and disilyl derivatives were observed simultaneously, but the response of the disilyl derivatives grew at the expense of the monosilyl derivative. At the end of 24 h, the monosilyl peak almost disappeared, indicating silylation was close to completion.

[c] The extent of reaction was not estimated since reaction was not completed at the end of the 24-h study period.

TABLE III

RELATIVE INTENSITIES OF THE MAJOR FRAGMENT IONS IN THE MASS SPECTRA OF THE tBDMS DERIVATIVES OF SULPHONATES

Compound	*Derivative*	*Mol. wt.*	*Base peak*	*Relative intensity (%)*								
				m/e 73	*m/e 75*	*m/e 115*	*m/e 133*	*[M−15]*	*[M−57]*	*[M−121]*[a]	*[M−179]*[a]	*[M−195]*[a]
1	$-SO_3$(tBDMS)	308	251	22	82	4	1	1	100	2	0	0.3
2, 3	$-SO_3$(tBDMS) –O(tBDMS)	354	73	100	30	24	26	2	56	0	0.2	4
4	–COO(tBDMS) –NH(tBDMS) $-SO_3$(tBDMS)	511	73	100	46	8	9	0.3	6	0.8	0	5
5	$-SO_3$(tBDMS)	300	243	11	11	0.2	0	0.4	100	9	0.2	28
6	$-SO_3$(tBDMS)	337	280	7	20	48	0	0.7	100	50	41	50
6	$-SO_3$(tBDMS) –NH(tBDMS)	451	184	83	45	17	0.7	8	37	14	20	10
7	$-SO_3$(tBDMS) $-SO_3$(tBDMS)	516	185	79	50	6	6	0.6	79	0	2	3
8	$-SO_3$(tBDMS)	335	75	11	100	2	0	0	70	22	4	12
8	$-SO_3$(tBDMS) –NH(tBDMS)	449	73	100	12	4	4	0.5	24	0	0.4	0
9	–COO(tBDMS) –COO(tBDMS) $-SO_3$(tBDMS)	588	73	100	43	3	13	0	16	0	0	0
10	–O(tBDMS) –O(tBDMS) $-SO_3$(tBDMS)	582	525	99	7	2	2	2	100	0.2	0.2	0.4

[a] [m − 121], [M–179] and [M − 195] correspond to the fragment ions [$M - SO_2 - 57$], [$M - SO_2$(tBDMS)] and [$M - SO_3$(tBDMS)] respectively.

In general, no difficulty was experienced in derivatizing aromatic sulphonates, although derivatives of higher degree of silylation were formed slower than those of lower degree of silylation (Table II). In all cases except compound 8, only one derivative was detected during the 24-h study period. For compound 8, both mono - and disilylated derivatives were observed simultaneously, with the quantity of the latter growing at the expense of that of the former. A strong GC response was observed after overnight derivatization for compound 10, although no kinetic or stability studies were carried out for this compound.

In case where there are more than one active site reacting such as in compounds 6 and 8, the detected monosilyl derivative is assummed to be the one with the sulphonate group derivatized, since aromatic compounds containing an amino group attached to the ring can elute under the described GC conditions but underivatized organic sulphonic acids or salts are too polar to pass through the DB5 column[10].

Stability of the tBDMS-sulphonates as a function of time

Those sulphonates which were completely derivatized in less than 24 h were subjected to stability test as described under Experimental. As presented in Tables I and II, all these tBDMS derivatives demonstrated excellent stability for at least 25 days.

Mass spectrometry

Each synthesized tBDMS-sulphonate was subjected to GC–MS analysis and each displayed a very sharp single chromatographic peak except the monosilyl derivatives of the two amino sulphonates (compounds 6 and 8) which exhibited a slight peak tailing.

Table III shows the MS results for the aliphatic and aromatic sulphonates, respectively. Both groups of tBDMS derivatives produced the same general fragmentation. All yielded a singular unique [M − 57] fragment ion in the high mass spectral region. As is typical of tBDMS derivatives, this fragment ion results from the elimination of one *tert.*-butyl function from the molecule. In monosilylated derivatives, this ion was very intense and often served as the base ion. The relative intensity of this fragment decreased as the degree of silylation increased. Each derivative also displayed both a weak molecular ion (<0.1%) and a low relative intensity [M − 15] fragment (0–8%) which was produced by the loss of a methyl group from the derivative.

In general, all these derivatives displayed fragment ions *m/z* 73, 75 and 115.

$^{+}O\text{-}C(CH_3)_3$	$H\overset{+}{O}=Si(CH_3)_2$	$[Si(CH_3)_2\text{-}tert.\text{-}C_4H_9]^{+}$
m/e 73	*m/e 75*	*m/e 115*

In addition to the ions already mentioned, di- or trisilylated derivatives also yielded the ion *m/e* 133 containing two silicone atoms..

$$(CH_3)_2HSi\overset{+}{O}=Si(CH_3)_2$$

Fragments characteristic of tBDMS–sulphonate function are $[M - SO_2 - 57]^{+}$, $[M - SO_2(tBDMS)]^{+}$ and $[M - SO_3(tBDMS)]^{+}$ corresponding to loss of

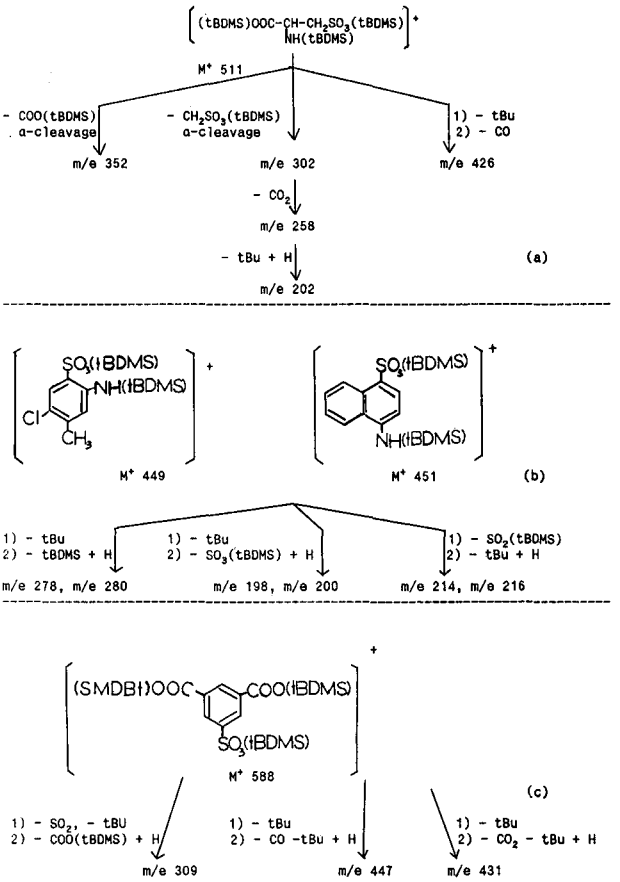

Fig. 2. Characteristic fragmentation patterns of tBDMS derivatives of (a) compound 4, (b) compounds 6 and 8 and (c) compound 9.

a.m.u. 121, 179 and 195 from the molecular ion. As shown in Table III, some or all of these fragments were observed in all of the derivatives except in the trisilylated derivative of compound 9, in which fragmentation involving the tBDMS–carboxylate function was competing with the cleavage at the tBDMS–sulphonate group.

Fig. 2 describes fragmentation patterns specific to the tBDMS derivatives of compounds 4, 6, 8 and 9.

Mass spectra of the trisilyl derivatives of compounds 4 and 9 are composed mainly of fragments of low intensities except the ions of *m/e* 73 and *m/e* 75. Ions resulting from the favorable cleavages α to the amino function were observed at *m/e* 302 and *m/e* 352 for compound 4 derivative as shown in Fig. 2a.

The disilylated derivative of compounds 6 and 8, both of which are aromatic aminosulphonates, share several similar fragmentation reactions as shown in Fig. 2b.

CONCLUSION

A method has been developed in which sulphonic acids or their sodium salts are derivatized to their respective tBDMS derivatives in a single-step reaction. These derivatives can be easily detected by FID. In addition, the tBDMS–sulphonates can be readily identified by their mass spectra characterized by the presence of [M − 57] fragment ion, and other ions resulting from cleavage at the SO_3(tBDMS) function.

ACKNOWLEDGEMENT

The authors thank Allan G. Harris for his encouragement to publish this work.

REFERENCES

1 K. A. Caldwell and A. L. Tappel, *J. Chromatogr.*, 32 (1968) 635.
2 O. Stokke and P. Helland, *J. Chromatogr.*, 146 (1978) 132.
3 J. J. Kirkland, *Anal. Chem.*, 32 (1960) 1388.
4 A. Amer, E. G. Alley and C. U. Pittman, Jr., *J. Chromatogr.*, 362 (1986) 413.
5 M. Nakada, A. Uzawa, S. Fukushi, H. Tomita and M. Hirota, *Nippon Kagaku Kaishi*, 5 (1984) 728.
6 L.-K. Ng, *U.S. Customs Bulletin*, 19 (1985) 40.
7 A. E. Pierce, *A Technique for Gas Phase Analysis, Silylation of Organic Compounds*, Pierce, Rockford, Il. 1968, ch. 1.
8 L.-K. Ng and M. Hupé, unpublished results.
9 C. J. Pedersen, *J. Am. Chem. Soc.*, 92 (1970) 386.
10 L.-K. Ng, unpublished results.

Journal of Chromatography, 513 (1990) 71–81
Elsevier Science Publishers B.V., Amsterdam

CHROM. 22 513

Simultaneous determination of neutral and amino sugars in biological materials

RICHARD J. KRAUS, FRED L. SHINNICK and JUDITH A. MARLETT*
Department of Nutritional Sciences, University of Wisconsin–Madison, 1415 Linden Drive, Madison, WI 53706 (U.S.A.)
(First received December 19th, 1989; revised manuscript received April 18th, 1990)

ABSTRACT

A method is described for the simultaneous analysis of nine neutral and three amino sugars. Mixtures of standard sugars and biological samples were acid hydrolyzed with a two step Saeman procedure, neutralized with $BaCO_3$, reduced with sodium borohydride, acidified, evaporated and alditol acetates prepared. Baseline resolution was achieved on a glass-capillary SP-2340 column in *ca.* 52 min. Reproducibility, response factors and hydrolysis losses were determined. Quantitation was linear over the range of 10–20 μg/ml to 2000 μg/ml. Conditions were defined for the reproducible quantitation of muramic acid.

INTRODUCTION

Several gas (GC) and high-performance liquid chromatographic and colorimetric methods have been used to measure the neutral sugars in the complex mixture of plant polysaccharides termed dietary fiber[1–3]. Understanding the role of dietary fiber in the gastrointestinal tract requires additional analytical capabilities to distinguish exogenous from endogenous carbohydrate polymers, and bacteria. Plant polysaccharides are comprised largely of neutral sugars whereas both neutral and amino sugars are present in bacteria and mucin. One amino sugar, muramic acid, has been used as a marker for bacteria[4]. Our interest in the analysis of polysaccharides typically found in the lumen of the gastrointestinal tract instituted a search for an analytical method that would allow complete determination of both neutral and amino sugars and wich would permit analysis over a wide range of absolute amounts of sugars in any particular sample. Earlier GC methods for measurement of both neutral and amino sugars as alditol acetate derivatives exhibited long retention times, poor chromatography of the amino sugars[5] or inadequate separation of the neutral sugars[6]. Deamination of amino sugars produced shorter retention times for amino sugar derivatives. However, multiple products were produced from each amino sugar and some neutral sugars partially decomposed under the deamination conditions[7].

Methods which give satisfactory results for specific types of samples have been

0021-9673/90/$03.50

reported, for example, non-starch polysaccharides in foods[2,3,8], plant cell walls[9], bacterial cell walls[10,11], and glycoproteins[12,13]. Each of these kinds of samples often contain relatively high concentrations of carbohydrates or specific polysaccharides, that simplify their analysis. We report here a method, derived by combining and modifying a number of existing methods, for the simultaneous analysis and quantitation of neutral and amino sugars, including muramic acid, in the CHO mixtures typically found in the lumen of the gastrointestinal tract.

EXPERIMENTAL

Chemicals

All sugars, sodium borohydride, acetic anhydride, octanol and methylene chloride were obtained from Sigma (St. Louis, MO, U.S.A.). All other chemicals were reagent grade. Whatman GF/A glass micro fiber filter paper (4.25 cm) was purchased through VWR Scientific (Chicago, IL, U.S.A.). 12 *M* H_2SO_4 was made by adding 1226 g ultra pure sulfuric acid, purchased from VWR, to 408 g of distilled water. The specific gravity was checked and adjusted, if necessary, to 1.63 g/ml and the solution stored in a desiccator. The standard sugar mixture consisted of 1 mg/ml of each of nine neutral and three amino sugars in distilled water.

Biological samples

All samples that were analyzed were obtained from experiments conducted in this laboratory. Rat feces were collected from animals fed an AIN 76A purified diet[14,15] into which 40% oat bran (Quaker Oats, Barrington, IL, U.S.A.) had been incorporated to make a diet containing 8% dietary fiber[16]. Complete fecal collections were made daily for 14 days from 10 animals, blended with distilled water and lyophilized. A single composite consisting of 10% of the dry output from each rat was prepared for analysis. One composite of human feces was prepared from samples collected during 5 to 7 days of ingestion of a mixed solid food diet supplemented with 30 g/day of soft white wheat bran (American Association of Cereal Chemists, St. Paul, MN, U.S.A.); dietary fiber intake was 33–35 g/day[17]. Nine stools from five male subjects were combined to prepare the composite. The other human feces sample was collected during consumption of a fiber free diet during the last 10 days of a 60-days study of a nutritionally complete liquid diet (Ensure®, Ross Labs. Columbus, OH, U.S.A.)[18]. A single composite from the 10 days of excreta of six subjects was prepared for analysis by combining 2% of dry stool from each subject.

Acid hydrolysis

All biological samples were acid hydrolyzed by a modified Saeman hydrolysis procedure. Dry ground samples or standards were thoroughly mixed with 12 *M* H_2SO_4 (1.0 ml acid/50 mg of sample)[19] and allowed to incubate at ambient temperatures for 1 h with mixing every 15 min; 11 ml water/ml of 12 *M* H_2SO_4 was added to produce 1 *M* H_2SO_4. Samples were then autoclaved for 1 h at 121°C (15 p.s.i.). After cooling to ambient temperature, 0.2 ml of the internal standards mixture was added. The internal standards were allose at 10 mg/ml and N-methylglucamine (N-methyl-2-amino-2-deoxy-D-glucose) at 10 mg/ml. The hydrolysates were filtered through tared filter paper (Whatman GF/A) and neutralized with $BaCO_3$ (ref. 20).

Sugar derivatization

Reduction was accomplished by heating 1 ml of the acid hydrolysate from 25 mg of a biological sample or 1 ml from 24 mg of the standard mixture with 0.1 ml of a sodium borohydride solution (100 mg/ml in 3 *M* ammonium hydroxide, 1 h, 40°C). Glacial acetic acid (0.1 ml) and 3 ml methanol were added and sample evaporated with simultaneous vortexing under vacuum to remove excess borate as methylborate and to remove water. The temperature of the evaporator was started at 40°C and raised to 60°C when the pressure gauge indicated most of the methanol had evaporated. This step was repeated three more times with drying time increased to 3 h for the last time. Derivatization was accomplished essentially by the method of Whiton *et al.*[21] with 2.0 ml acetic anhydride at 100°C for 16 h. If a larger aliquot of the hydrolysate was used, the amounts of reduction and acetylation reagents were proportionately increased. The procedure was modified to remove contaminants by incorporating the following extractive steps. After acetylation, samples were extracted three times with 1 ml of methylene chloride. The pooled methylene chloride extracts were backwashed with 2 ml of water, followed by 2 ml of 30% sodium hydroxide and finally 2 ml of water. The washed extracts were dried under a steam of nitrogen, redissolved in 0.5–1.0 ml of methylene chloride and stored at −20°C until analyzed.

Gas chromatography

GC analyses were carried out on a Model HP-5890 gas chromatograph (Hewlett-Packard, Palo Alto, CA, U.S.A.) equipped with a flame ionization detector, and containing a 30 m × 0.5 mm I.D. borosilicate glass column (SP-2340, Supelco, Bellefonte, PA, U.S.A.) fitted with 0.32 mm inert fused-silica tubing at both ends. Samples were injected (0.5–1.0 μl) using a split ratio of 10:1 and a column helium flow of 5.5 ml/min. The injection port temperature was 250°C, while the detector temperature was 300°C. The column oven program started at 185°C for 10 min then programmed at 3°C/min to 220°C, held at this temperature for 5 min, and then increased to a final temperature of 235°C at 15°C/min. The final temperature was held for 30 min. Data were collected on a Hewlett-Packard HP-3392A integrator.

Evaluation of method

Linearity of the method was determined by GC analysis of sets of sugar standards containing approximately 10, 20, 50, 500, 1000 and 2000 μg/ml of each sugar along with 0.2 ml of an internal standard mixture which contained 5.0 mg/ml of allose and 5.0 mg/ml of N-methylglucamine. Linearity was demonstrated by correlating the area ratio of each sugar, *i.e.*area of sugar/area of internal standard with the weighed amount of sugar. Response factors (*RF*) of standard sugar mixtures (24 mg sugar/ml) were determined by the equation: RF = (area of internal standard/mg of internal standard) × (mg of unknown/area of unknown). Hydrolysis losses were calculated as: [1.0 − (*RF* of sugars without acid treatment/*RF* of sugars with acid treatment)] × 100.

The effect of different concentrations of closely eluting pairs of neutral sugars, *i.e.* rhamnose and fucose, and ribose and arabinose, on the *RF* values for these sugars was evaluated by GC analysis of four mixtures of standard sugars without acid treatment: (1) the four sugars each at 2.0 mg/ml; (2) the four sugars each at 0.2 mg/ml; (3) rhamnose and ribose at 0.2 mg/ml, and fucose and arabinose at 2.0 mg/ml; and (4) rhamnose and ribose at 2.0 mg/ml and fucose and arabinose at 0.2 mg/ml.

Reproducibility of the method was evaluated by conducting all analyses in triplicate, determining the standard deviations and coefficients of variation. Reproducibility over time was determined by conducting triplicate analyses of four acid-treated standard sugar mixtures four times during two months.

RESULTS

Essentially baseline resolution was obtained for the nine neutral sugars, three amino sugars and two internal standards; the possible exceptions were the closely eluting pairs of rhamnose/fucose and ribose/arabinose (Fig. 1). The sugars eluted with these retention times: deoxyhexoses,at 8.02 and 8.60 min, pentoses, 12.06 to 16.39 min, hexoses 19.24 to 24.73 min, and amino sugars, 34.37 to 51.20 min (Table I).

Linearity for each neutral sugar was demonstrated over the range of 10 to 2000 μg/ml; the correlations between the area ratio of the sugar and the weighed amounts were $r \geqslant 0.999$. This linearity held throughout the entire range of concentrations tested; the coefficients of variation ($n=3$) for each neutral sugar at any concentration were all $\leqslant 4\%$. The mean coefficient of variation for all neutral sugars at 10 μg/ml was 1.9% (range: 1.0–3.6%), at 2000 μg/ml, 1.3% (range: 0.3–3.2%). None of the amino sugars were detectable at levels of 10 μg/ml; however, they were detected at 20 μg/ml. Linearity for each amino sugar was demonstrated over the range of 20 to 2000 μg/ml, with the correlations between the area ratio of the sugar and the weighed amounts of $r \geqslant 0.999$. At 20 μg/ml the mean coefficient of variation of triplicate analyses of two of the amino sugars, glucosamine and galactosamine, was 5.2%, and at 2000 μg/ml, 2.0%.

The individual sugars of the two closely eluting pairs, *i.e.* rhamnose/fucose and ribose/arabinose could be accurately measured whether concentrations of the two sugars in each pair varied by tenfold, 0.2 mg/ml and 2.0 mg/ml, or were at equal

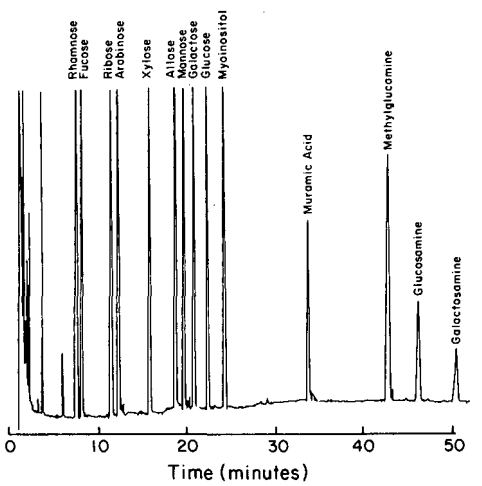

Fig. 1. Glass capillary column chromatogram of the alditol acetate derivatives of a mixture of hydrolyzed neutral and amino sugars each at a concentration of 2.0 mg/ml. Allose and methylglucamine were the internal standards.

TABLE I

RETENTION TIMES, RESPONSE FACTORS AND HYDROLYSIS LOSSES OF NEUTRAL AND AMINO SUGARS

I.S. = Internal standard.

Sugar	*Retention time (min)*	*Response factor (mean ± S.D., n=3)*		*Hydrolysis losses (%)*
		Without acid treatment	*With acid treatment*	
Rhamnose	8.02	0.94 ± 0.02	1.06 ± 0.03	11
Fucose	8.60	0.87 ± 0.01	0.98 ± 0.03	11
Ribose	12.06	0.89 ± 0.03	1.39 ± 0.04	36
Arabinose	12.85	0.88 ± 0.01	1.01 ± 0.03	13
Xylose	16.39	0.88 ± 0.01	1.18 ± 0.03	25
Allose (I.S.)	19.24	–	–	–
Mannose	20.19	0.95 ± 0.003	1.09 ± 0.03	13
Galatose	21.29	0.95 ± 0.004	1.09 ± 0.02	13
Glucose	22.80	0.94 ± 0.006	1.05 ± 0.03	11
Myoinositol	24.73	0.90 ± 0.01	0.97 ± 0.01	7
Muramic acid	34.37	–[a]	–[a]	–[a]
N-Methylglucamine (I.S.)	43.39	–	–	–
Glucosamine	46.02	1.90 ± 0.21	2.19 ± 0.05	13
Galactosamine	51.20	2.73 ± 0.06	3.26 ± 0.04	16

[a] See Table IV.

concentrations, 0.2 mg/ml or 2.0 mg/ml each. As shown in Table II, the *RF* for each individual sugar was essentially identical across the four different concentrations.

The extent of decomposition of monosaccharides during acid hydrolysis of carbohydrates was determined by subjecting a standard sugar mixture to the acid hydrolysis procedure and comparing the *RF* values of the same mixture without acid treatment. The *RF* values of standard sugar mixtures with and without acid treatment and the resulting hydrolysis losses are shown in Table I. The *RF* values of all of the neutral sugars without acid treatment were very similar, ranging from 0.87 for fucose

TABLE II

RESPONSE FACTORS OF TWO CLOSELY ELUTING PAIRS OF DERIVATIZED NEUTRAL SUGARS WITHOUT ACID TREATMENT

Concentrations (mg/ml)				R_F			
Rhamnose	*Fucose*	*Ribose*	*Arabinose*	*Rhamnose*	*Fucose*	*Ribose*	*Arabinose*
2.0	2.0	2.0	2.0	0.93[a]	0.86	0.85	0.85
0.2	0.2	0.2	0.2	0.87	0.80	0.80	0.80
0.2	2.0	0.2	2.0	0.85	0.82	0.80	0.83
2.0	0.2	2.0	0.2	0.93	0.86	0.86	0.81
Mean ± S.D.				0.90 ± 0.04	0.84 ± 0.03	0.83 ± 0.03	0.82 ± 0.02

[a] $n = 2$.

to 0.95 for both mannose and galactose. *RF* values for neutral sugars with acid treatment ranged from 0.97 for myoinositol to 1.39 for ribose; the *RF* values of the other neutral sugars were approximately 1.0 to 1.1. In contrast, the *RF* values of glucosamine and galactosamine without acid treatment were 1.90 and 2.73 and following acid treatment, 2.19 and 3.26, respectively (Table I). Seven of the nine neutral sugars showed about 10% to 15% decomposition during acid treatment while ribose and xylose exhibited 36 and 25% hydrolysis losses, respectively. Hydrolysis losses for glucosamine and galactosamine were 13 and 16%, respectively (Table I).

Reproducibility of the entire method, determined by analyzing four sets of triplicate aliquots of the standard sugar mixture, was very good, with coefficients of variation for the mean of means of the *RF* values of any sugar ranging from 1 to 4% (Table III). Precision within the sets of triplicates was also good, with coefficients of variation of 1 to 3%.

N-Acetylmuramic acid was included in the standard mixture and analyzed throughout these experiments. Data from four experiments in Table IV, part A, illustrate considerable variation within and between each set of triplicate analyses. Similar variability, with coefficients of variation, of 7 to 10% ($n=3$), was observed across the range of concentrations of 20 to 2000 mg/ml used to determine linearity of response. In addition, hydrolysis losses were variable and negative rather than positive numbers (Table IV, part A). The variability in the *RF* values suggested incomplete derivatization of N-acetylmuramic acid. The effects of the amounts of derivatizing reagents and total sugar content on the variability in N-acetylmuramic acid *RF* was evaluated by hydrolyzing and derivatizing N-acetylmuramic acid in the presence of constant amounts of derivatizing reagents and 8, 16 or 24 mg of total sugar. Indeed, the *RF* of N-acetylmuramic acid increased as the amount of total sugars increased in the mixture, indicating less complete derivatization of N-acetylmuramic acid in the presence of greater amounts of sugar (Table IV, part B). However, derivatizing

TABLE III

REPRODUCIBILITY OF RESPONSE FACTORS OF ALDITOL ACETATES OF MIXTURES OF NEUTRAL AND AMINO SUGARS WITH ACID TREATMENT

Sugar	*Response factor (mean ± S.D., n=3)*				*Mean of means ± S.D.*
	Day of Analysis				
	1	41	54	61	
Rhamnose	1.05 ± 0.03	1.06 ± 0.03	1.08 ± 0.01	1.08 ± 0.01	1.08 ± 0.02
Fucose	0.96 ± 0.03	0.97 ± 0.03	0.99 ± 0.01	0.98 ± 0.01	0.98 ± 0.01
Ribose	1.33 ± 0.03	1.39 ± 0.04	1.28 ± 0.01	1.36 ± 0.01	1.34 ± 0.05
Arabinose	0.99 ± 0.03	1.01 ± 0.03	1.03 ± 0.01	1.03 ± 0.01	1.02 ± 0.02
Xylose	1.14 ± 0.03	1.18 ± 0.03	1.14 ± 0.00	1.21 ± 0.01	1.17 ± 0.03
Mannose	1.03 ± 0.02	1.09 ± 0.02	1.10 ± 0.00	1.12 ± 0.01	1.09 ± 0.04
Galactose	1.04 ± 0.02	1.09 ± 0.02	1.11 ± 0.01	1.12 ± 0.01	1.09 ± 0.04
Glucose	1.00 ± 0.02	1.05 ± 0.03	1.04 ± 0.01	1.07 ± 0.01	1.04 ± 0.03
Myoinositol	1.03 ± 0.02	0.97 ± 0.02	1.00 ± 0.01	1.01 ± 0.01	1.00 ± 0.03
Glucosamine	2.10 ± 0.05	2.19 ± 0.05	2.16 ± 0.01	2.11 ± 0.03	2.14 ± 0.04
Galactosamine	3.09 ± 0.04	3.28 ± 0.04	3.27 ± 0.02	3.17 ± 0.03	3.20 ± 0.19

TABLE IV

RESPONSE FACTORS AND HYDROLYSIS LOSSES OF N-ACETYLMURAMIC AND MURAMIC ACID

	Response factor		*Hydrolysis loss (%)*
	Without acid treatment	*With acid treatment*	
(A) N-Acetylmuramic acid[a]			
Experiment 1	3.04 ± 0.30	2.29 ± 0.14	−33
Experiment 2	3.71 ± 0.29	2.48 ± 0.22	−50
Experiment 3	2.86 ± 0.80	2.90 ± 0.15	−16
Experiment 4	–	2.52 ± 0.10	–
(B) N-acetylmuramic acid[b]			
Sugar (mg) / *Reagents*			
8 standard[a]		2.17 ± 0.08	
16 standard		2.50 ± 0.10	
24 standard		2.76 ± 0.20	
24 3 × standard		2.27 ± 0.04	
(C) N-Acetylmuramic and muramic acids			
N-Acetylmuramic acid	2.80 ± 0.08	2.17 ± 0.07	−29
Muramic acid	1.64 ± 0.07	2.16 ± 0.12	+24

[a] Experiments used amounts of reduction and derivatization reagents reported in methods for 1 ml of acid hydrolysate from 25 mg of biological sample.

[b] N-Acetylmuramic acid derivatized in presence of varying amounts of neutral and amino sugars and with two amounts of derivatization reagents.

N-acetylmuramic acid in the presence of 24 mg sugar with 3 times more reductive and acetylating reagents produced a *RF* of 2.27, almost identical to the *RF* of 2.17 determined with the lowest amount of sugars (Table IV, part B). The concentrations of the reducing and acetylating reagents had no effect on the *RF* values of all other sugars.

The problem of a negative hydrolysis loss for N-acetylmuramic acid was addressed by testing the hypothesis that the acetyl group interfered with derivatization[22]. First, N-acetylmuramic and muramic acids (1 mg) were individually derivatized in triplicate with the standard amounts of reagents, i.e. 0.1 ml of sodium borohydrate and 2 ml acetic anhydride. Comparison of the *RF* values for muramic and N-acetylmuramic acid without acid treatment indicated the acetyl group interfered with derivatization (Table IV, part C). Muramic acid was approximately 55% more efficiently acetylated than N-acetylmuramic acid, with corresponding *RF* values of 1.64 and 2.80. The experiment was repeated but with acid treatment of the samples before derivatization. Following acid treatment, both sugars yielded essentially identical *RF* values, 2.16 ± 0.12 and 2.17 ± 0.07, for muramic acid and N-acetylmuramic acid, respectively, and a positive hydrolysis loss of 24% for muramic acid (Table IV, part C).

The method described here was successfully used to determine sugar content of typical biological samples analyzed in this laboratory (Table V). Total neutral sugars

TABLE V

SIMULTANEOUS DETERMINATION OF NEUTRAL AND AMINO SUGARS IN BIOLOGICAL MATERIALS

n.d. = None detected.

Sugar	*Content (mg/100 mg dry feces) (mean ± S.D., n=3)*		
	Rat feces, oat bran diet	*Human feces*	
		Wheat bran diet	*Fiber-free diet*
Rhamnose	0.7 ± 0.0	0.5 ± 0.0	0.5 ± 0.1
Fucose	0.3 ± 0.0	0.2 ± 0.0	0.1 ± 0.0
Ribose	0.5 ± 0.0	0.6 ± 0.0	0.2 ± 0.0
Arabinose	2.2 ± 0.1	4.8 ± 0.2	0.1 ± 0.0
Xylose	3.4 ± 0.1	5.2 ± 0.2	0.1 ± 0.0
Mannose	0.5 ± 0.0	0.5 ± 0.0	0.2 ± 0.0
Galactose	0.9 ± 0.0	1.3 ± 0.0	0.7 ± 0.1
Glucose	5.6 ± 0.1	8.1 ± 0.2	2.6 ± 0.2
Myoinositol	n.d.	n.d.	n.d.
Muramic acid	0.2 ± 0.1	0.2 ± 0.0	0.2 ± 0.0
Glucosamine	0.6 ± 0.0	0.5 ± 0.0	0.7 ± 0.0
Galactosamine	0.3 ± 0.0	0.3 ± 0.0	0.2 ± 0.1

in the three samples ranged from 4.4 to 21.1 mg/100 mg of dry feces. In all samples glucose was the dominant sugar, accounting for about 40% of the neutral sugar content in the fiber-containing samples and 60% in the fiber-free sample. The two fiber-containing samples also had significant amounts of arabinose and xylose, whereas the feces from humans fed the fiber-free diet had only negligible amounts. All three amino sugars were detected in the three samples, and all at low levels. Muramic acid content was about 0.2% for each sample, and galactosamine concentrations were slightly higher, ranging from 0.2 to 0.3%. Glucosamine was the most abundant amino sugar in all three samples.

DISCUSSION

Simultaneous quantitation of nine neutral and three amino sugars typically found in biological samples was achieved with the method we developed and evaluated. GC analysis of the alditol acetate derivatives of the sugars was achieved in less than one hour. The borosilicate glass column that was used showed excellent resolution for all desired sugar derivatives, including the closely eluting pairs of rhamnose/fucose and ribose/arabinose. Although the retention times of amino sugars were relatively long, the column and conditions used are an acceptable compromise which allows quantitation of both neutral and amino sugars.

The limit of detection of neutral sugars we observed was at a concentration of about 10 μg/ml when 1.0 ml of methylene chloride was used as the final solvent. This translated to limits of 0.04 mg/100 mg of starting material which is similar to the limits of 0.1 mg/100 mg of starting material reported by Fox *et al.*[10]. Since detection of amino

sugars was less sensitive than that of neutral sugars, the limits of detection on a starting weight basis for the three amino sugars would be about two to three times higher. Theoretically lower limits of detection per starting weight could be attained by dissolving the derivatized sample in smaller volumes of methylene chloride.

Sawardeker *et al.*[23] reported *RF* values of 1.0 for a series of the alditol acetates of neutral sugars without acid treatment when compared to xylitol. Since xylose is routinely present in samples analyzed in this laboratory, allose was chosen as an internal standard for neutral sugars. The *RF* values for neutral sugars when compared to allose were all very similar, ranging from 0.87–0.95, but were slightly less than 1.0 reported by Sawardeker *et al.*[23]. We used N-methylglucamine as the internal standard for amino sugars since Fox *et al.*[10] reported improved precision for the analysis of amino sugars when N-methylglucamine was used as an internal standard *versus* the neutral sugar xylose.

Hydrolysis losses of sugars are sugar specific and highly dependent on the severity of hydrolytic conditions[9,24,25]. We found xylose and ribose to be the neutral sugars most sensitive to hydrolytic decomposition. Hough *et al.*[24] also observed the most decomposition of these sugars when samples were heated to 100°C in 2 *M* H_2SO_4 for 6 h. They recovered only 48% of the ribose, and 67% of the xylose, while glucose and fucose recoveries were $\geqslant 90\%$, and mannose and galactose recoveries were 84 and 87% respectively. The higher recoveries we observed for ribose and xylose, 64 and 75% respectively, agree with the conclusions of Selvendran *et al.*[25], that Saeman hydrolysis methods result in less degradation than hydrolysis methods using only dilute H_2SO_4 and longer heating times. The need for anaerobic conditions for amino sugar acid hydrolysis is unclear[26,27]. Under our experimental conditions, the losses of glucosamine and galactosmine, 13% and 16% respectively, were similar to those of the neutral sugars even though they were hydrolyzed under aerobic conditions. Muramic acid, with hydrolysis losses of 24%, was decomposed to a greater extent than the two other amino sugars.

Difficulties in the GC analysis of amino sugars are well documented, regardless of the derivative prepared[28]. It was thought that these problems were due primarily to chromatographic problems rather than derivatization problems[12]. Hudson *et al.*[29] found the behavior of the alditol acetate derivatives of amino sugars to be highly dependent on the pretreatment of a capillary GC column. For example after pretreatment with basic conditions the amino sugar derivatives were completely adsorbed to or decomposed on the column. However, if deactivated inlets and capillary columns were used, they found that the response of the amino sugar derivatives were about 90% of that of the neutral sugar derivatives. Fox *et al.*[10] also have suggested that the sensitivity of amino sugars may be lower than those for neutral sugars because they may adsorb to the column. This lower sensitivity would explain the higher *RF* values we observed for the amino sugars and suggests some adsorption onto the column. The *RF* values we determined for the amino sugars have been reproducible and suitable for the quantitation of small amounts of amino sugars in biological samples.

Many of the currently available methods were designed for the carbohydrate analysis of specific types of samples with high levels of carbohydrates or specific polysaccharides, characteristics which simplified their analysis. The samples analyzed for sugar composition in this report not only contained a complex mixture of

polysaccharides derived from a variety of sources, plant cell walls, bacterial cell walls, bacterial exopolysaccharides and mucins, but also contained only very small amounts of some of the sugars. To determine complete sugar composition of these biological samples, it was necessary to take either a large portion of or the entire acid hydrolysate from 25 mg of sample for GC analysis. This was achieved by neutralization of the hydrolysate with barium carbonate and removal of the sulfate anion as barium sulfate by centrifugation. Part or all of the supernatant was then taken for subsequent reduction and derivatization.

Since muramic acid determination was desired, we found that the thorough evaporative and derivatizing procedures reported by others[21] were required. If muramic acid determination is not desired, derivatization of the supernatant by a methylimadizole catalized method[9] could be utilized. Muramic acid (13-O-lactyl-glucosamine) is chemically unique among amino sugars in that under dehydrating conditions it forms a lactam ring[10,21]. The acetylated lactam is the derivative analyzed by GC. Lactam formation is essential for muramic acid analysis by the method we report, as the free carboxyl would bind to the SP2340 GC column[21].

Acetylation of the amine nitrogen interferes with the lactam ring formation, explaining the less efficient derivatization of N-acetylmuramic acid we observed. Such interference would lead to an underestimation of the actual amount of muramic acid when starting with N-acetylmuramic acid. This underestimation would explain the negative hydrolysis losses of N-acetylmuramic acid in the standard sugar mixture. Since the acetyl group of N-acetylmuramic acid was cleaved during hydrolysis, thereby yielding muramic acid[22], identical *RF* values for the two sugars were achieved.

Following acetylation and extraction, it would be possible to inject samples directly into the GC system. However, we have found that sample clean up and drying prior to GC injection prolongs the life of the column; it may also eliminate extraneous peaks from the chromatogram. The clean up procedure we described should remove both acidic and basic contaminants and provide an essentially water-free extract for GC analysis.

ACKNOWLEDGEMENTS

This research was supported by National Institutes of Health grant DK 21712 and by the College of Agricultural and Life Science, University of Wisconsin–Madison.

REFERENCES

1 J. L. Slavin and J. A. Marlett, *J. Agric. Food Chem.*, 31 (1983) 467.
2 H. N. Englyst and J. H. Cummings, *Analyst (London)*, 109 (1984) 937.
3 O. Theander and E. A. Westerlund, *J. Agric. Food Chem.*, 34 (1986) 330.
4 A. Fox, H. Schwab and T. Cochran, *Infect. Immun.*, 29 (1980) 526.
5 R. Oshima, J. Kumantotani and C. Watanabe, *J. Chromatogr.*, 250 (1982) 90.
6 C. Green, V. M. Doctor, G. Holzer and J. Oro, *J. Chromatogr.*, 207(1981) 268.
7 R. J. Henry, A. B. Blakeney, P. J. Harris and B. A. Stone, *J. Chromatogr.*, 256 (1983) 419.
8 M. J. Nielson and J. A. Marlett, *J. Agric. Food Chem.*, 31 (1983) 1342.
9 A. B. Blakeney, P. J. Harris, R. S. Henry and B. A. Stone, *Carbohydr. Res.*, 113 (1983) 291.
10 A. Fox, S. C. Morgan, J. R. Hudson, Z. T. Zhu and P.Y. Lau, *J. Chromatogr.*, 256 (1983) 429.
11 M. D. Walla, P. Y. Lau, S. I. Morgan, A. Fox and A. Brown, *J. Chromatogr.*, 288 (1984) 399.

12 W. Niedermeier, *Anal. Biochem.*,40 (1971) 465.
13 L. A. Torello, A. J. Yates, D. K. Thompson, *J. Chromatogr.*, 202 (1980) 195.
14 American Institute of Nutrition, *J. Nutr.*, 107 (1977) 1340.
15 American Institute of Nutrition, *J. Nutr.*, 110 (1980) 1726.
16 H. L. Chen and J. A. Marlett, unpublished results.
17 K. B. Wright and J. A. Marlett, unpublished results.
18 B. H. Liebel, M. H. Fischer, S. C. Van Calcar and J. A. Marlett, *JPEN*, 14 (1990) 394.
19 R. J. Kraus and J. A. Marlett, *J. Sci. Food Agric.*, 52 (1990) in press.
20 F. L. Shinnick, M. J. Longacre, S. L. Ink and J. A. Marlett, *J. Nutr.*, 118 (1988) 144.
21 R. S. Whiton, P. Lau, S. I. Morgan, J. Gilbert and A. Fox, *J. Chromatogr.*, 347 (1985) 109.
22 A. Fox, personal communication.
23 J. S. Sawardeker, J. H. Sloneker and A. Jeanes, *Anal. Chem.*, 37 (1965) 1602.
24 L. Hough, J. V. S. Jones and P. Wasteman, *Carbohydr. Res.*, 21 (1972) 9.
25 R. R. Selvendran, J. F. March and S. G. Ring, *Anal. Biochem.*, 96 (1979) 282.
26 E. F. Walborg and D. N. Ward, *Biochim. Biophys. Acta*, 78 (1963) 304.
27 J. H. Kim, B. Shome, T. H. Liao and J. Pierce, *Anal. Biochem.*, 20 (1967) 258.
28 A. Fox, S. L. Morgan and J. Gilbart, in C. J. Biermann and G. D. McGinnis (Editors), *Analysis of Carbohydrates by GC and MS*, CRC Press, Boca Raton, FL, 1989, Ch. 5, p. 87.
29 J. R. Hudson, S. L. Morgan and A. Fox, *J. High Resolut. Chromatogr. Chromatogr. Commun.*, 5 (1982) 285.

Journal of Chromatography, 513 (1990) 83–91
Elsevier Science Publishers B.V., Amsterdam

CHROM. 22 447

Determination of 2-methylpyrazine and pyrazinamide in reaction mixtures by gas and high-performance liquid chromatography[a]

SAJID HUSAIN*, P. NAGESWARA SARMA, S. M. SAJJAD, R. NARSIMHA and M. SUBRAHMANYAM

Indian Institute of Chemical Technology, Hyderabad-500 007 (India)

(First received October 26th, 1989; revised manuscript received March 13th, 1990)

ABSTRACT

Pyrazinamide is an antitubercular drug, commonly prepared by ammoxidation of 2-methylpyrazine (2-MP), which also may be prepared by several routes. Rapid, sensitive and selective analytical methods are essential for monitoring the reactions during process development. Methods based on gas chromatography were developed for monitoring the reactions during the preparation of 2-MP and a high-performance liquid chromatographic procedure was used to separate and determine the ammoxidation products of 2-MP. The methods were utilized successfully in analysing the reaction streams.

INTRODUCTION

Pyrazinamide (PZA) is a drug used in the treatment of pulmonary tuberculosis[1,2] and is manufactured by several ways[3], including the hydrolysis of 2-cyanopyrazine (2-CP), obtained by ammoxidation of 2-methylpyrazine (2-MP). Pyrazine may be obtained as a byproduct during this ammoxidation process. The raw material, 2-MP, necessary for this ammoxidation is prepared by several routes. Pyrazine derivatives are useful not only in the preparation of pyrazinamide, but also in the manufacture of many other industrial products, *e.g.*, flavouring agents, pharmaceuticals and agricultural chemicals[4]. The reactions chosen for the preparation of 2-MP and PZA in the present studies are shown in Fig. 1.

PZA levels in biological fluids have previously been determined by spectrophotometric[5,6], gas chromatographic–mass spectrometric (GC–MS)[7] and high-performance liquid chromatographic (HPLC)[8–12] techniques. GC analysis of reaction mixtures obtained in the synthesis of 2-MP from EDA and PG (route I) and ammoxidation products of 2-MP (route IV) was reported by Forni *et al.*[13,14].

[a] IICT(H) Communication No. 2485.

0021-9673/90/$03.50

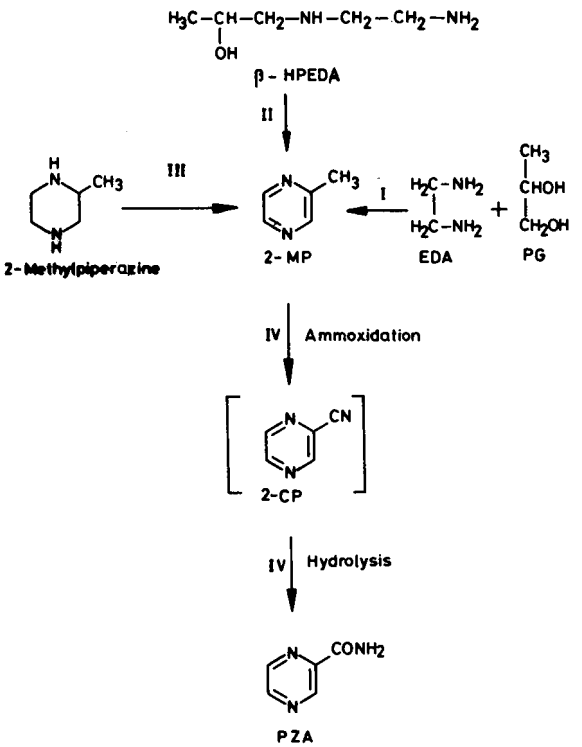

Fig. 1. Reactions for the preparation of 2-MP and PZA. β-HPEDA = β-hydroxypropylethylenediamine; PG = propylene glycol; EDA = ethylenediamine.

Attempts to standardize these methods in our laboratory are not successful. It was found that the stationary phase deteriorated quickly and that EDA was not eluted from the column.

In addition, no GC or HPLC methods are available for the analysis of reaction mixtures obtained in the preparation of 2-MP from β-hydroxypropylethylenediamine (β-HPEDA) (route II) and 2-methylpiperazine (route III). Therefore, there is an increasing need for rapid and selective methods for the determination of raw materials, intermediates and finished products in reaction streams during process development of 2-MP and PZA.

In this study, methods based on GC and HPLC were developed for the determination of 2-MP and PZA in reaction mixtures and their application to monitoring the reactions during process development is demonstrated.

EXPERIMENTAL

Reagents

2-MP and pyrazine were purchased from Aldrich (Milwaukee, WI, U.S.A.), PZA from IDPL (Hyderabad, India), 2-CP by Armour Chemicals (Bombay, India), EDA from Qualigens Fine Chemicals (Bombay, India) and PG from S.D. Fine

Chemicals (Bombay, India). All solvents used in HPLC except ethanol were obtained from Spectrochem (Bombay, India). Ethanol, 2-chloropyridine and 2,3-dichloropyridine (internal standards) were purchased from Fluka (Buchs, Switzerland). Chromosorb 101 was supplied by Sigma (St. Louis, MO, U.S.A.), other stationary phases employed in GC were purchased from Analabs (Norwalk, CT, U.S.A.) and stationary phases used in HPLC from Waters Assoc. (Milford, MA, U.S.A.). All other reagents were of analytical-reagent grade.

Doubly distilled water from a glass apparatus was used throughout. All glassware was cleaned, rinsed with acetone and silanized before use.

Instrumentation

The GC system consisted of Perkin-Elmer Model 910 chromatograph equipped with a flame ionization detector in conjunction with a Perkin-Elmer 1-mV potentiometric strip-chart recorder. The following GC conditions were used for the analysis of reaction mixtures of 2-MP obtained from route I: injection temperature, 300°C; detector temperature, 300°C; column, 10% Carbowax 20M (12 ft. × 1/8 in.) coated on Chromosorb W AW (80–100 mesh); carrier gas, nitrogen at a flow-rate of 45 ml/min; column temperature, programmed from 80 to 120°C at 5°C/min. The column was saturated with aliquots of ammonia before the sample was analysed. The following GC conditions were used for the analysis of reaction mixtures of 2-MP from routes II and III: injection temperature, 230°C; detector temperature, 250°C; stationary phase, Chromosorb 101 (6 ft. × 1/8 in.); oven temperature, 250°C; carrier gas, nitrogen at a flow-rate of 40 ml/min.

The HPLC system consisted of a Waters Assoc. Model ALC/GPC/244 chromatograph with an isocratic solvent delivery system (Model 6000A) equipped with a U6K injector, a Model 440 absorbance fixed-wavelength detector (254 nm at 0.1 a.u.f.s.), combined with a Chromatopak EIA integrator (Shimadzu, Kyoto, Japan). Analyses of process streams of PZA (route IV) were performed on a normal-phase μPorasil (10 μm particle size) column (30 mm × 3.9 mm I.D.) with isooctane–ethanol–acetic acid (75:24:1, v/v/v) as mobile phase at a flow-rate of 1.5 ml/min. The mobile phase was freshly prepared and filtered through Millipore HF 0.5-μm filters and the solvent was degassed before use.

Chromatographic analyses

Standard mixtures with different concentrations of 2-MP, EDA and PG together with 2-chloropyridine (internal standard) were prepared and analysed by GC. Standard solutions with different concentrations of 2-MP were prepared in order to construct a calibration graph for the determination of 2-MP reaction products by routes II and III. Sample volumes of 1 μl were injected in each instance.

Standard mixtures with different concentrations of 2-MP, pyrazine, 2-CP and PZA together with 2,3-dichloropyridine (internal standard) were prepared and analysed by HPLC; 5 μl of the sample were injected.

RESULTS AND DISCUSSION

GC analysis of reaction mixtures of 2-MP (route I)

The relative retention times of EDA, PG and 2-MP on Carbowax 20M

TABLE I

RELATIVE RETENTION TIMES (RRT) AND RESPONSE FACTORS OF EDA, PG AND 2-MP BY GC

Compound	*RRT*	*Response factor*
EDA	0.26	3.65
PG	0.41	2.17
2-MP	0.57	1.26
2-Chloropyridine (internal standard)	1.00	1.00

stationary phase are given in Table I. Stationary phases with different polarities such as Porapak Q, OV-17 and QF-1, and also Chromosorb 101[14], were tried for the separation of these compounds, but EDA was not quantitatively eluted and response factors calculated for PG and 2-MP were not reproducible. This problem was overcome by saturating the stationary phase with ammonia as the compounds under investigation are basic. It was observed that 5-μl aliquots of ammonia solution, injected six times, was sufficient for complete elution of all the compounds.

A typical chromatogram illustrating the separation of EDA, PG and 2-MP is shown in Fig. 2. Standard mixtures were prepared and analysed by GC. Response factors were calculated and presented in Table I. Results obtained in the analysis of standard mixtures are given in Table II, and are in close agreement with the true values. Reaction mixtures were analysed utilizing the developed method and the results are given in Table III.

GC procedure for the analysis of reaction mixtures of 2-MP (route II)

A procedure for monitoring the conversion of β-HPEDA to 2-MP by GC using

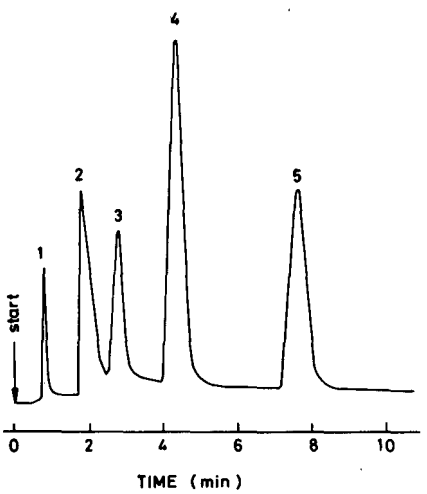

Fig. 2. Typical gas chromatogram showing the separation of the reaction mixture of 2-MP (route I). Peaks: 1 = solvent; 2 = EDA; 3 = PG; 4 = 2-MP; 5 = 2-chloropyridine (internal standard).

TABLE II

RESULTS OF ANALYSIS OF STANDARD MIXTURES OF EDA, PG AND 2-MP BY GC

Average of triplicate determinations.

Mixture No.	*EDA*		*PG*		*2-MP*	
	Taken (%)	*Found (%)*	*Taken (%)*	*Found (%)*	*Taken (%)*	*Found (%)*
1	25.31	25.46	24.89	24.70	49.80	49.33
2	21.43	21.27	22.86	22.72	55.71	55.89
3	16.58	16.40	20.08	20.19	63.34	63.12
4	34.92	35.61	32.23	32.05	32.85	32.64
5	10.47	10.41	13.74	13.91	75.79	76.50
6	5.58	5.65	8.28	8.38	86.14	86.09

TABLE III

RESULTS OF ANALYSIS OF REACTION MIXTURES OF 2-MP BY GC (ROUTE I)

Average values obtained from duplicate GC runs.

Mixture No.	*EDA (%)*	*PG (%)*	*2-MP (%)*
1	30.62	16.53	57.75
2	36.73	20.09	43.18
3	27.95	14.81	60.30
4	40.58	22.33	37.87
5	50.34	26.71	23.59

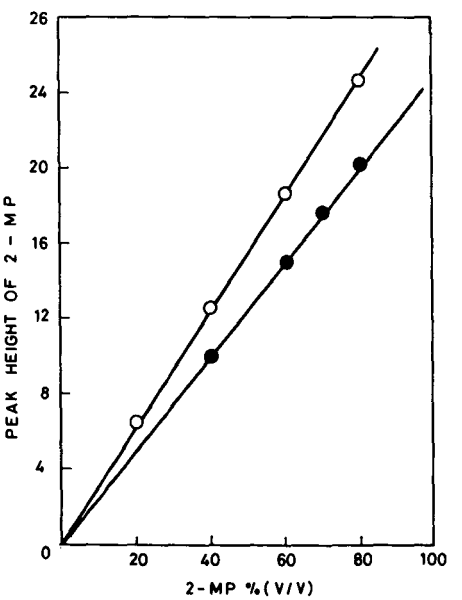

Fig. 3. Calibration graph for the determination of 2-MP in reaction mixtures obtained by routes II (○) and III (●).

TABLE IV

RESULTS OF ANALYSIS OF REACTION MIXTURES OF 2-MP BY GC (ROUTE II)

Mixture No.	*2-MP formed (%)*	*Unconverted β-HPEDA (%)*	*Pyrazine (%)*
1	53.50	35.00	9.50
2	57.00	40.00	2.50
3	73.50	20.00	6.50
4	72.00	22.00	4.00

the external standard method was developed. Mixtures with different concentrations of 2-MP and β-HPEDA were prepared and a calibration graph was constructed of peak height (ordinate) *versus* concentration of 2-MP (abscissa) (Fig. 3). Results of the analysis of reaction mixtures are given in Table IV.

GC procedure for the analysis of reaction mixtures of 2-MP (route III)

A similar method was developed for the analysis of reaction mixtures of 2-MP from route III. The calibration graph is shown in Fig. 3. Results of the analysis of reaction mixtures are given in Table V. The results obtained are in close agreement with the yields obtained after isolating the products.

HPLC analysis of 2-MP reaction mixtures of pyrazinamide (route IV)

Normal-phase HPLC with μPorasil as stationary phase and isooctane–ethanol–acetic acid (75:24:1, v/v/v) as mobile phase separated all the components, *i.e.*, 2-MP, 2-CP, PZA and pyrazine. A typical chromatogram is shown in Fig. 4. Relative retention times along with capacity factors are given in Table VI. Quantitative analysis was carried out by the internal standard method. Many compounds were tried as internal standards and 2,3-dichloropyridine was found to be most suitable. Response factors determined by well established procedures[15] are given in Table VI. It was found that the response factors for all the components are much less than 1, which indicates that the detector response is good.

The validity of the method was checked by analysing synthetic mixtures and the results are presented in Table VII. The results obtained are in good agreement with the true values.

TABLE V

RESULTS OF ANALYSIS OF REACTION MIXTURES OF 2-MP BY GC (ROUTE III)

Mixture No.	*2-MP formed (%)*	*Unconverted 2-methylpiperazine (%)*	*Pyrazine (%)*
1	64.00	35.00	2.00
2	57.50	40.50	2.50
3	80.50	17.00	2.50
4	85.50	12.50	2.00

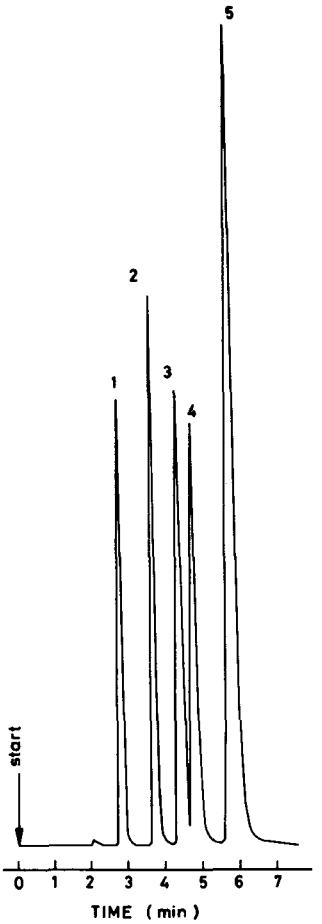

Fig. 4. Typical high-performance liquid chromatogram showing the separation of reaction mixtures of pyrazinamide (route IV). Peaks: 1 = 2,3-dichloropyridine (internal standard); 2 = 2-CP; 3 = 2-MP; 4 = pyrazine; 5 = PZA.

TABLE VI

RELATIVE RETENTION TIMES (RRT), RESPONSE FACTORS AND CAPACITY FACTORS OF THE CONSTITUENTS OF REACTION MIXTURES OF PYRAZINAMIDE BY HPLC

Compound	*RRT*	*Response factor*	*Capacity factor (k')*
2,3-Dichloropyridine (internal standard)	1.00	1.00	0.37
2-CP	1.88	0.25	0.82
2-MP	2.22	0.26	1.15
Pyrazine	2.43	0.13	1.36
PZA	2.93	0.23	1.84

TABLE VII

RESULTS OF ANALYSIS OF SYNTHETIC MIXTURES OF PYRAZINAMIDE BY HPLC

Average of triplicate determinations.

Mixture No.	*2-MP*			*2-CP*			*Pyrazine*			*PZA*		
	Taken (%)	*Found (%)*	*Error (%)*	*Taken (%)*	*Found (%)*	*Error (%)*	*Taken (%)*	*Found (%)*	*Error (%)*	*Taken (%)*	*Found (%)*	*Error (%)*
1	55.99	56.55	1.00	27.87	27.47	1.44	13.83	13.72	0.80	2.26	2.22	1.77
2	18.29	18.56	1.48	42.11	42.36	0.59	5.60	5.57	0.54	34.00	33.51	1.44
3	19.89	20.09	1.01	19.84	19.82	0.10	10.65	10.53	1.23	49.61	49.56	0.10
4	30.46	30.10	1.18	28.98	29.04	0.21	26.51	26.89	0.30	14.05	13.96	0.47
5	5.64	5.54	1.77	4.30	4.36	1.39	1.72	1.69	1.74	88.34	88.41	0.08

TABLE VIII

RESULTS OF ANALYSIS OF REACTION MIXTURES OF PYRAZINAMIDE BY HPLC

Average values obtained from duplicate GC runs.

Mixture No.	*2-MP (%)*	*2-CP (%)*	*Pyrazine (%)*	*PZA (%)*
1	97.23	1.96	–	0.82
2	85.85	0.70	11.90	0.01
3	47.78	28.73	22.43	1.08
4	42.51	–	24.16	33.32
5	44.45	52.11	0.96	2.46
6	41.87	54.67	0.77	2.66
7	47.71	47.69	3.15	1.43
8	37.26	2.70	8.51	51.54
9	34.78	–	10.47	54.75
10	40.54	–	4.23	55.22

Experiments on the ammoxidation of 2-MP were carried out under different conditions and with various catalysts. Typical samples of the reaction mixtures collected were analysed by the developed procedures and the results obtained are given in Table VIII. It can be seen that the amounts of PZA and 2-CP formed are different in each instance, depending on the experimental conditions.

CONCLUSIONS

A rapid and accurate GC method was developed for the determination of 2-MP, EDA and PG in reaction mixtures, in which presaturation of the column with ammonia before sample analysis enhanced the accuracy. A GC method was established for determining 2-MP in the conversion of β-HPEDA to 2-MP. Reaction mixtures obtained during the dehydrogenation of methylpiperazine were also monitored by GC under similar conditions.

In addition, an HPLC procedure for the determination of ammoxidation

products of 2-MP was developed. The time required for complete elution of the compounds is 10 min whereas the reported GC method requires nearly 20 min. Further, in the reported GC procedure, the stationary phase material deteriorates after a few months of use, whereas such a drawback is not observed in the developed HPLC method.

The methods developed are applicable to the assay of pyrazinamide and for monitoring the reactions during its process development. Further, the procedures are useful in the assay of the components of reaction mixtures in the process development of 2-methylpyrazine, which is the starting material for the manufacture of pyrazinamide.

ACKNOWLEDGEMENTS

The authors thank Dr. A. V. Rama Rao, Director, IICT(H), for his encouragement in carrying out this work. Thanks are also due to Dr. J. S. Yadav, Scientist, IICT(H), for his interest in this study.

REFERENCES

1 A. Brouard, H. Barreteau, H. Merdjan, M. Paillet and G. Fredj, *J. Chromatogr.*, 345 (1985) 453.
2 J. K. Landquist, in O. Meth-Cohn (Editor), *Comprehensive Heterocyclic Chemistry*, Vol. 1, Part I, Pergamon Press, New York, 1st ed., 1984, p. 180.
3 A. V. Rama Rao, J. S. Yadav, K. Ravichandran, A. B. Sahasrabudhe and S. S. Chaurassia, *Indian J. Chem.*, 23B (1984) 850.
4 A. E. A. Porter, in A. J. Boulton and A. AcKillop (Editors), *Comprehensive Heterocyclic Chemistry*, Vol. 3, Part 2B, Pergamon Press, New York, 1st ed., 1984, p. 158.
5 H. Foks and D. Panchechowska, *Acta Pol. Pharm.*, 33 (1976) 49; *C.A.*, 86 (1977) 72574p.
6 P. A. Caccia, *Am. Rev. Tuberc. Pulm. Dis.*, 75 (1957) 105; *C.A.*, 52 (1958) 1453a.
7 W. S. Allen, S. M. Aronovic, L. M. Bracone and J. H. Williams, *Anal. Chem.*, 25 (1953) 895.
8 J. Roboz, R. Suzuki and T. F. Yu, *J. Chromatogr.*, 147 (1978) 337.
9 B. Ratti, A. Toselli, E. Beretta, A. Bernareggi, *Farmaco, Ed. Prat.*, 37 (1982) 226; *C.A.*, 97 (1982) 84622t.
10 T. Yamamoto, Y. Moriwaki, S. Takahashi, T. Hada and K. Higashino, *J. Chromatogr.*, 382 (1986) 270.
11 K. Chan, C. L. Wong and S. Lok, *J. Chromatogr.*, 380 (1986) 367.
12 J. Woo, C. L. Wong, R. Teoh and K. Chan, *J. Chromatogr.*, 420 (1987) 73.
13 L. Forni, *Appl. Catal.*, 20 (1986) 219.
14 L. Forni, G. Stern and M. Gatti, *Appl. Catal.*, 29 (1987) 161.
15 F. J. Debbrecht, in R. L. Grob (Editor), *Modern Practice of Gas Chromatography*, Wiley, New York, 2nd ed., 1985, p. 409.

Journal of Chromatography, 513 (1990) 93–105
Elsevier Science Publishers B.V., Amsterdam

CHROM. 22 500

Fate of superabsorbents in the environment

Analytical techniques

S. S. CUTIÉ*, W. C. BUZANOWSKI and J. A. BERDASCO
Analytical Sciences, Polymeric Materials Research Center, 1897 Building, Midland, MI 48667 (U.S.A.)
(First received December 1st, 1989; revised manuscript received April 4th, 1990)

ABSTRACT

The Analytical and Environmental Committees of the Institute of Polyacrylate Absorbents (1330 Connecticut Avenue, N. W., Washington, DC 20036, U.S.A.), of which Dow is a member, requested the development of specific and sensitive analytical techniques to monitor the movement of soluble polyacrylates through soils. Three analytical techniques are explained that can be used to monitor effluents from columns or in studies where batch extraction of the soils are conducted. Concentrations of polyacrylic acid were studied from the ppm range for nuclear magnetic resonance spectroscopy and size-exclusion chromatography to the sub-ppm range for derivatization pyrolysis–gas chromatography. The soils under study were a sandy soil, a londo soil, and a clay type of soil. The investigation explained in this report was conducted with batch extractions. Included in this report is a soil adsorption capacity study that showed behavior opposite to what was expected to be the adsorption capacity of the soils. Also included are pH studies of the soils.

INTRODUCTION

The increased use of disposable diapers containing polyacrylate superabsorbents and their disposal in landfills has focused attention on the possible movement of the soluble polymer fraction and its penetration of soils. In the past, there have been reports[1,2] of studies designed to understand the dynamics of the movement of the soluble fraction of superabsorbent polymers. These studies were conducted with ^{14}C-tagged polyacrylate polymers, which made the study very expensive. Another study[3] used a Total Organic Carbon analyzer to monitor the effluent of a column loaded with soil to determine the movement of soluble polymer. The need to make this type of study more specific and available to investigators with limited resources prompted an investigation that resulted in the development of techniques that are specific and very sensitive.

The techniques investigated included size-exclusion chromatography (SEC) de-

rivatization pyrolysis–gas chromatography (Py–GC) with dual-column chromatography[4,7] and nuclear magnetic resonance (NMR) spectroscopy. Difficulties associated with the movement of polyelectrolytes through solids and the interactions these polymers will exhibit when contacted with water and soils have been explained before[5,6]. To add to these difficulties it was requested that the procedures developed be sensitive enough to detect the soluble fraction of the superabsorbent polymer at the sub-ppm level.

EXPERIMENTAL

Size-exclusion chromatography

Instrumentation. Column, 1 TSK G1000 PW; eluent, 0.3 *M* NaCl, 0.34 *M* Na_2HPO_4, pH adjusted to 6.8 with 3% H_3PO_4 and then filtered through a 0.1-μm filter; flow-rate, 1 ml/min; injection volume, 200 μl; detector, Waters differential refractometer Model 410; software, Nelson X-Chrom v. 7.1.

Sample preparation. The soluble polyacrylic acid was added to the soil in three different ways. (a) Linear polyacrylic acid (mol. wt. *ca.* 243 000 and 0% neutralization; Scientific Polymer Products, Ontario, NY, U.S.A.) was added directly to the soil and allowed to equilibrate for up to 4 h. (b) The same linear polymer was prepared by adding it to water and then contacting it with the soil. (c) soluble polymer was extracted with 0.9% NaCl from commercially available DRYTECH® (Dow Chemical, Midland, MI, U.S.A.) superabsorbent polymer which is partially neutralized. The soluble polymer in 0.9% NaCl was then contacted with the soils.

A 10-g amount of soil containing the polyacrylic acid was extracted with 100 ml of Millipore-filtered water in the case of sample a, a 10-g amount of soil was extracted with Millipore-filtered water containing soluble polyacrylic acid in the case of sample b, and a 10-g amount of soil was extracted with 100 ml of 0.9% NaCl containing the soluble polymer fraction in the case os sample c. The extraction was performed by shaking in a flatbed shaker for 16 h.

The samples were then placed in a centrifuge for 1 h with a relative centrifugal force of 1000 *g*.

The samples were then filtered through several filters. The filtration started with a 0.8-μm nylon plain filter (47 mm, Cat. No. N08SP04700 MSI) followed by a 0.45-μm nylon plain filter (47 mm, Cat. No. N04SP04700 MSI), then a 0.22-μm nylon plain filter (47 mm, Cat. No. N02SP04700 MSI), and, finally, a 0.1-μm nylon plain filter (47 mm, Cat. No. N01SP04700 MSI), all filters were obtained from Fisher Scientific (Midland, MI, U.S.A.).

The samples were then concentrated by freeze-drying to obtain the desired sensitivity.

Derivatization pyrolysis–gas chromatography

GC conditions. Instrument, Hewlett-Packard 5890 GC dual-column system; columns, (1) stainless steel, 6′ × ⅛″ I.D., packed with 0.1% SP-1000 Carbopack C and (2) 60 × 0.25 mm, 0.25 μm film tickness, capillary column DB-wax; temperatures, initial 50°C for 4 min, oven ramp 6°C/min, final 220°C for 40 min, injection 200°C, and flame ionization dectector 220°C; helium flow-rate, 16 ml/min.

Sample derivatization. The sample was prepared as explained in the *Size-exclu-*

sion chromatography section. A 250-μl aliquot of Methyl-8® [dimethylformamide (DMF) dimethyl acetal] was added. The sample was heated at 160°C for 16 h. Residual solvent was evaporated with a heat lamp under a nitrogen purge. Methanol, 0.5 ml, was added to dissolve the residue.

Sample analysis. The instrument was a CDS 120 pyrolyzer equipped with coil probe. The probe was placed in the GC interface and pyrolyzed under the following conditions: ramp, off; time, 20s; pyrolysis temperature, 700°C; interface temperature, 200°C. A 4-μl sample was placed in a quartz pyrolysis boat, the boat was placed in the CDS pyrolysis coil probe and the solvent was flashed off.

NMR analysis

Instrumentation. Instrument, IBM AF300 NMR spectrometer; spectrometer frequency, 300.132 MHz; sweep width, 5000 Hz; offset frequency, 5000 Hz; data size, 32K; acquisition time, 3.277 s; pulse width, 2.0 μs; receiver delay, 0.0 s; receiver gain, 40; apodization, 2–10 Hz[a].

Scans. Linearity (polyacrylic acid): 300–3700[b]. Soils (blank, spike): 1133[a].

Sample preparation. After the water was removed by free-drying as explained in the *Size-exclusion chromatography* section, the samples were dissolved in ^2H_2O and poured into 5-mm NMR tubes.

pH Determination. To 10 g of soil 100 ml of Millipore-filtered water was added. The samples were stirred for 10 min at a low-speed setting to avoid CO_2 absorption and the pH was determined using a pH meter.

RESULTS

Size-exclusion chromatography

In order to establish a limit of detection, the samples were analyzed after concentration. It was found that the Borden sand sample did not show any interferences with polyacrylic acid at the 0.5-ppm level. The Londo soil and the clay samples showed interferences ranging from 3 to 7 ppm. Humic acid naturally present in soils did not interfere with the analysis by SEC as shown in Fig. 1. Included in Fig. 1 are typical SEC traces of the extracted soils. Studies to determine the capacity of the soil to adsorb polyacrylic acid were conducted and they are shown in Tables I–IV. It was found that when the soil was extracted with water and the polymer was not neutralized, the Borden sand showed a greater capacity than the other soils to adsorb the polymer. When the solvent used was 0.9% NACl and the polymer was partially neutralized, the clay showed greater capacity as shown in Table III.

pH determination

The pH values of the soils were determined and the results can help explain the affinity of the polymer for the sand. The pH of the Borden sand sample (9.6) is higher than the other two soils, (Londo soil, pH 7.6; Fox Sandy Loam, pH 6.9).

---

[a] The number of scans and apodization was held constant for the blank and polyacrylic acid spiked soils.

[b] 39-ppm standard 3700 scans; 190-ppm standard, 1729 scans; 371-ppm standard, 313 scans.

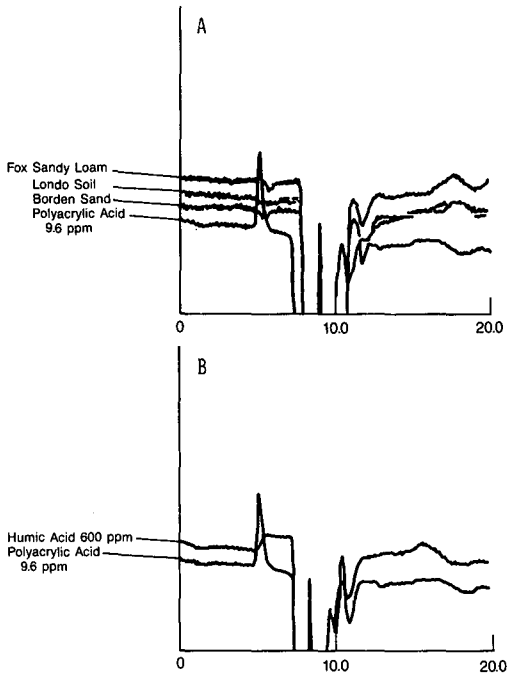

Fig. 1. SEC traces of (A) standard and soils (B) standard and humic acid. Horizontal axis represents time in minutes.

TABLE I

SOIL CAPACITY

Polymer was applied to the soil and the soil was extracted with water.

Soil type	*Polymer added (μg)*	*Recovery (%)*	*Lost (%)*	*Capacity (μg/g)*
Borden sand	400	0	100	>40
Londo soil	400	0	100	>40
Fox Sandy Loam	400	0	100	>40

TABLE II

SOIL CAPACITY OF BORDEN SAND

Polymer was applied to the soil and the soil was extracted with water.

Sample No.	*Polymer added (μg)*	*Recovery (%)*	*Lost (%)*	*Capacity (μg/g)*
1	400	0	100	> 40
2	1230	0	100	>120
3	2040	0	100	>200

TABLE III

SOIL CAPACITY

Soil type[a]	*Polymer added (μg)*	*Recovery (%)*	*Lost (%)*	*Capacity (μg/g)*
Borden sand[b]	14 000	70	30	460
Borden Sand	11 200	87	13	150
Londo soil	11 200	70	30	370
Fox Sandy Loam	11 200	24	76	850

[a] Polymer was added in 0.9% NaCl.
[b] Polymer was added in 0.7% NaCl.

Surface area

The surface areas of the three soils were determined following the BET Nitrogen Test with the following results: Borden sand, 0.3 m^2/g; Londo soil, 1.63 m^2/g; Fox Sandy Loam 8.78 m^2/g.

Derivatization pyrolysis–gas chromatography

In order to maximize the sensitivity of the method, the sample must be carefully concentrated and dried before derivatizing the polyacrylic acid. This was done by freeze-drying the extract in a 100-ml vial as explained before. The vial was washed with 5 ml of water which were then transferred to a 5-ml Reacti-vial. The sample was then evaporated to dryness by blanketing the sample with a stream of nitrogen and heating with an infrared heat lamp. Once the samples were dried, 250 μl of Methyl-8 were added and the vial was heated at 130°C for 16 h. After derivatization, the sample was again dried and the residue was redissolved in 0.5 ml of methanol. This second drying step was incorporated into the method because the derivatized polymer is not soluble in the methylating agent. A spin bar was used in the vial to aid in dissolution of the polymer. Using a 10-μl syringe the solution was then transferred to a quartz boat for pyrolysis. A quartz boat was used in favor of a platinum ribbon since the

TABLE IV

SOIL CAPACITY

Polymer was added to the water and extracted with water.

Soil type	*Polymer added (μg)*	*Recovery (%)*	*Lost (%)*	*Capacity (μg/g)*
Borden Sand	12 000	0	100	>1200
	24 300	0	100	>2430
	30 400	0	100	>3040
Londo Soil	12 000	0	100	>1200
	24 300	14	86	2100
	30 400	16	84	2540
Fox Sandy Loam	12 000	0	100	>1200
	24 300	3	97	2360
	30 400	30	70	2100

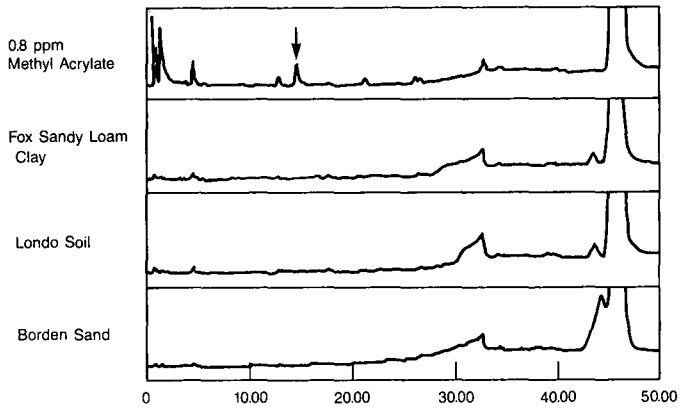

Fig. 2. Py–GC traces of an 0.8-ppm standard and soil samples using the packed column. Horizontal axis represents time in minutes.

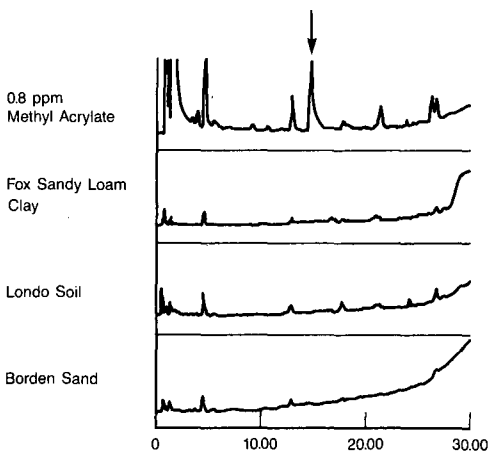

Fig. 3. Py–GC traces of an 0.8-ppm standard and soil samples using the packed column as in Fig. 2, but magnified electronically five-fold. Horizontal axis represents time in minutes.

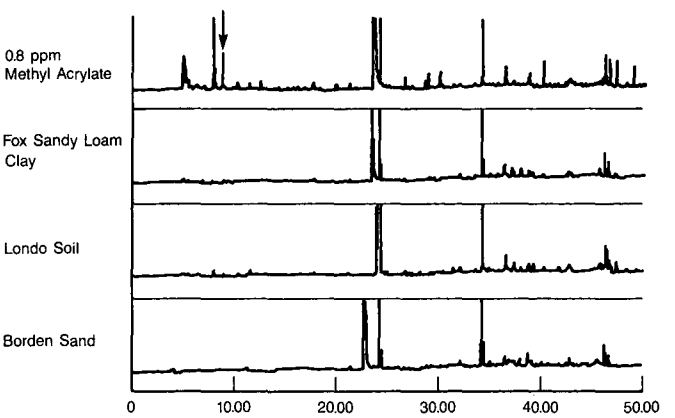

Fig. 4. Py–GC traces of an 0.8-ppm standard and soil samples using the capillary column. Horizontal axis represents time in minutes.

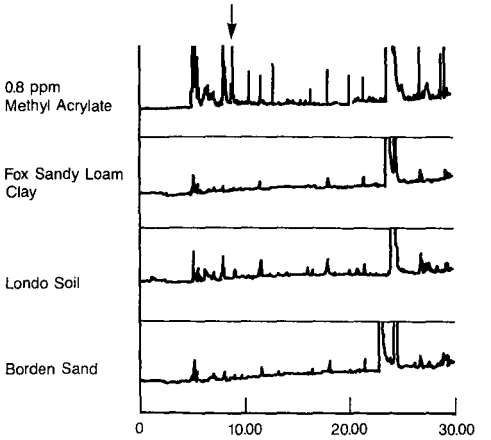

Fig. 5. Py–GC traces of an 0.8-ppm standard and soil samples using the capillary column as in Fig. 4, but magnified electronically five-fold. Horizontal axis represents time in minutes.

sample could contain salts. Rather than contaminating a ribbon with the salt, a boat was used which could be readily cleaned with acidified methanol.

The polyacrylic acid was derivatized to methylacrylate because the main pyrolysis products of the acid are carbon dioxide and water. Only a small amount of the monomer was produced under the pyrolysis conditions listed. By derivatizing the acid to methylacrylate, the main pyrolysis products are methanol and methylacrylate both

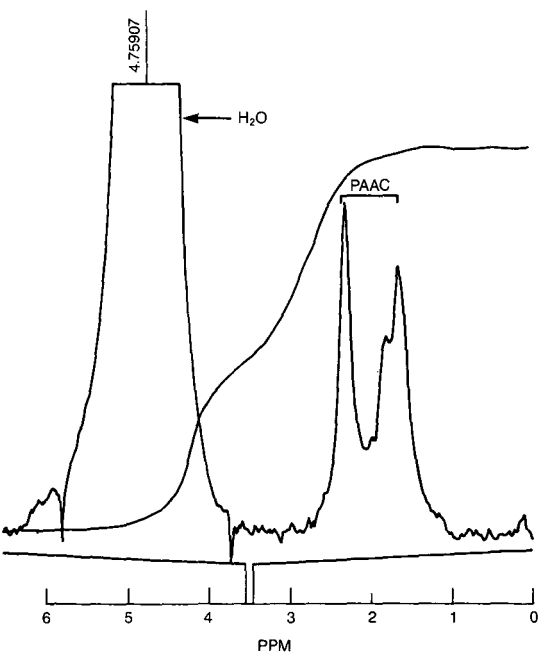

Fig. 6. NMR spectrum of 190 ppm polyacrylic acid (PAAC) in ^2H_2O.

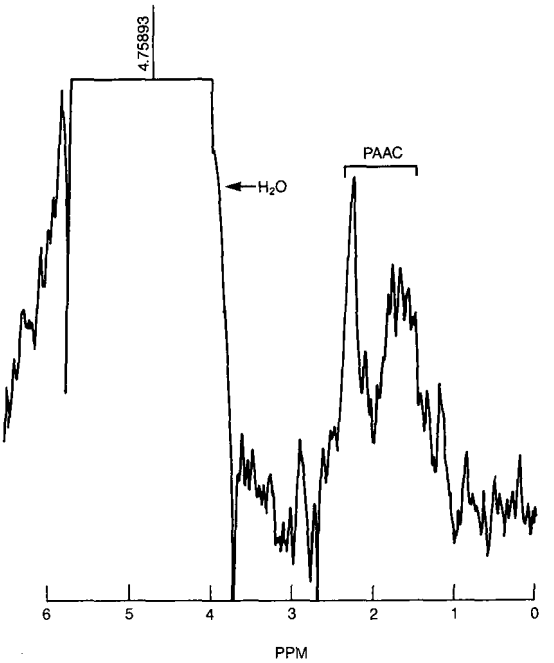

Fig. 7. NMR spectrum of 39.1 ppm polyacrylic axid (PAAC) in ^2H_2O.

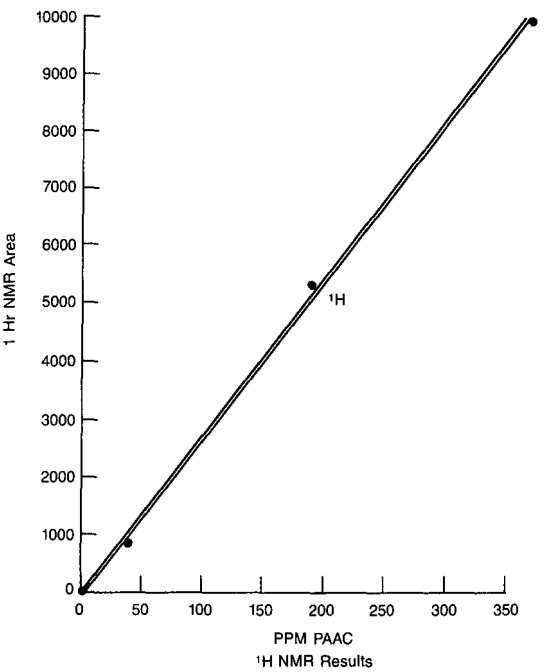

Fig. 8. Plot of the total area response for the polyacrylic acid (PAAC) backbone hydrogens *versus* PAAC concentration by NMR.

of which can be readily chromatographed and detected. The advantages of derivatizing the sample also include the fact that the pyrolysis products can be ratioed to each other, and when compared to a standard will indicate the presence of any interferences in the analysis. By using a dual-column system with columns of differing polarity or retention mechanisms, determination of the retention times of the main pyrolysis products becomes almost a definitive means of identifying the polymer present in the sample as polyacrylic acid. In Fig. 2 are shown Py-GC traces of an 0.8-ppm standard and soil samples using the packed column. In Fig. 3 are shown the same traces only magnified electronically five-fold. In Fig. 4 are shown the pyrograms of an 0.8-ppm standard and soil samples using the capillary column. In Fig. 5 the same traces are shown magnified electronically five-fold.

NMR spectroscopy

The spectra acquired for polyacrylic acid–^2H_2O solutions of 190 and 39.1 ppm are given in Figs. 6 and 7, respectively. The assignments for the polyacrylic acid backbone hydrogens and the residual hydrogens from the undeuterated water are included in the spectrum. A plot of the total area response for the polyacrylic acid backbone hydrogens versus concentration is given in Fig. 8. Although the signal-to-noise ratio in the spectrum given in Fig. 7 is not high, a reasonable estimate of the detection limit of the NMR experiment is approximately 20–40 ppm polyacrylic acid in ^2H_2O. The NMR spectrum of the polyacrylic acid standard spiked in ^2H_2O is given in Fig. 9. The area of the polyacrylic acid backbone hydrogens corresponds to approximately 128 ppm of polyacrylic acid. The spike was prepared to contain ap-

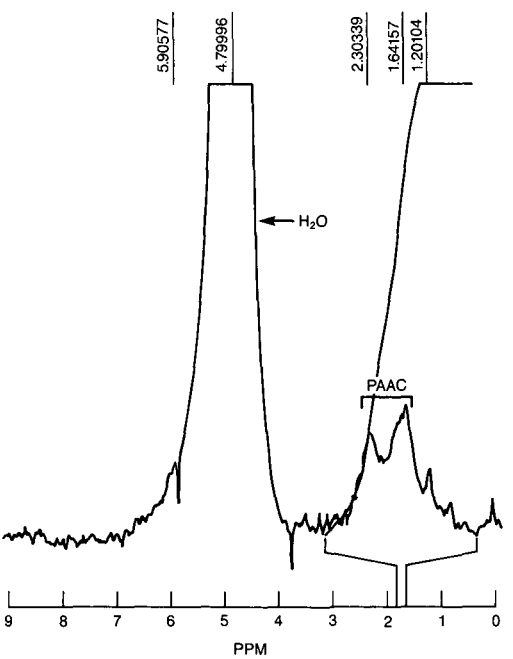

Fig. 9. NMR spectrum of the polyacrylic acid (PAAC) standard spike in ^2H_2O.

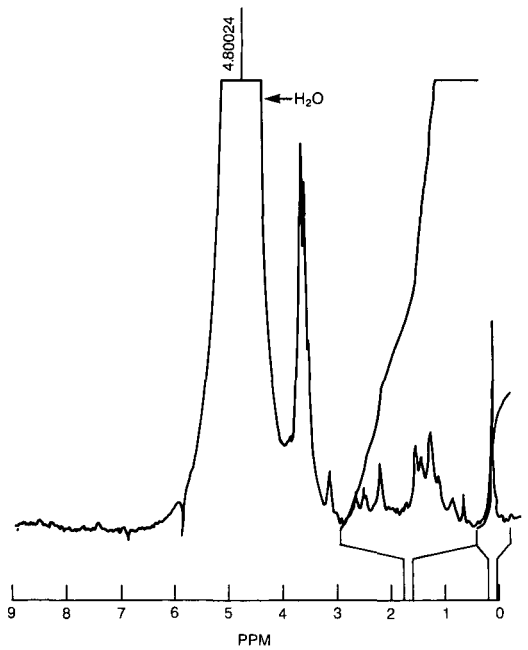

Fig. 10. NMR spectrum of a Fox Sandy Loam blank in ^2H_2O.

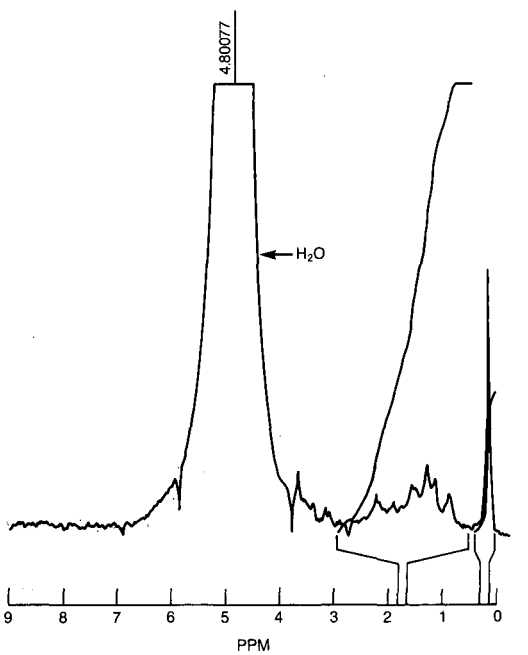

Fig. 11. NMR Spectrum of a Borden sand blank in ^2H_2O.

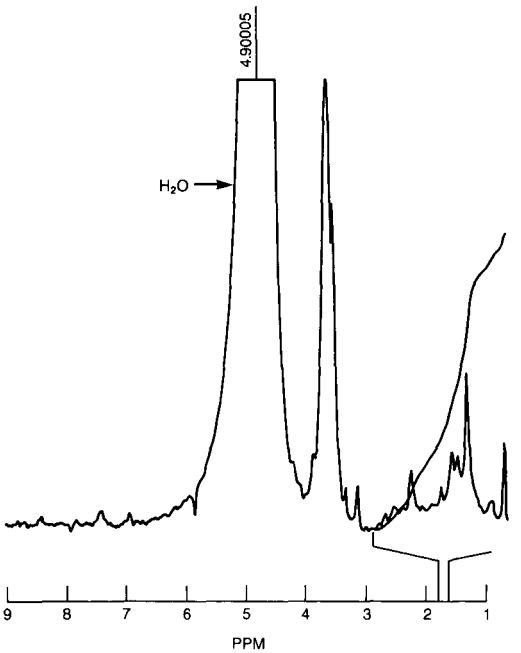

Fig. 12. NMR Spectrum of the Fox Sandy Loam soil spiked with 200 ppm polyacrilic acid in ^2H_2O.

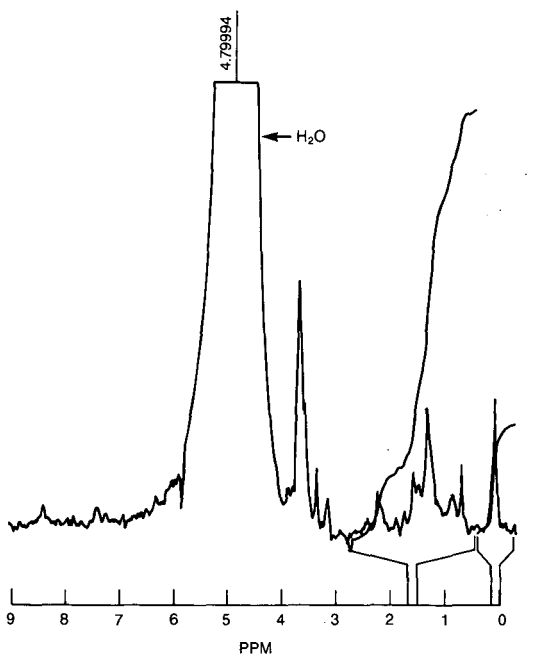

Fig. 13. NMR spectrum of the Borden sand soil spiked with 200 ppm of polyacrylic acid in ^2H_2O.

proximately 200 ppm of polyacrylic acid. The NMR result indicates a recovery of approximately 64%. The sample loss took place during the freeze-drying step and is probably due to irreversible adsorption of the polyacrylic acid to the glass of the bottle.

The hydrogen NMR spectra of the soils labeled Fox Sandy Loam and Borden sand are given in Figs. 10 and 11, respectively. There are peaks evident in the region 3–1 ppm. This is the region where the backbone hydrogens of polyacrylic acid resonate. Therefore, interferences exist in the soils which will interfere with the determination of low levels of polyacrylic acid.

The hydrogen NMR spectra for the Fox Sandy Loam and Borden sand soils spiked with 200 ppm of polyacrylic acid are given in Figs. 12 and 13, respectively Comparing these spectra with the spectra of the blank soils (Figs. 10 and 11), it is evident that very little, if any, polyacrylic acid is present in the samples. Further work is necessary to identify the components present in the soils.

DISCUSSION

The first approach was to use SEC, excluding the polymer totally to obtain a useable signal. Adsorption capacities of the soils for polyacrylic acid were obtained using this procedure. NMR spectroscopy was used as a characterization tool to verify the response obtained by SEC. Derivatization Py–GC with dual columns was then investigated. It was known that polyacrylic acids will degrade to CO_2 when heated at high temperatures for pyrolysis purposes. A derivatization procedure explained elsewhere[7] was successfully tried, and no interferences were found in any of the soils at the sub-ppm level.

The samples of soil extracts needed to be cleaned and concentrated to get the desired detection limits. The clean bottles normally used in the analytical laboratories for trace analysis were found to contain interferences in the area of elution of the polymer on the SEC system. The problem was solved by rinsing the bottles with Millipore-filtered water. Rinsing the bottles eliminated the interferences in the Borden sand sample, but the Londo soil and the Fox Sandy Loam sample still had some interferences at the 5-ppm level that were not introduced by the bottles. Humic acid naturally present in soils did not interefere with the SEC analysis. The use of batch extractions has advantages over the use of columns to study the movement of the polymer in soils. When batch extraction is used, all the intereferences that are naturally present in the soils will be present during extraction, while in the case of column studies the soil is constantly stripped of some of the components. Batch extractions monitored with SEC have been used to determine the capacity of soils which can be used to better understand the movement of polyelectrolytes through soils. As it was shown in Tables I–IV the selectivity of soils is not directly related to surface area.

Sand, which has a smaller surface area than clay (0.3 *versus* 1.63 and 8.78 m^2/g) has a greater selectivity for this type of polymers. On the other hand a decrease in particle size will increase the trapping of polymer molecules. In this case clay will perform better to stop the polymer movement. Water enhances the repulsive forces among the negatively charged carboxylic acid groups and expands the chains, increasing the hydrodynamic volume of the polymer. Salt solutions will have the opposite effect contracting the chains to their original size. The results presented in Tables

I–IV indicate that when this happens the capacity of soils to adsorb polyacrylates is enhanced when the polymer chains are at their larger volume. Concentration of the polymer under investigation is also a critical parameter, since the increase in concentration will increase the viscosity of the polymer and will affect the capacity of the soil to adsorb polyacrylates and the movement of the polymer.

CONCLUSIONS

SEC with batch extraction of the soils and NMR spectroscopy can be used to determine the capacity of soils to adsorb polyacrylates. Derivatization Py–GC with a dual-column system and a flame ionization detector or a single-column system with a mass spectrometer can be used to monitor effluents from columns or from batch extraction at the sub-ppm level.

ACKNOWLEDGEMENTS

The authors acknowledge the help and suggestions of C. G. Smith on the Py–GC part of the study and D. M. Williams in the surface area determinations.

REFERENCES

1 J. E. Martin, K. W. F. Howard and L. W. King, *Environmental Behavior of ^{14}C-Tagged Polyacrylate Polymer: Column Studies of Flow and Retardation in Sand* (*Nuclear and Chemical Waste Management*, Vol. 7), Pergamon Press, Elmsford, NY, 1987, pp. 265–271.
2 J. E. Martin, K. W. F. Howard and L. W. King, *Environmental Behavior of ^{14}C-Tagged Polyacrylate Polymer: Flow Tank Studies of Retention in Sand* (*Nuclear and Chemical Waste Management*, Vol. 7), Pergamon Press, Elmsford, NY, 1987, pp. 273–280
3 L. S. Sheldon, *Crosslinked Polyacrylate Fate Study*, Analytical and Chemical Sciences, Research Triangle Institute, Research Triangle Park, NC.
4 C. G. Smith, *J. Anal. Appl. Pyrolysis*, 15 (1989) 209–216.
5 H. G. Barth, in T. Provder (Editor), *Detection and Data Analysis in Size Exclusion Chromatography* (*ACS Symposium Series*, No. 352), American Chemical Society, Washington, DC, 1987, pp. 29–46.
6 P. L. Dubin, in P. L. Dubin (Editor), *Aqueous Size-Exclusion Chromatography* (*Journal of Chromatography Library*, Vol. 40), Elsevier, Amsterdam, 1988, Ch. 3, pp. 55–75.
7 J. L. Sharp and G. Paterson, *Analyst (London)*, 105 (1980) 517–520.

Journal of Chromatography, 513 (1990) 107–116
Elsevier Science Publishers B.V., Amsterdam

CHROM. 22 519

Solvatochromic hydrogen bond donor acidity of aqueous binary solvent mixtures for reversed-phase liquid chromatography

JUNG HAG PARK*, MYUNG DUK JANG and DONG SOO KIM
Department of Chemistry, College of Science, Yeungnam University, Gyongsan 713-749 (South Korea)
and
PETER W. CARR
Department of Chemistry, University of Minnesota, Minneapolis, MN 55455 (U.S.A.)
(First received February 1st, 1990; revised manuscript received April 26th, 1990)

ABSTRACT

Solvatochromic hydrogen bond (HB) donor acidity (α_m) values for aqueous mixtures of methanol, ethanol, isopropanol, acetonitrile and tetrahydrofuran were measured by electronic absorption spectroscopy employing bis[α-(2-pyridyl)-benzylidine-3,4-dimethylaniline]bis(cyano)iron(II) as an indicator, and compared to available literature values. The HB donor acidity of all the aqueous organic mixtures increases in a nonlinear fashion as water is added to the organic solvent. For mixtures of acetonitrile and tetrahydrofuran, which are not acidic or are only slightly acidic, with water α_m increases rapidly as a small amount of water is first added, then shows a plateau region, and finally slowly rises to the acidity value of water. In contrast, the α_m for the mixtures of methanol, ethanol and isopropanol, which are quite acidic, increase slowly as the first small amount of water is added and then increase rapidly as the mixture approaches pure water. Literature values of α_m for water-methanol mixtures, which were determined from the $E_T(30)$ values of Reichardt's betaine dye, showed a minimum in the plot of α_m *vs.* volume fraction of organic component. It was also shown that the solvophobicity parameter (S_p) of methanol– and ethanol–water mixtures can be described by a combination of the dipolarity (π_m^*) and HB donor acidity (α_m) of the mixtures.

INTRODUCTION

Retention in reversed-phase liquid chromatography (RPLC) is determined by the difference in various types of interactions which a solute can undergo in the mobile and stationary phase. According to the solvophobic theory of Horváth *et al.*[1] the stationary phase is considered to be more or less passive. It is now known that the structure and composition of the stationary phase plays an active role in the separation process and has a major effect on selectivity[2,3]. Since RPLC separations are often

0021-9673/90/$03.50

performed by employing a fixed stationary phase and examining the effect of different mobile phases to obtain optimal separation conditions, understanding the various interactions of solutes with the mobile phase is important for elucidating the retention mechanism and hence the prediction of selectivity in RPLC. There have been many studies of the effect of the mobile phase on retention. Solubility parameter theory[4,5], the interaction index[6], and statistical mechanics[7] have been applied in attempts to better understand the mechanism of retention, but none of these approaches makes quantitative predictions of retention.

Recently the $E_T(30)$ scale of mobile phase polarity[8–10] and linear solvation energy relationship (LSER) based on the Kamlet–Taft multiparameter scales[11,12] were successfully used to study retention in RPLC. Johnson *et al.*[8] have shown that plots of ln k' for a large number of solutes *vs.* the mobile phases' $E_T(30)$ solvatochromic parameters are very often more linear than are plots of ln k' *vs.* volume fraction of organic modifier. However, this approach only allows for the prediction of retention at different mobile compositions to be made, but provides no information about the relative strength of various interactions between a solute and the mobile phase, which are important in understanding the retention process. The $E_T(30)$ scale had been proposed as a single-parameter overall scale of solvent polarity, but Cheong and Carr[13] recently pointed out that there can be no global single-parameter solvent polarity scale except when the solute and solvent are incapable of forming hydrogen bonds. In contrast, LSER approaches based on multiparameter scales[11–13] seek to relate retention in a fixed mobile phase–stationary phase system to variations in the solute properties, or to variations in mobile phases' properties when the solute and stationary phase are fixed. The Kamlet–Taft multiparameter solvent scales are based on the differential evaluation of solvent dipolarity–polarizability (π^*), solvent HB donor acidity (α), and solvent hydrogen bond acceptor basicity (β)[14–17].

Kamlet and Taft and their co-workers have applied these measures of interaction strength based upon LSERs to about 600 processes[18], including a large number of systems of immediate relevance to chromatography, such as Rohrschneider's gas–liquid partition coefficients[19], Snyder's solvent strength scales for normal- and reversed-phase liquid chromatography[20,21], and retention in RPLC[11,12,22]. In this work we will adopt the LSER formalism and report, in particular, the measurement of Kamlet–Taft hydrogen bond (HB) donor acidity (α_m) values for RPLC mobile phases.

THEORY

The α parameter can be obtained from several different methodologies such as ^{13}C NMR, ^{19}F NMR, electronic absorption spectroscopy and reaction rate measurements[17], and is most conveniently obtained from measurements of the frequency of maximum absorption of carefully selected indicators. The LSER formalism[17] indicates that when solute-to-solvent hydrogen bonding effects are excluded, as when solutes or indicators are non-protic and when only solvents with similar polarizability characteristic are considered, a spectroscopic property (*XYZ*, *e.g.*, the frequency of maximum absorption) of a solute in various solvents will be well correlated through an equation of the form:

$$XYZ = XYZ_0 + s\pi^* + a\alpha \quad (1)$$

where XYZ_0 is the intercept of the regression equation, s and a are regression coefficients for the solvatochromic parameters (π^* and α). Inclusion of the dipolarity–polarizability parameter (π^*) comes about naturally since any compound which is able to donate or accept hydrogen bonding will also undergo dipolar interactions. When the value of π^* is available for a given solvent, the α parameter can be estimated by the following equation:

$$\alpha = (XYZ - XYZ_0 - s\pi^*)/a \tag{2}$$

To minimize possible errors, due to self-association of strong HB donors or solvents and to errors in the π^* values, Kamlet *et al.*[17] suggested that properties which meet the following criteria be chosen for formulating an α scale: (a) the properties should involve sufficiently strong HB acceptor that competitive solvent self-association should not materially influence the enhanced solvatochromic effects due to hydrogen bonding, (b) ratios of the a/s terms in eqn. 1 should not be too low (preferably > 1.0) so that uncertainties in the π^* values, which are necessarily less reliable for the HB donors than for the non-HB donor solvents, should not introduce unacceptable uncertainties in the α values.

To date there have been only a few studies on HB donor acidities of aqueous–organic mixtures[8,23,24]. Krygowski *et al.*[23] and Johnson *et al.*[8] reported measurement of $E_T(30)$ values, using Reichardt's betaine dye [4-(2,4,6-triphenylpyridinium)-2,6-diphenylphenoxide], for aqueous mixtures of a number of organic solvents including methanol, acetonitrile, tetrahydrofuran, isopropanol, etc. from 0% to 100% organic solvent. However, it has been shown that $E_T(30)$ values can be described by a combination of the Kamlet–Taft dipolarity parameter (π^*) and the related HB donor acidity scale (α) as follows[17]:

$$E_T(30) = 29.35 + 16.3\pi^* + 15.8\alpha \text{ (kcal/mol)} \tag{3}$$
$$n = 19,\ r = 0.993,\ \text{S.D.} = 0.89,\ (a/s = 0.97)$$

This equation holds for 19 solvents including aliphatic alcohols and other aliphatic HB donor solvents.

Recently, Cheong and Carr[24] reported measurement of Kamlet–Taft π^*_m values for a number of aqueous organic mixtures. The subscript m indicates that the values are for mixtures. They also estimated the α_m values of the same mixtures from Dorsey and Johnson's $E_T(30)$ values[10] and their π^*_m values by assuming that eqns. 2 and 3 for pure solvents could be applied to a mixture. Even though there are a number of serious approximations and assumptions in using pure solvent regression results to interpolate data on mixed solvents, the trends in the α_m values with volume fraction of organic cosolvent (φ_0) were in good agreement with chemical intuition. For example, they observed a rapid rise in α_m for tetrahydrofuran and acetonitrile mixtures upon addition of a small amount of water, a plateau region, and a final rise to the value of α in water. However, a peculiar result was observed for the α_m values in water–methanol mixtures, *i.e.*, they observed a minimum in the plot of α_m *vs.* φ_0. This is at variance with the chemical intuition. The HB acidity of the mixture is expected to increase as the more acidic solvent (water) is added. Cheong and Carr[24] suspected the existence of a specific solvation effect on Reichardt's betaine dye and concluded there must be an error in the α values of this mixture.

We believe it is likely that this unusual behavior of water–methanol mixture is due in part to the propagation of errors in the π_m^* values since the a/s ratio in eqn. 3 is not large and thus a small error in the π_m^* value might lead to a greater error in the estimated α_m value. In the present work errors of this kind were reduced by use of the wavenumber of the maximum absorption ($\bar{\nu}_{max}$) of bis[α-(2-pyridyl) benzylidine-3,4-dimethylaniline]bis(cyano)iron(II) (abbreviated Fe complex)[25] in the aqueous–organic mixtures and by utilizing eqn. 2 and the following solvatochromic regression equation for the $\bar{\nu}_{max}$ of this indicator in 13 pure solvents, where the ratio a/s is 1.59:

$$\bar{\nu}_{max} = 14.02 + 0.98\pi^* + 1.56\alpha \text{ (kK)}^a \quad (4)$$
$$n = 13,\ r = 0.999,\ \text{S.D.} = 0.04$$

The quality of the fit of $\bar{\nu}_{max}$ for the pure solvents is also better than that with $E_T(30)$ and thus the use of this relationship will minimize errors in the estimated α_m values due to the propagation of errors in the π_m^* values.

EXPERIMENTAL

All solvents used in this work were HPLC grade and were used without further purification. The solvent mixtures were prepared by mixing a known volume of each liquid. The indicator, Fe complex, was prepared and recrystallized twice using a procedure given in the literature[25]. Dilute solutions (typically 1 m*M* or less) were prepared in the solvent mixtures. The indicators for measurement of π_m^* for water–ethanol mixtures are 4-nitroanisole (1), 4-ethylnitrobenzene (4), N-methyl-2-nitroaniline (32), and 2-nitroanisole (45) were obtained commercially and recrystallized once before use. The number in parenthesis after each indicator refers to the Kamlet–Taft indicator designation[17]. All spectroscopic measurements were carried out by following the standard procedure[26] and repeated at least five times for each solution. A Hitachi Model 320 double-beam UV–VIS spectrophotometer was used to make measurements to ±0.2 nm. In order to check for any concentration dependence, measurements were repeated at five different concentrations ranging from 0.05 to 1 m*M* and in all the cases standard deviations in the wavelength of maximum absorption was found to be less than 0.3 nm and did not vary with concentration. Consequently the solvent mixtures were examined at a single solute concentration chosen within the above range. The agreement between our measurements of $\bar{\nu}_{max}$ of the Fe complex in 13 pure solvents and those in the literature[25] was within 0.1 kK except in water where the difference was about 0.3 kK. This led us to measure $\bar{\nu}_{max}$ for water using two different spectrophotometers over a period of two months, and our value of 17.09 kK was not changed. Thus in the subsequent work on solvent mixtures we chose to use our value.

RESULTS AND DISCUSSION

The α_m values for aqueous mixtures of methanol, isopropanol, acetonitrile and tetrahydrofuran at various organic compositions were computed as follows from literature values[24] of π_m^* and our measured $\bar{\nu}_{max}$ values for the Fe complex of the solvent mixtures:

$$\alpha_m = (\bar{\nu}_{max} - 14.02 - 0.98\pi_m^*)/1.56 \quad (5)$$

[a] kK = kiloKayser, *i.e.*, 1000 wavenumbers.

TABLE I

THE VALUES OF α_m FOR WATER–ORGANIC COSOLVENT MIXTURES

The α_m values based on $E_T(30)$ are in parentheses.

φ_0	*Methanol*	*Isopropanol*	*Acetonitrile*	*Tetrahydrofuran*
0.1	1.20(1.01)	1.16(0.92)	1.16(1.01)	1.11(0.89)
0.2	1.17(0.93)	1.02(0.76)	1.08(0.94)	0.98(0.72)
0.3	1.15(0.92)	0.90(0.70)	1.01(0.90)	0.90(0.62)
0.4	1.10(0.88)	0.88(0.67)	0.95(0.90)	0.86(0.60)
0.5	1.07(0.86)	0.89(0.69)	0.90(0.89)	0.83(0.58)
0.6	1.04(0.87)	0.89(0.69)	0.90(0.88)	0.78(0.57)
0.7	1.02(0.91)	0.88(0.71)	0.88(0.89)	0.74(0.56)
0.8	1.02(0.96)	0.86(0.70)	0.82(0.85)	0.68(0.53)
0.9	1.02(1.00)	0.81(0.69)	0.71(0.81)	0.58(0.46)
1.0	1.02(1.09)	0.78(0.74)	0.32(0.33)	0.04(−0.09)

Based on eqn. 5 an error of ± 0.03 in π_m^* gives an error of ± 0.006 in α_m. Our values for α_m are given in Table I along with the values given by Cheong and Carr[24] in parentheses, and are plotted *vs.* φ_0 in Fig. 1.

As can be seen in Fig. 1, the α_m values obtained from the Fe complex are generally greater than those from the $E_T(30)$ values of betaine dye but the trends in the

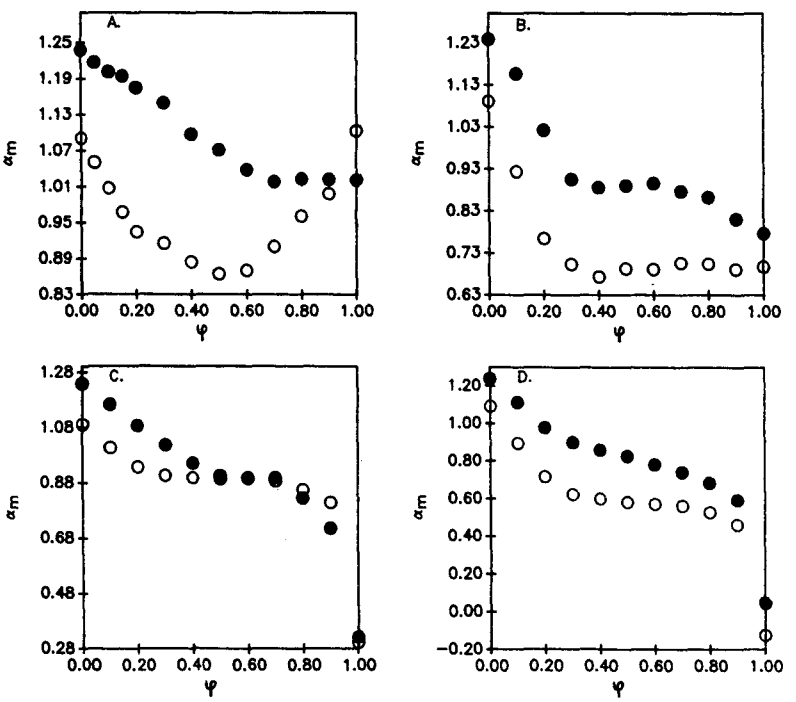

Fig. 1. Plots of α_m *vs.* volume fraction of organic cosolvents (φ_0). A, Methanol; B, isopropanol; C, acetonitrile; D, tetrahydrofuran. ○ = $E_T(30)$; ● = this work.

changes of α_m values with φ_0 are very similar in all the mixtures except the methanol mixtures. Differences in α_m values determined by using two different indicators are entirely possible, particularly in solvent mixtures. Although the two indicators sense via their solvatochromic shifts the same intermolecular interactions exerted by the solvent, the sensitivity of the two indicators to the effects can be different. It should, however, be noted that there is no distinct minimum in the plot for methanol mixtures when the α_m values are obtained with the Fe complex, while the same plot for α_m values obtained via the $E_T(30)$ values has a distinct minimum. Since both the betaine dye and the Fe complex are sensitive to their environment as a consequence of a large change in dipole moment upon excitation and are also very strongly dependent on the HB donor acidity of the solvent, as indicated by the *s* and *a* coefficients in both eqns. 3 and 4 for the pure solvents, variations in the E_T values (kcal) with φ_0 for the mixtures are expected to be very similar for the two indicators. Fig. 2 shows plots of the E_T values for the Fe complex *vs.* those for Reichardt's betaine dye [$E_T(30)$]. All the plots show good linear relatioships except the methanol mixtures, where a convex curve is evident. Non-linearity in the plot for the methanol mixtures is an indication that the cybotactic region about the two indicators have different compositions than the bulk mixtures, resulting in different effects on solvatochromic shifts of the two indicators.

In order to see if the behavior of betaine is unique to water–methanol mixtures, we measured α_m for water–ethanol mixtures with the Fe complex. We also measured the π_m^* values for ethanol–water mixtures with four indicators and determined two sets

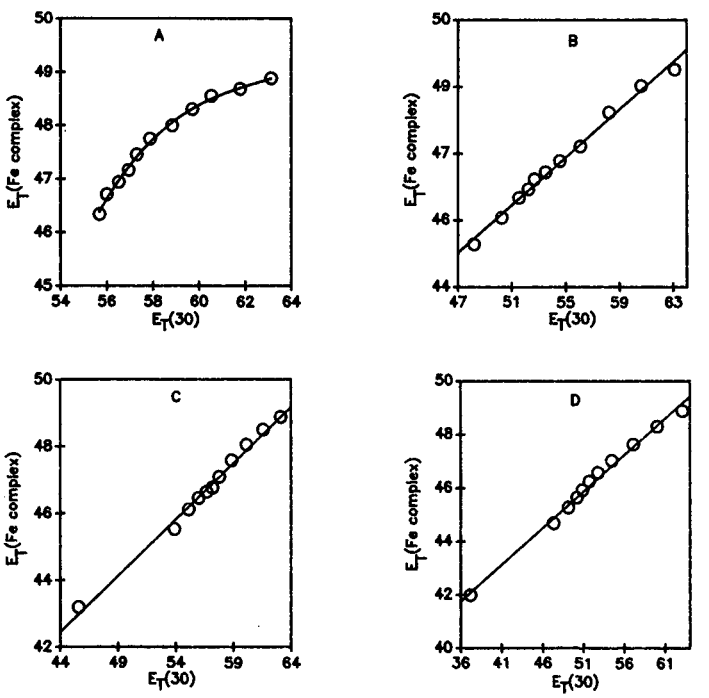

Fig. 2. Plots of E_T (kcal) for the Fe complex *vs.* $E_T(30)$ for the betaine. A, Methanol; B, isopropanol; C, acetonitrile; D, tetrahydrofuran.

TABLE II

THE VALUES OF π_m^* AND α_m FOR ETHANOL–WATER MIXTURES

φ_0	π_m^{*a}	$\alpha_m{}^b$	$\alpha_m{}^c$
0.0	1.16(0.17)	1.24	1.10
0.1	1.18(0.14)	1.17	0.99
0.2	1.18(0.14)	1.11	0.87
0.3	1.17(0.14)	1.05	0.75
0.4	1.08(0.12)	0.98	0.74
0.5	1.01(0.11)	0.94	0.73
0.6	0.94(0.10)	0.91	0.75
0.7	0.87(0.09)	0.90	0.76
0.8	0.79(0.09)	0.90	0.80
0.9	0.67(0.04)	0.91	0.86
1.0	0.54(0.06)	0.89	0.91

[a] The π_m^* values are the average based on four indicators. The figures in parentheses indicates standard deviation.

[b] The α_m values calculated from $\bar{\nu}_{max}$ values of the Fe complex using the corresponding solvatochromic equation.

[c] The α_m values calculated similarly from $E_T(30)$ values from literature[27].

of α_m values based on literature data[27] for $E_T(30)$ and our measurements of $\bar{\nu}_{max}$ for the Fe complex. The values are given in Table II and plotted *vs.* φ_0 in Fig. 3. There is a minimum in the plot of α_m values based on $E_T(30)$ while there is no minimum based on the Fe complex. We also note that the differences between the two sets of α_m values are smaller than those for the methanol mixtures.

Cheong and Carr[24] stated that within the framework of the solvatochromic LSER model of retention in RPLC the mobile phase HB acidity must increase as water is added and thus there should be no minimum in the plot of α_m *vs.* φ_0. Our results are in agreement with their conclusion and thus we believe that our α_m values are more reliable than those based on $E_T(30)$. The values of α_m calculated from $\bar{\nu}_{max}$ of the Fe

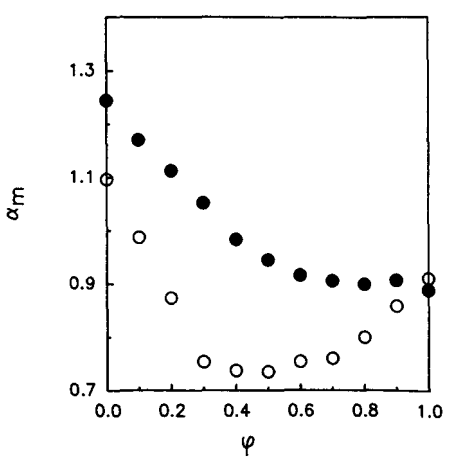

Fig. 3. Plots of α_m *vs.* volume fraction of ethanol. ○ = $E_T(30)$; ● = this work.

complex are 1.24, 1.02, 0.91, 0.78, 0.32 and 0.04 for water, methanol, ethanol, isopropanol, acetonitrile and tetrahydrofuran, respectively. These should be compared to the literature values[28] of 1.17, 0.93, 0.83, 0.76, 0.19 and 0.00. Recent work of Taft[29] indicates that α values determined by different methods have a variability of ± 0.10 units. Our values of α for these pure liquids are well within this range. In view of the fact that RPLC separation is more often applied to uncharged compounds, the HB donor acidity values measured via the uncharged Fe complex are expected to represent the HB acidity toward the solutes in the RPLC mobile phases in a more realistic fashion and to be more useful than those via a charged betaine.

The solvophobic strength of the mobile phases in RPLC has been of great interest to liquid chromatographers[1]. Recently, Abraham *et al.*[30] proposed a new measure of a solvent's solvophobic effect (S_p) for pure liquids and for aqueous mixtures based on the Gibbs free energies of transfer of inert solutes from water to the second liquid. Following Horváth's interpretation of hydrophobic interactions that they originate in the net repulsion between water and the non-polar stationary phase and the non-polar moiety of the solute, we expect that the S_p should be well correlated with the dipolarity (π_m^*) and HB acidity (α_m) and basicity (β_m) of the mobile phases. Thus we regressed S_p values for the methanol and ethanol mixturus against π_m^*, α_m and β_m. The β_m values for the mixtures are from Krygowski *et al.*[23]. The values of S_p for other aqueous–organic mixtures of interest to RPLC are not available. Based on previous experience, we have found that it is important to build up the regression in a stepwise fashion in order to avoid addition of unnecessary parameters. For S_p values at nine different volume fractions of organic cosolvent we obtain:

For methanol mixtures,

$$S_p = -0.77(\pm 0.17) + 1.43(\pm 0.17)\pi_m^* \quad (6)$$
$$r = 0.941, \text{ S.D.} = 0.10$$

For ethanol mixtures,

$$S_p = -0.88(\pm 0.18) + 1.40(\pm 0.18)\pi_m^* \quad (7)$$
$$r = 0.947, \text{ S.D.} = 0.09$$

RPLC mobile phases contain water, and water is very strong HB donor (see Table II). Thus the HB acidity parameter for the mobile phases was included in the regression equation:

For methanol mixtures,

$$S_p = -1.44(\pm 0.08) + 1.22(\pm 0.06)\pi_m^* + 0.81(\pm 0.12)\alpha_m \quad (8)$$
$$r = 0.998, \text{ S.D.} = 0.02$$

For ethanol mixtures,

$$S_p = -1.72(\pm 0.07) + 0.67(\pm 0.06)\pi_m^* + 1.58(\pm 0.12)\alpha_m \quad (9)$$
$$r = 0.998, \text{ S.D.} = 0.02$$

Incorporation of HB acidity obviously improves the quality of the fit very consider-

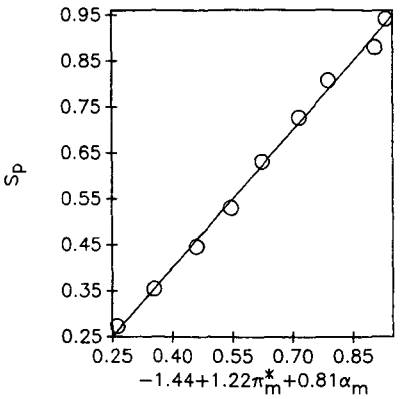

Fig. 4. Plot of experimental S_p *vs.* calculated S_p for water–methanol mixtures. Results calculated from eqn. 8.

ably. The Ehrenson test[31] indicates that the α_m parameter is significant at the 99.9% confidence level. Since methanol and ethanol are much more basic in HB interactions than water, it seems necessary to include the HB basicity of the mixtures in the regression equation. The three-parameter equations so obtained are:

For methanol mixtures,

$$S_p = -1.42(\pm 0.47) + 1.21(\pm 0.08)\pi^*_m + 0.79(\pm 0.32)\alpha_m - 0.01(\pm 0.26)\beta_m \quad (10)$$
$$r = 0.998, \text{ S.D.} = 0.02$$

For ethanol mixtures,

$$S_p = -1.68(\pm 0.26) + 0.67(\pm 0.06)\pi^*_m + 1.55(\pm 0.19)\alpha_m - 0.02(\pm 0.14)\beta_m \quad (11)$$
$$r = 0.999, \text{ S.D.} = 0.02$$

We find there is no improvement in the goodness of either fit and the b coefficients are very small (statistically zero). The Ehrenson test also shows that the β_m parameter is not significant. The quality of the fit for methanol mixtures based on eqn. 8 is demonstrated in Fig. 4 as an example. Based on the above regression results one can say that the solvophobic property of methanol and ethanol mixtures with water is a combination of the dipolarity and HB acidity of the mobile phases themselves. As described previously[18], transfer from one solvent to another should involve the difference in two cavity terms. Since no cavity formation parameter, such as Hildebrand solubility parameter (δ_H), was included in our model of S_p we believe that it is incomplete. Nonetheless rather good correlations were obtained most likely becaue δ_H covaries with π^* and α. Retention in RPLC involves transfer of the solute between the mobile and stationary phases. Thus, when regressions of retention in RPLC *vs.* mobile phase parameters include S_p, a parameter representing the cavity formation term should also be included. Work is in progress to correlate RPLC retention with the solvatochromic mobile phase properties.

ACKNOWLEDGEMENT

This work was supported by a grant from the Ministry of Education of Korea (1989).

REFERENCES

1 Cs. Horváth, W. Melander and I. Molnár, *J. Chromatogr.*, 125 (1976) 129–156.
2 R. K. Gilpin, *Anal. Chem.*, 57 (1985) 1465A–1474A.
3 K. B. Sentell and J. G. Dorsey, *J. Chromatogr.*, 461 (1989) 193–207.
4 B. L. Karger, L. R. Snyder and C. Eon, *Anal. Chem.*, 50 (1978) 2126–2136.
5 P. J. Schoenmakers, H. A. H. Billet and L. de Galan, *Chromatographia*, 15 (1982) 205–214.
6 P. Jandera, H. Colin and G. Guiochon, *Anal. Chem.*, 54 (1982) 435–441.
7 D. E. Martire and R. E. Bohem, *J. Phys. Chem.*, 87 (1983) 1045–1062.
8 B. P. Johnson, M. G. Khaledi and J. G. Dorsey, *Anal. Chem.*, 58 (1986) 2354–2365.
9 B. P. Johnson, M. G. Khaledi and J. G. Dorsey, *J. Chromatogr.*, 384 (1987) 221–230.
10 J. G. Dorsey and B. P. Johnson, *J. Liq. Chromatogr.*, 10 (1987) 2695–2706.
11 P. C. Sadek, P. W. Carr, R. M. Doherty, M. J. Kamlet, R. W. Taft and M. H. Abraham, *Anal. Chem.*, 57 (1985) 2971.
12 P. W. Carr, R. M. Doherty, M. J. Kamlet, R. W. Taft, W. Melander and Cs. Horváth, *Anal. Chem.*, 58 (1986) 2674.
13 W. J. Cheong and P. W. Carr, *Anal. Chem.*, 61 (1989) 1524–1529.
14 M. J. Kamlet, J. L. M. Abboud and R. W. Taft, *J. Am. Chem. Soc.*, 99 (1977) 6027.
15 M. J. Kamlet and R. W. Taft, *J. Am. Chem. Soc.*, 98 (1976) 377.
16 R. W. Taft and M. J. Kamlet, *J. Am. Chem. Soc.*, 98 (1976) 2886.
17 M. J. Kamlet, J. L. M. Abboud and R. W. Taft, *Prog. Phys. Org. Chem.*, 13 (1981) 485.
18 R. W. Taft, J. L. M. Abboud, M. J. Kamlet and M. H. Abraham, *J. Solution Chem.*, 14 (1985) 153.
19 M. J. Kamlet, R. W. Taft, P. W. Carr and M. H. Abraham, *J. Chem. Soc., Faraday Trans. 1*, 78 (1982) 1689.
20 J. H. Park and P. W. Carr, *J. Chromatogr.*, 465 (1989) 123–136.
21 S. C. Rutan, P. W. Carr, W. J. Cheong, J. H. Park and L. R. Snyder, *J. Chromatogr.*, 463 (1989) 21–37.
22 J. H. Park, P. W. Carr, M. H. Abraham, R. W. Taft, R. M. Doherty and M. J. Kamlet, *Chromatographia*, 25 (1988) 373.
23 T. M. Krygowski, P. K. Wrona and U. Zielkowska, *Tetrahedron*, 41 (1985) 4519–4527.
24 W. J. Cheong and P. W. Carr, *Anal. Chem.*, 60 (1988) 820–826.
25 J. Burgess, *Spectrochim. Acta*, 26A (1970) 1957–1962.
26 J. E. Brady and P. W. Carr, *J. Phys. Chem.*, 89 (1985) 1813.
27 C. Reichardt and K. Dimroth, *Top. Curr. Chem.*, 11 (1963) 1–73.
28 M. J. Kamlet, J. L. M. Abboud, M. H. Abraham and R. W. Taft, *J. Org. Chem.*, 48 (1983) 2877–2887.
29 R. W. Taft, unpublished results, July 1987.
30 M. H. Abraham, P. L. Grellier and R. A. McGill, *J. Chem. Soc., Perkin Trans. 2*, (1988) 339–345.
31 S. Ehrenson, *J. Org. Chem.*, 44 (1979) 1793.

Journal of Chromatography, 513 (1990) 117–135
Elsevier Science Publishers B.V., Amsterdam

CHROM. 22 492

Effect of temperature and organic modifier on the isocratic retention characteristics of nitrated polycyclic aromatic hydrocarbons on a reversed-phase octadecylsilane column

ALBERT ROBBAT, Jr.* and TYNG-YUN LIU

Chemistry Department, Trace Analytical Measurement Laboratory, Tufts University, Medford, MA 02155 (U.S.A.)

(First received January 30th, 1990; revised manuscript received April 3rd, 1990)

ABSTRACT

Nitrated polycyclic aromatic hydrocarbon (nitro-PAH) retention behavior was evaluated on a reversed-phase polymeric octadecylsilane column under isocratic conditions as a function of organic modifier and temperature. Several conclusions can be drawn from the retention and organic modifier study (*viz.*, methanol and acetonitrile–water). First, the logarithm of the capacity factor (log k') was linearly dependent on organic–water volume fraction (φ). Second, nitro-PAH k' values increased with decrease in organic modifier concentration. Third, the slopes of log k' *vs.* φ plots were solvent-dependent. Larger slope values were found for nitro-PAHs in methanol–water than in acetonitrile–water mixtures for a particular compound. Fourth, slope values were dependent on the molecular structure of individual nitro-PAHs.

Nitro-PAH retention times decreased with increase in column temperature. A linear dependence of log k' on the reciprocal of the absolute column temperature, the Van 't Hoff plot, was observed for both organic modifiers over the temperature range studied. The standard enthalpic change (ΔH^0) for nitro-PAH transfer from the mobile to the stationary phase was determined. ΔH^0 was dependent on organic modifier type and composition as well as solute structure. The enthalpy–entropy compensation effect was evaluated by plotting log k' *vs.* $-\Delta H^0$ and used to interpret nitro-PAH retention mechanisms. A compensation effect was found for some mononitrated PAHs for both organic modifiers. The compensation temperatures were within the accepted range described for reversed-phase high-performance liquid chromatography systems.

INTRODUCTION

Reversed-phase high-performance liquid chromatography (HPLC) retention and thus, solute selectivity, is influenced by several chemical (*e.g.*, type and concentration of organic modifier) and physical factors (*e.g.*, column temperature

0021-9673/90/$03.50

and/or stationary phase chain length, density, surface area, pore volume, monomeric/polymeric coatings). The retention process in reversed-phase HPLC is thought to be primarily controlled by solute interactions within the mobile phase[1–3]. Most research has focused on understanding the influence of mobile phase composition on retention. Studies have shown that variations in solvent composition (*i.e.*, water with one or more organic solvents) can produce dramatic retention differences[4–7]. Stationary phase studies are limited because details of the bonded-phase synthesis and silica substrates are not readily available. In addition to mobile–stationary phase effects on retention, changes in column temperature may alter retention characteristics as well[8–11].

In this investigation, the isocratic reversed-phase nitrated polycyclic aromatic hydrocarbon (nitro-PAH) retention behavior was studied as a function of mobile phase composition (acetonitrile–water and methanol–water) and column temperature (35–65°C) on a polymeric octadecylsilane column. For each organic modifier, the dependence of the logarithm of the capacity factor at a given volume fraction ($\log k'$) on the volume faction of organic modifier in the organic solvent–water mixture (φ) was evaluated. The slope, S, for $\log k'$ *vs.* φ plots was discussed in terms of solute type and organic modifier. Van 't Hoff plots, $\log k'$ *vs.* $1/T$ (T = temperature), were used to determine the effect of column temperature on nitro-PAH retention. Based on these results, the standard enthalpic change (ΔH^0) for nitro-PAH transfer from the mobile to the stationary phases was evaluated. An extra-thermodynamic approach, based on enthalpy–entropy compensation[12], was used to further define the nitro-PAH retention process.

EXPERIMENTAL

Reversed-phase HPLC separations were achieved using a Hewlett-Packard 1090M liquid chromatography system (Hewlett-Packard, Palo Alto, CA, U.S.A.) equipped with a DR5 binary solvent system, diode-array detector (standard flow cell), and temperature-controlled autosampler and column compartments. A Hewlett-Packard HPLC ChemStation was used to control the HPLC experiments, record and evaluate chromatograms and spectra. Sample injections were made using the autosampler and autoinjector system. A 25 cm × 2.1 mm, 5 μm particle size reversed-phase C_{18} column (Alltech, Deerfield, IL, U.S.A.) was used. A Rheodyne 3 mm × 0.5 μm column inlet filter was incorporated to protect the analytical column.

HPLC-grade acetontitrile and methanol (Fisher Scientific, Medford, MA, U.S.A.) were used as received. Water was purified by a Milli-Q water purification system (Millipore, Milford, MA, U.S.A.). All solvents were filtered through a 0.45-μm nylon-66 filter (Rainin, Woburn, MA, U.S.A.), ultrasonicated and vacuum degassed prior to use. Helium sparging was performed throughout the HPLC experiment. The mobile phase consisted of 50, 60 and 70% (v/v) of acetonitrile or methanol in water at flow-rate of 0.5 ml/min. HPLC experiments were performed at column temperatures of 35, 45, 55 and 65°C for each mobile phase composition. 2% Sodium dichromate in water was used to determine the elution time for the unretained solute for each mobile phase and temperature.

Sources of nitro-PAHs have been identified elsewhere[13]. Nitro-PAHs were used without further purification. Standard solutions were prepared by dissolving ap-

proximately 1 mg of nitro-PAH in 1 ml of acetonitrile or methanol. Samples were stored in the dark and refrigerated. After the column was equilibrated with solvent and the column temperature stabilized, 1 μl of a nitro-PAH solution mixture was injected. To reduce experimental time, multicomponent standard solutions were prepared. Identification of each compound peak was made by comparing HPLC retention times and UV absorption spectra with those of individual standards.

RESULTS AND DISCUSSION

Nitro-PAH retention as a function of mobile phase compostion

The intent of this study was to evaluate nitro-PAH isocratic reversed-phase HPLC retention characteristics, on a polymeric octadecylsilane column (250 × 2.1 mm, 5 μm particle size), at various acetonitrile–water and methanol–water mobile phase compositions and temperatures. Shown in Table I are nitro-PAHs and their corresponding compound numbers. Tables II–V illustrate nitro-PAH retention behavior, measured by log k', as a function of φ (50:50, 60:40 and 70:30, v/v) and T (35–65°C). Cross-comparison of acetonitrile and methanol log k' values at the same volume fraction and temperature revealed two readily apparent observations. First, nitro-PAH elution order was markedly different between the two organic modifiers. Second, nitro-PAHs were retained in the column much longer by methanol–water than by acetonitrile–water mixtures. For instance, 1-nitropyrene eluted at 22 min with acetonitrile–water (50:50) (35°C). The same compound eluted after 1.5 h with methanol–water (50:50) (35°C). Data for compounds eluting after 1.5 h are not included in this study. Retention time reproducibility was monitored over a nine-month time period with data incorporated in relevant tables.

The dependence of nitro-PAH retention on mobile phase composition was evaluated by plotting log k' *vs.* φ at constant column temperature

TABLE I

IDENTIFICATION OF NITRO-PAHs

No.	*Compound*	*No.*	*Compound*
1	5-Nitroquinoline	18	3-Nitro-9-fluorenone
2	6-Nitroquinoline	19	1-Nitro-2-methylnaphthalene
3	5-Nitro-6-methylquinoline	20	2,7-Dinitrofluorene
4	8-Nitroquinoline	21	3-Nitrobiphenyl
5	1,8-Dinitronaphthalene	22	2,2′-Dinitrobibenzyl
6	1,3,6,8-Tetranitronaphthalene	23	4-Nitrobiphenyl
7	1,5-Dinitronaphthalene	24	9-Nitrophenanthrene
8	1,4-Dinitronaphthalene	25	2-Nitrofluorene
9	1,3-Dinitronaphthalene	26	9,10-Dinitroanthracene
10	3-Nitrodibenzofuran	27	3-Nitrophenanthrene
11	2,4,7-Trinitro-9-fluorenone	28	9-Nitroanthracene
12	1-Nitronaphthalene	29	3-Nitrofluoranthene
13	2-Nitro-9-fluorenone	30	1-Nitropyrene
14	2,7-Dinitro-9-fluorenone	31	1-Methyl-10-nitroanthracene
15	2-Nitronaphthalene	32	6-Nitrochrysene
16	2,6-Dinitro-9-fluorenone	33	3-Nitroperylene
17	2-Nitrobiphenyl	34	6-Nitrobenzo[*a*]pyrene

TABLE II

DEPENDENCE OF log k' ON φ AT 35°C

No.	*Acetonitrile–water*						No.	*Methanol–water*					
	φ(%)			*Intercept*	*S(error)*	*r*		*φ(%)*			*Intercept*	*S(error)*	*r*
	50	*60*	*70*					*50*	*60*	*70*			
1	0.294	0.151	−0.004	1.04	1.49(0.04)	−0.999	4	0.620	0.325	0.076	1.97	2.72(0.13)	−0.999
2	0.354	0.170	0.024	1.17	1.65(0.11)	−0.998	2	0.662	0.397	0.158	1.92	2.52(0.08)	−0.999
3	0.407	0.197	0.024	1.36	1.92(0.11)	−0.998	5	0.695	0.358	0.080	2.22	3.08(0.17)	−0.999
4	0.491	0.213	0.042	1.60	2.25(0.31)	−0.991	1	0.697	0.409	0.167	2.01	2.65(0.13)	−0.999
5	0.498	0.220	0.074	1.54	2.12(0.38)	−0.984	6	0.699	0.367	0.070	2.27	3.15(0.10)	−0.999
6	0.599	0.280	0.063	1.92	2.68(0.29)	−0.994	3	0.925	0.593	0.293	2.50	3.16(0.09)	−0.999
7	0.677	0.377	0.202	1.84	2.38(0.36)	−0.989	7	1.063	0.703	0.380	2.76	3.42(0.11)	−0.999
8	0.729	0.418	0.234	1.95	2.48(0.37)	−0.989	8	1.147	0.772	0.434	2.92	3.57(0.11)	−0.999
9	0.740	0.431	0.246	1.95	2.47(0.37)	−0.990	26	1.157	0.867	0.595	2.56	2.82(0.05)	−0.999
10	0.746	0.476	0.256	1.96	2.45(0.14)	−0.998	11	1.179	0.798	0.418	3.08	3.81(0.01)	−1.000
11	0.753	0.427	0.114	2.35	3.20(0.04)	−0.999	9	1.193	0.827	0.495	2.93	3.49(0.01)	−0.999
12	0.759	0.473	0.306	1.87	2.27(0.34)	−0.989	12	1.218	0.850	0.525	2.94	3.47(0.12)	−0.999
13	0.787	0.518	0.268	2.09	2.61(0.05)	−0.999	13	1.252	0.838	0.471	3.19	3.91(0.14)	−0.999
14	0.801	0.458	0.184	2.33	3.09(0.20)	−0.998	17	1.272	0.830	0.441	3.34	4.16(0.15)	−0.999
15	0.808	0.543	0.311	2.05	2.49(0.10)	−0.999	14	1.300	0.873	0.497	3.30	4.02(0.15)	−0.999
16	0.819	0.481	0.195	2.37	3.12(0.15)	−0.999	15	1.313	0.916	0.556	3.20	3.79(0.11)	−0.999

17	0.858	0.567	0.272	2.32	2.93(0.01)	−1.000	21	1.366	0.954	0.582	3.32	3.92(0.12)	−0.999
18	0.881	0.539	0.279	2.37	3.01(0.24)	−0.997	16	1.401	0.974	0.601	3.39	4.00(0.16)	−0.999
19	0.938	0.612	0.409	2.24	2.65(0.36)	−0.991	19	1.457	1.029	0.637	3.50	4.10(0.10)	−0.999
20	0.952	0.636	0.331	2.50	3.11(0.03)	−0.999	20	1.514	1.029	0.605	3.78	4.55(0.10)	−0.999
21	1.021	0.704	0.423	2.51	2.99(0.10)	−0.999	23	1.616	1.150	0.725	3.84	4.46(0.12)	−0.999
22	1.042	0.693	0.379	2.69	3.32(0.10)	−0.999	18	1.654	1.189	0.762	3.88	4.46(0.12)	−0.999
23	1.046	0.709	0.414	2.62	3.16(0.12)	−0.999	10	1.666	1.213	0.857	3.67	4.05(0.28)	−0.999
24	1.072	0.811	0.522	2.45	2.75(0.08)	−0.999	22	1.686	1.164	0.698	4.15	4.94(0.16)	−0.999
25	1.125	0.782	0.483	2.72	3.21(0.13)	−0.999	25	1.761	1.280	0.845	4.04	4.58(0.13)	−0.999
26	1.169	0.882	0.579	2.65	2.95(0.05)	−0.999	28	1.916	1.379	0.904	4.44	5.06(0.18)	−0.999
27	1.213	0.889	0.589	2.77	3.12(0.07)	−0.999	24	1.950	1.449	1.012	4.28	4.69(0.18)	−0.999
28	1.247	0.888	0.582	2.90	3.33(0.15)	−0.999	27	1.999	1.514	1.072	4.31	4.64(0.12)	−0.999
29	1.272	1.028	0.712	2.68	2.80(0.21)	−0.997	29		1.609	1.185			
30	1.430	1.058	0.739	3.15	3.56(0.15)	−0.999	30		1.749	1.267			
31	1.484	1.043	0.728	3.35	3.78(0.36)	−0.995	32		1.933	1.505			
32	1.503	1.194	0.847	3.15	3.28(0.11)	−0.999	34			1.62			
33	1.606	1.377	1.026	3.08	2.90(0.35)	−0.993	33			1.713			
34	1.788	1.419	1.056	3.62	3.66(0.02)	−1.000							

TABLE III

DEPENDENCE OF log k' ON φ AT 45°C

No.	*Acetonitrile–water*						*No.*	*Methanol–water*					
	φ(%)			*Intercept*	*S(error)*	*r*		*φ(%)*			*Intercept*	*S(error)*	*r*
	50	*60*	*70*					*50*	*60*	*70*			
1	0.271	0.106	−0.035	1.03	1.53(0.07)	−0.999	4	0.536	0.259	0.047	1.75	2.45(0.19)	−0.999
2	0.333	0.121	0.003	1.14	1.67(0.27)	−0.988	6	0.568	0.284	0.012	1.96	2.78(0.03)	−0.999
3	0.361	0.164	−0.039	1.36	2.00(0.02)	−1.000	5	0.574	0.276	0.029	1.93	2.73(0.15)	−0.998
4	0.408	0.18	−0.009	1.44	2.09(0.11)	−0.999	2	0.579	0.314	0.096	1.78	2.42(0.14)	−0.998
5	0.410	0.188	0.041	1.32	1.85(0.22)	−0.993	1	0.599	0.333	0.120	1.79	2.40(0.15)	−0.998
6	0.500	0.210	0.021	1.68	2.39(0.29)	−0.993	3	0.836	0.504	0.238	2.32	2.99(0.19)	−0.999
7	0.595	0.334	0.162	1.66	2.17(0.26)	−0.995	7	0.939	0.613	0.312	2.50	3.14(0.07)	−0.999
8	0.640	0.381	0.193	1.75	2.23(0.20)	−0.996	8	1.020	0.684	0.363	2.66	3.29(0.04)	−0.999
9	0.641	0.391	0.201	1.73	2.20(0.17)	−0.997	9	1.065	0.729	0.415	2.69	3.25(0.06)	−0.999
11	0.684	0.357	0.057	2.25	3.14(0.08)	−0.999	11	1.069	0.682	0.347	2.87	3.61(0.15)	−0.999
12	0.684	0.446	0.264	1.72	2.10(0.16)	−0.997	13	1.075	0.688	0.356	2.86	3.60(0.16)	−0.999
10	0.697	0.421	0.244	1.83	2.27(0.29)	−0.992	26	1.086	0.805	0.544	2.44	2.71(0.06)	−0.999
14	0.710	0.389	0.131	2.15	2.90(0.18)	−0.998	14	1.101	0.705	0.369	2.92	3.66(0.17)	−0.998
16	0.745	0.415	0.149	2.22	2.98(0.18)	−0.998	12	1.102	0.771	0.499	2.60	3.02(0.17)	−0.999
18	0.749	0.484	0.239	2.02	2.55(0.06)	−0.998	17	1.156	0.745	0.391	3.06	3.83(0.16)	−0.998

13	0.761	0.463	0.221	2.10	2.70(0.17)	−0.998	15	1.169	0.793	0.497	2.84	3.36(0.23)	−0.999
15	0.785	0.493	0.260	2.09	2.63(0.17)	−0.998	21	1.198	0.819	0.518	2.89	3.40(0.23)	−0.999
17	0.816	0.507	0.229	2.28	2.94(0.09)	−0.999	16	1.230	0.832	0.492	3.07	3.69(0.17)	−0.999
19	0.859	0.568	0.362	2.09	2.49(0.25)	−0.995	20	1.313	0.859	0.477	3.39	4.18(0.21)	−0.999
20	0.920	0.563	0.267	2.54	3.27(0.17)	−0.999	19	1.313	0.927	0.558	3.20	3.78(0.05)	−0.999
23	0.986	0.662	0.361	2.54	3.13(0.07)	−0.999	23	1.469	1.031	0.639	3.54	4.15(0.13)	−0.999
24	0.997	0.641	0.396	2.48	3.01(0.32)	−0.994	18	1.499	1.065	0.706	3.47	3.96(0.22)	−0.997
21	1.002	0.658	0.366	2.58	3.19(0.01)	−0.999	22	1.502	1.008	0.629	3.67	4.37(0.35)	−0.999
22	1.021	0.636	0.320	2.76	3.15(0.20)	−0.998	10	1.512	1.112	0.762	3.37	3.75(0.14)	−0.999
25	1.056	0.735	0.419	2.65	3.19(0.01)	−1.000	25	1.597	1.144	0.746	3.72	4.26(0.16)	−0.999
26	1.089	0.781	0.461	2.66	3.14(0.03)	−0.999	28	1.746	1.245	0.810	4.08	4.68(0.19)	−0.999
28	1.176	0.827	0.519	2.81	3.29(0.12)	−0.999	24	1.790	1.325	0.914	3.97	4.38(0.16)	−0.999
29	1.177	0.929	0.625	2.57	2.76(0.16)	−0.998	27	1.847	1.384	0.949	4.09	4.49(0.08)	−0.999
27	1.192	0.811	0.519	2.86	3.37(0.27)	−0.997	29	1.974	1.485	1.065	4.25	4.55(0.20)	
32	1.306	1.094	0.735	2.76	2.85(0.42)	−0.989	30		1.589	1.149			
30	1.342	0.993	0.661	3.04	3.41(0.05)	−0.999	32		1.883	1.369			
31	1.379	0.979	0.647	3.20	3.66(0.20)	−0.999	34		1.977	1.472			
33	1.503	1.248	0.902	3.02	3.01(0.26)	−0.996	33			1.554			
34	1.671	1.298	0.943	3.49	3.64(0.05)	−0.999							

TABLE IV

DEPENDENCE OF log k' ON φ AT 55°C

No.	*Acetonitrile–water*						*No.*	*Methanol–water*					
	φ(%)			*Intercept*	*S(error)*	*r*		*φ(%)*			*Intercept*	*S(error)*	*r*
	50	*60*	*70*					*50*	*60*	*70*			
1	0.254	0.064	−0.060	1.03	1.57(0.19)	−0.993	4	0.467	0.200	−0.012	1.66	2.40(0.16)	−0.998
2	0.261	0.108	−0.047	1.03	1.54(0.01)	−1.000	6	0.469	0.205	−0.038	1.74	2.54(0.06)	−0.999
3	0.330	0.129	−0.054	1.29	1.92(0.05)	−0.999	5	0.481	0.200	−0.025	1.74	2.53(0.16)	−0.998
4	0.341	0.133	0.005	1.17	1.68(0.23)	−0.991	1	0.508	0.255	0.070	1.59	2.19(0.20)	−0.996
5	0.359	0.144	−0.040	1.35	2.00(0.09)	−0.999	2	0.536	0.243	0.052	1.73	2.42(0.29)	−0.993
6	0.413	0.156	−0.026	1.50	2.20(0.22)	−0.995	3	0.725	0.428	0.175	2.09	2.75(0.13)	−0.999
7	0.520	0.285	0.121	1.51	2.00(0.21)	−0.995	7	0.834	0.529	0.246	2.30	2.94(0.06)	−0.999
8	0.574	0.324	0.150	1.62	2.12(0.22)	−0.995	8	0.916	0.599	0.294	2.47	3.11(0.03)	−0.999
9	0.583	0.332	0.161	1.63	2.11(0.23)	−0.994	11	0.934	0.584	0.275	2.57	3.29(0.13)	−0.999
11	0.610	0.304	−0.016	2.18	3.13(0.04)	−0.999	14	0.944	0.585	0.282	2.59	3.31(0.16)	−0.999
12	0.615	0.386	0.224	1.58	1.96(0.19)	−0.995	9	0.951	0.644	0.338	2.48	3.06(0.01)	−1.000
14	0.622	0.324	0.077	1.98	2.73(0.15)	−0.999	13	0.993	0.575	0.279	2.76	3.57(0.35)	−0.999
10	0.638	0.389	0.215	1.68	2.12(0.22)	−0.995	12	1.001	0.718	0.382	2.56	3.10(0.15)	−0.999
16	0.656	0.347	0.092	2.06	2.82(0.16)	−0.999	26	1.014	0.734	0.500	2.29	2.57(0.13)	−0.999

13	0.683	0.402	0.166	1.97	2.59(0.13)	−0.999	15	1.043	0.699	0.397	2.65	3.23(0.12)	−0.999
15	0.718	0.441	0.218	1.96	2.50(0.16)	−0.998	17	1.047	0.657	0.335	2.82	3.56(0.20)	−0.999
18	0.721	0.428	0.186	2.05	2.68(0.15)	−0.999	21	1.063	0.696	0.392	2.73	3.36(0.18)	−0.999
17	0.759	0.455	0.190	2.18	2.85(0.11)	−0.999	16	1.093	0.724	0.417	2.77	3.38(0.18)	−0.999
19	0.786	0.514	0.321	1.94	2.33(0.23)	−0.995	20	1.151	0.739	0.392	3.04	3.80(0.19)	−0.999
20	0.831	0.490	0.208	2.38	3.12(0.17)	−0.999	19	1.216	0.831	0.483	3.04	3.67(0.11)	−0.999
24	0.915	0.599	0.355	2.30	2.80(0.21)	−0.997	10	1.327	1.011	0.655	3.01	3.36(0.12)	−0.999
23	0.917	0.594	0.316	2.41	3.01(0.13)	−0.999	23	1.337	0.921	0.562	3.27	3.88(0.16)	−0.999
21	0.925	0.596	0.320	2.43	3.03(0.15)	−0.999	22	1.345	0.888	0.503	3.44	4.21(0.21)	−0.999
22	0.941	0.575	0.262	2.63	3.40(0.15)	−0.999	18	1.364	0.950	0.590	3.29	3.87(0.16)	−0.999
25	0.980	0.652	0.368	2.50	3.06(0.13)	−0.999	25	1.446	1.025	0.657	3.41	3.95(0.15)	−0.999
26	1.013	0.679	0.413	2.50	3.00(0.20)	−0.998	28	1.589	1.122	0.722	3.75	4.34(0.19)	−0.999
29	1.086	0.862	0.556	2.42	2.65(0.24)	−0.996	24	1.651	1.214	0.830	3.69	4.11(0.15)	−0.999
28	1.101	0.748	0.463	2.68	3.19(0.20)	−0.998	27	1.704	1.269	0.881	3.75	4.12(0.14)	−0.999
27	1.103	0.750	0.458	2.71	3.23(0.18)	−0.999	30	1.941	1.467	1.044	4.18	4.49(0.15)	−0.999
32	1.221	1.014	0.690	2.57	2.66(0.34)	−0.992	29	1.827	1.345	0.934	4.05	4.47(0.20)	−0.999
30	1.254	0.890	0.594	2.89	3.30(0.20)	−0.998	32		1.736	1.252			
31	1.288	0.901	0.585	3.03	3.52(0.21)	−0.998	34		1.811	1.308			
33	1.414	1.152	0.820	2.91	2.97(0.20)	−0.998	33			1.414			
34	1.561	1.206	0.856	3.32	3.53(0.01)	−1.000							

TABLE V

DEPENDENCE OF log k' ON φ AT 65°C

No.	*Acetonitrile–water*						*No.*	*Methanol–water*					
	φ(%)			*Intercept*	*S(error)*	*r*		*φ(%)*			*Intercept*	*S(error)*	*r*
	50	*60*	*70*					*50*	*60*	*70*			
1	0.207	0.043	−0.090	0.94	1.49(0.09)	−0.998	6	0.376	0.135	−0.088	1.53	2.32(0.05)	−0.999
2	0.219	0.073	−0.108	1.04	1.64(0.10)	−0.998	5	0.391	0.137	−0.072	1.54	2.32(0.13)	−0.998
5	0.295	0.096	−0.036	1.11	1.66(0.19)	−0.993	2	0.397	0.176	0.009	1.36	1.94(0.16)	−0.997
3	0.311	0.082	−0.096	1.32	2.04(0.15)	−0.997	4	0.409	0.156	−0.043	1.53	2.26(0.16)	−0.998
4	0.315	0.104	−0.095	1.34	2.05(0.03)	−0.999	1	0.412	0.199	0.017	1.39	1.98(0.09)	−0.999
6	0.350	0.098	−0.062	1.36	2.06(0.27)	−0.992	3	0.639	0.357	0.117	1.94	2.61(0.12)	−0.999
7	0.470	0.237	0.084	1.42	1.93(0.23)	−0.993	7	0.738	0.448	0.188	2.11	2.75(0.09)	−0.999
8	0.522	0.283	0.110	1.54	2.06(0.27)	−0.996	8	0.812	0.507	0.233	2.25	2.90(0.09)	−0.999
9	0.530	0.286	0.124	1.53	2.03(0.24)	−0.993	13	0.818	0.483	0.205	2.34	3.07(0.16)	−0.999
11	0.540	0.243	−0.045	2.00	2.93(0.03)	−1.000	14	0.823	0.487	0.189	2.40	3.17(0.11)	−0.999
14	0.543	0.240	0.012	1.86	2.66(0.23)	−0.997	11	0.824	0.494	0.208	2.36	3.08(0.13)	−0.999
12	0.570	0.340	0.189	1.51	1.91(0.23)	−0.993	9	0.853	0.551	0.270	2.31	2.92(0.06)	−0.999
16	0.575	0.263	0.028	1.93	2.74(0.22)	−0.997	12	0.940	0.593	0.310	2.50	3.15(0.18)	−0.998
10	0.597	0.359	0.174	1.65	2.12(0.15)	−0.997	26	0.942	0.676	0.447	2.17	2.48(0.11)	−0.999
13	0.610	0.325	0.100	1.88	2.55(0.17)	−0.998	15	0.946	0.619	0.336	2.46	3.05(0.13)	−0.999

18	0.650	0.347	0.117	1.97	2.67(0.21)	−0.997	21	0.949	0.604	0.324	2.50	3.13(0.19)	−0.998
15	0.651	0.369	0.176	1.82	2.38(0.26)	−0.994	17	0.953	0.581	0.276	2.63	3.39(0.19)	−0.998
19	0.697	0.468	0.272	1.76	2.13(0.10)	−0.999	16	0.981	0.635	0.345	2.56	3.18(0.16)	−0.999
17	0.702	0.423	0.151	2.08	2.76(0.02)	−1.000	20	1.025	0.639	0.316	2.79	3.54(0.18)	−0.999
20	0.740	0.397	0.139	2.23	3.01(0.25)	−0.997	19	1.111	0.741	0.417	2.84	3.47(0.13)	−0.999
24	0.846	0.529	0.295	2.21	2.76(0.24)	−0.996	22	1.215	0.786	0.419	3.19	3.98(0.18)	−0.999
23	0.853	0.541	0.271	2.30	2.91(0.12)	−0.999	23	1.221	0.829	0.484	3.06	3.69(0.14)	−0.999
21	0.860	0.530	0.255	2.36	3.03(0.16)	−0.999	18	1.254	0.858	0.525	3.07	3.65(0.18)	−0.999
22	0.863	0.491	0.176	2.57	3.44(0.16)	−0.999	10	1.254	0.89	0.579	2.93	3.38(0.15)	−0.999
25	0.912	0.599	0.313	2.41	3.00(0.08)	−0.999	25	1.321	0.921	0.569	3.19	3.76(0.14)	−0.999
26	0.941	0.608	0.355	2.39	2.93(0.23)	−0.997	28	1.459	1.017	0.635	3.51	4.12(0.17)	−0.999
29	0.999	0.777	0.491	2.28	2.54(0.18)	−0.997	24	1.518	1.091	0.728	3.48	3.95(0.18)	−0.999
28	1.018	0.706	0.409	2.54	3.05(0.04)	−0.999	27	1.566	1.140	0.783	3.51	3.92(0.20)	−0.999
27	1.023	0.656	0.378	2.62	3.23(0.26)	−0.997	30	1.667	1.319	0.931	3.56	3.77(0.17)	−0.999
32	1.135	0.925	0.606	2.48	2.65(0.31)	−0.993	32	2.094	1.570	1.125	4.50	4.85(0.23)	−0.999
30	1.178	0.840	0.531	2.79	3.24(0.08)	−0.999	29	1.683	1.215	0.836	3.79	4.24(0.26)	−0.999
31	1.205	0.812	0.506	2.94	3.49(0.25)	−0.997	34		1.649	1.189			
33	1.321	1.053	0.732	2.80	2.95(0.15)	−0.998	33		1.732	1.269			
34	1.335	1.108	0.775	2.75	2.80(0.31)	−0.996							

$$\log k' = \log k_0 - S\varphi \quad (1)$$

where k_0 is the (extrapolated) value of k' for pure water as the mobile phase ($\varphi = 0$). The slope, S, should be related to the solvent strength of the pure organic solvent[14]. Tables II–V also list the corresponding slopes (slope error), intercepts and correlation coefficients. Several conclusions were drawn from the data. First, log k' was linearly related to φ. Second, as might be expected[15], the slope, S, for a particular nitro-PAH was significantly different between the two mobile phases. Nitro-PAHs had larger S values with methanol–water than with acetontitrile–water, *e.g.*, the slope for 9-nitroanthracene was 5.06 *vs.* 3.33, respectively, at 35°C. Third, at each temperature studied, a wide range of slope values were found for both mobile phases. For example, the S values ranged between 1.49 and 3.66 for nitro-PAHs in acetonitrile–water at 35°C. This resulted in nitro-PAH elution order sequence reversals for some compounds (see tables). Several researchers have observed this phenomena as well[2,7,16–18].

Eqn. 2 relates S with log k_0

$$S = p \log k_0 + q \quad (2)$$

where p and q are assumed to be constants for a given experimental condition. Schoenmakers *et al.*[2] plotted S *vs.* log k_0 for 32 benzene derivatives (having a wide range of functionality and molecular structure) in methanol–water ($p = 0.79$, $r = 0.98$) and acetonitrile–water ($r = -0.06$). The data revealed that the relationship between S and log k_0 was solvent-dependent. Moreover, the slope value greatly differed from one suggesting that the same solute properties effected S and log k_0 in much different ways. In contrast, Quarry *et al.*[7] plotted S *vs.* log k_0 for seven nitroaromatics in methanol–water. For these compounds, the same solute properties appeared to influence S and log k_0 in a similar manner ($p = 1.0$, $r = 0.99$). Shown in Table VI are the results of S *vs.* log k_0 plots for nitro-PAHs. Higher correlation coefficients were found for the compounds studied in methanol–water ($r = 0.98$) than in acetonitrile–water ($r = 0.94$). Nevertheless, the relatively small deviation in slope from one suggests that the same solute properties contribute to S and log k_0 in the same way. The extent to which these properties contribute in each organic modifier however was greatly different as evidenced by the k' values.

TABLE VI

S *vs.* LOG k_0 PLOTS AT VARIOUS TEMPERATURES

Temperature (°C)	*r*	*p*	*q*	*n*
Acetonitrile–water				
35	0.94	0.83 ± 0.05	0.87 ± 0.19	34
45	0.95	0.88 ± 0.05	0.77 ± 0.18	34
55	0.95	0.91 ± 0.05	0.72 ± 0.18	34
65	0.94	0.91 ± 0.06	0.74 ± 0.19	34
Methanol–water				
35	0.98	0.94 ± 0.04	0.82 ± 0.15	28
45	0.98	0.91 ± 0.04	0.85 ± 0.14	29
55	0.98	0.90 ± 0.03	0.89 ± 0.13	30
65	0.98	0.90 ± 0.03	0.87 ± 0.13	31

Braumann and co-workers[17,18] proposed the concept of using log k_0 as a measure of the intrinsic property of the solute to partition itself between the mobile–stationary phases. For all common nitro-PAHs, the correlation coefficient for $\log k_{0(CH_3OH)}$ *vs.* $\log k_{0(CH_3CN)}$ averaged 0.84 ± 0.01 over the temperature range studied. The moderate correlation in retention data also suggested that the same molecular properties contribute to the separation process to much different degrees. These solute property differences result in greatly different retention behavior for nitro-PAHs in the two organic modifiers.

Nitro-PAH retention as a function of temperature

The extent to which individual nitro-PAH retention decreased was a function of column temperature. This resulted in elution order reversals for some nitro-PAHs (see Tables II–V). Eqn. 3 describes the relationship between solute retention and column temperature[12]

$$\log k' = -\Delta H^0/2.3RT + (\Delta S^0/2.3R) + \log \theta \quad (3)$$

where R is the gas constant, T is the absolute temperature, θ is the mobile–stationary phase ratio, ΔH^0 is the standard enthalpy change of solute transfer from the mobile phase to the stationary phase, and ΔS^0 is the associated change in the standard entropy.

Summarized in Tables VII and VIII are the results of log k' *vs.* $1/T$ plots at constant mobile phase composition. (Note: The data for these plots are given in Tables II–V). The standard enthalpy change, ΔH^0, was constant and independent of temperature. The negative value indicated that nitro-PAH transfer from the mobile phase to the C_{18} stationary phase was enthalpically favored.

Nitro-PAH ΔH^0 values varied widely in a particular mobile phase composition. For example, at acetonitrile–water (50:50), ΔH^0 was between 1.32 and 6.96 kcal/mol (see Tables VII and VIII for other comparisons). In general, as the concentration of organic in the mobile phase increased, ΔH^0 decreased or remained constant (at the 95% confidence level). Further inspection revealed that nitro-PAHs were between 0.24 and 4.4 kcal/mol more favorable to transfer from methanol–water to the C_{18} stationary phase than were nitro-PAHs in acetonitrile-water. Nitro-PAH ΔH^0 values were dependent on solute structure as well as the type and concentration of organic modifier.

Eqn. 4 was used to examine the nitro-PAH transfer mechanism between the mobile and stationary phases[12]. If a linear dependence is observed between log k' (determined at or close to the harmonic mean temperature, T_{eval}) and ΔH^0, it implies that the retention mechanism is similar and that an enthalpy–entropy effect exists in the solute retention process. The compensation temperature, β, can be determined from the slope of log k' *vs.* $-\Delta H^0$ plot

$$\log k'_T = -\Delta H^0/2.3R\,(1/T - 1/\beta) - (\Delta G^0_\beta/2.3R\beta) + \log \theta \quad (4)$$

where, k'_T is the capacity factor at temperature T and ΔG^0_β is the Gibbs free energy at the compensation temperature. If a family of compounds exhibit enthalpy–entropy compensation, the values of β and ΔG^0_β will be invariant and the solute transfer process

TABLE VII

ΔH^0 CALCULATED FROM log k' *VS.* $1/T$ AT VARIOUS ACETONITRILE–WATER COMPOSITIONS

No.	*Acetonitrile–water*								
	50:50			*60:40*			*70:30*		
	Intercept	$-\Delta H^0$ *(kcal/mol)*	*r*	*Intercept*	$-\Delta H^0$ *(kcal/mol)*	*r*	*Intercept*	$-\Delta H^0$ *(kcal/mol)*	*r*
1	−0.63 ± 0.01	1.32 ± 0.25	0.967	−1.09 ± 0.01	1.76 ± 0.15	0.998	−0.96 ± 0.002	1.35 ± 0.04	0.999
2	−1.23 ± 0.02	2.26 ± 0.39	0.972	−0.87 ± 0.01	1.46 ± 0.18	0.985	−1.45 ± 0.02	2.11 ± 0.38	0.969
3	−0.68 ± 0.01	1.53 ± 0.15	0.992	−1.08 ± 0.01	1.81 ± 0.17	0.992	−1.26 ± 0.01	1.81 ± 0.25	0.982
4	−1.48 ± 0.01	2.77 ± 0.21	0.994	−1.01 ± 0.01	1.73 ± 0.11	0.996	−1.45 ± 0.01	2.11 ± 0.15	0.995
5	−1.82 ± 0.01	3.25 ± 0.22	0.996	−1.21 ± 0.01	2.03 ± 0.20	0.991	−1.16 ± 0.01	1.74 ± 0.12	0.995
6	−2.23 ± 0.01	3.99 ± 0.17	0.998	−1.75 ± 0.001	2.87 ± 0.03	0.999	−1.36 ± 0.004	2.01 ± 0.08	0.998
7	−1.69 ± 0.01	3.33 ± 0.17	0.997	−1.20 ± 0.01	2.23 ± 0.12	0.997	−1.13 ± 0.003	1.88 ± 0.06	0.999
8	−1.61 ± 0.01	3.30 ± 0.17	0.997	−1.13 ± 0.01	2.20 ± 0.19	0.993	−1.16 ± 0.003	1.98 ± 0.07	0.999
9	−1.61 ± 0.01	3.31 ± 0.25	0.994	−1.23 ± 0.01	2.35 ± 0.19	0.994	−1.13 ± 0.001	1.94 ± 0.02	0.999
10	−0.96 ± 0.01	2.41 ± 0.13	0.997	−0.83 ± 0.01	1.84 ± 0.14	0.995	−0.65 ± 0.01	1.30 ± 0.26	0.961
11	−1.65 ± 0.01	3.40 ± 0.14	0.998	−1.62 ± 0.002	2.89 ± 0.05	0.999	−1.75 ± 0.01	2.63 ± 0.27	0.990
12	−1.40 ± 0.01	3.05 ± 0.16	0.997	−1.06 ± 0.01	2.17 ± 0.29	0.983	−1.02 ± 0.002	1.87 ± 0.04	0.999
13	−1.23 ± 0.02	2.88 ± 0.51	0.973	−1.63 ± 0.01	3.04 ± 0.27	0.992	−1.61 ± 0.01	2.66 ± 0.23	0.992
14	−2.11 ± 0.004	4.12 ± 0.09	0.999	−1.96 ± 0.01	3.42 ± 0.23	0.996	−1.73 ± 0.01	2.71 ± 0.18	0.996
15	−0.97 ± 0.02	2.54 ± 0.46	0.969	−1.38 ± 0.01	2.73 ± 0.26	0.991	−1.20 ± 0.00	2.14 ± 0.003	1.000

16	−1.94 ± 0.01	3.91 ± 0.23	0.997	−1.94 ± 0.01	3.44 ± 0.25	0.995	−1.67 ± 0.01	2.65 ± 0.23	0.993
17	−0.90 ± 0.01	2.49 ± 0.21	0.993	−1.08 ± 0.01	2.32 ± 0.15	0.996	−1.09 ± 0.002	1.92 ± 0.04	0.999
18	−1.60 ± 0.03	3.48 ± 0.56	0.975	−1.58 ± 0.01	3.00 ± 0.29	0.990	−1.52 ± 0.01	2.56 ± 0.30	0.986
19	−1.74 ± 0.01	3.79 ± 0.20	0.997	−1.02 ± 0.01	2.31 ± 0.13	0.997	−1.12 ± 0.004	2.16 ± 0.09	0.998
20	−1.45 ± 0.03	3.42 ± 0.61	0.970	−2.02 ± 0.01	3.76 ± 0.26	0.995	−1.81 ± 0.01	3.03 ± 0.14	0.999
21	−0.83 ± 0.02	2.64 ± 0.51	0.964	−1.25 ± 0.01	2.77 ± 0.26	0.997	−1.43 ± 0.01	2.62 ± 0.16	0.996
22	−1.00 ± 0.03	2.91 ± 0.58	0.962	−1.54 ± 0.01	3.17 ± 0.31	0.991	−1.86 ± 0.01	3.17 ± 0.31	0.990
23	−1.13 ± 0.01	3.09 ± 0.16	0.997	−1.21 ± 0.01	2.72 ± 0.21	0.994	−1.19 ± 0.001	2.27 ± 0.02	0.990
24	−1.49 ± 0.01	3.63 ± 0.14	0.999	−2.26 ± 0.04	4.30 ± 0.77	0.969	−1.96 ± 0.02	3.49 ± 0.39	0.980
25	−1.28 ± 0.01	3.41 ± 0.15	0.998	−1.34 ± 0.01	3.00 ± 0.30	0.990	−1.42 ± 0.002	2.68 ± 0.03	0.999
26	−1.40 ± 0.003	3.63 ± 0.08	0.999	−2.25 ± 0.01	4.42 ± 0.19	0.998	−1.89 ± 0.02	3.48 ± 0.40	0.987
27	−0.96 ± 0.03	3.11 ± 0.63	0.961	−1.67 ± 0.01	3.62 ± 0.27	0.995	−1.75 ± 0.01	3.31 ± 0.19	0.997
28	−1.32 ± 0.01	3.63 ± 0.21	0.997	−1.22 ± 0.01	2.98 ± 0.23	0.994	−1.36 ± 0.002	2.75 ± 0.03	0.999
29	−1.80 ± 0.005	4.34 ± 0.10	0.999	−1.75 ± 0.01	3.92 ± 0.11	0.999	−1.77 ± 0.002	3.50 ± 0.05	0.999
30	−1.42 ± 0.01	4.03 ± 0.11	0.996	−1.49 ± 0.02	3.61 ± 0.36	0.990	−1.60 ± 0.001	3.30 ± 0.04	0.999
31	−1.66 ± 0.002	4.44 ± 0.05	0.999	−1.54 ± 0.01	3.66 ± 0.32	0.993	−1.73 ± 0.01	3.48 ± 0.12	0.999
32	−2.58 ± 0.003	5.74 ± 0.72	0.985	−1.81 ± 0.003	4.24 ± 0.07	0.999	−1.77 ± 0.01	3.69 ± 0.32	0.993
33	−1.58 ± 0.003	4.51 ± 0.07	0.999	−2.24 ± 0.002	5.11 ± 0.07	0.999	−2.25 ± 0.01	4.62 ± 0.15	0.999
34	−3.11 ± 0.05	6.96 ± 0.50	0.976	−2.05 ± 0.002	4.90 ± 0.05	0.999	−2.01 ± 0.04	4.45 ± 0.10	0.999

TABLE VIII

ΔH^0 CALCULATED FROM log k' *VS.* $1/T$ AT VARIOUS METHANOL–WATER COMPOSITIONS

No.	*Methanol–water*								
	50:50			*60:40*			*70:30*		
	Intercept	$-\Delta H^0$ *(kcal/mol)*	*r*	*Intercept*	$-\Delta H^0$ *(kcal/mol)*	*r*	*Intercept*	$-\Delta H^0$ *(kcal/mol)*	*r*
1	−2.49 ± 0.004	4.51 ± 0.14	0.999	−1.99 ± 0.01	3.38 ± 0.14	0.998	−1.51 ± 0.01	2.38 ± 0.13	0.997
2	−2.15 ± 0.03	3.98 ± 0.68	0.997	−2.09 ± 0.001	3.51 ± 0.03	0.999	−1.51 ± 0.003	2.35 ± 0.07	0.999
3	−2.34 ± 0.01	4.62 ± 0.26	0.997	−2.06 ± 0.001	3.75 ± 0.03	0.999	−1.70 ± 0.01	2.82 ± 0.14	0.997
4	−1.76 ± 0.004	3.36 ± 0.09	0.999	−1.59 ± 0.01	2.71 ± 0.10	0.999	−1.32 ± 0.01	1.98 ± 0.24	0.986
5	−2.71 ± 0.004	4.81 ± 0.08	0.999	−2.14 ± 0.004	3.53 ± 0.08	0.999	−1.64 ± 0.004	2.43 ± 0.09	0.999
6	−2.93 ± 0.01	5.11 ± 0.12	0.999	−2.25 ± 0.004	3.70 ± 0.08	0.999	−1.70 ± 0.001	2.50 ± 0.02	0.999
7	−2.60 ± 0.002	5.17 ± 0.06	0.999	−2.16 ± 0.004	4.05 ± 0.08	0.999	−1.78 ± 0.003	3.07 ± 0.07	0.999
8	−2.61 ± 0.00	5.30 ± 0.01	1.000	−2.19 ± 0.01	4.20 ± 0.17	0.998	−1.84 ± 0.003	3.21 ± 0.07	0.999
9	−2.65 ± 0.01	5.42 ± 0.10	0.999	−2.26 ± 0.01	4.36 ± 0.11	0.999	−2.05 ± 0.004	3.59 ± 0.08	0.999
10	−3.78 ± 0.03	7.73 ± 0.86	0.994	−2.05 ± 0.01	4.62 ± 0.27	0.999	−2.40 ± 0.01	4.61 ± 0.43	0.996
11	−2.86 ± 0.01	5.72 ± 0.32	0.997	−2.62 ± 0.002	4.83 ± 0.05	0.999	−1.95 ± 0.004	3.35 ± 0.11	0.999
12	−1.96 ± 0.01	4.48 ± 0.31	0.995	−1.91 ± 0.02	3.92 ± 0.55	0.981	−2.00 ± 0.03	3.60 ± 0.69	0.965
13	−3.44 ± 0.03	6.62 ± 0.57	0.993	−3.16 ± 0.01	5.65 ± 0.25	0.998	−2.51 ± 0.01	4.20 ± 0.18	0.998
14	−4.10 ± 0.02	7.61 ± 0.35	0.998	−3.48 ± 0.02	6.13 ± 0.33	0.997	−2.94 ± 0.01	4.84 ± 0.14	0.999
15	−2.85 ± 0.01	5.87 ± 0.20	0.999	−2.43 ± 0.01	4.72 ± 0.17	0.999	−2.00 ± 0.02	3.62 ± 0.35	0.991

16	−3.34 ± 0.01	6.69 ± 0.24	0.999	−2.85 ± 0.01	5.39 ± 0.22	0.998	−2.27 ± 0.01	4.04 ± 0.15	0.999
17	−2.33 ± 0.01	5.09 ± 0.10	0.999	−1.99 ± 0.01	3.98 ± 0.13	0.999	−1.41 ± 0.01	2.62 ± 0.16	0.996
18	−2.87 ± 0.01	6.39 ± 0.17	0.999	−2.56 ± 0.01	5.30 ± 0.14	0.999	−2.01 ± 0.02	3.93 ± 0.48	0.986
19	−2.40 ± 0.01	5.44 ± 0.16	0.999	−2.21 ± 0.004	4.58 ± 0.09	0.997	−1.85 ± 0.003	3.51 ± 0.07	0.989
20	−4.02 ± 0.02	7.81 ± 0.33	0.998	−3.36 ± 0.02	6.19 ± 0.33	0.999	−2.64 ± 0.01	4.57 ± 0.25	0.997
21	−3.33 ± 0.01	6.64 ± 0.20	0.999	−3.02 ± 0.01	5.61 ± 0.20	0.999	−2.44 ± 0.02	4.28 ± 0.50	0.987
22	−3.64 ± 0.01	7.51 ± 0.19	0.999	−3.10 ± 0.01	6.01 ± 0.21	0.999	−2.53 ± 0.02	4.58 ± 0.48	0.989
23	−2.84 ± 0.05	6.30 ± 0.10	0.999	−2.48 ± 0.01	5.13 ± 0.11	0.999	−1.98 ± 0.04	3.82 ± 0.07	0.999
24	−2.91 ± 0.003	6.86 ± 0.05	0.999	−2.55 ± 0.01	5.65 ± 0.18	0.999	−2.14 ± 0.01	4.46 ± 0.18	0.998
25	−3.22 ± 0.01	7.03 ± 0.16	0.999	−2.77 ± 0.004	5.72 ± 0.09	0.999	−2.25 ± 0.02	4.38 ± 0.07	0.999
26	−1.61 ± 0.01	3.42 ± 0.13	0.999	−1.30 ± 0.01	3.07 ± 0.14	0.998	−1.05 ± 0.004	2.33 ± 0.09	0.998
27	−2.87 ± 0.001	6.88 ± 0.15	0.999	−2.66 ± 0.01	5.90 ± 0.22	0.999	−2.10 ± 0.01	4.48 ± 0.23	0.998
28	−3.26 ± 0.01	7.31 ± 0.17	0.999	−2.71 ± 0.01	5.78 ± 0.11	0.999	−2.12 ± 0.004	4.27 ± 0.10	0.999
29				−2.65 ± 0.02	6.03 ± 0.56	0.996	−2.87 ± 0.01	5.73 ± 0.47	0.997
30				−3.03 ± 0.01	6.75 ± 0.18	0.999	−2.49 ± 0.01	5.31 ± 0.14	0.999
32				−2.16 ± 0.05	5.83 ± 0.11	0.965	−2.74 ± 0.01	6.00 ± 0.13	0.999
33							−3.26 ± 0.01	7.03 ± 0.13	0.999
34							−3.42 ± 0.02	7.12 ± 0.62	0.996

is assumed to be identical. On the other hand, differences in ΔG^0_β and β suggest differing solute retention processes. Thus, the compensation temperature provides an indication of the retention process as a function of the nature and composition of organic modifier studied.

Plots of log k'_{45} *vs.* $-\Delta H^0$ yielded an average correlation coefficient of 0.80 $\pm$ 0.07 for both organic modifiers at the mobile phase compositions studied ($n=18$, 3 compositions $\times$ 3 runs per composition $\times$ 2 organic modifiers). The relatively moderate correlation suggested different retentive processes for the family of nitro-PAHs studied. However, much higher correlation, $r=0.96 \pm 0.03$ ($n=18$), was found for some mononitrated PAHs (*viz.* 1, 3, 10, 15, 17, 23, 25, 28, 30, 31 and 33). For these compounds an enthalpy–entropy compensation effect existed over a wide range of mobile phase conditions. The plots further suggested that changes in ΔH^0 were countered by changes in ΔS^0 at temperatures near β, 565 $\pm$ 54 K. Moreover, the compensation temperature fell within the accepted range (554–755 K) reported by other researchers [10,12,19,20] and thus, the retention process for these compounds appeared to be same.

CONCLUSION

The data revealed that nitro-PAH log k_0 values (defined as the solute capacity factor at 100% water) were dependent on organic modifier. Thus, the assumption that reversed-phase retention was primarily controlled by solute–mobile phase interactions was supported by the observed differences in log $k_{0(CH_3CN)}$ and log $k_{0(CH_3OH)}$. The extent to which the organic modifier influenced the retention process and therefore, log k' was significant. Nevertheless, the moderate correlation between log $k_{0(CH_3CN)}$ and log $k_{0(CH_3OH)}$ purported that the same solute properties contributed to the separation process to varying degrees. This was probably due to differences in nitro-PAH conformation in the two solvent systems. Why some mononitrated PAHs exhibit enthalpy–entropy compensation was unclear. The relationship cannot be explained by simple steric or electronic arguments.

ACKNOWLEDGEMENT

The authors thank Hewlett-Packard (Palo Alto, CA, U.S.A.) for providing the 1090M HPLC system through their university grants program.

REFERENCES

1 C. M. Riley, E. Tomlinson and T. M. Jefferies, *J. Chromatogr.*, 185 (1979) 197.
2 P. J. Schoemakers, H. A. H. Billiet and L. de Galan, *J. Chromatogr.*, 185 (1979) 179.
3 P. Jandera, H. Colin and G. Guiochon, *Anal. Chem.*, 54 (1982) 435.
4 X. Geng and F. E. Regnier, *J. Chromatogr.*, 296 (1984) 15.
5 X. Geng and F. E. Regnier, *J. Chromatogr.*, 332 (1985) 147.
6 L. R. Snyder, M. A. Quarry and J. L. Glajch, *Chromatographia*, 24 (1987) 33.
7 M. A. Quarry, R. L. Grob, L. R. Snyder, J. W. Dolan and M. P. Rigney, *J. Chromatogr.*, 384 (1987) 163.
8 J. A. Schmit, R. A. Henry, R. C. Williams and J. F. Dieckman, *J. Chromatogr. Sci.*, 9 (1971) 645.
9 J. Chmielowiec and H. Sawatzky, *J. Chromatogr. Sci.*, 17 (1979) 245.
10 G. Vigh and Z. Varga-Pauchony, *J. Chromatogr.*, 196 (1980) 1.
11 H. J. Issaq, S. D. Fox, K. Lindsey, J. H. McConnell and D. E. Weiss, *J. Liq. Chromatogr.*, 10 (1987) 49.
12 W. Melander, D. E. Campbell and Cs. Horváth, *J. Chromatogr.*, 158 (1978) 215.

13 P. J. Doherty, *Master thesis,* Tufts University, Medford, MA, 1985.
14 P. J. Schoenmakers, H. A. H. Billiet, R. Tijssen and L. de Galan, *J. Chromatogr.*, 149 (1978) 519.
15 L. R. Snyder, J. L. Glajch and J. J. Kirkland, *Practical HPLC Method Development,* Wiley-Interscience, New York, 1988.
16 A. Opperhuizen, T. L. Sinnige, J. M. D. van der Steen and O. Hutzinger, *J. Chromatogr.*, 338 (1987) 51.
17 T. Braumann, G. Weber and L. H. Grimme, *J. Chromatogr.*, 261 (1983) 329.
18 T. Braumann and L. H. Grimme, *J. Chromatogr.*, 206 (1981) 7.
19 J. H. Kruz and G. Vasvari, *J. Chromatogr.*, 83 (1973) 181.
20 K. Jinno and N. Ozaki, *J. Liq. Chromatogr.*, 7 (1984) 887.

Journal of Chromatography, 513 (1990) 137–143
Elsevier Science Publishers B.V., Amsterdam

CHROM. 22 496

Correlation of protein partitioning in aqueous polymer two-phase systems

ALAN D. DIAMOND and JAMES T. HSU*

Bioprocessing Institute, Department of Chemical Engineering, Lehigh University, Bethlehem, PA 18015 (U.S.A.)

(First received June 22nd, 1989; revised manuscript received March 1st, 1990)

ABSTRACT

A correlation is presented for the partitioning of proteins in aqueous two-phase systems. The correlation relates the natural logarithm of the protein partition coefficient to the polyethylene glycol (PEG) concentration difference between the phases, $(w_1'' - w_1')$, by the equation, $\ln K = A(w_1'' - w_1') + b(w_1'' - w_1')^2$. This relationship was shown to fit protein partitioning data obtained from eight two-phase systems at pH 7.0, four consisting of PEG 8000–Dextran T-500–water systems and four consisting of PEG 3400–potassium phosphate–water systems. Seven different proteins, ribonuclease, lysozyme, trypsin, rhodanese, transferrin, hexokinase and invertase, with a molecular weight range of 10 000–270 000, were utilized in this work. Each of the proteins partitioned with different values of the empirical constants A and b.

INTRODUCTION

Aqueous polymer two-phase systems such as those composed of polyethylene glycol (PEG)–dextran–water and PEG–potassium phosphate–water provide both a gentle and economical means for the purification of biological materials[1,2]. In order to facilitate their use, a simple method is needed for correlation of partition coefficients. Such a correlation would provide the groundwork necessary for the selection of an appropriate system for separation, and the eventual scale up of the purification process.

The partition coefficient, K, has been postulated as a function of many parameters, including electrical charge, hydrophobicity, biospecificity, size and conformation[1]. Much work has been done to elucidate the effects of pH[3], the influence of salts[4,5], hydrophobicity[6,7] and biomolecule and polymer molecular weight[8,9] on protein partitioning. Several theoretical models have been proposed for the thermodynamic behavior of protein partitioning in aqueous polymer two-phase systems. Walter *et al.*[2] and Albertsson *et al.*[9] have shown that the lattice model of Flory[10] and Huggins[11] could be used to qualitatively predict protein partitioning. Baskir *et al.*[12]

have modified the theory of Scheutjens and Fleer[13,14], while King *et al.*[15] extended the model of Edmond and Ogston[16] to take into account electrostatic charge. However, a simple correlation still has not resulted. Diamond and Hsu[17] presented a linear semilogarithmic relationship for correlating biomolecule partitioning, with respect to the PEG concentration difference between the phases, based on Flory–Huggins solution thermodynamics. The relationship proved to be adequate for dipeptide and low-molecular-weight protein partitioning. However, the correlation was not appropriate for high-molecular-weight proteins, which apparently exhibited partitioning with non-linear dependence on the PEG concentration difference. In this paper, the correlation of Diamond and Hsu is generalized to include a quadratic dependence on PEG concentration difference for high-molecular-weight protein partitioning. The generalized expression is shown to be applicable to both PEG–dextran–water and PEG–potassium phosphate–water two-phase systems for seven proteins.

MATERIALS AND METHODS

Materials

Dextran T-500 (Lot 06905) was obtained from Pharmacia (Piscataway, NJ, U.S.A.). PEGs of molecular weights 3400 (Lot 00304 EV) and 8000 (Lot 02316 EV) were purchased from Aldrich (Milwaukee, WI, U.S.A.).

Ribonuclease (bovine pancreas), trypsin, lysozyme (chicken egg), rhodanese (bovine liver), hexokinase (bakers yeast), invertase (bakers yeast) and transferrin (human) were obtained from Sigma (St. Louis, MO, U.S.A.).

Partition experiments

The PEG 8000–Dextran T-500–water systems at 4°C and the PEG 3400–potassium phosphate–water systems at 20°C were prepared as described earlier[17–19] and had the following phase compositions (in %, w/w):

(1) Bottom phase: 8.83% dextran–1.63% PEG, top phase: 0.86% dextran–4.91% PEG

(2) Bottom phase: 14.11% dextran–0.73% PEG, top phase: 0.11% dextran–7.03% PEG

(3) Bottom phase: 18.73% dextran–0.43% PEG, top phase: 0.03% dextran–9.27% PEG

(4) Bottom phase: 21.61% dextran–0.30% PEG, top phase: 0.01% dextran–10.83% PEG

(5) Bottom phase: 14.06% phosphate–4.23% PEG, top-phase: 8.19% phosphate–15.96% PEG

(6) Bottom phase: 15.46% phosphate–2.54% PEG, top phase: 7.01% phosphate–19.16% PEG

(7) Bottom phase: 17.41% phosphate–1.30% PEG, top phase: 5.56% phosphate–23.90% PEG

(8) Bottom phase: 19.41% phosphate–0.78% PEG, top phase: 4.55% phosphate–28.15% PEG

The PEG–dextran phase diagram data were taken from Diamond and Hsu[17], while the composition of systems 5–8 of the PEG–potassium phosphate phase diagram were obtained from Albertsson[1].

Partition experiments were performed as previously described[17], in which the PEG–dextran–water systems were maintained at pH 7.0 with 0.01 *m* potassium phosphate buffer. The potassium phosphate in the PEG–potassium phosphate–water systems consisted of a mono- to dibasic weight ratio of 0.55, thus maintaining at pH 7.0. A 10-ml volume of phase system was poured into 15 ml polypropylene centrifuge tubes. A 10-mg amount of protein was added, and the tubes tightly sealed. The protein was then dissolved by gently mixing the contents of the centrifuge tube with a vortex mixer. The phases of the PEG–dextran system were allowed to settle for 24 h at 4.0 $\pm$ 0.1°C in a temperature controlled refrigerator, while the PEG–phosphate systems were permitted to settle for 24 h at 20.0 $\pm$ 0.5°C in the laboratory environment. A pasteur pipet was used to collect the top phase, while the lower phase was drained from the tube by piercing a hole at its bottom.

Protein concentration was determined by diluting the phase aliquot with water, and measuring absorbance at 280 nm *versus* an equally diluted phase blank. The partition coefficient, K, was defined as protein concentration in the top phase divided by that in the bottom. Two or more partition experiments were performed for a protein in a particular system, and the resulting partition coefficients did not differ by more than 5%. The K values used in this work represent the average value of the measured partition coefficients.

RESULTS AND DISCUSSION

It has been demonstrated that for low-molecular-weight proteins and small molecules such as dipeptides, the natural logarithm of the partition coefficient may be correlated with the PEG concentration difference in a system composed of PEG, dextran and water[17]. Zaslavsky *et al.*[20], using dinitrophenylated amino acids, have also shown that the Gibbs free energy of transfer of a CH_2 group varied linearly with the PEG concentration difference between the phases for a PEG–dextran–water system. However, they did not provide a theoretical basis for their plot. The linear relationship between ln K and the PEG concentration difference, as derived from Flory–Huggins polymer solution thermodynamics, was found to be[17]:

$$\ln K = A(w_1'' - w_1') \tag{1}$$

where w is weight percent, the subscript 1 refers to PEG, and the double and single prime superscripts represent the top and bottom phase, respectively. The slope, A, is a function of biomolecule and polymer molecular weight, and the interaction of the biomolecule with the polymers and water. The above relationship was not applicable to high-molecular-weight proteins which tended to deviate from eqn. 1. Introducing a second degree term into eqn. 1 yields the following relationship:

$$\ln K = A(w_1'' - w_1') + b(w_1'' - w_1')^2 \tag{2}$$

Although empirical in nature, the coefficient b, like A, may reflect the interaction of the protein with the polymers and water. Eqn. 2 may be simplified by dividing through by $w_1'' - w_1'$ to yield the linear relationship:

$$\frac{\ln K}{w_1'' - w_1'} = A + b(w_1'' - w_1') \tag{3}$$

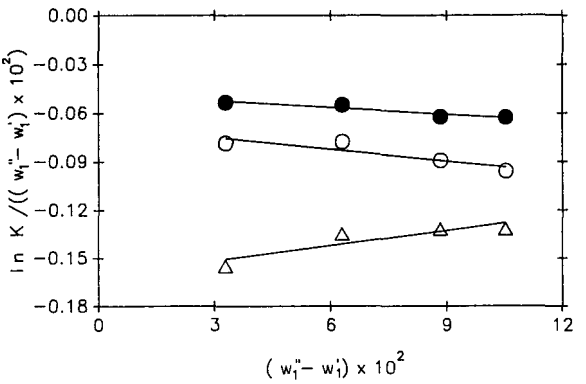

Fig. 1. Correlation of low-molecular-weight protein partitioning data in the PEG 8000–Dextran T-500–water system according to eqn. 3. ○ = Ribonuclease; ● = trypsin; △ = lysozyme.

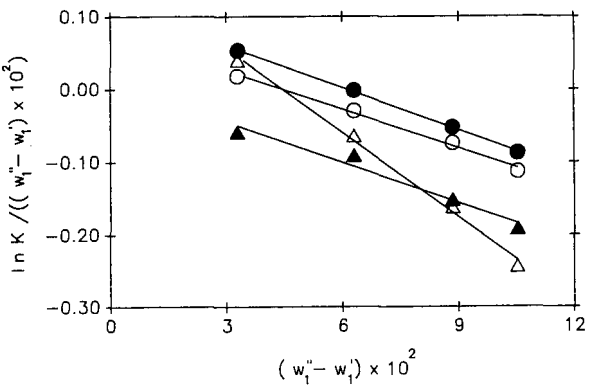

Fig. 2. Correlation of high-molecular-weight protein partitioning data in the PEG 8000–Dextran T-500–water system according to eqn. 3. ○ = Rhodanese; ● = hexokinase; △ = invertase; ▲ = transferrin.

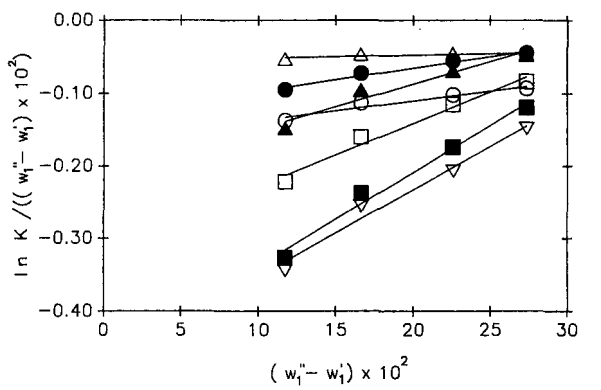

Fig. 3. Correlation of protein partitioning data in the PEG 3400–potassium phosphate–water system according to eqn. 3. ○ = Ribonuclease; ● = trypsin; △ = lysozyme; ▲ = rhodanese; □ = hexokinase; ■ = invertase; ▽ = transferrin.

TABLE I

THE CORRELATION CONSTANTS, A AND B, OF EQN. 3 FOR PROTEIN PARTITIONING IN THE PEG 8000–DEXTRAN T-500–WATER AND PEG 3400–POTASSIUM PHOSPHATE–WATER PHASE SYSTEMS

Protein	*Molecular weight*	*Isoelectric pH*	*PEG 8000–Dextran T-500*[a]		*PEG 3400–potassium phosphate*	
			A	*b*	*A*	*b*
Ribonuclease	12 600	9.3	− 6.7	− 30	−16.4	30
Lysozyme	13 900	11.0	−16.1	30	− 5.6	4
Trypsin	23 200	8.7	− 4.8	− 20	−12.9	30
Rhodanese	37 570	4.7	8.0	−180	−21.1	60
Transferrin	77 000	5.9	1.1	−190	−47.3	120
Hexokinase	102 000	4.7	11.9	−190	−31.5	90
Invertase	270 000	4.0	17.3	− 39	−46.9	130

[a] System contains 0.01 *m* potassium phosphate buffer, pH 7.0.

Eqn. 3 was tested by partitioning seven proteins in two types of aqueous two-phase systems. Figs. 1 and 2 represent the partitioning data for three low-molecular-weight proteins and four high-molecular-weight proteins, respectively. The system utilized was PEG 8000–Dextran T-500–water at 4°C. Similarly, in Fig. 3, the same seven proteins have been partitioned in the system composed of PEG 3400–potassium phosphate–water at 20°C. The values of A and b for each of the proteins in the two systems as obtained by unweighted least squares fitting of eqn. 3, along with protein molecular weight and isoelectric pH, are presented in Table I. It should be pointed out that the A values for ribonuclease, lysozyme, and trypsin were found to be −9.0, −13.4 and −6.1, respectively, when correlated according to eqn. 1[17]. These values differ slightly from those reported in Table I due to the equation of regression.

Examination of Fig. 1 reveals that, although the regression lines are not perfectly horizontal, the second term of eqn. 3 appears to be small compared to the first term (the intercept, A) for the low-molecular-weight proteins. Since the low-molecular-weight proteins in the PEG–dextran system partitioned according to eqn. 1[17], then b will be small, and the plot of eqn. 3 will approximate a horizontal line.

In Fig. 2, the linear relationship of eqn. 3 was tested in the PEG–dextran system for the high-molecular-weight proteins, rhodanese, hexokinase, invertase and transferrin. The linearity obtained for each of the proteins suggests that the addition of the second degree term was appropriate.

The partitioning data for the seven proteins in the PEG–phosphate system was correlated according to eqn. 3 and is presented in Fig. 3. The linear relationships for all of the proteins verify the applicability of eqn. 3 to protein partitioning in the PEG–salt system. Since the PEG–salt systems are more economical than PEG–dextran two-phase systems for protein purification[2], the results should be useful for the selection of the proper phase system.

Although eqn. 3 must at present be considered empirical, a trend is observed when the A values for the proteins are compared with their molecular weights. The A term was found to be both a function of protein molecular weight and the interaction

of the protein with the polymers and water. Examination of the PEG–dextran data in Table I reveals that as protein molecular weight is increased, the A value shows an increasing trend. A similar trend is observed for the PEG–phosphate data where A, in general, becomes more negative as protein molecular weight is increased. However, a definite relationship can not be established between protein partitioning and molecular weight unless the protein–polymer and protein–water interaction can be measured. In addition to these interactions, the protein tertiary structure must be known at each tie of the phase diagram since the interactions will change with the three-dimensional structure of the protein. It also has been shown that the primary structure of a protein has an effect on partitioning behavior in PEG–phosphate system[19].

It should be pointed out that eqn. 3 is applicable over a region of the phase diagram where partitioning experiments are most frequently performed. When using eqn. 3, the question arises as to what happens when $w_1'' - w_1' = 0$, *i.e.*, the plait point is reached, or when $w_1'' - w_1'$ becomes very large, *i.e.*, far removed from the plait point. At the plait point, the composition of the two phases is identical, and the partition coefficient is unity. Therefore, $\ln K/(w_1'' - w_1') = 0/0$, and is undefined. However, according to eqn. 3, it can be seen that $\ln K/(w_1'' - w_1')$ approaches A as $w_1'' - w_1'$ approaches zero. To verify whether this limit is true, partition experiments must be performed close to the plait point. At present, no such data exists in the literature due to the sensitivity of the two-phase systems near the plait point, and the closeness of the K values to unity. Similarly, when $w_1'' - w_1'$ becomes large, $\ln K/(w_1'' - w_1')$ should large. However, partitioning far removed from the plait point is difficult to perform due to the high viscosity of the phases, limited solubility of the protein at high polymer concentrations, and the problem of denaturation and precipitation at the interface.

CONCLUSIONS

Based on the relationship of eqn. 3, an empirical equation has been presented for correlating protein partitioning in PEG–dextran–water and PEG–potassium phosphate–water two-phase systems at pH 7.0. The relationship was found to apply to the seven proteins partitioned in the above two-phase systems. Future work involves applying the equation to other aqueous two-phase systems, and varying environmental parameters such as temperature, pH and ionic composition.

ACKNOWLEDGEMENT

This research was supported by the National Science Foundation Grant Nos. EET-8708839 and CBT-8702912.

REFERENCES

1 P.-Å. Albertsson, *Partition of Cell Particles and Macromolecules*, Wiley, New York, 3rd ed., 1986.
2 H. Walter, D. E. Brooks and D. Fisher, *Partitioning in Aqueous Two-Phase Systems—Theory, Methods, Uses and Applications to Biotechnology*, Academic Press, Orlando, FL, 1985.
3 P.-Å. Albertsson, S. Sasakawa and H. Walter, *Nature (London)*, 228 (1970) 1329.
4 P.-Å. Albertsson, *Partition of Cell Particles and Macromolecules*, Wiley, New York, 2nd ed., 1971.
5 G. Johansson, *Biochim. Biophys. Acta*, 221 (1970) 387.

6 V. P. Shanbhag and C. G. Axelsson, *Eur. J. Biochem.*, 60 (1975) 17.
7 B. Yu Zaslavsky, L. M. Miheeva, N. M. Mestechkina, V. M. Pogorelov and S. V. Rhogozhin, *FEBS Lett.*, 94 (1978) 77.
8 H. Hustedt, K. H. Kroner, W. Stach and M.-R. Kula, *Biotech. Bioeng.*, 20 (1978) 1989.
9 P.-Å. Albertsson, A. Cajarville, D. E. Brooks and F. Tjerneld, *Biochim. Biophys. Acta*, 926 (1987) 87.
10 P. J. Flory, *J. Chem. Phys.*, 9 (1941) 660.
11 M. L. Huggins, *J. Chem. Phys.*, 9 (1941) 440.
12 J. N. Baskir, T. A. Hatton and U. W. Sutter, *Macromolecules*, 20 (1987) 1300.
13 J. M. H. M. Scheutjens and G. J. Fleer, *J. Phys. Chem.*, 83 (1979) 1619.
14 J. M. H. M. Scheutjens and G. J. Fleer, *J. Phys. Chem.*, 84 (1980) 178.
15 R. S. King, H. W. Blanch and J. M. Prausnitz, *AIChE J.*, 34 (1988) 1585.
16 E. Edmond and A. G. Ogston, *Biochem. J.*, 109 (1968) 569.
17 A. D. Diamond and J. T. Hsu, *Biotech. Bioeng.*, 34 (1989) 1000.
18 A. D. Diamond and J. T. Hsu, *Biotechnol. Tech.*, 3 (1989) 119.
19 A. D. Diamond, X. Lei and J. T. Hsu, *Biotechnol. Tech.*, 3 (1989) 271.
20 B. Yu. Zaslavsky, L. M. Miheeva, G. Z. Gasanova and A. U. Mahmudov, *J. Chromatogr.*, 403 (1987) 123.

Journal of Chromatography, 513 (1990) 145–158
Elsevier Science Publishers B.V., Amsterdam

CHROM. 22 395

Investigation of the reversed-phase high-performance liquid chromatographic ligand-exchange retention mechanism on a triamine stationary phase

THEODORE R. KOZIOL[a] and MARY LYNN GRAYESKI*
Department of Chemistry, Seton Hall University, South Orange, NJ 07079-2694 (U.S.A.)
(First received July 18th, 1988; revised manuscript received February 7th, 1990)

ABSTRACT

A tridentate ligand, trimethoxysilylpropyldiethylenetriamine, was bound to silica and studied as a stationary phase for reversed-phase ligand-exchange chromatography. The tridentate stationary phase "triamine" yielded more stable metal complexes, *i.e.*, better metal loading efficiencies than previously reported diamine and monoamine stationary phases. This triamine packing with its enhanced metal loading properties was evaluated to identify the key factors that affect solute retention and selectivity. Mobile phase properties like buffer ionic strength and metal concentration greatly affected retention, while type of metal, *i.e.*, Zn^{II}, Cd^{II}, Hg^{II}, Cu^{II} or Ni^{II} greatly affected selectivity. The choice of mobile phase organic modifier significantly affected both retention and selectivity. Methanol–water mobile phases elicited relatively little metal binding per triamine site, with Hg^{II}, Zn^{II}, Ni^{II} and Cd^{II} occupying 32, 9.5, 7.8 and 5.7%, respectively. Changing the organic modifier from methanol to acetonitrile provoked a dramatically different but consistent pattern of metal loading to the triamine. The ratio of loaded metal with the acetonitrile modifier was 2.3 ± 0.1 fold higher than that observed for the methanol modifier in each of the cases tested. Factors found to affect metal loading to the stationary phase were the type of metal and the mobile phase solvent. The loading of metals onto the silica-bound triamine correlated directly to metal basicity. The variety of solute selectivities obtained in this study indicate that the key solute–metal interactions are a function of metal and solute functional group basicities and the number and spacing of solute functional groups possessing lone-pair electrons capable of interacting with the metal. Retention can be greatly enhanced when multiple functional groups possessing donatable electrons are present: functionalities containing nitrogen, sulfur or oxygen. Ring-substituted nitrogen, sulfur or oxygen atoms *i.e.* piperdines, pyrimidines, purines, xanthines and triazoles, enhance retention more than non-ring-substituted functionalities, such as carboxylic and sulfonic acids. The presence of non-electron-

[a] Present address: Berlex Laboratories Inc., 110 East Hanover Avenue, Cedar Knolls, NJ 07927 U.S.A.

0021-9673/90/$03.50

donating functionalities in close proximity to strong interacting groups resulted in significant decreases in retention due to steric hindrance of solute lone-pair electrons to the metal coordination sphere. It is suggested that the mechanism of ligand-exchange retention on this triamine phase involves the reversible binding of a metal to the stationary phase followed by outer-sphere solute–metal complexation.

INTRODUCTION

In 1961, Helfferich[1] first introduced the term "ligand exchange" illustrating how metal ions (Cu^{I}, Cu^{II}, Ni^{II}, Ag^{I} and Co^{III}) when loaded onto an ion exchanger could separate or isolate ammonia, organic amines, polyhydric alcohols, olefins and anions of organic acids and amino acids by forming complexes of varying strengths with these metals. In ligand-exchange chromatography (LEC) the interaction between solute and stationary phase is accomplished primarily via the coordination sphere of the complex-forming metal ion. Reviews of early work in LEC have been published by Davankov and Semechkin[2], Walton[3], and Chow and Grushka[4].

Compounds amenable to separation by LEC include those which contain lone-pair electrons or π-orbitals, *e.g.*, isomers or homologues of organic compounds containing nitrogen, oxygen and sulfur. Examples of LEC separations of amino acids and peptides[5–10], nucleosides and nucleotides[11], olefins[12–15], heterocyclics[16,17] and aromatic amines[18,19] now appear in the literature.

The purpose of this work was first to identify an amine-based packing that could give enhanced ligand-exchange retention and selectivity over previously reported mono- and diamine packings; second, to study those parameters and conditions that affect retention and selectivity in reversed-phase LEC using a silica-bonded triamine stationary phase; and last to characterize the stationary ligand (triamine)–metal interaction and the stationary ligand–metal–solute interaction as influenced by metal type and mobile phase organic modifier.

The metal loading of the triamine stationary phase, expressed as the moles/gram of Cu^{II} loaded divided by the molar quantity of ligand per gram, was superior to either the mono- of diamine packings. The metal loading of Cu^{II} to each packing was approximately 0.1, 0.2 and 0.5 for the mono-, di- and triamine stationary phases, respectively. Chromatographic utility of the triamine was investigated by evaluating retention characteristics of compounds with various functional groups. Substituted naphthalenes, benzoic acids and compounds containing one or more heterocyclic nitrogen were chosen as study solutes. All solutes could be detected by UV without metal interference. The substituted naphthalenes were used to quantify the magnitude of the effect of different exocyclic and heterocyclic functionalities on LEC retention, the substituted benzoic acids were used to determine the effect of substitution of a non-ligand-exchanging group, and, finally, the substituted xanthines were used to elucidate the LEC retention mechanism.

The metals used in this study, Zn^{II}, Cd^{II}, Hg^{II}, $Ni^{II}$and Cu^{II}, were chosen based on their properties. The former three metals are water-soluble, have a wide range of basicities and represent a homologous series with filled *d*-shells. Consequently, the stereochemistry of the complexes of these metals will be based solely on considerations of size, electrostatic forces and covalent binding forces. Ni^{II} was chosen for study as it is

a water-soluble *d*-8 metal that contains a large crystal field component. The choice of these metals allowed the use of UV detection in the range 240–290 nm. An experiment was also conducted utilizing Cu^{II} because its use has been described extensively in the LEC literature.

EXPERIMENTAL

Chromatographic apparatus

A modular chromatographic system consisting of a WISP 710B (Waters Assoc., Milford, MA, U.S.A.) autosampler, Model 400 solvent-delivery system (Kratos Analytical, Ramsey, NJ, U.S.A.), Model 773 variable-wavelength detector (Kratos), normally at 254 nm, and an HP 3388 integrator–computer (Hewlett-Packard, Palo Alto, CA, U.S.A.) was used. The pH of aqueous solutions was determined using a digital Orion pH meter. To avoid baseline instability from variation in temperature columns were jacketed at 30 ± 1°C using a column oven (Jones Chromatography, U.K.).

Reagents and chemicals

Reagent-grade trimethoxysilylpropyldiethylenetriamine was obtained from Petrarch (Bristol, PA, U.S.A.). The 10-μm irregular silica gel of 60 Å pore diameter and 500 m^2/g surface area, Polygosil 60-10 (Macherey-Nagel), was obtained from Ace Scientific (East Brunswick, NJ, U.S.A.). Metal salts and buffers were obtained from Aldrich (Milwaukee, WI, U.S.A.). The solvents used for HPLC were obtained from Burdick & Jackson (Muskegon, MI, U.S.A.). All xanthines were kindly supplied by Berlex Labs. (Cedar Knolls, NJ, U.S.A.). The remaining solutes were obtained from Aldrich or Sigma (St. Louis, MO, U.S.A.).

Preparation of bonded phase

A 250-ml aliquot of toluene was added to a 500-ml round-bottom flask and heated with slow stirring. Once the temperature of the toluene reached 50°C, 50.00 g of Polygosil 60-10 silica gel were slowly added to the flask. Following the addition of the silica gel, a 1.00-ml aliquot of distilled water was added to the flask. The temperature was increased to allow azeotropic distillation of all water and *ca.* 50 ml of toluene thereby obtaining dry toluene and silica.

The reaction mixture was allowed to cool to 60°C with constant stirring. A 25.8-ml aliquot of trimethoxypropyldiethylenetriamine was added to the flask. The reaction mixture was refluxed for 20 h with constant stirring. At the conclusion of the reaction the mixture was cooled to room temperature and the toluene decanted. The silica-bonded triamine was washed with *ca.* 1 l of chromatographic-grade methanol and dried for 12 h at 70°C in a vacuum oven. The phase was slurry-packed into 15 cm × 4.6 mm I.D. stainless-steel columns.

Measurement of metal loading

The measurement of metal breakthrough volume was determined colorimetrically using a dye solution containing a 0.2 mg/ml solution of pyridine-2-azo-*p*-dimethylanaline (Sigma). The mobile phase was concomitantly monitored at 210 nm (290 nm for nickel) during metal loading.

TABLE I

METAL LOADING ON THE TRIAMINE PHASE

% = mole% of triamine sites occupied by metal.

Mobile phase	*Loading*							
	Ni^{II}		Zn^{II}		Cd^{II}		Hg^{II}	
	mol/g × 10^{-5}	%	*mol/g* × 10^{-5}	%	*mol/g* × 10^{-5}	%	*mol/g* × 10^{-5}	%
Water–methanol (65:35, v/v)	5.1	7.8	6.3	9.5	3.8	5.7	15	23
Water–acetonitrile (1:1, v/v) containing 0.1 *M* ammonium acetate	15	23	34	52	1.5	2.5	–	–

Mobile phase metal content and detection sensitivity

Solute sensitivity using UV detection at 254 nm was affected only when either Cu^{II} or Hg^{II} was present in the mobile phase. Hg^{II} mobile phases were operated at 268 nm where the metal has a lower absorption band. Because of the strength of the Trien–Cu^{II} complex, columns loaded with Cu^{II} could be operated without metal in the mobile phase for up to 4 h.

RESULTS AND DISCUSSION

Characterization of the triamine stationary phase

Based on C, H and N analysis, the surface coverage of the triamine to the Polygosil 60-10 was calculated to be 1.3 μmol/m^2, with $6.57 \cdot 10^{-4}$ mol triamine per g packing or a 13.4% triamine loading.

The triamine stationary phase dissociation constants were determined by titration. Two pK_a values were observed in the 9.5–10 range while the third was observed in the acidic range of 4.2. For steric reasons the latter pK_a was attributed to the central amine of the triamine. These numbers are in rough agreement with those reported for a similar compound, 1-amino-2-(2-aminoethyl)amino ethane: 9.9, 9.1 and 4.3 (ref. 20).

Metal loading on triamine stationary phase

The extent of loading of the triamine sites at equilibrium with a given metal were calculated for the mobile phases and are presented in Table I. The methanol–water mobile phases elicited relatively little metal binding per triamine site, with Hg^{II}, Zn^{II}, $Ni^{II}$and Cd^{II} occupying 23, 9.5, 7.8 and 5.7%, respectively. The loading of the above metals onto the triamine from methanolic mobile phase was proportional to the basicity of the metal.

Changing the organic modifier from methanol to acetonitrile provoked a dramatically different but consistent pattern of metal loading to the triamine. Again, the extent of metal loading onto triamine sites followed the metal basicity in all cases. Interestingly, the ratio of metal loaded with the acetonitrile modifier was 2.3 ± 0.1 fold higher than that observed for the methanol modifier in each of the cases tested.

The volume of mobile phase for metal breakthrough was determined by appearance of metal in the effluent. At that point, each metal was at equilibrium for a given mobile phase except for Ni^{II} in methanol which continued to bind for 48 ml.

The triamine–metal complexes, except in the case of Cu^{II} where a fairly stable complex was formed, were fairly weak and easily reversed by passing through a mobile phase without metal. All the *d*-10 metals tested eluted from the triamine stationary phase at essentially the same rate. The metals possessing unfilled *d*-orbitals and more rigid coordination formed the more stable complexes owing to lower exchange rate of metal–triamine ligands with mobile phase ligands.

Following the use of an LEC mobile phase, a column was washed with approximately fifty column volumes of an acidic mobile phase, 35:65, (v/v) acetonitrile–water containing 5 ml glacial acetic acid.

Triamine as an ion exchanger

For proper assessment of the solute functional group effect in LEC, solute–

TABLE II

CAPACITY FACTORS OF SUBSTITUTED NAPHTHALENES AND OTHER COMPOUNDS ON THE TRIAMINE PHASE OPERATED IN THE ION-EXCHANGE AND LIGAND-EXCHANGE MODES

Chromatographic conditions: 15 cm × 4.6 mm I.D. triamine column; mobile phase, methanol–water (35:65, v/v) containing 0.004 *M* ammonium acetate or 0.004 *M* metal (as acetate or chloride), pH 6.9; flow-rate, 2.0 ml/min; UV detection, 254 nm.

Solute	*Abbreviation*	*No metal (II)*	Cd^{II}		Zn^{II}		Ni^{II}		Hg^{II}	
			k'	*k''*	*k'*	*k''*	*k'*	*k''*	*k'*	*k''*
1-Naphthylamine	N-AM	1.09	1.18	0.08	1.15	0.06	1.15	0.06	1.50	0.38
1-Naphthoic acid	N-COOM	5.18	11.6	1.2	7.0	0.35	12.1	1.3	4.83	0.00
1-Naphthalenesulfonic acid	NSA	4.91	8.0	0.63	5.07	0.03	9.73	0.98	3.10	0.00
8-Aminonaphthalenesulfonic acid	ANSA	7.43	17.9	1.4	8.63	0.16	34.5	3.6	2.75	0.00
Quinoline	QIN	1.00	1.13	0.13	1.85	0.85	1.15	0.15	1.72	0.72
Cinnoline	CIN	0.94	1.10	0.17	1.22	0.30	1.37	0.46	1.30	0.38
Quinazoline	QAZ	0.88	1.03	0.17	1.47	0.67	1.05	0.19	1.42	0.61
Quinoxaline	QOX	0.88	1.00	0.14	1.08	0.23	1.03	0.17	1.02	0.16
8-Hydroxyquinoline	HQIN	1.75	7.80[a]	3.5	17.6[a]	9.1	6.57[a]	2.8	Inf.	Inf.
p-Aminobenzoic acid	PABA	4.33	10.9	1.6	11.9	1.7	13.3	2.1	6.5	0.50

[a] Peak was very broad but symmetric.

stationary phase interaction in the ion-exchange mode (mobile phase minus metal) was established first. A series of substituted naphthalenes were injected into the HPLC system operated in the ion-exchange mode as presented in Table II.

Introduction of the functionalities hydroxy, amino, cyano and aldehyde to the naphthalene backbone contributed little to retention on the triamine when operated in the anion-exchange mode. Furthermore, naphthalenes with single or multiple heterocyclic nitrogen substitutions were generally less retained than naphthalene mainly because the heterocyclic naphthalenes and the triamine possess common functionalities. Predictably, significant increases in retention were observed when anions such as carboxylic acids and sulfonic acids are substituted onto naphthalene.

Triamine as a ligand exchanger

Study of substituted naphthalenes and similar compounds. The capacity factors (k') of the substituted naphthalenes on the triamine phase, operated in the ligand-exchange mode, were determined with the mobile phase containing Cd^{II}, Zn^{II}, Ni^{II} or Hg^{II} (Table II). In order to separate the pure solute ligand-exchange retention effects from those inherent in the silica-bonded triamine alone (*i.e.* no metal present) a so-called ligand-exchange capacity factor, k'', was calculated for each solute as follows:

$$k'' = \frac{k'(\mathrm{LE}) - k'(\mathrm{IE})}{k'(\mathrm{IE})} \tag{1}$$

where k'(LE) is the capacity factor of a solute *versus* a non-retained species when a metal is present in the mobile phase and k'(IE) is the capacity factor of a solute *versus* a non-retained species when no metal is present in the mobile phase. Using eqn. 1 the "pure" ligand-exchange effects on a solute can be evaluated. If ligand-exchange retention was less than ion-exchange retention, k'' was defined as zero. Solutes with $k'' \leqslant 0.2$ for all metals (naphthalene, 1-naphthol, 1-cyanonaphthalene, 1-naphthaldehyde and 1,4-naphthoquinone) have been omitted from Table II.

Where single functional groups are concerned, the difference in basicity of solute and metal was the key determinant to retention. In the case of molecules containing an alcohol, aldehyde or quinone functionality, the basic metals Ni^{II}, Cd^{II} and Zn^{II} had essentially no effect on ligand-exchange retention, and cyano and amino functionalities show very minor effects. Conversely, these "basic" functional groups displayed a much greater affinity for, and were retained in the presence of acidic Hg^{II}.

Modest retention increases were noted for solutes with various heterocyclic nitrogen ring substitutions. The difference in the basicity of solute and metal appears to be the controlling factor to each ligand-exchange interaction. The role of metal coordination sphere size and "fit", however, also appear to influence retention. In the case of Zn^{II} and Hg^{II} complexation, the fit also appears better for quinazoline while quinoline appears better for Cd^{II}.

Study of substituted benzoic acids. The ligand-exchange retention properties of benzoic acids substituted at the *p*-position were studied on the triamine phase loaded with Cd^{II} in order to quantify the effect on retention of substitution of a non-ligand exchanging group away from the exchanging functionality. Alkyl substitution at the *p*-position of C_1–C_5 had no significant effect on retention. Also, mono-, di- or

trimethyl substitution close to the ligand-exchanging carboxyl group (2,4-, 2,5-, 2,6- or 2,4,6-methyl substitution) had little effect on retention. Steric hindrances to the carboxy functionality were not sufficiently established by methyl substitutions near the acidic carboxyl group.

Study of substituted xanthines. A series of substituted xanthines were studied to further elucidate the retention mechanism in LEC (Table III). Essentially no retention was observed for these solutes when injected into the system operated in the ion-exchange mode; therefore, retentions observed in LEC could only be attributed to metal–solute interactions.

The xanthine backbone is rigid and essentially planar[21–23], allowing the effect of the solute in metal–solute interactions to be more easily interpreted. Also, deprotonated xanthine bases exhibit a variety of nucleophilic sites which do not differ significantly in their electronic properties[24]. The literature[25–30] illustrates that metal–xanthine binding, via inner-sphere complexation, takes place mainly in the imidizole ring, at atoms N-7 and N-9, under basic conditions where the heterocyclic nitrogens are not protonated. Stability studies of theophylline–Zn^{II} complexes[31] have shown that the complex rapidly breaks down below a pH of 9.0 where atom N-7 is protonated.

The LEC retention of xanthines within each metal studied appears to be controlled by electrostatic effects between multiple functional group interactions and the metal. Xanthine was the most retained solute in all cases; in fact, the interaction was so strong that it only eluted in the ligand-exchange mode on the lightly loaded Ni^{II}–triamine. Based on molecular distances between functionalities of xanthine possessing lone-pair electrons, the molecule is capable of ten metal interactions at atoms N-7 O-6–N-7, N-7–N-9, N-9, N-3–N9, N3, N-1, O-6–N-1, O-2–N-1 and O-2–N-3 (ranked in order of importance).

TABLE III

RETENTION OF SUBSTITUTED XANTHINES ON THE TRIAMINE PHASE USING ACETONITRILE–BUFFER MOBILE PHASES CONTAINING VARIOUS METALS

Chromatographic conditions: 15 cm × 4.6 mm I.D. triamine column; mobile phase, acetonitrile–water (3:7, v/v) containing 0.0667 *M* ammonium acetate, 0.133 *M* sodium chloride and 0.004 *M* metal acetate, pH 6.9; flow-rate, 2.0 ml/min, detection, UV at 254 or 268 nm (for Hg). In the study of Hg^{II} the chloride salt was used. The Cu^{II} data were collected by first pre-loading the column with metal then switching to a mobile phase minus metal; the system was stable for several hours.

	k'				
Solute	*No metal(II)*	*Ni^{II}*	*Zn^{II}*	*Hg^{II}*	*Cu^{II}*
Xanthine	0.19	5.0	DNE[a]	DNE	DNE
1-Methylxanthine	0.12	3.2	DNE	16.0	DNE
3-Methylxanthine	0.01	1.2	21.0	7.30	DNE
3,7-Dimethylxanthine	0.01	0.34	0.54	1.80	1.10
1,3-Dimethylxanthine	0.01	0.87	14.7	2.40	17.6
1,7-Dimethylxanthine	0.01	0.60	DNE	1.86	2.09
1,3,7-Trimethylxanthine	0.00	0.14	0.22	0.61	0.46

[a] DNE: solute did not elute in 60 min.

In the xanthine molecule, the most important binding site, atom N-7, is only partially ionized as compared to the other substituted xanthines. This is advantageous to stronger binding at the N-7 atom with concomitant O-6 hydrogen bonding to other ligands, probably water or solvent, in the metal coordination sphere. The N-9 atom can be considered to moderately affect retention, while binding influences from atoms N-1, N-3 and O-2 are considered to be small. The N-1 position is protonated and sterically hindered by the two neighboring oxo functionalities, while N-3 is also protonated.

The effect of changing mobile phase metal on the retention of substituted xanthines was also studied in a methanol–water mobile phase (Table IV). Substituted xanthines were slightly retained on the triamine phase operated in the ion-exchange mode. The slight retention by ion exchange was caused by the poor solubilities of the xanthines in this mobile phase. Retention was, therefore, achieved by the aversion of the solute for the mobile phase which allowed longer interaction with the stationary phase.

TABLE IV

RETENTION OF SUBSTITUTED XANTHINES ON THE TRIAMINE PHASE USING METHANOL–WATER MOBILE PHASES CONTAINING VARIOUS METALS

Chromatographic conditions: 15 cm × 4.6 mm I.D. triamine column; mobile phase, methanol–water (35:65, v/v) containing either no metal or 0.005 *M* metal acetate, pH 6.9; flow-rate, 2.0 ml/min; detection, UV at 254 or 268 nm (for Hg). In the study of Hg^{II} the chloride salt was used.

	k'				
Solute	*No metal(II)*	*Zn^{II}*	*Cd^{II}*	*Ni^{II}*	*Hg^{II}*
Xanthine	1.26	DNE[a]	DNE	DNE	DNE
1-Methylxanthine	0.85	DNE	DNE	24.2	DNE
3-Methylxanthine	0.61	DNE	2.31	4.45	DNE
3,7-Dimethylxanthine	0.32	0.55	0.39	0.43	5.87
1,7-Dimethylxanthine	0.37	DNE	1.00	1.88	14.4
1,3-Dimethylxanthine	0.50	9.86	1.51	3.07	0.43
1,3,7-Trimethylxanthine	0.32	0.32	0.33	0.36	0.89
1,3,7,9-Tetramethylxanthine	0.32	0.32	0.36	0.36	0.44

[a] DNE: solute did not elute in 60 min.

Spectroscopic studies of xanthine and metals were carried out in the mobile phases tested in order to determine the mechanism of complexation between the various metals and the xanthine at pH 6.9. Based on the experimental results, the possibility of solute–metal inner-sphere complexation was ruled out. It can then be assumed that the electron transfer process in reversed-phase LEC on the triamine phase involves intact coordination spheres. The reactant ions do not come into intimate contact but are separated by ligands at the time of electron transfer, *i.e.* outer-sphere complexation. This result would be expected based on the previously reported xanthine–metal complexation data and because almost all the nitrogens are ionized.

Study of other chromatographic parameters affecting LEC retention on the triamine phase

Mobile phase metal concentration. The effect of varying mobile phase Zn^{II} concentration from 0.0002 to 0.02 *M* on a set of test solutes was determined using Zn^{II} as the acetate salt in the mobile phase. The ionic strength of the mobile phase was kept constant using ammonium acetate. Dramatic increases in solute retention were observed accompanied by changes in separation factor (Fig. 1). Over a limited range of Zn^{II} concentrations, *e.g.* 2–8 m*M*, a linear relationship was observed between the molar concentration of metal and the *k'* of a solute.

Ionic strength. The effect of mobile phase ionic strength on retention of solutes on the triamine phase was evaluated by varying the amount of ammonium acetate buffer in acetonitrile–water (1:1, v/v) containing 0.004 *M* Zn^{II} at pH 6.9. Increasing ionic strength of the mobile phase from 0.13 to 0.23 and then to 0.33 resulted in approximately a 2.5-fold loss in capacity factor per increment for the solutes 8-chlorobenzotriazole, 1,7-dimethylxanthine and theophylline.

To evaluate the effect of counter-ion type on retention, the ionic strength of a mobile phase containing Zn^{II} was held constant while a portion of the ammonium acetate buffer was replaced with sodium chloride. Significantly increased retention was observed with the weaker chloride anion.

Mobile Phase pH. pH 6.8–6.9 was chosen for these comparative ligand-exchange studies based on the criteria that a common mobile phase had to be found that could solubilize all metals under investigation. Studies on the effect of mobile phase pH on the ligand-exchange retention based on extent of solute ionization have been conducted by Lindner *et al.*[32].

Column quality under LEC conditions

Column stability and reproducibility. In order to test column stability and column reproducibility, a column was selected from each of three different triamine reaction

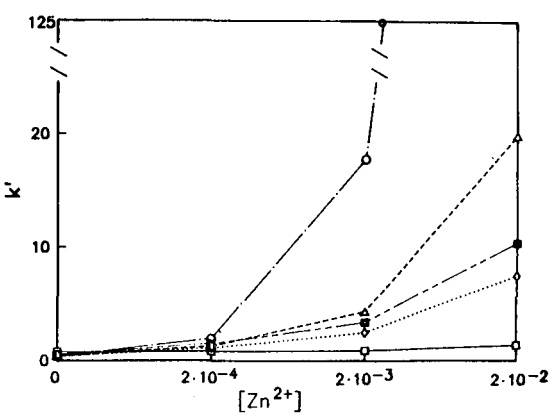

Fig. 1. Effect of metal concentration (wide range). Chromatographic conditions: 15 cm × 4.6 mm I.D. triamine column; mobile phase, acetonitrile–water (35:65, v/v) containing 0.2 *M* ammonium acetate and various concentrations of zinc acetate, pH 6.9; flow-rate, 2.0 ml/min; detection, UV at 254 nm. ◘ = 3-Methylxanthine; ○ = 1,7-dimethylxantine; △ = 5-chlorobenzotriazole; ◇ = theophylline; □ = *p*-aminobenzoic acid.

batches and operated with various mobile phases and metals. A test solute, *p*-aminobenzoic acid, was injected into a mobile phase of acetonitrile–water (1:1, v/v) containing 0.1 *M* ammonium acetate at pH 6.9 onto each column before and after use with each mobile phase containing metal. The k' of the test solute did not change (range 6.87–6.97), illustrating that not only could each metal be removed, but also no column degradation took place.

Chromatographic quality. Chromatograms of *p*-aminobenzoic acid under the ion-exchange and ligand-exchange chromatographic conditions illustrated in Table II are shown in Fig. 2. The peak shapes shown for *p*-aminobenzoic acid are typical and represent a compound that had moderate increased capacity over the ion-exchange mode when chromatographed in the LEC mode. The number of theoretical plates (N), calculated by

$$N = 5.54\ [\text{retention time (s)}]/\text{peak width at half-height (s)}]^2,$$

observed for the solutes tested in Table II ranged from 1000 to 2000. Asymetry, assessed as tailing factor (calculated at 10% peak height: peak width front/peak width tail, generated from construction of perpendicular line from peak maximum), averaged approximately 0.8. The latest eluted solute, 8-aminonaphthalene sulfonic acid with $k' = 34.5$, exhibited a tailing factor of 0.34. The solute, 8-hydroxyquinaline, exhibited the poorest mass transfer characteristics of all compounds tested ($n = 10$). It

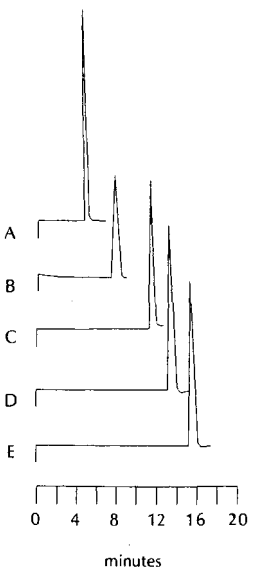

Fig. 2. Chromatograms of *p*-aminobenzoic acid when chromatographed in a common mobile phase containing different metals. Chromatographic conditions: 15 cm × 4.6 mm I.D. triamine column; mobile phase, methanol–water (35:65. v/v) containing 0.004 *M* ammonium acetate or 0.004 *M* metal (as acetate or chloride), pH 6.9; flow-rate, 2.0 ml/min; detection, UV at 254 nm. (A) No metal added to mobile phase; (B) mobile phase containing Hg: (C) mobile phase containing Cd; (D) mobile phase containing Zn, (E) mobile phase containing Ni.

is postulated that this compound can inner-sphere coordinate with the metals tested making it a poor candidate for LEC.

Application of LEC

The separation of xanthines has historically been a difficult task. In order to study the metabolism and pharmacokinetics of theophylline (1,3-dimethylxanthine) one must first chromatographically separate it from its metabolites as well as caffeine (1,3,7-trimethylxanthine). It is particularly diffficult to separate the metabolite 1,7-dimethylxanthine from its parent compound[31,33].

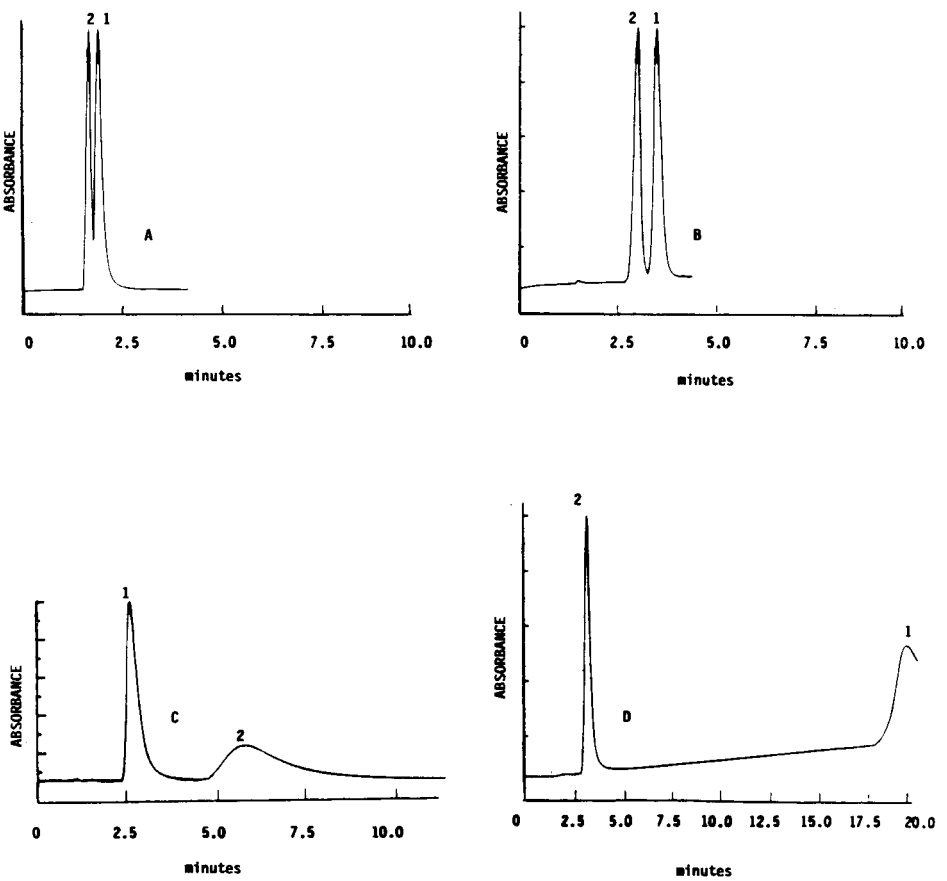

Fig. 3. Examples of ligand-exchange separations of 1,3-dimethylxanthine from 1,7-dimethylxanthine. Chromatographic conditions: 15 cm × 4.6 mm I.D. triamine column; mobile phase, acetonitrile–water (3:7, v/v) containing ammonium acetate and/or sodium chloride and 0.005 *M* metal acetate, pH 6.9; flow-rate, 2.0 ml/min; detection, UV at 254 or 268 nm (for Hg). Solutes, 1,3-dimethylxanthine (1) and 1,7-dimethylxanthine (2). (A) Mobile phase containing Ni, 0.1333 *M* sodium chloride and 0.0667 *M* ammonium acetate; (B) mobile phase containing Hg, 0.1333 *M* sodium chloride and 0.0667 *M* ammonium acetate; (C) mobile phase containing Zn and 0.2 *M* ammonium acetate; (D) mobile phase equilibrated with Cu, 0.1333 *M* sodium chloride and 0.0667 *M* ammonium acetate.

Using the LEC systems described in this paper, a wide range of selectivities can be attained for xanthines. Separation factors between theophylline and 1,7-dimethylxanthine in the methanol–water mobile phase were 1.51, 1.63, 33.5 and infinity for Cd^{II}, Ni^{II}, Hg^{II} and Zn^{II}, respectively, while separation factors in the acetonitrile–buffer mobile phase were 1.45, infinity, 1.3 and 8.4, for Ni^{II}, Zn^{II}, Hg^{II} and Cu^{II}, respectively.

Comparison of the separation factors obtained for the theophylline/1,7-dimethylxanthine separation for Ni^{II} and Hg^{II} loaded onto triamine when mobile phase organic solvent was changed from acetonitrile to methanol resulted in selectivity changes of 100 and 600%, respectively. These changes again illustrate the effect of solvent and the wide range of separations that are possible (Fig. 3).

CONCLUSION

The silica-bonded tridentate amine stationary ligand yields more stable metal complexes, resulting in better metal loading efficiencies, than previously reported bidentate and monodentate amine silica-bonded ligands studied in reversed-phase LEC.

LEC can be applied to routine, yet specific chromatographic separation problems encountered in the analytical laboratory. Compounds amenable to separation by LEC include those which contain lone-pair electrons or π-orbitals, *e.g.*, isomers or homologues of organic compounds containing nitrogen, oxygen and sulfur.

Solute–metal interactions in ligand-exchange chromatography are determined by factors such as the number of sites capable of donating electron pairs, the ionizability of each site, steric hindrances imposed by bound and/or neighboring functionalities, the hardness of a metal, the intermolecular distances between key functionalities and the ability of other ligands in the metal sphere to form hydrogen bonds to solute functionalities creating a more stable chelated outer-sphere complex.

Retention can be greatly enhanced when multiple functional groups possessing donatable electrons are present: N-, S- and O-containing functionalities. Ring-substituted N, S and O atoms, *i.e.*, piperidines, pyrimidines, purines and triazoles, enhance retention more than non-ring -substituted functionalities, such as carboxylic and sulfonic acids.

Key mobile phase factors affecting solute retention include the metal concentration, buffer ionic strength and percentage organic modifier, while solute selectivity is mainly governed by the choice of metal and organic modifier.

The mechanism of chromatographically useful ligand-exchange retention on the triamine phase is postulated to involve a process in which metal is reversibly "bound" to the stationary triamine phase through chelation of the metal coordination sphere to the amine functionalities of the triamine. This triamine–metal(II) complex can then interact with sterically unhindered functional groups containing lone-pair electrons according to the scheme

triamine ---- metal(II) **** solute,

where **** represents an outer-sphere attraction and ---- represents an inner-sphere coordination.

The limitations of reversed-phase LEC are related to the requirement that

a metal be present in the mobile phase. Consequently, practical considerations can include metal precipitation, limited UV detection and waste disposal.

REFERENCES

1 F. G. Helfferich, *Nature (London)*, 189 (1961) 1001.
2 V. A. Davankov and A. V. Semechkin, *J. Chromatogr.*, 141 (1977) 313.
3 H. F. Walton, *Sep. Purif. Methods*, 4 (1975) 189.
4 F. K. Chow and E. Grushka, *Anal. Chem.*, 50 (1978) 1346.
5 S. K. Lam and F. K. Grushka, *J. Liq. Chromatogr.*, 3 (10) (1980) 1579.
6 J. N. LePage, W. Lindner, G. Davies, D. Seitz and B. L. Karger, *Anal. Chem.*, 51 (1979) 433.
7 Y. A. Zolotarev, N. F. Myasoedov, V. I. Penkina, I. N. Dostovalov, O. V. Petrenik and V. A. Davankov, *J. Chromatogr.*, 207 (1981) 231.
8 A. Foucault, M. Claude and L. Oliveros, *J. Chromatogr.*, 185 (1979) 345.
9 V. A. Davankov, A. S. Bochkov, A. A. Kurganov, P. Roumeliotis and K. K. Unger, *Chromatographia*, 13 (1980) 677.
10 G. Gubitz, W. Jellenz and W. Santi, *J. Liq. Chromatogr.*, 4 (4) (1981) 701.
11 E. Grushka and F. Chow, *J. Chromatogr.*, 199 (1980) 283.
12 E. A. Emken, J. C. Hartman and C. R. Turner, *J. Am. Oil Chem. Soc.*, 55 (1978) 561.
13 B. Vonach and G. Schomburg, *J. Chromatogr.*, 149 (1978) 417.
14 D. Tabak and M. N. Dos Santos, *J. Chromatogr.*, 106 (1975) 471.
15 R. R. Heath, J. H. Tumlinson, R. E. Doolittle and A. T. Proveaux, *J. Chromatogr. Sci.*, 13 (1975) 380.
16 N. H. C. Cooke, R. L. Viavattene, R. Eksteen, W. S. Wong, G. Davies and B. L. Karger, *J. Chromatogr.*, 149 (1978) 391.
17 R. Vivilecchia, M. Thiebauld and R. W. Frei, *J. Chromatogr. Sci.*, 10 (1972) 411.
18 D. Kunzru and R. W. Frei, *J. Chromatogr. Sci.*, 12 (1974) 191.
19 F. K. Chow and E. Grushka, *Anal. Chem.*, 49 (1977) 1756.
20 D. D. Perrin (Editors), *Dissociation Constants of Organic Bases in Aqueous Solution*, Butterworths, London, 1965.
21 M. J. Gardner, F. X. Smith and E. Shefter, *J. Pharm. Sci.*, 72 (1983) 346.
22 E. Shefter and P. Sackman, *J. Pharm. Sci.*, 60 (1971) 282.
23 E. Schefter, *J. Pharm. Sci.*, 58 (1969) 710.
24 R. Bonaccoral, A. Pullman, E. Scrocco and J. Tomasi, *Theor. Chim. Acta*, 24 (1972) 51.
25 G. M. Blackburn and A. W. Johnson, *J. Chem. Soc.*, (1960) 4347.
26 A. R. Norris, R. Kumar, E. Buncel and A. L. Beauchamp, *J. Inorg. Biochem.*, 21 (1984) 277.
27 R. Weiss and H. Venner, *Hoppe-Seyler's Z. Physiol. Chem.*, 340 (1965) 138.
28 D. J. Salda, T. J. Kistenmacher and L. G. Marzilli, *Inorg. Chem.*, 15 (1976) 2783.
29 A. T. Tu and M. J. Heller, *Metal Ions in Biological Systems*, Vol. I, Marcel Dekker, New York, 1974.
30 F. Allaire and A. L. Beauchamp, *Can. J. Chem.*, 62 (1984) 2249.
31 K. T. Muir, J. H. G. Jonkman, D. Tang, M. Kunitan and S. Riegelman, *J. Chromatogr.*, 221 (1980) 85.
32 W. Lindner, J. N. LePage, G. Davies, D. E. Seitz and B. L. Karger, *J. Chromatogr.*, 185 (1979) 323.
33 J. J. Grygiel, M. W. Lindon, M. B. Wing, J. Farkas and D. J. Burkett, *Clin. Pharmacol. Ther.*, 26 (1979) 660.

Journal of Chromatography, 513 (1990) 159–166
Elsevier Science Publishers B.V., Amsterdam

CHROM. 22 484

Evaluation of an alternating current plasma emission detector for high-performance liquid chromatography

LUIS A. COLÓN and EUGENE F. BARRY*
Department of Chemistry, University of Lowell, 1 University Avenue, Lowell, MA 01854 (U.S.A.)
(First received November 14th, 1989; revised manuscript received March 5th, 1990)

ABSTRACT

The details of construction and operation of an alternating current plasma (ACP) detector supported with helium gas for reversed-phase high-performance liquid chromatography is described. The system is evaluated as a selective detector for the determination of organomercury compounds. The chromatographic eluent is introduced into the plasma by means of a frit nebulizer and the plasma can tolerate the nebulization of 100% methanol without extinguishment. Detection limits of methylmercury chloride and ethylmercury chloride were found to be 4.5 and 2.2 ng Hg/sec, respectively. In the nanogram to microgram mass range studied the precision was found to be less than 10% (relative standard deviation). The detection of organomercurials in complex sample matrices illustrates the selectivity of the ACP detector.

INTRODUCTION

The advantages of high-performance liquid chromatography (HPLC) in combination with plasma emission detectors has been described during the last decade[1–4]. One attractive feature of this type of detectors is their capability for elemental speciation permitting the determination of organic molecules containing a specific heteroatom in a very complex sample matrix, where resolution of a desired compound and matrix interferences may affect its detection. The choice of a suitable detector is one area that should be considered for the utilization of HPLC for speciation purposes[5].

There are three principal plasma sources that have been evaluated as specific detection modes in HPLC: direct current plasma (DCP), inductively coupled plasma (ICP) and microwave-induced plasma (MIP). Most studies have focused on the combination of HPLC with ICP and many applications have been reported[6–11]. The introduction of the direct injection nebulizer (DIN) has made the technique more attractive[12,13]. The extensively reported fact that the DCP is compatible with a wide variety of solvents has facilitated its combination with HPLC[14–17]. However, the interface of HPLC and MIP has been more challenging because of the low tolerance of the MIP towards organic solvents typically used in HPLC although this situation has

0021-9673/90/$03.50

been addressed by mixing the plasma gas with oxygen[18] and modification of the design of the discharge tube. In addition, this type of plasma can accommodate solutions containing up to 90% (v/v) methanol in water. More powerful and costly He-MIP (500-W) detectors have been also investigated[19,20]. A low power (100-W) He-MIP with a moving wheel sample transport-desolvation interface has also been described[21]. The aqueous solvent is evaporated with a nitrogen flow at elevated temperatures in order to reduce interferences due to the solvent. However, this device is in a preliminary stage and the effect of organic solvents was not reported.

In a recent communication our laboratory reported an alternating current plasma (ACP) detector for gas chromatography (GC)[22]. The self-seeding plasma could tolerate high mass flow-rates of organics without extinguishment. The performance of the ACP detector was comparable with that of the MIP detector for GC. The compatibility with large injected aliquots of organics strongly suggested the possibility of extending its application into HPLC as an inexpensive detector, simple in construction and operation. In this communication the interface and operation of the detector in tandem with HPLC in the reversed-phase mode are reported.

EXPERIMENTAL

Reagents

All the solvents used were HPLC grade. The organomercury compounds, methylmercury chloride (MMC) and ethylmercury chloride (EMC), were purchased from Morton Thiokol (Alfa Products, Danvers, MA, U.S.A.). Stock solutions were prepared by dissolving the appropriate amount of the organomercurial in methanol (J. T. Baker, Phillipsburg, NJ, U.S.A.). Subsequent solutions were prepared by serial dilution of the stock solutions.

Chromatographic equipment

Fig. 1 shows a schematic diagram of the components of the system used in this study. A Spectra-Physics solvent delivery system (Model SP8700, Spectra-Physics, San

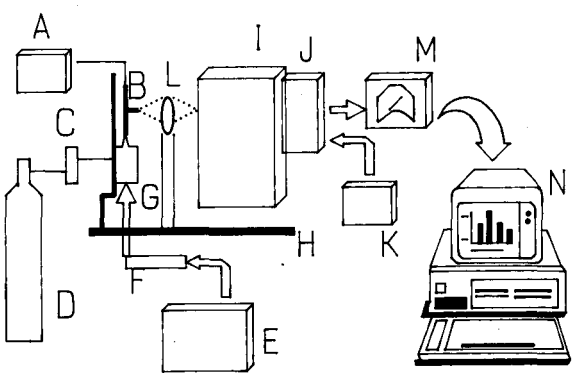

Fig. 1. Schematic diagram of the HPLC–ACP system. A = a.c. power supply; B = discharge tube; C = gas flow controller; D = solvents and solvent delivery system; F = HPLC column; G = nebulizer; H = optical bench; I = monochromator; J = PMT; K = PMT power supply; L = focussing lens; M = picoammeter; N = data acquisition system.

Jose, CA, U.S.A.) delivered the mobile phase to the sample loop injector (Model 7125, Rheodyne, Cotati, CA, U.S.A.) which was connected to a Hypersil ODS column, 100 × 4.6 mm I.D., 5 μm (Hewlett-Packard, Palo Alto, CA, U.S.A.). UV monitoring was performed using a TriDent detector (Perkin-Elmer, Norwalk, CT, U.S.A.).

Spectroscopic equipment

A single-beam McPherson grating monochromator EU700 (McPherson, Acton, MA, U.S.A.) was equipped with a R212 photomultiplier tube (Hamamatsu, Middlesex, NJ, U.S.A.) which was coupled to a voltage power supply (McPherson, Model 7640) and operated at −900 V. An optical bench was equipped with an adjustable optical mount and a 75-mm biconvex quartz lens (Oriel, Stratford, CT, U.S.A.) to focus the plasma into the monochromator with a slit height and width setting of 5 mm and 300 μm, respectively. For spectral background measurements, a slit width of 50 μm was selected. A picoammeter (Model 414s, Keithley Instruments, Cleveland, OH, U.S.A.) monitored the current generated by the photomultiplier tube. A mercury hollow cathode lamp (Perkin-Elmer) was employed to accurately select the analytical emission line (253.7 nm). Data acquisiton was achieved with the Chrom-1AT chromatography data acquisition board controlled by the Lab Calc software (Galactic Industries, Salem, NH, U.S.A.) in conjunction with a Zenith AT compatible microcomputer (Zenith Data Systems, St. Joseph, MI, U.S.A.). The Lab Calc software package provided data smoothing algorithms to reduce random noise and permitted selectable sampling rates. In this investigation a rate of 5 points per second was utilized which is more than adequate to define the peak shape in LC applications where peak widths are typically 15 to 60 s (ref. 13).

Discharge tube and interface operation

The discharge tube was constructed from quartz tubing, 6 mm O.D. × 4 mm I.D, and it was similar to that previously reported in our GC study[22]. The discharge tube was attached to an adjustable optical mount (Edmund Scientific, Barrington, NJ, U.S.A.) which was fastened to the optical bench. The plasma was generated across two copper electrodes (1 mm diameter) with an a.c. power supply, operated at 10 000 V, Furnace Ignition Transformer (France, Fairview, TN, U.S.A.). The gap between the electrodes was maintained at 13 mm (ref. 23).

A glass-frit nebulizer was used as the interface between the HPLC column and the ACP and a schematic of the interface is illustrated in Fig. 2. The design closely resembled that which has been used in other studies[24,25]. It consisted of a modified 15-ml Pyrex sintered glass funnel filter, 20 mm in diameter and 4.5–5.0 μm in porosity (Corning Glass, Corning, NY, U.S.A.). A 15 cm length of Flexon high-pressure tubing (0.063 in. O.D. × 0.007 in. I.D.) served as the connecting line from the column eluent to the glass frit. The volume of the chamber was approximately 5 ml. The upper arm of the modified funnel was connected to the bottom end of the PTFE tee union attached to the discharge tube. Helium flow of 6 l/min was introduced into the opposite side of the frit as the nebulizer gas and simultaneously supported the ACP. The drain of the nebulizer was closed to the environment allowing the fine mist produced to be transported toward the plasma. The largest droplets were removed and discarded through the drain to a closed waste collector.

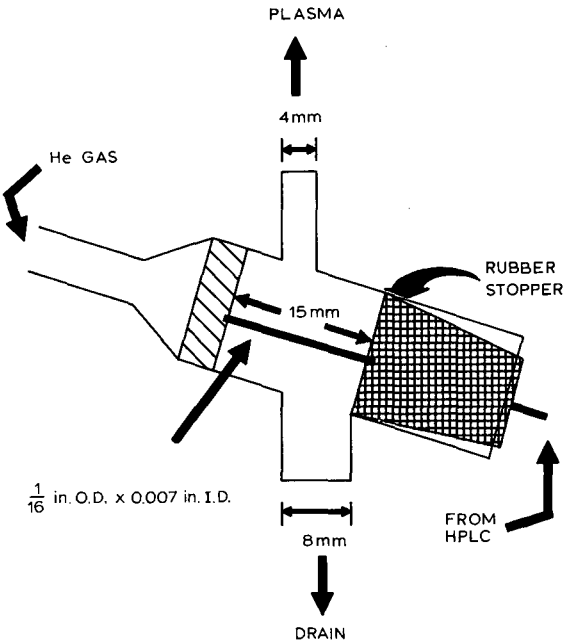

Fig. 2. Schematic of the glass-frit nebulizer.

RESULTS AND DISCUSSION

Interface

The frit nebulizer generates a very fine mist with droplet size distribution smaller than the pneumatic nebulizer[26] and greatly enhances the introduction of organic solvents to the plasma[25]. The nebulizer performed more favorably when the sintered glass disc was positioned in a vertical or angular orientation with respect to the discharge tube, as shown in Fig. 2, as opposed to the preferred horizontal position used with the ICP[24].

The inherently high efficiency of the frit nebulizer[24,25] and the small inner diameter of the transfer tube were responsible for small droplets of the nebulized solution to be deposited as small droplets on the walls of the transfer tube. After several minutes the droplets filled part of the transfer tube presenting disturbances to the plasma and even trapped most of the aerosol at flow-rates greater than 3 l/min. These problems were overcome by maintaining the transfer tube and the connection to the discharge tube at 100°C. Pressures up to 100 p.s.i. can be applied to the nebulizer without producing damage to the sintered glass frit. The ACP response showed a dependence on the gas flow-rate across the frit nebulizer. The maximum response was associated with a He gas flow-rate of 6 l/min delivered at a pressure of 78 p.s.i.

Plasma stability

The presence of organic solvents in the ACP increases the noise level of the

detector; therefore, the high-frequency random noise was digitally removed by smoothing the data once collected, improving signal to noise ratio. Since methanol and acetonitrile are the most commonly used organic modifiers in reversed-phase HPLC, the characteristics of the plasma were further studied with the binary mixtures of these solvents with water. The color of the plasma (pink-purple with the introduction of pure water) changed to a bluish green color when aqueous solutions of the organic solvents were introduced. This color change, resulting from CN molecular emission, became more intense with increasing concentration of the organic solvent. However, if increased oxygen levels are present in the plasma, such as is the case when aqueous solutions of methanol are introduced, decreasing cyanogen formation occurs and the more stable CO molecular species are formed instead resulting in decreased intensity of the bluish-green color[27]. The CN molecular species formation results from nitrogen impurities in the He gas, when acetonitrile is not used as the organic modifier. The ACP did not extinguish when pure methanol was nebulized into the plasma at a rate of 1 ml/min for a period of 30 min and the recorded baseline (noise) did not show any irregular perturbation. However, the introduction of aqueous mobile phase containing 10% acetonitrile did extinguish the plasma after 5 min. In addition, with acetonitrile entering the plasma in place of methanol, the formation of carbon species increases with a concurrent decrease in the amount of oxygen-containing species and results in the accumulation of combustion deposits in the vicinity of the plasma. Carbon deposition with acetonitrile was also observed on the walls of the discharge tube above the plasma plume but with methanol very little residue was noted in this vicinity.

Organomercury detection

The analytical emission line used throughout this study was the Hg(I) 253.7-nm line. In order to observe the influence of the mobile phase in the vicinity of the analytical line, a profile of the plasma emission was generated. No interference is observed at the wavelength corresponding to Hg(I) line.

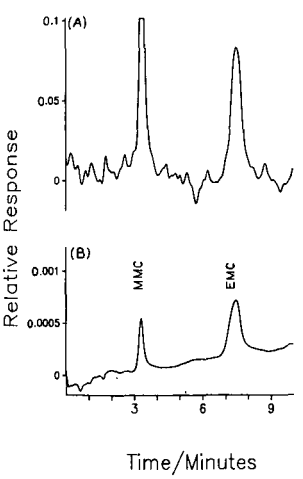

Fig. 3. Chromatograms of MMC (669 ng as Hg) and EMC (505 ng as Hg) with (A) ACP detection and (B) UV detection; mobile phase, 0.01% 2-mercaptoethanol in methanol–water (22:78); column, Hypersil ODS 5 (100 mm × 4.6 mm I.D.); flow-rate, 1.0 ml/min; injection volume, 25 μl; wavelength, 253.7 nm.

The HPLC–ACP chromatograms of MMC and EMC were monitored with a fixed-wavelength UV detector (254 nm) operated at its maximum output sensitivity. In Fig. 3 parallel chromatograms of MMC and EMC which clearly display the improved sensitivity of the ACP detector are presented.

Linearity and detection limits

Calibration plots for MMC and EMC were prepared by injecting six repetitive injections of known amounts into the HPLC–ACP system linearity of over three orders of magnitude for both probe solutes in the range studied was observed. Correlation coefficients of the log–log plots were 0.999 and 0.998 for MMC and EMC, respectively. Detection limits (D) were calculated based on the integrated baseline noise[6,28] and according to eqn. 1

$$D = 3\sigma/m \tag{1}$$

where σ refers to the standard deviation of the noise and m is the sensitivity. The sensitivity is defined as the slope of the calibration curve[29] multiplied by the peak width at 0.607 height of the analyte peak[30] to account for the capacity factor, k'. The detection limits for MMC and EMC, expressed in terms of elemental Hg, were calculated to be 4.5 ng/s and 2.2 ng/s, respectively. The actual values observed corresponded to 25 μl injection of 2.8 ng/μl MMC (2.2 ng/μl or 70 ng as Hg) and 4.0 ng/μl EMC (3.0 ng/μl or 70 ng as Hg). The repeatability of a standard solution at twice the detection limit was under 10% relative standard deviation ($n = 5$) for both MMC and EMC. Detection limits for similar compounds analyzed by HPLC interfaced with ICP by means of a conventional nebulizer have been reported to be 232 and 302 ng/μl as Hg for MMC and EMC, respectively; improved results were also reported but the cold vapor generation technique for mercury was used after the analytical column[31].

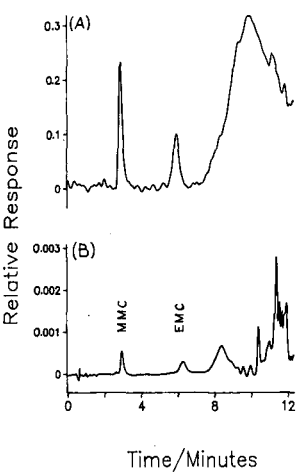

Fig. 4. Chromatograms of a water sample taken from a local river spiked with MMC and EMC, with (A) ACP detection and (B) UV detection: mobile phase, 0.01% 2-mercaptoethanol in methanol–water (22:78), after 5 min methanol was increased to 100%; column, Hypersil ODS 5 (100 mm × 4.6 mm I.D.); flow-rate, 1.0 ml/min; injection volume, 25 μl; wavelength, 253.7 nm.

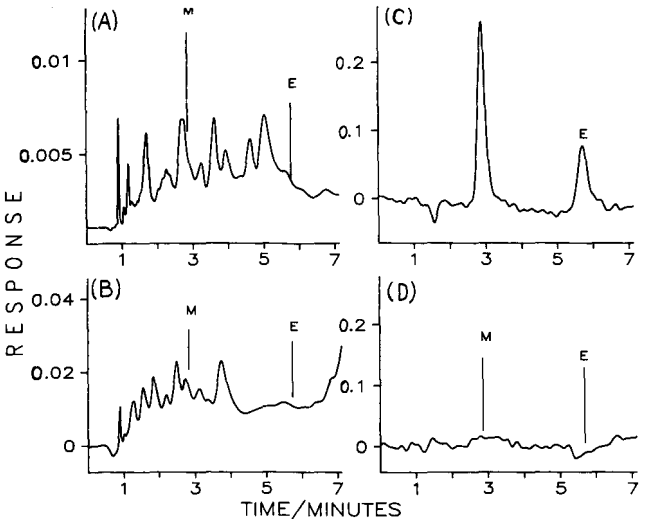

Fig. 5. Chromatograms of (A) diluted gasoline spiked with MMC and EMC by UV detection, (B) unspiked gasoline with UV detection, (C) ACP detection of the spiked gasoline and (D) unspiked gasoline detected by ACP; M and E points out the elution time of MMC and EMC, respectively. Conditions as in Fig. 4.

Selectivity

In order to demonstrate the selectivity of the ACP, known, amounts of MMC and EMC were spiked to samples of different matrix composition, namely, a sample of local river water and gasoline. Chromatograms of each spiked sample in Figs. 4 and 5 were monitored in parallel by UV detection at 254 nm and the ACP. The samples were spiked in such a manner that a 25-μl injection corresponded to 840 ng (669 ng Hg) and 668 ng (505 ng Hg) of MMC and EMC, respectively. In order to elute all strongly retained components from the column, the amount of methanol in the mobile phase was increased after 5 min from injection (from 22% to 100%). In Fig. 5 the selectiviy of the ACP detector is further demonstrated with chromatograms of gasoline: UV detection of (A) gasoline spiked with MMC and EMC and (B) unspiked gasoline, and ACP detection of (C) spiked and (D) unspiked gasoline. The rapid increase of methanol in the mobile phase (after 5 min of injection) also yielded a higher plasma background emission when the methanol reached the plasma as a "plug" of solvent. After approximately 4 min the baseline restabilized but at an elevated level. Moreover, the baseline stability of the ACP detector in HPLC was not affected by injection of a complex matrix whereas in our GC studies we found baseline instability to be problematic at the beginning of chromatograms associated with high organic solvent concentrations in the plasma[22].

CONCLUSION

The ACP detector described here offers a number of attractive features as an element-selective detector for the reversed-phase mode of HPLC. The detector is inexpensive, simple in design and can accept pure methanol with no adverse

performance. The ACP offers considerable potential for the determination of organomercurials by HPLC, especially where complex sample matrix may be a difficulty with other types of detectors. The nebulizer used as the interface contributed to the development of the ACP detector for reversed-phase HPLC. Further improvements in detector design including the use of other nebulizing systems should provide even improved performance of the ACP. One such area is the use of discharge tubes of smaller inner diameters to further reduce the overall dead volume of the system.

ACKNOWLEDGEMENTS

The authors wish to acknowledge the Seed Money Research Program at the University of Lowell for providing financial support and one of us (L.A.C.) wishes to further acknowledge the Graduate School at the University of Lowell for providing a summer research fellowship in 1989. Also, the authors are deeply appreciative for the data acquisition system donated by Galactic Industries Corporation (Salem, NH, U.S.A.) and various chromatographic supplies very generously donated by Alltech Associates, Inc. (Chicago, IL, U.S.A.).

REFERENCES

1 J. C. VanLoon, *Anal. Chem.*, 51 (1979) 1139A.
2 K. L. Jewett, and F. E. Brinckman, *J. Chromatogr. Sci.*, 23 (1983) 205.
3 P. C. Uden, *Trends Anal. Chem.*, 6 (1987) 239.
4 L. Ebdon, S. Hill and R. W. Ward, *Analyst (London)*, 112 (1987) 1.
5 C. J. Cappon, *LC · GC*, 6 (1988) 584.
6 C. H. Gast, J. C. Kraak, H. Poppe and J. M. Maessen, *J. Chromatogr.*, 185 (1979) 549.
7 M. Morita, T. Uehiro and K. Fuwa, *Anal. Chem.*, 53 (1981) 1806.
8 K. J. Irgolic, R. A. Stockton, D. Chakraborti and W. Beyer, *Spectrochim. Acta*, 38B (1983) 437.
9 M. Ibrahim, W. Nisamaneepong, D. L. Hass and J. A. Caruso, *Spectrochim. Acta*, 40B (1985) 367.
10 D. M. Fraley, D. A. Yates, S. E. Manahan, D. Stalling and J. Petty, *Appl. Spectrosc.*, 35 (1981) 525.
11 K. Jinno, H. Tsuchida, S. Natanishi, Y. Hirata and C. Fujimoto, *Appl. Spectrosc.*,37 (1983) 258.
12 K. E. Lawrence, G. W. Rice and V. A. Fassel, *Anal. Chem.*, 56 (1984) 289.
13 K. E. LaFreniere, V. A. Fassel and D. E. Eckels, *Anal. Chem.*, 59 (1987) 879.
14 P. C. Uden, B. D. Quimby, R. M. Barnes and W. G. Elliott, *Anal. Chim. Acta*, 101 (1978) 99.
15 D. J. Mazzo, W. G. Elliott, P. C. Uden and R. M. Barnes, *Appl. Spectrosc.*, 38 (1984) 585.
16 W. R. Biggs, J. T. Gano and R. J. Brown, *Anal. Chem.*, 56 (1984) 2653.
17 W. R. Biggs, J. C. Fetzer and R. J. Brown, *Anal. Chem.*, 59 (1987) 2798.
18 D. Kollotzek, D. Oechsle, G. Kaiser, P. Tschopel and G. Tolg, *Fresenius Z. Anal. Chem.*, 318 (1984) 485.
19 D. L. Hass, J. W. Carnahan and J. A. Caruso, *Appl. Spectrosc.*, 37 (1983) 82.
20 K. G. Michlewicz and J. W. Carnahan, *Anal. Lett.*, 20 (1987) 193.
21 L. Zhang, J. W. Carnahan, R. E. Winans and P. H. Neil, *Anal. Chem.*, 61 (1989) 826.
22 R. B. Costanzo and E. F. Barry, *Anal. Chem.*, 60 (1988) 826.
23 R. S. Braham and A. Dynako, *Anal. Chem.*, 40 (1968) 95.
24 M. Ibrahim, W. Nisamaneepong, D. L. Hass and J. A. Caruso, *Spectrochim. Acta*, 40B (1985) 367.
25 W. Nisamaneepong, D. L. Hass and J. A. Caruso, *Spectrochim. Acta*, 40B (1985) 3.
26 L. R. Layman and F. E. Lichte, *Anal. Chem.*, 54 (1982) 638.
27 R. J. Skelton, Jr., P. B. Farnsworth, K. E. Markides and M. L. Lee, *Anal. Chem.*, 61 (1989) 1815.
28 H. C. Smith and H. L. Walg, *Chromatographia*, 8 (1975) 311.
29 W. P. Carey and B. R. Kowalski, *Anal. Chem.*, 58 (1986) 3077.
30 R. P. W. Scott, *Liquid Chromatography Detectors*, (*Journal of Chromatography Library*, Vol. 33), Elsevier, Amsterdam, New York, 2nd ed., 1986, p. 18.
31 I. S. Krull, D. S. Bushee, R. G. Schleicher and S. B. Smith, Jr., *Analyst (London)*, 11 (1986) 345.

Journal of Chromatography, 513 (1990) 167–179
Elsevier Science Publishers B.V., Amsterdam

CHROM. 22 433

Molecular recognition in synthetic polymers: preparation of chiral stationary phases by molecular imprinting of amino acid amides

LARS I. ANDERSSON, DANIEL J. O'SHANNESSY[a] and KLAUS MOSBACH*
Department of Pure and Applied Biochemistry, Chemical Center, University of Lund, P.O. Box 124, S-221 00 Lund (Sweden)

(First received February 1st, 1990; revised manuscript received March 9th, 1990)

ABSTRACT

Methacrylate-based molecular imprints were prepared using a number of L-amino acid aromatic amide derivatives as print molecules. Methacrylic acid was used as a functional monomer such that the acid function of the monomer interacts ionically with the amine function and via hydrogen bonding with the amide function of the print molecule. Bulk polymers were prepared and were ground and sieved to particles <25 μm, packed into high-performance liquid chromatographic (HPLC) columns and used for enantiomeric separations in the HPLC mode. The polymers were shown to exhibit efficient enantiomeric resolution of a racemic mixture of the amino acid amide used as the print molecule and in many instances were also able to resolve the enantiomers of amino acid amides other than the print molecule, depending on the substituents on the amine and amide functionalities. Allowing an increased number of monomers to interact with the print molecule, *i.e.*, by introducing an additional amide function or a pyridyl ring to the print molecule, led to an improved separation in most instances, although increased band broadening was observed, especially when isocratic elutions were performed. With all polymers, acetic acid gradient elution improved the peak shape, leading to increased resolution and shorter analysis times. The implications of these findings with respect to the mechanism of recognition and the ability to predict the enantiomeric resolution of substances on molecularly imprinted polymers are discussed.

INTRODUCTION

Molecular imprinting in synthetic polymers is a new and potentially very interesting technique for preparing specialized separation media for chromatography,

[a] Present address: Smith Kline Beecham, Research and Development Division, L-47, Department of Macromolecular Sciences, 709 Swedeland Road, P.O. Box 1539, King of Prussia, PA 19406, U.S.A.

0021-9673/90/$03.50

especially for enantiomeric separations. Polymerization is allowed to occur in the presence of a template, the print molecule, which is subsequently removed from the rigid polymer, thereby producing sites within the polymer with affinity for the original print molecule, the so called "memory" effect. Polymerizable monomers are chosen to allow specific and definable interactions with the print molecule. Such interactions are subsequently responsible for the recognition of the substrate by the polymer. The interactions can be either non-covalent forces such as ionic and hydrogen bonding[1,2] or the formation of reversible covalent bonds, such as ketals[3], boronic esters[4,5] and Schiff's bases[6,7].

We have previously described the preparation of molecular imprints of amino acid derivatives[2] and in particular we have been interested in the application of the technique of molecular imprinting to the optical resolution of such compounds. Previously described polymers showed very high enantio selectivity and were sufficiently rigid to be used in the high-performance liquid chromatography (HPLC) mode[8]. In addition, the enantiomers of structurally related compounds could be resolved on a polymer of predefined specificity[9]. A solution NMR study gave evidence for the formation of complexes between a print molecule (L-phenylalanine anilide) and functional monomers (methacrylic acid) defined by ionic and hydrogen bonds[10]. It was argued that these complexes were preserved during the polymerization process, resulting in an arrangement of methacrylic acid residues in the polymer responsible for subsequent recognition of molecules. From the ability of the polymer to resolve the enantiomers of an array of structural analogues of the print molecule, it was possible to draw some conclusions about the mechanism of recognition[9]. It was proposed that the substrate was initially bound to the polymer via "ion pairing" between the primary amine of the substrate and a carboxylic acid residue on the polymer. Additional interactions between the polymer and substrate, such as hydrogen bonding between the amide on the substrate and carboxylic acid residues in the polymer, were then "induced".

We have extended these earlier investigations and describe here the molecular imprinting of eight amino acid derivatives based on the same structural elements previously shown to be important for enantiomeric resolution in this system. All print molecules used in this study were amino acid amide derivatives. The aromatic amide was either an anilide or a β-naphthylamide and various substituents were coupled to the amino nitrogen. The versatility of the resulting polymers to resolve the enantiomers of amino acid amide derivatives was analysed in the HPLC mode. The aim was to correlate the chromatographic properties of the polymers with the structures of the print molecules. The effect of increasing the number of interactions between the print molecule and monomers during polymerization on the ability of the resulting polymers to separate enantiomers and the applications of these polymers as chiral stationary phases in column chromatography are discussed.

EXPERIMENTAL

Methacrylic acid (MAA) and ethylene glycol dimethacrylate (EDMA) were obtained from Aldrich Chemie (Steinheim, F.R.G.), 2,2'-azobis(2-methylpropionitrile) (AIBN) from Janssen Chemica (Beerse, Belgium), L-leucine-β-naphthylamide (LeuβNA) and L-phenylalanine-β-naphthylamide (PheβNA) from Sigma (St. Louis,

MO, U.S.A.) and D-leucine-β-naphthylamide from Bachem (Bubendorf, Switzerland). D- and L-phenylalanine anilides (PheAn), D- and L-proline anilides (ProAn) and D- and L-phenylalanylglycine anilides (PheGlyAn) were all synthesized by a procedure similar to that described previously for L-phenylalanine anilide[8]. D- and L-N,N-dimethylphenylalanine anilides (Me_2PheAn) were prepared by reductive methylation of phenylalanine anilide analogously to a literature method[11]. D- and L-N-pyridoxylphenylalanine anilides (PLPheAn) were prepared essentially as described elsewhere[12]. The syntheses of D- and L-N-(pyridylmethyl)phenylalanine anilides (PyMePheAn) were developed in our laboratory and will be described in detail elsewhere[13]. Briefly, phenylalanine anilide was reacted with pyridine-4-carbaldehyde in acetonitrile to produce the imine, which was then reduced by sodium cyanoborohydride.

All solvents used were of the highest available grade. HPLC analyses were performed with an LKB (Bromma, Sweden) system consisting of a Model 2152 HPLC controller two Model 2150 HPLC pumps and a Model 2151 variable-wavelength monitor. Fourier transform IR (FT-IR) analyses were performed with a Nicolet 20 SXC instrument.

Polymer preparation

Polymers were prepared as described previously[8,14] using EDMA as cross-linker and MAA as the functional monomer. The compositions of the polymerization mixtures are shown in Table I. The molar ratio of cross-linker to functional monomer to print molecule was 30:6:1.5 in entries A–C, E and F; in entries D, G and H a molar ratio of 30:6:1 was used. MAA, EDMA, initiator (AIBN), chloroform and the appropriate amount of crystalline print molecule were weighed into 50-ml borosilicate glass ampoules (Wheaton Scientific, Melvill, NJ, U.S.A.). The mixtures were cooled on ice, degassed under vacuum in a sonicating bath and sparged with nitrogen for 5 min. The ampoules were then sealed with Parafilm and placed under a UV source (366 nm) at 4°C overnight (16 h). The bulk polymers were ground in a mechanical

TABLE I

POLYMER PREPARATIONS

All polymers were prepared using EDMA (52.4 mmol) as cross-linking monomer, chloroform (16 ml) as solvent and AIBN (0.76 mmol) as the initiator at 0°C as described previously.

Polymer	*Print molecule*			*MAA (mmol)*	*Ratio MAA:pm*[a]	*Inner surface area* (m^2/g)[b]
	Abbreviation	*mg*	*mmol*			
A	L-PheβNA	760	2.62	10.48	4	3.8
B	L-LeuβNA	671	2.62	10.48	4	3.3
C	L-PheAn	629	2.62	10.48	4	6.2
D	L-PheGlyAn	520	1.75	10.48	6	5.6
E	L-ProAn	498	2.62	10.48	4	4.2
F	L-Me_2PheAn	702	2.62	10.48	4	2.8
G	L-PyMePheAn	579	1.75	10.48	6	3.5
H	L-PLPheAn	684	1.75	10.48	6	3.6

[a] Ratio MAA:pm refers to the molar ratio of functional monomer (MAA) to print molecule (pm).
[b] Inner surface area was determined by nitrogen adsorption measurements.

mortar (Retsch, Haan, F.R.G.) and wet sieved (water) through a 25-μm sieve (Retsch). The fraction that passed through the sieve was collected and the remainder was re-ground. This procedure was repeated until all polymer particles passed through the sieve. The fines were removed from the preparation by repeated settling in acetonitrile and the particles were finally dried under vacuum.

High-performance liquid chromatography

Particles were suspended in chloroform by sonication and packed into 200 mm $\times$ 4.5 mm I.D. stainless-steel columns using acetonitrile as solvent with an air-driven fluid pump (Haskel Engineering Supply, Burbank, CA, U.S.A.) at 300 bar. The columns were then washed on-line with methanol–acetic acid (9:1, v/v) until a stable baseline was obtained. HPLC analyses were performed under either isocratic or gradient elution conditions. Isocratic elutions were performed with acetonitrile containing the appropriate percentage of acetic acid (5–12.5%, v/v) at a flow-rate of 1 ml/min and with detection at 250 nm. Gradient elutions were performed using a linear gradient of 0–30% (v/v) acetic acid in acetonitrile over 30 min at a flow-rate of 1 ml/min. Samples consisted of a mixture of 5 μg of each of the L- and D-enantiomers of a given compound, prepared in acetonitrile, and injected in a total volume of 20 μl.

Enantiomeric resolution was confirmed by separate injections of each of the enantiomers. The void volume of the columns were determined by injection of glacial acetic acid. Capacity factors (k'), separation factors (α) and plate numbers (N) were calculated using standard chromatographic theory[15]. The resolution (R_s) was calculated according to Wulff *et al.*[4].

RESULTS AND DISCUSSION

Polymer preparations

A recently developed polymerization procedure, based on photolytic initiation, was used in this study as the chromatographic properties of the resulting polymers have previously been shown to be superior to polymers prepared by thermal initation[8]. All polymerizations were performed under equivalent conditions to ensure that the physical properties of the polymers were as equivalent as possible. In addition, the composition of the polymerization mixture was kept constant throughout all experiments, with the exception of added print molecule. The molar ratio of cross-linker (EDMA) to functional monomer (MAA) was 5:1. The optimum molar ratio of MAA to print molecule was previously shown to be about 4:1[9,14] and this ratio was used here, except in entries D, G and H (Table I). To allow for the possibility of an additional interaction point to the print molecules L-PheGlyAn, L-PyMePheAn and L-PLPheAn, the ratio of functional monomer to print molecule was increased to 6:1 by decreasing the amount of print molecule added to the polymerization mixtures of these polymers (Table I). As the formation of complexes between print molecule and functional monomers in the prepolymerization mixture is an equilibrium process, the introduction of additional interaction points on the print molecule must be accompanied by a corresponding increase in the amount of functional monomer. This was achieved by keeping the number of moles of interacting sites constant, rather than the number of moles of print molecule, by decreasing the amount of print molecule added to the polymerization mixture. In this way the ratio of functional monomer (MAA) to

the number of "potential" interaction sites was constant in all polymerization mixtures.

As a routine measure of the equivalence of physical properties between polymer preparations, the specific surface areas were determined. As can be seen from the data in Table I, all polymer preparations had comparable surface areas. In this context it should be noted that a "reference" polymer, prepared in the absence of print molecule, possessed different physical properties. The specific surface area was 13 m^2/g of polymer for the reference polymer compared with 3–6 m^2/g for imprinted polymers A–H (Table I) and the pore volume of the reference polymer was 0.08 cm^3/g compared with 0.04–0.05 cm^3/g for polymers C and F (not shown).

The polymer particles were packed into stainless-steel columns (200 × 4.5 mm I.D.) and washed on-line with 10% (v/v) acetic acid in methanol to remove print molecules from the polymer. The amount of irreversibly incorporated print molecules, determined by FT-IR difference spectra between polymer C (Table I) and a reference polymer (prepared in the absence of print molecule), was calculated to be less than 1% of the total amount of print molecules added, as no IR bands originating from PheAn could be detected (not shown).

Chromatography

Polymers were evaluated in the HPLC mode using either isocratic or gradient elution schemes. When using isocratic elution conditions the composition of the eluent was optimized for each stationary phase by changing the concentration of acetic acid. In order to compare chromatographic data from all stationary phases, the eluent was chosen to give a capacity factor, k', for the D-form of the print molecule of *ca.* 1. Eight polymers were prepared (see Table I) using print molecules containing the same basic structural elements; all were aromatic amides of amino acids, as shown in Fig. 1. Racemic mixtures of all amino acid amides were analysed on all eight columns and the results are presented as separation factors, α, in Table II, and a few representative chromatograms are depicted in Fig. 2.

The broad elution peaks obtained in the present system, particularly for the more strongly retained L-forms of the substrates, may be due to several factors, including the size distribution and shape irregularity of the polymer particles. In addition, broad elution peaks may be due to differences in the number and complementarity of interactions between the print molecule and functional monomers, prior to and during polymerization, giving rise to a wide range of non-equivalent sites in the polymer. A third explanation for peak broadening may be that the kinetics of release are slow such that $K_{ass} \gg K_{diss}$, as discussed previously[9]. The observed peak broadening is probably due to a combination of all of these factors. Peak broadening was most pronounced on polymers D, G and H (Table I), imprinted against compounds L-PheGlyAn, L-PyMePheAn and L-PLPheAn, respectively, with an increased number of interaction points with the functional monomer. Despite the increase in separation factor on polymers D and G (see below), the resolution was not improved and therefore lower than expected for these columns; $R_s = 0.5$ (polymer D) and $R_s = 1.1$ (polymer G) compared with $R_s = 0.7$ (polymer B) and $R_s = 1.0$ (polymer C). This was probably due to band-broadening effects, particularly as all the columns used in this study resulted in symmetrical void peaks with plate numbers between 500 to 650 using glacial acetic acid (not shown).

TABLE II

SEPARATION FACTORS[a] FOR THE DIFFERENT AMINO ACID DERIVATIVES ON POLYMERS A–H (TABLE I)

A mixture of 5 μg of each of the enantiomers of the amino acid derivatives was injected onto the column in a total volume of 20 μl of acetonitrile and eluted at room temperature under isocratic conditions using the appropriate percentage of acetic acid in acetonitrile. Detection was at 250 nm. Plate numbers, calculated for a non-retained void marker (acetic acid), were approximately the same for all columns, between 500 and 650. The separation factors obtained for print molecule on respective columns are underlined.

Polymer	*Print molecule*[b]	*Acetic acid concentration (%)*[c]	*Substrate*						
			LeuβNA	*PheAn*	*PheGlyAn*	*ProAn*	*Me_2PheAn*	*PyMePheAn*	*PLPheAn*
A	L-PheβNA[d]	12.5	(2.4	5.5	3.0	1.0	1.0	1.0	1.0)[d]
B	L-LeuβNA	10	3.8	4.8	2.2	1.0	1.0	1.0	1.0
C	L-PheAn	10	2.6	4.1	2.1	1.2	1.0	1.0	1.0
D	L-PheGlyAn	7.5	1.0	3.0	5.1	1.0	1.0	1.0	1.0
E	L-ProAn	7.5	2.8	2.5	1.0	4.5	1.0	1.0	1.0
F	L-Me_2PheAn	7.5	1.0	1.0	1.0	1.0	3.7	1.0	1.0
G	L-PyMePheAn	5	1.0	1.0	1.0	1.0	1.0	8.4	1.0
H	L-PLPheAn	5	1.0	1.0	1.0	1.0	1.0	1.6	2.7

[a] Separation factor, α, is the ratio k'_L/k'_D.
[b] Structures are shown in Fig. 1.
[c] Acetic acid concentration (%) refers to the percentage of acetic acid in acetonitrile used during chromatography.
[d] Only the L-form of PheβNA was applied as substrate and separation factor, α, could not be calculated for this compound.

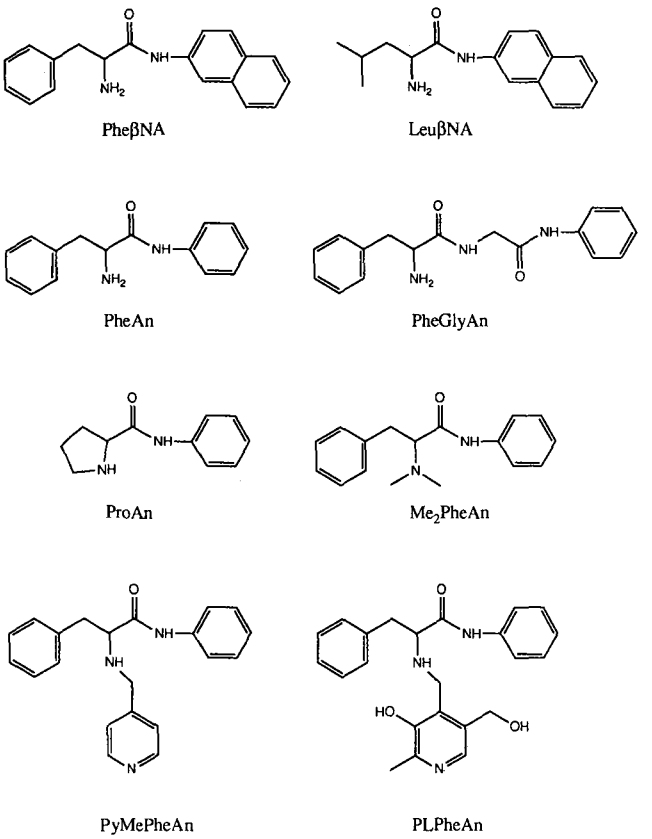

Fig. 1. Structures of the compounds used as print molecules. Abbreviations: PheβNA, phenylalanine-β-naphthylamide (polymer A); LeuβNA, leucine-β-naphthylamide (polymer B); PheAn, phenylalanine anilide (polymer C); PheGlyAn, phenylalanylglycine anilide (polymer D); ProAn, proline anilide (polymer E); Me_2PheAn, N,N-dimethylphenylalanine anilide (polymer F); PyMePheAn, N-pyridylmethylphenylalanine anilide (polymer G); PLPheAn, N-pyridoxylphenylalanine anilide (polymer H).

As acetic acid is a competing ligand, it follows that by increasing the acetic acid concentration in the eluent, the equilibrium would be shifted towards dissociation, or elution of the substrate, and the higher the K_a the higher is the concentration of acetic acid required to effect elution. It was considered, therefore, that gradient elution [0–30% (v/v) acetic acid in acetonitrile] would both improve the peak shape and give some information on the relative affinities of the substrates for the various polymers, as reflected in the percentage of acetic acid required for elution (see Table III). Fig. 3 shows the elution profiles for the enantiomers of PLPheAn on polymer H using both isocratic and gradient elution. In this instance, the resolution showed a modest increase from 0.4 to 0.5 and the analysis time decreased from 30 to 20 min when gradient elution was used.

Specificity of recognition

In a previous study we showed that it was possible to resolve the enantiomers of

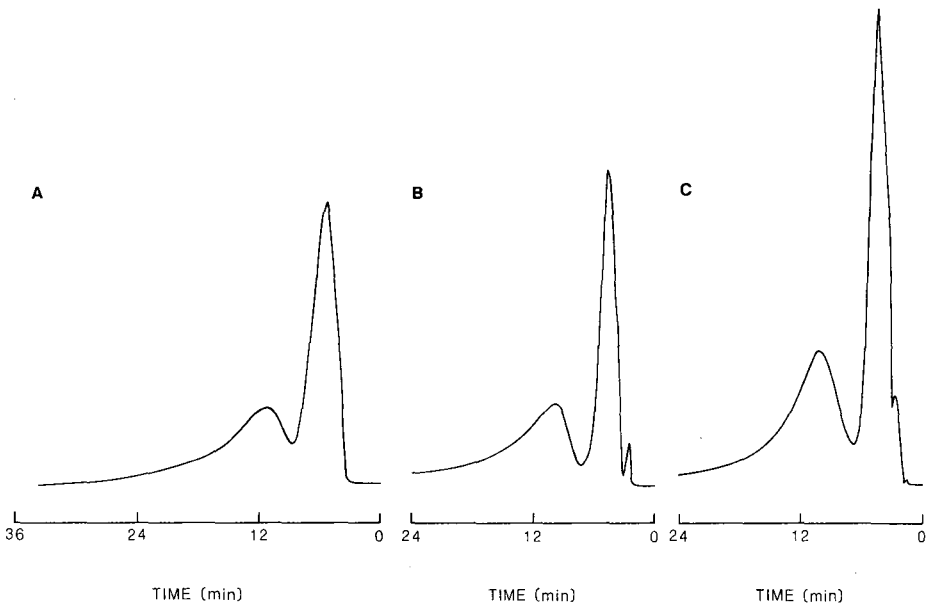

Fig. 2. Enantiomeric resolution of amino acid amides. Particles of <25 μm were packed into 200 $\times$ 4.5 mm I.D. columns. Analyses were performed isocratically using (A) 10% (v/v) or (B and C) 7.5% (v/v) acetic acid in acetonitrile as the eluent at 1 ml/min at room temperature. Detection was at 250 nm. In all experiments, a mixture of 5 μg of each of the enantiomers of the compound was analysed. Analyses shown: (A) D,L-PheAn on polymer C (prepared against L-PheAn, Table I); (B) D,L-Me_2PheAn on polymer F (prepared against L-Me_2PheAn, Table I); and (C) D,L-ProAn on polymer E (prepared against L-ProAn, Table I).

TABLE III

SEPARATION OF THE ENANTIOMERS OF THE PRINT MOLECULE BY GRADIENT ELUTION ON POLYMERS A–H (TABLE I)

A mixture of 5 μg of each of the enantiomers of the corresponding amino acid derivative was injected onto the column in a total volume of 20 μl of acetonitrile and eluted with acetonitrile–acetic acid using a linear gradient of 0–30% acetic acid in 30 min. Detection was at 250 nm.

Polymer	*Print molecule*	*Elution*[a]	
		L	*D*
A	L-PheβNA	15.7	–
B	L-LeuβNA	11.0	6.6
C	L-PheAn	14.5	10.7
D	L-PheGlyAn	9.5	8.4
E	L-ProAn	10.1	7.3
F	L-Me_2PheAn	10.5	7.1
G	L-PyMePheAn	10.1	6.9
H	L-PLPheAn	7.9	6.3

[a] Percentage of acetic acid at which the compound eluted.

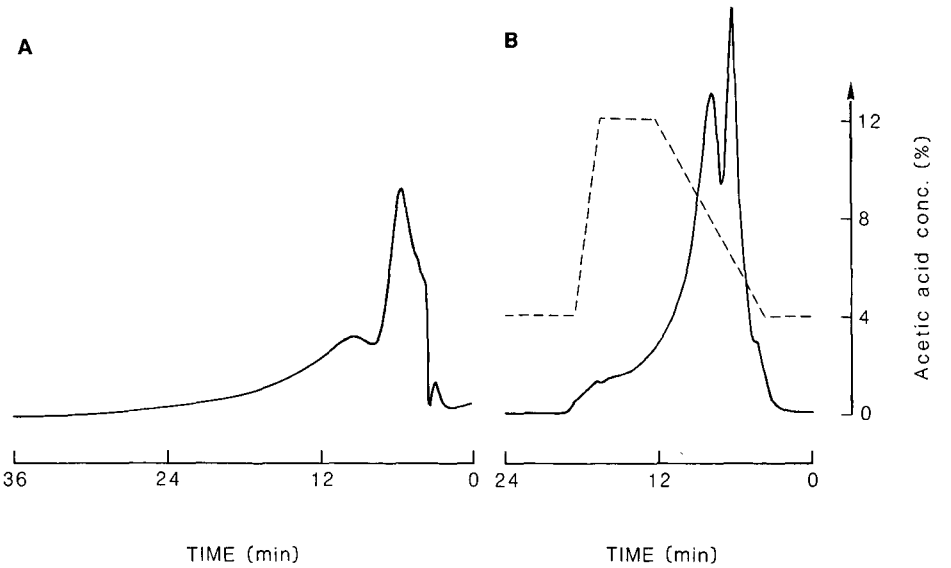

Fig. 3. Resolution of the enantiomers of the print molecule on polymer H (prepared against L-PLPheAn, Table I). Particles of <25 μm were packed into a 200 × 4.5 mm I.D. column. (A) Analysis performed at room temperature with acetonitrile–acetic acid (19:1, v/v) as the eluent at 1 ml/min; (B) analysis with the following gradient of acetic acid in acetonitrile at 1 ml/min: 0–4 min, 4%; 4–12 min, 4–12%; 12–16 min, 12%; 16–18 min, 12–4%. Detection was at (A) 250 nm and (B) 290 nm. Samples consisted of 5 μg of each of the enantiomers of PLPheAn in a total volume of 20 μl of acetonitrile. The resolution (R_s), calculated as in ref. 4, was *ca.* (A) 0.4 and (B) 0.5. Asymmetry factors (A_s) at 10% of the peak height were calculated to be (A) 3.7 and (B) 2.7 for the L-peak and (A) 1.5 and (B) 0.9 for the D-peak.

a number of compounds on a polymer molecularly imprinted against L-PheAn[9] and that an amine and an amide, in the correct geometry around the chiral carbon, were necessary for resolution. In this work we extended previous investigations by preparing molecular imprints against eight aromatic amides of amino acids. The structural differences between the print molecules were small; the amide moiety was either an anilide or β-naphthylamide, and the amine moiety was either primary, secondary or tertiary (see Fig. 1). All compounds had the same arrangement of amine and amide around the chiral carbon, previously shown to be essential for enantiomeric resolution on a polymer prepared against L-PheAn[9]. This ensures, as far as possible, that the types of interactions involved in the recognition process are the same on all polymers, *viz.*, ionic bonding to the amine and hydrogen bonding to the amide. The introduction of additional interactions, such as hydrogen bonding in PheGlyAn and ionic bonding in PyMePheAn (see below), should not alter the type of interactions but only increase their number. The recognition sites formed after polymerization would, in principle therefore be very similar in structure and any differences would be indicative of changes in the three-dimensional arrangement, spatial or distal, of carboxylic acid residues, the number of carboxylic acids or the shape (volume) of the sites. The elution data for the various amino acid amides should then reflect differences in the conformation, configuration and number of interactions introduced into the recognition sites by a particular print molecule.

Racemic mixtures of all amino acid amides were analysed on all eight stationary phases prepared and the data are presented in Table II as separation factors, α. It is important to note that enantiomeric resolution was observed for all stationary phases, at least for the print molecule. In this context, a polymer imprinted against a racemic mixture of D,L-PyMePheAn, did not display any enantiomeric resolution (not shown).

In almost all instances the best separation was achieved when the enantiomers of the print molecule were applied to the column (Table II). Although the polymers were able to resolve the enantiomers of compounds other than the print molecule, the separation factor, α, was less than that for the racemate of the print molecule. Unexpectedly, on many polymer preparations only the enantiomers of a few amino acid amides, in some instances only of the print molecule, were resolved, at least using the present elution schemes.

The first group of polymers to be discussed are polymers A, B, C and D, prepared against L-PheβNA, L-LeuβNA, L-PheAn and L-PheGlyAn, respectively. On all four polymers enantiomeric resolution was observed when a racemic mixture of each of the compounds LeuβNA, PheAn and PheGlyAn was applied to the columns, with the exception of LeuβNA on polymer D. These observations extend and support the hypothesis that an amine moiety and an amide moiety, in the correct geometry around the chiral carbon, are the major criteria for enantiomeric recognition on molecularly imprinted polymers[9]. When applying compounds containing a substituted amine, as with ProAn, Me_2PheAn, PyMePheAn and PLPheAn, no enantiomeric resolution could be detected on polymers A–D. Therefore, these polymers have the ability to distinguish, at least to some extent, primary from substituted amines.

Polymers E, F, G and H prepared against the "substituted" amines L-ProAn, L-Me_2PheAn, L-PyMePheAn and L-PLPheAn, respectively, showed little tendency to resolve the enantiomers of compounds other than the original print molecule, with a few exceptions (see Table II). It must be stressed, however, that the possibility exists that a polymer prepared against L-Me_2PheAn, for example, may be able to resolve the enantiomers of a number of other N,N-dimethylated amino acid amides, analogous to polymers A–D and previous observations[9].

The mutual inability of polymers prepared against substituted and unsubstituted amines to resolve the enantiomers of the other type of amine can not be accounted for by differences in ionic interactions, as the pK_a values for the corresponding acids of primary, secondary and tertiary amines are generally in the same range of 10–11. The substituents on the amino groups would therefore only cause the participants in the ionic bond to become more distanced from each other, but as coloumbic interactions are long range on the molecular level the ionic bond is not expected to be weakened to any great extent. This is supported by the observation that regardless of the number of substituents on the amine moiety, all amino acid amides were bound approximately equally strongly to the polymers in the present solvent system, in that all D-forms and L-forms of the non-resolved substances eluted at approximately the same position on any given polymer (data not shown). Perhaps the most striking examples of the selectivity for unsubstituted and substituted amines are polymers C and F, imprinted against L-PheAn and L-Me_2PheAn, respectively (see Table II), where the addition or removal of two methyl groups to the amine of the print molecule resulted in total loss of enantiomeric resolution. This effect cannot be simply

explained by differences in ionic bonding to carboxylic acid residues on the polymer but may be related to the shape of the molecules[16] and hence the shape of the binding sites on the polymers and/or additional interactions such as hydrophobic interactions or changes in hydrogen bonding abilities. It is also unlikely that the bulkiness of the two methyl groups would be a major factor responsible for the observed effect.

By increasing the number of possible interactions between polymer and substrate it was expected that the resolution of the enantiomers would improve. The introduction of an additional point of interaction into the print molecule should allow coordination of more functional monomers during polymerization and subsequent incorporation of additional carboxylic acid residues into the recognition sites. This concept was investigated on polymers D, G and H, imprinted against L-PheGlyAn, L-PyMePheAn and L-PLPheAn, respectively. PheGlyAn has a peptide bond in the molecule (Fig. 1) and therefore additional hydrogen bonding potential. PyMePheAn has a pyridine ring coupled to the amine (Fig. 1), which should result in an additional ionic bond to the pyridine nitrogen, albeit weak as the pK_a of the pyridine ring is *ca.* 5. PLPheAn was included in the investigation because of its complexity, being a more functionalized molecule than the other compounds investigated. It is similar in structure to PyMePheAn but contains an additional hydroxyl group and a hydroxymethyl group on the pyridine ring (Fig. 1). In each of the three compounds, these "additional" points of interaction are situated at a distance from the chiral carbon, but if this interaction is participating in the chiral recognition event an improved enantiomeric separation would be expected. Polymer D, prepared against L-PheGlyAn, produced a significantly higher separation factor for the enantiomers of the print molecule compared with polymers B and C, prepared against "similar" print molecules, L-LeuβNA and L-PheAn (Table II). Polymer G, imprinted against L-PyMePheAn, resolved the enantiomers of the print molecule very efficiently (Table II). It is in fact one of the highest α-values ever obtained in our laboratories and among the highest ever reported in the literature in the field of molecular imprinting[2]. Peak broadening of the L-enantiomer was considerable but the D-enantiomer eluted as a narrow, symmetrical peak (not shown). Analysis of a racemic mixture of D- and L-PLPheAn on polymer H produced a lower separation factor than expected.

Although the second amide moiety in PheGlyAn and the pyridyl nitrogen in PyMePheAn are situated at a distance from the chiral carbon in these molecules, the additional interactions had a positive effect on the separations. In general, the results indicate that additional points of interaction between the print molecule and functional monomers during polymerization gives rise to polymers possessing improved separation abilities, exemplified by polymers D and G, imprinted against L-PheGlyAn and L-PyMePheAn, respectively. However, this is not universally applicable, as shown by polymer H, imprinted against L-PLPheAn.

CONCLUSIONS

It is clear from the results presented here and in previous publications[8–10,12,14] that some form of chiral information is introduced into the polymer during polymerization in the presence of a template, the print molecule. This information is preserved during work-up of the polymer and removal of print molecule, resulting in the "memory effect". The polymeric material can then be used as a chiral stationary

phase in column chromatography. It is unlikely that the observed enantiomeric separations are due to irreversible incorporation of chiral molecules as the template is almost quantitatively removed after polymerization, as determined in the present study by FT-IR measurements. The enantiomeric separations observed are more likely due to specific interactions between the substrate and chiral recognition sites within the polymer. The fact that the best separation is almost always recorded for the enantiomers of the print molecule supports this hypothesis. Although it is extremely difficult to "map" the actual structure of these sites, several assumptions may be made. It seems clear that one or several carboxylic acid residues from functional monomers are incorporated into the sites[10]. These acid functionalities are responsible for the initial binding of substrate to the polymer via ionic interaction with the amino function(s) on the substrate[9]. The forces giving rise to enantiomeric separations are more difficult to study.

An indirect approach to obtaining information about the enantiomeric separation event is to investigate different racemates and record which compounds are resolved, as described here. It was shown previously that an amine and an amide in the correct geometry around the chiral carbon are crucial for a substrate to be resolved on a polymer prepared against L-phenylalanine anilide[9]. The side-chain on the amino acid derivative is of little importance for enantiomeric resolution. Here we have presented data showing that the moieties important for binding to the polymer are of extreme importance for chiral resolution, *e.g.*, the type of amine in the amine–carboxylic acid interaction. It should be stressed that binding and chiral resolution are two distinct events. Increasing the number of interactions between the substrate and the polymer results in higher separation factors but the unfavourable kinetics on such polymers lead to peak broadening. For practical reasons it is neither necessary nor advantageous to increase the number of interactions in order to achieve better separations, at least for small organic molecules. Although the type of amine determines if a given amino acid amide is resolved on a particular polymer, it is recognized that all amino acid amides are bound equally strongly to each polymer. We conclude that the initial binding of the substrate to the polymers occurs via ionic bonding between the amine on the substrate and carboxylic acid residues on the polymer. The second step in the recognition process is the formation of other interactions, such as hydrogen bonds and hydrophobic forces, and it is these "secondary" interactions which give rise to the enantiomeric separations observed.

Molecular imprinting is an interesting and simple technique for preparing chiral stationary phases for enantiomeric separations. The relatively high separation factors achieved in the present system and in previous studies[8–10,14] are promising for future developments of polymers with practical applications in column chromatography. The polymers are rigid and stable enough to be used at high pressures and are also resistant to most of the commonly used solvents[9]. The major shortcoming of these polymer preparations in column chromatography is the sometimes pronounced broadening of peaks. Gradient elution schemes improve the peak shape, increase the resolution and shorten analysis times. However, further improvements in the chromatographic applications of these polymers are desirable and may include the preparation of beaded molecular imprints and a thorough investigation of the kinetics of association and dissociation.

ACKNOWLEDGEMENTS

This investigation was supported by grants from the Swedish Natural Science Research Council and the Riksbankens Jubileumsfond foundation.

REFERENCES

1 R. Arshady and K. Mosbach, *Makromol. Chem.*, 182 (1981) 687.
2 B. Ekberg and K. Mosbach, *Trends Biotechnol.*, 7 (1989) 92.
3 K. J. Shea and T. K. Dougherty, *J. Am. Chem. Soc.*, 108 (1986) 1091.
4 G. Wulff, H.-G. Poll and M. Minárik, *J. Liq. Chromatogr.*, 9 (1986) 385.
5 O. Norrlöw, M.-O. Månsson and K. Mosbach, *Swed. Pat. Appl.*, 8605372-5, 1986; *J. Chromatogr.*, 396 (1987) 374.
6 Y. Fujii, K. Matsusani and K. Kikuchi, *J. Chem. Soc, Chem. Commun.*, (1985) 415.
7 G. Wulff, B. Heide and G. Helfmeier, *J. Am. Chem. Soc.*, 108 (1986) 1089.
8 D. J. O'Shannessy, B. Ekberg and K. Mosbach, *Anal. Biochem.*, 177 (1989) 144.
9 D. J. O'Shannessy, L. I. Andersson and K. Mosbach, *J. Mol. Recogn.*, 2 (1989) 1.
10 B. Sellergren, M. Lepistö and K. Mosbach, *J. Am. Chem. Soc.*, 110 (1988) 5853.
11 R. Borch and A. Hassid, *J. Org. Chem.*, 37 (1972) 1673.
12 L. I. Andersson and K. Mosbach, *Makromol. Chem., Rapid Commun.*, 10 (1989) 491.
13 L. I. Andersson unpublished results.
14 D. J. O'Shannessy, B. Ekberg, L. I. Andersson and K. Mosbach, *J. Chromatogr.*, 470 (1989) 391.
15 A. Fallon, R. F. G. Booth and L. D. Bell, in R. H. Burdon and P. H. van Knippenberg (Editors), *Laboratory Techniques in Biochemistry and Molecular Biology, Vol. 17, Applications of HPLC in Biochemistry*, Elsevier, Amsterdam, 1987.
16 K. J. Shea and D. Y. Sasaki, *J. Am. Chem. Soc.*, 111 (1989) 3442.

Journal of Chromatography, 513 (1990) 181–194
Elsevier Science Publishers B.V., Amsterdam

CHROM. 22 435

(*S*)-2-Hydroxypropyl-β-cyclodextrin, a new chiral stationary phase for reversed-phase liquid chromatography

APRYLL M. STALCUP, SAN-CHUN CHANG and DANIEL W. ARMSTRONG*
Department of Chemistry, University of Missouri-Rolla, Rolla, MO 65401 (U.S.A.)
and
JOSEF PITHA
National Institute of Health, NIA/GRC, Baltimore, MD 21224 (U.S.A.)
(First received December 22nd, 1989; revised manuscript received February 19th, 1990)

ABSTRACT

(*S*)-2- and (*R,S*)-2-hydroxypropyl-β-cyclodextrin have been bonded to silica gel and evaluated as stationary phases for reversed-phase liquid chromatography. Stationary phases also were prepared on two silicas having different pore sizes and surface areas. Dissimilarities were observed in enantiomeric selectivities between these columns and also between these and the native β-cyclodextrin columns. With the exception of compounds **5** and **10**, all other racemates reported here which have been successfully resolved on the new phases are enantiomers which have not been previously reported as separated on the β-cyclodextrin stationary phase. In some cases, there were also differences in enantioselectivities observed between the (*S*)- and the (*R,S*)-hydroxypropyl-β-cyclodextrin phases on the same silica. The results are discussed in terms of the retention mechanism and compared to results reported earlier for β-cyclodextrin columns.

INTRODUCTION

Cyclodextrins (CDs), cyclic oligomers of glucose bonded through α-1,4 linkages, have been used successively and extensively both as mobile phase additives (CMA)[1–4] and as chiral bonded stationary phases (CBP)[5–7] in liquid chromatography for the separation of enantiomers. Although the native CDs have proven useful as stationary phases for liquid chromatographic applications, their use as mobile phase additives has been restricted because of the low solubility of the native CDs in aqueous solutions. Derivatizing the CD increases the solubility of the CD; however, derivatization has been found to cause changes in the chromatographic behavior[8]. In reversed-phase applications, the separation mechanism is thought to be the result of the formation of inclusion complexes in which the solute is included into the cavity of the CD. For enantiomers, separation is possible if these inclusion complexes have different binding

0021-9673/90/$03.50

constants. The mouth of the CD hydrophobic cavity is surrounded by secondary hydroxyls which are locked into position and are considered to be important in chiral recognition. In the derivatized CD, some of these hydroxyls are substituted with hydroxypropyl groups. When using hydroxypropyl-β-CD as a CMA, it has been found that as the degree of substitution on the derivatized CD increases, it can sometimes affect the binding process as well as the enantioselectivity. It is probable that the hydroxypropyl groups partially occlude the mouth of the CD cavity and sterically influence the formation of inclusion complexes. Computer modeling[9,10] as well as considerable chromatographic data have revealed that enantioselectivity using CDs is enhanced when there is close proximity of substituents on the "chiral center" of the enantiomer capable of forming hydrogen bonds with the secondary hydroxyls of the CD. Unfortunately, many chiral compounds do not meet this requirement. In an effort to extend the range of chiral separations obtainable using CD-based stationary phases, an additional chiral center was incorporated as a side-chain on β-CD and the derivatized CD was used to synthesize a bonded stationary phase. Both the racemic and the optically pure forms of the hydroxypropyl-β-CD were used. The (*R*) and (*S*) designations are used to specify only the configuration of the hydroxypropyl group and not the configuration of the CD. The resultant hydroxypropyl-β-CD stationary phases were evaluated chromatographically. Numerous separations were obtained on the new hydroxypropyl-β-CD bonded phases that were not possible on the β-CD stationary phase. Differences in selectivity also were observed between the racemic and enantiomerically pure stationary phases. In addition, the effect of bonded-phase loading on selectivity was examined.

EXPERIMENTAL

Materials

The 5-μm silica (Nucleosil, 300 Å, and Spherisorb, 120 Å) was obtained from Alltech. (*R,S*)-2- and (*S*)-2-hydroxypropyl-β-CD were synthesized as previously described[11]. Briefly, β-CD was dissolved in aqueous sodium hydroxide (5%, w/w) and the solution was cooled in an ice bath. Propylene oxide of the desired chirality was slowly added with stirring. After about 6 h in an ice bath, the reaction was allowed to proceed for a day at room temperature, neutralized and dialyzed briefly in order to remove the contaminating salts. The retained solution was filtered and the product obtained by freeze drying. The (*S*)-2-hydroxypropyl-β-CD used for the bonded phase was a mixture of homologues with an average molar substitution of 7.9, calculated per cyclodextrin molecule.

The structures of the solutes used are presented in the tables. Idazoxan and methylidazoxan are drugs under investigation at Reckitt & Colman and were supplied by N. A. Hyde from Danson Lane, Kingston-upon-Hull, U.K. Compounds **8**–**14** were supplied by Dr. David Kimball at the Squibb Institute for Medical Research, Princeton, NJ, U.S.A., and are listed in the tables using the Squibb designation. The thyroid drugs, 3,3′,5-triiodo-D,L-thyronine and 3,5-diiodo-D,L-thyronine, were obtained from Dr. H. J. Cahnmann of the National Institutes of Health, Bethesda, MD, U.S.A. The other solutes were obtained from various sources and used without further purification. Methanol, acetonitrile, triethylamine and glacial acetic acid were obtained from Fisher Scientific (St. Louis, MO, U.S.A.). Water was distilled,

TABLE I

LIST OF BONDED SORBENTS

Column, length × I.D. (cm)	*Bonded ligand*	*Pore size (Å)*	*Surface area (m^2/g)*	*Spacer ($\mu mol/m^2$)*	*CD ($\mu mol/m^2$)*	*%C*
A, 25 × 0.46	*S*-Hydroxypropyl	300	100	1.16	0.19	3.1
B, 15 × 0.46	*rac*-Hydroxypropyl	300	100	0.97	0.21	4.3
C, 25 × 0.46	*S*-Hydroxypropyl	120	170	3.77	0.12	5.6

subsequently deionized using a Barnstead Cartridge, filtered and used without further purification.

Columns

The bonded phases were prepared under anhydrous conditions as reported previously[12]. The bonded sorbents were submitted for carbon analysis. The pertinent sorbent parameters are listed in Table I. The surface concentration was calculated according to the equation[13]

$$\text{surface concentration } (\mu\text{mol/m}^2) = \frac{\%\text{C} \cdot 10^6}{1200N_c - \%\text{C}(M-1)} \cdot \frac{1}{S}$$

where %C is the percent carbon (w/w) from elemental analysis, N_c is the total number of carbons in the bonded ligand, S is the surface area of the bare silica and M is the molecular weight of the bonded ligand. The molecular weight used for the derivatized CD determination of the surface concentration is based on an average molar substitution of 7.9.

RESULTS AND DISCUSSION

Bonding results

As can be seen from Table I, better CD coverages were obtained on the silica with the larger pore size (300 Å). This is indicative of some exclusion of the CD from the smaller pores of the silica used in the preparation of column C. Although column C has a lower CD density, the absolute amount of bonded CD is greater because of the greater surface area of the substrate.

Chromatographic results

The chromatographic data for the solutes used to evaluate the columns are tabulated in Tables II–IV. If racemates were unresolved on a particular column (A, B or C) no data were reported for these columns in Tables II, III or IV. Unfortunately, due to the different bonding characteristics of each sorbent, it was not possible to obtain a given separation under identical mobile phase conditions on all three columns. Mobile phase conditions were therefore optimized for each column.

The solutes that were used to evaluate the columns can be loosely classified into

TABLE II

ENANTIOMERIC SEPARATION OF RACEMATES IN WHICH THE CHIRAL CENTER IS A PART OF A RING

k' = Capacity factor of the first eluted enantiomer; α = separation factor; R_s = resolution; Et = ethyl; Me = methyl; t = *tert*. The buffer used for all of these separations was 1% triethylamine acetate, pH 4.1.

Compound	*Structure*	*Column*[a]	k'	α	R_s	*Mobile phase*
(1) (±)-1-Benzocyclobutene carboxylic acid	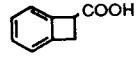	A	2.98	1.14	1.0	100% Buffer
		B	1.60	1.10	0.6	95% Buffer in acetonitrile
		C	3.30	1.09	0.6	90% Buffer in acetonitrile
(2) 1-Indanol	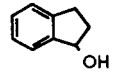	A	1.27	1.07	0.6	100% Buffer
		B	1.00	1.11	0.6	100% Buffer
		C	3.00	1.04	0.5	95% Buffer in acetonitrile
(3) (±)-1,2,3,4-Tetrahydro-1-naphthol		A	2.36	1.08	0.7	100% Buffer
		B	1.92	1.08	0.5	100% Buffer
		C	1.71	1.03	0.6	80% Buffer in acetonitrile
(4) 3-Phenylphthalide	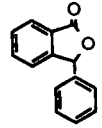	B	5.92	1.04	0.5	90% Buffer in acetonitrile
(5) Chlorthalidone	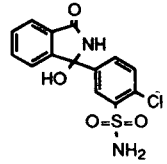	A	1.33	1.38	2.2	95% Buffer in acetonitrile
		B	1.50	1.31	2.8	95% Buffer in acetonitrile
		C	2.80	1.21	1.6	90% Buffer in acetonitrile
(6) Idazoxan	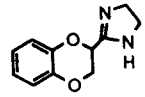	A	0.89	1.07	0.55	100% Buffer
		B	0.63	1.06	0.50	100% Buffer

(7) Methylidazoxan	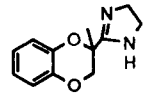	A	0.75	1.19	1.09	100% Buffer
		B	0.62	1.11	0.60	100% Buffer
		C	1.17	1.08	0.55	95% Buffer in acetonitrile
(8) BAY COOH		A	1.16	1.28	1.56	98% Buffer in acetonitrile
		B	0.65	1.12	0.8	95% Buffer in acetonitrile
		C	3.74	1.11	0.7	95% Buffer in acetonitrile
(9) SQ 28 873		A	2.66	1.06	0.6	95% Buffer in acetonitrile
(10) SQ 30 840	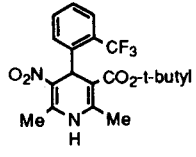	A	4.32	1.22	2.00	85% Buffer in acetonitrile
		B	1.33	1.38	1.50	80% Buffer in acetonitrile
		C	5.46	1.14	1.07	80% Buffer in acetonitrile
(11) BAY CNET	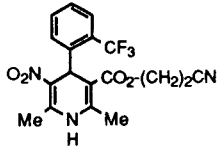	A	3.27	1.10	0.7	98% Buffer in acetonitrile
		B	1.54	1.12	0.5	95% Buffer in acetonitrile

(Continued on p. 186)

TABLE II *(continued)*

Compound	*Structure*	*Column*[a]	*k'*	*α*	R_s	*Mobile phase*
(**12**) Nisoldipine		A	4.81	1.13	1.04	90% Buffer in acetonitrile
		C	3.17	1.07	0.6	80% Buffer in acetonitrile
(**13**) SQ 31 236	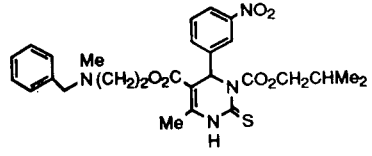	A	2.00	1.21	2.00	85% Buffer in acetonitrile
		B	10.86	1.28	1.25	80% Buffer in acetonitrile
		C	2.54	1.13	0.83	95% Buffer in acetonitrile
(**14**) SQ 31 579	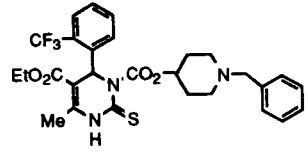	A	5.08	1.14	0.55	95% Buffer in acetonitrile

[a] See Table I for column designation.

TABLE III

ENANTIOMERIC SEPARATION OF RACEMATES IN WHICH THE CHIRAL CENTER IS EXTERNAL TO A RING

k' = Capacity factor of the first eluted enantiomer; buffer A = 1% triethylamine acetate, pH 4.1; buffer B = 1% triethylamine acetate, pH 7.1.

Compound	*Structure*	*Column*[a] *k'*	α	R_s	*Mobile phase*
(15) 3,3',5-Triiodo-D,L-thyronine	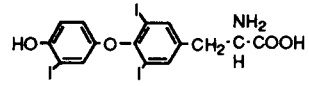	A 7.18	1.05	0.65	85% Buffer A in acetonitrile
(16) 3,5-Diiodo-D,L-thyronine	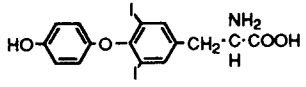	A 8.42 C 4.16	1.07 1.05	1.12 0.5	90% Buffer A in acetonitrile 80% Buffer A in acetonitrile
(17) α-(1-Naphthyl)ethylamine	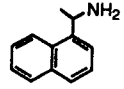	A 2.10 B 2.58 C 5.40	1.05 1.06 1.06	0.3 0.6 0.4	100% Buffer B 90% Buffer B in methanol 80% Buffer B in methanol
(18) DL-3-(α-Acetonyl-4-chlorobenzyl)-4-hydroxycoumarin	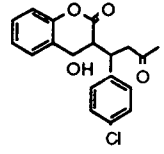	A 4.41 B 5.38	1.06 1.04	0.6 0.6	95% Buffer B in acetonitrile 95% Buffer B in acetonitrile

[a] See Table I for column designation.

TABLE IV

ENANTIOMERIC SEPARATION OF ATROPIC ANALYTES

k' = Capacity factor of the first eluted enantiomer. Buffer = 1% triethylamine acetate, pH 4.1.

Compound	*Structure*	*Column*[a]	k'	α	R_s	*Mobile phase*
(19) (±)-1,1′-Bi-2-naphthol	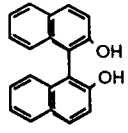	A	4.40	1.08	0.6	20% Buffer in methanol
(20)	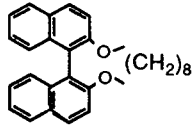	A	0.64	1.08	0.5	30% Acetonitrile in water
		C	4.16	1.15	1.1	30% Acetonitrile in water

[a] See Table I for column designation.

three groups. The first group consists of those compounds in which the chiral center is incorporated into a ring system. The data for these solutes are tabulated in Table II. Table III contains the data for solutes for which the chiral center is external to an aromatic ring. The third group of solutes consists of atropic compounds, or compounds which contain an axis of dyssymmetry. In almost all cases, the best selectivities were achieved on the larger-pore silica. This is undoubtedly due to the higher derivatized CD density on the silica surface (see Table I).

The spacer chain concentration on the smaller-pore silica is approximately twice that found on the wider-pore silica. This suggests the possibility of an alternative retention mechanism in which the solute interacts with the spacer chain rather than with the CD. The spacer chain, lacking a chiral center, does not confer any enantioselectivity but can contribute to retention. This may account for the lower enantioselectivity of column C despite the generally larger capacity factors relative to the other 25-cm column. Alternatively, there is more likelihood of the CD being linked by more than one spacer chain to the smaller-pore silica. This could limit the mobility of the CD and also sterically restrict access of the CD to the chiral analytes.

As stated in the introduction, the mechanism thought to be responsible for enantiomeric separations using underivatized CDs is related to the formation of a diastereomeric inclusion complex between the CD and the chiral compound. Earlier chromatographic studies using CDs have revealed several solute structural factors affecting chiral recognition[14]. Hydrogen bonding groups adjacent to the "chiral center" capable of interacting with the hydroxyls which line the mouth of the CD cavity enhance enantioselectivity. The hydrophobic interior of β-CD can accommodate a solute of about the same size as a naphthyl or biphenyl group. There must be a relatively tight fit between the solute and the CD cavity for chiral recognition. Better resolution is obtained when the solute has between two and four rings with at least one being aromatic. It also has been found that enantioselectivity is enhanced when the chiral center is "sandwiched" between π systems. In general, the more rigid the substituents on the "chiral center", the better the resolution between enantiomers.

In the case of derivatized CDs, the additional hydroxyl groups external to the CD may play more than one role in chiral recognition. In some cases, the external hydroxyl groups may provide additional sites for hydrogen bonding and may assist in "immobilizing" the solute in the diastereomeric inclusion complex. In contrast to the secondary hydroxyls which are locked into position on the native CD, the OH moiety of the hydroxypropyl groups is free to rotate. This flexibility may allow for a closer approach between the OH and any hydrogen bonding moiety present in the solute leading to stronger or more stereospecific interactions than are possible with the native CD. This effect would be more important for the smaller solutes such as indanol (**2**) and 1,2,3,4-tetrahydro-1-naphthol (**3**). In these cases, the optical purities of the additional chiral centers on the derivatized CD would not play a role in the chiral recognition process. This type of role is also demonstrated by the fact that some enantiomeric pairs (*i.e.*, **5** and **10**) are well resolved on the racemic stationary phase despite the fact that the racemic column was shorter than the optically pure columns (Table II). The fact that the additional hydroxyls do make a contribution to chiral recognition is established because most of these solutes were unresolved on a β-CD column. Compounds **5** and **10** were recently reported as separated on a β-CD column[15]. The β-CD column exhibited better selectivity for these compounds.

In the case of compounds **8**–**14**, the aromatic ring presumably is the portion of the molecule included into the CD cavity (Fig. 1). The presence of the polar trifluoromethyl (or nitro, compound **12**) substituent on the aromatic ring probably precludes full penetration of the aromatic ring into the CD cavity. Others have found that for geometrical isomers of dipolar substituted aromatics, *ortho*-substituted isomers elute before the *para* isomers[8]. Although the exact substitution patterns of the hydroxypropyl groups on the CD are not known, the presence of these groups no doubt alters the types of interactions possible at the mouth of the CD cavity. These alternate types of interactions possible with the hydroxypropyl-β-CD include not only the hydrogen bonding interactions with the hydroxypropyl OH mentioned above but also include steric interactions with these groups as well. These additional steric

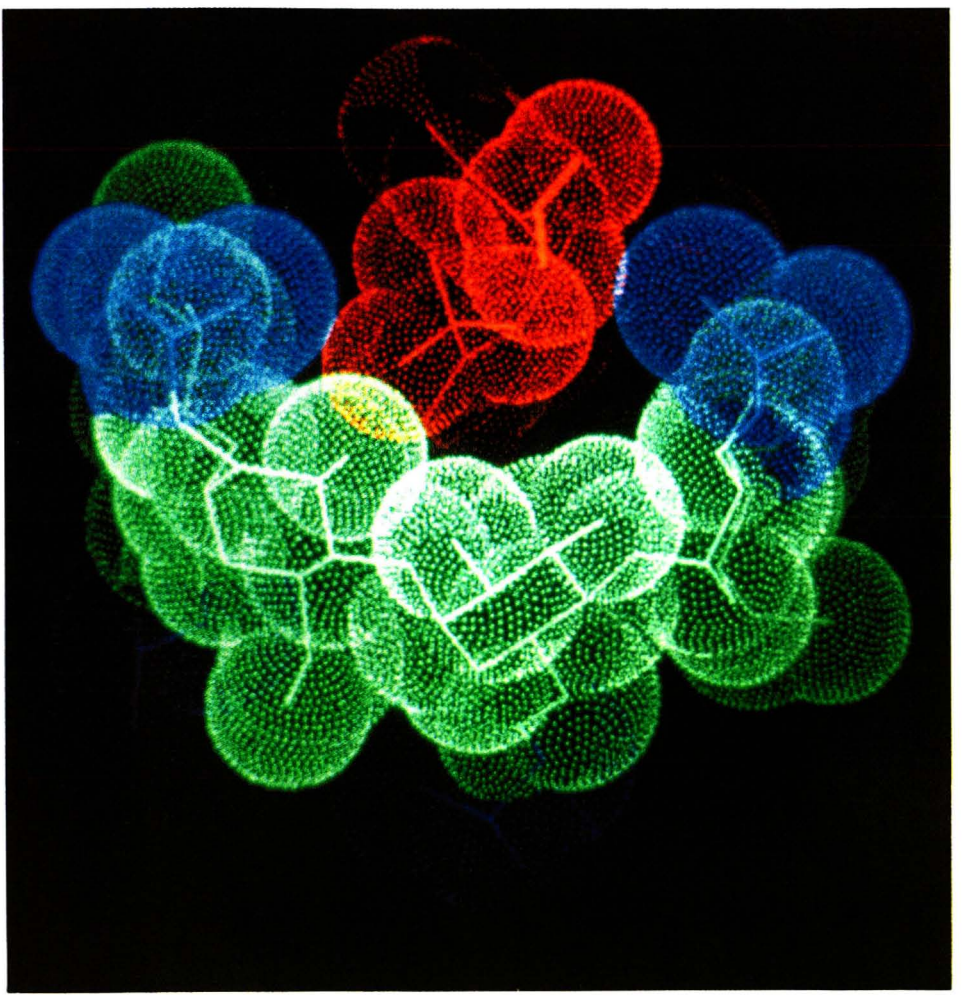

Fig. 1. Computer graphic image of the inclusion complex of BAY COOH (compound **8**), a calcium-channel blocker, and hydroxypropyl-β-CD.

interactions may account for some of the enantioselectivity observed for enantiomers which have bulky substituents on the heterocyclic ring β to the chiral center (*i.e.*, **13** in Fig. 2).

As in the case of β-CD-based separations, selectivity is more likely if the substituents on the chiral center are capable of hydrogen bonding or if the chiral center is adjacent to an aromatic ring. However, the restriction that the hydrogen bonding or aromatic substituents be α to the chiral center seems to be much less stringent for the hydroxypropyl phases. The effect of substitution on selectivity can be seen by comparing the selectivities obtained for compounds with different substituents (Table II). The relative selectivity obtained for the enantiomers of Idazoxan (**6**) is less than that obtained when the chiral center has an additional methyl substituent (**7**). Compounds **9–11** are esterified derivatives of compound **8**. The acid is fairly well resolved on all three columns (Fig. 3). This is probably due to hydrogen-bonding interactions through the acid. Some of this resolution is lost, however, when the ester is formed (compounds **9** and **11**) unless the ester has a bulky substituent which can hinder the possible orientations of the molecule in the diastereomeric association complex (compound **10**). In this case, the hydrogen bonding interactions are replaced by steric interactions. Also, for compounds **9** and **12**, the external chiral center of the derivatized CD seems to play a role in the chiral recognition process because the racemic column was unable to resolve the enantiomers. However, the racemic column exhibited better selectivity than the other two columns for compounds **10** and **11**, probably because of the higher bonded CD density.

For some compounds (*i.e.*, **9**, **12**, **15**, **16** and the atropic compounds **19** and **20**), the additional chiral centers undoubtedly play a role in the chiral recognition process because of the significantly greater selectivities achieved on the A and C columns as opposed to the selectivity obtained on the B column (Tables II–IV). Bulky substituents on the chiral centers of the optically active molecules sterically restrict access to the CD cavity and preclude full penetration of the solute into the CD cavity. For example, the presence of an additional iodine on the phenolic ring of 3,3′,5-triiodo-D,L-thyronine (**15**) interferes with the formation of an inclusion complex. Only the optically pure column with the highest bonded ligand density is able to resolve the enantiomers

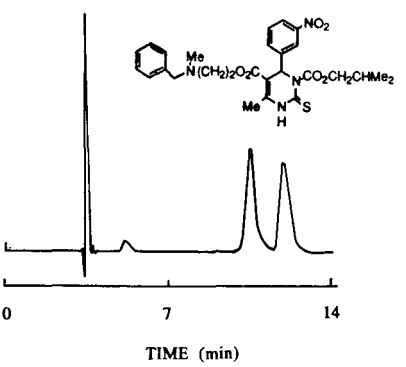

Fig. 2. Chromatogram of a calcium-channel blocker (compound **13**) on the wide-pore (*S*)-hydroxypropyl-β-CD column A. Mobile phase as specified in Table II.

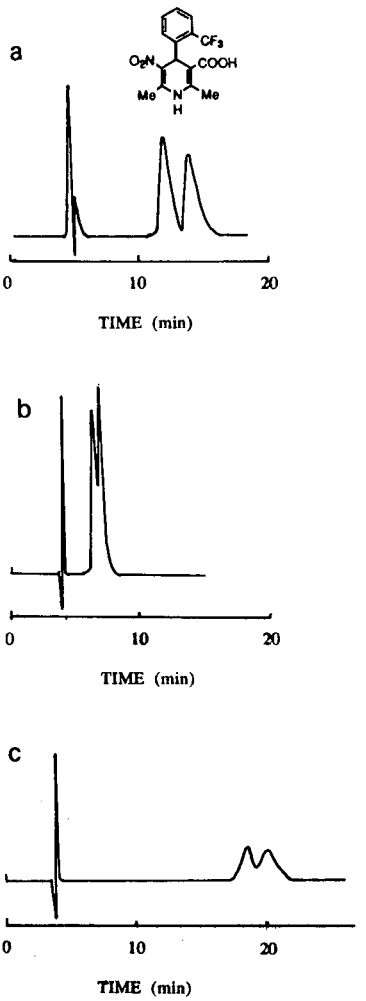

Fig. 3. Chromatograms of BAY COOH (compound **8**) on (a) column A (wide pore, (*S*)-hydroxypropyl); (b) column B (wide pore, racemic hydroxypropyl and (c) column C (narrow pore, (*S*)-hydroxypropyl). Mobile phase as specified in Table II.

(Fig. 4). 3,3′,5,5′-Tetraiodo-D,L-thyronine was unresolvable on any of the columns. The atropic molecules also are sterically restricted from fully entering the CD cavity; therefore, the enantioselectivity must arise through interaction with the chiral center external to the CD. As pointed out by Han and Armstrong[16], it is not necessary for the entire molecule to be included in the CD cavity. In the case of hydroxypropyl-β-CD, it is possible for the hydroxypropyl groups to assume a configuration which would allow stereoselective hydrogen bonding with the chiral portion of the molecule even though the chiral center sits outside the CD cavity as long as a portion of the molecule is tightly complexed within the CD cavity. In order for enantioselectivity to occur, however, the hydroxypropyl groups would have to be optically pure. This would explain the lack of stereoselectivity on the racemic column (B) for these particular solutes.

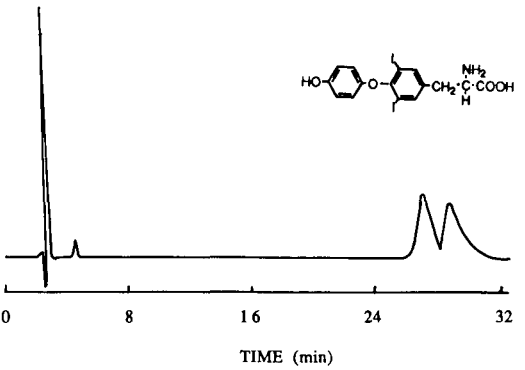

Fig. 4. Chromatogram of 3,5-diiodo-D,L-thyronine (compound **17**) on the wide-pore (*S*)-hydroxypropyl-β-CD column A. Mobile phase as specified in Table III.

In summary, hydroxypropyl-β-CD has been shown to be a useful liquid chromatography packing for the separation of enantiomers which are difficult or impossible to separate using β-CD columns. In most cases, the separation mechanism appears to be, as in the case of the native CD, due to the formation of diastereomeric inclusion complexes. However, the hydroxypropyl-CD phase seems to have more than one mechanism for distinguishing between enantiomers. For smaller solutes, the flexibility of the hydroxypropyl group allows for a closer approach between the hydroxyls and any hydrogen bonding moiety present in the analyte leading to stronger but not necessarily stereospecific interactions than is possible with the native CD. The hydroxypropyl groups can provide not only additional sites for hydrogen bonding but steric interactions as well. In addition, the additional centers of chirality on the hydroxypropyl group may also contribute to enantioselectivity through stereospecific hydrogen-bonding interactions. This is particularly important in cases where the analyte is too big to fully enter the CD cavity.

ACKNOWLEDGEMENT

The support of this work by the Missouri Research Assistance Act (MRAA/Monsanto) and the Department of Energy, Office of Basic Sciences (DE FG02 88ER13819) is gratefully acknowledged.

REFERENCES

1 J. Debowski, D. Sybilska and J. Jurczak, *J. Chromatogr.*, 237 (1982) 303.
2 J. Debowski, J. Jurczak, D. Sybilska and J. Zukowski, *J. Chromatogr.*, 329 (1985) 206.
3 J. Zukowski, D. Sybilska and J. Bojarski, *J. Chromatogr.*, 364 (1986) 225.
4 D. W. Armstrong, F. He and S. M. Han, *J. Chromatogr.*, 448 (1988) 345.
5 D. W. Armstrong and W. DeMond, *J. Chromatogr. Sci.*, 22 (1984) 411.
6 T. J. Ward and D. W. Armstrong, *J. Liq. Chromatogr.*, 9 (1986) 407.
7 D. W. Armstrong, A. Alak, K. H. Bui, W. DeMond, T. Ward, R. E. Riehl and W. L. Hinze, *J. Inclusion Phenom.*, 2 (1984) 533.
8 D. W. Armstrong, J. R. Faulkner, Jr. and S. M. Han, *J. Chromatogr.*, 452 (1988) 323.

9 D. W. Armstrong, T. J. Ward, R. D. Armstrong and T. E. Beesley, *Science (Washington, D.C.)*, 232 (1986) 1132.
10 R. D. Armstrong, T. J. Ward, N. Pattabiraman, C. Benz and D. W. Armstrong, *J. Chromatogr.*, 414 (1987) 192.
11 D. W. Armstrong, W. Li, C. Chang and J. Pitha, *Anal. Chem.*, 62 (1990) 914.
12 D. W. Armstrong, *U.S. Pat.*, 4 539 399 (1985).
13 G. E. Berendsen, K. A. Pikaart and L. de Galan, *J. Liq. Chromatogr.*, 3 (1978) 561.
14 S. M. Han, Y. I. Han and D. W. Armstrong, *J. Chromatogr.*, 441 (1988) 376.
15 A. Berthod, H. L. Jin, T. E. Beesley, J. D. Duncan and D. W. Armstrong, *J. Pharm. Biomed. Anal.*, (1990) in press.
16 S. M. Han and D. W. Armstrong, in A. M. Krstulovic (Editor), *Chiral Separations by HPLC—Applications to Pharmaceutical Compounds*, Ellis Horwood, Chichester, 1989, pp. 208–284.

Journal of Chromatography, 513 (1990) 195–207
Elsevier Science Publishers B.V., Amsterdam

CHROM. 22 465

Coupled column chromatography in chiral separations

I. Enantiomeric separation on swollen microcrystalline cellulose triacetate columns after a preseparation on a non-chiral alkylsilica column[a]

ANDREAS M. RIZZI
Institute of Analytical Chemistry, University of Vienna, Währingerstrasse 38, A-1090 Vienna (Austria)
(First received February 15th, 1990; revised manuscript received March 26th, 1990)

ABSTRACT

A two-dimensional chromatographic system was evaluated that combines a column packed with swollen crystalline cellulose triacetate for optical resolution of enantiomers with a non-chiral column for the preseparation of these enantiomers from other analytes or impurities. This two-dimensional approach greatly enhances the low peak capacities usually obtained with swollen microcrystalline cellulose triacetate columns. In this way determination of enantiomers can be achieved also in more complex samples and the significance of the purity determination of the enantiomeric peaks can be improved. The coupled column system was evaluated with respect to the compatability of the mobile phases and the possibilities of achieving peak compression at the top of the second column.

INTRODUCTION

In the last 10 years, the separation of enantiomers has attracted great interest for a wide spectrum of compounds. Chiral stationary phases based on cellulose derivatives have been applied for this purpose in many instances[1–3]. Microcrystalline cellulose triacetate (CTA) and cellulose tribenzoate (CTB) can be used directly in a swollen state as packing materials with small particle sizes (down to 7–10 μm) in high-performance liquid chromatographic (HPLC) columns[4–7]. These adsorbents provide high enantioselectivity for a great variety of substances, including those with only one polar functional group. This feature and a surprisingly high loadability without loss of performance are the main advantages of these materials[5,6,8,9]. Their main drawback, however, is the very large peak dispersion for most types of analytes.

[a] Dedicated to Professor J.F.K. Huber on the occasion of his 65th birthday.

0021-9673/90/$03.50

Recent papers[8,9] discussed certain stategies for improving the efficiency of chiral separations by means of swollen crystalline cellulose triacetate (swcrCTA) packings. In spite of significant improvements in peak dispersion on optimizing the chromatographic conditions, the plate height values still remain high for many types of substances. The resulting lack of theoretical plates can be overcome in many instances by the high enantioselectivity obtainable by swcrCTA adsorbents to give good enantiomeric resolution. The low peak capacity of a swcrCTA column, however, which results from the low plate number, remains a problem. A low peak capacity implies that one has only a small chance of finding separation conditions where the enantiomers will be sufficiently separated from each other and from other compounds present. Even with well separated and seemingly pure enantiomeric peaks one needs a certain peak capacity to ensure and to demonstrate that no trace peak is hidden underneath the analyte peak. This is also important for more or less pure chiral substances, because high accuracy and precision are usually required for the determination of the enantiomeric excess.

An effective technique for enhancing the peak capacity is the use of a multi-column set-up with column switching[10]. The whole potential of on-line column switching techniques can only be utilized if the two following conditions are met: the mobile phase carryover from the first column should not cause a severe and detrimental deconditioning of the second column, and proper selection of the mobile phases should make it possible to achieve a peak compression effect in the second column[11]. In our case the question also has to be discussed of whether the carryover severely affects or disturbs the swelling state of the swcrCTA material.

In this work the possibilities and limitations of column switching in a coupled system consisting of a non-chiral alkylsilica column operated in a reversed-phase system and a subsequent chiral swcrCTA column were examined with respect to the above criteria: compatability of the mobile phases and possibilities for obtaining peak compression effects.

Conclusions drawn for this column-switching system may also be useful for the optimization of off-line preseparations, especially when considering deconditioning of the CTA column by the injected solvent and the determination of the maximum allowable injection volume.

EXPERIMENTAL

Instrumentation

Chromatographic experiments were carried out with an HPLC pump (Model L-6200 intelligent pump, Merck–Hitachi, Tokyo, Japan), a syringe-valve injector (Model 7161, Rheodyne, Cotati, U.S.A.) equipped with a 20-μl loop, a column oven (Model 655A-52, Merck–Hitachi), two switching valves (Model 7000, Rheodyne) and a UV detector (Model L-4000, Merck–Hitachi) connected to an integrator (Model D-2000 chromato-integrator, Merck–Hitachi).

Columns

Non-chiral column. Prepacked stainless-steel columns (250 mm × 4.0 mm I.D.) filled with chemically bonded octylsilica material, particle diameter 5 μm (LiChrosorb RP-8; E. Merck, Darmstadt, F.R.G.).

Chiral column. Prepacked columns (250 mm × 4.0 and 10.0 mm I.D.) filled with swollen crystalline cellulose triacetate, mean particle diameter 10 μm (Hibar; E. Merck).

Reagents and samples

Organic solvents were obtained from E. Merck: methanol of LiChrosolv quality and absolute ethanol of analytical-reagent grade. Water was distilled twice from a quartz apparatus and additionally purified by passing it through an RP-8 column before eluent preparation. Alcohol–water mixtures were partially premixed and degassed in an ultrasonic bath.

Pure standard solutions of the racemic test analytes were used for the evaluation of the peak compression effect. Solutions of less pure standard analytes were employed to demonstrate the separation power of the column-switching set-up.

Chromatographic procedure

A schematic diagram of the two-column set-up is shown in Fig. 1 and a general chromatographic elution and column switching protocol is given in Table I. The procedure starts with the injection of the sample onto the non-chiral alkylsilica column and the elution on this first column with ethanol–water mixtures suitable for the entire separation problem. In this step, the racemic analytes are separated from matrix constituents and impurities. A small fraction of the eluate which contains the chiral analyte is transferred to the CTA column. After the transfer of this fraction to the second column, the elution on the first column is finished. Thereafter, column 1 is switched off and the capillary bypass is used. At the same time the eluent composition is changed to an ethanol–water mixture suitable for the separation on the CTA column, and the capillaries are rinsed. After rinsing, the CTA column is switched on and the analyte stored in this column is eluted. The temperature of the first column was ambient and of the CTA column 50°C. UV detection at 254 nm was used. Mobile phase void volumes of the CTA columns were calculated by assuming a packing porosity of 0.71[8].

RESULTS AND DISCUSSION

Peak capacities

The peak capacity, $n_{(R_s)}$, *i.e.*, the maximum number of peaks that can be separated in a chromatogram with a desired resolution, R_s, in a given time, in the ideal

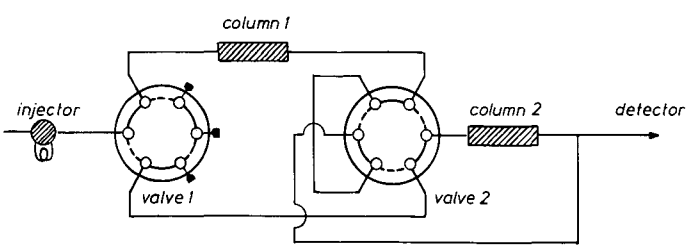

Fig. 1. Schematic diagram of the coupled column chromatographic system used: column 1, alkylsilica (OS or ODS); column 2, swollen crystalline cellulose triacetate (CTA). Valves: rotor position A, solid lines; rotor position B, broken lines.

TABLE I

GENERAL ELUTION AND COLUMN-SWITCHING PROGRAMME

Time interval[a]	*Position of valve*		*Column*	*Eluent*[b]	*Flow-rate*[c]	*Comment*
	1	*2*				
0–*t*1	A	A	RP	1	1	Preseparation of the sample
*t*1–*t*2	A	B	RP + CTA	1	2[d]	Transfer of the racemic analyte
*t*2–*t*3	A	A	RP	1	1	End of RP elution
*t*3–*t*4	B	B	Capillaries	2	1 or higher	Change of eluent Rinsing of capillaries
*t*4–*t*5	B	A	CTA	2	2	Chiral separation

[a] *t*1 = Beginning of analyte transfer, *e.g.*, at the beginning of the appearance of the racemic analyte; *t*2 = end of transfer; *t*3 = end of the chromatogram on the RP column; *t*3–*t*4 = time for eluent change and rinsing the capillaries (3–5 min); *t*4 = beginning of elution of CTA column; *t*5 = end of elution of CTA column, end of chromatogram.

[b] Eluent 1, eluent optimized for separation in column 1; eluent 2, eluent optimized for separation in column 2.

[c] Flow-rates 1 and 2: optimum flow-rates for columns 1 and 2, respectively.

[d] If the pressure of both columns is too high, a lower flow-rate can be selected.

case that all possible peak positions can be utilized, is calculated here by means of the equation.

$$n_{(R_s)} = \log(1 + k'_n)/\log(1 + R_s/\sqrt{\bar{N}}) \quad (1)$$

where k'_n is the capacity factor of the last eluted peak, n, and $\bar{N}$ is the mean plate number. For the desired resolution of subsequently eluting peaks, R_s, we chose a value of 6[a].

Assuming for a typical octylsilica (OS) column of length 25 cm an average plate number of 9000 and choosing a k'_n value of 20 as the upper limiting value for the practical use, the peak capacity value is *ca.* 50.

The plate numbers achievable of swcrCTA columns depend very much on the chemical structures of the analytes. Assuming $\bar{N}$ to be 900, which is obtained with a column of length 25 cm under favourable conditions, and k'_n to be 5, the maximum number of separable peaks is about ten. When looking for average values in typical chiral separations by means of swcrCTA adsorbents, an $\bar{N}$ value of about 600 seems to be more realistic[8,9]. In addition, a lower value should be assumed for k'_n, *e.g.*, 3, as in practice very few analytes are eluted with $k' > 3$ when using commonly applied mobile phases (low capacity factors are also convenient in order to keep the analysis time acceptably short). With these more realistic assumptions, a peak capacity of *ca.* 6 is obtained. This is a very low value compared with that obtainable with other chromatographic support materials.

[a] The resolution, R_s, is defined here by $R_s = (V_{R_j} - V_{R_i})/\sigma_{V_i}$), where V_R are retention volumes and σ_{V_i} is the volume standard deviation of the first-eluted peak. For peaks of equal height, R_s values of 6 mean just baseline separation. The numerical values of R_s calculated according to this definition are about four times larger than would be obtained by using the definition given by Snyder and Kirkland[12].

A peak capacity value of 6 may be sufficient for the separation of two enantiomers. It is, however, too low, to allow separation also from impurities or to demonstrate their absence with confidence. The large increase in peak capacity is the main reason for introducing a two-column set-up for this type of separation. In principle and under certain conditions, peak capacity values can be obtained in two-column systems which are as high as the product of the peak capacity values of the individual columns. These conditions are met if peak dispersion resulting from the first column is negligible with respect to the overall dispersion or is overcome by peak compression.

Peak compression at the top of the second column

Peak-sharpening effects generally can be obtained by enhancing the elution power of the eluents. These effects are well known from gradient elution. In coupled column chromatography, those column combinations are especially useful, where at a given eluent composition the analyte is retained more strongly on the second column than on the first: $k_{i_{co}}^{col.2} > k_{i_{co}}^{col.1}$ (co represents carryover). In such a case one may apply a step gradient after the transfer of the analyte onto column 2 by using a stronger eluent for the second column than for the first at the time of transfer (*i.e.*, during the carryover). The peak compression effect which is obtained on applying a step gradient at the top of the second column can be quantified by the peak compression factor, *pcf*. This factor can be evaluated to a certain approximation by the equation[13]

$$pcf_i = \sigma_{V_i}(\text{before compr.})/\sigma_{V_i}(\text{after compr.}) = k'^{col.2}_{i_{co}}/k'^{col.2}_{i_{el.2}} \quad (2)$$

where el.2 indicates the eluent used for the second column.

Table II shows that, with water–ethanol eluents and with the same eluent composition, all analytes investigated are in fact retained more strongly by the CTA than by the OS adsorbent used. A strong step gradient can therefore be applied at the top of column 2.

The influence of the eluent composition on the retention is illustrated in Fig. 2 for ethanol–water mixtures. These data are required when applying eqn. 2. With the alkylsilica phases, the capacity factors of the given analytes show a monotonic decrease with increasing alcohol concentration. This is a typical and well known behaviour for non-ionic solutes at not too high alcohol concentrations. There one may even assume an approximately linear correlation between ln k' and the volume fraction of the alcohol in the aqueous mobile phase.

With CTA columns the dependence of k' on the ethanol concentration is not monotonic in the region of ethanol concentrations usually applied with this adsorbent. The decrease in retention with increasing ethanol concentration follows the opposite trend at high concentrations of ethanol.

The observed behaviour is due to the special adsorption mechanism on swcrCTA adsorbents[14]. The strength of the competitive effect of solvent components is significantly influenced by the steric size of the solvent molecules. Hence the competitive effect of water on this adsorbent is stronger than that of ethanol. This effect acts in the direction of reducing the capacity factor values with increasing concentration of water. On the other hand, the smaller solvation power of water compared with ethanol for many analytes causes the activity coefficients of the

TABLE II

CAPACITY FACTORS WITH OCTYLSILICA AND swcrCTA STATIONARY PHASES AS A FUNCTION OF THE CONCENTRATION OF ETHANOL IN WATER–ETHANOL MOBILE PHASES

Compound		*Octylsilica*						
		80%[a]	*72%*	*64%*	*40%*	*24%*		
Phenyloxazolone			0.03	0.09	0.50	2.69		
Phenyldioxolone		0.07	0.09	0.14	1.00	3.72		
Hexobarbital		0.08	0.11	0.20	1.59			
Spirobiindanone		0.11	0.19		3.88			
Methaqualone		0.13	0.28	0.44	4.50			
Tröger's base			1.26	2.27	4.77			
		swcrCTA						
		96%[a]	*86.4%*	*80%*	*76.8%*	*72%*	*60%*	*40%*
Phenyloxazolone	I[b]	0.54	0.34	0.23		0.30	0.56	1.87
	II[b]	0.88	0.57	0.43		0.70	0.89	2.71
Phenyldioxolone	I	1.84			1.66			
	II	3.47			3.66			
Hexobarbital	I	0.83	0.60	0.59		0.85	1.42	
	II	1.21	0.99	1.02		1.22	2.50	
Spirobiindanone	I	0.95	0.67		1.08			
	II	2.03	1.80		3.14			
Methaqualone	I	0.27	0.18		0.29			
	II	0.42	0.29		0.44			
Tröger's base	I	1.10	0.74		1.24			
	II	2.31	1.67		2.99			

[a] Ethanol concentration in mobile phase (%, v/v).
[b] I and II indicate first and second enantiomer, respectively.

analytes in the mobile phase, and hence the capacity factors, to increase with increasing concentration of water. The superposition of both effects produces the capacity factor dependence given in Fig. 2.

By use of eqn. 2 and the data from Fig. 2, one can evaluate the conditions under which and the extent to which peak compression can be obtained. As a rule, peak compression can simply be obtained in most instances by choosing a higher alcohol concentration in eluent 2 than in the carryover, with the exception of ethanol concentrations higher than 75–80% (v/v).

Exploitable peak compression effect

To evaluate the optimum eluent compositions for eluent 2, one must consider the optimum separation conditions for the racemic analytes on the CTA column together with the peak compression potential at the top of this column given under these conditions. One should consider that the peak compression factor at the top of column 2 is not required to be the maximum attainable. It is sufficient if the peak variance in the carryover is reduced to such an extent that it does not affect the resolution to more

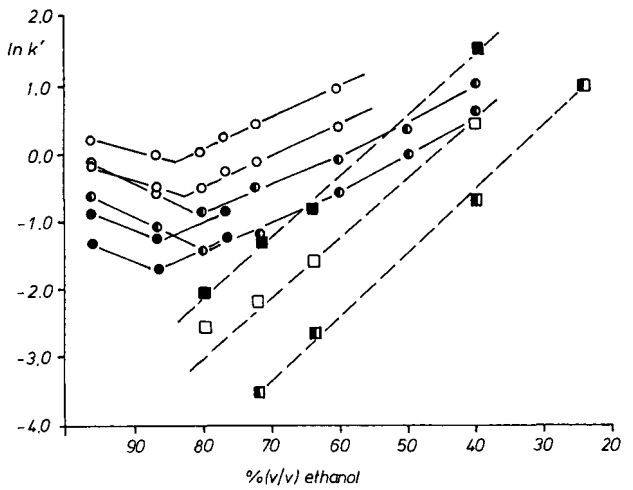

Fig. 2. Logarithm of the capacity factors of test analytes on swcrCTA and octylsilica adsorbents as a function of the volume fraction of ethanol in ethanol–water mobile phases. Temperature, 50°C. Analytes: hexobarbital (open symbols), 5-phenyltetrahydrooxazol-2-one (half filled symbols) and methaqualone (full symbols). Circles, swcrCTA adsorbent; squares, octylsilica adsorbent.

than a few percent. The maximum exploitable compression factor therefore obviously depends on the peak variance in the carryover and the variance resulting during elution in column 2.

The influence of the peak variance in the carryover on the total resolution is evaluated by means of eqn. 3, assuming that more or less the whole analyte peak is transfered to column 2:

$$\frac{R_s^{(1+2)}}{R_s^{(2)}} = \left[1 + \left(\frac{\sigma_V^{col.1}}{\sigma_V^{col.2}}\right)^2\right]^{-1/2} \tag{3}$$

where $R_s^{(2)}$ means the resolution obtained by use of column 2 and $R_s^{(1+2)}$ that obtained by the use of a combination of both column; σ_V is the standard deviation of the eluted peaks in volume units.

For reasonable capacity factors and plate numbers in the first (OS) and second (CTA) columns, and considering typical inside diameters of the columns (4 mm for the OS and 4 and 10 mm for the CTA column), the relative decrease in enantiomeric resolution due to the first column is shown in Table III, under the assumption that peak compression is not performed. Conversely, these data illustrate the maximum effect on the peak widths in the final chromatograms that can be expected from peak compression at the top of the column under the optimum conditions. For columns with equal diameter, the decrease in resolution is sometimes significant and may be up to 30% for compounds weakly retained on the CTA column. Here, the application of peak compression will result in a decisive improvement. If one combines the OS column of 4 mm I.D. with the chiral column of 10 mm I.D., the decrease in resolution is very small and in fact negligible. In this instance, a peak compression at the top of column 2 will produce no observable effect on the final chromatogram.

TABLE III

CALCULATED PEAK PROFILE STANDARD DEVIATIONS, σ_V, OF THE COLUMNS USED AND CALCULATED DECREASE IN CHROMATOGRAPHIC RESOLUTION ON USING TWO-COLUMN CHROMATOGRAPHY WITHOUT PEAK COMPRESSION

Column 1 (N = 8000,[a] *I.D. = 4 mm, V_0 = 2.4 ml)*		*Column 2 (N = 600)*[b]				
		I.D. = 4 mm, V_0 = 2.4 ml			*I.D. = 10 mm, V_0 = 15 ml*	
k'	σ_V (μl)	k'	σ_V (μl)	$R_s^{(1+2)}/R_s^{(2)}$	σ_V (μl)	$R_s^{(1+2)}/R_s^{(2)}$
3	107	0.5	147	0.808	919	0.993
		1.0	196	0.877	1225	0.996
		1.5	255	0.916	1531	0.998
5	161	0.5	147	0.674	919	0.985
		1.0	196	0.772	1225	0.991
		1.5	255	0.835	1531	0.995

[a] Typical value for RP columns.
[b] Typical value for swcrCTA columns.

Chromatograms of 5-phenyltetrahydrooxazol-2-one, hexobarbital and Tröger's base obtained by the OS–CTA coupled column system are shown in Figs. 3–5. In each instance, the eluents for the first column were selected such that reasonable capacity factors are obtained on the OS column and a too high concentration of water is avoided (*cf.*, discussion on the compatibility of mobile phases). The eluents for the second column were selected such that the requirements for enantiomeric resolution and short analysis time were satisfied[14]. The separation of the enantiomers obtained with the coupled column system is seen to be as good as that given by a single CTA column.

Table IV shows the capacity factor, enantioselectivity and peak dispersion data corresponding to these chromatograms together with the data obtained by single CTA chromatography. Experimental peak compression factors, determined from peak widths in the chromatograms according to eqn. 4, and the maximum obtainable compression factors at the top of column 2, as calculated from capacity factor data according to eqn. 2, are also given.

$$pcf^{exp} = \left[\frac{(\sigma_V^{col.1})^2 + (\sigma_V^{col.2})^2 + (\sigma_V^{ex})^2}{(\sigma_V^{col.1+col.2})^2 + (\sigma_V^{ex})^2} \right]^{1/2} \quad (4)$$

where the superscript ex indicates contributions from the injector, detector, capillaries and switching valves. $(\sigma_V^{col.1})^2$ has to be substituted by the peak variance in the carryover if only parts of the analyte are transferred to column 2.

First, and most important for practical applications, one can see in Table IV that the final peak widths (σ_V data) remain essentially unchanged in all instances, whether using a single CTA column or a column-switching system. Because of the higher elution strength of eluent 2 with respect to the carryover, peak compression can be expected to take place at the top of the CTA column in all instances (*cf.*, pcf^{max} data). It

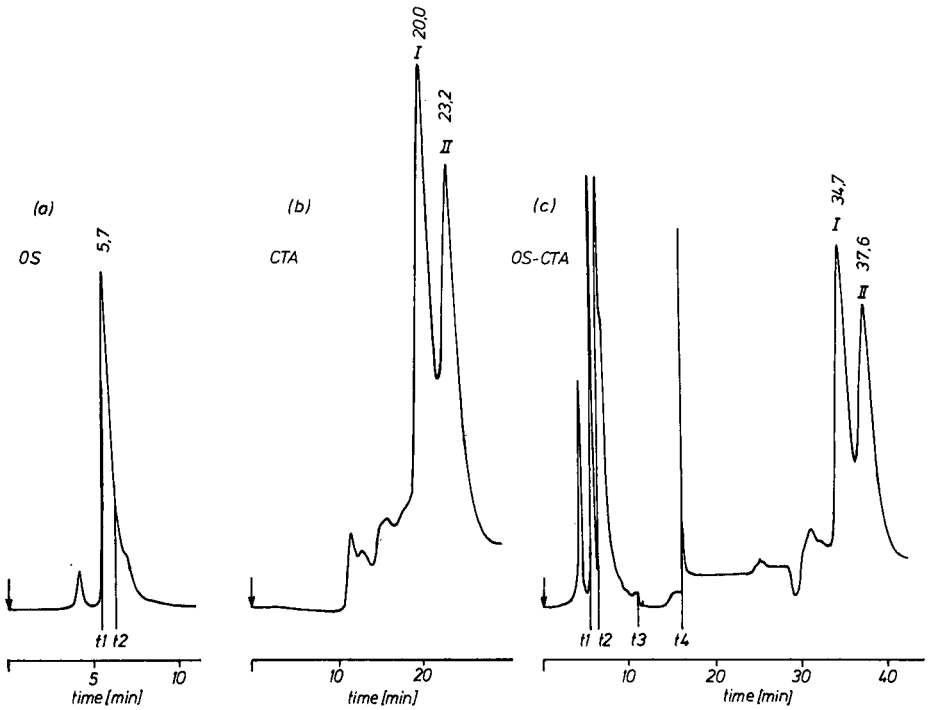

Fig. 3. Chromatograms of 5-phenyltetrahydrooxazol-2-one obtained in single column systems and in the octylsilica–swcrCTA two-column system including column switching. Separated enantiomers are indicated by I and II. (a) OS column only; (b) $CTA_{(II)}$ column only; (c) OS-$CTA_{(II)}$ with column switching. Column dimensions: OS, 250 × 4 mm I.D.; $CTA_{(II)}$, 250 × 10 mm I.D. Temperature: column 1, ambient; column 2, 50°C. Eluent 1, ethanol–water (40:60); eluent 2, ethanol–methanol–water (67.2:20:12.8). Flow-rate 1, 0.5 ml/min; flow-rate 2, 1.0 ml/min. Times of events: $t1$ = 5.5; $t2$ = 6.5; $t3$ = 11.0; $t4$ = 16.0; $t5$ = 42.0 min.

is obvious that a significant peak compression effect in the final chromatograms (see pcf^{exp} data) can be observed only in instances where the small-diameter CTA column was employed. Otherwise the effect vanishes because of the dispersion in the wide-diameter column.

From Table IV a decrease in the capacity factors on the CTA adsorbent by the column switching procedure can be seen. It is probably due to a slightly higher temperature in the CTA column when operated in the column-switching mode, which results from different working temperatures in columns 1 and 2 in our set-up. The increase in enantioselectivity is probably caused by the high water content in the carryover. Increasing enantioselectivity with increasing water concentration in the eluent can be observed for many analytes with CTA adsorbents[7,14]. The higher water contents in the carryover thus produces a useful side effect in this type of column-switching system.

General compatibility of the mobile phases

The use of coupled column chromatography requires that the carryover from the first column is fully compatible with the stationary phase and the eluent used in the

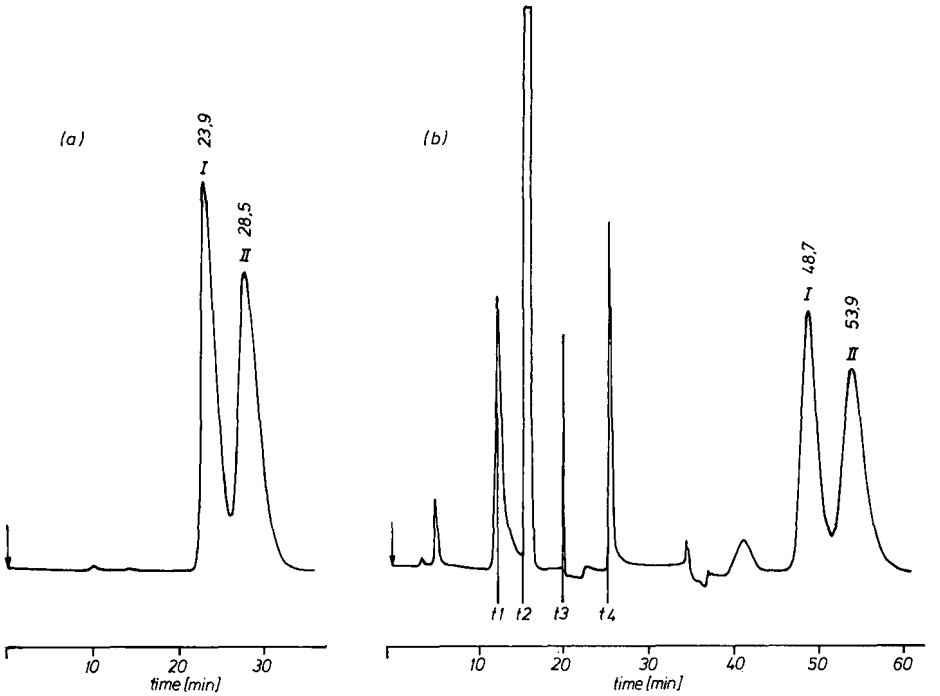

Fig. 4. Chromatograms of hexobarbital obtained from a single CTA column and in the octylsilica–swcrCTA two-column system including column switching. (a) $CTA_{(l)}$ column only; (b) OS-$CTA_{(l)}$ with column switching. Column dimensions: OS, 250 × 4 mm I.D.; $CTA_{(l)}$ 250 × 4 mm I.D. Temperature: column 1, ambient; column 2, 50°C. Eluent 1, ethanol–water (40:60); eluent 2, ethanol–methanol–water (67.2:20:12.8). Flow-rate 1, 0.5 ml/min; flow-rate 2, 0.16 ml/min. Times of events: $t1$ = 12.25; $t2$ = 15.20; $t3$ = 20.0; $t4$ = 25.0; $t5$ = 61.0 min.

second column. This means, first, that for our column-switching system, solvents which may solvate the CTA adsorbent (chloroalkanes, THF, ketones) must be excluded from the carryover.

Second, with swcrCTA stationary phases, an additional constraint results from the swollen state of the packed bed. Previous investigations[14] have shown that changes in the eluent composition probably also affect the swelling state of the CTA packing. It is therefore necessary to prevent an irreversible change in the swelling state of the bed by the eluent carryover. With regard to the proposed two-column combination, too high a water concentration in the carryover may be problematic for the CTA column. In our experience, the packing of the column is not disturbed, at least up to a concentrations of 76% (v/v) water in the ethanolic mobile phase, although temporary changes in the swelling state are very likely. The critical content of water at which breakdown of the packing occurs has not been determined. Up to 76% of water all the changes in the swelling state did not cause problems with the stability of the packed bed. Plate-number data indicate that these changes are fully reversible on returning to the initial eluent composition that was used for the packing of the column [in this instance ethanol–water (96:4)].

TABLE IV

CAPACITY FACTOR (k'), ENANTIOSELECTIVITY (α) AND PEAK STANDARD DEVIATION (σ_V) DATA OF ANALYTES IN SINGLE-COLUMN AND COUPLED-COLUMN CHROMATOGRAPHY, AND PEAK COMPRESSION FACTORS (pcf) DERIVED THEREFROM

$CTA_{(I)}$, column with I.D. 4 mm, flow-rate = 0.16 ml/min; $CTA_{(II)}$, I.D. 10 mm, flow-rate = 1.0 ml/min; OS, octylsilica, flow-rate = 0.5 ml/min. Other chromatographic conditions as given in Figs. 3–5; co indicates the carryover; pcf^{exp}, experimental peak compression factor, determined according to eqn. 4; pcf^{max}, maximum obtainable peak compression factor at the top of column 2, evaluated according to eqn. 2. Enantioselectivity coefficients in the coupled-column system are calculated according to $\alpha = (t_{R_2}^{OS-CTA} - t_4 - t_{R_0}^{CTA})/(t_{R_1}^{OS-CTA} - t_4 - t_{R_0}^{CTA})$, t_{R_1} and t_{R_2} being the retention times of the two enantiomers, t_4 the time of starting the elution on the CTA column (*cf.*, Table I) and t_{R_0} the elution time of the system peak of the eluent component methanol (*i.e.*, 14 min in both columns at the flow-rates applied).

Compound	*Parameter*	$CTA_{(I)}$	$OS\text{–}CTA_{(I)}$	$CTA_{(II)}$	$OS\text{–}CTA_{(II)}$
5-Phenyltetrahydrooxazol-2-one[a]	$k'^{CTA}_{1\,el.2}$	0.65[b]	0.31[b]	0.43	0.33
	$k'^{CTA}_{2\,el.2}$	0.85[b]	0.48[b]	0.66	0.53
	α	1.31[b]	1.52[b]	1.55	1.61
	$(\sigma_V)_1$ (μl)	86[b]	96[b]	680	680
	$(\sigma_V)_2$ (μl)	106[b]	102[b]	760	760
	$(\sigma_V)^{co}$ (μl)		500		130
	pcf_1^{exp}		5.3		1.02
	pcf_2^{exp}		5.0		1.01
	$k'^{CTA}_{1\,el.1}$			1.87[c]	
	$k'^{CTA}_{2\,el.1}$			2.71[c]	
	pcf_1^{max}		6.0[d]		4.3
	pcf_2^{max}		5.6[d]		4.1
Hexobarbital[a]	$k'^{CTA}_{1\,el.2}$	0.71	0.66	0.67	0.55
	$k'^{CTA}_{2\,el.2}$	1.04	1.03	1.05	0.90
	α	1.46	1.56	1.57	1.62
	$(\sigma_V)_1$ (μl)	131	140	880	810
	$(\sigma_V)_2$ (μl)	173	182	1200	1090
	$(\sigma_V)^{co}$ (μl)		500		300
	pcf_1^{exp}		3.7		1.15
	pcf_2^{exp}		2.9		1.00
	$k'^{CTA}_{1\,el.1}$			3.6[c]	
	$k'^{CTA}_{2\,el.1}$			6.0[c]	
	pcf_1^{max}			5.4	
	pcf_2^{max}			5.7	
Tröger's base[e]	$k'^{CTA}_{1\,el.2}$			1.13	0.96
	$k'^{CTA}_{2\,el.2}$			2.41	2.23
	α			2.14	2.33
	$(\sigma_V)_1$ (μl)			1410	1420
	$(\sigma_V)_2$ (μl)			2960	2800
	$(\sigma_V)^{co}$ (μl)				310
	pcf_1^{exp}				1.02
	pcf_2^{exp}				1.06
	$k'^{CTA}_{1\,el.1}$			1.5[c]	
	$k'^{CTA}_{2\,el.1}$			3.6[c]	
	pcf_1^{max}			1.3	
	pcf_2^{max}			1.5	

[a] Eluent 1, ethanol–water (40:60); eluent 2, ethanol–methanol–water (67.2:20:12.8).
[b] Flow-rate, 0.08 ml/min; temperature of CTA column, 60°C.
[c] Obtained by extrapolation (Fig. 2).
[d] Calculated from the k'^{CTA} data given under $OS\text{–}CTA_{(I)}$.
[e] Eluent 1, ethanol–water (72:28); eluent 2, ethanol–water (96:4).

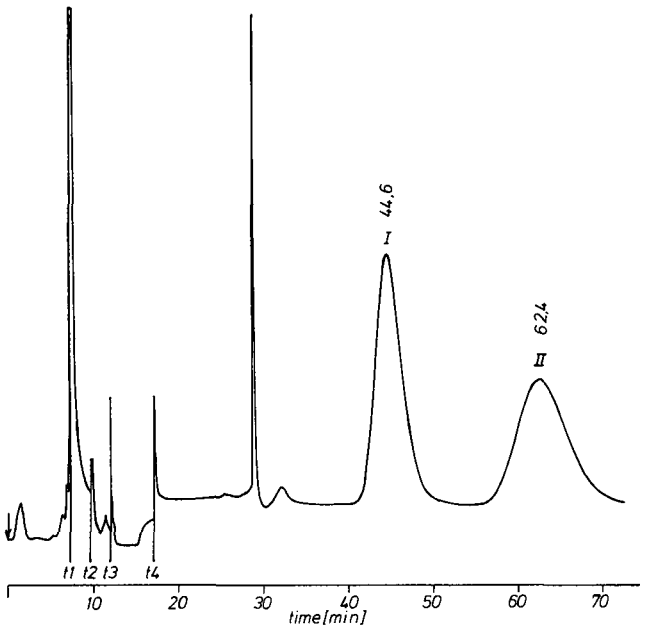

Fig. 5. Chromatogram of Tröger's base obtained with the octylsilica–swcrCTA two-column system with column switching. Column 1, octylsilica; column 2, swcrCTA$_{(II)}$. Column dimensions: OS, 250 × 4 mm I.D.; CTA$_{(II)}$, 250 × 10 mm I.D. Temperature: column 1, ambient; column 2, 50°C. Eluent 1, ethanol–water (72:28); eluent 2, ethanol–water (96:4). Flow-rate 1, 0.5 ml/min; flow-rate 2, 1.0 ml/min. Times of events: $t1$ = 7.0; $t2$ = 9.50; $t3$ = 12.0; $t4$ = 17.0; $t5$ = 72.0 min.

CONCLUSION

For optical purity control and enantiomeric excess determination, a high peak capacity is required in order to exclude the possibility with sufficiently high significance that small impurity peaks interfere with the peaks of the enantiomers. Even for apparently pure substances one needs a minimum peak capacity to make purity evaluation possible at a certain level of accuracy and precision. To increase the low peak capacity of swcrCTA columns, a two-column set-up with column switching can be used which combines a non-enantioselective separation step on an alkylsilica column with an enantioselective separation step on the swcrCTA column. In order to take advantage of the maximum achievable peak capacity in a column-switching system, the variance of the transferred peak must be negligible with respect to the variance originating from the second column, or has to be made negligible by peak compression.

Owing to the strong peak dispersion in swcrCTA columns, the peak broadening produced by the alkylsilica columns can often be neglected. This is obvious when using CTA columns of 25 cm × 10 mm I.D., as they are commercially available, and OS columns of 4 mm I.D. Using columns of equal diameter, peak compression is worthwhile. Peak compression may also be of interest for semi-preparative separations, for which swcrCTA adsorbents are especially suitable. Overloading effects

expected in column 1 (OS) when using swcrCTA columns for semi-preparative purposes can be compensated for in this way.

Peak compression at the top of the CTA column can be achieved in most instances simply by choosing a higher concentration of alcohol in eluent 2 than in the carryover, when applying mixed water–alcohol mobile phases. This strategy may not be successful at very high concentrations of ethanol. Compatibility of the mobile phases for both columns is given for ethanol–water mixtures with a water concentration of least up to 75% (v/v) in the carryover. Up to this value, the CTA packing has been proved to be stable. The exact limit at which the packing breaks down has not been determined. For not very hydrophilic analytes, the given concentration range should be sufficient for successful reversed-phase chromatography. Obviously, with respect to the solubility of the CTA material, chloroalkanes, ketones of THF must not be present in the carryover.

ACKNOWLEDGEMENTS

This study was made possible by a grant from the Austrian Fond zur Förderung der Wissenschaftlichen Forschung (FWF). The author appreciates this support and thanks E. Merck (Darmstadt, F.R.G.) for kindly donating the chiral CTA columns.

REFERENCES

1 T. Shibata, I. Okamoto and K. Ishii, *J. Liq. Chromatogr.*, 9 (1986) 313.
2 G. Blaschke, *J. Liq. Chromatogr.*, 9 (1986) 341.
3 Y. Okamoto, M. Kawashima, K. Yamamoto and K. Hatada, *Chem. Lett.*, (1984) 739.
4 K. R. Lindner and A. Mannschreck, *J. Chromatogr.*, 193 (1980) 308.
5 H. Koller, K.-H. Rimböck and A. Mannschreck, *J. Chromatogr.*, 282 (1983) 89.
6 A. Mannschreck, H. Koller and R. Wernicke, *Kontakte (Darmstadt)*, 1985, No. 1 (1985) 40.
7 K.-H. Rimböck, M. A. Cuyegkeng and A. Mannschreck, *Chromatographia*, 21 (1986) 223.
8 A. Rizzi, *J. Chromatogr.*, 478 (1989) 71.
9 A. Rizzi, *J. Chromatogr.*, 478 (1989) 87.
10 J. F. K. Huber, R. van der Linden, E. Ecker and M. Oreans, *J. Chromatogr.*, 83 (1973) 267.
11 C. Fioresi, *Thesis*, University of Vienna, 1980.
12 L. R. Snyder and J. J. Kirkland, *Introduction to Modern Liquid Chromatography*, Wiley, New York, 1979, p. 35.
13 R. Hirz, *Thesis*, University of Vienna, 1982.
14 A. Rizzi, *J. Chromatogr.*, 478 (1989) 101.

Journal of Chromatography, 513 (1990) 209–218
Elsevier Science Publishers B.V., Amsterdam

CHROM. 22 480

Determination of enantiomeric purity of paclobutrazol and fluazifop-P-butyl using a diode-laser-based polarimetric high-performance liquid chromatography detector

ZECAI WU, DAVID M. GOODALL* and DAVID K. LLOYD[a]
Chemistry Department, University of York, York, YO1 5DD (U.K.)
and
PETER R. MASSEY and KATHIE C. SANDY
ICI Agrochemicals, Jealott's Hill Research Station, Bracknell, Berkshire RG12 6EY (U.K.)
(First received February 12th, 1990; revised manuscript received April 3rd, 1990)

ABSTRACT

Enantiomeric purities of resolved enantiomers of the agrochemicals paclobutrazol (I) and fluazifop-P-butyl (II) have been determined using a diode-laser-based polarimetric high-performance liquid chromatography detector. Reversed-phase achiral chromatography was used with polarimetric and absorbance detectors in series to measure optical rotation, α, and absorbance, A. In blind trials enantiomer mole fractions in unknowns, x_u, were calculated from a standard, x_s, and α/A values using the equation

$$(\alpha/A)_u/(\alpha/A)_s = (2x_u - 1)/(2x_s - 1).$$

The method always gave x_u within 1% of actual values. 95% confidence limits were roughly twice those from chiral chromatography and better than conventional polarimetry. The linear range of the polarimetric detector was 0.02 – 10 mg ml^{-1} for I and 0.1 – 10 mg ml^{-1} for II (20 μl injection). Limits of detection for I and II of 0.19 and 1.0 μg correlate with specific rotations of the compounds.

INTRODUCTION

With the advent of laser-based polarimetric detectors specially designed for high-performance liquid chromatography (HPLC)[1–4], the reduction of noise to microdegree levels in optical rotation (OR) measurements has allowed chiral molecules to be quantitated with detection limits in the 0.1–1-μg range. Applications of

[a] Present address: Department of Clinical Pharmacy, University of Tennessee, 26 South Dunlap St., Memphis, TN 38163, U.S.A.

0021-9673/90/$03.50

polarimetric detection in HPLC have been recently reviewed[5]. The use of absorbance and polarimetric detectors coupled in series to monitor peaks eluting from an achiral chromatography column has been shown to provide a simple method for determination of the enantiomeric purity of compounds for which a standard of known purity is available[2,6,7]. This technique was first applied to a permethrinic acid insecticide[6] and a detailed account of the precision and accuracy of the method has recently been given for the pharmaceuticals ephedrine hydrochloride and pseudoephedrine hydrochloride[8].

In the present paper the technique is applied to two agrochemicals, paclobutrazol and fluazifop-P-butyl, with particular reference to establishing 95% confidence limits and comparison with alternative procedures using chiral separation or polarimetry of bulk samples for quality control of these compounds which are used in enantiomerically pure form.

Paclobutrazol, (2*RS*,3*RS*)-1-(4-chlorophenyl)-4,4-dimethyl-2-(1H-1,2,4-triazol-1-yl)pentan-3-ol (I, Fig. 1), is one of a new class of plant growth regulators that affect both vegetative and reproductive components of fruit tree growth[9] and is a broad-spectrum growth retardant with a wide range of uses[10]. Paclobutrazol possesses two chiral centres, so four optical isomers may be separated. The 2*S*,3*S* enantiomer, the active ingredient in plant growth regulation, inhibits the biosynthesis of gibberellins, the plant hormones that primarily regulate the elongation of shoots[10] while the 2*R*,3*R* component has low plant-growth activity but high fungicidal activity[11]. The 2*R*,3*S* and 2*S*,3*R* diastereoisomers of paclobutrazol are potent inhibitors of plant sterol biosynthesis[12].

Fluazifop-butyl, butyl(*RS*)-2-[4-(5-trifluoromethyl-2-pyridyloxy)phenoxy]propionate (II, Fig. 1), is the active ingredient of a highly selective systemic postemergence herbicide for use against annual and/or perennial grasses in cotton, soybean and other broad leaf crops. Compound II has one chiral centre and only the *R*-(+) form, termed fluazifop-P-butyl, is generally herbicidally active.

Because the enantiomers display large differences in the nature and degree of biological activity, analyses which quantitate the enantiomeric forms are of considerable importance in studies of activity, mode of action, translocation, metabolism and persistence of these agrochemicals in the environment[13]. Many methods have been developed for chiral analysis, the most useful being those based on chromatographic separation. Achiral chromatography may be carried out after chiral derivatisation of I[12] and II[14], but this is a lengthy process. Such procedures require the chiral reagent to be optically pure and the reaction to proceed to completion without racemisation at any stage[15]. Separations using a chiral stationary phase (CSP)[14] are generally taken to

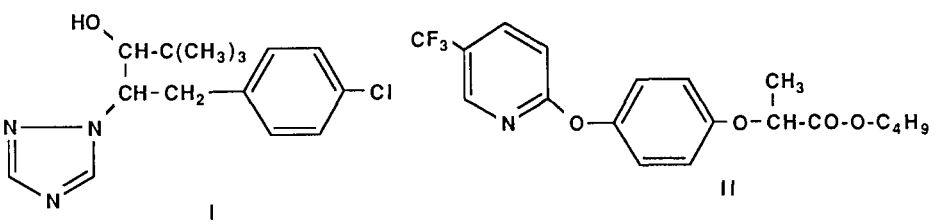

Fig. 1. Structural formulae of paclobutrazol (I) and fluazifop-butyl (II).

be the standard methods of analysis. Such analyses are not ideal for quality control because many CSPs are less robust and considerably more expensive than those for normal achiral chromatography.

EXPERIMENTAL

Reagents and chemicals

Experimental samples, supplied by ICI Agrochemicals, were fluazifop-P-butyl, the racemate fluazifop-butyl, and the 2*R*,3*R* and 2*S*,3*S* enantiomers of paclobutrazol. Solutions of all compounds were prepared immediately prior to use, and filtered through a 0.45-μm filter. The HPLC mobile phases were prepared using deionized water (Elgastat UHQ water purifier), methanol, ethanol, hexane (all HPLC grade) and trifluoroacetic acid (analytical-reagent grade).

Instrumentation

The HPLC system consisted of a ternary gradient pump (ACS, Model 352), an injection valve (Rheodyne 7152) with a 20-μl loop, a variable-wavelength UV detector (ACS 750/12) operating at 265 nm for paclobutrazol and 300 nm for fluazifop-P-butyl, and a polarimetric HPLC detector (ACS ChiraMonitor) which utilises a diode laser light source at 820 nm and a cell with pathlength 0.16 dm and volume 23 μl. The UV data were collected and analysed on an integrator (Trivector Trio), whilst a chart recorder (Chessell) recorded the output from the polarimetric detector. A polarimeter (Perkin-Elmer 141) with a 1-dm pathlength silica cell thermostatted at 20°C was used to measure the optical rotation of fluazifop-P-butyl and both enantiomers of paclobutrazol at the sodium D line (589 nm) and mercury arc wavelengths (579, 546, 436, 405, 365, 313 and 302 nm). A UV spectrophotometer (Shimadzu UV 260) was used to measure absorbance spectra.

Chromatographic conditions

In the analysis of paclobutrazol, a Chiralcel OC column (25 cm × 4.6 mm I.D.) was used for chiral separation with a hexane–ethanol (95:5) mobile phase at a flow-rate of 2.0 ml min^{-1}. The achiral determination used a C_{18} column (Hichrom, 10 cm × 4.6 mm I.D.) with a methanol–water (70:30) mobile phase at a flow-rate of 1.0 ml min^{-1}.

In the determination of fluazifop-P-butyl, the chiral column was a Pirkle type (CPIA-3, 25 cm × 4.6 mm I.D.) packed with covalent D-phenylglycine. A mixture of hexane–methanol–trifluoroacetic acid (1000:0.9:0.5) was used as the mobile phase at flow-rates of 1.0 or 2.0 ml min^{-1}. Conditions for the achiral analysis were the same as for paclobutrazol with the exception of the mobile phase composition (methanol–water, 75:25).

All chromatographic experiments were carried out at ambient temperature.

RESULTS AND DISCUSSION

Paclobutrazol

Chiral chromatography. Chiral chromatography was carried out as described in the experimental section to establish the enantiomeric purity of 2*R*,3*R* and 2*S*,3*S* samples of paclobutrazol. The enantiomer mole fractions determined from UV peak areas are given in Table I.

TABLE I

ENANTIOMERIC PURITY OF PACLOBUTRAZOL SAMPLES

Sample	*Enantiomer mole fractions*	
	(2R,3R)	*(2S,3S)*
2*R*,3*R*	0.97	0.03
2*S*,3*S*	0.074	0.926

(2*R*,3*R*)-Paclobutrazol elutes first, and because of peak tailing and lack of baseline resolution the small mole fraction of the 2*S*,3*S* enantiomer in the (2*R*,3*R*) paclobutrazol sample carries higher uncertainty than does the 2*R*,3*R* content of the 2*S*,3*S* sample. The (2*S*,3*S*)-paclobutrazol sample was consequently taken as the standard for enantiomeric purity determinations in subsequent work.

Polarimetry. The observed rotation, α, of a compound containing mole fractions of (+)- and (−)-enantiomers x and $(1 - x)$ respectively is given from Biot's law as

$$\alpha = [\alpha](2x - 1)cl \tag{1}$$

where c is the mass concentration, l the cell pathlength, and $[\alpha]$ the specific rotation of the (+)-enantiomer. For the racemate, with $x = 0.5$, $\alpha = 0$; for the pure (+)-form, with $x = 1$, $\alpha = [\alpha]cl$; for the pure (−)-form, with $x = 0$, $\alpha = -[\alpha]cl$.

Eqn. 1 was used to obtain specific rotations at the sodium D line and mercury arc wavelengths using the (2*S*,2*S*)-(−)-paclobutrazol reference standard for which x had been found from chiral chromatography as described in the previous section.

Extrapolation of $[\alpha]$ to the wavelength of the diode laser, 820 nm, was carried out using the Drude equation applicable to a material with one dominant chiral chromophore[16]

$$\lambda^2[\alpha]_\lambda = \lambda_0^2[\alpha]_\lambda + K \tag{2}$$

where λ is the wavelength of measurement and λ_0 (the wavelength of the dominant chiral chromophore) and K are constants. Fig. 2 shows the plot of $\lambda^2[\alpha]_\lambda$ *versus* $[\alpha]_\lambda$, from which $[\alpha]_{820}^{20}$ was deduced to be 65.6 ± 2.4° ml g^{-1} dm^{-1} and $\lambda_0 = 217 \pm 2$ nm. Paclobutrazol has two chiral centres, and λ_0 coincides with the 220 nm UV peak maximum which may be assigned to a π–π^* transition on the triazole ring attached to the C2 chiral centre[17].

Achiral chromatography. A representative achiral chromatogram of (2*R*,3*R*)-paclobutrazol is shown in Fig. 3 and the calibration plot of the OR response, log (peak height) *versus* log(concentration) is given in Fig. 4. The linear range of the method is from 0.02 to 10 mg ml^{-1} (for a 20-μl injection) of (2*R*,3*R*)-paclobutrazol with correlation coefficient of 0.99998 and slope of 1.005 ± 0.005. The limit of detection of the technique is 9.5 μg ml^{-1} injected concentration (0.19 μg on column) calculated using the equation[18]:

$$\text{LOD} = 3s_{y/x}/b \tag{3}$$

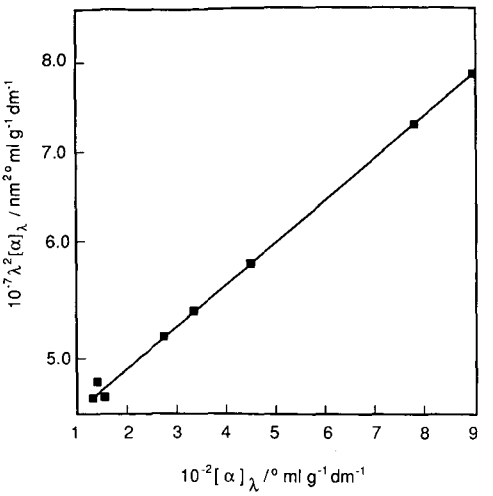

Fig. 2. Wavelength dependence of the optical rotation of (2*R*,3*R*)-paclobutrazol in methanol–water (70:30) measured at the sodium D line (589 nm) and mercury arc wavelengths (436, 405, 365, 313 and 302 nm) at 20°C.

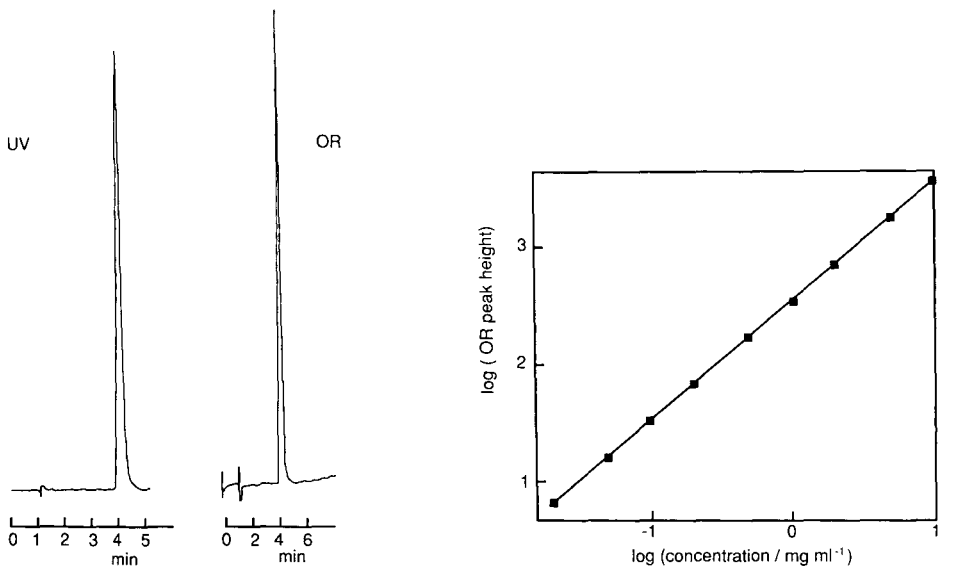

Fig. 3. Achiral chromatograms of (2*R*,3*R*)-paclobutrazol with dual optical rotation and UV absorbance detection. Column: Hichrom C_{18} (10 cm × 4.6 mm I.D.). Mobile phase: methanol–water (70:30). Flow-rate: 1.0 ml min^{-1}. Injection, 40 μg. ChiraMonitor attenuation 2, time constant 1 s and chart recorder 200 mV fsd.

Fig. 4. Linear response of the polarimetric detector. Plot of log(OR peak height) *versus* log(concentration/mg ml^{-1}) for (2*R*,3*R*)-paclobutrazol.

where $s_{y/x}$ is the root mean square (RMS) error on the data points and b the slope of the plot of OR peak height *versus* concentration using the lowest concentration points in Fig. 4. Eqn. 3 may be shown to follow[18] from the IUPAC recommendation[19] for the definition limit of detection $= 3\ s_B$, where s_B is the standard deviation on the blank signal.

Enantiomeric purity determination. From eqn. 1, the simplest method of determining the enantiomer mole fraction in a chemically-pure compound when an enantiomeric standard is available is to measure α/c values for unknown, u, and standard, s,

$$\frac{(\alpha/c)_u}{(\alpha/c)_s} = \frac{2x_u - 1}{2x_s - 1} \tag{4}$$

This is the procedure normally used when carrying out enantiomeric purity determination using conventional polarimetry.

Using the (2*S*,3*S*)-(−)-paclobutrazol as standard, with $x_s = 0.074$, x_u for the 2*R*,3*R*-(+)-sample was deduced from α/c ratios measured at 365 nm (the wavelength at which the highest sensitivity was obtained) to be 0.983 ± 0.010 (three replicate measurements).

An alternative procedure is to use achiral chromatography with polarimetric and spectrophotometric detectors in series, and calculate the enantiomeric purity from the ratio of the optical rotation and the absorbance (A) response, α/A, for unknown and standard samples[8],

$$\frac{(\alpha/A)_u}{(\alpha/A)_s} = \frac{2x_u - 1}{2x_s - 1} \tag{5}$$

This follows from eqn. 4 since A is directly proportional to c. As in previous sections the 2*S*,3*S* sample was used as standard, giving $x_u = 0.963 \pm 0.006$ (three measurements) for the (2*R*,3*R*)-(+)-paclobutrazol sample.

Table II compares the three methods for determination of enantiomeric purity. Mean values are given with their 95% confidence limits, calculated knowing the number of replicate measurements, n, and the t value for a confidence interval of 95%, t_{95} (ref. 18).

The achiral HPLC method with dual detectors is seen to give results in good agreement with chiral chromatography, and carries less uncertainty than does polarimetry on bulk samples. Perhaps of greatest importance when considering applications in quality control of agrochemicals is that the α/A method does not require chemically pure samples, and that it can be orders of magnitude more economical in material. To obtain the data in Table II, 40 μg was loaded for each HPLC injection whereas about 6 mg was required to fill the 6-ml polarimeter cell.

Fluazifop-P-Butyl

Chiral chromatography. Fig. 5 shows the chromatogram of fluazifop-P-butyl obtained using a chiral column under the conditions given in the experimental section. The mole fractions of each enantiomer in this sample and in the racemate

TABLE II

(2*R*,3*R*)-(+)-PACLOBUTRAZOL MOLE FRACTION DETERMINED BY THREE METHODS

Method	$\bar{x}_u \pm t_{95}s_{x_u}/\sqrt{n}$	n
(1) Chiral chromatography	0.97	
(2) Polarimetry	0.978 ± 0.010	3
(3) Achiral chromatography with OR and UV detectors	0.963 ± 0.006	3

fluazifop-butyl were calculated from the ratio of the peak areas of (+)- and (−)-forms. The results, given in Table III, establish the precision and accuracy of the method. It should be noted that the mole fractions for fluazifop-butyl agree within 95% confidence limits with those expected for the racemate.

Polarimetry. In the same way as for paclobutrazol, the optical rotations of fluazifop-P-butyl were measured at the sodium D line and mercury arc wavelengths (579, 546, 436, 405 and 365 nm) and $[\alpha]_\lambda$ calculated with eqn. 1. The $\lambda^2[\alpha]$ *versus* $[\alpha]$ plot (eqn. 2) gave $\lambda_0 = 237 \pm 5$ nm which corresponds to the 230 nm peak maximum in the UV spectrum, and $[\alpha]^{20}_{820} = 18.1 \pm 0.4°$ ml g^{-1} dm^{-1} (in methanol–water, 75:25).

Achiral chromatography. Fig. 6 gives an achiral chromatogram of fluazifop-P-butyl. Under the achiral conditions described in the experimental section, the linear range of the technique for the analysis of fluazifop-P-butyl was found to be 0.10–10 mg ml^{-1} with a correlation coefficient of 0.9989 for the log (OR peak height) *versus* log(concentration) plot (*cf.* Fig. 4). The slope and the RMS error of the plot of the OR height *versus* the concentration of II gave a detection limit of 1.0 μg using eqn. 3.

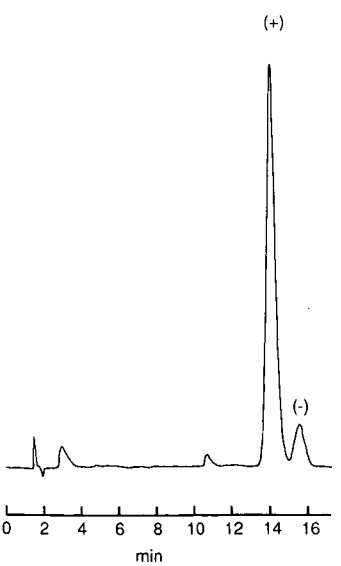

Fig. 5. Chiral chromatogram of fluazifop-P-butyl spiked with racemate fluazifop-butyl. Column: Pirkle CIPA-3 (25 cm × 4.6 mm I.D.). Mobile phase: hexane–methanol–trifluoroacetic acid (1000:0.9:0.5). Flow-rate: 1.0 ml min^{-1}. Total amount injected was 3.8 μg.

TABLE III

ENANTIOMERIC PURITY OF FLUAZIFOP-BUTYL SAMPLES FROM CHIRAL CHROMATOGRAPHY

Sample	*Enantiomer mole fraction* ($\bar{x}_u \pm t_{95}s_{x_u}/\sqrt{n}$)		n
	(+)-form	*(−)-form*	
Fluazifop-P-butyl	0.948 ± 0.005	0.052 ± 0.005	9
Fluazifop-butyl	0.501 ± 0.004	0.499 ± 0.004	4

The detection limits for I and II may be compared with the theoretical values obtained by considering the noise level on the detector. The RMS noise was measured to be 2.3 ± 0.6 microdegrees (1 s time constant). This is taken as the theoretical figure for the standard deviation in the blank signal, s_B (eqn. 3). Theoretical limits of detection of $3s_B$ are presented in Table IV. Eqn. 1 was used to convert from rotation to concentration, and the measured peak width to determine dilution between concentrat ions at injection and at peak maximum in the OR cell. There is good agreement between the theoretical and the observed LOD values, 0.19 μg for I and 1.0 μg for II injected on column (1-s detector time constant). It should be noted that the LOD is inversely proportional to the specific rotation and directly proportional to the peak width. The former factor contributes × 3.6 and the latter × 1.4 to the ratio $(LOD)_{II}/(LOD)_I = 5$.

Enantiomeric purity determination. In blind trials, mixtures of fluazifop-P-butyl (0.185 mg ml^{-1}) and the racemate fluazifop-butyl (0.304 mg ml^{-1}) were prepared to

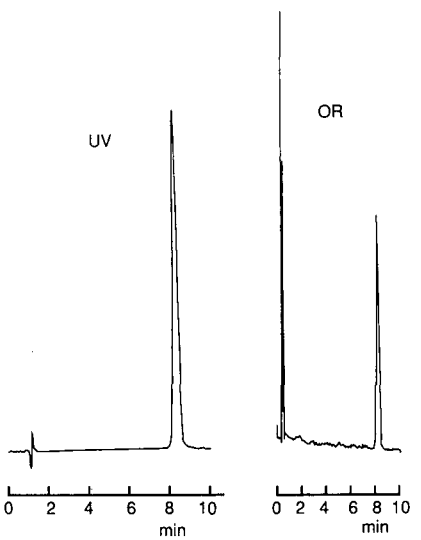

Fig. 6. Achiral chromatograms of fluazifop-P-butyl with dual optical rotation and UV absorbance detection. Column: Hichrom C_{18} (10 cm × 4.6 mm I.D.). Mobile phase: methanol–water (75:25). Flow-rate: 1.0 ml min^{-1}. Injection, 20 μg. ChiraMonitor attenuation 2, time constant 1 s and chart recorder 50 mV fsd.

TABLE IV

LIMITS OF DETECTION (LOD) FOR PACLOBUTRAZOL (I) AND FLUAZIFOP-P-BUTYL (II)

Time constant = 1 s.

	I	*II*
$[\alpha]_{820}$/° ml g^{-1} dm^{-1}	66	18
Half height peak width/ml	0.22	0.30
Dilution factor	12	16
Theoretical LOD/μg	0.15 ± 0.04	0.8 ± 0.2
Observed LOD/μg	0.19	1.0

give samples with x_u around 0.90. Assays were then carried out with both achiral chromatography and (for samples 5–7) chiral chromatography. For samples 1–4, solutions of the mixtures were prepared in the same solvent as the achiral mobile phase (methanol–water, 75:25). For samples 5–7, the mixture solutions were prepared in hexane–methanol (1000:0.9). As the different mobile phases used in chiral and achiral chromatographies were immiscible, the solution of each sample (Nos. 5–7) was divided into two portions. One of them was for direct chiral chromatographic assay. With the other portion for achiral chromatography, solvent was evaporated and methanol–water (75:25) added to redissolve the sample to a concentration of ~1 mg ml^{-1}. The enantiomer mole fractions of (+)-form in each of the mixture solutions were calculated from the ultraviolet peak ratio in chiral chromatography and from the α/A ratio (eqn. 5) in achiral chromatography. The results of the blind trials are shown in Table V. The quality of the achiral technique for enantiomeric purity determination is evident. Although the achiral chromatography carries a little more uncertainty than does the chiral chromatography, it is in good agreement with that from the chiral separation as well as with the actual mole fractions.

TABLE V

ENANTIOMER MOLE FRACTION OF FLUAZIFOP-P-BUTYL IN BLIND TRIALS

Sample	x_u[a] *(actual)*	$\bar{x}_u \pm t_{95}s_{x_u}/\sqrt{n}$ *(n)*	
		Chiral separation	*Achiral chromatography*
Standard		0.948 ± 0.005 (9)	
1	0.940		0.942 ± 0.016 (5)
2	0.931		0.938 ± 0.012 (5)
3	0.919		0.923 ± 0.008 (7)
4	0.910		0.901 ± 0.010 (7)
5	0.926	0.928 ± 0.004 (4)	0.916 ± 0.010 (6)
6	0.902	0.904 ± 0.008 (6)	0.902 ± 0.012 (8)
7	0.886	0.884 ± 0.007 (7)	0.880 ± 0.011 (6)

[a] The calculated uncertainty in all x_u values is 0.005, the dominant error being the enantiomer mole fraction of the standard.

CONCLUSION

Using a diode-laser-based polarimetric detector in series with a UV detector, the enantiomeric purities of paclobutrazol and fluazifop-P-butyl have been assayed and calculated from the α/A ratios of unknown and standard samples eluting from an achiral column. The accuracy of the technique has been confirmed by comparison with chiral separations on the same samples.

The precision using achiral chromatography is comparable to that of the chiral separations and the 95% confidence limits are better than those from conventional polarimetry. The achiral chromatography technique with dual OR/UV detection offers advantages for routine quality control of (i) using a normal achiral column instead of a less robust and more expensive chiral column, (ii) using μg of sample which need not be chemically pure, whereas conventional polarimetry requires mg amounts of chemically pure sample.

The detection limit of the technique is dependent on specific rotation and the quality of the chromatographic peak. Any increase in $[\alpha]$ or decrease in peak width will improve the limit of detection.

It is anticipated that this technique will provide a convenient routine analytical method for the enantiomeric purity determination of chiral agrochemicals and pharmaceuticals[8] with the precision dependent upon the availability of well-characterised standard samples and the number of replicate measurements taken.

ACKNOWLEDGEMENT

We wish to thank ICI Agrochemicals and the Laboratory of the Government Chemist for a studentship to Z.W.

REFERENCES

1 E. S. Yeung, L. E. Steenhoek, S. D. Woodruff and K. C. Kuo, *Anal. Chem.*, 52 (1980) 1399.
2 B. H. Reitsma and E. S. Yeung, *J. Chromatogr.*, 362 (1986) 353.
3 D. R. Bobbitt and E. S. Yeung, *Appl. Spectrosc.*, 40 (1986) 407.
4 D. K. Lloyd, D. M. Goodall and H. Scrivener, *Anal. Chem.*, 61 (1989) 1238.
5 D. K. Lloyd and D. M. Goodall, *Chirality*, 1 (1989) 251.
6 W. Boehme, G. Wagner and U. Oehme, *Anal. Chem.*, 54 (1982) 709.
7 B. D. Scott and D. L. Dunn, *J. Chromatogr.*, 319 (1985) 419.
8 Z. Wu, D. M. Goodall and D. K. Lloyd, *J. Pharm. Biomed. Anal.*, (1990) in press.
9 E. A. Stahly and D. A. Buchanan, *HortScience*, 21 (1986) 534.
10 F. J. Schwinn, *Pestic. Sci.*, 15 (1984) 40.
11 B. Sugavanam, *Pestic. Sci.*, 15 (1984) 296.
12 R. S. Burden, A. H. B. Deas and T. Clark, *J. Chromatogr.*, 391 (1987) 273.
13 E. J. Ariens, J. J. S. van Rensen and W. Welling, *Stereoselectivity of Pesticides*, Elsevier, Amsterdam, 1988.
14 M. D. Muller and H. P. Bosshardt, *J. Assoc. Off. Anal. Chem.*, 71 (1986) 614.
15 W. J. Lough, *Chiral Liquid Chromatography*, Blackie & Son, London, 1989, p. 24.
16 C. Tanford, *Physical Chemistry of Macromolecules*, Wiley, New York, 1961.
17 M. H. Palmer, *The Structure and Reactions of Heterocyclic Compounds*, Arnold, London, 1967.
18 J. C. Miller and J. N. Miller, *Statistics for Analytical Chemistry*, Ellis Horwood, Chichester, 2nd ed., 1988.
19 IUPAC Analytical Chemistry Division, *Anal. Chem.*, 48 (1976) 2294.

Journal of Chromatography, 513 (1990) 219–225
Elsevier Science Publishers B.V., Amsterdam

CHROM. 22 453

Separation and determination of acidic herbicides on a PRP-1 polymeric column

ADALBERTO BETTI*, GAETANO LODI and SIMONA COPPI[a]
Department of Chemistry, University of Ferrara, Via Borsari, 46 Ferrara (Italy)
(First received December 15th, 1989; revised manuscript received March 19th, 1990)

ABSTRACT

The chromatographic behaviour of some acidic herbicides (phenoxyacetic acids, bentazon and dicamba) was investigated on a column laboratory-packed with PRP-1, using acetonitrile–water as mobile phase. Detection was performed with a UV detector set at 220 nm. This wavelength was selected as the optimum for the simultaneous determination of the herbicides. The elution of acidic compounds is affected by the pH of the mobile phase. The greatest retention and the best peak symmetry were observed at pH 2.3. The relationships between log k' and acetonitrile volume fraction (φ) in the mobile phase are parabolic. The detection limits of the tested substances were about 0.2 ng in the volume injected. The capacity factors in pure water (k'_w), extrapolated by a quadratic expression, showed that PRP-1 could be effective in extracting the examined compounds from water. Various experiments, carried out on spiked water samples using commercial PRP-1 cartridges, showed that the recovery of examined herbicides is nearly 100%. Further, such traps could make it possible to concentrate aqueous samples containing acidic herbicides at very low levels (ppt).

INTRODUCTION

Phenoxy acid herbicides are used extensively in agriculture for weed control and ultimately find their way into lakes, streams and groundwaters. Sometimes they may be found in tap water at very low concentrations (ppt). The common procedure for determining these pollutants in water involves extraction and derivatization prior to analysis by gas chromatography[1–5]. The main disadvantages are the time-consuming sample preparation and the hazards associated with handling organic solvents.

High-performance liquid chromatography (HPLC) appears to be an atractive alternative as phenoxy acids absorb strongly in the UV region. Both reversed-phase[6–9] and normal-phase[6,9,10] applications have been reported. Ion-pair chromatography on octadecylsilica columns has also been employed[11]. Chiral stationary phases were used

[a] Present address: Servizio Multizonale di Prevenzione, USL 31, C.so Giovecca 169, Ferrara, Italy.

0021-9673/90/$03.50

to separate enantiomers of MCPP [2-(4-chloro-2-methylphenoxy)propionic acid] and of 2,4-DP [2-(2,4-dichlorophenoxy)propionic acid] in formulations[12,13].

In previous work, many substituted benzoic acids were studied on styrene–divinylbenzene columns and a polymeric packing, such as PRP-1, showed good properties for the elution of acidic compounds[14]; in fact, polymeric columns have better stability than silica-bonded phases at lower pH. It should be pointed out that phenoxy acids are usually separated on a C_{18} reversed phase at a mobile phase pH of 3[6–9]. However, at this pH, some herbicides (such as 2,4-D and 2,4,5-TP) having $pK_a < 3$ are partially ionized during chromatographic runs[15].

The aim of this work was to investigate the elution behaviour of some phenoxy acid herbicides on PRP-1 polymeric laboratory-prepared columns. The influence of the mobile phase pH on the retention data and the relationship between the capacity factor (k') and the mobile phase composition were investigated using water–acetonitrile eluents. Experiments were also carried out to find the optimum wavelength for the simultaneous determination of the herbicides; some workers have set the detector at 280 nm[8,9] and others at lower wavelengths[16,17]. The use of styrene copolymers as solid-phase extraction materials for the determination of phenoxy acids in water is discussed.

EXPERIMENTAL

The retention parameter measurements were carried out on a Waters Assoc. Model 501 solvent-derivery system (Millipore, Milford, MA, U.S.A.), equipped with a Waters, Assoc. Model 484 tunable absorbance detector. Chromatograms were recorded on a Spectra-Physics (San Jose, CA, U.S.A.) SP 4270 integrator. Samples were introduced with a Rheodyne Model 7125 injector (supplied by Millipore), equipped with a 10-μl sampling loop. HPLC-quality acetonitrile (Rudi Pont, Eurobase, Milan, Italy) and deionized, distilled water were filtered through a 0.45-μm Millipore filter and degassed with a helium purge. The pH was controlled with 0.05 *M* phosphoric acid and 0.05 *M* potassium dihydrogenphosphate or sodium monohydrogenphosphate. The reported pH values are those of the solution before the addition of acetonitrile. Solvent mixtures are expressed as percent by volume. The solutes, listed in Table I (Chem. Service, West Chester, PA, U.S.A.), were dissolved in acetonitrile. Bentazon and dicamba also were considered as they are the most effective herbicides under our environmental conditions. The solute concentrations were about 1 mg/l and allowed suitable detector responses without overloading the column. A PRP-1 (Hamilton, Bonaduz, Switzerland) column (150 × 4.6 mm I.D.) was prepared as described previously[18]. Potassium nitrate was used as the unretained solute. All experiments were run in triplicate at a flow-rate of 1 ml/min. The repeatibility of retention times was better than ±1%.

PRP-1 commercial cartridges, supplied by Alltech (Milan, Italy), were employed in enrichment experiments. Before use the traps were treated as described previously[19].

RESULTS AND DISCUSSION

Preliminary runs were performed to choose the optimum wavelength for the maximum absorbance. These experiments were carried out with a Waters Assoc.

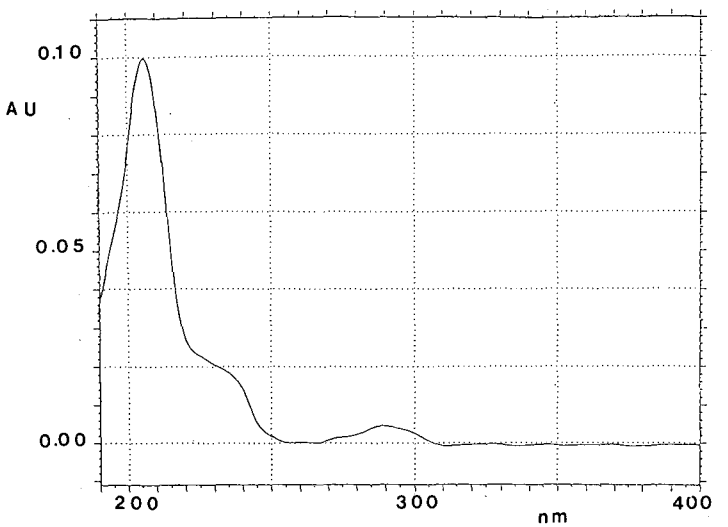

Fig. 1. UV spectrum of 2,4,5-TP. Mobile phase: acetonitrile–water (50:50) at pH 2.3.

Model 990 photodiode-array detector using acetonitrile–water (50:50) at pH 2.3. This pH (corresponding to a 0.05 *M* phosphoric acid solution) allows the phenoxy acids to be completely non-ionized.

The solutes showed absorbance bands at various wavelengths; some had a band with a maximum at a wavelength below the cut-off of acetonitrile (190 nm) and a shoulder between about 220 and 230 nm; others had a band with a maximum slightly above 190 nm and a similar shoulder. All the compounds examined showed bands between 250 and 320 nm.

The UV spectrum of 2,4,5-TP is reported in Fig. 1 as an example. In Table I the wavelengths of the maxima and of the shoulders are reported. For analytical purposes, 220 nm is a good compromise wavelength for all the solutes examined. Moreover, the molar absorptivities at 220 and 280 nm (Table I) show that a greater sensitivity may be obtained at the lower wavelength.

The retention mechanism of ionizable compounds in reversed-phase chromatography is highly dependent on the pH of the mobile phase[20]. Measurements of k' in the pH range 2.3–5 were carried out with acetonitrile–water (50:50) as eluent. The maximum k' values were obtained at pH 2.3 and decreased as the pH was increased. At pH >5 many solutes were eluted with the solvent. Further, the peak asymmetry factors were about 1 at pH 2.3 and became worse as the pH was increased. The data in Table II show that solute retention increases with increase in the number of methylene groups in the aliphatic chain and with an increase in the number of methyl and/or chloro substituents on the benzene ring. In fact, 2,4,5-TP is more retained than MCPP and 2,4,5-T more than MCPA. However, some pairs of phenoxy acid herbicides, such as 2,4-DB–MCPB and 2,4-D–MCPA, cannot be separated.

The behaviour of phenoxy acid herbicides on PRP-1 columns may be explained with the solvophobic theory[20] and is similar to the behaviour observed by other

TABLE I

UV SPECTRA OBTAINED WITH ACETONITRILE–WATER (50:50) OF pH 2.3 AS MOBILE PHASE

Compound	*Systematic name*	*Wavelength of maximum absorbance (nm)*			*Molar absorptivity, $\varepsilon \times 10^{-3}$ ($l\ mol^{-1}cm^{-1}$)*	
					220 nm	*280 nm*
2,4-DB	4-(2,4-Dichlorophenoxy) butanoic acid	<190	220	280	9.97	1.78
2,4-D	2,4-Dichlorophenoxy acetic acid	<190	220	280	9.20	1.68
2,4,5-TP	(+)-2-(2,4,5-Trichloro phenoxy)propionic acid	205	220–230	290	9.05	0.98
2,4,5-T	2,4,5-Trichlorophenoxy acetic acid	200	220–230	290	9.12	1.01
MCPB	4-(4-Chloro-2-methyl phenoxy)butanoic acid	198	230	290	9.88	1.70
MCPP	(+)-2-(4-Chloro-2-methyl phenoxy)propanoic acid	198	230	290	10.10	1.55
MCPA	(4-Chloro-2-methyl phenoxy)acetic acid	198	230	280	10.90	1.62
Dicamba	3,6-Dichloro-2-methoxy benzoic acid	202	220–230	280	10.90	0.65
Bentazon	3-Isopropyl-(1*H*)-2,1,3-benzothiadiazin-4(3*H*)-one 2,2 dioxide	215	220–230	310	14.90	1.30

workers[9] using octadecylsilica columns. The relationships between log k' and the acetonitrile volume fraction (φ) were investigated and the plots for some phenoxy acids are shown in Fig. 2. Regression analysis between log k' and φ showed that all data points may be fitted to a quadratic expression[21]:

$$\log k' = A\varphi^2 + B\varphi + C$$

TABLE II

k' VALUES OF HERBICIDES OBTAINED WITH ACETONITRILE–WATER (50:50) AS THE MOBILE PHASE AT VARIOUS pH

Compound	*pH*					
	2.3	*2.5*	*3.0*	*3.5*	*5.0*	*5.3*
2,4-DB	5.15	5.07	4.94	4.63	2.89	2.15
2,4-D	2.65	2.49	1.96	0.99	0.15	–
2,4,5-TP	6.02	5.71	4.61	2.49	0.31	0.22
2,4,5,-T	4.02	3.82	2.92	1.42	0.21	–
MCPB	5.33	5.18	5.15	4.87	3.12	2.82
MCPP	3.87	3.70	3.31	2.20	0.27	0.20
MCPA	2.71	2.56	2.19	1.27	0.17	–
Dicamba	2.09	1.74	0.86	0.29	–	–
Bentazon	3.28	2.96	1.89	0.80	0.52	–

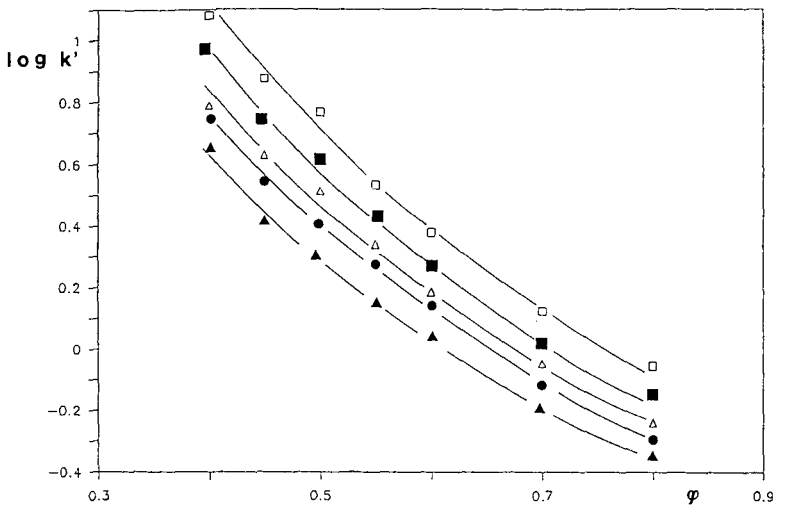

Fig. 2. Plot of log k' *versus* φ on PRP-1 column. Mobile phase: acetonitrile–water (pH 2.3). □ = MCPB; ■ = 2,4,5-T; △ = bentazon; ● = 2,4-D; ▲ = dicamba.

The regression parameters and correlation coefficients are reported in Table III. A similar behaviour was found for triazines on polymeric columns with water–acetonitrile eluents[19].

Extrapolation to 0% organic modifier yields the logarithm of the capacity factor in pure water (k'_w). The high k'_w values suggest that PRP-1 could be effective in extracting phenoxy acids from water. In fact, herbicides are usually present at concentrations below the detection limits, so that a preconcentration step is necessary.

The suitability of PRP-1 for enrichment from aqueous solutions was evaluated by sampling distilled water containing herbicides at concentrations below the

TABLE III

REGRESSION PARAMETERS OF LOG k' *VS.* φ

Log $k' = A\varphi^2 + B\varphi + C$.

Compound	*A*	*B*	*C*	*Correlation coefficient*
2,4-DB	3.1	−6.6	3.2	0.999
2,4-D	2.4	−5.4	2.5	0.998
2,4,5-TP	3.4	−6.8	3.2	0.999
2,4-T	3.0	−6.2	2.7	0.999
MCPB	3.0	−6.5	3.2	0.996
MCPP	2.8	−6.2	2.9	0.999
MCPA	2.7	−5.9	2.6	0.998
Dicamba	1.9	−4.5	2.1	0.998
Bentazon	1.8	−4.8	2.4	0.995

TABLE IV

RECOVERIES OF HERBICIDES AT VARIOUS CONCENTRATION LEVELS IN DISTILLED WATER

Concentrations: column 1, 0.05 ppm; column 2, 0.5 ppm; column 3, 1.0 ppm; column 4, 0.5 ppm. pH of the aqueous sample = 2.3 with phosphoric acid (columns 1, 2 and 3) and 2 with hydrochloric acid (column 4).

Compound	*Recovery (%)*			
	1	*2*	*3*	*4*
2,4-DB	101	99	99	98
2,4-D	99	98	101	100
2,4,5-TP	99	103	101	101
2,4-T	97	99	100	99
MCPB	101	100	103	99
MCPP	100	98	98	100
MCPA	96	99	99	98
Dicamba	98	93	99	98
Bentazon	102	100	100	102

detection limits. These detection limits (signal-to-noise ratio = 3) were about 0.2 ng of the tested substance in the injected volume, *i.e.*, 0.01–0.05 p.p.m.

Commercial cartridges containing about 100 mg of PRP-1 were employed. Before use, the traps were washed with 2 ml of acetonitrile and 2 ml of water at pH 2.3. A vacuum was applied by a water pump and, after 250 ml of aqueous sample had

Fig. 3. Chromatogram obtained by concentrating 1000 ml of tap water spiked with 0.1 μg/l of dicamba (peak 1), 0.1 μg/l of 2,4-D (peak 2) and 0.2 μg/l of bentazon (peak 3) using a PRP-1 cartridge. Mobile phase: acetonitrile–water (40:60), pH 2.

passed through, the herbicides were desorbed by passing 1 ml of acetonitrile and collected in a glass vial.

The recoveries of the herbicides were evaluated by comparing the peak height obtained with the sample and with a standard solution. The results obtained in three runs are reported in Table IV (first three columns of recoveries). These data do not vary with increase in the volume of the water samples (up to 1000 ml) or with increase in herbicide concentration (up to 1 mg/l). The repeatibility of the percentage recovery data is $\pm 2\%$.

The re-usability of the cartridges was investigated by making repeated pre-concentration runs and by restoring the adsorbents with 10 ml of acetonitrile. After five extractions the recovery of herbicides had not decreased significantly.

Fig. 3 shows a typical chromatogram obtained by this procedure for a tap-water sample (1000 ml) acidified with hydrochloric acid to pH 2 and spiked with dicamba, bentazon and 2,4-D. The use of phosphoric acid in natural and in tap-water samples should be avoided in order to prevent the precipitation of insoluble phosphates. On the other hand, hydrochloric acid does not affect the recovery efficiency reported in Table IV (last column).

The results obtained showed that polymeric columns could be usefully employed in the determination of phenoxy acid herbicides. Further, such material could also make it possible to concentrate aqueous samples of these herbicides at very low concentration levels.

REFERENCES

1 A. E. Greenberg, J. J. Connors and D. Jenkins (Editors), *Standard Methods for the Examination of Water and Waste*, American Public Health Association, Washington, DC, 15th ed., 1981.
2 H.-B. Lee, Y. D. Stokker and A. S. Y. Chau, *J. Assoc. Off. Anal. Chem.*, 69 (1986) 557.
3 A. J. Cessna, *J. Agric. Food Chem.*, 33 (1985) 504.
4 M. J. Bertand, A. W. Ahmed and B. D. Sorasin, *Anal. Chem.*, 59 (1987) 1302.
5 J. Haislova, F. Pudil, Z. Jemlickova, I. Viden and J. Davidek, *J. Chromatogr.*, 438 (1988) 55.
6 J. F. Lawrence and D.Turton, *J. Chromatogr.*, 159 (1978) 207.
7 A. D. Drinkwine, D. W. Bristol and J. R. Fleeker, *J. Chromatogr.*, 174 (1979) 264.
8 T. S. Stevens, *Adv. Chromatogr.*, 19 (1981) 91.
9 P. Jandera, L. Svoboda, J. Kubat, J. Schvantner and J. Churacek, *J. Chromatogr.*, 292 (1984) 71.
10 J. C. van Damme and M. Galoux, *J. Chromatogr.*, 190 (1980) 401.
11 M. Armjand, R. H. Hamilton and R. O. Mumma, *J. Agric. Food Chem.*, 26 (1988) 971.
12 B. Blessington and J. O'Sullivan, *J. Chromatogr.*, 396 (1987) 177.
13 B. Blessington and N. Crabb, *J. Chromatogr.*, 454 (1988) 450.
14 S. Coppi, A. Betti and S. Caldari, *J. Chromatogr.*, 395 (1987) 159.
15 C. R. Worthing and S. B. Walker (Editors), *The Pesticide Manual*, British Crop Protection Council, 7th ed., 1983.
16 S. H. Hoke, E. E. Brueggemann, L. J. Baxter and T. Trybus, *J. Chromatogr.*, 357 (1986) 429.
17 R. Hamann and A. Kettrup, *Chemosphere*, 16 (1988) 97.
18 S. Coppi, A. Betti, C. Bighi, G. P. Cartoni and F. Coccioli, *J. Chromatogr.*, 442 (1988) 97.
19 S. Coppi and A. Betti, *J. Chromatogr.*, 472 (1989) 406.
20 D. J. Pietrzyk, E. P. Kroeff and T. D. Rotsch, *Anal. Chem.*, 50 (1978) 497.
21 P. J. Schoenmakers, H. A. H. Billiet and L. de Galan, *J. Chromatogr.*, 185 (1979) 179.

Journal of Chromatography, 513 (1990) 227–235
Elsevier Science Publishers B.V., Amsterdam

CHROM. 22 440

Studies on the chromatographic behaviour of some uronic acids and neutral sugars on an amino-bonded phase column

YUAN-AN WEI* and JI-NIAN FANG
Shanghai Institute of Materia Medica, Academia Sinica, 319 Yue-yang Road, Shanghai 200031 (China)
(First received August 8th, 1989; revised manuscript received December 29th, 1989)

ABSTRACT

The differences in the chromatographic behaviour of glucuronic and galacturonic acids and some common neutral sugars on an amino-bonded phase column (LiChrosorb NH_2) were studied. The mobile phase was either acetonitrile–water or acetonitrile–sodium dihydrogenphosphate buffer. The influences of the presence of an anion ($H_2PO_4^-$) in the mobile phase, the pH and the composition of eluent were investigated. The results contributed to the elucidation of the mechanism of the elution of uronic acids and the simultaneous determination of uronic acids and neutral sugars.

INTRODUCTION

The use of amino-bonded phase columns with a mixture of acetonitrile and water as eluent in high-performance liquid chromatographic (HPLC) separations of carbohydrates has been studied by numerous investigators[1–7]. However, most of the previous work dealt with the separation of neutral sugars and little attention has been paid to the separation of uronic acids with this method because uronic acids are not readily eluted from this type of column with aqueous acetonitrile systems. A few reports have been published on the separation of some organic acids on amino-bonded phase column[8–10]. An attempt to separate some uronic acids using a LiChrosorb 10 NH_2 column in a weak anion-exchange mode with sodium acetate buffers as eluent was not successful[10]. Further, the mechanism of the elution of uronic acids on this type of column is poorly known.

An alternative approach is to use ion-exchange columns for such separations. Most current procedures for separating acidic monosaccharides are carried out on anion- or cation-exchange resins[10–14]. In comparison with amino-bonded phase columns, ion-exchange columns offer different selectivities and elution sequences, but have to be run at high temperatures and are either prone to rapid degeneration[10,15] or have little facility for retention time adjustment[15,16]. Comparative studies[15] and critical reviews[16] concerning liquid chromatographic carbohydrate separations on the above columns have been published.

0021-9673/90/$03.50

Based on these observations, we were interested in extending the potential of amino-bonded phase columns to the simultaneous analysis of neutral sugars and uronic acids. It is of value to analyse directly the uronic acids and neutral sugar residues in order to identify the polysaccharides as it is the first step in the structural analysis of polysaccharides. In this paper, we report an investigation of the chromatographic behaviour of uronic acids and neutral sugars on an amino-bonded phase column and discuss the results from the viewpoint of structural features and elution mechanism. The possibility of the simultaneous determination of uronic acids and neutral sugars is considered.

EXPERIMENTAL

Materials

Standard saccharide samples were obtained from Sigma and Aldrich. HPLC-grade acetonitrile (Fluka) and analytical-reagent grade sodium dihydrogenphosphate (NaH_2PO_4) were used.

Preparation of hydrolysate of acidic polysaccharides. An acidic polysaccharide, PIA-I, prepared in our laboratory, was hydrolysed with 2 *M* trifluoroacetic acid (TFA) at 120°C for 1 h in a sealed tube. After the TFA had been removed by evaporation, the hydrolysate was dissolved in water, filtered to remove any particulate matter and then subjected to HPLC analysis.

Apparatus

The equipment consisted of a programmable HPLC pump (Waters Model 590) a differential refractometer (Shodex Model SE-51) and a high-pressure sampling valve (Bio-Rad Model 7125). The detector output was recorded with a flat-bed recorder (LKB Model 2210) and an integrator (CDMC-2, China).

Chromatography was carried out with a 200 × 5 mm I.D. stainless-steel column packed with 5-μm LiChrosorb NH_2 (E. Merck) and a 5 × 5 mm I.D. guard column packed with the same material.

Chromatographic conditions

The mobile phase was a mixture of acetonitrile and phosphate buffer or water. All solvents were filtered and degassed ultrasonically before use. The column was equilibrated overnight with the respective eluent at a flow-rate of 0.5 ml/min and then the flow-rate was maintained at 1 ml/min during chromatography. A 20-μl volume of a sample solution containing 0.5–2% (w/w) of each saccharide was applied to the column. All separations were done at room temperature and no attempt was made to control the temperature of the mobile phase and the column.

RESULTS AND DISCUSSION

A typical separation of some common mono- and disaccharides using acetonitrile–water (80:20, v/v) (pH 8.4) as eluent is shown in Fig. 1. The elution sequence and resolution are similar to those reported using the same column[1,3–5]. With this LiChrosorb NH_2 column and acetonitrile–water as eluent, however, uronic acids such as glucuronic acid (GlcA) and galacturonic acid (GalA) could not be eluted as

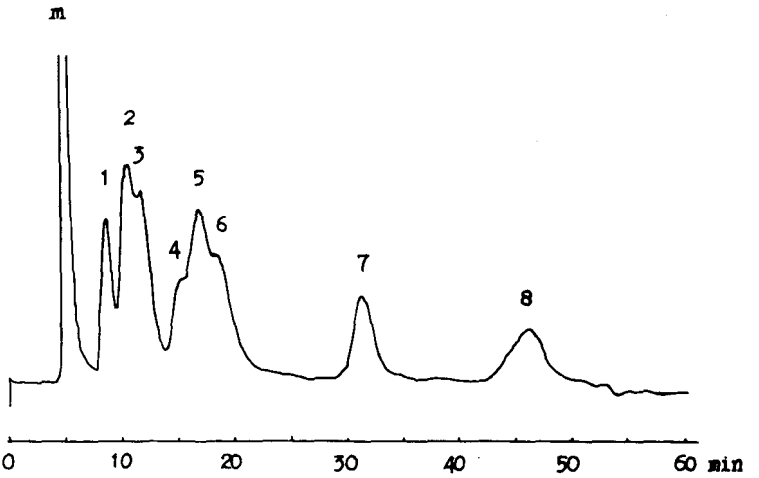

Fig. 1. Separation of a neutral mono- and disaccharide mixture on LiChrosorb NH_2 column. Flow-rate, 1.0 ml/min. Eluent, acetonitrile–water (80:20, v/v) (pH 8.4). Peaks: 1 = rhamnose; 2 = xylose + fucose; 3 = arabinose; 4 = mannose; 5 = glucose; 6 = galactose; 7 = sucrose; 8 = lactose; m = mobile phase.

measurable peaks within a reasonable time. For the separation of these acids, a phosphate buffer–acetonitrile solvent was tested[6]. Fig. 2 shows the chromatogram obtained on the same column with acetonitrile–0.015 *M* NaH_2PO_4 buffer (80:20, v/v) (pH 7.3) as eluent for the separation of a standard mixture of uronic acids and neutral sugars. GlcA was eluted as a comparatively broad peak but GalA was still not eluted.

The marked difference in the elution behaviour of the uronic acids with the two solvent systems led us to investigate the effects of the composition and pH of the buffered mobile phase on the separation of the acids.

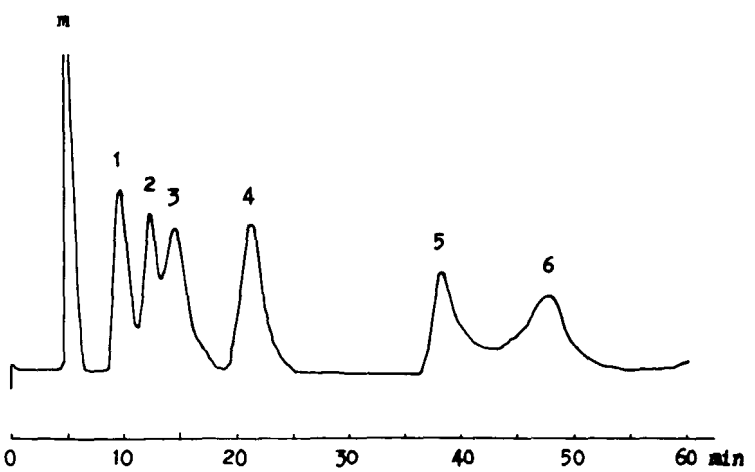

Fig. 2. Separation of (1) rhamnose, (2) xylose, (3) arabinose, (4) glucose, (5) sucrose, (6) glucuronic acid and galacturonic acid on the same column. Flow-rate, 1.0 ml/min. Eluent, acetonitrile–0.015 *M* NaH_2PO_4 (80:20, v/v) (pH 7.3).

At fixed acetonitrile to buffer ratio of 75:25 (v/v), the pH of the mobile phase was adjusted to 7.2 and 6.9 with 0.015 and 0.018 *M* NaH_2PO_4, respectively. Using these eluents, the same test mixture as in Fig. 2 was chromatographed and the results are shown in Fig. 3. On comparing the elution profiles of GlcA and GalA in Fig. 3B with that in Fig. 3A, the improvement in peak width and peak tailing obtained with the eluent of lower pH is obvious, especially for GalA, although a negative peak appeared at the retention time of GalA and split the relatively broad peak of GalA into two. This negative peak has also been reported by Hendrix *et al.*[17] using a similar system with amine-modified silica as the stationary phase, and was found to be a function of the eluent pH. The acidic eluents resulted in a strong negative peak following trisaccharide elution.

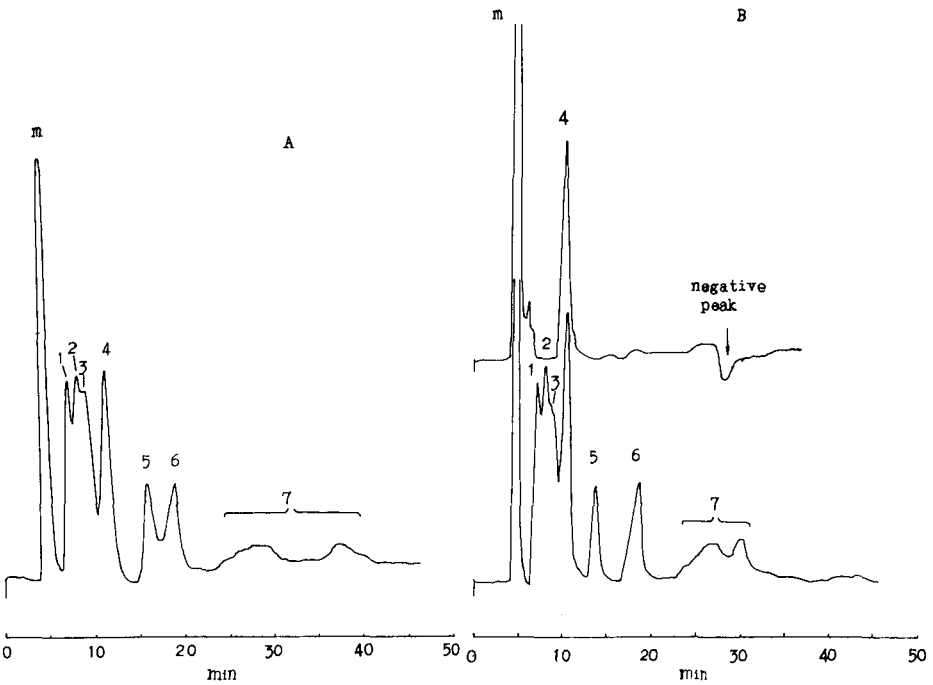

Fig. 3. Effect of increasing the acidity of eluent on solute elution. Flow-rate, 1.0 ml/min. Eluents: A, acetonitrile–0.015 *M* NaH_2PO_4 (75:25, v/v) (pH 7.2); B, acetonitrile–0.018 *M* NaH_2PO_4 (75:25, v/v) (pH 6.9). Note that a negative peak appears at the GalA elution position. Peaks: 1 = rhamnose; 2 = xylose; 3 = arabinose; 4 = glucose; 5 = sucrose; 6 = glucuronic acid; 7 = galacturonic acid.

In our system, a solvent with a higher water content was employed to elminate this undesirable negative peak. Fig. 4 illustrates the results for the test mixture and GalA alone with acetonitrile–0.015 *M* NaH_2PO_4 (70:30, v/v) (pH 7.0) as eluent. GlcA and GalA were eluted as symmetrical peaks and a baseline separation was obtained.

In Table I, the retention times and capacity factors (k') of the carbohydrates determined with various solvents are presented. The retention of the carbohydrates on the amino-bonded phase is strongly dependent on structural features. It has been proposed that the number and geometry of hydroxyl groups on the neutral sugars are

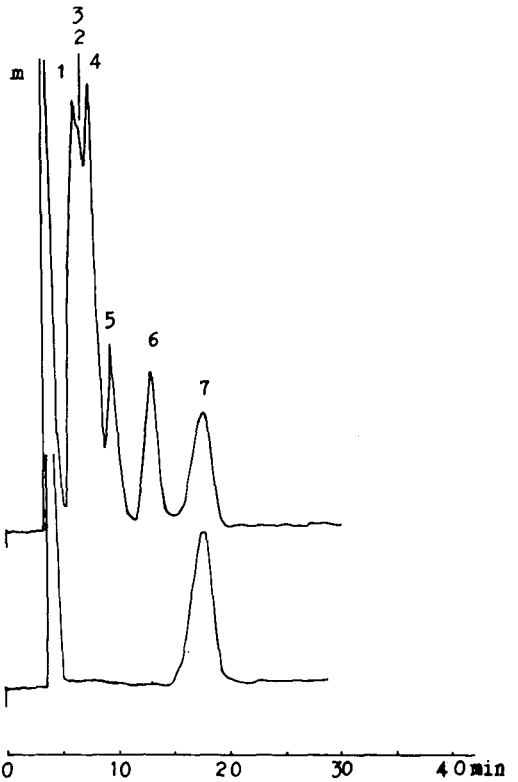

Fig. 4. Chromatogram obtained with a higher water content in the buffered solvent. Flow-rate, 1.0 ml/min. Eluent, acetonitrile–0.015 *M* NaH_2PO_4 (70:30, v/v) (pH 7.0). Peaks as in Fig. 3.

important factors for separation[18]. In general, more hydroxyl groups would result in more hydrogen bonds with the stationary phase, therefore increasing the retention. The uronic acids are distinguished from neutral monosaccharides in the replacement of the 6-hydroxyl group with a carboxylate group:

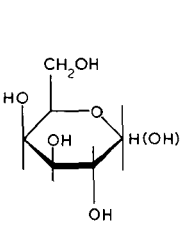

D-Galactose

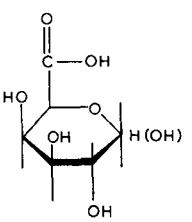

D-Galacturonic acid

Our data indicate that a uronic acid either cannot be eluted from the column or is eluted much later than the corresponding neutral sugar. This different behaviour cannot be explained by the difference in the number of hydrogen bonds.

TABLE I

RETENTION DATA FOR NEUTRAL SUGARS AND URONIC ACIDS ON AN AMINO-BONDED PHASE COLUMN WITH DIFFERENT MOBILE PHASE SYSTEMS

Sample	*No. of hydroxyl groups*	*System I: CH_3CN–water (80:20, v/v) (pH 8.4)*		*System II: CH_3CN–0.015 M NaH_2PO_4 (80:20, v/v) (pH 7.3)*		*System III: CH_3CN–0.015 M NaH_2PO_4 (75:25, v/v) (pH 7.2)*		*System IV: CH_3CN–0.018 M NaH_2PO_4 (75:25, v/v) (pH 6.9)*		*System V: CH_3CN–0.015 M NaH_2PO_4 (70:30, v/v) (pH 7.0)*	
		t_r (min)	k'	t_r (min)	k'	t_r (min)	k'	t_r (min)	k'	t_r (min)	k'
Rhamnose	4	8.84	0.740	9.73	0.966	7.38	0.689	6.90	0.612	6.44	0.656
Xylose	4	10.50	1.067	12.42	1.509	8.48	0.941	7.76	0.813	6.68	0.717
Fucose	4	10.70	1.106	12.71	1.568	8.62	0.973	7.86	0.836	6.71	0.725
Arabinose	4	12.10	1.382	14.59	1.947	9.27	1.121	8.63	1.016	6.82	0.753
Mannose	5	15.79	2.108	18.76	2.790	10.75	1.460	9.49	1.217	7.57	0.946
Glucose	5	17.10	2.366	21.56	3.356	11.54	1.641	10.09	1.357	7.99	1.054
Galactose	5	18.30	2.602	22.85	3.616	12.03	1.753	10.39	1.428	8.21	1.111
Sucrose	8	30.67	5.037	38.09	6.695	16.12	2.689	13.61	2.180	9.73	1.501
Lactose	8	46.31	8.116	53.33	9.774	20.12	3.604	17.81	3.161	11.35	1.918
GlcA	4	[a]	–	47.12	8.519	19.26	3.407	18.49	3.320	13.14	2.378
GalA	4	[a]	–	[a]	–	[b]	–	[b]	–	17.85	3.589
t_0		5.08		4.95		4.37		4.28		3.89	

[a] Sample cannot be eluted from the column.
[b] Peaks too broad to measure.

It is also interesting that GlcA was eluted before or after the disaccharide lactose with the different mobile phases employed. It has been observed previously that when neutral mono- or disaccharides were separated on an amino-bonded phase column, although the capacity factors were a function of the eluent pH, composition and the column used, the elution order was not significantly effected by them[6,7,17,19]. Our results on neutral sugars are also in agreement with these reports. This can probably be attributed to the dominant force in the separation of these neutral sugars on the amino-bonded phase column being the same as forces such as hydrogen bonding force[1,6,18]. If the retention of uronic acids on the columns were also caused by this force, GlcA would follow the same rule and the above factors would not change its elution sequence. When the eluent pH and composition were varied, however, the experimental results did not support the above assumption. The influence of the pH and composition of the eluent on the retention order of uronic acids and neutral sugars is demonstrated in Fig. 5.

These results may lead to a better understanding of the elution mechanism of the acids. It seems more likely that the retention of uronic acids is mainly derived from other kinds of molecular forces. This may also explain why the uronic acid cannot be eluted from LiChrosorb NH_2 with an acetonitrile–water system. Some similar organic acids on an amino-bonded phase column were presumed to form salts with the amino groups in the normal-phase mode[8].

From literature data and our studies, it appeared that the retention of carbohydrates decreased with decreasing eluent pH. However, we also noticed that

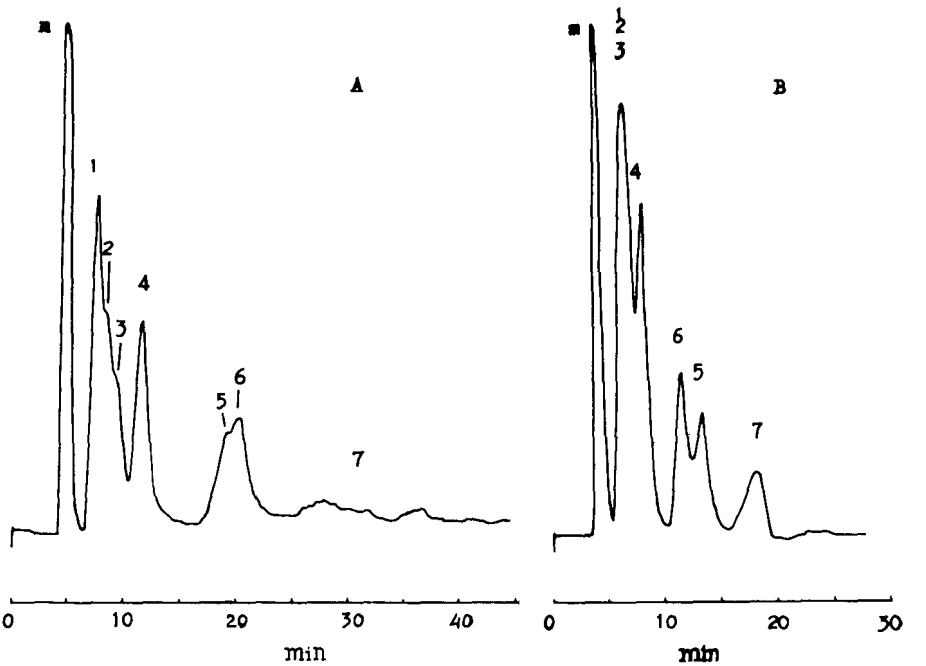

Fig. 5. Influence of eluent modification on the elution order of uronic acids and neutral sugars. Flow-rate, 1.0 ml/min. Eluents: A, acetonitrile–0.015 *M* NaH_2PO_4 (75:25, v/v) (pH 7.2); B, acetonitrile–0.015 *M* NaH_2PO_4 (70:30, v/v) (pH 7.0). Peaks: 1 = rhamnose; 2 = xylose; 3 = arabinose; 4 = glucose; 5 = glucuronic acid; 6 = lactose; 7 = galacturonic acid.

increased retention times for neutral sugars were obtained in system II, the eluent pH being changed from 8.4 in system I to 7.3 with phosphate buffer. It was considered possible that the role of the anion ($H_2PO_4^-$) in the mobile phase is not only to adjust the eluent pH, but also to form a complex with the bonded phase. The complex is probably similar to the amine phosphate salt [$RNH^-O^+PO(OH)_2$] obtained on a phosphoric acid-modified amino-bonded phase column[20]. Preliminary investigations indicated this modified amino-bonded phase column did not change the elution order of neutral sugars but had a significant influence on the elution of GlcA and GalA. Further work is in progress.

From the above it is evident that the addition of NaH_2PO_4 to buffer the eluent is essential for elution of the acids from the column and a higher water content of the eluent can eliminate the negative peak found with acidic eluents and have a promoting effect on the elution of the uronic acids.

Accordingly, under the appropriate mobile phase conditions, the method described makes it possible to analyse directly the hydrolysate of polysaccharides which contain uronic acid units. Fig. 6 demonstrates the result for a real sample on the amino-bonded phase column. Filtration of the sample is the only pretreatment and no derivatization is required. The column used in our system appeared to be stable.

In conclusion, owing to the different chromatographic behaviour between uronic acids and neutral sugars on an amino-bonded phase column, the use of

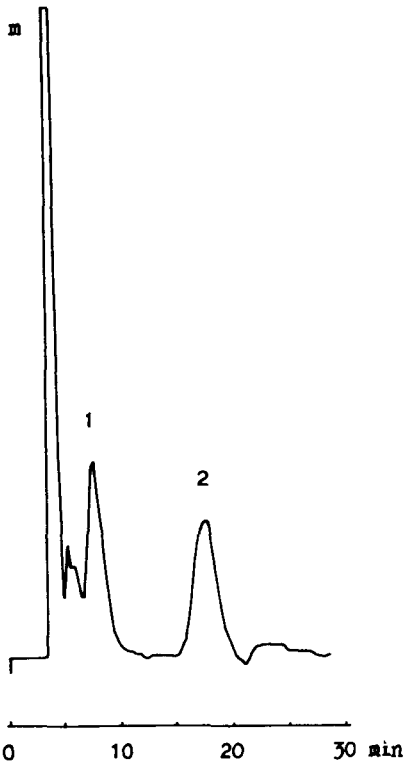

Fig. 6. Separation and determination of (1) galactose and (2) galacturonic acid in the hydrolysate of the acidic polysaccharides PIA-I. Flow-rate, 1.0 ml/min. Eluent: acetonitrile–0.015 *M* NaH_2PO_4 (70:30, v/v) (pH 7.0).

a buffered mobile phase and control of the eluent pH and composition are necessary for the simultaneous and direct analysis of these carbohydrate mixtures. This HPLC method has proved helpful in the study of the structural analysis of acidic polysaccharides such as plant gums and mucilages.

ACKNOWLEDGEMENT

The authors are grateful to the Chinese Foundation of Natural Sciences for financial support of this work.

REFERENCES

1 H. Binder, *J. Chromatogr.*, 189 (1980) 414.
2 V. Kahle and K. Tesařík, *J. Chromatogr.*, 191 (1980) 121.
3 M. T. Yang, L. P. Milligan and G. W. Mathison, *J. Chromatogr.*, 209 (1981) 316.
4 D. P. Lu, K. W. Huang and R. C. Li, *Acta Biochim. Biophys. Sin.*, 14 (1982) 501.
5 W. Blaschek, *J. Chromatogr.*, 256 (1983) 157.
6 W. M. Blanken, M. L. E. Bergh, P. L. Koppen and D. H. Van Den Eijnden, *Anal. Biochem.*, 14 (1985) 322.

7 Z. L. Nikolov, M. M. Meagher and P. J. Reilly, *J. Chromatogr.*, 319 (1985) 51.
8 E. Laakso, R. A. Tokola and E. Hirvisalo, *J. Chromatogr.*, 278 (1983) 406.
9 E. Rajakylä, *J. Chromatogr.*, 218 (1981) 695.
10 A. G. J. Voragen, H. A. Schols, J. A. De Vries and W. Pilnik, *J. Chromatogr.*, 244 (1982) 327.
11 P. Gacesa, A. Squire and P. J. Winterburn, *Carbohydr. Res.*, 118 (1983) 1.
12 K. B. Hicks, P. C. Lim and M. J. Haas, *J. Chromatogr.*, 319 (1985) 159.
13 K. B. Hicks, *Carbohydr. Res.*, 145 (1986) 312.
14 S. Honda, *Anal. Biochem.*, 140 (1984) 1.
15 J. G. Baust, R. E. Lee, R. R. Rojas, D. L. Hendrix, D. Friday and H. James, *J. Chromatogr.*, 261 (1983) 65.
16 M. Verzele, G. Simoens and F. Van Damme, *Chromatographia*, 23 (1987) 292.
17 D. L. Hendrix, R. E. Lee, Jr., J. G. Baust and H. James, *J. Chromatogr.*, 210 (1981) 45.
18 M. D'Amboise, D. Noël and T. Hanai, *Carbohydr. Res.*, 79 (1980) 1.
19 L. A. Th. Verhaar and B. F. M. Kuster, *J. Chromatogr.*, 220 (1981) 313.
20 J. W. Haas, III, W. F. Joyce, Y. J. Shyu and P. C. Uden, *J. Chromatogr.*, 457 (1988) 215.

Journal of Chromatography, 513 (1990) 237–246
Elsevier Science Publishers B.V., Amsterdam

CHROM. 22 466

Applications of high-performance liquid chromatography to quantitation of metabolites and enzymes of the patulin pathway from *Penicillium patulum*

JEFFREY W. PRIEST[a] and ROBLEY J. LIGHT
Department of Chemistry and Institute of Molecular Biophysics, Florida State University, Tallahassee, FL 32306 (U.S.A.)
(Received January 2nd, 1990)

ABSTRACT

Conditions for extraction and high-performance liquid chromatographic (HPLC) analysis for fourteen of the patulin pathway metabolites from *Penicillium patulum* are described which allow quantitation of the metabolite content of cultures at hourly intervals. The HPLC analysis is more sensitive than gas–liquid chromatographic analysis and is more quantitative than thin-layer chromatographic analysis. Separations on a preparative column allow for the collection and identification of new metabolites. The column elution program can be varied to optimize analysis time for individual metabolites, allowing individual enzymes of the pathway to be assayed by following the conversion of substrate to product. Analysis of product formation in crude enzyme mixtures can be used to assay an enzyme in the presence of subsequent enzymes of the pathway and to establish the pathway reaction sequence.

INTRODUCTION

Fig. 1 shows the polyketide family of products derived from the simple aromatic polyketide 6-methylsalicylic acid (6-MS) in the organism *Penicillium patulum* and in several related fungal species. The metabolites and the enzymes producing them are absent from young cultures undergoing balanced "trophophase" growth, and they are not produced until the culture enters "idiophase"growth where some essential nutrient has become limiting[1] (these terms were suggested by Bu'Lock *et al.*[2]). Patulin is the major end product accumulating under some culture conditions but changes in media composition, pH, temperature, aeration rate, etc. can affect not only the relative amounts of the metabolites but also the timing of their appearance[1,3,4]. Variations in the induction rates and final activities of the several enzymes involved are presumably responsible for the variability in metabolite profile, though limitations on transport in

[a] Present address: Department of Biochemistry, University of Alabama at Birmingham, Birmingham, AL 35297, U.S.A.

0021-9673/90/$03.50

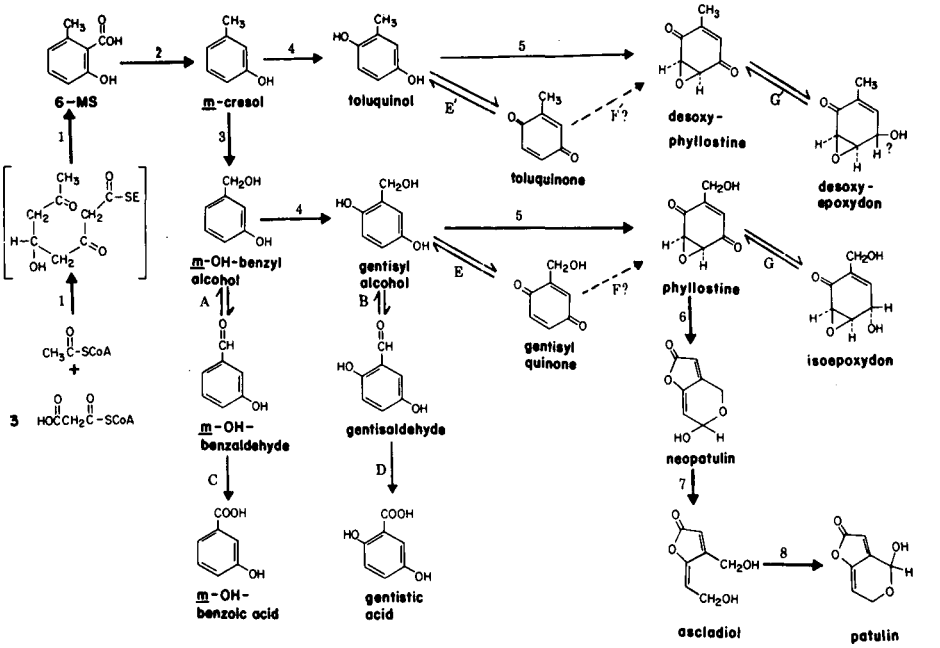

Fig. 1. Products derived from polyketide 6-methylsalicylic acid in the organism *Penicillium patulum* and related species.

and out of the cells may also play a role in what is found in the culture medium at any one time.

While this polyketide "pathway" is one of the most studied examples of secondary metabolism, a thorough study of many of the subtleties involved in induction of the pathway enzymes has been hindered by the lack of a rapid, sensitive, and quantitative assay for the metabolites and a sensitive, general assay for the enzymes. A crude measure such as the color intensity with $FeCl_3$ can quickly quantitate total 6-MS in the absence of significant amounts of the other metabolites[5], but is an inadequate indication of total "phenolic" metabolite production. Thin-layer chromatography (TLC) provides sensitive information[4,6], but spots on thin-layer plates are difficult to quantitate, interpretation can be difficult when compounds comigrate, and the collection of data is time-consuming. Gas–liquid chromatography (GLC) has been used in some laboratories for metabolite quantitation but this method is less sensitive and requires preparation of silylated derivatives[7]. The dehydrogenase enzymes of the pathway which employ NAD^+ or $NADP^+$ cofactors are simple to assay spectrophotometrically[8,9] but the other enzymes studied have required a specialized assay development for each enzyme, usually involving the use of isotopically labeled precursors and the chromatographic isolation and counting of a radiolabeled product[5,10,11].

We report here the application of HPLC to the rapid (1 h) simultaneous analysis of metabolites with a sensitivity one to two orders of magnitude higher than GLC, and with only two cases of peak overlap requiring special attention. Minor variations of the

procedure allow a generalized assay of any enzyme in the pathway for which substrate is available.

EXPERIMENTAL

Metabolite standards

Several compounds were obtained from commercial sources and purified by recrystallization or, in the case of *m*-cresol, redistillation. These include *m*-cresol, *m*-hydroxybenzyl alcohol, *m*-hydroxybenzaldehyde, and gentisaldehyde from Aldrich, toluquinol from Matheson, and patulin from Applied Science. Gentisaldehyde was also synthesized from *p*-hydroquinone (Matheson) by the Riemer-Tieman reaction[12]. 6-MS was synthesized by the method of Eliel *et al.*[13]. Toluquinone was synthesized by oxidation of toluquinol with Ag_2O (ref 14). Gentisyl alcohol was prepared by the $NaBH_4$ reduction of gentisaldehyde, and gentisyl quinone by the further oxidation of this product with $NaIO_4$ (ref. 15). Ascladiol was synthesized by the $NaBH_4$ reduction of patulin[16]. Phyllostine was kindly supplied by Dr. G. M. Gaucher, University of Calgary, Canada[17]. Desoxyphyllostine and neopatulin were isolated from preparative scale *in vitro* enzyme incubations[18]. Standard curves were obtained by dissolving a known quantity of standard (10 to 160 μg) to two or more 0.5 ml samples of HPLC buffer (14 m*M* potassium phosphate, pH 6.0 and 20% methanol) and analyzing 20 μl aliquots by HPLC. The integrated peak areas on the recorder were used to calculate the conversion factor "pmoles/10^3 area units" (Table I).

HPLC conditions

The HPLC system consisted of two Model 114M solvent pumps, a Model 421A controller, a Model 210A sample injection valve, a Model 160 UV detector with 280 nm and 254 nm filters (all Beckman), and a Shimadzu model C-R3A integrator. Reversed-phase columns were packed with Altex Ultrasphere ODS C_{18} for either analytical (25 cm × 4.6 mm I.D., 5 μm packing or 7.5 × 4.6 mm I.D., 3 μm packing) or preparative (25 × 1.0 cm I.D., 5 μm packing) analyses. Samples isolated by ether extraction followed by drying and removal of ether *in vacuo* were dissolved in 14 m*M* potassium phosphate buffer, pH 6.0, containing 20% methanol [and 0.7 m*M* tetrabutylammonium phosphate (Sigma, 90%) if this ion-pair reagent was being used in the elution]. Analytical samples were cleared of fine particles by a 30-s high-speed centrifugation in an Eppendorf tube prior to injection of a 20-μl aliquot. Preparative samples were centrifuged for 30 min at 30 000 *g* prior to injection of 500 μl aliquots. The eluting solvents were HPLC grade and de-aerated prior to use. The elution programs are described in the figure legends.

Metabolite extraction

Fermentor cultures of *P. patulum* were grown as described previously[18]. Aliquots of the culture were harvested at various times and the mycelium separated by filtration. For analytical runs, a 30-ml portion of the filtered culture medium was acidified to pH 2–3 with concentrated HCl and extracted twice with 30-ml portions of anhydrous ether. The ether was dried over 20 g of anhydrous Na_2SO_4 and removed by rotary evaporation under an aspiration vacuum. The residue was redissolved in 10 ml of buffer as described above. For preparative isolations, usually one liter of medium

was acidified and extracted with two 500-ml portions of anhydrous ether. The combined ether extracts were equilibrated with saturated aqueous NaCl solution, dried over anhydrous Na_2SO_4, and the ether was removed by rotary evaporation. The residue was redissolved in 3 ml of buffer as described above.

Enzyme assays

Mycelial samples of *P. patulum* were harvested from cultures grown as previously described[18], washed with 0.5 volumes of 20 m*M* potassium phosphate, pH 7.5, and suspended in this same buffer for lyophilization. Lyophilized samples were stored at −70°C until utilized for enzyme isolation or analysis. To facilitate cell breakage and to remove phenolic metabolites which might inhibit activity[19] the lyophilized mycelium was frozen in liquid nitrogen, ground to a fine powder with a mortar and pestle, and stirred into 10 ml of −20°C acetone per gram of powder. The acetone was removed by filtration through a sintered glass filter, and the mycelial powder was rinsed with 10 ml of −20°C anhydrous ether and dried thoroughly by suction filtration. A 0.5-g portion of the dried mycelium was mixed in a cold mortar with 5 ml of extraction buffer (100 m*M* potassium phosphate, pH 7.5, 2.5 m*M* dithiothreitol, and 15% glycerol) and 0.5 g of sand. The sample was ground with a pestle to a paste and the thick suspension centrifuged at 4°C for 10 min at 10 000 *g* in a Sorvall RC-2B centrifuge with an SS-34 rotor. The supernatant was transferred to a second tube and centrifuged at 4°C for 30 min at 30 000 *g*. This process yielded approximately 3.5 ml of crude extract with a protein concentration of 18–48 mg/ml. Aliquots of this crude extract were utilized for the enzyme assays. The conditions for each assay are described in the figure legends. The metabolite extraction efficiency for the enzyme assay (Table I) was determined by adding known quantities of metabolite (10 to 160 μg) to two or more 5.0 ml portions of 100 m*M* potassium phosphate buffer, pH 7.5, acidifying to pH 1–2, and extracting twice with two volumes of ether. The ether was dried over sodium sulfate and evaporated as in the enzyme assay extraction, the residue was dissolved in 0.5 ml of HPLC buffer (14 m*M* potassium phosphate, pH 6.0 and 20% methanol) and 20 μl aliquots were analyzed by HPLC. Integrated peak areas were compared with those obtained from an equivalent amount of standard added directly to 0.5 ml of HPLC buffer.

RESULTS AND DISCUSSION

Fig. 2 shows an analytical HPLC profile of eight of the more common metabolites from 6-MS (Fig. 1), including the most polar (gentisyl alcohol, peak a) and the least polar (*m*-cresol, peak i). A gradient elution was necessary to achieve the best separation of the early peaks while keeping elution of *m*-cresol within 30 min. An ion-pair reagent, tetrabutylammonium phosphate, was necessary to alter the elution position of 6-MS (peak h), the one carboxylic acid in the set of standards. In the absence of the ion pair the carboxylate ion of 6-MS elutes very early as a broad, polar peak and interferes with detection of the other polar metabolites. At the indicated concentration of 0.7 m*M* ion pair reagent, 6-MS eluted in a region clear of other metabolites. Instability of the column at low pH precluded attempts to suppress ionization using an acidic elution mixture. For samples not containing 6-MS or another carboxylic acid, the ion-pair reagent can be omitted. Only two pairs of

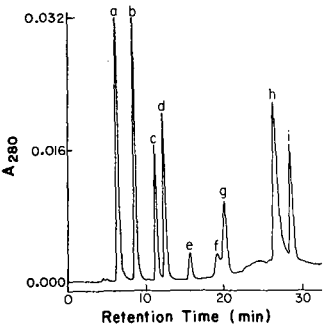

Fig. 2. HPLC profile of metabolite standards. A 20-μl sample of a mixture of standards in a buffer containing 14 mM potassium phosphate at pH 6.0, 0.7 mM tetrabutylammonium phosphate, and 20% (v/v) methanol was injected on a 25 cm × 4.6 mm I.D., 5 μm C_{18} column. The column was eluted at a flow-rate of 0.6 ml/min using a gradient of solvent B [14 mM potassium phosphate at pH 6.0, 0.7 mM tetrabutylammonium phosphate, and 50% (v/v) methanol] in solvent A (14 mM potassium phosphate at pH 6.0 and 0.7 mM tetrabutylammonium phosphate). The elution program was 40% B to 60% B (linear gradient) in 10 min, 60% B to 100% B (linear gradient) in 10 min, and 100% B (isocratic) for 10 min. The metabolite standards are: a = gentisyl alcohol, 0.4 μg; b = patulin, 0.05 μg; c = toluquinol, 0.2 μg; d = *m*-hydroxybenzyl alcohol, 0.4 μg; e = impurity; f = gentisaldehyde, 0.5 μg; g = *m*-hydroxybenzaldehyde, 0.4 μg; h = 6-MS, 1.0 μg; and i = *m*-cresol, 0.4 μg.

compounds tested did not give satisfactory resolution under these conditions. On a preparative column ascladiol co-eluted with gentisyl alcohol at 10.8 min, and toluquinone co-eluted with *m*-hydroxybenzaldehyde at 32.8 min. For the culture induction and enzymatic assays reported here, this lack of resolution did not cause ambiguity in interpretation of results. Gentisyl alcohol and ascladiol are not likely to be present in the same enzymatic assays, and in culture analyses gentisyl alcohol should be the first of the pair appearing. The presence of toluquinone would be indicated if toluquinol were also found. Nevertheless, should it be necessary to verify the content of these peaks, one can re-run the sample at a different detector wavelength or collect material from the peaks to analyze by UV–VIS spectroscopy or by TLC.

Ideally, one would like to inject a culture medium or an enzymatic reaction mixture directly on the HPLC. The major components of either the culture medium (glucose, salts, nutrients) or the enzyme solution (proteins, buffers) would likely interfere or drastically shorten the life of the column, so metabolites were first extracted with ether prior to analysis. While ether extraction adds some time to the analysis, it also adds flexibility in manipulating sample size and ultimate sensitivity. One can vary the volume of sample extracted, the volume of elution buffer used to reconstitute the extract, and the volume of the aliquot injected.

The sensitivity, of course, also varies with the compound and the wavelength of the detector. The quantity of standards shown in Fig. 2 ranged from 50 ng (0.32 nmol) for patulin (peak b) to 1.0 μg (6.6 nmol) for 6-MS (peak h) in a 20-μl injection, or 2.5 ng/μl and 50 ng/μl respectively. Discernable peaks could be seen with as little as 2% of this quantity, whereas detection limits reported for GLC by Ehman and Gaucher[7] range from 4–18 ng/μl of extract for a 1-μl injection.

In addition to monitoring the appearance of known metabolites, the HPLC procedure provides the possibility of observing new metabolites. Samples can be

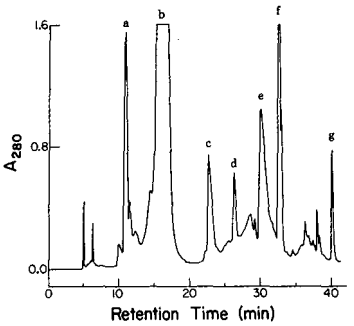

Fig. 3. Preparative HPLC metabolite profile of extract from an induced culture of *Penicillium patulum*. One liter of medium from a 32-h culture was extracted and reconstituted in 3.0 ml of buffer containing 14 m*M* potassium phosphate at pH 6.0 and 20% (v/v) methanol. A 500-μl aliquot was injected on a 25 × 1.0 cm I.D., 5 μm C_{18} column. The column was eluted at a flow-rate of 2.0 ml/min using a methanol–water solvent as follows: 17.5% methanol(isocratic) for 15 min, 17.5% methanol to 100% methanol (linear gradient) in 30 min, and 100% methanol (isocratic) for 5 min. Metabolite identities were determined by comparison with retention times and by examining the UV spectra of collected material as described in the text (the ion-pair reagent was not included because no 6-MS was detected in the culture at that time).

collected from a preparative column for structural verification of identification using other spectral techniques.

Fig. 3 shows a typical preparative HPLC elution profile of a culture extract obtained from a 32-h fermentor culture. The lettered peaks were identified both by comparison of retention times to standards and by collecting the corresponding eluent and comparing its UV spectrum to that of a standard. Peak a contained a mixture of gentisyl alcohol and ascladiol. Peak b contained neopatulin in early fractions and patulin in late fractions (neopatulin can be seen as a distinct shoulder on the patulin peak with a smaller sample). Peak c contained toluquinol with a small unknown contaminant. Peaks d and g contained *m*-hydroxybenzyl alcohol ad *m*-cresol respectively. Material from peak e had four absorption maxima at 210, 242, 285, and 350 nm and that from peak f had a broad absorption band with a maximum at about 270 nm. These latter two substances may turn out to be new compounds related to the pathway, but have yet to be identified.

The HPLC procedure was easily adapted to assay of individual enzymes of the patulin pathway. We modified the extraction method to start with a smaller sample volume and achieve a greater concentration of extract in the elution buffer in order to increase sensitivity. The gradient elution profile was modified for each specific assay to minimize elution time while still achieving separation of substrate and product. The ion-pair reagent was unnecessary for reactions not involving 6-MS, nor was it necessary for 6-MS decarboxylase since the product *m*-cresol elutes much later than 6-MS. Details are given under Experimental.

Figs. 4 and 5 show an example of the assay of 6-MS decarboxylase in crude extract. The production of *m*-cresol is linear with respect to both time up to one hour (Fig. 4) and extract concentration up to 20 μl (Fig. 5). Fig. 6 shows similar results for *m*-hydroxybenzyl alcohol dehydrogenase. A more convenient spectrophotometric assay has been developed for the dehydrogenase[8], but the HPLC method can be used to verify activity in crude extract where competing reactions of NADH could

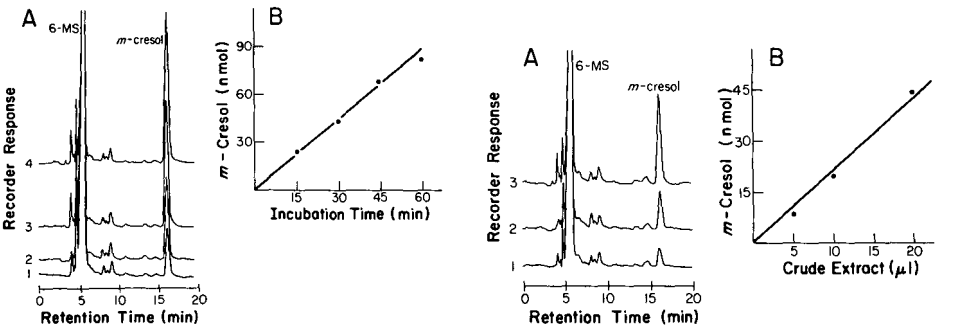

Fig. 4. HPLC assay of 6-MS decarboxylase: effect of incubation time on product formation. Each assay tube contained 0.50 μmol of 6-MS, 7.5 mg of serum albumin, and 20 μl of crude extract in 5.0 ml of 100 m*M* potassium phosphate buffer, pH 7.5. Tubes were incubated at 28°C for the indicated time, acidified to pH 1–2 with concentrated HCl, and the products were extracted with ether as described under Experimental. Aliquots of the reconstituted extract (20 μl of 500 μl) were injected on a 25 cm × 4.6 mm I.D., 5 μm C_{18} column which was eluted isocratically with 50% methanol at a flow-rate of 0.6 ml/min. (A) Tracing of the recorder response at 280 nm from (1) 15 min, (2) 30 min, (3) 45 min, and (4) 60 min incubations respectively. (B) Plot of the quantity of *m*-cresol in the extract determined from the integrated peak areas in A. These values were not corrected for extraction efficiency.

Fig. 5. HPLC assay of 6-MS decarboxylase: effect of crude extract concentration on product formation. Assays were carried out as in Fig. 4 except incubations were for 60 min at crude extract concentrations of (1) 5 μl, (2) 10 μl, and (3) 20 μl in the 5.0-ml incubation mixture. (A) Tracing of the recorder response at 280 nm from the HPLC analysis. (B) Plot of the quantity of *m*-cresol in the extract determined from the integrated peak areas in A. These values were not corrected for extraction efficiency (this extract had been stored longer than that used in Fig. 4, consequently its decarboxylase activity was lower).

complicate the assay with a high background. A similar assay procedure has been reported for toluquinol and gentisyl alcohol epoxidase activity[18].

The data in Figs. 4–6 were not corrected for extraction efficiency. If one desires

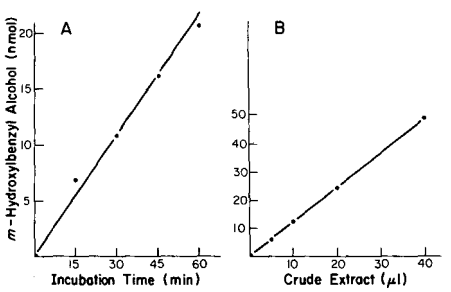

Fig. 6. HPLC assay of *m*-hydroxybenzyl alcohol dehydrogenase: effect of incubation time and enzyme extract concentration on product formation. Each assay tube contained 0.50 μmol of *m*-hydroxybenzaldehyde, 0.50 μmol of NADPH, 50 nmol of ATP, 5 μmol of $MgCl_2$ and the indicated amount of crude extract in 5.0 ml of 100 m*M* phosphate buffer, pH 7.5. The enzyme extract was a saturated ammonium sulfate precipitate of crude extract resuspended in an equivalent volume of enzyme buffer. Tubes were incubated at 28°C for various times with 40 μl of enzyme extract (A) or for 60 min with varying amounts of enzyme extract (B). After acidification and extraction with ether as described under Experimental, aliquots of the reconstituted extract (20 μl of 500 μl) were injected on a 25 cm × 4.6 mm I.D., 3 μm C_{18} column which was eluted at a flow-rate of 0.6 ml/min with a gradient of 20% methanol to 50% methanol in 4 min followed by 50% methanol for 14 min. The quantity of *m*-hydroxybenzyl alcohol (retention time, 4.8 min) produced was determined from the integrated peak areas. These values were not corrected for extraction efficiency.

to calculate enzyme activities on an absolute basis for comparison with each other, then the extraction efficiency of the method must be determined. Table I shows the efficiency under conditions we employed for our enzymatic assays as determined for thirteen of the metabolites we have studied. These are clearly lower than those reported by Ehman and Gaucher[7] who were preparing samples for GLC analysis, and who obtained extraction efficiencies above 90% for all but the very polar gentisyl alcohol at 78%. Different sample sizes and volume ratios of extracting solvent to sample probably account for these different results, and our method could be modified to improve efficiency if necessary. Table I also compares the detector sensitivity at 280 nm for each of the compounds. Multiplying the factor in the table by the integrated peak area gives the quantity of material in the injected sample. The retention times for standards are given for both the analytical column with the ion-pair reagent and the preparative column without the ion-pair reagent under the gradient elution programs described in Figs. 2 and 3.

TABLE I

PARAMETERS FOR QUANTITATING METABOLITE CONCENTRATIONS BY HPLC ANALYSIS

The metabolite extraction efficiency for enzyme assays, and the recorder response for each metabolite were determined as described under Experimental. Retention times on an analytical (25 cm × 4.6 mm I.D.) and a preparative (25 cm × 1.0 cm I.D.) column were determined using the elution programs described in Figs. 2 and 3, respectively. They varied by less than 5% in any one day's experiments and less than 15% between two columns over a period of eighteen months. The elution order is constant.

Metabolite	*Extraction efficiency*[a] *(%)*	*Detector response*[b] *280 nm (pmoles/10³ area units)*	*Retention time (min)*	
			Analytical	*Preparative*
Gentisyl alcohol[c]	32 ± 3	9.6	6.61	10.8
Phyllostine	68 ± 4	16.7	n.d.[e]	12.2
Neopatulin	n.d.[d]	2.7	n.d.[e]	15.1
Patulin	49 ± 9	1.5	8.8	15.6
Gentisyl quinone	66 ± 5	34.7	n.d.[e]	16.8
Toluquinol	76 ± 10	12.1	11.5	22.5
m-Hydroxybenzyl alcohol	68 ± 5	18.2	12.6	25.6
Desoxyphyllostine	60 ± 5	12.8	n.d.[e]	29.1
Gentisaldehyde	77 ± 12	62.5	19.3	31.9
m-hydroxybenzaldehyde	76 ± 8	28.6	20.4	32.8
Toluquinone	43 ± 1	62.6	n.d.[e]	32.8
6-Methylsalicylic acid	80 ± 5	15.1	26.9	n.d.[d]
m-Cresol	74 ± 7	22.0	28.9	39.1

[a] Average of 3–5 extractions.

[b] Arbitrary area units on a Shimadzu model C-R3A integrator at a setting of 0.04 a.u.f.s. This factor converts peak area to pmoles of analyte.

[c] Ascladiol co-elutes with gentisyl alcohol. We did not determine extraction efficiency or a standard peak response for this compound.

[d] Not determined.

[e] Not determined under the specific elution conditions described in Fig. 2.

We did not systematically study the sensitivity of the method for different assays, but Fig. 5 can give one a feeling for the sensitivity of the decarboxylase assay. The lowest point (5 μl of extract) gives a small but clearly discernable peak when the recorder is set at 0.04 a.u.f.s. After correction for 74% extraction efficiency, this value corresponds to about 10 nmoles or about 1 μg of *m*-cresol in 5 ml of assay mixture. By comparing the 280 nm recorder responses shown in Table I, one can calculate that other compounds would be detected with one-third to ten times the sensitivity of *m*-cresol.

The HPLC procedure also provides an advantage beyond speed and sensitivity in studying the pathway enzymes. Assays based on incorporation of substrate radioactivity into product involve isolation and counting of product accumulated after a given time of incubation. The presence of other enzymes in the crude extract, especially the next pathway enzyme, can prevent product accumulation by further metabolizing it. Thus assay values in crude extract can be misleading. The HPLC analysis allows one to observe accumulation of other products as well as the one being assayed and to determine whether subsequent reactions are occuring. One also need not go to the trouble and expense of preparing radiolabeled substrate.

Finally, the ability to observe several products at once has proven useful in determining the reaction sequence of the pathway. As an example, Fig. 7 shows the complexity of products formed after incubation of crude extract with gentisyl alcohol. Four products are observed: gentisyl quinone (d), which might have been produced chemically or enzymatically; gentisaldehyde (e), product of gentisyl alcohol dehydrogenase; phyllostine (b), the epoxidase reaction product on the way to patulin; and neopatulin (c), the product of phyllostine ring opening[20]. Fig. 7 describes a preparative HPLC run used for the purpose of collecting and identifying these metabolites. An analytical column was used under similar conditions [isocratic elution with methanol–water (10:90) at a flow-rate of 0.35 ml/min] to assay different enzyme fractions. These assays played an important role in unraveling the reaction sequence as gentisyl

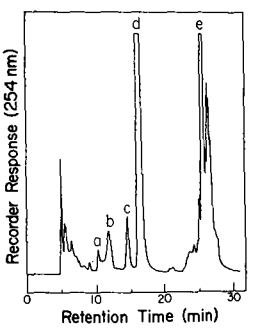

Fig. 7. Preparative-scale HPLC of products from the incubation of crude extract with gentisyl alcohol. A 1.0-l assay containing 30 mg of gentisyl alchol, 100 m*M* potassium phosphate buffer, pH 7.5, and 6.0 ml of mycelial crude extract from a 32-h culture was incubated for 2 h at 28°C. The product was isolated by ether extraction, the ether removed *in vacuo* and the residue dissolved in 4.0 ml of 17.5% methanol–water. A 0.5-ml aliquot was injected on a 1.0 × 25 cm 5 μm C_{18} column which was eluted isocratically with 17.5% methanol–water at a flow-rate of 2.0 ml/min. The detector was set at 254 nm and the recorder response at 2.0 a.u.f.s. Material in the lettered peaks was collected and identified as: a = gentisyl alcohol; b = phyllostine; c = neopatulin; d = gentisyl quinone; e = gentisaldehyde.

alcohol → phyllostine → neopatulin, with gentisaldehyde and gentisyl quinone as products of side reactions[18].

With the relatively rapid HPLC method it becomes possible to assay metabolite production at hourly intervals while the culture is in progress. Culture experiments from several laboratories have shown similarity in induction patterns, but the time of induction varies considerably[1,2,4,5]. Even in our hands under carefully controlled conditions the induction time may differ by a couple of hours. Timely assay of the induction state of the culture is important if one wants to harvest large samples of mycelia at a given stage of induction. We will report elsewhere the use of these assays to carefully define the condition of culture samples for the purpose of isolating mRNA from uninduced and early induction-stage cells and the use of this mRNA in isolating induction-specific genes from a genomic library.

ACKNOWLEDGEMENTS

This work was supported in part in its early stages by Grant PCM-8213610 from the National Science Foundation. We also acknowledge the support of Hank Henricks and the Biochemical Analysis and Synthesis Service facility of the Department of Chemistry for access to HPLC equipment and of Beckman Instruments for donation of an analytical column.

REFERENCES

1 J. W. D. Grootwassink and G. M. Gaucher, *J. Bacteriol.*, 141 (1980) 443.
2 J. D. Bu'Lock, D. Hamilton, M. A. Hulme, A. J. Powell, H. M. Smalley, D. Shepherd and G. N. Smith, *Can. J. Microbiol.*, 11 (1965) 765.
3 L. B. Bullerman, *Lebensm.-Wiss.-Technol.*, 18 (1985) 197.
4 P. I. Forrester and G. M. Gaucher, *Biochemistry*, 11 (1972) 1102.
5 R. J. Light, *J. Biol. Chem.*, 242 (1967) 1880.
6 J. Sekiguchi and G. M. Gaucher, *Appl. Environ. Microbiol.*, 33 (1977) 147.
7 J. Ehman and G. M. Gaucher, *J. Chromatogr.*, 132 (1977) 17.
8 P. I. Forrester and G. M. Gaucher, *Biochemistry*, 11 (1972) 1108.
9 J. Sekiguchi and G. M. Gaucher, *Can. J. Microbiol.*, 25 (1979) 881.
10 R. J. Light, *Biochem. Biophys. Acta*, 191 (1969) 430.
11 H. Iijima, Y. Ebizuka and U. Sankawa, *Chem. Pharm. Bull.*, 34 (1986) 3534.
12 H. H. Hodgson and T. A. Jenkinson, *J. Chem. Soc.*, 131 (1929) 469.
13 E. L. Eliel, D. E. Rivard and A. W. Burgstahler, *J. Org. Chem.*, 18 (1953) 1679.
14 R. Willstatter and A. Pfannenstiel, *Ber.*, 37 (1904) 4744.
15 J. M. Bruce and P. Knowles, *J. Chem. Soc. (C)*, (1966) 1627.
16 T. Suzuki, M. Takeda and H. Tanabe, *Chem. Pharm. Bull.*, 19 (1971) 1786.
17 J. Sekiguchi and G. M. Gaucher, *Biochemistry*, 17 (1978) 1785.
18 J. W. Priest and R. J. Light, *Biochemistry*, 28 (1989) 9192.
19 W. G. Niehaus, Jr. and R. P. Dilts, Jr., *J. Bacteriol.*, 151 (1982) 243.
20 J. Sekiguchi, G. M. Gaucher and Y. Yamada, *Tetrahedron Lett.*, (1979) 41.

Journal of Chromatography, 513 (1990) 247–254
Elsevier Science Publishers B.V., Amsterdam

CHROM. 22 460

Determination of nine flavonoids and coumarins in licorice root by high-performance liquid chromatography

LU ZENG, RU-YI ZHANG, TONG MENG and ZHI-CEN LOU*
School of Pharmaceutical Sciences, Beijing Medical University, Beijing 100083 (China)
(First received January 3rd, 1990; revised manuscript received March 20th, 1990)

ABSTRACT

A rapid high-performance liquid chromatographic method for the simultaneous separation and determination of five flavonoids and four coumarins, *viz.*, liquiritin, isoliquiritin, liquiritigenin, isoliquiritigenin, glycycoumarin, isoglycycoumarin, licochalcone A, glycyrol and isoglycyrol, in licorice root is described. The separation system consists of a reversed-phase column and a gradient elution system containing acetonitrile and 3% acetic acid in water. The compounds were detected at 310 and 365 nm successively. The recoveries of the flavonoids and coumarins were 95.6–105.2% with relative standard deviations of 0.62–4.24%. The contents of the above nine compounds in three species of licorice root produced in China were determined.

INTRODUCTION

Licorice root, the roots and rhizomes of *Glycyrrhiza* spp., family Leguminosae, has long been used as an important drug in China and also in Europe. It attracted special attention when Revers[1] in 1946 discovered and investigated the effect of licorice extract in the treatment of gastric and duodenal ulcers. Since then, a large amount of work on the chemical, pharmacological and clinical studies have been reported[2–5]. It has been found that the main active constituents of licorice root are saponins, flavonoids and coumarins, among which glycyrrhizinic acid and its aglycone showed anti-inflammatory, antitussive and antiallergic activities[3], liquiritin and isoliquiritin and their aglycones antiulcerogenic and spasmolytic activities[3,5], glycycoumarin antibacterial activity and licochalcone A anti-HIV activity[6].

Methods for the determination of glycyrrhizinic acid using precipitation[7], thin-layer chromatography[8], gas–liquid chromatography[9] and high-performance liquid chromatography (HPLC)[10–13] have been reported. No method for the determination of other constituents of licorice root has been found in literature. We describe here an HPLC method for the separation and determination of five flavonoids and four coumarins, *viz.*, liquiritin (**I**), isoliquiritin (**II**), liquiritigenin (**III**), isoliquiritigenin (**IV**), glycycoumarin (**V**), isoglycycoumarin (**VI**), licochalcone A (**VII**), glycyrol (**VIII**)

0021-9673/90/$03.50

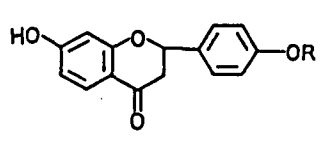

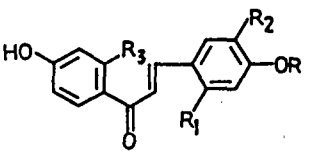

		R
I	Liquiritin	Glu
III	Liquiritigenin	H

		R	R_1	R_2	R_3
II	Isoliquiritin	Glu	H	H	OH
IV	Isoliquiritigenin	H	H	H	OH
VII	Licochalcone A	H	OCH_3	$CMe_2CH{=}CH_2$	H

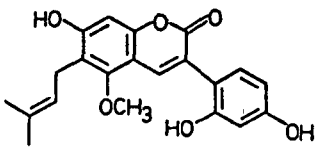

V Glycycoumarin

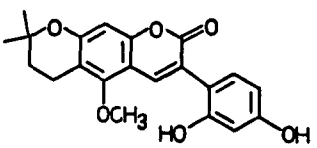

VI Isoglycycoumarin

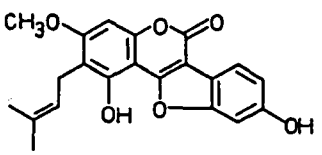

VIII Glycyrol

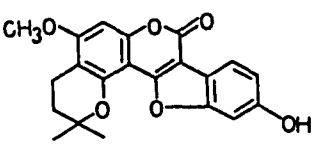

IX Isoglycyrol

Fig. 1. Structures of compounds I–IX. Me = CH_3.

and isoglycyrol (**IX**). These compounds are known to be present in certain *Glycyrrhiza* spp.[4,16–18] and their structures are shown in Fig. 1.

EXPERIMENTAL

Plant material

Glycyrrhiza uralensis Fisch. was collected in Linxian County, Shanxi Province, and purchased from Nei Monggol Autonomous Region (July, 1987), *G. inflata* Bat. in Yianqi County, Xinjiang Autonomous Region (July 1986) and *G. glabra* L. in Hejing County, Xinjiang Autonomous Region (July, 1986). Roots and rhizomes of the above species were used in all analyses. Voucher specimens of the plants and crude drugs are deposited in the drug museum of the Department of Pharmacognosy, School of Pharmaceutical Sciences, Beijing Medical University.

Apparatus

HPLC analysis was carried out using a Varian 5500 instrument with a Varian UV-200 spectrophotometric detector, a Varian 4270 data processor and a Zorbax ODS stainless-steel column (15 cm × 4.6 mm I.D.) (Shimadzu, Kyoto, Japan).

Reagents

Freshly distilled acetonitrile and acetic acid of analytical-reagent grade and freshly distilled water were used for all HPLC analyses. Other solvents were of analytical-reagent grade. The reference compounds used were isolated from licorice root and characterized in our laboratory by spectroscopic methods. Each compound shows a single peak in HPLC. Their melting points are as follows: liquiritin, 213–215°C (lit.[14], 212°C); isoliquiritin, 188–190°C (lit.[15], 187–189°C); liquiritigenin, 203–205°C (lit.[16], 201–203°C); isoliquiritigenin, 198–200°C (lit.[16], 198–200°C); glycycoumarin, 236–238°C (lit.[16], 231–233°C); isoglycycoumarin, 236–237°C (lit.[17], 236–237°C); licochalcone A, 102–103°C (lit.[18], 102°C); glycyrol, 247–249°C (lit.[19], 243–245°C); and isoglycyrol, 301–303°C (lit.[19], 298–300°C).

Chromatographic conditions

The temperature of the column oven was 28–30°C. The programme for the mobile phase, flow-rate and UV detector wavelength is given in Table I.

Analytical procedure

A 100-mg amount of powdered crude drug was weighed into a micro-Soxhlet extractor and refluxed with 10 ml of methanol for 2 h in a water-bath (70°C). The methanolic extract was concentrated at 70°C to less than 3 ml, transferred to a measuring flask and, after cooling to room temperature, was made up to 5 ml with methanol. Volumes of 4–10 μl of this solution were used for HPLC analysis.

RESULTS AND DISCUSSION

Selection of separation system

In order to separate the five flavonoids and four coumarins, we tried a number of columns, *viz.*, MicroPak MCH-5 (15 cm × 4.6 mm I.D.) (Varian), Zorbax ODS (15 cm x 4.6 mm I.D.) (Shimadzu) and μBondapak CN (30 cm × 7.8 mm I.D.)

TABLE I

PROGRAMME FOR MOBILE PHASE COMPOSITION, FLOW-RATE AND UV DETECTOR WAVELENGTH FOR QUANTITATIVE ANALYSIS OF LICORICE ROOT BY HPLC

Time (min)	*Mobile phase (%, v/v)*		*Flow-rate (ml/min)*	*UV detector (nm)*
	3% acetic acid	*Acetonitrile*		
0 (start)	80	20	1.0	310
13.0	↓	↓	↓	365
15.0	50	50	1.2	365
25.0	20	80	1.2	365
30 (stop)	20	80	1.2	365

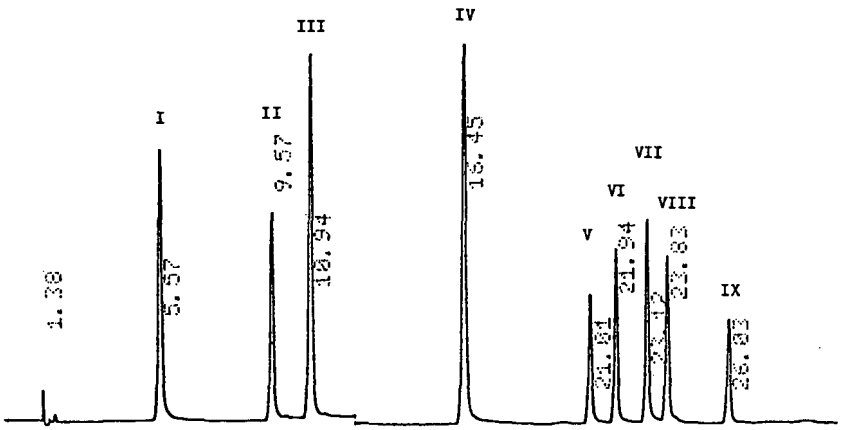

Fig. 2. HPLC of compounds **I–IX**. Numbers at peaks indicate retention times in min.

(Waters Assoc.), and several gradient elution systems, *i.e.*, methanol–water, methanol–water–acetic acid and acetonitrile–3% acetic acid and found that the Zorbax ODS column combined with acetonitrile–3% acetic acid gives the best separation and resolution for all nine compounds in 30 min (Table I and Fig. 2).

Selection of wavelength

The maximum absorption wavelengths (nm) and intensities (log ε) of the nine compounds are as follows: liquiritin, 220 (4.10), 275 (4.00), 312 (3.75); isoliquiritin, 232 (4.20 sh), 362 (4.43); liquiritigenin, 231 (4.33), 275 (4.24), 312 (3.95); isoliquiritigenin, 262 (4.10 sh), 365 (4.45); glycycoumarin, 252 (4.36), 258 (4.30), 352 (4.60); isoglycycoumarin, 253 (4.28), 256 (4.24), 353 (4.48); licochalcone A, 264 (3.79), 304 (3.94), 370 (4.20); glycyrol 231 (4.49), 243 (4.36), 347 (4.42), 353 (4.38 infl.); and isoglycyrol, 224 (4.38 sh), 247 (4.34), 347 (4.40), 363 (4.36 infl.). Further, other substances in licorice can interfere with the detection, such as the coexisting glycyrrhizin-

TABLE II

REGRESSION EQUATIONS AND CORRELATION COEFFICIENTS FOR COMPOUNDS **I** TO **IX**

Function: $y = ax + b$, where y = peak area and x = amount (μg).

Compound	*Regression equation*	*Correlation coefficient*
I	$y = 83.49x + 2.23$	0.9935
II	$y = 155.33x - 1.12$	0.9989
III	$y = 87.29x - 0.23$	0.9979
IV	$y = 685.24x - 0.23$	0.9983
V	$y = 246.32x + 0.47$	0.9969
VI	$y = 269.62x - 0.61$	0.9985
VII	$y = 1586.12x - 0.91$	0.9978
VIII	$y = 313.31x - 1.08$	0.9988
IX	$y = 352.91x - 0.47$	0.9985

ic acid, which shows a retention time close to that of isoliquiritigenin in our analytical system. Considering the above factors, we chose wavelengths of 310 and 365 nm for detection, not only to avoid the interference from glycyrrhizinic acid, which gives a maximum absorption at 248 nm ($\log \varepsilon = 2.16$), but also to make the baseline of the chromatogram smooth. The programme for the mobile phase, flow-rate and UV detector wavelength for the analysis of the above nine compounds is given in Table I.

Linearity and precision

In order to check the linearity of the relationship between amount of compound and peak area using the above separation system, suitable amounts of each of the nine compounds were weighed and mixed in a measuring flask, dissolved and suitably diluted with methanol to serve as a standard solution. Various amounts of the standard solution were injected and chromatographed. The regression equation $y = ax + b$, where x is the amount of compound (μg) and y is the peak area (absorbance $\times 10^{-3}$), and the correlation coefficients of compounds **I–IX** are given in Table II. All the graphs exhibit good linearity and obey Beer's law. The concentration ranges for a linear relationship between amount and peak area are as follows (all 10^{-4} μmol): liquiritin, 2.536–12.68; isoliquiritin, 2.244–11.22; liquiritigenin, 3.203–16.02; isoliquiritigenin, 0.9766–4.883; glycycoumarin, 0.6576–6.576; isoglycycoumarin, 0.8696–13.9; licochalcone A, 0.1746–2.793; glycyrol, 0.7104–11.37; and isoglycyrol, 0.4180–6.667. Volumes of 10 μl of the mixed solution of the nine compounds were chromatographed and the experiments repeated six times. The results showed that the relative standard deviations for the nine compounds were between 1.38 and 3.70%.

Selection of extraction methods

Four methods of extracting the flavonoids and coumarins from licorice root were compared for efficiency. Amounts of 100 mg of the powdered drug were weighed and extracted by one of the following methods: (i) hot reflux with ethyl acetate in a

TABLE III

EFFICIENCY OF DIFFERENT METHODS FOR EXTRACTING COMPOUNDS I–IX FROM *GLYCYRRHIZA URALENSIS* ROOT

Compound	*Amount of compound extracted (%)*			
	Hot ethyl acetate reflux	*Hot ethanol reflux*	*Cold methanol maceration*	*Hot methanol reflux*
I	0.481	0.918	1.016	1.152
II	0.444	0.770	0.843	0.949
III	0.384	0.697	0.666	0.662
IV	0.082	0.120	0.114	0.136
V	0.048	0.048	0.041	0.048
VI	Trace	Trace	Trace	0.002
VII	Trace	Trace	Trace	Trace
VIII	0.016	0.018	0.014	0.019
IX	0.003	0.003	Trace	0.003
Total	0.458	2.574	2.694	2.971

TABLE IV

RECOVERIES OF COMPOUNDS **I–IX** FROM LICORICE ROOT (*GLYCYRRHIZA URALENSIS* FISCH.)

Compound	*Added (mg)*	*Recovered (mg)*	*Recovery (%)*	*Mean recovery ± S.D. (%)*	*Relative standard deviation (%)*
I	1.060	1.055	99.5	96.2 ± 2.96	3.08
	1.590	1.489	93.7		
	2.385	2.278	95.5		
II	0.992	0.998	100.6	99.1 ± 2.86	2.89
	1.488	1.426	95.8		
	2.323	2.252	100.9		
III	0.820	0.827	100.9	99.1 ± 3.06	3.08
	1.230	1.176	95.6		
	1.845	1.862	100.9		
IV	0.250	0.252	100.7	100.3 ± 0.72	0.72
	0.375	0.373	99.5		
	0.563	0.568	100.8		
V	0.386	0.362	93.8	95.6 ± 1.70	1.70
	0.579	0.554	95.7		
	0.869	0845	97.2		
VI	0.512	1.515	100.6	101.7 ± 1.92	1.79
	0.768	0.797	103.8		
	1.152	1.160	100.7		
VII	0.094	0.098	104.1	101.5 ± 4.30	4.24
	0.141	0.136	96.5		
	0.212	0.220	103.8		
VIII	0.416	0.414	99.5	99.4 ± 0.153	0.62
	0.624	0.620	99.4		
	0.936	0.929	99.2		
IX	0.244	0.255	104.5	105.2 ± 0.651	0.62
	0.366	0.385	105.2		
	0.549	0.581	105.8		

TABLE V

CONTENTS OF COMPOUNDS **I–IX** IN THREE SPECIES OF CHINESE LICORICE ROOT (%)

Compound	*G. uralensis*[a]	*G. uralensis*[b]	*G. inflata*	*G. glabra*
I	3.649	1.152	0.593	0.470
II	2.328	0.949	0.508	0.425
III	0.121	0.662	0.032	0.014
IV	0.121	0.136	0.016	0.016
V	0.138	0.048	0.017	0.011
VI	0.018	0.002	0.009	0.005
VII	Trace	Trace	0.138	0.025
VIII	0.044	0.019	Trace	0.008
IX	0.027	0.003	Trace	Trace
Total	6.446	2.971	1.313	0.974

[a] From Shanxi.
[b] From Nei Monggol.

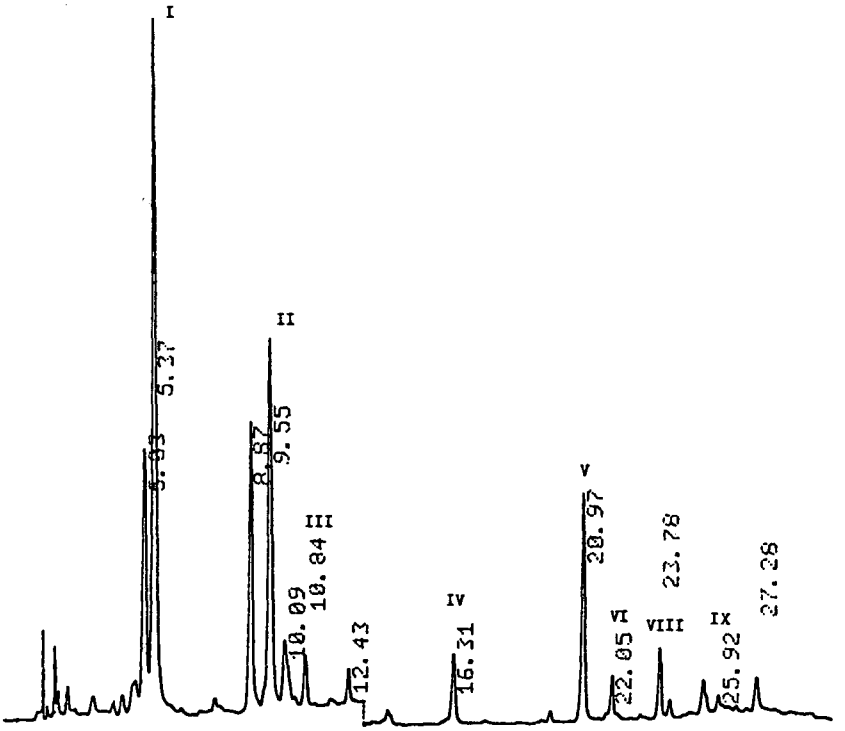

Fig. 3. HPLC of Chinese licorice root (*Glycyrrhiza uralensis* Fisch.). Numbers at peaks indicate retention times in min.

micro-Soxhlet extractor in a water-bath (80°C) for 2 h; (ii) hot reflux with ethanol in a micro-Soxhlet extractor in a water-bath (85°C) for 2 h; (iii) cold maceration with methanol in a stoppered centrifuge tube at room temperature for 24 h and (iv) hot reflux with methanol in a micro-Soxhlet extractor in a water-bath (70°C) for 0.5, 1.0, 1.5 and 2 h. The results showed that method iv (hot reflux with methanol for 2 h) is the best (Table III).

Recovery of compounds ***I–IX***

Suitable amounts of compounds **I–IX** were added to a sample of powdered licorice root with known contents of the nine compounds and the whole was extracted and analysed by the above procedure. The recoveries of the flavonoids and coumarins were 95.6–105.2% with relative standard deviations of 0.62–4.24% (Table IV).

Contents of compounds ***I–IX*** *in licorice root*

In order to demonstrate the validity of this method, the contents of the nine compounds in three species of Chinese licorice root were determined. The peaks were checked by adding a mixed solution of reference compounds to the sample solution before injection. The results are given in Table V. A chromatogram of the extract of *G. uralensis* root is illustrated in Fig. 3.

REFERENCES

1 F. E. Revers, *Ned. Tijdschr. Geneeskd.*, 90 (1946) 135.
2 B. H. Zhang, *Acta Pharm. Sin.*, 10 (1963) 688.
3 W. Watanabe, *Taisha*, 10 (1973) 626.
4 J. Lutomski, *Pharm. Unserer Zeit*, 12 (1983) 49.
5 *Drugs in Japan*, Japan Pharmacetical Information Centre, Tokyo, 9th ed., 1985, p. 12.
6 T. Hatano, H. Kagawa, T. Yashuhara and T. Okuda, *Chem. Pharm. Bull.*, 36 (1988) 2090.
7 P. A. H. Houseman, *J. Assoc. Off. Anal. Chem.*, 36 (1922) 191.
8 Y. Tokino, M. Koshioka, M. Shiokawa, Y. Ishii, S. Maruyama, M. Higashino and T. Hayashi, *Planta Med.*, 36 (1979) 74.
9 T. Vandenhaf, K. W. Glombitza and M. Steiner, *Sci. Pharm.*, 41 (1973) 155.
10 S. Ogawa, A. Yoshida and Y. Mitani, *Yakugaku Zasshi*, 96 (1976) 122 and 1488.
11 Y. Akada and Y. Tanase, *Yakugaku Zasshi*, 96 (1976) 1035.
12 J. Killacky, M. S. F. Ross and T. D. Turner, *Planta Med.*, 30 (1976) 310.
13 K. Okada, J. Tanaka, A. Miyashita and K. Iwoto, *Yakugaku Zasshi*, 101 (1981) 822.
14 J. Shinoda and J. Ueeda, *Yakugaku Zhasshi*, 54 (1934) 1.
15 V. I. Litvinenko, *Dokl. Akad. Nauk SSSR*, 169 (1966) 347.
16 D. Y. Zhu, G. Q. Song and F. X. Jian, *Acta Chim. Sin.*, 42 (1984) 1080.
17 L. Zeng, R. Y. Zhang, D. Wong and Z. C. Lou, *Acta Bot. Sin.*, in press.
18 S. L. Yang and Y. L. Liu, *Acta Bot. Sin.*, 30 (1988) 176.
19 T. Saitoh and S. Shibata, *Chem. Pharm. Bull.*, 17 (1969) 729.

Journal of Chromatography, 513 (1990) 255–262
Elsevier Science Publishers B.V., Amsterdam

CHROM. 22 474

Identification of ferrioxamines by high-performance liquid chromatography and diode-array detection

H.-P. FIEDLER*, J. MEIWES and I. WERNER
Universität Tübingen, Biologisches Institut, LB Mikrobiologie/Antibiotika, Auf der Morgenstelle 28, D-7400 Tübingen (F.R.G.)
and
S. KONETSCHNY-RAPP and G. JUNG
Universität Tübingen, Institut für Organische Chemie, Auf der Morgenstelle 18, D-7400 Tübingen (F.R.G.)
(First received December 18th, 1989; revised manuscript received March 23rd, 1990)

ABSTRACT

High-performance liquid chromatography and diode-array detection were employed for the determination and identification of new ferrioxamines, produced by directed fermentations with *Streptomyces olivaceus* TÜ 2718. Supplementation of the production medium with L-ornithine, 1,6-diaminohexane, bis(2-aminoethyl) ether, S-(2-aminoethyl)-L-cysteine and N-glycyl-1,2-ethylenediamine resulted in the production of thirteen new compounds which were identified during the fermentation process in the culture filtrate by this technique.

INTRODUCTION

Ferrioxamines belong to the group of sideramines, natural iron-chelating compounds, produced in the desferri form by microorganisms[1,2]. Desferrioxamine B, a non-cyclic, positively charged sideramine[3,4], is produced industrially by fermentation of *Streptomyces pilosus* and used medically against a variety of disorders related to iron overload and pathological iron deposition in man and aluminium chelation during dialysis[5]. Desferrioxamine E (Fig. 1) is a cyclic sideramine consisting of three

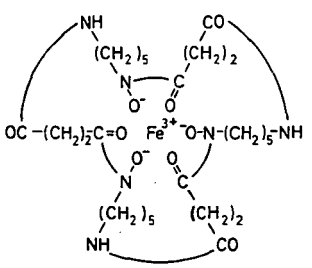

Fig. 1. Ferrioxamine E iron complex.

0021-9673/90/$03.50

units of 5-succinyl-1-amino-5-hydroxyaminopentane, which is derived from L-lysine[6]. The three hydroxamate groups of the molecule are responsible for specific iron chelation. The compound is produced by *Streptomyces olivaceus* TÜ 2718 at a concentration up to 12 g/l in an optimized fermentation process by feeding of L-lysine[7]. This microorganism therefore seemed to be an ideal tool for our studies on the biological derivatization of desferrioxamine E by feeding precursors structurally related to L-lysine. The interpretation of such investigations demands a rapid, selective and sensitive method to identify the newly synthesized compounds during the fermentation process.

As reported previously, high-performance liquid chromatography (HPLC) and diode-array detection represent a highly efficient technique for the classification of structurally related compounds by comparing the UV–VIS spectra of peaks during the HPLC analysis[8–10]. As ferrioxamines show a characteristic maximum in the visible spectrum at 435 nm, it should be possible to detect related compounds directly in the culture filtrate of the fermentation broth of *Streptomyces olivaceus*.

EXPERIMENTAL

Chemicals

Acetonitrile (HPLC grade) and orthophosphoric acid (analytical-reagent grade) were obtained from Merck (Darmstadt, F.R.G.). Water was purified by means of a Milli-Q system (Millipore, Eschborn, F.R.G.).

L-Lysine and L-ornithine were obtained from Deutsche Ajinomoto (Hamburg, F.R.G.), 1,4-diaminobutane and 1,6-diaminohexane from Fluka (Neu-Ulm, F.R.G.) and S-(2-aminoethyl)-L-cysteine from Diamalt (Munich, F.R.G.). Bis(2-aminoethyl) ether was a kind gift from Dow Chemical (Midland, MI, U.S.A.).

Chromatographic system

The chromatographic system consisted of an HP-1090M liquid chromatograph equipped with a diode-array detection system and work station (Hewlett-Packard, Waldbronn, F.R.G.). A detection wavelength of 435 nm with a band width of 10 nm was used.

The column (125 × 4.6 mm I.D.) was fitted with a guard column (20 × 4.6 mm I.D.) and filled with 5-μm Nucleosil-100 C_{18} (Grom, Herrenberg, F.R.G.).

The biological samples were separated by gradient elution. Solvent A was 0.1% phosphoric acid, solvent B was acetonitrile and the linear gradient was from 5 to 25% solvent B in 10 min, with a flow-rate of 2 ml/min.

Sample preparation

A sample of the fermentation broth was centrifuged. The supernatant was diluted with methanol to a ferrioxamine concentration below 2 m*M*. A 5-μl volume of 1 *M* $FeCl_3$ was added to 1 ml of the sample and, after centrifugation, 10 μl of the supernatant were injected automatically onto the column.

RESULTS

The results of the optimization of fermentation conditions for the production of desferrioxamine E and analogues are described elsewhere[7].

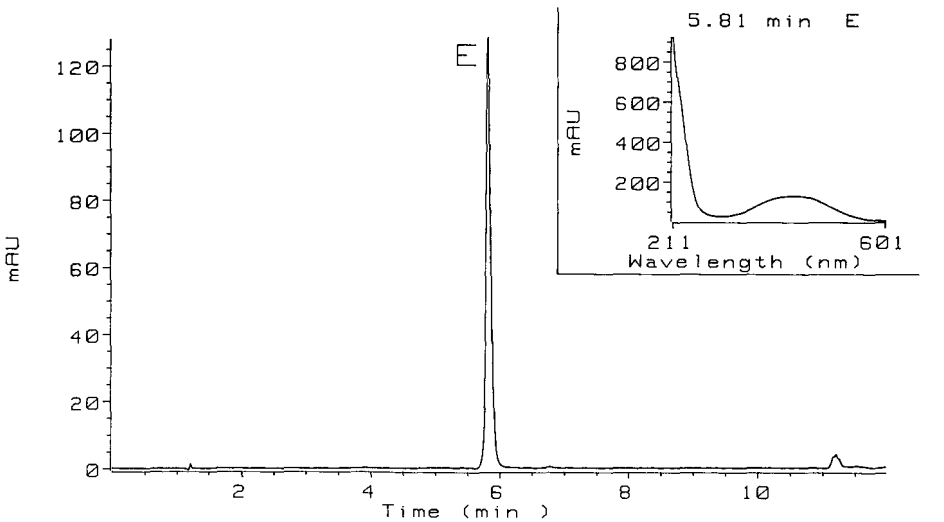

Fig. 2. HPLC of ferrioxamine E (1 mg/ml), plotted at 435 nm, and UV–VIS spectrum, recorded during chromatography of the standard solution.

Fig. 2 shows the HPLC analysis and UV–VIS spectrum of ferrioxamine E. Supplementing the production medium with different analogues (20 m*M*, summarized in Table I) led to the formation of thirteen new desferrioxamines. The new compounds

TABLE I

PRECURSORS FOR BIOLOGICAL PRODUCTION OF FERRIOXAMINE DERIVATIVES BY DIRECTED FERMENTATIONS WITH *STREPTOMYCES OLIVACEUS*

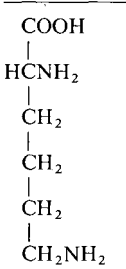	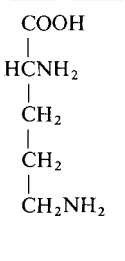	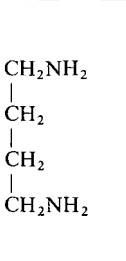	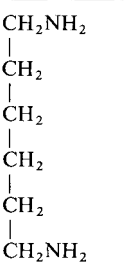
L-Lysine	L-Ornithine	1,4-Diaminobutane	1,6-Diaminohexane
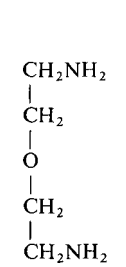	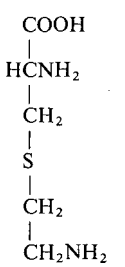	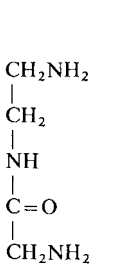	
Bis(2-aminoethyl) ether	S-(2-Aminoethyl)-L-cysteine	N-Glycyl-1,2-ethylenediamine	

were characterized by HPLC and diode-array detection, comparing the retention times and UV–VIS spectra with those of known ferrioxamines.

Supplementation with L-ornithine or 1,4-diaminobutane (putrescine) resulted in the production of four compounds. In addition to the primary products ferrioxamine E and D_2, which have no or one, respectively, exchange of 1,5-diaminopentane with 1,4-diaminobutane, two new ferrioxamines, X_1 and X_2, were produced, having two and three, respectively, exchanges of 1,5-diaminopentane with 1,4-diaminobutane. The HPLC analysis of the culture filtrate and the corresponding UV–VIS spectra of the modified ferrioxamines are shown in Fig. 3.

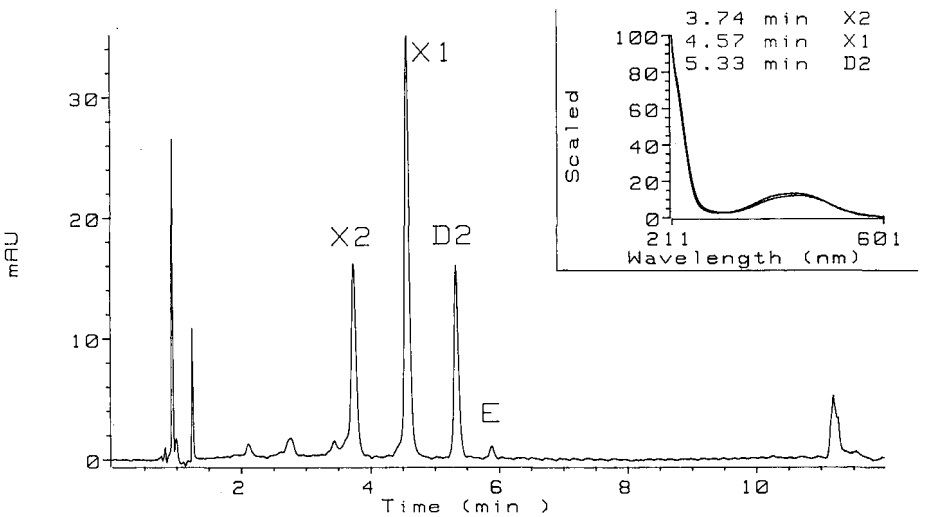

Fig. 3. HPLC of culture filtrate from directed fermentation by supplementation with 1,4-diaminobutane, plotted at 435 nm, and UV–VIS spectra of the produced ferrioxamines X_2, X_1 and D_2.

The supplementation with 1,6-diaminohexane led to four new desferrioxamine analogues. Two of them, ferrioxamine X_4 and X_6, could not be detected directly in the culture filtrate because of their low concentration, but were isolated during downstream processing. HPLC of the culture filtrate and UV–VIS spectra of the new compounds are shown in Fig. 4. The shifted maximum in the visible spectral range of ferrioxamine X_5, which was also found for ferrioxamine X_6, is due to partial hydroxylation of the desferrioxamine molecule. The first hydroxamate group is lacking, and hence iron chelates are formed by the remaining two hydroxamate groups. A desferrioxamine containing three 1,6-diaminohexane molecules was not detected.

In the case of supplementation with bis(2-aminoethyl) ether three new desferrioxamines, Et_1, Et_2 and Et_3, were produced, as could be expected. The compounds differed in their retention times compared with ferrioxamine E but showed identical UV–VIS spectra (Fig. 5).

Addition of S-(2-aminoethyl)-L-cysteine led to incorporation into the sideramine molecule and the production of three new compounds, desferrioxamine Te_1,

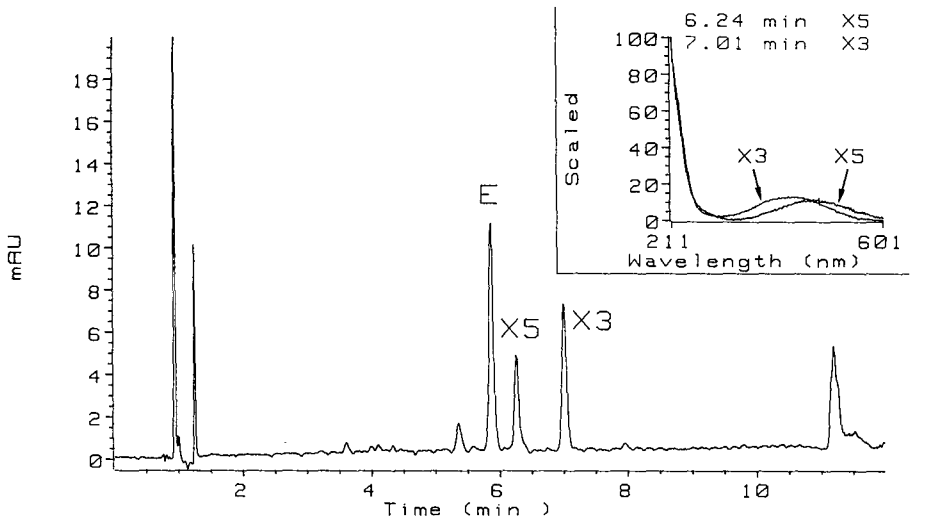

Fig. 4. HPLC of culture filtrate from directed fermentation by supplementation with 1,6-diaminohexane, plotted at 435 nm, and UV–VIS spectra of the produced ferrioxamines X_5 and X_3.

Te_2 and Te_3 (Fig. 6). In contrast to all other investigated ferrioxamines, no baseline separation was achieved.

On supplementing the production medium with N-glycyl-1,2-ethylenediamine, only one desferrioxamine analogue, P_1, could be detected in the culture filtrate and characterized as a new ferrioxamine, as shown in Fig. 7. In ferrioxamine P_1 one

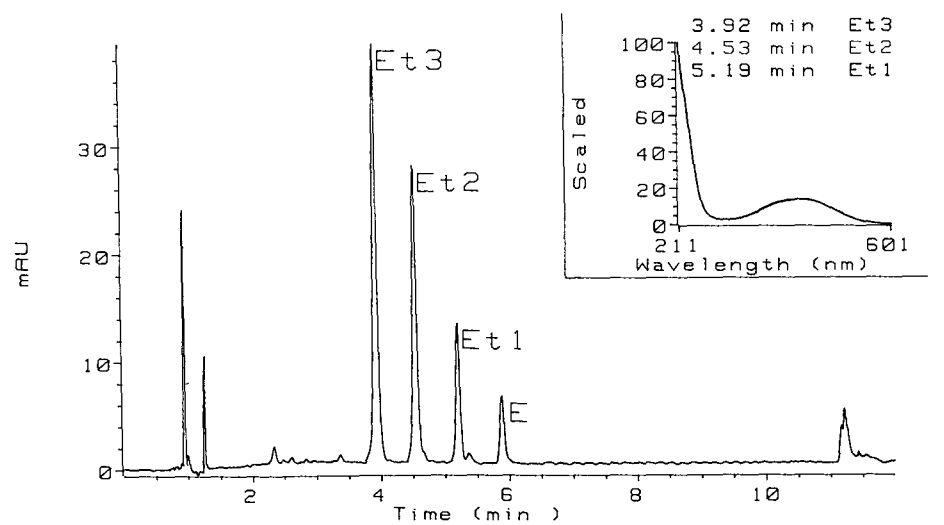

Fig. 5. HPLC of culture filtrate from directed fermentation by supplementation with bis(2-aminoethyl) ether, plotted at 435 nm, and UV–VIS spectra of the produced ferrioxamines Et_3, Et_2 and Et_1.

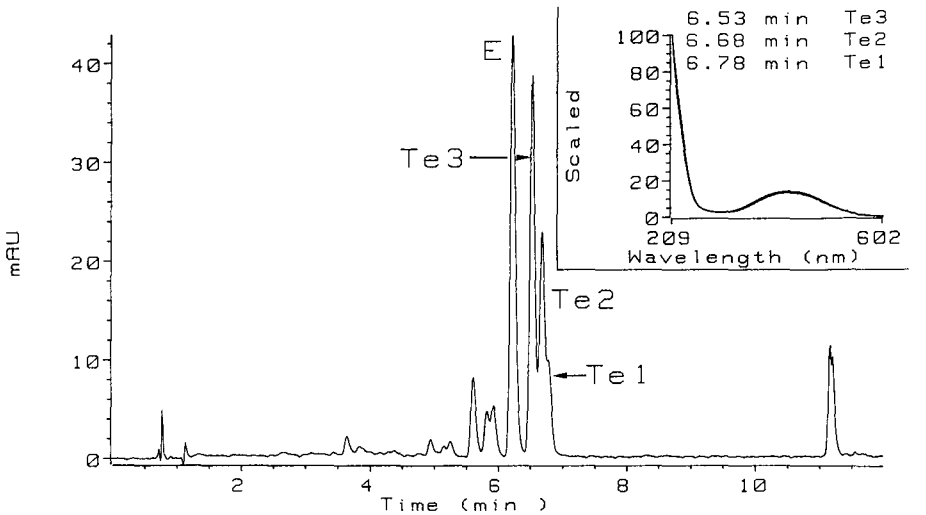

Fig. 6. HPLC of culture filtrate from directed fermentation by supplementation with S-(2-aminoethyl)-L-cysteine, plotted at 435 nm, and UV–VIS spectra of the produced ferrioxamines Te_3, Te_2 and Te_1.

1,5-diaminopentane is substituted by N-glycyl-1,2-ethylenediamine, resulting in an altered retention time of the substance compared with ferrioxamine E.

The isolation and structure elucidation of all the detected new ferrioxamines confirmed the HPLC and spectral data with respect to their identification as new structures[7]. These are summarized in Table II.

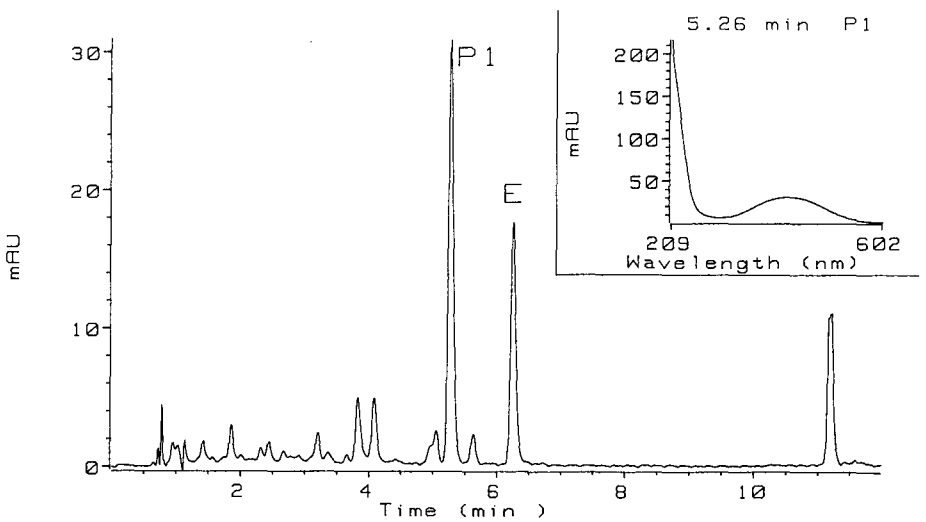

Fig. 7. HPLC of culture filtrate from directed fermentation by supplementation with N-glycyl-1,2-ethylenediamine, plotted at 435 nm, and UV–VIS spectrum of the produced ferrioxamine P_1.

TABLE II

STRUCTURES OF THE CYCLIC DESFERRIOXAMINES PRODUCED BY DIRECTED FERMENTATIONS WITH *STREPTOMYCES OLIVACEUS*

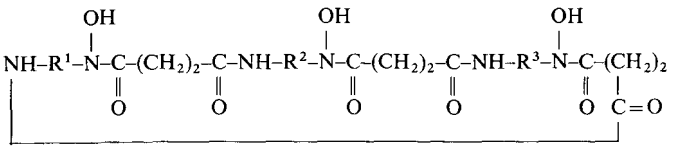

Ferrioxamine	R^1	R^2	R^3
X_2	$(CH_2)_4$	$(CH_2)_4$	$(CH_2)_4$
X_1	$(CH_2)_5$	$(CH_2)_4$	$(CH_2)_4$
D_2	$(CH_2)_5$	$(CH_2)_5$	$(CH_2)_4$
E	$(CH_2)_5$	$(CH_2)_5$	$(CH_2)_5$
X_3	$(CH_2)_6$	$(CH_2)_5$	$(CH_2)_5$
X_4	$(CH_2)_6$	$(CH_2)_6$	$(CH_2)_5$
X_5[a]	$(CH_2)_6$	$(CH_2)_5$	$(CH_2)_5$
X_6[a]	$(CH_2)_6$	$(CH_2)_6$	$(CH_2)_5$
Et_1	$(CH_2)_2$–O–$(CH_2)_2$	$(CH_2)_5$	$(CH_2)_5$
Et_2	$(CH_2)_2$–O–$(CH_2)_2$	$(CH_2)_2$–O–$(CH_2)_2$	$(CH_2)_5$
Et_3	$(CH_2)_2$–O–$(CH_2)_2$	$(CH_2)_2$–O–$(CH_2)_2$	$(CH_2)_2$–O–$(CH_2)_2$
Te_1	$(CH_2)_2$–S–$(CH_2)_2$	$(CH_2)_5$	$(CH_2)_5$
Te_2	$(CH_2)_2$–S–$(CH_2)_2$	$(CH_2)_2$–S–$(CH_2)_2$	$(CH_2)_5$
Te_3	$(CH_2)_2$–S–$(CH_2)_2$	$(CH_2)_2$–S–$(CH_2)_2$	$(CH_2)_2$–S–$(CH_2)_2$
P_1	$(CH_2)_2$–NH–CO–CH_2	$(CH_2)_5$	$(CH_2)_5$

[a] The first hydroxamate moiety is lacking.

CONCLUSIONS

The coupling of HPLC with computer-assisted diode-array detection represents a powerful tool for the identification of structurally related compounds. The comparison of the retention time and UV–VIS spectrum of the primary product, stored in a computer library, with those of compounds produced by altered fermentation conditions, such as directed fermentations, permit a rapid classification of peaks during HPLC analysis. This technique simplifies the interpretation of time-consuming feeding experiments by determining the new product spectrum during the fermentation process.

ACKNOWLEDGEMENTS

This work was supported by the Deutsche Forschungsgemeinschaft (SFB 323) and the Bundesministerium für Forschung und Technologie (BCT 0501 4). J.M. was supported by a Dechema grant and S.K.-R. thanks the Studienstiftung des Deutschen Volkes for a doctoral scholarship.

REFERENCES

1 H. Bickel, E. Gäumann, W. Keller-Schierlein, V. Prelog, E. Vischer, A. Wettstein and H. Zähner, *Experientia*, 16 (1960) 129.
2 W. Keller-Schierlein, V. Prelog and H. Zähner, *Fortschr. Chem. Org. Naturst.*, 22 (1964) 279.
3 H. Bickel, R. Bosshardt, E. Gäumann, P. Reusser, E. Vischer, W. Voser, A. Wettstein and H. Zähner, *Helv. Chim. Acta*, 43 (1960) 2118.
4 H. Bickel, G. E. Hall, W. Keller-Schierlein, V. Prelog, E. Vischer and A. Wettstein, *Helv. Chim. Acta*, 43 (1960) 2129.
5 H. H. Peter, in M. Aksoy and G. F. B. Bindwood (Editors), *Hypertransfusion and Iron Chelation in Thalassaemia*, Huber, Berne, 1985.
6 T. Schupp, C. Toupet and M. Divers, *Gene*, 64 (1988) 179.
7 J. Meiwes, H.-P. Fiedler, H. Zähner, S. Konetschny-Rapp and G. Jung, *Appl. Biotechnol. Microbiol.*, 32 (1990) 505.
8 H.-P. Fiedler, *J. Chromatogr.*, 316 (1984) 487.
9 H.-P. Fiedler, *J. Chromatogr.*, 361 (1986) 432.
10 S. Konetschny-Rapp, H.-G. Huschka, G. Winkelmann and G. Jung, *Biol. Met.*, 1 (1988) 9.

Journal of Chromatography, 513 (1990) 263–269
Elsevier Science Publishers B.V., Amsterdam

CHROM. 22 526

High-performance liquid chromatographic method for the comparison of tanning capacity of tannic acid batches used in the manufacture of pregnancy testing kits

DECLAN J. TURLEY
Organon Technika, Finglas, Dublin 11 (Ireland)
and
MARY T. KELLY and MALCOLM R. SMYTH*
School of Chemical Sciences, Dublin City University, Dublin 9 (Ireland)
(First received May 3rd, 1989; revised manuscript received May 1st, 1990)

ABSTRACT

A high-performance liquid chromatographic (HPLC) method was developed for the quantitative comparison of various batches of tannic acid from the same manufacturer used to aid the binding of human chorionic gonadotropin to sheep erythrocytes in the manufacture of pregnancy testing kits. The tannic acids were separated by reversed-phase HPLC on a C_{18} column using gradient elution with aqueous methanolic eluents at low pH. A portion of the chromatogram corresponding to the compounds involved in the tanninisation process was integrated and a linear relationship was established between this peak area and tannic acid concentration. The correlation coefficient was greater than 0.993 even in the absence of an internal standard. Tanning capacity was evaluated on the basis of the amount of tannic acid which remained following incubation with a known quantity of erythrocytes. The application of this procedure to three batches of tannic acid is demonstrated.

INTRODUCTION

Tannins comprise a heterogeneous group of polyphenols which can combine with skin proteins, *e.g.* gelatin, in such a way as to render them insoluble and resistant to putrefaction. They are of high molecular weight, containing sufficient phenolic hydroxyl groups to permit stable cross-links with proteins. Tannins are nowadays classified as "condensed"[1] or "hydrolysable"[2], depending on their structure. Hydrolysable tannins consist of gallotannins, ellagitannins and caffetannins. Of these, the gallotannins (which are composed of galloyl groups bound to a central polyol by a hydrolysable ester bond) are the most important. Besides the galloyl components, tannin extracts in general contain small amounts of free gallic, digallic and trigallic acids[3,4]. Condensed tannins consist of acacatechin, isoacacatechin and the gambin

0021-9673/90/$03.50

catechin tannins. Of the two classes, the condensed tannins are more widely distributed in higher plants.

Tannic acid is the usual form of tannin used in industry and is obtained by purification of hydrolysable tannins. Tannic acid is widely used in the pharmaceutical industry as an astringent, and in the brewing industry as a clarifier for wine and beer. It has many applications in the chemical industry, including leather tanning, ink compounding, as a reagent in analytical chemistry, and (of particular interest in the present study) as a coupling agent used to bind human chorionic gonadotropin (hCG) to erythrocytes in the manufacture of pregnancy testing kits.

The components of tannic acid have been separated by gel filtration[5], thin layer chromatography[6] and high-performance liquid chromatography (HPLC)[7–11]. Both normal-phase[7,8,11] and reversed-phase[9,10] HPLC techniques have been employed, and in both cases a gradient was required to separate gallic, digallic and trigallic acids from the tannic acid mixture. Quantitative analysis of tannic acids from different commercial sources was carried out by Verzele and Delahaye[8]. The normal-phase HPLC of tannic acid had a regular pattern of about six peaks with a general Gaussian shape pattern. They concluded from this that different sources of tannic acid could be identified on the basis of total peak pattern of the chromatogram and 2,3,4-trihydroxybenzoic acid was proposed as a suitable internal standard. Single peaks obtained by normal-phase HPLC could be further separated into two or three peaks by reversed-phase HPLC with a gradient of methanol–water containing phosphoric acid. Gallic, digallic, trigallic and ellagic acids have also been separated by reversed-phase HPLC[10]. In this case, on ODS column was used with an aqueous methanol mobile phase (adjusted to pH 2.5 with $HClO_4$) operated over a linear gradient ramp.

Tanning capacity (*i.e.* protein precipitating or binding power) is routinely determined by the "hide powder assay" prescribed by the American Leather Chemists Association[12–14]. This method, however, also determines non-tannins in an extract, and therefore gives purity percentages which do not always reflect the real tanning power[15]. As an alternative to the hide powder assay, tanning capacity may be evaluated by binding with bovine serum albumin (BSA), where it is expressed in terms of the number of milligrammes of protein bound to 1 mg of tannic acid[11]. Other methods used to study tannin–protein interactions include complexation with dinitrophenol-derivatised gelatin[16] and ^{125}I-labelled BSA[17]. In general, tanning power is considered to be related to molecular weight (optimum 3000), though it has also been reported that tanning capacity is improved if specific groups in a molecule are sterically well-positioned to permit binding to the protein surface. The latter hypothesis is used to explain the high tanning capacity of some tannic acids despite their low molecular weight.

There are, to date, no reports on the binding of tannic acid to erythrocytes although Schultz *et al.*[18] have described the use of haemoglobin in a quantitative assay for plant tannins. This method was based on the decrease in absorbance of haemoglobin at 578 nm following precipitation with tannins. They found that the tannin-protein binding reaction exhibited co-operativity, in that the first tannin bound facilitated binding of successive tannin molecules. The problem with this technique is that it necessitates the ready availability of large batches of fresh blood, as preserved human blood cannot be used due to the addition of anticoagulants.

The objective of the present study was to develop a suitable analytical method

for the quantitation of tannic acids and to use this method to compare the tanning capacity of new batches of tannic acid in the tanninisation of erythrocytes during the manufacture of pregnancy testing kits. Such a method might obviate the current requirement for expensive, time-consuming and sometimes inconclusive production trials in the quality control screening of new batches of tannic acid.

EXPERIMENTAL

Reagents and solvents

Tannic acid was supplied as pharmaceutical grade by Merck (Darmstadt, F.R.G.). Methanol (HPLC grade) was obtained from Fisons (Loughborough, U.K.). Disodium hydrogen phosphate, potassium dihydrogen phosphate and orthophosphoric acid (AnalaR grade) were purchased from BDH (Dorset, U.K.). Purified water was produced by passing distilled water through a Millipore (Milford, MA, U.S.A.) Milli-Q water purification system. Whole blood from sheep was decanted into an isotonic citrate buffer. The packed cell volume of a representative sample was measured following centrifugation and adjusted to a pre-determined value by addition of more citrate buffer or removal of supernatant as the case demanded. The erythrocytes were then separated, washed with more buffer and stored in isotonic saline under refrigeration until required for use.

Instrumentation and operating conditions

The tannic acids were separated on a Rosil (Alltech, Deerfield, IL, U.S.A.) C_{18} (5-μm) column, 15 × 4.6 cm I.D. Samples were introduced onto the column using a Perkin-Elmer (Beaconsfield, U.K.) Model LC600 autosampler with an injection volume of 10 or 100 μl. Detection was achieved by ultraviolet absorption at 280 nm using a Perkin-Elmer Model LC15 spectrophotometric detector and the resultant chromatograms were recorded using a Perkin-Elmer chart recorder at a chart speed of 5 mm/min. The mobile phase consisted of 0.5% aqueous phosphoric acid (A) and methanol–phosphoric acid [100:0.5, v/v] (B), delivered from a starting concentration of 30% B over a gradient ramp of 2% B per min for a run time of 23 min. The mobile phase components were filtered through a 0.45-μm membrane, degassed by helium sparging, and delivered by a Perkin-Elmer Series 2 dual pump at a flow-rate of 1.5 ml/min.

Procedure

Erythrocytes were tanninised by mixing 5 ml erythrocyte suspension with an equal volume of 1.0% tannic acid in 0.01 *M* phosphate buffer, pH 7.2, and incubating (in a standing position) the suspension at 56°C for 30 min. The supernatant was separated from the erythrocytes by centrifugation at 2000 *g* for 10 min. Erythrocyte-free tannic acid in phosphate buffer, pH 7.2, was treated in the same manner and used as a control.

Standard solutions in the concentration range 0.01–0.07% tannic acid in 0.01 *M* phosphate buffer were prepared for each batch of tannic acid resulting in a separate calibration curve for each new batch. Following incubation of the control and erythrocyte-treated samples, the supernatants were diluted 1 in 20 to bring them into the range of the calibration curve. The total peak area along the chromatogram from

11.5 to 23 min was integrated electronically and plotted as a function of concentration to yield a linear calibration curve. The peak area corresponding to the tannic acid remaining following treatment with erythrocytes was subtracted from the control peak area. The concentration of tannic acid bound to erythrocytes was determined through interpolation of this figure on the calibration curve and tanning capacity was expressed in terms of the percentage of the original concentration added which became bound to the erythrocytes.

RESULTS AND DISCUSSION

Development of chromatography

The chosen starting point was the mobile phase reported by Verzele and Delahaye[8]. A typical chromatogram resulting form this mobile phase programme is shown in Fig. 1A. Shown in Fig. 1B is a typical chromatogram which demonstrates the somewhat improved resolution of the main tannin band achieved with the modified mobile phase as indicated in this figure.

The stability of tannic acid solutions was determined by comparing chromatograms of a fresh 50% (v/v) solution in purified water and the same solution stored at 4-8°C over a 2-week period. Based on the fact that the number and magnitude of peaks remained constant, it was decided that the tannic acid solution was stable under these storage conditions. Tannic acid solutions prepared in buffer were stable for 5 h at room temperature. After this time, the early eluting peaks began to increase in intensity and there was a change in the peak pattern of the main band.

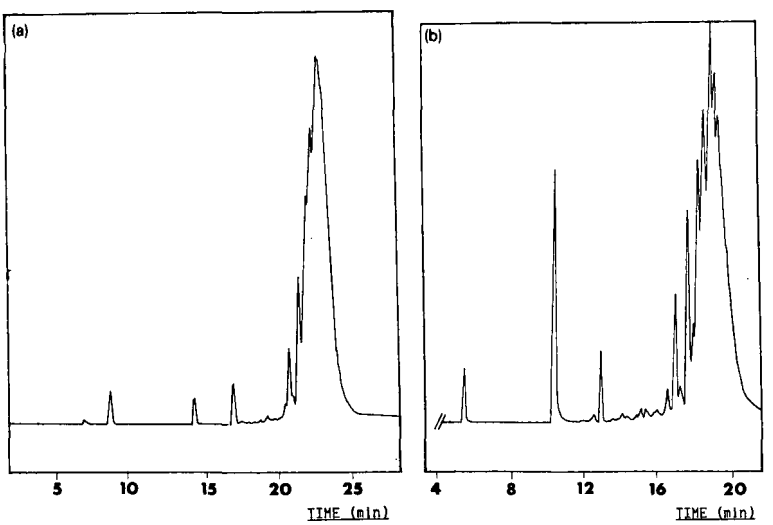

Fig. 1. Typical chromatograms of tannic acid constituents A, before and B, after mobile phase modification. (A) Mobile phase: methanol–water–orthophosphoric acid (10:90:0.5. v/v/v) increasing after 1 min to methanol–orthophosphoric acid (100:0.5, v/v) over a linear gradient ramp of 3% methanol–orthophosphoric acid/min. (B) Mobile phase: methanol–water–orthophosphoric acid (30:70:0.5, v/v/v) increasing after 1 min to methanol–orthophosphoric acid (100:0.5, v/v) over a linear gradient ramp of 2% methanol–orthophosphoric acid/min. Sensitivity = 0.256 a.u.f.s., injection volume = 10 μl, sample = 1 mg/ml tannic acid in purified water.

Selection of a tanninisation procedure

Initially, erythrocytes were tanninised by mixing with 0.01% tannic acid in phosphate buffer, pH 7.2, and incubating the suspension at 56°C for both 10 and 30 min. Following centrifugation, the supernatants of the two incubated suspensions, in addition to a suspension which had not been incubated, were tested for remaining tannic acid. Erytrocyte-free tannic acid solutions (in phosphate buffer, pH 7.2) were subjected to the same treatment and compared with the supernatants. No tannic acid was detected in the supernatant after 10 or 30 min incubation. In the incubated controls there appeared only a small change in the peak pattern along the chromatograms and a slight increase in the height of the early eluting peaks.

Since all of the 0.01% tannic acid solution had become bound to the erythrocytes after 10 min incubation, it was decided to increase the concentration of tannic acid to establish at what point it would be in excess of the erythrocytes binding sites. 0.1, 0.15, 0.18, 0.2, 0.25, 0.5 and 1.0% solutions of tannic acid were investigated and it was found that with the 0.5% solution, 12% (as compared with the corresponding erythrocyte-free control) remained after incubation, and that almost 60% remained using the 1% tannic acid solution. In order to allow for batch-to-batch variations of greater than 12% in tannic acid, it was decided to use the 1.0% solution in all subsequent tannisation procedures. Chromatograms of 1% tannic acid solutions following 30 min incubation both with and without erythrocytes are presented in Fig. 2.

Verzele and Delahaye[8] found that (i) high molecular weight polygalloyl glucose

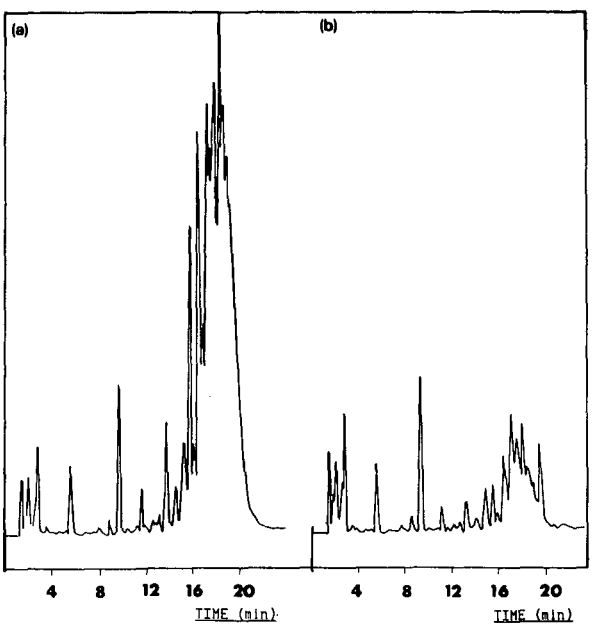

Fig. 2. Typical chromatograms of tannic acid constituents after incubation, A, with erythrocytes and B without erythrocytes. A = Control tannic acid; B = Erythrocyte-treated sample. Mobile Phase = methanol–water–orthophosphoric acid (30:70:0.5, v/v/v) increasing to methanol–orthophosphoric acid (100:0.5, v/v) over a linear gradient ramp of 2% methanol–orthophosphoric acid/min.

constituents preferentially bound to BSA, (ii) that low-molecular-weight polygalloyl glucose components bound preferentially to beer proteins, and (iii) that gallic acid and its oligomers, di- and tri-gallic acid, have no tanning capacity under these circumstances. In the present work it was found that all polygalloyl glucose constituents complexed with erythrocytes during tanninisation, since all peaks in the main peak pattern of the chromatogram reduced proportionally during tanninisation. Therefore, the total area of this band was used as measure of tanning capacity. The early peaks, corresponding to low-molecular-weight gallic acid-type consitituents, and which have no tanning capacity, were subtracted from the total area of the chromatogram. Furthermore, following processing, it was found that there was greater variation in the peak areas of the early-eluting peaks than in the main band within a given batch of tannic acid. Peak area integration was, therefore, commenced at 11.5 min following injection.

Evaluation of tanning capacity of three tannic acid batches

Quantitative measurements were based on the difference in tannin concentrations after tanninisation of erythrocytes compared to tannic acid control solutions which were subjected to the same incubation conditions. It was found that the chosen internal standard, 2,4,6-trihydroxybenzoic acid, co-eluted with the early eluting peaks, so attempts were made to extract the constituents responsible for these peaks since they are known not to partake in the tanninisation process. Peak removal was attempted using a cation exchanger but this approach resulted in a reduction of the peaks of interest as well as the interfering peaks. It was decided, therefore, to proceed with the analysis without an internal standard, and even under these circumstances there is a linear relationship between peak area and concentration with a correlation coefficient greater than 0.993. The correlation coefficients were compared for the total peak area in the chromatogram and for the corrected peak area, *i.e.*, the area of analytical interest along the chromatogram. There was no significant change in correlation when the corrected (as opposed to the total) peak area was integrated. The three batches tested had tanning capacities of 62%, 68% and 80% respectively. The 80% value was yielded by a batch manufactured in 1985 and the other two were manufactured in 1981. This suggests a fall-off in tanning capacity with time, though further investigations to confirm these findings have not yet been concluded.

CONCLUSION

Reversed-phase HPLC can be used to determine the reduction in tannic acids by incubation with erythrocytes. Using the described method, it was found that there appeared to be a decrease with time in the concentration of pollygalloyl constituents which are responsible for the tanninisation process. Potentially, this method can be used in the quality control screening of batches for the binding of antigens to erythrocytes.

REFERENCES

1 E. Haslam, *Chemistry of Vegetable Tannins,* Academic Press, London, 1966, p. 10.
2 M. Metche, *Tannins, Nature et Properties, Bulletin de Liasion nr. 10,* Groupe Polyphenols, Neuchatel, 1980.

3 M. Verzele, P. Delahaye and J. Van Dyck, *Bull. Soc. Chim. Belges*, 93 (1983) 181.
4 M. Verzele, A. De Bruyn, F. Van Damme and P. Delahaye, *Bull. Soc. Chim. Belges*, 92 (1983) 469.
5 H. C. G. King and G. Pruden, *J. Chromatogr.*, 52 (1970) 285.
6 E. P. Kemertelidze, P. A. Yavich, A. G. Sarabunovich, L. T. Churadze, M. I. Khechumashvili, G. E. Elerdashvili and D. D. Dolidze, *Farmatsiya (Moscow)*, 33 (1984) 34; *Anal. Abstr.*, 47 (1985) 248.
7 P. Delahaye and M. Verzele, *J. Chromatogr.*, 265 (1983) 363.
8 M. Verzele and P. Delahaye, *J. Chromatogr.*, 268 (1983) 469.
9 G. Belleau and M. Dadic, *J. Am. Soc. Brew.*, 37 (1979) 175.
10 M. H. Salagoity-Auguste, C. Tricard, F. Marsal and P. Sudraud, *Am. J. Enol. Vitic.*, 37 (1986) 301.
11 M. Verzele, P. Delahaye and F. J. Van Damme, *J. Chromatogr.*, 362 (1986) 363.
12 American Leather Chemists Association, Subcommittee report, *J. Am. Leather Chem. Assoc.*, 51 (1956) 353.
13 C. Gordon-Gray, *J. Soc. Leather Trades Chem.*, 61 (1957) 269.
14 D. Roux, *J. Soc. Leather Trades Chem.*, 61 (1957) 275.
15 T. Beasley, H. Ziegler and A. Bell, *Anal. Chem.*, 49 (1977) 238.
16 J. Van Buren and W. Robinson, *J. Agric. Food Chem.*, 17 (1969) 773.
17 A. Hagerman and L. Butler, *J. Agric. Food Chem.*, 28 (1980) 945.
18 J. C. Schultz, I. T. Baldwin and P. J. Nothagle, *J. Agric. Food Chem.*, 29 (1981) 823.

Journal of Chromatography, 513 (1990) 271–278
Elsevier Science Publishers B.V., Amsterdam

CHROM. 22 520

Applications of gel filtration chromatography for resole phenolic resins using aqueous sodium hydroxide as solvent

TERRY SELLERS, Jr.* and M. LYNN PREWITT

Mississippi Forest Products Utilization Laboratory, Mississippi State University, P.O. Drawer FP, Mississippi State, MS 39762 (U.S.A.)

(First received November 1st, 1989; revised manuscript received April 24th, 1990)

ABSTRACT

Suggested applications are demonstrated for a gel filtration technique previously described with a suitable gel packing material (Sephacryl) for the analysis of phenol–formaldehyde resins (resoles) and phenolic-like compounds. An alkaline solution was used as eluent which saved preparation time for the alkaline resole resins. Sodium polystyrene sulphonates were used as standards. Several chromatographic systems were used to study the phenolic resins which are typically used to bond wood composite panels including plywood, hardboard, oriented strandboard and waferboard. The studies focused on commercial and laboratory resins, formulation process variables, freeze-dried and liquid treatments of resins, varying gel packing materials, various end-use type resins, lignin-modified phenolic polymers, and lignin raw materials. The system is suitable for characterizing the molecular weight of resoles and as a quality control tool.

INTRODUCTION

Size-exclusion chromatography (SEC), such as gel filtration chromatography (GFC) and gel permeation chromatography (GPC), is a useful technique for the analysis of macromolecules. The technique is a type of chromatography that separates molecules according to molecular size. Gels of very narrow sieve fractions (approximately 5–40 μm) are used as stationary phase. The chromatograph of such a system reveals a fingerprint of the molecular weight distribution of a resin. In this article, GFC refers to aqueous SEC at less than 1 atm (1 kPa); whereas, systems using higher pressures in non-aqueous solvents are referred to as GPC.

In the U.S.A., where phenol–formaldehyde (PF) resins consume over 35% of the phenol produced, resole-type PF resins are the preferred binder for structural wood composites[1,2]. While some chromatography data have been reported about molecular weights for resoles used by the wood industry[3–7], faster methods would be more practical for a quality control tool.

Efforts to develop more accurate and faster chromatographic techniques for

0021-9673/90/$03.50

phenolic resins have been ongoing since the instrumentation has been developed. Many polymers such as resole phenolic resins are not totally soluble in common GPC solvents such as N,N-dimethylformamide (DMF) and tetrahydrofuran (THF), and altering the polymers' solubility changes their hydrodynamic volume and behaviors in GPC systems[6,8]. Precipitating or drying the resoles causes the molecular weight to increase and solvation in such solvents as THF to decrease[6]. Acetylation of resole resins in THF did not eliminate all artifacts associated with dissolving the high-molecular-weight fractions in some studies[6]. However, artifacts of high-molecular-weight groups in phenolic resins on Merckogel Si were reported eliminated by acetylation of these groups or by the addition of lithium chloride to the mobile phase (DMF)[9]. But acetylation procedures for a phenolic resin sample take about 24 h and such time-consuming techniques do not facilitate speedy monitoring of resin production or quality control.

The development of suitable chromatography systems that use an alkaline solution as eluent, which is the medium of the alkaline resoles (*ca.* 10% caustic solids in phenol–formaldehyde wood binders), would provide a faster method for characterizing resins and serve as a quicker quality control tool when compared to current GPC methods. The time saved is related to the preparation time (5 min) and not the analytical separating flow-rate (30 to 60 min). This article summarizes some applications of just such a system.

EXPERIMENTAL

GFC system

The GFC system used in this study has been previously reported[10] and may be summarized as follows: A peristaltic pump was connected to a Pharmacia preparative or an analytical chromatographic column with two adapters. The columns contained Sephadex G-100 or Sephacryl S-200 (HR). The eluent was 0.10 *M* sodium hydroxide. Blue dextran was used to determine the exclusion volume and phenol was used to determine the permeated volume. A standardization curve was produced by using sodium polystyrene sulphonate (SPS) standards (Polymers Labs.). Because of the low polydispersities, the standards M_p (peak molecular weights) were considered weight-average molecular weights (M_w) in the standardization calculations. The column was connected to an ultraviolet detector with a 280-nm filter and interfaced with a chromatographic data acquisition system. Resin samples (25 μl) were injected onto the column using a low-pressure injector valve. The sample preparation consisted of 0.1 g of resin diluted to 10 ml with 0.1 *M* sodium hydroxide. Chromatographs were produced on a graphics plotter. Tabular molecular weight data were generated by the Nelson Chromatograph GPC software.

High-pressure GPC system

A high-pressure GPC system used for comparison is described as follows: Waters Assoc. Model 510 solvent delivery system, Model U6K injector, Model 481 Lambda-Max UV spectrophotometer, and calculations on Waters Assoc. software using commercial polystyrene molecular weight standards. The separation was performed on a Polymer Laboratory 60 cm × 1 cm mixed gel of 10 μm, a mobile phase of mainly DMF, a flow-rate of 1 ml/min, an injection volume of 25 μl, a sample

preparation of 0.1 g of resin in 3 drops of water added to 5 ml of mobile phase and a run time of 31 min.

RESULTS AND DISCUSSION

Table I shows the molecular weight distribution of three commercial phenolic resins used to bond plywood, hardboard and oriented strandboard wood composites. The chromatographs for these resins are shown in Fig. 1. The plywood resin (A) has the highest $\bar{M}_w$ average (11 237), followed by the dry-process hardboard resin (B) (3903 $\bar{M}_w$) and the oriented strandboard resin (C) (1574 $\bar{M}_w$). In terms of distribution, the plywood resin has over 40% above 10 000 $\bar{M}_w$ and less than 5% below 2000 $\bar{M}_w$; the hardboard resin has 11% above 10 000 $\bar{M}_w$ and over 50% below 2000 $\bar{M}_w$; and the OSB resin has less than 2% above 10 000 $\bar{M}_w$ and over 70% below 2000 $\bar{M}_w$ (with over 50% below 1000 $\bar{M}_w$).

As shown in Fig. 2, resoles used to make similar wood composite products are diverse in molecular weight. This diversity is dictated by the resin raw materials, composite process, wood species and the end use (exterior *vs.* interior) of the wood composite products. In this hardboard case, the wet process depends heavily on precipitating of the phenolic resin solids prior to final cure and the dry process depends on accelerated condensation at immediate high temperatures.

Most PF resin types have molecular weights below 18 000. However, column packing material should be able to accommodate the higher ranges (*ca.* 35 000 $\bar{M}_w$) of molecular weight distribution such as occurs in North American plywood PF resins.

TABLE I

COMPARISON OF GFC MOLECULAR WEIGHT DISTRIBUTION (AREA PERCENT) OF THREE LIQUID COMMERCIAL RESOLE RESINS USED TO BOND WOOD COMPOSITES

M_w = weight-average molecular weight; M_n = number-average molecular weight.

Molecular weight range	*Area percent*[a,b]		
	OSB (C)	*Hardboard (B)*	*Plywood (A)*
>35 000	0.0(0.0)	0.3(0.3)	0.4(0.4)
35 000–18 000	0.3(0.3)	5.7(6.0)	25.9(26.3)
18 000–10 000	1.3(1.6)	5.1(11.1)	16.0(42.3)
10 000–5000	5.1(6.7)	6.5(17.6)	14.6(56.9)
5000–3000	8.0(14.7)	12.3(29.9)	23.6(80.5)
3000–2000	8.7(23.4)	13.8(43.7)	15.3(95.8)
2000–100	18.8(42.2)	19.8(63.5)	3.9(99.7)
1000–500	20.0(62.2)	17.4(80.9)	0.3(100.0)
500–100	37.8(100.0)	19.1(100.0)	0.0(100.0)
$\bar{M}_w$	1574	3904	11237
$\bar{M}_n$	343	769	5079
$\bar{M}_w/\bar{M}_n$	4.58	5.07	2.21

[a] The results were obtained using Sephacryl S-200 HR and were based on sodium polystyrene sulphonate standards. The area percent values in this table correlate to the letters in Fig. 1 with (C) oriented strandboard (OSB), (B) dry-process hardboard and (A) plywood-type phenolics.

[b] The numbers in parentheses represent accumulations.

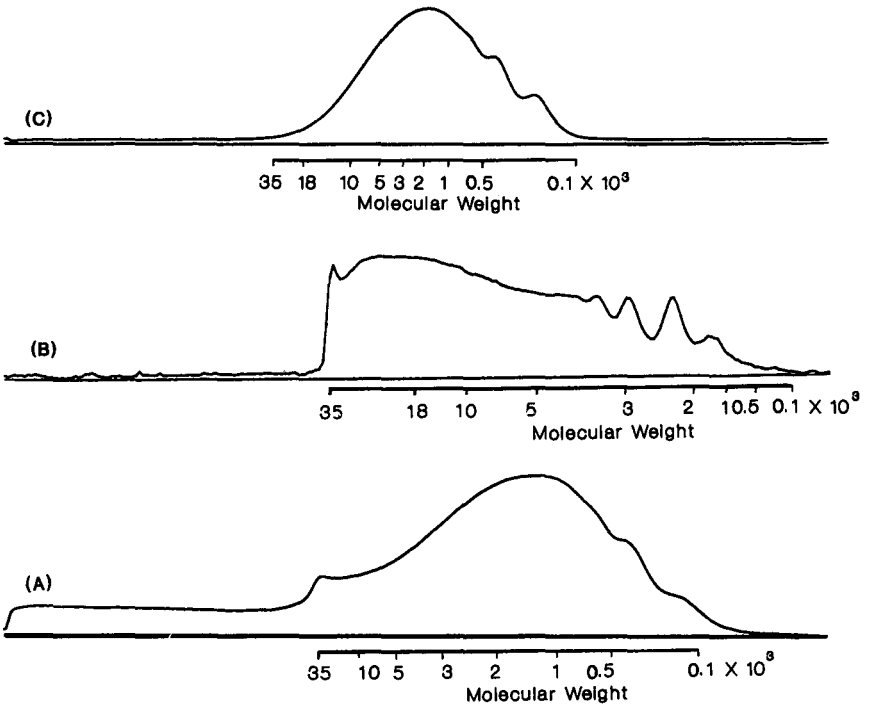

Fig. 1. Chromatographs of GFC molecular weight of three commercial phenolic resins used to bond wood composites. (A) Plywood; (B) dry-process hardboard; (C) Oriented strandboard. (See Table I).

Fig. 3 compares chromatographs using Sephadex G-100 and Sephacryl S-200 HR for a single commercial oriented strandboard PF resin (results exclude urea content). While providing a higher molecular weight range for delineation than Sephadex, Sephacryl also enhances the percent of the area within the 2000–5000 $\bar{M}_w$ range. However, above Sephadex's upper limit, the reaction of higher molecular weight

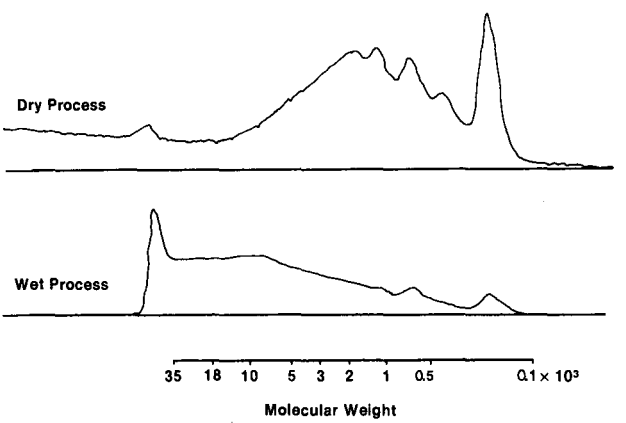

Fig. 2. Chromatographs of GFC molecular weight of two commercial resoles used to bond hardboard manufactured by two different processes.

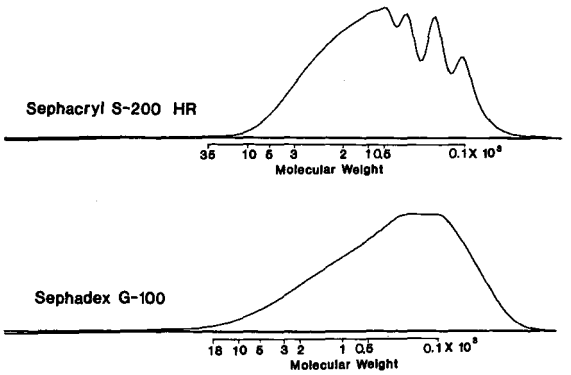

Fig. 3. Chromatographs of GFC molecular weight for an oriented strandboard phenolic resin using Sephadex G-100 and Sephacryl S-200 HR column packing materials (SPS standards).

materials in plywood resoles is unknown, although higher standards (35 000 $\bar{M}_p$ SPS) are available for comparison (Table I). Therefore, Sephacryl S-200 HR is the gel of preference in this GFC system.

One use of GFC is to examine the progression of a phenolic resin synthesis during the cook compared to the final finished form (Table II). This application is particularly useful when formulation changes are made such as adding a two-charge sodium hydroxide catalyst instead of a single-charge caustic catalyst to plywood-type phenolic formulations[11,12].

Comparisons of typical high pressure GPC results to the GFC data obtained in

TABLE II

MOLECULAR WEIGHT DISTRIBUTION OF PLYWOOD-TYPE PHENOLIC RESIN SAMPLES TAKEN AT SEVEN POINTS DURING THE COOK AND AT THE END OF THE COOK

Molecular weight range	*Area percent by sample number*[a]							
	1	*2*	*3*	*4*	*5*	*6*	*7*	*8*[b]
>35 000	0.0	0.0	0.0	0.0	0.3	0.5	1.0	0.0
35 000–18 000	0.0	0.0	0.1	0.2	0.2	0.3	0.4	2.2
18 000–10 000	0.0	0.1	0.7	1.6	2.9	3.9	4.3	5.9
10 000–5000	0.0	0.8	2.6	5.0	6.0	6.7	7.6	8.7
5000–3000	0.0	6.4	11.2	13.6	14.9	16.2	16.5	16.6
3000–2000	1.2	13.9	16.4	17.3	17.2	17.0	16.5	16.2
2000–1000	7.0	20.6	20.1	19.3	18.4	17.7	16.8	16.1
1000–500	17.2	20.5	18.1	16.3	15.2	14.5	14.0	13.2
500–100	74.6	37.7	30.8	26.7	24.9	23.2	22.9	21.2
$\bar{M}_w$	406	1166	1722	1997	2640	3622	6610	7174
$\bar{M}_n$	225	417	492	555	589	620	625	675
$\bar{M}/\bar{M}_n$	1.80	2.79	3.50	3.59	4.48	5.84	10.57	10.62

[a] The analyses are based on sodium polystyrene sulphonate standards and using Sephacryl S-200 HR.

[b] Sample No. 8 is the finished resin.

this work are shown in Figs. 4 and 5. While both methods provide qualitative and semi-quantitative data relative to any series of tests, it is thought that greater association of organic solvents with phenolic methoxy groups yield higher molecular weight values in the GPC method compared to the GFC method.

Phenolics are "living polymers" that are constantly changing toward gelation and decreasing in stability with increasing time and temperature. In the U.S.A., a plywood phenolic resin may increase from 600 to 2000 mPa · s (cP) in two weeks at 25°C. Due to these changes, the essence of physical characteristics of these synthetic resins over time is difficult to capture, even with experimental precautions. GFC offers an opportunity to observe or monitor changes which occur with alterations in conditions. Freeze-drying may offer an opportunity to protect the integrity of the GFC data on sample retains of PF resins for periods of up to six months or more (Table III).

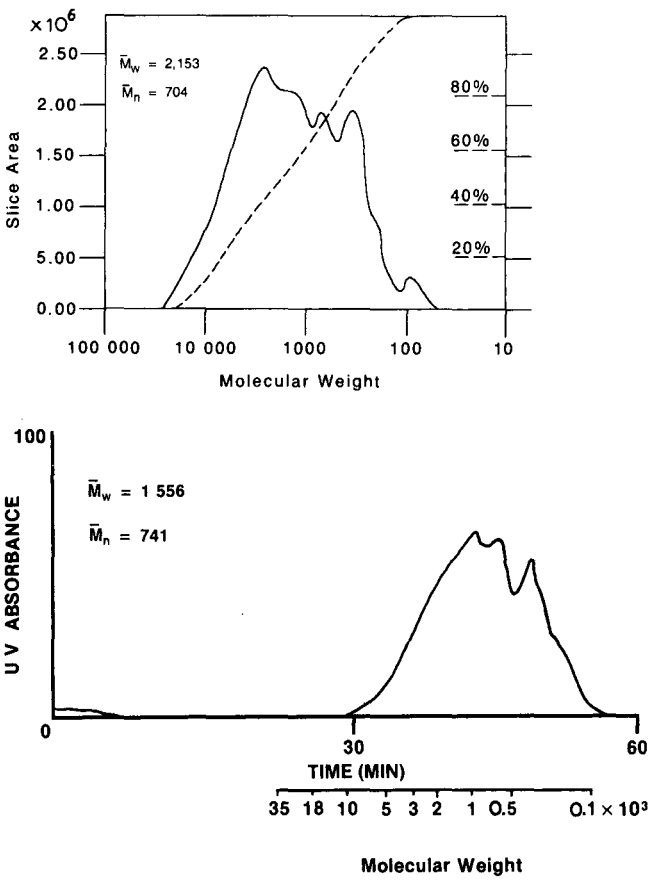

Fig. 4. Chromatographs of a flakeboard phenolic resin using high-pressure GPC (upper) and GFC (lower).

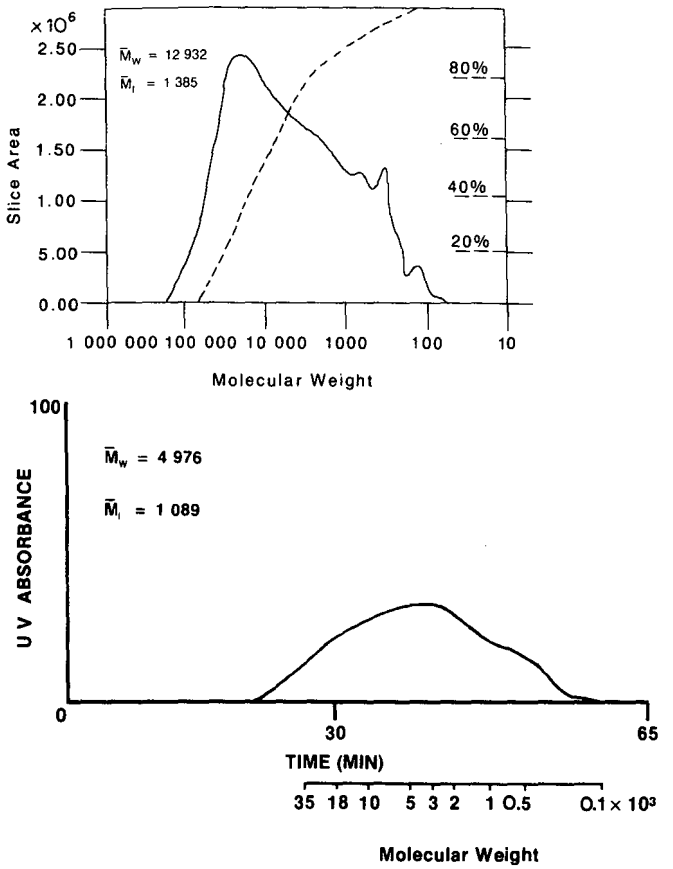

Fig. 5. Chromatographs of a plywood phenolic resin using high-pressure GPC (upper) and GFC (lower).

TABLE III

COMPARISON OF MOLECULAR WEIGHT DISTRIBUTION OF A PHENOLIC RESIN BEFORE AND AFTER FREEZE-DRYING USING SEPHACRYL S-200 HR COLUMN-PACKING MATERIAL

Molecular weight range	*Area percent*[a]	
	Before	After
>35 000	0.3(0.3)	0.1(0.1)
35 000–18 000	5.9(6.2)	3.8(3.9)
18 000–10 000	6.0(12.2)	5.4(9.3)
10 000–5000	7.6(19.8)	7.8(17.1)
5000–3000	12.9(32.7)	12.9(30.0)
3000–2000	12.7(45.4)	12.8(42.8)
2000–1000	16.8(62.2)	17.0(59.8)
1000–500	14.6(76.8)	17.0(76.8)
500–100	23.2(100.0)	23.2(100.0)
$\bar{M}_w$	4075	3397
$\bar{M}_n$	670	716
$\bar{M}_w/\bar{M}_n$	6.08	4.74

[a] The numbers in parentheses represent accumulations.

CONCLUSIONS

The GFC technique developed in this work showed usefulness in many applications analyzing the PF resins and phenolic-like compounds as manufactured with a minimal alteration of their molecular structures. The procedure uses aqueous sodium hydroxide as solvent reducing resin preparation time by not requiring acetylation or conversion to a non-aqueous solvent system. Having relative GFC data over time for various types of common phenolic-like polymers allowed comparative evaluation of similar resins and potential raw material extenders. The technique described in this study can be used to characterize resoles with a wide range of molecular weight (low and high) and to serve as a quality control tool. Eventually correlation of $\bar{M}_w$ data of resins to end-use performance of bonded wood composites is a likely goal[13–16].

ACKNOWLEDGEMENTS

Financial support from the U.S. Department of Agriculture Wood Utilization Research Grant Program and the Mississippi Forest Products Utilization Laboratory is gratefully acknowledged.

REFERENCES

1 *Chem. Eng. News*, 25 (1988) 42.
2 G. E. Myers, *Adhesive Age*, 11 (1988) 31–36.
3 R. C. Vasishth, F. E. Schwarz and S. Y. Leong, *Spectrovisions*, No. 20, Perkin-Elmer, Norwalk, CT, 1968, pp. 4–7.
4 J. E. Armonas, *For. Prod. J.*, 7 (1970) 22–23.
5 J. B. Wilson, G. L. Jay and R. L. Krahmer, *Adhesive Age*, 22 (1979) 26–30.
6 J. D. Wellons and L. Gollob, *Wood Sci.*, 2 (1980) 68–74.
7 B. Riedl, L. Calve and L. Blanchette, *Holzforschung*, 42 (1988) 315–318.
8 A. Rudin, C. Fyfe and S. M. Vines, *J. Appl. Polym. Sci.*, 28 (1983) 2611–2622.
9 G. Schulz, R. Gnauck and G. Ziebarth, *Paste Kautsch.*, 29 (1982) 398–401.
10 A. L. Wooten, M. L. Prewitt, T. Sellers, Jr. and D. C. Teller, *J. Chromatogr.*, 445 (1988) 371–376.
11 E. R. Wagner and R. J. Greff, *J. Polym. Sci., Part A-1*, 9 (1971) 2193–2207.
12 Jack Cazes and Nina Martin, *Proc. Wash. State Univ. Symp. Particleboard*, 10 (1977) 209–222.
13 L. Gollob, *Wood Adhesives: Chemistry and Technology*, Vol. 2, Marcel Dekker, New York, 1989, pp. 121–153.
14 P. M. Tahir, *M. Sci. Thesis*, Mississippi State University, Mississippi State, MS, 1989; on file: Mississippi Forest Products Laboratory.
15 T. Sellers, Jr., A. L. Wooten and P. M. Cook, *Structural Wood Composites: New Technologies for Expanding Markets, Symp. Proc., No. 47359* Forest Products Research Society, Madison, WI, 1988, pp. 43–50.
16 L. Jin, T. Sellers, Jr., T. P. Schultz and D. D. Nicholas, *Holzforschung*, 44 (1990) 207–210.

Journal of Chromatography, 513 (1990) 279–295
Elsevier Science Publishers B.V., Amsterdam

CHROM. 22 441

Separation and determination of lipophilic corticosteroids and benzothiazepin analogues by micellar electrokinetic chromatography using bile salts

HIROYUKI NISHI*, TSUKASA FUKUYAMA and MASAAKI MATSUO

Analytical Chemistry Research Laboratory, Tanabe Seiyaku, Co., Ltd., 16–89, Kashima 3-chome, Yodogawa-ku, Osaka 532 (Japan)

and

SHIGERU TERABE

Department of Industrial Chemistry, Faculty of Engineering, Kyoto University, Sakyo-ku, Kyoto 606 (Japan)

(First received September 26th, 1989; revised manuscript received February 22nd, 1990)

ABSTRACT

The separation of corticosteroids and benzothiazepin analogues by micellar electrokinetic chromatography (micellar EKC) was studied in comparison with capillary zone electrophoresis. The separation of these substances was not succesful under neutral and alkaline conditions because they migrated with the same velocity as that of the electroosmotic flow. Micellar EKC with sodium dodecyl sulphate (SDS) solutions was also not successful because these substances migrated with almost the same velocity as that of the SDS micelle, owing to their high lipophilicity. The use of bile salts, which have a similar skeleton to corticosteroids, as the micellar phase permitted the separation of these substances with high theoretical plate numbers (150 000–350 000) within a short time (*ca.* 15 min). Sodium cholate was particularly useful. The effects of bile salt concentration, pH and the addition of methanol were investigated. Micellar EKC was also applied to the determination of the drug substances in tablets and cream using the internal standard method and to purity testing of drug substances and tablets.

INTRODUCTION

Micellar electrokinetic chromatography (micellar EKC) is a type of liquid chromatography based on micellar solubilization and the instrumental technique of capillary zone electrophoresis (CZE)[1,2]. CZE has been shown to be a very powerful separation technique for ionic and biological substances[3,4]. Although CZE separation can be applied only to ionic species, owing to the separation mechanism involved, micellar EKC permits the separation of neutral substances[5–7] because its separation principle is the same as that of chromatography.

0021-9673/90/$03.50

The greatest advantage of this technique is its capability to separate neutral substances. In addition, selectivity and peak shapes can be much improved with this technique for some ionic substances[8–13] in comparison with CZE because of the presence of the micellar phase.

The determination of antibiotics in plasma by micellar EKC was reported by Nakagawa and co-workers[14,15] using a direct sample injection method. According to their method, pretreatment of the plasma sample was not necessary because the plasma proteins, which can interfere with drug analysis, were solubilized by the micelles and hence eluted later than the drugs. The use of surfactants in high-performance liquid chromatography (HPLC) was established by Armstrong and Terrill[16] as micellar chromatography, in which serum or plasma is injected directly without any pretreatment[17].

Chiral separation by micellar EKC was also successful, using chiral surfactants such as bile salts[18,19] or mixed micelles[20], in which chiral additives are solubilized into the micelle. In the former method, the chiral separation was achieved with chiral micelles alone without any metals that form chelate complexes.

Recently, Bushey and Jorgenson[21] reported the separation of dansylated methylamine and dansylated trideuteromethylamine by micellar EKC. The closely related isotopic compounds were also successfully separated under the optimum conditions by CZE[22]. These results show that ultra-high resolution can be obtained by micellar EKC or CZE.

Application of CZE and micellar EKC to the separation of water-soluble substances has been well studied recently[8–13,23–26]. However, few papers have considered the separation of lipophilic substances. These non-ionic solutes cannot be separated by CZE owing to its separation principle, or by micellar EKC using sodium dodecyl sulphate (SDS) because of the strong solubilization effect of the micelle, that is, such solutes migrate with almost the same migration time as that of the micelle. The utility of micellar EKC for the separation of hydrophobic substances has only recently begun to be explored. The use of organic modifiers in the operating buffer solution has been reported to be effective for the separation of such compounds[27,28].

This paper concerns the separation of corticosteroids and benzothiazepin analogues, which are relatively lipophilic, by micellar EKC with bile salts. Bile salts seem to have a relatively small solubilization effect compared with SDS micelles from the smaller micelle–water partition coefficients for 1-pentanol and 1-heptanol than those of SDS[29]. We would expect some characteristic solubilization effect from the structures of bile salts similar to those of corticosteroids. The effects of the pH of the buffer, organic modifier content and surfactant concentrations were studied and the separation mechanism is discussed with respect to the structures of four bile salts. The application of this technique to the determination of drug substances in commercial preparations by the internal standard method and the purity testing of drug substances and tablets are also described. The results obtained are compared with those obtained by HPLC.

EXPERIMENTAL

Apparatus and procedure for micellar EKC

Micellar EKC was performed with the same apparatus as described previous-

ly[12]. A fused-silica capillary tube (650 mm × 50 μm I.D.) (Scientific Glass Engineering, Ringwood, Victoria, Australia) was used as a separation tube. A d.c. voltage was applied between the two ends of the tube through platinum electrodes dipped into the buffer solution in the reservoirs with a Model HJLL-25PO high-voltage d.c. power supply (Matsusada Precision Devices, Kusatsu, Shiga, Japan), which delivered up to +25 kV. The electric current was monitored between the negative electrode and the negative terminal of the power supply with an ammeter throughout the operation. Migrating solute bands were detected by the on-column measurement of UV absorption (210 or 220 nm) across the axis of the tube at a position 150 mm from the negative end with a Uvidec-100-VI (Jasco, Tokyo, Japan). A Chromatopac C-R2AX (Shimadzu, Kyoto, Japan) was used for data processing. Sample solution was injected by siphoning from the positive end into the fused-silica tube filled with the buffer solution in advance. Micellar EKC was carried out at ambient temperature (*ca.* 25°C). Regarding the reproducibility of the system, the coefficients of variation of the migration times of the solutes with repeated injections (n = 5–7) were within 1% from run to run and within 3% from day to day in micellar EKC.

Reagents

Hydrocortisone, triamcinolone, betamethasone, hydrocortisone acetate, dexamethasone acetate, triamcinolone acetonide, fluocinolone acetonide and fluocinonide were obtained from Sigma (St. Louis, MO, U.S.A.). Fourteen benzothiazepin analogues (diltiazem and its derivatives and metabolites) were obtained from our laboratory (Tanabe Seiyaku, Osaka, Japan). These test samples are listed with their structures in Tables I and II. Sample 1 in Table II is diltiazem, which is a calcium antagonist with coronary vasodilatory activity[30]. All samples were used as received and dissolved in methanol at a concentration of *ca.* 0.5–1 mg/ml to give adequate peak heights in the study of the separation. Several kinds of diltiazem hydrochloride and its tablets from different companies were used as samples for the purity testing. Diltiazem tablets (Herbessor) and fluocinonide cream (Topsym) (Tanabe Seiyaku) were used for the analysis of commercial preparations.

Sodium dodecyl sulphate (SDS) from Nacalai Tesque (Kyoto, Japan) and sodium cholate (SC), sodium taurocholate (STC), sodium deoxycholate (SDC) and sodium dehydrocholate (SDHC) from Tokyo Kasei Kogyo (Tokyo, Japan) were used as anionic surfactants. Sudan III from Nacalai Tesque was used as a tracer of the micelle[2]. These were dissolved in a buffer solution prepared by mixing 0.02 *M* sodium dihydrogenphosphate solution with 0.02 *M* sodium tetraborate solution to give appropriate pH values. These solutions were filtered through a 0.45-μm membrane filter prior to use. All other chemicals and solvents were of analytical-reagent grade from Katayama Kagaku Kogyo (Osaka, Japan).

Procedure for purity testing

About 0.03 g of diltiazem hydrochloride was weighed and dissolved in 20 ml of methanol. The solution was used as the sample solution. Diltiazem tablets were ground and the resulting powder was weighed in an amount approximately equivalent to 0.03 g of diltiazem according to the label claim and placed in a test-tube, then 20 ml of methanol were added for extraction. The tube was warmed in a water-bath at *ca.* 40°C

TABLE I

CORTICOSTEROIDS

Hydrocortisone

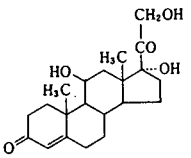

Triamcinolone

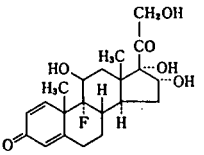

Betamethasone

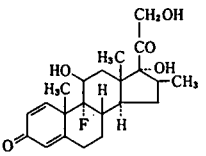

Hydrocortisone acetate

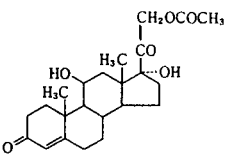

Dexamethasone acetate

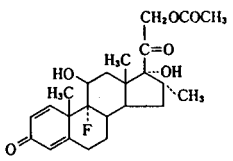

Triamcinolone acetonide

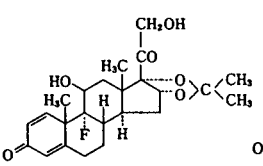

Fluocinolone acetonide

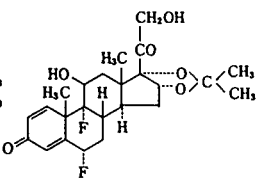

Fluocinonide

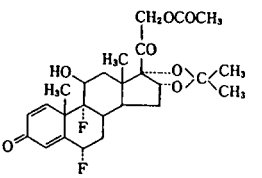

Symbol	*Name*	*Symbol*	*Name*
a	Hydrocortisone	e	Dexamethasone acetate
b	Triamcinolone	f	Triamcinolone acetonide
c	Betamethasone	g	Fluocinolone acetonide
d	Hydrocortisone acetate	h	Fluocinonide

TABLE II

DILTIAZEM AND ITS RELATED COMPOUNDS

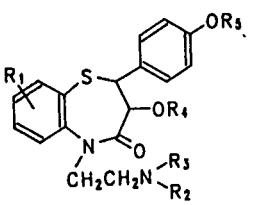

No.	R_1	R_2	R_3	R_4	R_5
1	H	CH_3	CH_3	$COCH_3$	CH_3
2	H	CH_3	CH_3	H	CH_3
3	H	H	CH_3	H	CH_3
4	H	CH_3	CH_3	H	H
5	H	H	CH_3	H	H
6	H	(NH[a]	−)	$COCH_3$	CH_3
7	Cl	CH_3	CH_3	$COCH_3$	CH_3
8	Cl	H	CH_3	H	CH_3
9	Cl	H	H	$COCH_3$	CH_3
10	Cl	CH_3	CH_3	H	H
11	Cl	(NH[a]	−)	$COCH_3$	CH_3
12	H	CH_3	CH_3	Aromatic[b]	CH_3

[a] Des-$CH_2CH_2NR_2R_3$ form (thiazepin form).

[b] Substituted benzoyl.

for 10 min with occasional shaking, then cooled. The solution was filtered through a membrane filter (0.45 μm) and used as the sample solution. The peak areas of the substances obtained from each solution were measured with the data processor and the content of impurities was determined by the area percentage method.

Procedure for determination of drug substances in products

Ten diltiazem tablets (Herbessor, 30-mg tablets) were weighed and ground. One tenth of the powder was weighed accurately into a 50-ml volumetric flask and 30 ml of methanol were added for extraction. The flask was warmed in a water-bath at *ca.* 40°C for 10 min with occasional shaking, then cooled. Internal standard solution (exactly 10 ml), which was prepared by dissolving 0.3 g of diltiazem derivative (sample 7 in Table II) in 100 ml of acetonitrile, was added and then sufficient water was added to the flask to make 50 ml. This solution was filtered and used as the sample solution. Authentic diltiazem (*ca.* 0.03 g) was weighed accurately into a 50-ml volumetric flask and exactly 10 ml of internal standard solution were added and then sufficient water to make 50 ml. This solution was used as the standard solution.

About 1 g of fluocinonide cream was weighed accurately into a test-tube and 5 ml of methanol and 5 ml of internal standard solution, which was prepared by dissolving 0.02 g of diltiazem derivative (sample 11 in Table II) in 100 ml of methanol, were added. The tube was then warmed at *ca.* 40°C for 5 min. After cooling, this methanol solution was filtered with a membrane filter (0.45 μm) and 0.1 ml of water was added to 1.0 ml of this filtrate. This solution was filtered again with a membrane filter (0.45 μm) and used as the sample solution. Authentic fluocinonide (about 5 mg) was weighed accurately and dissolved in exact 50 ml of methanol. Exactly 5 ml of this solution were combined with exactly 5 ml of internal standard solution and 1 ml of water. This solution was used as the standard solution.

The sample solution and the standard solution were introduced into the capillary tube by siphoning (about 10 cm height, 10 s) for micellar EKC analysis. The injection volume in the system was of the order of 1 nl[12]. The ratios of the peak area of each ingredient to that of the internal standard were measured with the data processor and the content of each ingredient in a tablet or cream was calculated.

Procedure for capillary washing

To maintain good peak shapes and reproducible retention data, the capillary tube was flushed with the working buffer solution from a manually operated syringe for 1 min each time after a sample solution had been injected. The tube was washed according to the following procedure each time when the solution was replaced: the capillary was flushed with water for *ca.* 1 min, then swept with 0.1 *M* potassium hydroxide solution and allowed to stand for *ca.* 30 min, flushed with water again until the eluted solution showed neutral using a pH test paper and finally filled with the working solution and allowed to stand for at least 30 min before operation.

RESULTS AND DISCUSSION

CZE separation and micellar EKC with SDS solutions

Corticosteroids are very lipophilic and are not soluble in water, hence the octanol–water partition coefficients are infinity. Benzothiazepin analogues (diltiazem

and related compounds) are soluble in water in their salt forms, however. Their octanol–water partition coefficients change in accordance with the pH values of aqueous solutions and are also infinity under neutral and alkaline conditions because their pK_a values are around 7. Corticosteroids are electrically neutral in the range pH 7–9, and consequently they migrated with almost the same velocity as the electroosmotic velocity, which was evaluated from the migration time of methanol[2], with very broad and tailing peaks in the CZE mode using pH 7–9 buffer solutions. Diltiazem analogues also eluted with around the migration time of the electroosmotic flow with very broad and tailing peaks in the CZE mode using pH 7–9 buffer solutions.

As micellar EKC has been applied successfully to the separation of electrically neutral or non-ionic compounds[5–7], we tried to separate these corticosteroids and diltiazem-related compounds by micellar EKC with SDS solutions. The solutes migrated with almost the same migration time as that of Sudan III with 0.05–0.1 *M* SDS at pH 7–9. This result shows that these solutes are almost totally solubilized by the SDS micelle, because Sudan III is considered to be a marker of the micelle[2]. The separation of these solutes was slightly improved by decreasing the SDS concentration to 0.01–0.02 *M*, but the peaks were very broad and showed tailing as in CZE separation. These results may indicate that adsorption of these solutes on the capillary wall occurs in the absence of SDS or at low SDS concentrations.

The use of organic modifiers in the operating solutions has been reported to be effective for the separation of such compounds by reducing the capacity factors[28]. However, addition of organic modifiers results in long migration times owing to a decrease in electroosmotic flow and selectivity is not much improved.

Micellar EKC with bile salts

Bile salts, which have a skeleton similar to that of corticosteroids, are biological surfactants synthesized in the liver. They form small aggregates because of the bulky structure of the monomer. The structures of the bile salts used are shown in Table III with critical micellar concentrations (CMC)[31]. Three (or two) hydroxyl groups at the 3α-, (7α-) and 11α-positions of bile salts are all oriented in the same direction, nearly perpendicular to the steroidal frame, and consequently the bile salts have both a hydrophilic and a hydrophobic face in the molecule. Therefore, the bile salt molecules tend to combine with each other at the hydrophobic face in an aqueous phase, as shown diagrammatically in Fig. 1[32]. Hence bile salts are considered to form a primary micelle with up to ten monomers.

Micellar EKC was performed with buffer solutions of pH 9.0 containing bile salts. First, a mixture of seven alkyl *p*-hydroxybenzoates (see Fig. 2) was injected to examine the power of micellar solubilization. These solutes migrated with almost identical velocities and coeluted at *ca.* 7 min in CZE at pH 9.0. However, micellar EKC using 0.05 *M* SDS or N-lauroyl-N-methyltaurate permitted a successful separation[12]. Micellar EKC using bile salts was also successful except for sodium dehydrocholate (SDHC). A typical electropherogram of seven alkyl *p*-hydroxybenzoates in CZE and chromatograms obtained by employing sodium cholate (SC) and sodium deoxycholate (SDC) are shown in Fig. 2. The elution pattern of these solutes in SDHC was almost the same as that of the electropherogram in CZE, indicating that SDHC has no effect on micellar solubilization or does not form micelles, although it has been reported that SDHC has a capability for inclusion complex formation with various organic solvents[33].

TABLE III

STRUCTURE OF BILE SALTS

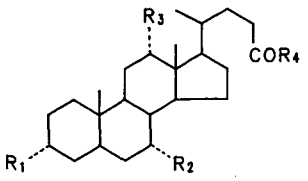

Bile salt	*Abbreviation*	R_1	R_2	R_3	R_4	*CMC (mM)*	N^a
Sodium cholate	SC	OH	OH	OH	ONa	12.5	3
Sodium taurocholate	STC	OH	OH	OH	$NHCH_2CH_2SO_3Na$	4.0	3.5
Sodium deoxycholate	SDC	OH	H	OH	ONa	6.4	14
Sodium dehydrocholate	SDHC	=O	=O	=O	ONa	–	–

[a] Aggregation number.

In general, the migration time varies in a regular and predictable fashion with repeated substitution of a group in a sample molecule. Often the capacity factor will depend linearly on the number of repeating groups. This relationship is well known as Martin's rule in chromatography. In micellar EKC, the capacity factor is given by[1]

$$\tilde{k}' = \frac{t_R - t_0}{t_0(1 - t_R/t_{mc})} \tag{1}$$

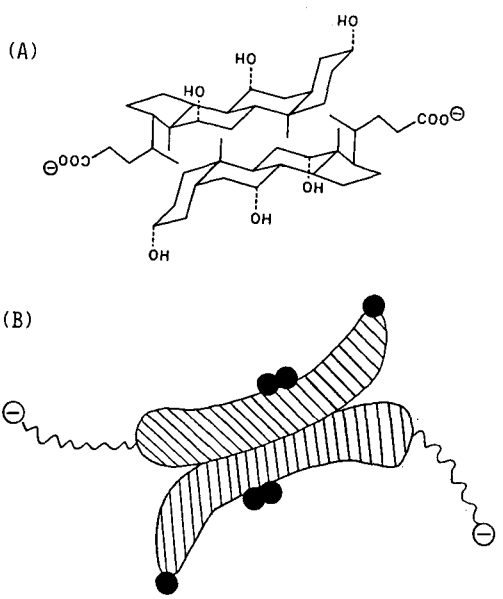

Fig. 1. (A) A possible structure and (B) its diagrammatic representation of a two-molecular aggregate of sodium cholate in aqueous solution. The hydroxy groups are representated by the filled circles and the carboxylate groups by the open circles.

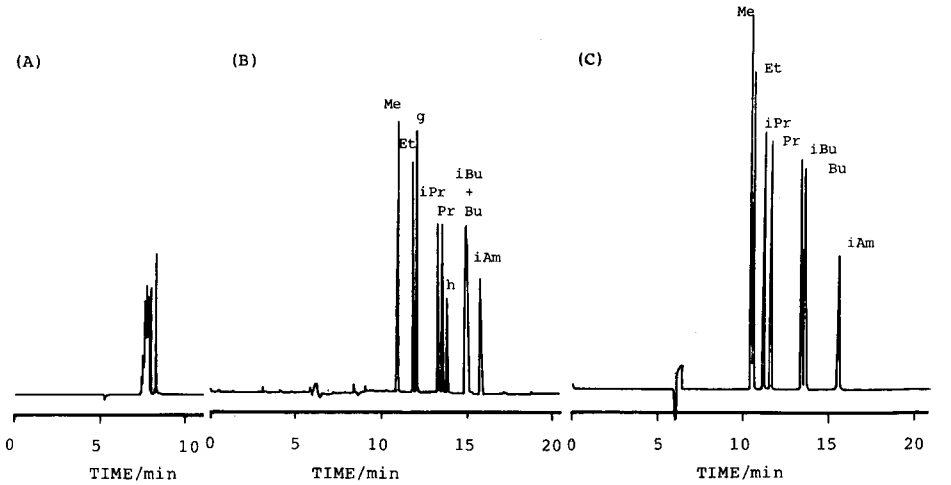

Fig. 2. (A) Separation of seven alkyl *p*-hydroxybenzoates by CZE with a 0.02 *M* phosphate–borate buffer solution (pH 9.0), and separation of those with fluocinolone acetonide (g) and fluocinonide (h) by micellar EKC with (B) 0.1 *M* sodium cholate (pH 9.0) and with (C) 0.05 *M* sodium deoxycholate (pH 9.0). Me, methyl; Et, ethyl; iPr, isopropyl; Pr, *n*-propyl; iBu, isobutyl; Bu, *n*-butyl; iAm, isoamyl *p*-hydroxybenzoate. Applied voltage, 20 kV.

where t_0, t_R and t_{mc} are the migration times of an unincorporated solute, the solute and the micelle, respectively.

The $\tilde{k}'$ values of seven alkyl *p*-hydroxybenzoates were calculated according to this equation from the data shown in Fig. 2, where these esters and samples g and h are separated by micellar EKC with 0.1 *M* SC solution of pH 9.0. The plots of log $\tilde{k}'$ versus *n* (carbon number of the alcohol part in alkyl *p*-hydroxybenzoates) are approximately

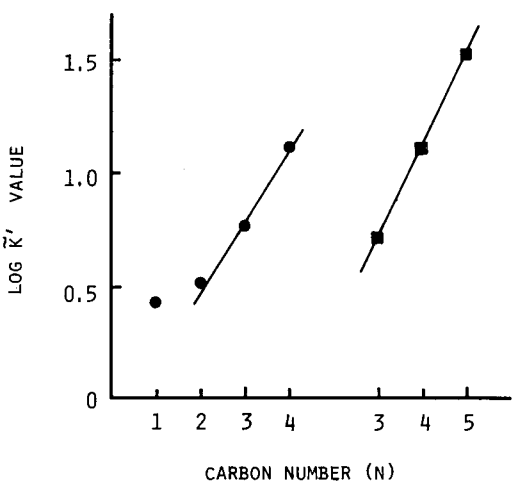

Fig. 3. Dependence of log $\tilde{k}'$ on the carbon number (*n*) of the alcohol part of alkyl *p*-hydroxybenzoates in micellar EKC with sodium cholate. Conditions as given in Fig. 2B. ●, Me, Et, Pr and Bu; ■, iPr, iBu and iAm.

linear, as shown in Fig. 3, except for $n = 1$. This indicates that partition or interaction between the solutes and the micelle in micellar EKC employing bile salts follows a retention mechanism similar to that in reversed-phase HPLC.

From the results, corticosteroids and diltiazem-related compounds were analysed by micellar EKC with SC, sodium taurocholate (STC) and SDC solutions. Typical chromatograms are shown in Fig. 4. The solutes were successfully separated within *ca.* 15 min by use of bile salts in comparison with CZE or micellar EKC with SDS solutions. The theoretical plates numbers calculated from the equation[34]

$$N = 2\pi(t_R h/A)^2 \quad (2)$$

where t_R, h and A are migration time, peak height and peak area, respectively, were 200 000–350 000.

The relative migration order observed in Fig. 4 almost follows the lipophilicity of the solutes. Among corticosteroids, the solutes which have the foundamental steroid structure, that is, having no ester structure at the hydroxy group on the C-21 position and having no acetonide structure at the hydroxy groups on the C-16 and C-17 positions (samples a, b and c in Table I) eluted first, followed by the acetate type (d and e), the acetonide type (f and g) and finally fluocinonide, which has both acetate and acetonide structures. The lipophilicity of corticosteroids also increases in the order mentioned above. For diltiazem-related compounds, elution of the solutes follows in the order diltiazem analogues (samples 1–6), their chlorinated derivatives (7–11) and

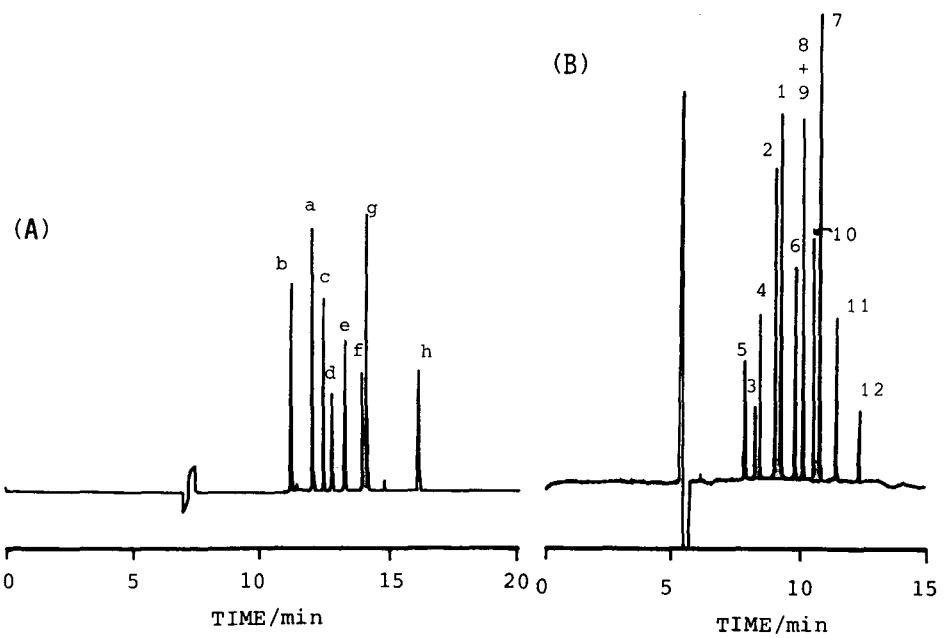

Fig. 4. Typical chromatograms of (A) eight corticosteroids and (B) twelve benzothiazepin analogues. Conditions: buffer, 0.02 *M* phosphate–borate (pH 9.0) containing (A) 0.1 *M* sodium cholate and (B) 0.05 *M* sodium taurocholate; applied voltage, 20 kV; temperature, ambient; detection wavelength, 210 nm. Solutes are given in Tables I and II.

substituted benzoyl compound (12). Samples 2–5 are metabolites of diltiazem (1) and samples 8–10 are metabolites of its chlorinated compound (7). These metabolites migrated faster than their original compounds because of an increase of hydrophilicity.

Micellar EKC with 0.05 *M* SDC solution (pH 9.0) was also performed and typical chromatograms are shown in Fig. 5. The migration pattern of corticosteroids is almost the same as that in 0.1 *M* SC shown in Fig. 4, except for sample f. For sample b, the migration time was shorter than for other samples over the all bile salts and the elution order was altered by the bile salt concentrations, as mentioned later. The separation of twelve benzothiazepin analogues by use of SDC was not successful. Six diltiazem analogues and five chlorinated analogues were eluted as groups of incompletely resolved peaks even at pH 9.0 (Fig. 5B). From these results, we selected SC or STC as the surfactant for micellar EKC in the following experiments.

Among four bile salts, SDHC had no effect on solubilization of the solutes. SDC, in contrast, had the greatest solubilization effect, although the selectivity decreased in comparison with SC and STC. No distinct difference in the migration of the solutes was observed between SC and STC, between which only the ionic groups are different. The effect of ionic interaction observed in the separation of ionic solutes by micellar EKC[12,13,35] did not contribute to the migration of the solutes, because the solutes are electrically neutral. The structural difference in the steroidal part between SDC and SC or STC is only in one hydroxyl group (see Table III); the hydroxyl group at the C-7 position in SC or STC is replaced with a hydrogen atom in SDC. The solubilization effect of SDC seems to be much increased by this substitution from the data on the effect of surfactant concentration on the migration times of the solutes (see below). The reported CMC of SDC is smaller than that of SC[31]. This supports the observation of stronger solubilization of SDC.

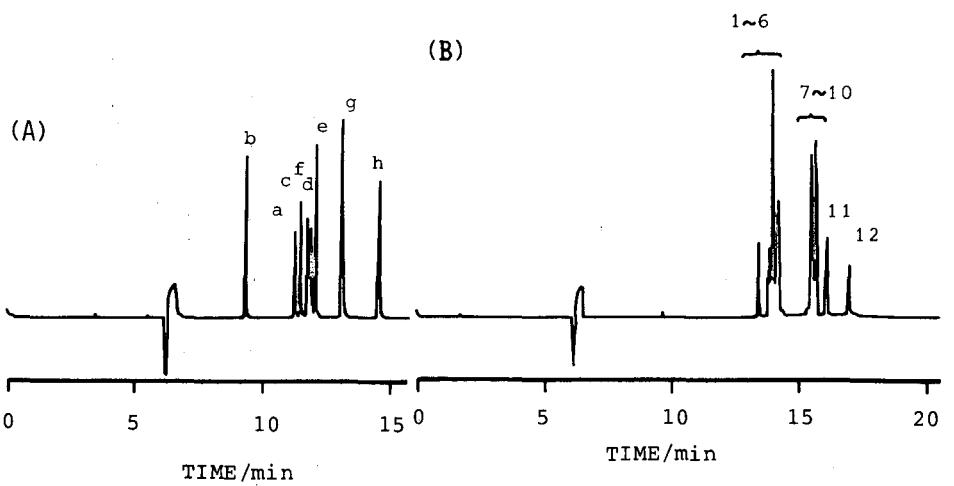

Fig. 5. Typical chromatograms of (A) eight corticosteroids and (B) twelve benzothiazepin analogues by micellar EKC with sodium deoxycholate (0.05 *M*). Other conditions as in Fig. 4.

Effect of bile salt concentration and pH on the separation

The effect of the bile salt concentration on the migration times of the solutes was investigated with SC and STC solutions (pH 9.0). The results are shown in Fig. 6 for corticosteroids and Fig. 7 for benzothiazepin analogues. The migration times increased with increase in bile salt concentration, although the electroosmotic flow did not change significantly over the whole concentration range. The migration time of Sudan III was almost the same as for sample 12 in Fig. 7. This can be ascribed to a larger micelle phase ratio at high than at low SC concentrations. However, the increase in migration times was very slight when the SC concentration was increased from 0.1 to 0.15 *M* in comparison with the increase from 0.05 to 0.1 *M*, as shown in Figs. 6 and 7.

In micellar EKC, the total range of migration of electrically neutral solutes is limited between the migration time of water (t_0), which is measured with methanol, and that of the micelle (t_{mc}), which is measured with Sudan III. The value of t_{mc}/t_0 can be regarded as a parameter indicating the total width of the migration time window. The value of t_{mc}/t_0 calculated from Fig. 2, in which Sudan III migrated just after isoamyl *p*-hydroxybenzoate, is 2.7. The value of t_{mc}/t_0 observed in micellar EKC with SDS solutions usually lies between 4 and 5[7]. The slight change in migration times between 0.1 and 0.15 *M* SC and the narrow migration time window at 0.15 *M* SC can be ascribed to the small t_{mc}/t_0 value in micellar EKC with bile salts. It is interesting that a typical solute concentration would be 3 m*M* (calculated for hydrocortisone), and the greatest change in migration behaviour in Figs. 6 and 7 occurred as the concentration of micelles changed from about 5 to about 10 m*M*, assuming an aggregation number of 10. Optimum separation was obtained at *ca.* 0.1 *M* SC.

The use of STC instead of SC did not bring about any significant change in selectivity in comparison with the results shown in Figs. 6 and 7. When concentrations of STC higher than 0.1 *M* were employed, the baselines became noisy. The purity of the STC used might be responsible.

The pH dependence of the migration time was examined with 0.1 *M* SC solutions

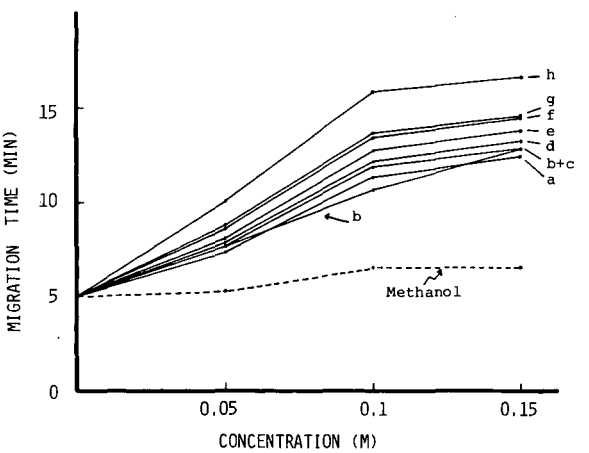

Fig. 6. Effect of bile salt concentration on the migration time of corticosteroids. Buffer, 0.02 *M* phosphate–borate (pH 9.0) containing sodium cholate. Other conditions as in Fig. 4.

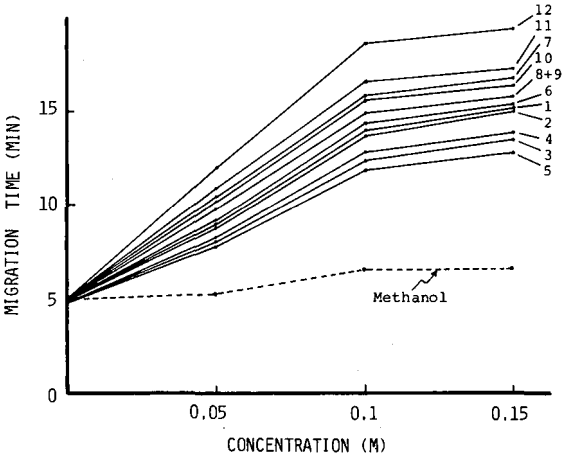

Fig. 7. Effect of bile salt concentration on the migration time of benzothiazepin analogues. Conditions as in Fig. 6.

in the pH range 7–9 and the results are shown in Fig. 8. The migration behaviour of corticosteroids did not alter over the whole pH range, because they are electrically neutral. However, the selctivity between diltiazem (sample 1) and its metabolites or chlorinated diltiazem (sample 7) and its metabolites deteriorated at low pH. It was useful to use high pH solutions to improve the separation of benzothiazepin analogues. The ionic effect due to an ionizable phenol will probably contribute to migration at high pH (9.0), because metabolic solutes have phenolic hydroxy groups. That is, electrostatic repulsion between the solutes and the anionic micelle will decrease the incorporation of these solutes by the micelle. Unincorporated anionic solutes,

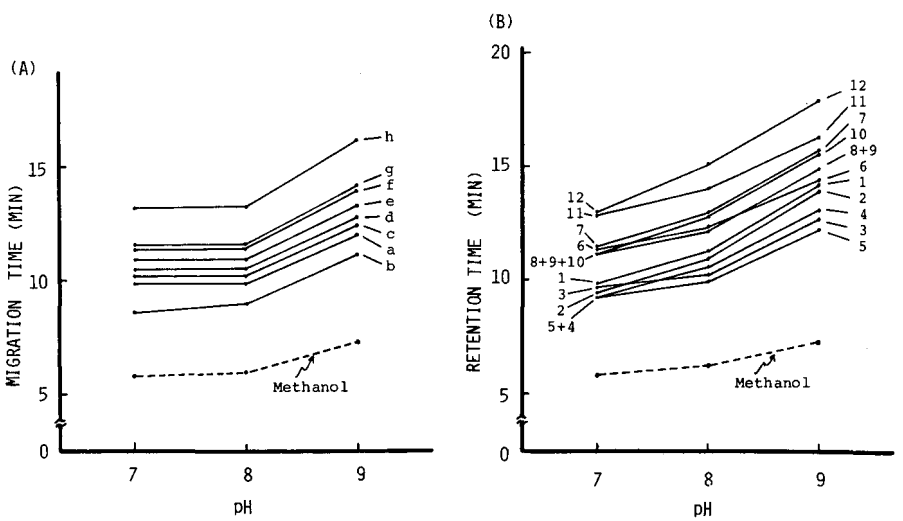

Fig. 8. pH dependence of the migration time of (A) cortocosteroids and (B) benzothiazepin analogues. Buffer, 0.02 *M* phosphate–borate containing 0.1 *M* sodium cholate. Applied voltage, 20 kV.

however, will migrate in the opposite direction to the electroosmotic flow by electrophoresis of solutes themselves. Therefore, it is difficult to predict how the migration time of ionizable solutes will be altered by changes in pH.

Effect of organic modifiers

Optimization of resolution has been also attained through adding an aqueous organic modifier[27,28,36] in addition to the parameters mentioned above. The effect of an organic solvent on the separation of the solutes was investigated by use of methanol at concentrations up to 20%. The result for corticosteriods is shown in Fig. 9. The migration times of the solutes increased with increase in the methanol concentration. This is ascribed to the decrease in the electroosmotic flow. The addition of 20% of methanol decreased the electroosmotic flow by about half (from 1.24 to 0.64 mm/s). The migration order and selectivity were not influenced except for sample b, probably because these solutes have nearly the same structure and they are electrically neutral. For the benzothiazepin analogues the same tendency (increase in migration time) was observed with increase in the methanol concentration without a change in elution order. However, the selectivety was much improved in the separation of a mixture of fourteen cold medicines, in which ionic compounds were mixed with neutral compounds[37].

Qualitative analysis of diltiazem hydrochloride and its tablets

On the basis of the results mentioned above, a buffer solution of pH 8.0 containing 0.1 *M* SC was selected for qualitative and quantitative analysis of diltiazem hydrochloride and its tablets from the viewpoint of successful separation and short analysis times. A chromatogram of diltiazem containing 0.3–0.5% of its related substances (samples 2–5) is shown in Fig. 10B, indicating a satisfactory separation. A typical chromatogram obtained from diltiazem hydrochloride (supplied by FE)

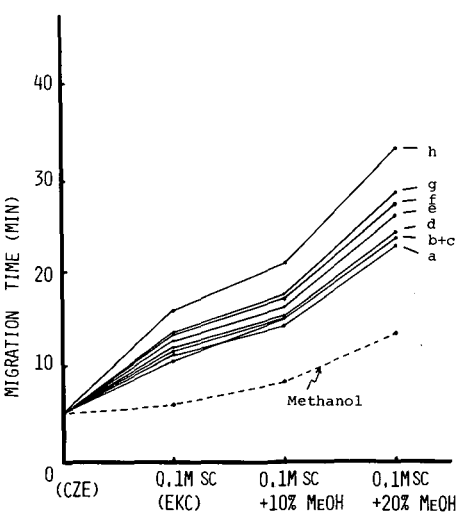

Fig. 9. Effect of organic modifier (methanol) in micellar EKC of corticosteroids in comparison with 0.02 *M* phosphate–borate buffer solution without bile salts (CZE) and with 0.1 *M* sodium cholate (EKC).

according to the procedure described under Experimental is shown in Fig. 10A. About 0.2% of an impurity (sample 2) was detected. The detection limit was *ca.* 0.1% at a signal-to-noise ratio of 3. Other results with samples from commercial sources and our laboratory are summarized in Table IV. These values agreed well with the values obtained by HPLC. Qualitative analysis was thus successfully performed by micellar EKC with the same precision as in an HPLC analysis.

Quantitative analysis of diltiazem tablets and fluocinonide cream

Diltiazem tablets were analysed by the internal standard (I.S.) method using sample 7 as an I.S.. The conditions are the same as in Fig. 10. The reproducibilities (coefficients of variation, C.V.) of the migration times and peak area ratios obtained with the standard solution by repeated injections ($n = 5$) were 0.7% and 2.2% respectively, were comparable to those obtained in previous studies[37–39]. The calibration graph for diltiazem obtained by the peak-area ratio method gave excellent linearity over the range 40–120% of the assay concentration with a correlation coefficient $r = 0.998$ and passed through the origin. The recovery was almost 100%.

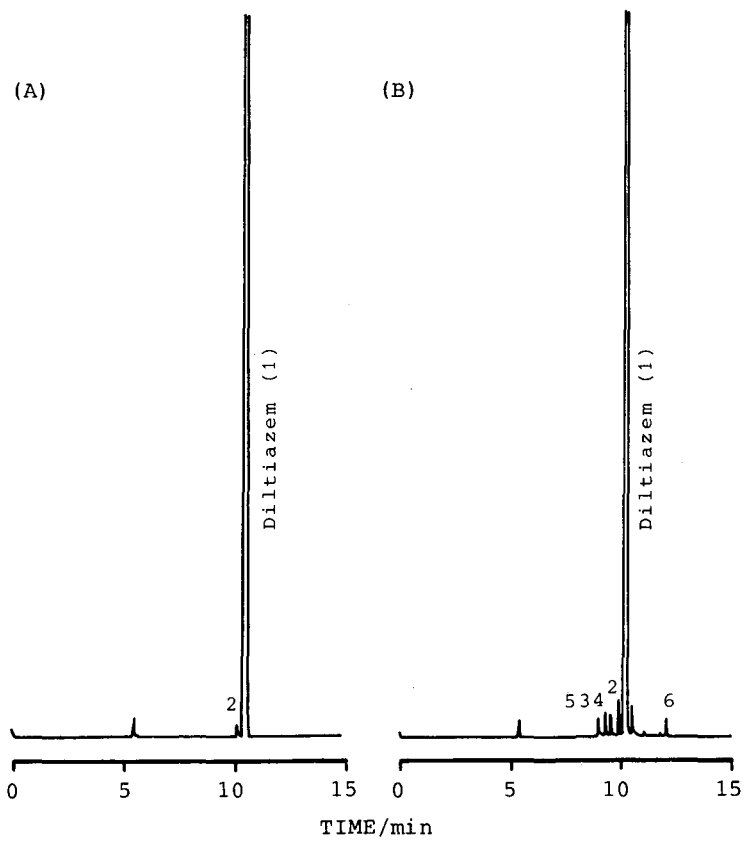

Fig. 10. Typical chromatograms obtained in the purity testing of diltiazem. (A) Diltiazem hydrochloride supplied by FE and (B) authentic diltiazem with 0.3–0.5% of related substances added. Buffer, 0.02 *M* phosphate–borate (pH 8.0) containing 0.1 *M* sodium cholate. Other conditions as in Fig. 4.

TABLE IV

RESULTS OF PURITY TESTING OF DILTIAZEM HYDROCHLORIDE AND ITS TABLETS

Source	*Sample*	*Impurity (%)*
TA	Diltiazem	ND[a]
FE	Diltiazem	0.22
FA	Diltiazem	0.27
TA	Tablets	ND[a]
TO	Tablets	1.46

[a] Not detected.

The assay results are summarized in Table V and typical chromatograms are shown in Fig. 11A. The average assay value for six replicate analyses was 101.5% and the C.V. was 1.7%.

Topsym cream containing 0.5% of fluocinonide was also analysed by the I.S. method using sample 11 as an I.S. Buffer solution of pH 9.0 containing 0.1 *M* SC was used and typical chromatograms are shown in Fig. 11B. The accuracy and reproducibility of the determination are given in Table VI. The C.V. obtained by repeated injections ($n = 6$) of the same sample solution in the peak-area ratio mode was worse than that in the peak-height ratio mode. The reason is unclear but the matrix of the formulation (non-ionic surfactant) might have affected the results. The peak-height ratio mode was used in the actual assay of cream. The capillary tube was washed with the operating buffer solutions as described in the procedure for capillary washing. Tables V and VI demonstrate the capability of this technique as a quantification method.

In conclusions, it was found that corticosteroids and benzothiazepin analogues can be successfully separated by micellar EKC using bile salts with high theoretical plate numbers within *ca.* 15 min, although the separation of these solutes could not be achieved by conventional CZE or micellar EKC with SDS solutions. The successful separation indicates that it might be useful in cases of poor resolution to explore various kinds of surfactants having different molecular structures in order to improve the selectivity in micellar EKC. The results of the quantitative and the qualitative analyses suggest that micellar EKC can be a helpful complement to HPLC in the field of separation science.

TABLE V

REPRODUCIBILITY AND ASSAY RESULTS FOR DILTIAZEM TABLETS

Peak area ratio (C.V.)	*Assay values (%)*		
2.2%	99.4	102.5	99.9
	101.3	104.3	101.6

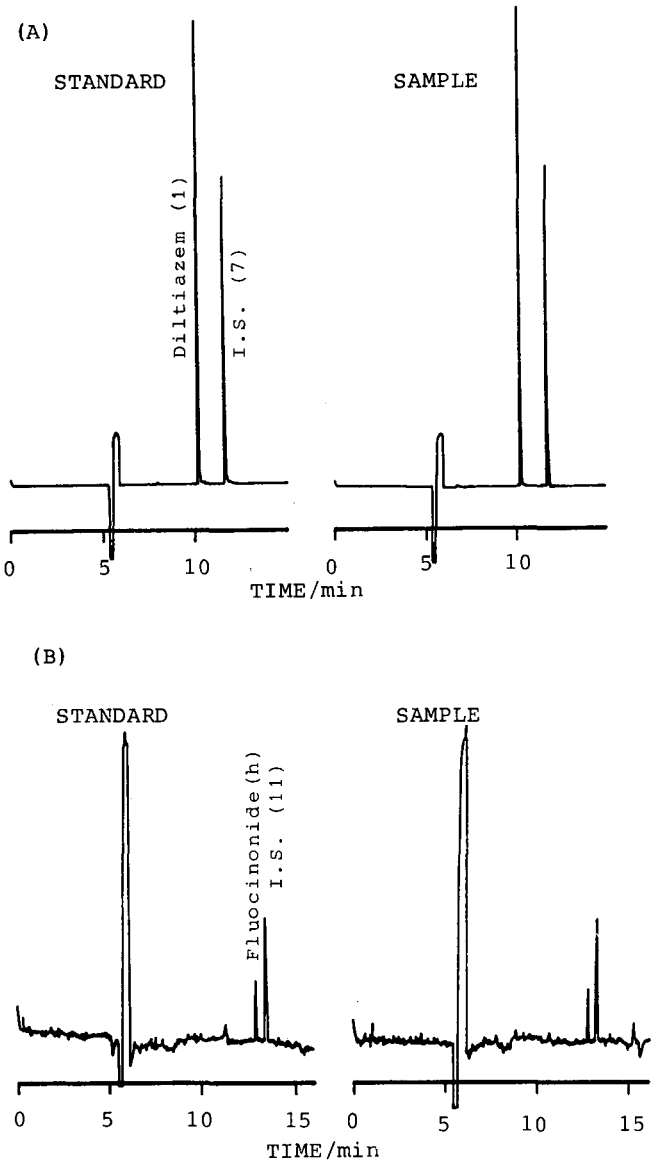

Fig. 11. Typical chromatograms obtained in the assay of (A) diltiazem tablets and (B) fluocinonide cream. Conditions: (A) as in Fig. 10; (B) as in Fig. 2B.

TABLE VI

REPRODUCIBILITY (C.V.) AND ASSAY RESULTS FOR FLUOCINONIDE CREAM

Standard solution (C.V.)		*Sample solution (C.V.)*		*Assay values (%)*		
Peak area ratio	*Peak height ratio*	*Peak area ratio*	*Peak height ratio*			
3.17%	4.59%	9.32%	2.77%	102.5 104.4	100.2 93.0	101.4 103.6

ACKNOWLEDGEMENTS

We thank Professor Terumichi Nakagawa (Faculty of Pharmaceutical Sciences, Kyoto University) for helpful advice. We also thank Dr. Toshio Kakimoto (Analytical Chemistry Research Laboratory, Tanabe Seiyaku) for his encouragement throughout this study.

REFERENCES

1 S. Terabe, K. Otsuka, K. Ichikawa, A. Tsuchiya and T. Ando, *Anal. Chem.*, 56 (1984) 111.
2 S. Terabe, K. Otsuka and T. Ando, *Anal. Chem.*, 57 (1985) 834.
3 J. W. Jorgenson and K. D. Lukacs, *Anal. Chem.*, 53 (1981) 1298.
4 J. W. Jorgenson and K. D. Lukacs, *Science*, 222 (1983) 266.
5 K. Otsuka, S. Terabe and T. Ando, *J. Chromatogr.*, 332 (1985) 219.
6 K. Otsuka, S. Terabe and T. Ando, *J. Chromatogr.*, 348 (1985) 39.
7 K. Otsuka, S. Terabe and T. Ando, *Nippon Kagaku Kaishi*, (1986) 950.
8 D. E. Burton, M. J. Sepaniak and M. P. Maskarinec, *J. Chromatogr. Sci.*, 24 (1986) 347.
9 K. H. Row, W. H. Griest and M. P. Maskarinec, *J. Chromatogr.*, 409 (1987) 193.
10 D. E. Burton, M. J. Sepaniak and M. P. Maskarinec, *Chromatographia*, 21 (1986) 583.
11 A. S. Cohen, S. Terabe, J. A. Smith and B. L. Karger, *Anal. Chem.*, 59 (1987) 1021.
12 H. Nishi, N. Tsumagari, T. Kakimoto and S. Terabe, *J. Chromatogr.*, 465 (1989) 331.
13 H. Nishi, N. Tsumagari, T. Kakimoto and S. Terabe, *J. Chromatogr.*, 477 (1989) 259.
14 T. Nakagawa, Y. Oda, A. Shibukawa and H. Tanaka, *Chem. Pharm. Bull.*, 36 (1988) 1622.
15 T. Nakagawa, Y. Oda, A. Shibukawa, H. Fukuda and H. Tanaka, *Chem. Pharm. Bull.*, 37 (1989) 707.
16 D. W. Armstrong and R. Q. Terrill, *Anal. Chem.*, 51 (1979) 2160.
17 J. D. Dorsey, *Adv. Chromatogr.*, 27 (1987) 167.
18 S. Terabe, M. Shibata and Y. Miyashita, *J. Chromatogr.*, 480 (1989) 403.
19 H. Nishi, T. Fukuyama, M. Matsuo and S. Terabe, *J. Microcolumn Sep.*, 1 (1989) 234.
20 A. S. Cohen, A. Paulus and B. L. Karger, *Chromatographia*, 24 (1987) 15.
21 M. M. Bushey and J. W. Jorgenson, *Anal. Chem.*, 61 (1989) 491.
22 S. Terabe, T. Yashima, N. Tanaka and M. Araki, *Anal. Chem.* 60 (1988) 1673.
23 R. M. McCormick, *Anal. Chem.*, 60 (1988) 2322.
24 R. G. Nielsen, G. S. Sittampalam and E. C. Rickard, *Anal. Biochem.*, 177 (1989) 20.
25 R. A. Wallingford, Jr, P. D. Curry and A. G. Ewing, *J. Microcolumn Sep.*, 1 (1989) 23.
26 Y. Walbroehl and J. W. Jorgenson, *J. Microcolumn Sep.*, 1 (1989) 41.
27 Y. Walbroehl and J. W. Jorgenson, *Anal. Chem.*, 58 (1986) 479.
28 J. Gorse, A. T. Balchunas, D. F. Swaile and M. J. Sepaniak, *J. High Resolut. Chromatogr. Chromatogr. Commun.*, 11 (1988) 554.
29 W. L. Hinze, *Ordered Media in Chemical Separations* (*ACS Symposium Series*, 342), American Chemical Society, Washington, DC, 1987, p. 19.
30 M. Nakazawa and S. Imai, *Pharma Med.*, 7 (1989) 13.
31 W. L. Hinze, *Ordered Media in Chemical Separations* (*ACS Symposium Series*, 342), American Chemical Society, Washington, DC, 1987, pp. 3–7.
32 D. Attwood and A. T. Florence, *Surfactant Systems. Their Chemistry, Pharmacy and Biology*, Chapman and Hall, London, 1983, pp. 185–196.
33 S. Sasaki, M. Miyata and K. Takemoto, unpublished data.
34 L. R. Snyder and J. J. Kirkland, *Introduction to Modern Liquid Chromatography*, Wiley, New York, 2nd ed., 1979, pp. 222–223.
35 H. Nishi, N. Tsumagari and S. Terabe, *Anal. Chem.*, 61 (1989) 2434.
36 S. Fujiwara and S. Honda, *Anal. Chem.*, 59 (1987) 487.
37 H. Nishi, T. Fukuyama, M. Matsuo and S. Terabe, *J. Chromatogr.*, 498 (1990) 313.
38 K. Otsuka, S. Terabe and T. Ando, *J. Chromatogr.*, 396 (1987) 350.
39 H. Nishi, T. Fukuyama, M. Matsuo and S. Terabe, *J. Pharm. Sci.*, 79 (1990) in press.

Journal of Chromatography, 513 (1990) 297–310
Elsevier Science Publishers B.V., Amsterdam

CHROM. 22 475

Preparative isotachophoretic analyser equipped with a dropwise fractionating device

TAKESHI HIROKAWA*, JIAN-YING HU, KEIJI UMEDA, GOJI KIMURA, HIROMI IKEDA, FUMITAKA NISHIYAMA and YOSHIYUKI KISO

Applied Physics and Chemistry, Faculty of Engineering, Hiroshima University, Shitami, Saijo, Higashi-Hiroshima 724 (Japan)

(First received September 26th, 1989; revised manuscript received March 27th, 1990)

ABSTRACT

A preparative isotachophoretic analyser with a series of four separation tubes of I.D. 0.5–5 mm was constructed and its fundamental efficiency was evaluated. The maximum injectable sample volume was 2.5 ml. The heat convection in the separation tube (I.D. = 5 mm) was suppressed by adding hydroxypropylcellulose to the leading electrolyte (1%) and sucrose to the terminating electrolyte (20%). The entire separated zones were fractionated dropwise (5.4 μl each) through a narrow-bore nozzle by a counter flow of the leading electrolyte. Variations in the course of dropping due to electrostatic forces were suppressed by a simple electrostatic device. The recoveries of several micrograms of separands were determined by photometric and PIXE analysis and were almost 100%. The separability and apparent sensitivity were very good; *e.g.*, 150 ppb (10^9) Sm^{3+} (10^{-6} *M*, 2 ml) was separated from a mixture with Dy^{3+}, Tm^{3+} and Lu^{3+}.

INTRODUCTION

Capillary isotachophoresis (IP) is an important method for preparative separations because of its high separation power. In addition to the purification of a sample by fractionation, preparative isotachophoresis is useful for various purposes such as the determination of unknown constituents in combination with different analytical methods. In such a case, preparative isotachophoresis is regarded as a pretreatment technique with high selectivity for further characterization and identification.

Preparative capillary isotachophoretic analysers can be classified into two types with respect to the method of fractionation. A type for the fractionation of the entire sample zones was reported by Arlinger[1]. The zones were swept gradually by a counter flow of the leading electrolyte on applying a migration current and the fractions were fixed on a cellulose acetate strip. For this purpose, the apparatus was equipped with a pump to provide the counter flow and a strip-winding device. The fractions on the strip are eluted and the fractions are analysed by different methods.

0021-9673/90/$03.50

On the other hand, in the type reported by Kobayashi *et al.*[2], the separated sample zone was fractionated using a microsyringe. They reported a potential gradient detector equipped with a sample removal port to fractionate the target zone immediately after the tail of the zone was detected. Although the method was not intended for the successive fractionation of the entire sample zones the operational facility is notable. Kaniansky *et al.*[3] reported a similar discontinuous fractionation technique with the use of a specially designed fractionating valve. The fractionated solution itself is convenient as a sample for further analysis.

Considering the characteristics of these methods, an isotachophoretic analyser was constructed to fractionate the entire separated zones dropwise by using a counter flow of leading electrolyte. Complete recovery of the mobile components in the injected samples was expected with the minimum risk of loss and contamination, although the mixing of adjacent sample zones could not be avoided in principle.

The other aim was to increase the amount of sample that can be separated for trace analysis. Dolnik *et al.*[4] suggested strategies for isotachophoretic trace analysis and developed an isotachophoretic analyser with rectangular tubes. In trace analysis, a large sample volume is required with application of a high electric charge[5]. There are three ways to increase the load of the leading electrolyte according to the sample amount to be separated[4]: as (1) a hydrodynamic counter flow; (2) a concentration cascade; and (3) enhancement of the separation volume. We used method (3), utilizing the column coupling technique[6].

In this paper the design, operation and basic efficiency are reported for a preparative isotachophoretic analyser using a separation tube of I.D. 5 mm. The maximum sample volume is 2.5 ml.

EXPERIMENTAL

Instrumentation

Fig. 1 shows a schematic diagram of the apparatus. The double lines represent the electrolyte tubing and single lines the electric wiring. Valves are represented by circles. Sample migration in this apparatus can be divided into three stages. In the first stage, the sample solution (2.5 ml or less) was separated roughly. We shall call this stage the "preseparation stage". The second stage was used for the complete separation of the preseparated samples or the separation of the relatively small amounts of samples of the order of 10^2 nmol or less. Part of the unnecessary constituents migrating in front of the target zones was isolated at this stage. We shall call this stage the "separation stage". In the last stage, the separated zones were fractionated dropwise by a counter flow of leading electrolyte.

Four tubes with different inner diameters (I.D.) were coupled to increase both the separable amount of sample and the volume of the sample solution; the I.D.s were 5, 2, 1 and 0.5 mm and typical lengths for effective separations were 10, 10, 15 and 30 cm, respectively. The lengths of three tubes were easily adjustable except for the tube with an I.D. of 5 mm.

The tubes with I.D. 1 and 0.5 mm were connected by using a PTFE joint for a Shimadzu IP-2A with a tapered structure. The other joints for the tubes with larger I.D. were made from a block of acrylic resin. The migration around the joint was carefully checked visually using dyes; good separation and recovery could not be

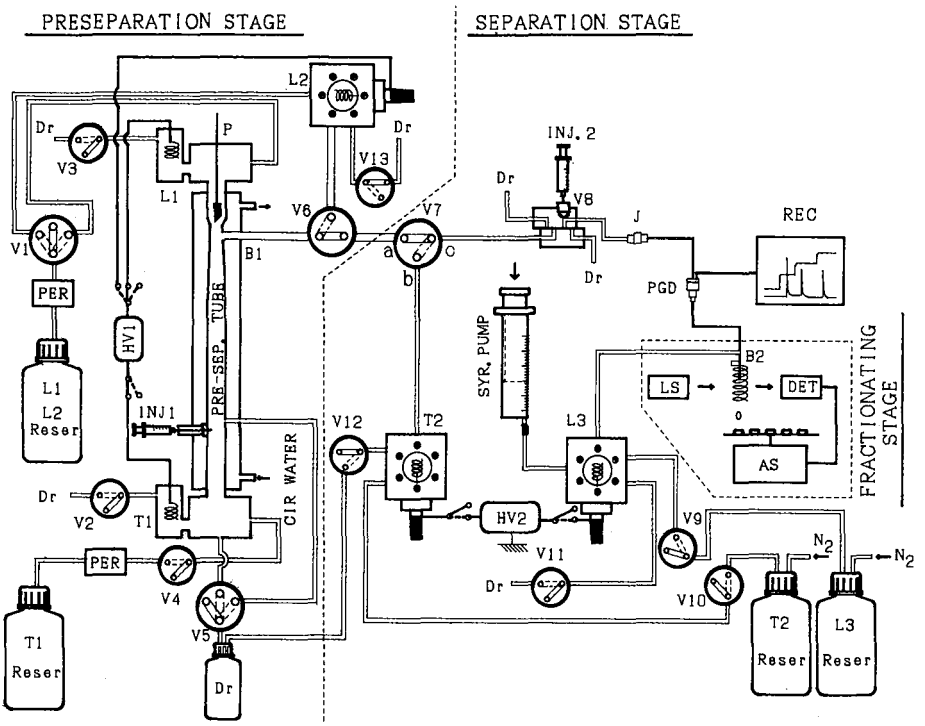

Fig. 1. Schematic diagram of preparative IP equipment. L1,L2,L3 = Leading electrolyte compartments; T1,T2 = terminating electrolyte compartments; V1–V5, V9–V13 = valves to fill and to drain the electrolyte compartments; V8 = injection valve; J = tube joint; V6,V7 = valves to change the current path; INJ1,INJ2 = injection ports; P = PTFE plug to cut off L1 compartment; PRE-SEP. TUBE = presep-aration tube; B1,B2 = branch of separation tubes; Reser = electrolyte reservoir; PER = peristaltic pump; PGD = potential gradient detector; REC = amplifier and recorder; SYR.PUMP = syringe pump to give a counter flow of leading electrolyte for fractionation; AS = automatic sampler driven by stepping motor; LS = light source; DET = photodetector and amplifier for triggering the automatic sampler; Dr = electrolyte drain; HV1,HV2 = high-voltage power supplies; N_2 = nitrogen pneumatic device. Separation tubes: B1–V6–V7 and V6–L2, I.D. = 2 mm and O.D. = 3 mm; T2–V7–J and B2–L3, I.D. = 1 mm and O.D. = 2 mm; J–B2, I.D. = 0.5 mm and = O.D. = 1 mm; preseparation, I.D. = 5 mm and O.D. = 7 mm.

expected if the joint had an electrophoretically dead space. The load of the leading electrolyte in the thus connected tubes was *ca.* 3.1 ml, which is at least ten times larger than that of the ordinary apparatus. This permits the separation of micromole amounts of samples, although the amount depends on the difference in the mobilities of the separands.

Three leading electrolyte compartments (L1, L2 and L3 in Fig. 1) and two terminating compartments (T1 and T2) were used for the rapid migration of samples through the different stages. The migration current was applied selectively to the electrodes of these compartments. The apparatus was equipped with two injection ports (INJ1 and INJ2 in Fig. 1). One of them was used selectively according to the amount and/or volume of sample.

The details of each stage are considered in the following sub-sections.

Preseparation stage

The preseparation tube was made of acrylic resin. The tube was tapered as illustrated in Fig. 1 and the I.D. and O.D. were 5 and 7 mm at the maximum and 3 and 4 mm at the minimum at branch B1. At the branch the tube of the preseparation stage was connected with that of the separation stage. The preseparation tube was surrounded by a water-jacket and was cooled by circulating water (room temperature) during operation.

The leading and terminating electrolyte compartments (L1 and T1) were made of acrylic resin blocks and the volume of the solution was *ca.* 30 ml. The electrode compartments (volume *ca.* 8 ml) were set apart from the electrolyte compartments and were connected with a tube (O.D. = 12 mm, I.D. = 8 mm, length = 55 mm). The electrode used was a coiled platinum wire. The hydrogen and oxygen generated were trapped in the electrode compartments and released after the operation. It seemed that some electrode reaction took place and the reactive ions formed hindered the electrophoretic migration of samples if the electrode compartments were not separated. When histidine was present in the leading electrolyte, for example, the colour of the electrolyte solution gradually turned brown during migration.

The migration voltage applied between L1 and T1 was 1000–500 V under typical operation conditions, and the current varied from 5 to 3 mA during the migration. The distance between INJ1 and B1 was *ca.* 10 cm and it took *ca.* 20 min for the migration. Then the current path was changed from L1–T1 to L2–T1 and the preseparated zones were led to the separation stage by applying 1500 V (*ca.* 1.5 mA) using the high-voltage power supply HV1. The separation tube connecting L2 and branch B1 was made of PTFE and the I.D. and O.D. were 2 and 3 mm, respectively. When the edge of the preseparated sample zone reached valve V6, HV1 was turned off.

Appropriate dyes were used as position markers to monitor the migration process and to switch the valves appropriately. When the leading edge of the sample zone reached branch B1, HV1 was turned off. The course of the separation tube (L1–T1) was blocked by a PTFE plug (P) at B1. The role of the plug was to prevent the gradual mixing of the leading ion or the rejected sample constituents with the target zones; if the plug was not used, the separation in the subsequent stage was unfavourable owing to the elution by the leading ion from L1.

As the heat conductivity of acrylic resin was poor and the wall of the preseparation tube was relatively thick (1 mm), the electrolyte in the tube could not be cooled sufficiently. Therefore, the temperature of the electrolyte near the inner surface wall was significantly different from that in the centre of the tube. To suppress heat convection, which disturbed the formation of sharp zone boundaries, the viscosity of the electrolytes in L1 and L2 was increased by adding hydroxypropylcellulose (HPC, 1%, w/w), obtained from Tokyo Kasei (Tokyo, Japan). The viscosity of the 2% aqueous solution was 1000-4000 cP at 20°C according to the specification. A 2% stock solution was prepared and used after deionization with an ion-exchange resin.

Deionized sucrose solution was added to the terminating electrolyte in T1 (20%, w/w) to prevent the heat convection in the terminating zone. Two peristaltic pumps PER in Fig. 1; Model MP-3 (EYELA, Tokyo, Japan) were used to fill L1, L2 and T1 with the leading and terminating electrolytes. First, T1 was filled with the heavy terminating electrolyte up to the level of the drain tube near INJ1. Then L1 was filled with the viscous leading electrolyte and finally L2 was filled. Owing to the

difference between the specific gravities of the leading and terminating electrolytes, the initial boundary between these electrolytes was sufficiently stable. The boundary was clearly visible, because the refractive indices of the solutions were different from each other. The sample solution was injected into the tube containing terminating electrolyte through a rubber septum at INJ1 in Fig. 1. The initial boundary was not perturbed during sample injection, provided that the injection was slow.

The temperature of the electrolyte in the preseparation tube was at most *ca.* 50°C at the narrowest position. This was seen from the fact that the solubility of HPC decreased with increase in temperature and the transparency of the 1% solution was lost completely at *ca.* 50°C. In fact, the current applied was adjusted so that this temperature was not exceeded.

In the preseparation stage, a Toyo Seisakusyo Model 2515 high-voltage power supply (2500 V maximum HV1) was used in the constant-voltage mode, and stop valves V1, V2, V3, V4, V5, V6 and V13 were used for the liquid chromatograph (Gasukuro Kogyo, Models LPV-2, LPV-3 and LPV-4.

Separation stage

After the leading edge of the preseparated sample zone had reached at the valve V6, a migration current (300 μA) was applied between L3 and T1 by using HV2. After the final sample zone had passed V7, the current path was changed from L3-T1 to L3-T2, and the migration current was decreased from 300 to 150 μA. This change in current path was very important, as discussed later. Until fractionation, the sample zones migrated through the separation tube.

When the sample amount was small, the preseparation procedure was not necessary. In such cases the sample solution was injected using the second injection port (INJ2) at sampling valve V8. Coupled PTFE tubes (O.D. = 2, I.D. = 1 mm and O.D. = 1, I.D. = 0.5 mm) connected V8 with the leading electrolyte compartment L3. Half way along the tube of I.D. 0.5 mm a potential gradient detector (PGD, for Shimadzu IP-2A) and a fractionation compartment were fitted.

The electrolytes used in the separation stage were the same as those used in the preseparation stage except that the concentration of HPC in the former electrolytes was 0.2%. The temperature at this stage was not as high as in the preseparation stage because the applied current was low. The main role of HPC at this stage is to suppress not the heat convection but the electroendosmosis. Hence, if the presence of HPC in the fractions is undesirable, it should not be contained in the leading electrolyte solution.

In this separation stage, the sampling valve V8 and the stop valves V9, V10, V11 and V12 were used (Shimadzu IP-1B). The valve V7 was that used for Gasukuro Kogyo Models LPV-2, LPV-3 and LPV-4 liquid chromatographs. To fill L3 and T2, a pneumatic device was used.

Fractionation stage

After the migration in the separation stage had started, a counter flow of leading electrolyte was fed continuously by a syringe pump (Model JP-V, Furue Science, Tokyo, Japan). The leading electrolyte used was the same as that used to fill compartment L3. Until the leading edge of the sample zone reached the fractionation compartment, the overflow of leading electrolyte was discarded through a nozzle at the

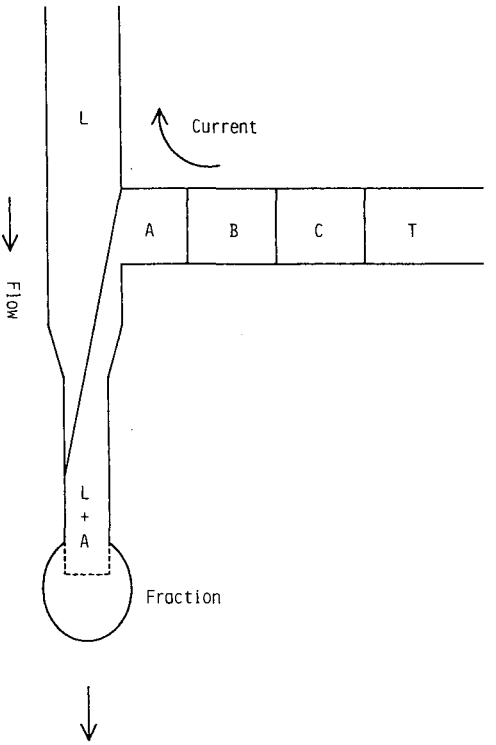

Fig. 2. T-shaped branch of the fractionation compartment and illustration of fractionation. L = leading zone; T = terminating zone; A, B and C = sample zones.

T-branch of B2 in Fig. 1. Hence it should be noted that the counter flow was not effective through the whole capillary. After the sample zones had reached B2, the dropwise fractionation was started. As shown in Fig. 2, the edge of the migrating zones was swept by the counter flow, and the samples diluted with the leading electrolyte dropped onto a sample collector through the nozzle (a platinum capillary, I.D. = 0.3 mm and O.D. = 0.5 mm). The dropping of fractions was monitored by an optical device.

The voltage applied between L3 and T2 was up to *ca.* 10 kV under typical experimental conditions. The power supply used (HV2) was a constant-current type for a Shimadzu IP-2A. As it was a bipolar type, for example, -5 kV were applied to the leading electrode and 5 kV to the terminating electrode. If the potential at the fractionating nozzle was made equal to the ground level, there could be no electrostatic hindrance to the drop. However, it was not easy to maintain such a situation because the potential gradient varied according to the electrolyte used and during the migration process. Unless a positive counter measure was devised, the fractions scattered widely and did not form drops. To regulate such an electrostatic influence, a copper coil (six turns) was located under the nozzle and was connected to the nozzle. The O.D. of the coil was 16 mm, the length was 20 mm and the O.D. of the copper

wire was 1 mm. The size of the drops and the dropping course could be stabilized by the use of such a simple device.

An automatic sampler (AS in Fig. 1) was used for the fractional collection of the dropped samples. Twenty-five fractions were collected in small sampling tubes or on Nuclepore filters which were set on the exchangeable turntable of the sampler. The turntable was revolved by a stepping motor (Model PH264M-32, Oriental Motor, Tokyo, Japan) with a pulse generator (Model UG601) and a driver (Model UD210). The pulse generator was triggered by a delayed photometric signal caused by a fraction dropping through a light path. A small lamp was used as the visible light source (LS) and the detector (DET) used was a photodiode (Model S1226-5BQ), Hamamatsu Photonics, Hamamatsu, Japan). The distance between LS and DET was *ca.* 40 mm.

The concentration of samples in the fractionated drops or the amount of the target substance in a fraction was adjustable by changing the rate of pumping of the leading electrolyte solution. The rate was determined by considering the isotachophoretic velocity under the operating conditions and the linear velocity of the counter flow. In a typical experiment, the linear velocity of the counter flow was four times larger than the isotachophoretic velocity and the flow-rate was variable in the range 10-50 μl/min. Under the condition of 12 μl/min and a driving current of 150 μA, the time interval for fractionation was *ca.* 30 s. The averaged volume of a drop was estimated to be 5.4 μl by weighing out 200 drops of sample. The consistency of the volume was *ca.* $\pm$ 10% when the above-mentioned difficulties were removed. The volume of one drop was affected by the diameter and seemingly by the material of the nozzle. A platinum nozzle was preferable to PTFE for making the volume small and constant.

Samples

Using the present analyser, to mark the migration process and to monitor the timing of valve opening or closing (as mentioned above), the selection of suitable dye markers is important. In this experiment, the R_E (effective mobility of leading ion/effective mobility of sample) values of eighteen kinds of cationic dyes were obtained.

Two cationic dyes, toluidine blue (TB) and astrazon pink (AP), were used in order to evaluate the basic efficiency of fractionation of the present apparatus. A mixture of Ce^{3+}, Sm^{3+}, Dy^{3+} and Tm^{3+} was also separated and fractionated for the same purpose. To exemplify trace analysis, a mixture of Sm^{3+}, Dy^{3+}, Tm^{3+} and Lu^{3+} was used. The concentration of Sm^{3+} was varied from $1.25 \cdot 10^{-5}$ to $1 \cdot 10^{-6}$ *M* whereas the concentration of Dy^{3+}, Tm^{3+} and Lu^{3+} was kept constant as $1.25 \cdot 10^{-5}$ *M*.

The dyes and other chemicals were obtained from Tokyo Kasei in the purest form available. The standard lanthanoids were purchased as the chlorides containing six molecules of water of crystallization and the purity was above 99.9%. They were dissolved in deionized water (5 m*M*).

Electrolyte system

The electrolyte system used in the fractionation and trace analysis is shown as system 1 in Table I. The concentration of HPC in the leading electrolyte for the preseparation stage was 1% and that for the separation and fractionation stages was

TABLE I

ELECTROLYTE SYSTEM USED IN ISOTACHOPHORETIC SEPARATION

HIB = α-Hydroxyisobutyric acid; CARH = carnitine hydrochloride; HPC = hydroxypropylcellulose.

Parameter	*System 1*	*System 2*
Leading electrolyte	20 m*M* KOH or 1 m*M* KOH + 19 m*M* NH_4OH[a]	10 m*M* KOH
Complexing agent	10 m*M* HIB	None
pH buffer	Acetic acid	Acetic acid
pH of leading electrolyte	4.8	4.57, 4.8, 5.0
Terminating electrolyte	20 m*M* CARH	10 m*M* CARH
Additive	0.2–1% HPC (leading) 20% sucrose (terminating)	0.2% HPC (leading)

[a] When the fractions were analysed by the PIXE method.

0.2%. The terminator (carnitine hydrochloride) was recrystallized from methanol, unless stated otherwise. The pH measurements were carried using a Horiba (Tokyo, Japan) Model F7ss expanded pH meter.

Analytical methods

The fractions of dyes were analysed with a Hitachi Model 356 double-beam spectrophotometer. One fraction (average volume = 5.4 μl) was dissolved in 5 ml of distilled water and the spectrum of the solution was obtained in the range 300–700 nm. By determining the maximum absorption at 532 and 623 nm of astrazon pink and toluidine blue, respectively, the concentration of the fractions was obtained.

PIXE (particle-induced X-ray emission) was used to analyse the lanthanoid fractions. The fractions were dropped directly on a Nuclepore filter mounted on a aluminium frame. After drying in a desiccator, they were used as the targets. The targets were irradiated by a 2.0-MeV proton beam generated by a Van de Graaff accelerator (Nisshin High Voltage, Tokyo, Japan). The PIXE spectra were obtained by a multi-channel analyser equipped with an hp (high pure)-Ge detector. A typical single run took *ca.* 1000 s (beam current = 20 nA). The details of the PIXE analysis of lanthanoids and their isotachophoretic analysis have been reported elsewhere[7,8].

In the fractionation of lanthanoids, mixed leading ions were used (1 m*M* KOH and 19 m*M* NH_4OH, see Table I) because the sensitivity of potassium is very high in PIXE analysis and it disturbed the rapid collection of the signals of the target elements. The mobilities of K^+ and NH_4^+ are of the same magnitude and the mixing has no adverse effect on isotachophoresis.

RESULTS AND DISCUSSION

Migration markers

In the measurement of the R_E values of eighteen kinds of cationic dye markers, electrolyte system 2 in Table I was used. Table II gives the observed R_E values, with carnitine as terminator and tris(hydroxymethyl)aminomethane (Tris) as an internal standard to correct the asymmetric potential of the potential gradient detector[9]. Most

TABLE II

THE OBSERVED R_E VALUES AND EFFECTIVE MOBILITIES OF CATIONIC DYES AT pH 4.57, 4.8 AND 5

R_E = effective mobility of leading ion/effective mobility of sample. $\bar{m}$ = effective mobility × 10^5 cm^2 V^{-1} s^{-1}. For the electrolyte system, see system 2 in Table I.

Dye	*pH of leading electrolyte*					
	4.57		*4.80*		*5.00*	
	R_E	$\bar{m}$	R_E	$\bar{m}$	R_E	$\bar{m}$
Bismark brown	1.47	(48.6)	1.46	(48.9)	1.48	(48.2)
Acridine orange	1.76	(40.6)	1.79	(39.9)	1.75	(40.8)
Toluidine blue (TB)	1.80	(39.7)	1.79	(39.9)	1.83	(39.0)
Neutral red	1.88	(38.0)	1.84	(38.8)	1.93	(37.0)
Pyronine Y	1.90	(37.6)	1.96	(36.4)	1.93	(37.0)
Methylene blue	1.94	(36.8)	1.97	(36.2)	1.96	(36.4)
Astrazon green	1.96	(36.4)	1.94	(36.8)	1.93	(37.0)
Astrazon blue	2.06	(34.7)	2.11	(33.8)	2.09	(34.2)
Astrazon Bordeaux	2.21	(32.3)	2.25	(31.7)	2.24	(31.9)
Safranine O	2.24	(31.9)	2.23	(32.0)	2.28	(31.3)
Crystal violet	2.25	(31.7)	2.24	(31.9)	2.25	(31.7)
Astrazon red	2.44	(29.3)	2.49	(28.7)	2.55	(28.0)
Methyl violet	2.66	(26.8)	2.70	(26.4)	2.76	(25.9)
Basic fuchsin	2.83	(25.2)	3.01	(23.7)	2.99	(23.9)
Pyronine G	2.90	(24.6)	3.04	(23.5)	3.06	(23.3)
Brilliant green	2.96	(24.1)	3.23	(22.1)	3.65	(19.6)
Astrazon pink (AP)	3.41	(20.9)	3.53	(20.2)	3.40	(21.0)
Astrazon yellow	3.69	(19.3)	3.69	(19.3)	3.69	(19.3)
Carnitine (Terminating)	5.43	(13.1)	6.18	(11.6)	6.53	(10.9)
Tris (standard)	2.66	(26.8)	2.67	(26.7)	2.67	(26.7)

of the dyes treated contained impurities. The listed R_E values were those for the coloured main components. Apparently from Table II, the R_E values of the treated dyes were not affected by changes in the pH of the leading electrolyte, except for brilliant green. It should be emphasized that most of these cationic dyes may form complexes with metal ions. When the complex-forming interaction occurs, the R_E values may be different from those listed in Table I.

Evaluation of fractionation

To examine the separability and consistency of the fractionation, 30 μl of a mixture of AP and TB (5 m*M*, 150 nmol each) was separated and fractionated. As the amount of sample was small, the preseparation stage was not used. A separation tube with an I.D. of 0.5 mm and a length of 30 cm was used, and the driving current was 150 μA. It took *ca.* 30 min to start fractionation. The observed isotachopherogram is shown in Fig. 3. The impurity zone with a large step height was due to the terminating electrolyte used, as in this particular instance the terminating carnitine hydrochloride was not purified. The impurity zone with a small step height was due to TB.

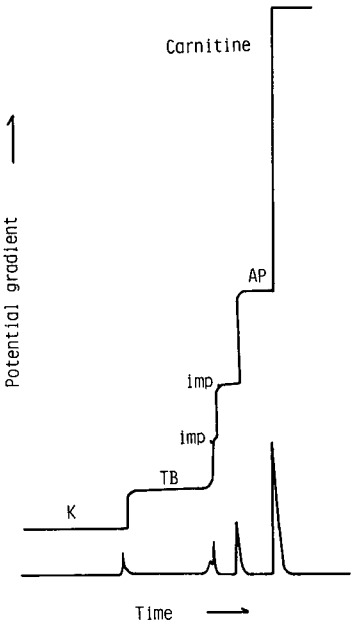

Fig. 3. Observed isotachopherogram of astrazon pink (AP) and toluidine blue (TB) mixture. Leading electrolyte, 1 m*M* KOH + 19 m*M* NH_4OH + 10 m*M* α-hydroxyisobutyric acid + 0.2% hydroxypropylcellulose, pH 4.8 (adjusted with acetic acid); terminating electrolyte, 10 m*M* carnitine hydrochloride. The migration current was 150 μA.

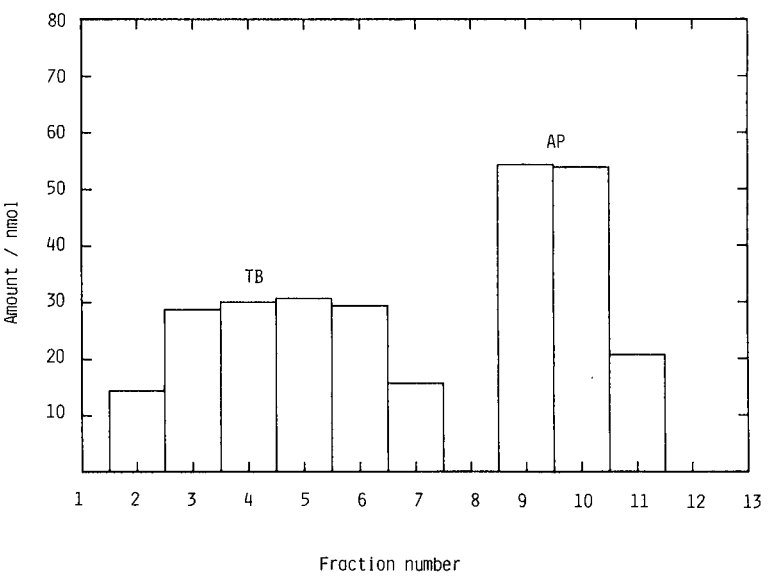

Fig. 4. Constituents and concentrations in the fractions of astrazon pink (AP) and toluidine blue (TB) mixture. Electrolyte system as in Fig. 3.

Ten fractions were obtained at a flow-rate of 24 μl/min. The visible spectra of the fractions were then obtained and the amounts of the components were determined (Fig. 4). Fractions 1–8 were TB and 9–11 were AP. The differences between the observed concentrations of TB and AP are due mainly to the differences in the effective charges of the ions. The fractionated amounts of AP and TB were 148.2 and 131 nmol, respectively, and the recoveries were 98.8 and 87.3%, respectively. The recovery of TB was relatively low because some UV-transparent impurity was present in the sample. The lack of mixing of TB and AP in the fractions was due to the existence of UV-transparent zones between the TB and AP zones.

For the same purpose, a mixture of Ce^{3+}, Sm^{3+}, Dy^{3+} and Tm^{3+} was separated and fractionated. The volume injected was 20 μl, which nominally contained 25 nmol of lanthanoids (3.50, 3.76, 4.06 and 4.22 μg, respectively). Twenty-five fractions were obtained in 6 min. Fig. 5 shows the observed isotachopherogram for Ce^{3+}, Sm^{3+}, Dy^{3+} and Tm^{3+} and Fig. 6 shows the constituents and amounts found in the fractions; these are the results of the PIXE analysis. Apparently the fractionation was very good. At the plateaux in Fig. 6, the deviation of the fractionated amounts was less than 10%. The total amounts of the lanthanoids recovered were 3.77, 4.00, 3.98 and 4.41 μg and the recoveries were 108, 106, 98 and 104% for Ce, Sm, Dy and Tm, respectively. These values are satisfactory taking into account the experimental and analytical errors of the PIXE method.

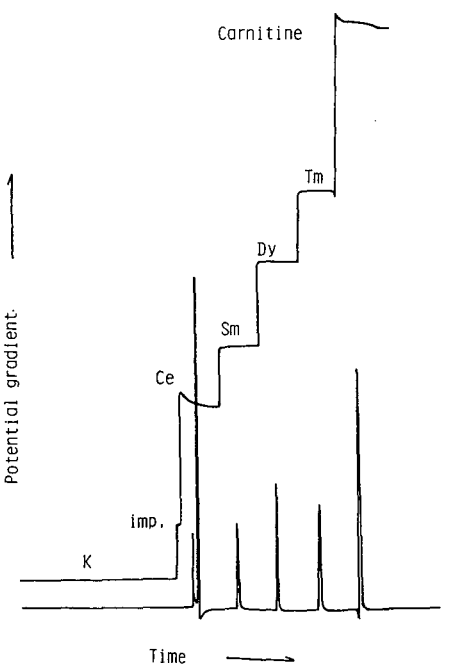

Fig. 5. Observed isotachopherogram of Ce^{3+}, Sm^{3+}, Dy^{3+} and Tm^{3+} mixture (25 nmol of each). Electrolyte system as in Fig. 3.

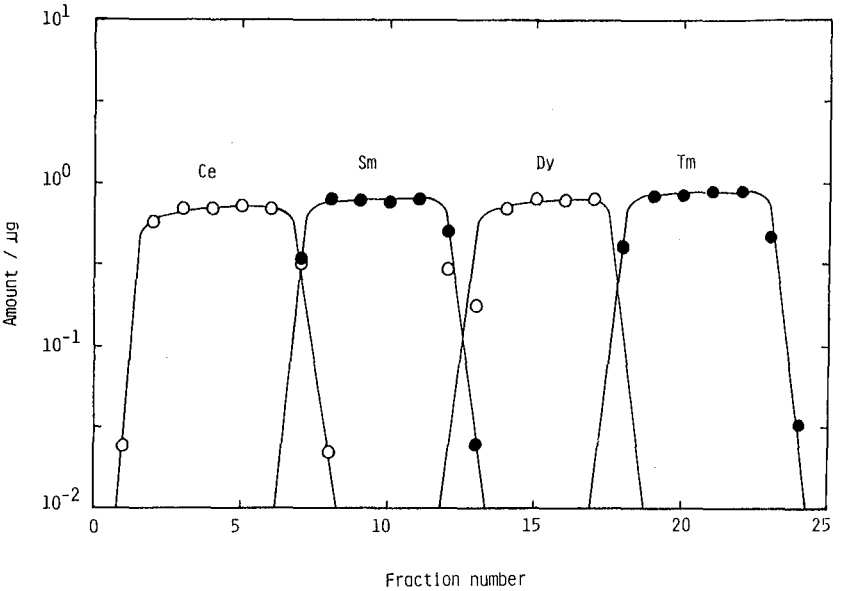

Fig. 6. Constituents of the 25 fractions of Ce, Sm, Dy and Tm mixture and the amounts evaluated by the PIXE method.

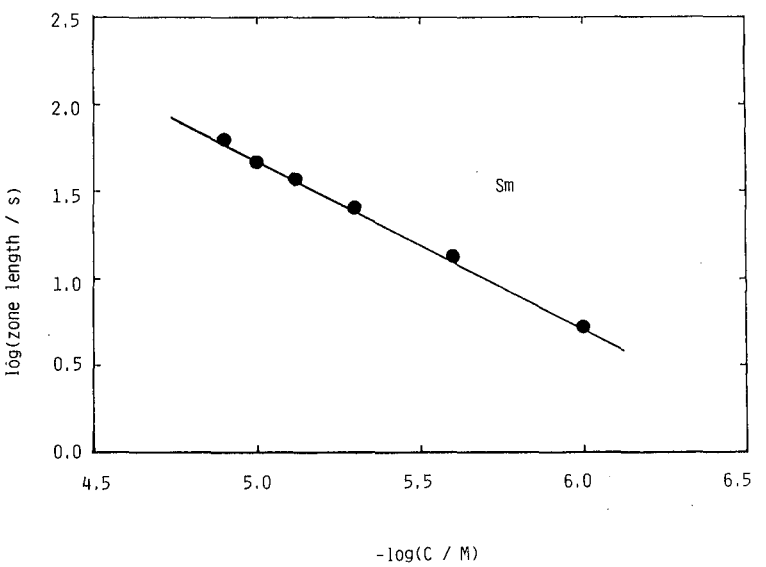

Fig. 7. Zone length of Sm^{3+} with time *vs.* the concentration of the solution injected. The solution was a mixture of Sm^{3}, Dy^{3+}, Tm^{3+} and Lu^{3+}. The concentrations of Dy^{3+}, Tm^{3+} and Lu^{3+} were $1.25 \cdot 10^{-5}$ *M* each. The volume injected was 2 ml. Leading electrolyte as in System 1 in Table I.

Trace analysis

As the expected performance of the developed system with respect to fractionation was confirmed, the limits were studied using a mixture of Sm^{3+}, Dy^{3+}, Tm^{3+} and Lu^{3+} as the sample. The concentration of Sm^{3+} was varied from $1.25 \cdot 10^{-5}$ to $1 \cdot 10^{-6}$ *M* while the concentrations of the other lanthonoids were kept constant at $1.25 \cdot 10^{-5}$ *M*. The sample (volume 2 ml) was injected from the injection port in the preseparation stage (INJ1 in Fig. 1). A potential gradient detector was used and the current applied during the sample detection was 150 μA. It took *ca.* 120 min for analysis and the time-based zone lengths were in the range 63.0–5.25 s.

Fig. 7 shows the observed zone length of Sm^{3+} and the concentration of solution. Good linearity was obtained, confirming the high sensitivity and reproducibility. The minimum concentration of 10^{-6} *M* corresponds to 150 ppb (10^9). A higher sensitivity may be expected when a narrower separation tube is used.

If the migration was carried by applying a current between L3 and T1 instead of L3 and T2, the detected zone boundaries were obscure. Moreover, a linear relationship between the amounts of sample injected and the detected zone lengths could not be obtained. This can be explained as follows: during the migration in the preseparation stage, the temperature of the electrolyte between L1 and T1 increased considerably owing to the high current (3-5 mA) and the geometry of the separation tube (acrylic resin) changed slightly. After the current had been lowered to 150 μA, the electrolyte and the tube were cooled gradually and hydrostatic flow occurred owing to the contraction. Consequently, the isotachophoretic migration of the separated zone was disturbed by the flow along the direction of the capillary.

In conclusion, the present apparatus was very useful both for the fractionation of sample constituents and for the analysis of trace components. The zone of the markers formed in the preseparation stage (tube of I.D. 5 mm) was very sharp, suggesting that the use of a larger I.D. may be allowed. As the amount of electrolyte constituents which concern the electrophoretic process was relatively large, in particular in the preseparation stage, the chemicals used for the preparation of the leading and terminating electrolytes should be extremely pure. In the present experiments, a considerable amount of Na^+ was detected in KOH. Unless the HPC was deionized and the terminating carnitine was recrystallized from methanol, the disturbance due to the impurities was serious. This is really an adverse effect due to the high load of the electrolytes.

The coupled IP–PIXE method proposed here has been applied to the determination of trace amounts of lanthanoids in crude rare earth metal chlorides and misch metal. The results will be published in due course.

REFERENCES

1 L. Arlinger, *J. Chromatogr.*, 119 (1976) 9.
2 S. Kobayashi, Y. Shiogai and J. Akiyama, in F. M. Everaerts (Editor), *Analytical Isotachophoresis —Proceedings of the 2nd International Symposium on Isotachophoresis, Eindhoven, 1980*, Elsevier, Amsterdam, 1981, p. 47.
3 D. Kaniansky, V. Zelenska and I. Zelensky, *J. Chromatogr.*, 256 (1983) 126.
4 V. Dolnik, M. Deml and P. Bocek, *J. Chromatogr.*, 320 (1985) 89.
5 P. Bocek, M. Deml, B. Kaplanova and J. Janak, *J. Chromatogr.*, 160 (1978) 1.
6 F. M. Everaerts, Th. P. E. M. Verheggen and F. E. P. Mikkers, *J. Chromatogr.*, 169 (1979) 21.

7 T. Hirokawa, F. Nishiyama and Y. Kiso, *Nucl. Instrum. Methods*, B31 (1988) 525.
8 T. Hirokawa, N. Aoki and Y. Kiso, *J. Chromatogr.*, 312 (1984) 11.
9 T. Hirokawa, M. Nishino, N. Aoki, Y. Kiso, Y. Sawamoto, T. Yagi and J. Akiyama, *J. Chromatogr.*, 271 (1983) D1.

Journal of Chromatography, 513 (1990) 311–314
Elsevier Science Publishers B.V., Amsterdam

CHROM. 22 497

Note

Possible value of a liquid crystal stationary phase for the gas chromatographic study of aromatic constituents of essential oils

T. J. BETTS
School of Pharmacy, Curtin University of Technology, GPO Box U1987, Perth, Western Australia 6001 (Australia)

(First received January 8th, 1990; revised manuscript received April 5th, 1990)

This author has previously recorded[1] the use of a mixed liquid crystal as a gas chromatographic (GC) stationary phase for resolving the most volatile constituents of essential oils such as limonene, cineole, etc. The potential of liquid crystal phases for studying the other less volatile constituents of essential oils has not been studied, and an initial evaluation is given here. These oils are often complex mixtures of aromatics and terpenoids, and results on liquid crystals could usefully supplement those obtained using conventional isotropic phases with their randomly distributed molecules.

In 1965, Dewar and Schroeder[2] described the use of eight liquid crystals for the GC of aromatic solutes and commented that "the effectiveness of II (a chlorinated tetra-aromatic di-anil) as a stationary phase agreed with our expectations, since II has a very long nematic (existing as a liquid crystal) range (180°) and a high transition temperature" at which it changes to a normal isotropic liquid. Although they record that "II decomposed slowly even at temperatures just above its melting point" they used it at 200°C as well as 158°C.

As this liquid crystal "II" is relatively cheap and commercially available under various names, it was selected for an initial study, despite its possible decomposition hazard, but only used up to 190°C. It is $(CH_3O\text{–}C_6H_4\text{–}CH=N\text{–}C_6H_3Cl\text{–})_2$ and is bis-4-(4-methoxybenzylidineanil-2-chloroaniline) $(MBCA)_2$.

EXPERIMENTAL

Apparatus

A Pye GCD gas chromatograph fitted with flame ionisation detector and a Hewlett-Packard 3380A recorder/integrator were used. A glass column (1.5 m × 4 mm I.D.) was packed with 2.5% $(MBCA)_2$ [*p*-dianisal-3,3′-dichlorobenzidine (TCI, Tokyo, Japan), melting point observed 142°C]. The weighed $(MBCA)_2$ was dissolved in dichloromethane and taken to dryness in a rotary evaporator with weighed Chromosorb W AW, 80–100 mesh. The column, after packing, was heated at 190°C

0021-9673/90/$03.50

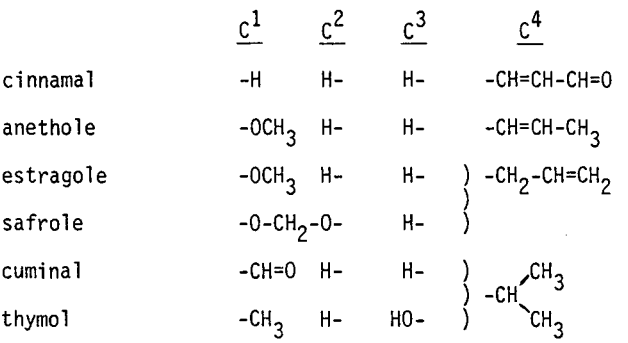

Fig. 1. Formulae of some benzene derivatives studied.

TABLE I

RELATIVE RETENTION TIMES (LINALOL = 1.00 AFTER SUBTRACTION OF HOLD-UP TIME)[a] ON PACKED COLUMN OF 2.5% $(MBCA)_2$

Mobile phase, nitrogen at a flow-rate of 3.75 to 5.00 ml min^{-1} at the flame ionization detector outlet. Averages (in italics) and ranges of values shown.

Essential oil constituent (and source)	*Relative retention time*				
	Column temperature (°C)				
	134.7 134.2–135.2	*149.8* 148.0–151.6	*160.3* 159.0–161.3	*175.4* 174.7–176.3	*189.3* 186.8–191.1
α-Pinene (BDH)	*0.15*	*0.18* 0.16–0.19	*0.20* 0.18–0.22	*0.19* 0.18–0.20	*0.25* 0.21–0.27
1,8-Cineole (Faulding)	*0.37*	*0.38*	*0.46* 0.44–0.48	*0.46* 0.44–0.50	*0.52* 0.47–0.55
Estragole (Sigma)	*1.58* 1.53–1.63	*1.58* 1.52–1.63	*1.71* 1.63–1.76	*1.58* 1.52–1.65	*1.81* 1.69–1.91
Safrole (Fritzsche)	*2.67* 2.61–2.70	*2.61* 2.45–2.77	*2.55* 2.41–2.73	*2.51* 2.45–2.59	*2.63* 2.53–2.79
Thymol (Sigma)		*3.92* 3.87–3.98	*3.40* 3.24–3.61	*3.27* 3.15–3.35	*3.06* 2.87–3.19
Cuminal (Eastman)			*3.90* 3.66–4.24	*3.45* 3.30–3.59	*3.61* 3.21–3.91
Anethole (*trans*) (Sigma)	*3.74* 3.64–3.82	*3.73* 3.62–3.85	*3.78* 3.50–4.07	*3.48* 3.25–3.64	*3.64* 3.42–3.83
Perillal[b] (Koch-Light)			*4.95* 4.46–5.26	*4.50* 4.40–4.55	*4.84* 4.74–5.00
Cinnamal (Ajax)				*9.02* 8.70–9.44	*9.45* 9.00–9.63

[a] Average retention times for linalol (Sigma) at each of the above temperatures were 0.79, 0.44, 0.32, 0.25 and 0.19 min, respectively.

[b] Perillal is not an aromatic substance but an unsaturated cyclic mono-terpenoid structurally like cuminal.

for a few hours with a flow of mobile phase (nitrogen) before analytical use. It could be used repeatedly.

A Technoterm 7300 probe was used to observe oven temperatures to 0.1°C.

Materials

The materials used are indicated in Table I and Fig. 1.

Method

Repeated injections were made from a microsyringe which had been filled then "emptied" of materials. Relative retention times were calculated against linalol, a "standard" used previously[3], after deducting hold-up time. Various column temperatures (isothermal) were used, indicated in Table I.

RESULTS AND DISCUSSION

Results are given in Table I. An unusually low mobile phase flow-rate of 5 ml min^{-1} or less was needed, and then sharp symmetrical peaks were only obtained with aromatic substances and with compounds having short retention times. Terpenoids such as carvone, citral and geraniol exhibited considerable "tailing" and were subject to excessively varying relative retention times, thus appearing unsuited to analysis on $(MBCA)_2$. The terpenoid perillal was, however, satisfactory. The variations often involved an atypical increase in retention time as the quantity of solute injected was reduced. Dewar and Schroeder[2] recommended using small samples, and this was found necessary in this study to approach consistent results. The short retention times involved also increased the chance of variation.

Six of Dewar and Schroeder's liquid crystals[2] were di-, tri- or tetra-aromatics, and it is likely that the use of such phases for GC will be best for aromatic solutes, as found here. Ignoring estragole, which always emerges first, results for some aromatics on $(MBCA)_2$ are safrole (first) — thymol — anethole — cinnamal (last). This is interestingly different from results on polyethylene glycol[3] where anethole precedes safrole, and thymol is a long last. It seems that the double bond conjugated with the aromatic ring present in anethole and cinnamal (see Fig. 1) is preferentially retained by $(MBCA)_2$. On polyethylene glycol it is the polar nature of the phenol (thymol) and aldehyde (cinnamal) groups which show greatest affinity, so deciding the elution sequence.

Liquid crystals have been used for the GC resolution of geometric isomers since 1977, when Vetrova *et al.*[4] separated *cis*- from *trans*-decalin. It was thus disappointing that $(MBCA)_2$ used here failed to resolve *cis*- from *trans*-citral (neral from geranial). Nor did it resolve the *dextro*- and *laevo*-isomers of carvone and linalol.

At 80°C $(MBCA)_2$ resolved cineole from α-pinene (separation factor, $\alpha = 3.15$) almost as efficiently as the previously used[1] mixed liquid crystal ($\alpha = 3.45$). It is amazing that $(MBCA)_2$ with a melting point above 140°C functions as a stationary phase at a temperature well below this, even as low as 50°C, where it resolves β- from α-pinene. However, Witkiewicz[5] records, in his recent review, that "several examples are known of the use of liquid crystals in the solid state". $(MBCA)_2$ gave "normal" results at 135°C, just below its melting point (given as 154°C by Dewar and Schroeder[2] for their synthesised product), fitting into the pattern given at higher temperatures

when it had reliably become a liquid crystal. The melt, observed on a microscope slide between crossed polarisers, showed a striated birefringence of liquid crystallinity, with spherulites of solid growing in it as it cooled.

A change in behaviour was observed for $(MBCA)_2$ at temperature above 175°C, when relative retention times increased instead of decreasing as usual, apart from thymol. This has been observed by Janini *et al.*[6] using another di-anil liquid crystal GC phase for which "retention increases due to the enhanced retention property of the nematic state".

Substances with short retention times gave relative (linalol) retention times on $(MBCA)_2$ falling between those previously observed[3] on packed columns of conventional phases. The low-polarity solute cineole shows the highest relative retention time on the low-polarity methylpolysiloxane, whilst "polar" aromatic solutes like estragole and safrole show the highest relative retention times on the polar polyethylene glycol. Other aromatic solutes with longer retention times give greater relative retention times on $(MBCA)_2$ than on either conventional phase, although these are still fairly brief retentions.

$(MBCA)_2$ thus may have potential for the analysis of essential oils which are rich in aromatic constituents such as aniseed, basil, cinnamon, cumin, fennel, sassafras, tarragon and thyme, where it could supplement conventional phase work. It does not seem suited to the GC of oils containing terpenoids apart from coriander and lavender, which contain linalol.

ACKNOWLEDGEMENT

Thanks are due to Mr. B. MacKinnon for preparing the liquid crystal column.

REFERENCES

1 T. J. Betts, *J. Chromatogr.*, 467 (1989) 272.
2 M. J. S. Dewar and J. P. Schroeder, *J. Org. Chem.*, 30 (1965) 3485.
3 P. N. Breckler and T. J. Betts, *J. Chromatogr.*, 53 (1970) 163.
4 Z. P. Vetrova, N. T. Karabanov and I. A. Jashin, *Chromatographia*, 10 (1977) 341.
5 Z. Witkiewicz, *J. Chromatogr.*, 466 (1989) 37.
6 G. M. Janini, G. M. Muschik and W. L. Zielinski, *Anal. Chem.*, 48 (1976) 809.

Journal of Chromatography, 513 (1990) 315–320
Elsevier Science Publishers B.V., Amsterdam

CHROM. 22 472

Note

Gas chromatographic separation of monoterpene hydrocarbon enantiomers on α-cyclodextrin[a,b]

MIKAEL LINDSTRÖM and TORBJÖRN NORIN
Department of Organic Chemistry, Royal Institute of Technology, S-100 44 Stockholm (Sweden)
and
JOHAN ROERAADE*
Department of Analytical Chemistry, Royal Institute of Technology, S-100 44 Stockholm (Sweden)
(First received September 25th, 1989; revised manuscript received March 28th, 1990)

Monoterpene hydrocarbons are common natural products, and are the major constituents in turpentine and other essential oils[1]. Several monoterpenes are important mediators in the chemical communication between organisms and are essential in insect–plant interactions[2]. Most of these monoterpenes are chiral with the (+)- and (−)enantiomers often having different biological properties. The individual enantiomers of a compound such as α-pinene can be transformed to chiral auxiliaries, which are used in organic synthesis, *e.g.*, hydroboration reactions[3]. Hence there is a need for rapid and accurate methods for the determination of the enantiomeric composition of monoterpene hydrocarbons. The classical polarimetric method and NMR techniques require large amounts of sample and are not suitable for complex mixtures or impure compounds. Chromatographic techniques are therefore more attractive [4–6]. A perpentyl-β-cyclodextrin phase has been reported[5] for gas chromatographic (GC) separations of some chiral olefins, including α-pinene and limonene. However, the enantioselectivity of such columns is limited, requiring high plate numbers, which lead to long analysis times.

We have reported that the enantiomeric purity of monoterpene hydrocarbons can be determined by GC via transformation to carbamates that can be separated on a Chirasil-Val column[7]. Chiral olefins have also been converted to the corresponding diastereomeric ketal of (2*R*,3*R*)-2,3-butanediol that can be separated on standard GC columns[8]. However, these procedures are experimentally laborious and are therefore not suitable for routine analysis.

In 1983, Koscielski *et al.*[9] described a promising method for the enantiomeric separation of both α- and β-pinenes using α-cyclodextrin in formamide as the stationary phase. Later, the same workers separated the enantiomers of pinanes and

[a] Dedicated to Günther Ohloff on the Occasion of his 65th Birthday.
[b] Presented in part at the *1st International Symposium on the Separation of Chiral Molecules, Paris, 1988.*

0021-9673/90/$03.50

2-carene[10] using the same procedure. The aim of the present investigation was to study and develop further this method in order to obtain a reliable technique for the determination of the enantiomeric composition of monoterpene hydrocarbons in biological samples, such as spruce phloem.

EXPERIMENTAL

Apparatus

A Pye Unicam 304 gas chromatograph, equipped with a split/splitless injector and a flame ionization detector, was used with helium as the carrier gas. A Pye GCV chromatograph equipped with an effluent splitter (1:100) was used for preparative work and fraction collection. Merck–Hitachi D-2000 integrators were used. The different fractions from the biological samples were collected in gas-tight syringes (SGE, 100 μl) and cooled by wrapping in aluminium foil together with dry-ice. Before the analysis, the syringes were heated in an oven at 100°C.

Chemicals

α-Cyclodextrin was purchased from Aldrich as the hydrate. The individual enantiomers, (+)- and (−)-α-pinene, (−)-β-pinene, (+)- and (−)-limonene and (+)-3-carene, were commercial samples. (+)-2-Carene and racemic 2-carene were obtained by isomerization from (+)-3-carene and racemic 3-carene, respectively. Racemic 3-carene and (+)-β-pinene were gifts from A. M. Mosieenkow (Selinskii Institute, Moscow, U.S.S.R.) and P. Baeckström (Royal Institute of Technology, Stockholm, Sweden), respectively. The (+)- and (−)-enatiomers of camphene were obtained by preparative GC on an α-cyclodextrin column (2.1 m × 4 mm I.D.) at 45°C of a commercial racemate, and the identification of the enantiomers was carried out by NMR spectroscopy and polarimetry.

Procedure

To prepare the packing material for the analytical column, 200 mg of α-cyclodextrin hydrate were dissolved in 1 g of formamide, which was diluted with water (10 ml). This solution was poured into a round-bottomed flask containing 5 g of Chromosorb W AW (45–60 mesh). The slurry was dried under reduced pressure (15–20 mmHg) using a rotary evaporator at 50°C for 30 min, then packed into a glass capillary (1.8 m × 0.8 mm I.D.) using an ultrasonic bath. Fused-silica capillaries (20 cm × 0.53 mm I.D.) were epoxy-glued to the ends of the filled column before it was mounted in the chromatograph. The carrier gas was saturated with water vapour by passing it through a stainless-steel cylinder packed with water-impregnated glass-wool, and then through a second stainless-steel cylinder loosely packed with glass-wool to remove water aerosol.

Phloem samples (1 cm^2), taken 1.5 m above the ground, were collected from a Norway spruce [*Picea abies* (L.) Karst], then chopped with a knife and extracted with 1.5 ml of methanol in an ultrasonic bath for 15 min. Saturated aqueous sodium chloride (1.5 ml) and pentane (1 ml) were added to the methanol extracts. The mixture was shaken and the layers separated. The pentane phase was passed through a short silica column to remove oxygenated compounds in order to shorten the GC separation time. A 5-μl volume of the mixture was fractionated on a preparative column

(Carbowax 20M, 10% on Chromosorb W, 80–120 mesh) (2.1 m × 3 mm I.D.), and the individual monoterpenes were subsequently analysed on an α-cyclodextrin column.

RESULTS AND DISCUSSION

During initial attempts to separate the two enantiomeric pairs of α- and β-pinene at 35°C with dry helium, according to the method of Koscielski *et al.*[9], we were not able to obtain stable conditions. The retention times fluctuated, the peak shape deteriorated with time and the enantioselectivity was rapidly reduced. This behaviour was attributed to dehydration of the stationary phase matrix by the dry carrier gas. Earlier, Andera and Smolkova-Keulemansova[11] pointed out the beneficial effect of water in the carrier gas on the peak shape with cyclodextrin-based columns. Support for our assumption was obtained by measurement of the weight loss of the column. The column weight decreased from 11.38 to 11.24 g in 19 h, after which it remained almost constant. The selectivity factor, α, correspondingly fell from over 2.2 to less than 1.5 for α-pinene enantiomers. To improve this situation, the experiments were repeated with the carrier gas saturated with water vapour. Stable enantioselectivity and resolution were obtained with only a slight weight loss of the column. The increased stability of the "wetted" column allowed us to separate (+)- and (−)-limonene. For this separation, the humidification of the carrier gas is of critical importance, as can be seen in Fig. 1.

Initially, separations were carried out at 35°C, but better results can often be obtained at lower temperatures, as in Fig. 2, where the chromatograms of the enantiomeric pairs of 3-carene, camphene and limonene are shown. The elution order was determined by injecting the individual reference enantiomers. The retention times still fluctuated over a long period and also a slight deterioration of the peak shape after several days of use was noticed. This can be attributed to the pressure drop over the column, eventually resulting in an uneven water distribution along the column. It was

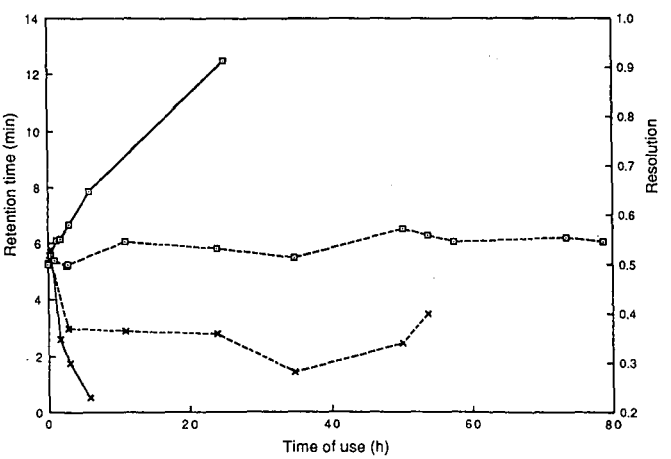

Fig. 1. (□) Change in retention time for (−)-limonene on α-cyclodextrin columns and (×) change in resolution of the limonene enantiomers with time in "unwetted" (solid line) and "wetted" (dashed line) systems.

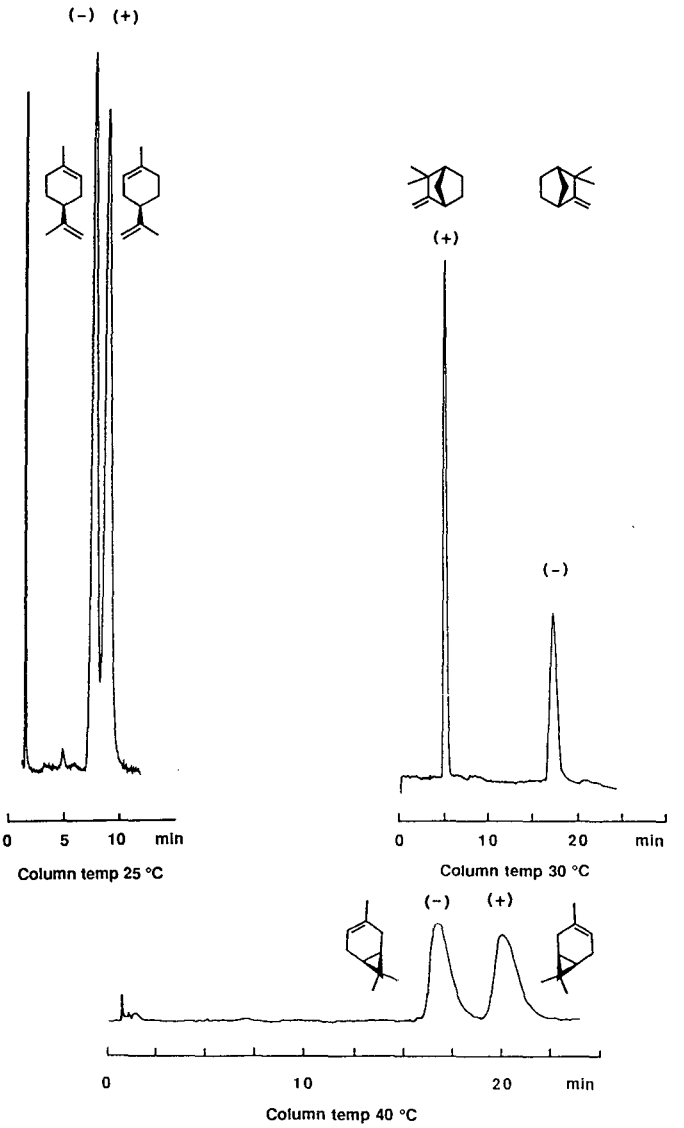

Fig. 2. Chromatograms of the enantiomeric pairs of some monoterpene hydrocarbons.

found that the peak shape could be restored by periodically reversing the direction of flow in the column.

The "wetted" α-cyclodextrin columns have the disadvantage of a limited temperature range and a low efficiency; however, this is outweighed by their high enantioselectivity. Thus, it is possible to obtain short analysis times making these columns suitable for preparative fractionation. Our pure (+)-and (−)-camphene reference material was obtained by such a preparative GC method from a commercial racemate of camphene.

TABLE I

THE ENANTIOMERIC COMPOSITION OF SOME CHARACTERISTIC MONOTERPENE CONSTITUENTS IN A PHLOEM EXTRACT OF *PICEA ABIES* (L.) KARST

Compounds are listed in elution order from the Carbowax column. Elution temperature on the cyclodextrin column was 30°C, except for 3-carene (40°C) and limonene (25°C).

Compound	*P. abies extract composition (%)*	*Enantiomeric composition (%) [(+):(−)]*	*Retention time α-CD column (min) [(+):(−)]*
α-Pinene	34	42:58	6.1:11.7
Camphene	9	8:92	5.4:17.6
β-Pinene	16	3:97	8.0:10.4
Myrcene	12	Not chiral	—
3-Carene	6	>99.5:<.5	19.8:16.5
Limonene	8	10:90	8.2:7.3
α-Phellandrene	13	[a]	—
Unidentified constituents	2	—	—

[a] The α-phellandrene enantiomers could not be determined owing to lack of reference material.

The improved "wetted" system was used to determine the enantiomeric composition of the major monoterpene hydrocarbons in a phloem extract of Norway spruce. A direct separation of the enantiomers was not possible owing to the complex nature of the extract. Therefore, the extract was first fractionated on the preparative Carbowax column and the individual monoterpene hydrocarbons were collected by a simple off-line procedure. The results from the final enantiomeric determinations on the α-cyclodextrin column are presented in Table I. In a previous paper[7] we have shown that there exists a large variation in the enantiomeric composition of α-pinene in Swedish spruce trees. A systematic investigation concerning the genetic dependence on the enantiomeric composition of monoterpene hydrocarbons in Swedish conifers is in progress.

To optimize the performance of α-cyclodextrin columns further, one can change the organic liquid in the stationary phase. Some promising results were obtained with triethanolamine instead of formamide as the stationary phase matrix component. This should be further investigated.

ACKNOWLEDGEMENTS

Financial support from the Swedish Council for Forestry and Agricultural Research and the Swedish Natural Science Research Council is gratefully acknowledged.

REFERENCES

1 S. Dev, *CRC Handbook of Terpenoids*,Vol. 1, CRC Press, Boca Raton, FL, 1982.
2 J. B. Harborne, *Introduction to Ecological Biochemistry*, Academic Press, London, 1977.
3 G. Zweifel and H. C. Brown, *J. Am. Chem. Soc.*, 86 (1964) 393.
4 V. Schurig, *Angew. Chem., Int. Ed. Engl.*, 16 (1977) 110.

5 V. Schurig and H. P. Novotny, *J. Chromatogr.*, 441 (1988) 155.
6 J. Ehlers, W. A. König, S. Lutz, G. Wenz and H. tom Dieck, *Angew. Chem., Int. Ed. Engl.*, 27 (1988) 1556.
7 M. Lindström, T. Norin, G. Birgersson and F. Schlyter, *J. Chem. Ecol.*, 15 (1989) 541.
8 D. M. Satterwhite and R. B. Croteau, *J. Chromatogr.*, 407 (1987) 243.
9 T. Koscielski, D. Sybilska and J. Jurczak, *J. Chromatogr.*, 280 (1983) 131.
10 T. Koscielski, D. Sybilska and J. Jurczak, *J. Chromatogr.*, 364 (1986) 299.
11 L. Andera and E. Smolkova-Keulemansova, *J. Inclus. Phenom.*, 5 (1987) 397.

Journal of Chromatography, 513 (1990) 321–326
Elsevier Science Publishers B.V., Amsterdam

CHROM. 22 452

Note

Determination of sunscreen agents in cosmetic products by gas chromatography and gas chromatography–mass spectrometry

KAZUO IKEDA*, SUKEJI SUZUKI and YOHYA WATANABE
Tokyo Metropolitan Research Laboratory of Public Health, 24–1, Hyakunicho 3 chome, Shinjuku-ku, Tokyo 169 (Japan)
(First received October 31st, 1989; revised manuscript received February 2nd, 1990)

Sunscreen agents are widely used to protect the skin against sunburn and to prevent the degradation of cosmetic products by sunglight, and a simple and reliable method for the determination and confirmation of sunscreen agents in cosmetic products is required in order to check whether the products were prepared in accordance with official regulations.

Several methods have been reported, including gas–liquid chromatography (GC)[1–3] and high-performance liquid chromatography (HPLC)[2–8]. Confirmation of sunscreen agents in these methods is usually done on the basis of retenion times, and a method based on UV spectral characteristics of sunscreen agents was proposed by Gagliardi *et al.*[5]. However, a more definite identification of sunscreen agents by gas chromatography–mass spectrometry (GC–MS) has not been reported.

In a previous paper[8], a simple method based on HPLC was proposed for the determination of six sunscreen agents {(2-hydroxy-4-methoxyphenyl)phenylmethanone (Oxybenzone), 2-ethoxyethyl 3-(4-methoxyphenyl)-2-propenoate (Cinoxate), 2-ethylhexyl 4-(dimethylamino)benzoate (Escalol 507), 2-ethylhexyl 3-(4-methoxyphenyl)-2-propanoate (Parsol MCX), 1-[4-(1-methylethyl)phenyl]-3-phenyl-1,3-propanedione (Eusolex 8020) and 1-[4-(1,1-dimethylethyl)phenyl]-3-(4-methoxyphenyl)-1,3-propanedione (Parsol 1789)} in cosmetic products. HPLC is useful for routine analysis but now difficult to use in combination with mass spectrometry in our laboratory. In this paper, we describe the application of GC to the determination of the six sunscreen agents and GC–MS to their confirmation using a DB-17 megabore capillary column.

EXPERIMENTAL

Reagents and materials

Oxybenzone, Cinoxate, Escalol 507, Parsol MCX, Eusolex 8020 and Parsol 1789 were used as reference standards as reported previously[8]. Water was deionized and distilled from glass apparatus. All other chemicals were of analytical-reagent grade.

0021-9673/90/$03.50

Standard solutions

Stock standard solutions were prepared by dissolving the appropriate amount of sunscreen agent in tetrahydrofuran (THF). A set of working standard solutions were produced by diluting aliquots of the stock standard solutions with THF to 50 ml in volumetric flasks. The concentration of each compound for the calibration graphs ranged from 20 to 100 μg/ml.

Sample solution

An amount of a cosmetic product equivalent to about 1–5 mg of a sunscreen agent was weighed accurately in a 50-ml beaker, dissolved in about 20 ml of THF by sonication and transferred into a 50-ml volumetric flask. The beaker was rinsed twice with 5-ml portions of THF and the rinsings were combined in a volumetric flask. The solution was diluted to volume with THF.

Gas chromatography

Determination of sunscreen agents was performed on a Model GC-15A gas chromatograph (Shimazu, Kyoto, Japan) equipped with a flame ionization detector. All samples were automatically injected into the gas chromatograph by a Model AOC-9 automatic sampler (Shimazu). Chromatograms and peak areas were obtained with a Model C-R5A reporting integrator (Shimazu). The megabore column used (15 m × 0.53 mm I.D.) contained DB-17 (50% phenylmethylpolysiloxane, 1.0-μm film thickness; J & W Scientific, Folsom, CA, U.S.A.). The injection temperature was 280°C. The oven temperature was set at 160°C for 10 min, then programmed from 160 to 250°C at 5°C/min followed by a 10-min hold at 250°C. Helium was used as the carrier gas at a flow-rate of 20 ml/min.

By means of the automatic sampler, 5 μl of the prepared sample solution and standard solution were chromatographed under the operating conditions described above. Quantification was based on peak areas.

Gas chromatography–mass spectrometry

Confirmation of sunscreen agents was performed on a Model HP 5890A gas chromatograph (Hewlett-Packard, Avondale, PA, U.S.A.) interfaced to a VG Analytical (Manchester, U.K.) Model 70S high-resolution mass spectrometer. Electron impact (EI) mass spectra were recorded at an ionization potential of 70 eV. The megabore column used and the operating conditions for GC–MS analysis were the same as described under *Gas chromatography*. The mass spectrometer was scanned repetitively from m/z 50 to 400 at a rate of one scan per second.

RESULTS AND DISCUSSION

A representative chromatogram obtained with the proposed GC method is shown in Fig. 1. Under the experimental conditions, the six sunscreen agents were well resolved. Calibration graphs were constructed by plotting the peak area against the concentration of standard injected. Good linearity over the range 20–100 μg/ml for each sunscreen agent was obtained. The detection limits were 1 μg/ml for Oxybenzone, Cinoxate, Escalol 507 and Parsol MCX, 3 μg/ml for Eusolex 8020 and 5 μg/ml for Parsol 1789.

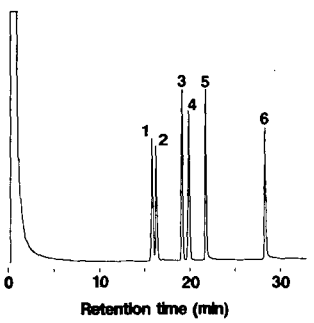

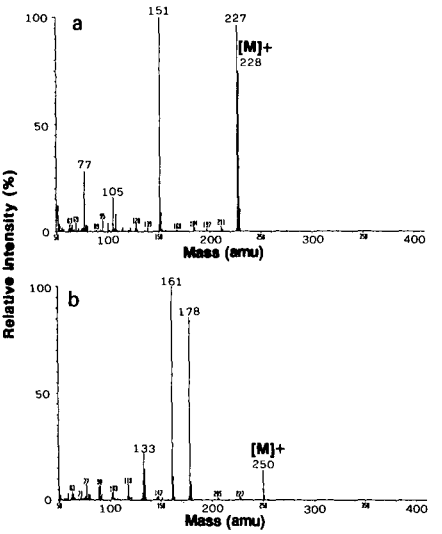

Fig. 1. GC of sunscreen agents. Amount injected: 500 ng of each sunscreen agent. Peaks: 1 = Oxybenzone; 2 = Cinoxate; 3 = Escalol 507; 4 = Parsol MCX; 5 = Eusolex 8020; 6 = Parsol 1789.

Fig. 2. EI mass spectra for (a) Oxybenzone and (b) Cinoxate.

The total ion current chromatogram of a full-scan GC–EI-MS analysis of 500 ng of each sunscreen agents is essentailly identical with the gas chromatogram in Fig. 1. Figs. 2, 3 and 4 show the EI mass spectra of the sunscreen agents. Each spectrum showed an $[M]^+$ ion and Oxybenzone and Eusolex 8020 also showed a strong $[M - H]^+$ ion. The base peaks of the sunscreen agents were as follows: Oxybenzone,

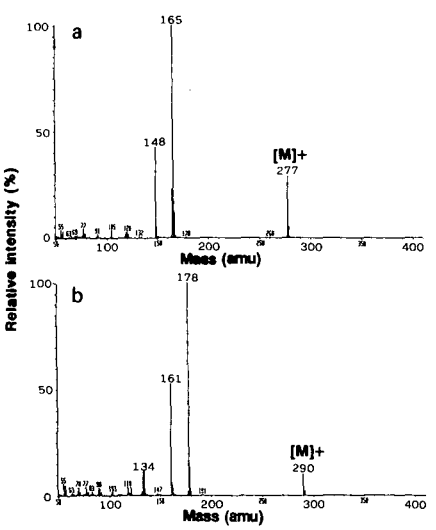

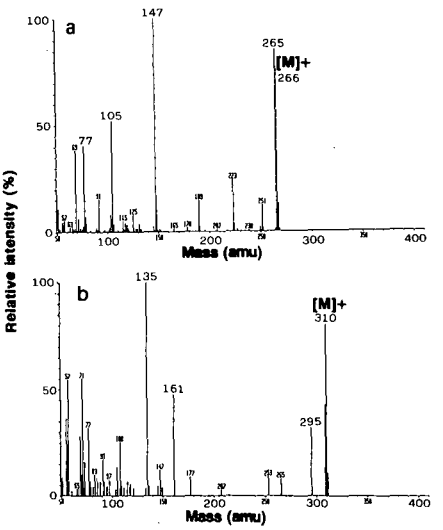

Fig. 3. EI mass spectra for (a) Escalol 507 and (b) Parsol MCX.

Fig. 4. EI mass spectra for (a) Eusolex 8020 and (b) Parsol 1789.

m/z 151 ($[M - C_6H_5]^+$); Cinoxate, *m/z* 161 ($[M - C_4H_9O_2]^+$); Escalol 507, *m/z* 165 ($[M - C_8H_{16}]^+$); Parsol MCX, *m/z* 178 ($[M - C_8H_{16}]^+$); Eusolex 8020, *m/z* 147 ($[M - C_8H_7O]^+$); and Parsol 1789, *m/z* 135 ($[M - C_{12}H_{15}O]^+$). Cinoxate and Parsol MCX showed intense peaks at *m/z* 178 and 161 due to the 3-(4-methoxyphenyl)-2-propenoic acid moiety.

The peaks of the sunscreen agents in practical GC analysis sometimes overlap those of other ingredients containing in cosmetic products. In such a case, the information obtained from monitoring the characteristic ions (molecular ion and major ion) by GC–MS is useful to confirm whether particular sunscreen agents are present or not. The characteristic ions are as followed: Oxybenzone, *m/z* 228 ($[M]^+$), 227 ($[M - H]^+$) and 151; Cinoxate, *m/z* 250 ($[M]^+$), 178 ($[M - C_4H_8O]^+$) and 161; Escalol 507, *m/z* 277 ($[M]^+$), 165 and 148 ($[M - C_8H_{17}O]^+$); Parsol MCX, *m/z* 290 ($[M]^+$), 178 and 161 ($[M - C_8H_{17}O]^+$); Eusolex 8020, *m/z* 266 ($[M]^+$), 265 ($[M - H]^+$) and 147; and Parsol 1789, *m/z* 310 ($[M]^+$), 295 ($[M - CH_3]^+$), 161 ($[M - C_9H_9O_2]^+$) and 135.

Recovery tests were carried out on cosmetic products to evaluate the reproducibility and accuracy of the proposed GC method. Three cosmetic products were spiked with the amounts of the agents reported in Table I and subjected to the whole procedure. As shown in Table I, excellent recoveries and precision were observed.

TABLE I

RECOVERIES OF SUNSCREEN AGENT FROM COSMETICS

Amounts of standard samples added were as follows: suntan lotion, 2.5% (w/w); foundation, 1% (w/w); lipstick, 2% (w/w).

Sunscreen agent	*Suntan lotion*		*Foundation*		*Lipstick*	
	Recovery (%)	*R.S.D. (%)*[a]	*Recovery (%)*	*R.S.D. (%)*[a]	*Recovery (%)*	*R.S.D. (%)*[a]
Oxybenzone	99.9	1.8	100.9	1.2	101.2	1.4
Cinoxate	99.8	0.4	99.9	1.5	97.0	2.1
Escalol 507	100.0	1.2	103.5	1.5	98.7	1.5
Parsol MCX	100.0	0.5	100.0	2.8	99.9	1.9
Eusolex 8020	100.4	0.3	98.3	1.1	104.2	1.0
Parsol 1789	101.2	0.4	95.8	3.3	103.7	1.7

[a] Relative standard deviation ($n = 5$).

The proposed GC method was applied to the determination of sunscreen agents in various cosmetic products (suntan lotion, foundation and lipstick). A representative chromatogram of a commercial suntan lotion is shown in Fig. 5. Analytical results are given in Table II. These results agreed with those obtained by HPLC[8]. The suntan lotion, foundation and lipstick contained about 1–7% of sunscreen agents.

The concentrations of sunscreen agents in the cosmetic products could be determined by monitoring the characteristic ions because the absolute intensity of each ion increases in proportion with the amount of compound injected. Fig. 6 shows total

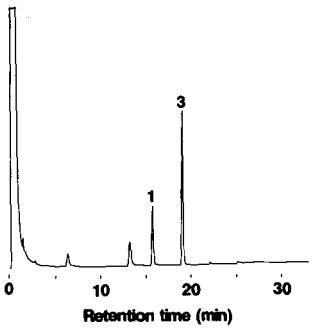

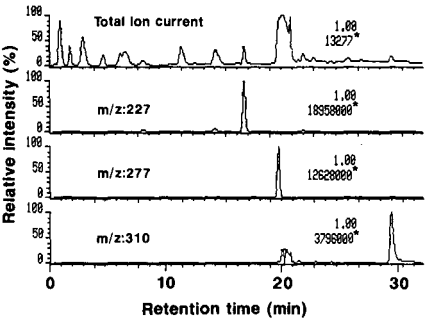

Fig. 5. GC of sunscreen agents in a commercial suntan lotion (No. 2 in Table II). Peaks: 1 = Oxybenzone; 3 = Escalol 507.

Fig. 6. Total ion current and mass chromatograms from the GC–EI-MS analysis of a commercial milk lotion. The values with asterisks are the absolute intensities on the 100% intensity axis.

ion current and mass chromatograms obtained from the GC–EI-MS analysis of a commercial milk lotion. It was confirmed from these chromatograms that the lotion contained Oxybenzone, Escalol 507 and Parsol 1789. The concentrations of each of these sunscreen agents were also determined from intensities of the characteristic ions; the results of 0.1% for Oxybenzone, 0.1% for Escalol 507 and 0.05% for Parsol 1789 were in agreement with the results obtained by GC analysis. The detection limits were the same as those in GC.

In conclusion, a simple, precise and accurate method has been developed for the determination of sunscreen agents in cosmetic products by GC using a megabore capillary column without any derivatization such as silanization as reported by Cumpelik[1]. It is suitable for the routine analysis of cosmetic products. The GC–MS method allows the determination and confirmation of sunscreen agents even if the cosmetic products contain many ingredients.

TABLE II

CONTENTS OF SUNSCREEN AGENTS IN COSMETICS

Values in parentheses obtained by HPLC[8].

Sample	*No.*	*Concentration (%, w/w)*		
		Oxybenzone	*Escalol 507*	*Parsol MCX*
Suntan lotion	1	3.2 (3.5)	6.6 (7.0)	2.2 (2.1)
	2	3.1 (2.8)	7.1 (6.9)	
Foundation	1		3.0 (2.8)	
	2			1.3 (1.3)
Lipstick	1			0.96 (0.95)
	2	2.7 (2.8)		

ACKNOWLEDGEMENTS

The authors thank Kokuritu Eisei Shikenjo, Kanto Chemical, Ina Trading and Givadan (all Tokyo, Japan) for supplying Cinoxate, Eusolex 8020, Escalol 507, Parsol 1789 and Parsol MCX, respectively.

REFERENCES

1 B. M. Cumpelik, *Cosmet. Toiletries*, 97 (1982) 67.
2 H. Koenig and R. Ryschka, *Fresenius' Z. Anal. Chem.*, 315 (1983) 434.
3 H. Koenig, *Fette Seifen Anstrichm.*, 86 (1984) 37.
4 H. S. I. Tan, R. Sih, S. E. Moseley and J. L. Lichtin, *J. Chromatogr.*, 291 (1984) 275.
5 L. Gagliardi, A. Amato, A. Basili, G. Cavazzutti and D. Tonelli, *J. Chromatogr.*, 408 (1987) 409.
6 T. Ohshima and E. Saito, *Gekkan Yakuji*, 29 (1987) 2477.
7 L. Gagliardi, G. Cavazzutti, L. Montanarella and D. Tonelli, *J. Chromatogr.*, 464 (1989) 428.
8 K. Ikeda, S. Suzuki and Y. Watanabe, *J. Chromatogr.*, 482 (1989) 290.

Journal of Chromatography, 513 (1990) 327–332
Elsevier Science Publishers B.V., Amsterdam

CHROM. 22 463

Note

Gas–liquid chromatographic method for the determination of marine wax esters according to the degree of unsaturation[a]

GERHARD KATTNER*, MARTIN GRAEVE and WOLFGANG ERNST
Alfred-Wegener-Institut für Polar- und Meeresforschung, Sektion Chemie, Am Handelshafen 12, D-2850 Bremerhaven (F.R.G.)
(Received March 22nd, 1990)

Wax esters constitute an important lipid class in the marine environment and are found in many marine organisms[1], in particulate[2] and dissolved matter[3] and in sediments[4]. They are energy-storage molecules in the marine food chain, especially in calanoid copepods, which represent a large fraction of the zooplankton biomass in most parts of the world's oceans. Calanoid copepods from high latitudes generally contain high levels of wax esters with high degrees of unsaturation[5–9].

Marine wax esters are composed of long-chain saturated and monounsaturated fatty alcohols and fatty acids with up to six double bonds. Therefore, the wax esters may exhibit up to seven double bonds in the molecule. In previous work various phases for the separation of wax esters were described, such as OV-1[10,11], OV-101[12], Dexil 300[13] and SE-52[14]. With these phases separations could be achieved based on chain length but hardly on the degree of unsaturation.

In order to obtain clear separations also of the various unsaturated wax esters, high-temperature gas chromatography (GC) on a special triglyceride stationary phase using a capillary column was applied in this work.

EXPERIMENTAL

The method was developed by using a complex mixture of wax esters isolated from lipids of the calanoid copepod *Calanus hyperboreus* originating from the Greenland Sea (Arctic). The organisms had to be sorted immediately after catching and preserved in chloroform–methanol (2:1) to avoid deterioration and loss of substance. Samples were frozen and stored at −25°C until analysis[9].

Lipid was extracted by homogenizing the animals in the storage solution with a Potter homogenizer (Braun, Melsungen, F.R.G.) at 1000 U/min. Insoluble particles settled out within a few hours or after slight centrifugation. From an aliquot of the supernatant, wax esters were separated by thin-layer chromatography (TLC) on silica gel 60 (Merck, Darmstadt, F.R.G.) with hexane–diethyl ether–acetic acid (90:10:1)[15].

[a] Contribution No. 270 of the Alfred Wegener Institute for Polar and Marine Research.

0021-9673/90/$03.50

Bands corresponding to wax esters were scraped off and eluted with chloroform, evaporated and dissolved in hexane. Additional TLC separations were made on silica gel 60 impregnated with 3% silver nitrate to differentiate between the polyunsaturated and the mono- and diunsaturated wax esters. Plates were developed with chloroform–methanol (95:5)[16].

GC of the wax esters was carried out under the following conditions: instrument, Carlo Erba Model 5370 Mega Series; carrier gas, hydrogen at 100 kPa; column, 25 m × 0.25 mm I.D. wall-coated open-tubular bonded fused-silica column coated with a 0.10-μm film of 50% methyl–50% phenylpolysiloxane [Triglyceride Analysis Phase (TAP); Chrompack, Mühlheim, F.R.G.]; injection, 0.2–0.5 μl of hexane solution

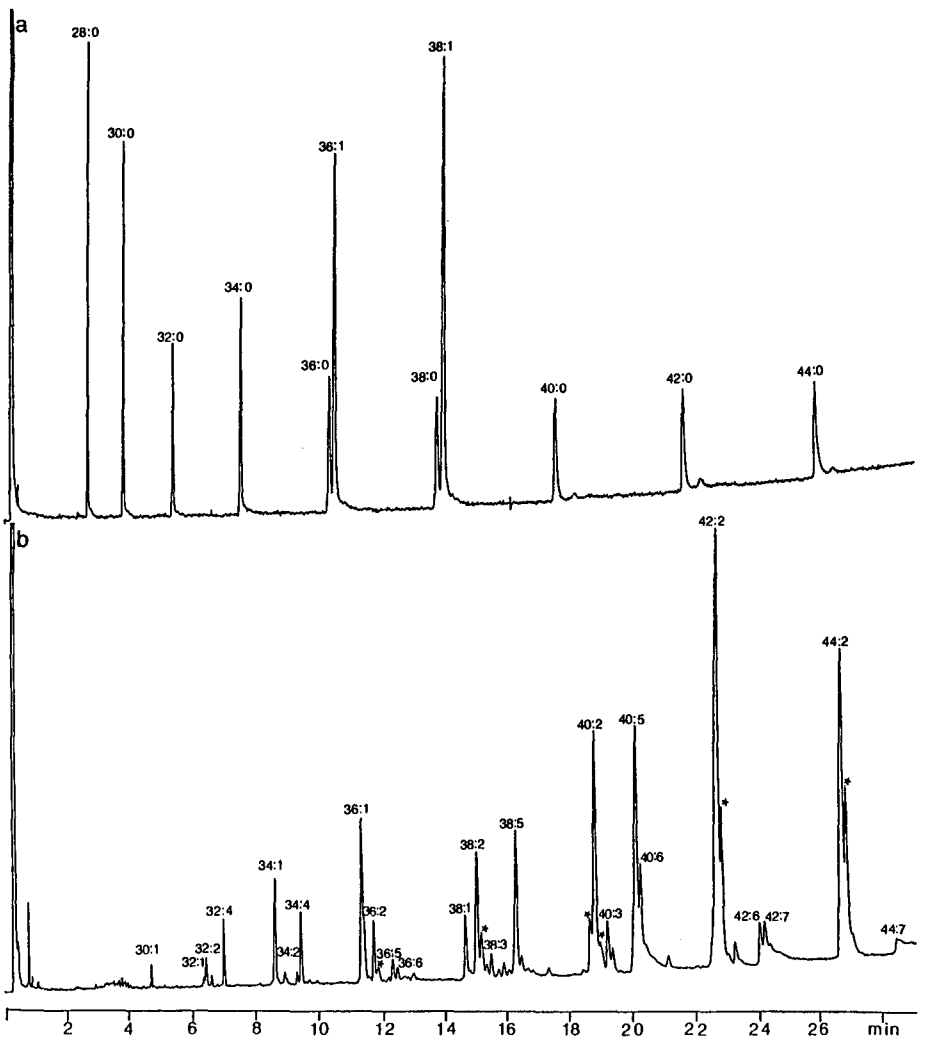

Fig. 1. Gas chromatograms of wax esters. (a) Commercial mixture; (b) natural wax esters isolated from lipids of *Calanus hyperboreus*. Asterisks indicate corresponding isomers.

on-column at 280°C oven temperature with 30-s auxiliary cooling; temperature programme, 2 min at 280°C, increased at 1°C/min to 320°C; detector, flame ionization (380°C).

To confirm the identification of peaks, commercial standards of saturated wax esters from C_{28} to C_{44} and monounsaturated 36:1 and 38:1 wax esters (Sigma, Deisenhofen, F.R.G.) were used. For the determination of possible wax ester combinations, an aliquot of the wax ester extract was transesterified. The resulting fatty acid methyl esters and fatty alcohols were analysed by GC according to the method described by Kattner and Fricke[17].

RESULTS

The samples of *Calanus hyperboreus* contained a mixture of wax esters in the range C_{30}–C_{44} with different degrees of unsaturation. In Fig. 1 the chromatogram of these wax esters is compared with that of a standard mixture of commercially available saturated and monounsaturated wax esters. Saturated wax esters were not detected in

TABLE I

ALL POSSIBLE COMBINATIONS OF THE WAX ESTERS OF *CALANUS HYPERBOREUS* CALCULATED BY ALCOHOL AND FATTY ACID ANALYSIS

C:X = number of carbon atoms:number of double bonds; wax ester combination = alcohol/fatty acid.

C:X	*Main compounds*	*Minor compounds*	*Traces*	*C:X*	*Main compounds*	*Minor compounds*	*Traces*
28:0	14:0/14:0			38:1	22:1/16:0	16:0/22:1	20:1/18:0
30:0	14:0/16:0			38:2	20:1/18:1		16:1/22:1
	16:0/14:0				22:1/16:1		
30:1	14:0/16:1	16:1/14:0		38:3	20:1/18:2		22:1/16:2
30:2	14:0/16:2			38:4	20:1/18:3		22:1/16:3
30:3	14:0/16:3			38:5	20:1/18:4		22:1/16:4
30:4	14:0/16:4			38:6	16:0/22:6		16:1/22:5
32:0	16:0/16:0		14:0/18:0	40:2	20:1/20:1	22:1/18:1	
32:1	16:0/16:1	14:0/18:1	16:1/16:0	40:3	22:1/18:2		
32:2	14:0/18:2	16:0/16:2	16:1/16:1	40:4	22:1/18:3		
32:3	14:0/18:3	16:0/16:3	16:1/16:2	40:5	22:1/18:4		
32:4	14:0/18:4	16:0/16:4	16:1/16:3	40:6	20:1/20:5		
32:5	16:1/16:4			42:2	20:1/22:1		
34:1	20:1/14:0	14:0/20:1	16:0/18:1		22:1/20:1		
34:2	16:0/18:2		16:1/18:1	42:6	22:1/20:5		20:1/22:5
34:3	16:0/18:3		16:1/18:2	42:7	20:1/22:6		
34:4	16:0/18:4		16:1/18:3	44:2	22:1/22:1		
34:5	14:0/20:5		16:1/18:4	44:6	22:1/22:5		
36:1	22:1/14:0	16:0/20:1		44:7	22:1/22:6		
	20:1/16:0	14:0/22:1					
36:2	20:1/16:1		16:1/20:1				
36:3	16:0/18:3		16:1/18:2				
36:4	20:1/16:3						
36:5	20:1/16:4	16:0/20:5	14:0/22:5				
36:6	14:0/22:6	16:1/20:5					

the copepod. The 36:1 and 38:1 wax esters were directly identified by comparison of their retention times. By using the standard mixture (Fig. 1a) the range of retention times for the unsaturated wax esters could be deduced, as it has already been established that TAP retards the unsaturated more than the saturated components.

Identification is further possible from the known linear relationship between the logarithm of the retention times and the number of carbon atoms for members of a homologous series. Most important for the identification was the analysis of the fatty acid and alcohol components of the wax esters. On the basis of these results all possible wax ester combinations can be calculated (Table I). The compositions were classified on the basis of the amounts of the major fatty acids and alcohols. Traces of fatty acids and alcohols may contribute very small amounts to some wax ester peaks. These combinations are also given in Table I. In Table II the wax ester composition of *Calanus hyperboreus* in combination with the resulting fatty acid and alcohol composition is presented. The fatty alcohols were less complex than the fatty acids. Only five alcohols were found, of which the principle components were the 20:1 and 22:1 alcohols. Nineteen fatty acids were identified with about seven major acids. Owing to their different proportions, the identities of the major wax esters could be established.

TABLE II

COMPOSITION OF WAX ESTERS, FATTY ACIDS AND ALCOHOLS OF *CALANUS HYPERBOREUS*

C:X ($n-y$) = number of carbon atoms:number of double bonds; y is the number of carbon atoms between the methyl end and the first double bond. Trace amounts are neglected.

Wax esters	*Content) (%,w/w)*	*Fatty acids*	*Content (%,w/w)*	*Alcohols*	*Content (%,w/w)*
30:1	0.42	14:0	3.84	14:0	2.22
32:1	0.51	16:0	2.12	16:0	3.23
32:2	0.21	16:1 ($n-7$)	5.37	20:1 ($n-9$)	27.97
32:4	1.31	16:2 ($n-6$)	0.51	22:1 ($n-11$)	65.61
34:1	3.04	16:3 ($n-3$)	0.43		
34:2	0.32	16:4 ($n-3$)	0.66		
34:4	2.12	18:0	0.32		
36:1	5.45	18:1 ($n-9$)	2.73		
36:2	2.09	18:1 ($n-7$)	0.45		
36:5	0.54	18:2 ($n-6$)	2.44		
36:6	0.24	18:3 ($n-3$)	1.28		
38:1	1.95	18:4 ($n-3$)	19.94		
38:2	5.64	20:1 ($n-9$)	20.81		
38:3	0.39	20:1 ($n-7$)	1.45		
38:5	6.17	20:5 ($n-3$)	4.79		
40:2	9.98	22:1 ($n-11$)	21.10		
40:3	1.99	22:1 ($n-9$)	4.69		
40:5	8.73	22:5 ($n-3$)	1.14		
40:6	5.05	22:6 ($n-3$)	5.83		
42:2	21.79				
42:6	1.28				
42:7	1.90				
44:2	17.38				
44:7	1.40				

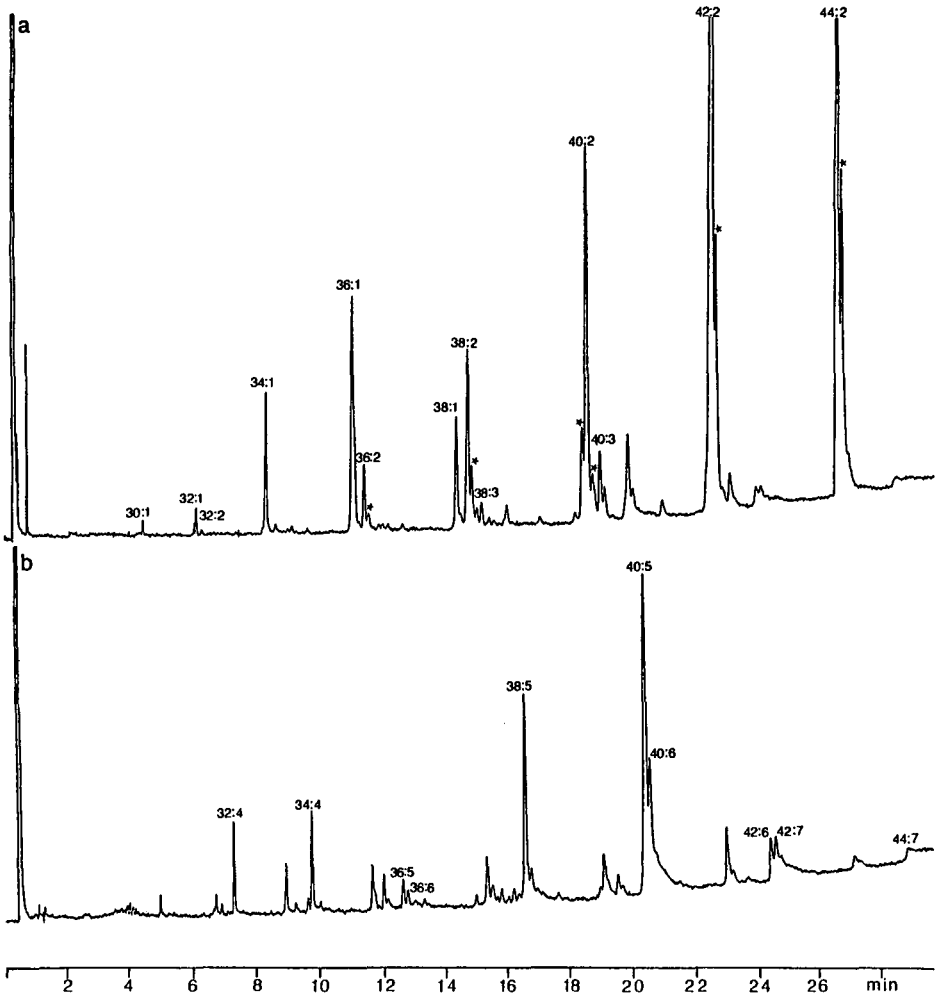

Fig. 2. Gas chromatograms of natural wax esters, isolated from lipids of *Calanus hyperboreus*, after separation by silver ion thin-layer chromatography. (a) Mono- and diunsaturated wax esters; (b) polyunsaturated wax esters. Asterisks indicate corresponding isomers.

Small amounts of the different isomers of the wax esters were found but are not listed in Table I. They appear as peak shoulders and as broadening of the bases of the corresponding peaks (Figs. 1 and 2). For the 42:2 wax ester, for example, theoretically at least eight isomers are possible owing to the different double bond positions in the fatty acids and alcohols.

From combined TLC and GC it could be concluded that the major mono- and diunsaturated wax esters are 36:1, 38:1, and 40:2, 42:2, 44:2, respectively (Fig. 2a). In the polyunsaturated fraction the 40:5 and 38:5 wax esters are most abundant as a combination of the 20:1 and 22:1 alcohol with the 18:4 fatty acid. The 40:6 and the 38:6 wax esters are not clearly separated from 40:5 and 38:5 (Fig. 2b). Owing to incomplete TLC separation in both chromatograms small amounts of the other fraction are detected.

DISCUSSION

In previous studies, high-temperature GC was performed to characterize especially commercial waxes according to chain length with and without derivatization[13]. Most data on marine wax esters are based on the GC identification of fatty acids and alcohols after hydrolysis. The calculation of possible wax ester combinations from those data has some limitations, of course. On the other hand, the few methods used so far were performed on columns with non-polar phases. They provided only total values for all wax esters having the same carbon number and gave no information about their degree of unsaturation[10–13] or at most they only differentiated between saturated and mono- and diunsaturated wax esters[14].

The Triglyceride Analysis Phase used in our method allows the separation of wax esters of the same chain length according to the number of double bonds without derivatization. The peaks appear in order from the saturated to the most unsaturated components, similarly to standard fatty acid methyl ester separation methods[17]. It is also possible to separate isomeric components. However, most of the peaks may be composed of a number of wax esters which differ in the alkyl and acyl moieties but having the same total carbon number and the same number of double bonds. Supported by the analysis of fatty acids and alcohols, most of the wax esters can be identified as a major single component (Table I). Hence the combination of the two methods allows a nearly complete elucidation of the wax ester composition of the studied material. Quantification is possible by adding internal standards, *e.g.*, a saturated wax ester such as 40:0 or 42:0.

This method was developed to study the wax esters of marine calanoid copepods from temperate and high latitudes, which are known to contain high amounts of wax esters often with large moieties of polyunsaturated fatty acids[7–9]. Now it will be possible to investigate, *e.g.*, species variabilities and distributions of copepods based on more detailed data for intact wax ester molecules.

REFERENCES

1 J. R. Sargent, R. F. Lee and J. C. Nevenzel, in P. E. Kolattukudy (Editor), *Chemistry and Biochemistry of Natural Waxes*, Elsevier, Amsterdam, 1976, p. 50.
2 S. G. Wakeham, *Geochim. Cosmochim. Acta*, 46 (1982) 2239.
3 J. K. Volkman, R. R. Gatten and J. R. Sargent, *J. Mar. Biol. Assoc. U.K.*, 60 (1980) 759.
4 S. G. Wakeham, C. Lee, J. W. Farrington and R. B. Gagosian, *Deep-Sea Res.*, 31 (1984) 509.
5 J. R. Sargent, R. R. Gatten and R. McIntosh, *Mar. Chem.*, 5 (1977) 573.
6 J. R. Sargent, *Sci. Prog.*, 65 (1978) 437.
7 R. F. Lee, *Mar. Biol.*, 26 (1974) 313.
8 J. R. Sargent, R. R. Gatten and R. J. Henderson, *Oceanis*, 7 (1981) 623.
9 G. Kattner, M. Krause and H. J. Hirche, *Mar. Biol.*, 102 (1989) 473.
10 R. F. Lee, J. C. Nevenzel and G. A. Paffenhöfer, *Mar. Biol.*, 9 (1971) 99.
11 R. F. Lee, J. C. Nevenzel and A. G. Lewis, *Lipids*, 9 (1974) 891.
12 J. J. Boon and J. W. de Leeuw, *Mar. Chem.*, 7 (1979) 117.
13 J. F. Lawrence, J. R. Iyengar, B. D. Page and H. B. S. Conacher, *J. Chromatogr.*, 236 (1982) 403.
14 S. G. Wakeham and N. M. Frew, *Lipids*, 17 (1982) 831.
15 H. K. Mangold, in E. Stahl (Editor), *Aliphatische Lipide*, Springer, Berlin, 1967, p. 350.
16 L. J. Morris, *J. Lipid Res.*, 7 (1966) 717.
17 G. Kattner and H. S. G. Fricke, *J. Chromatogr.*, 361 (1986) 263.

Journal of Chromatography, 513 (1990) 333–337
Elsevier Science Publishers B.V., Amsterdam

CHROM. 22 462

Note

Behaviour of 23 persistent organochlorine compounds during sulphuric acid clean-up on a solid-matrix column

ALFONSO DI MUCCIO*
Laboratorio Tossicologia Applicata, Istituto Superiore di Sanità, Viale Regina Elena 299, 00161 Rome (Italy)
ANGELA SANTILIO
Ospite del Laboratorio di Tossicologia Applicata, Istituto Superiore di Sanità, Viale Regina Elena 299, 00161 Rome (Italy)
ROBERTO DOMMARCO, MARINA RIZZICA and LUISA GAMBETTI
Laboratorio Tossicologia Applicata, Istituto Superiore di Sanità, Viale Regina Elena 299, 00161 Rome (Italy)
and
ANTONELLA AUSILI and FABIO VERGORI
Ospite del Laboratorio di Tossicologia Applicata, Istituto Superiore di Sanità, Viale Regina Elena 299, 00161 Rome (Italy)
(First received November 22nd, 1989; revised manuscript received March 22nd, 1990)

The most frequently used methods for the determination of organochlorine pesticide (OCP) residues in fatty samples involve adsorption chromatography on Florisil[1–3], alumina[4,5] or silica gel[6,7] as a clean-up step before determination by gas chromatography (GC) with electron-capture detection (ECD).

During analyses of lipid-rich samples such as human milk, cow milk and vegetable oils for OCP residues with Florisil clean-up[3], we frequently observed in the GC–ECD trace negative peaks which interfere with, and in some instances prevent, the determination of some OCP residues. Further, some large negative peaks, observed especially with vegetable oils, elute very late and their removal is very useful for decreasing the analysis time. Treatment with concentrated sulphuric acid has already been reported as the sole[8,9] or supplementary[10,11] clean-up of fatty extracts for the determination of OCP residues by GC–ECD. The treatment has been carried out either by shaking the sample extract dissolved in hydrocarbon solvents with concentrated sulphuric acid[8,10] or by passing it through a column of acid-impregnated Celite[11,12] or silica gel[9]. However, both approaches have some drawbacks. Shaking is not a safe procedure because sputtering of sulphuric acid may occur and, further, it requires centrifugation for clear separation of the phases. Impregnation by thoroughly mixing concentrated sulphuric acid with granular materials such as Celite is time consuming and also not safe because of the possible volatilization and inhalation of acid-charged particles. Both approaches involve the recovery of reusable glassware.

0021-9673/90/$03.50

This paper describes a sulphuric acid treatment for removing negative peaks from extracts of fatty samples which are insufficiently cleaned up by adsorption methods. The treatment is carried out on disposable solid-matrix columns in a simple, safe and efficient manner. The behaviour of selected OCPs toward this treatment has been studied.

EXPERIMENTAL

Reagents and materials

Analytical-reagent grade chemicals were used. Light petroleum (b.p. 40–60°C) and isooctane were redistilled from an all-glass apparatus. Sulphuric acid (95%, density 1.824 g/ml) was used. Organochlorine pesticide reference standards were from the collection in this laboratory.

Apparatus

Extrelut-1 columns (E. Merck, Darmstadt, F.R.G.; code 15371) are ready-to-use, disposable columns filled with a macroporous Kieselghur-type material with a nominal volume of 1 ml. Remove the upper paper disk before use and attach the supplied needle (Luer Lock 0.65/32) at the column end as a flow regulator in the elution step.

The analyses were carried out on a DANI 6800 gas chromatograph equipped with an electron-capture detector. A glass column (1.8 × 4 mm I.D.) was packed with OV-17 + QF-1 (1.5% + 1.95%) on Chromosorb W HP (100–120 mesh). The temperatures were oven 210, inlet block 230, outlet block 250 and detector 250°C. The carrier gas was nitrogen at a flow-rate of 55 ml/min.

A rotatory evaporator (bath temperature 40°C; reduced pressure) was used to concentrate solutions.

Procedure

Pipette 1 ml of sulphuric acid onto the Extrelut column, avoiding touching the inner walls. Allow the acid to drain and wait 10 min to obtain an even distribution into the filling material. Transfer onto the Extrelut column the sample extract cleaned up by Florisil adsorption chromatography, *e.g.*, according to Suzuki *et al.*[3] with three 1-ml portions of light petroleum. Wait 5 min, then elute the OCP residues with 10 ml of light petroleum. Collect the eluate and concentrate it carefully to dryness, dissolve the residue in 1 ml of isooctane and analyse the solution by GC–ECD.

RESULTS AND DISCUSSION

Some applications of solid-matrix columns and their advantages in pesticide residue analysis over conventional techniques have been reported previously[13–15]. In this application, the columns were used as a solid support to carry out a sulphuric acid clean-up of fatty extracts for the determination of OCP residues by GC–ECD.

The proposed procedure overcomes the problems mentioned in the Introduction because the acid is held in a solid matrix, the columns are prepared just prior to use with simple and safe operation and there is no need to recover reusable glassware. It is noteworthy that with this treatment emulsions do not occur, the elution is accom-

TABLE I

RECOVERIES OF ORGANOCHLORINE COMPOUNDS USING THE DESCRIBED PROCEDURE

Extrelut columns with 1 ml of 95% or 90% sulphuric acid, eluted with 10 ml of light petroleum.

Compound	*Amount present (μg)*	*Average recovery ±S.D. (n = 6) (%)*	
		95% H_2SO_4	*90% H_2SO_4*
HCB	0.01	76 ± 18	89 ± 7
α-HCH	0.01	90 ± 14	99 ± 6
τ-HCH	0.01	89 ± 10	98 ± 9
β-HCH	0.02	84 ± 16	94 ± 9
δ-HCH	0.01	100 ± 9	117 ± 20
Aldrin	0.01	91 ± 12	104 ± 15
Dieldrin	0.05	n.r.[a]	n.r.[a]
Endrin	0.05	–[b]	–[b]
HEPO	0.01	95 ± 8	102 ± 13
τ-Chlordane	0.03	95 ± 8	93 ± 9
α-Chlordane	0.03	95 ± 7	89 ± 8
τ-Chlordene	0.02	61 ± 12	–[c]
α-Chlordene	0.02	68 ± 15	–[c]
p,p'-DDE	0.03	98 ± 6	98 ± 10
o,p'-TDE	0.05	92 ± 8	94 ± 9
o,p'-DDT	0.05	88 ± 7	88 ± 9
p,p'-TDE	0.05	95 ± 5	92 ± 9
p,p'-DDT	0.05	86 ± 8	90 ± 11
Mirex	0.11	94 ± 7	95 ± 11
Metoxychlor	0.15	19 ± 17	49 ± 12
Oxychlordane	0.02	97 ± 8	–[c]
trans-Nonachlor	0.02	77 ± 10	–[c]

[a] Not recovered.

[b] Recovered as endrin ketone, which appears as a peak with a retention time longer than that of the parent compound.

[c] Not investigated.

plished in a few minutes with a reduced volume of solvent and the eluate is neutral and does not need to be centrifuged, washed and dried as in shaking methods[8].

The performance of the method was studied with respect to the recovery of selected OCPs, the quality of the GC–ECD trace and the weight of lipidic material left in the extract after the treatment.

In Table I are reported the average recoveries and standard deviations for 23 organochlorine compounds subjected to the described procedure in amounts ranging from 0.01 μg for HCB to 0.15 μg for metoxychlor. Acceptable recoveries were observed for most of the compounds. Exceptions included α-chlordene, τ-chlordene and metoxychlor, which were recovered only partly and with high variability; dieldrin was not visible in the GC–ECD trace at the sensitivity used; endrin, according to the published data[16], is converted to the ketone, which appears as a peak with a retention time longer than that of the parent compound.

With respect to the quality of the GC–ECD trace, Fig. 1 shows the substantial improvement in the gas chromatogram of a human milk extract obtained according to the method of Suzuki *et al.*[3] after the described treatment. Similarly, tissues from

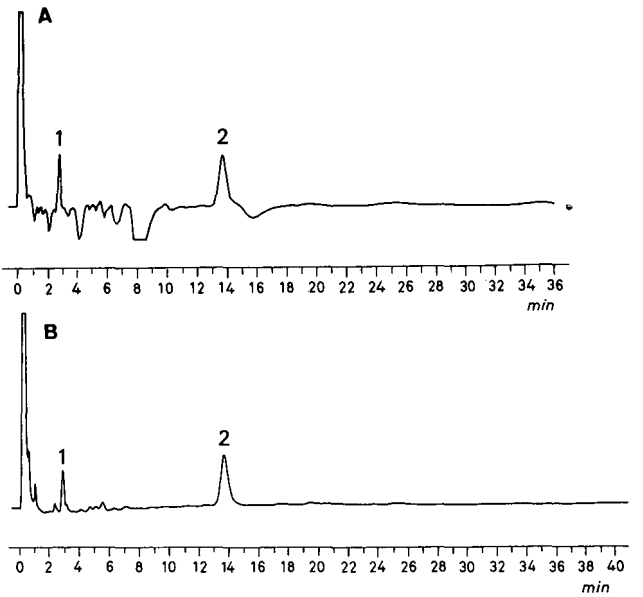

Fig. 1. Gas chromatogram of human milk extract obtained according to the method of Suzuki *et al.*[3], (A) before and (B) after the sulphuric acid clean-up. Peaks: 1 = HCB; 2 = *p,p'*-DDE. For conditions, see text.

marine organisms such as mussels and seal liver could be analysed for OCP residues only after applying the described sulphuric acid clean-up. The blank of the method is satisfactory under the GC–ECD conditions used, allowing the determination of OCP residues in milk at ppb (μg/kg) levels.

With respect to the ability of the described clean-up method to destroy unwanted lipidic material, it was found that extracts from ham, milk, mussels and seal liver and muscle after Florisil chromatography[3] normally contain 10–50 mg of lipidic material, which was reduced to just a few milligrams after the sulphuric acid clean-up. This is very important when capillary GC, especially with on-column injection, is used.

CONCLUSIONS

The described method offers a simple, rapid and safe method for a supplemental clean-up of difficult fatty extracts which are insufficiently cleaned up by adsorptive methods. As the procedure requires only disposable items and almost unattended operation, it offers a means of improving the throughput of residue laboratories with significant savings of reagents, glassware and time.

REFERENCES

1 B. McMahon and J. A. Burke, *J. Assoc. Off. Anal. Chem.*, 61 (1978) 640.
2 T. Stijve and F. Brand, *Dtsch. Lebensm.-Rundsch.*, 73 (1977) 41.

3 T. Suzuki, K. Ishikawa, N. Sato and K.-I. Sakai, *J. Assoc. Off. Anal. Chem.*, 62 (1979) 681.
4 A. V. Holden and K. Marsden, *J. Chromatogr.*, 44 (1969) 481.
5 P. A. Greve and W. B. F. Grevenstuck. *Meded. Rijksfac. Landbouwwet. Gent*, 40 (1975) 1115.
6 H. Steinwandter and H. Schluter, *Fresenius' Z. Anal. Chem.*, 286 (1977) 90.
7 H. Steinwandter and H. Schluter, *Dtsch. Lebensm.-Rundsch.*, 74 (1978) 139.
8 S. M. Waliszewski and G. A. Szymcsynski, *J. Assoc. Off. Anal. Chem.*, 65 (1982) 677.
9 A. L. Smrek and L. L. Needham, *Bull. Environ. Contam. Toxicol.*, 28 (1982) 718.
10 W. Specht and M. Tilkes, *Fresenius' Z. Anal. Chem.*, 322 (1985) 443.
11 K. Kypke-Hutter, J. Vogelgesang, R. Malish, P. Binneman and H. Wetzlar, *Z. Lebensm.-Unters.-Forsch.*, 182 (1986) 464.
12 R. L. Stanley and H. T. Le Favoure, *J. Assoc. Off. Anal. Chem.*, 48 (1965) 666.
13 A. Di Muccio, A. M. Cicero, I. Camoni, D. Pontecorvo and R. Dommarco, *J. Assoc. Off. Anal. Chem.*, 70 (1987) 106.
14 A. Di Muccio, M. Rizzica, A. Ausili, I. Camoni, R. Dommarco and F. Vergori, *J. Chromatogr.*, 456 (1988) 143.
15 A. Di Muccio, A. Ausili, I. Camoni, R. Dommarco, M. Rizzica and F. Vergori, *J. Chromatogr.*, 456 (1988) 149.
16 A. S. Y. Chau, *Bull. Environ. Contam. Toxicol.*, 8 (1972) 169.

Journal of Chromatography, 513 (1990) 338–343
Elsevier Science Publishers B.V., Amsterdam

CHROM. 22 467

Note

Gas–liquid chromatographic analysis of carboxymethylcellulose and carboxymethylstarch

SHIGEO UKAI*, ATSUKO HONDA, KATSUYUKI NAGAI and TADASHI KIHO
Gifu Pharmaceutical University, 6–1, Mitahora-higashi 5-chome, Gifu 502 (Japan)
(Received January 8th, 1990)

Carboxymethylcellulose (CMC) and carboxymethylstarch (CMS) have been employed as important industrial polymers in textile processing, detergents, drilling fluids and protective coatings. The purified grades have been used extensively in the pharmaceutical, cosmetic and food industries. The suitability of CMC or CMS in actual applications is influenced by the degree of substitution (the average number of carboxymethyl groups substituted per anhydroglucose unit) and the distribution of the carboxymethyl substituents. Various methods have been reported for the determination of the DS (degree of sustitution) in CMC and CMS, such as chemical titration[1–4], spectrophotometry[1,5] and electrometric titration[1,6]. However, these methods determine only the DS without providing information on the distribution of the carboxymethyl substituents. Recently, Ho and Klosiewicz[7] reported on the distribution of the substituents on CMC by proton nuclear magnetic resonance spectrometry.

This paper deals with determination of the DS and the distribution of the carboxymethyl groups in both CMC and CMS by a gas–liquid chromatographic (GLC) method based on a modification of previous work[8].

EXPERIMENTAL

Reagents

All chemicals were of analytical-reagent grade. Sodium borohydride was purchased from Kishida (Osaka, Japan) and other reagents from Nacalai Tesque (Kyoto, Japan). Amberlite CG-120 was purchased from Organo (Tokyo, Japan). CMC (DS = 0.6–0.8) and CMC (DS = 1.0–1.5) were kindly provided by Daicel (Osaka, Japan) and CMS (DS = 0.3–0.5) was obtained from Nikka (Fukui, Japan).

Evaporation

All evaporations were conducted under reduced pressure at bath temperatures not exceeding 40°C.

Reduction of carboxymethylglucans

CMC (DS = 0.6–0.8) (100 mg) was dissolved in water (30 ml), then 1-ethyl-3-

0021-9673/90/$03.50

(3-dimethylaminopropyl)carbodiimide (EDC) (1 g) was added. As the reaction proceeded, the pH of the reaction mixture was maintained at 4.75 by titration with 0.1 *M* hydrochloric acid (HCl) with stirring for 2 h. Then 2 *M* sodium borohydride ($NaBH_4$) (10 ml) was added slowly to the reaction mixture at room temperature. The pH of the mixture rose rapidly to 7.0 and the mixture was maintained at this pH by titration with 4 *M* HCl. The solution was dialysed against water overnight, then the non-dialysable solution was concentrated to *ca.* 30 ml. The product was reduced twice more under the same conditions. The final non-dialysable solution was lyophilized to yield 85.3 mg as the hydroxyethyl product HCMC-1. CMC (DS = 1.0–1.5) (100 mg) was reduced under the same conditions to give 82.2 mg as the hydroxyethyl product HCMC-2. CMS (DS = 0.3–0.5) (100 mg) was treated in the same manner to yield 62.3 mg as hydroxyethyl product HCMS.

Preparation for GLC analysis

Reduced carboxymethylglucans (5 mg), *i.e.*, hydroxyethylglucans (HCMC-1, HCMC-2 and HCMS), were hydrolysed with 90% formic acid (1.5 ml) at 100°C for 5 h and the solution was evaporated to dryness. The residue was dissolved in 2 *M* trifluoroacetic acid (TFA) (1 ml) and heated at 100°C for 4 h. The solution was evaporated to dryness and the dried hydrolysates were reduced with $NaBH_4$ (5 mg) in water (2 ml) for 3 h at room temperature, then passed through a column of Amberlite CG-120(H^+). The eluate was evaporated to dryness and the resulting boric acid in the residue was removed as trimethyl borate by repeated evaporation with methanol. The sample was dried and acetylated with acetic anhydride–pyridine (1:1) (1 ml) at 95°C for 2 h. Toluene (1 ml) was added to the reaction mixture in order to remove the residual acetic anhydride and pyridine as an azeotropic mixture[8], then evaporated to dryness. The residue was dissolved in chloroform (50 μl) and the solution was injected into the gas chromatograph.

Gas–liquid chromatography

The samples were analysed using a Shimadzu 4 CM chromatograph equipped with a hydrogen flame ionization detector. A glass column (1.5 m × 0.3 cm I.D.) packed with 2% EGSS-X on Chromosorb W AW DMCS (60–80 mesh) was used at 215°C and a nitrogen flow-rate of 60 ml/min. Peak areas and retention times were measured by use of a Shimadzu Chromatopac C-R5A integrator. The samples were also analysed with a CP-Sil 88 FS-WCOT fused-silica capillary column (25 m × 0.25 mm I.D.) with temperature programming (after injection at 180°C, held for 70 min, the temperature was increased at 0.5°C/min to 190°C, held for 70 min, at 0.5°C/min to 200°C held for 70 min, at 0.5°C/min to 210°C, held for 70 min, and finally at 0.5°C/min to 220°C) at a pressure of 60 kPa (1.3 kg/cm^2) of helium, with a splitting ratio of 1:157.

RESULTS AND DISCUSSION

The reduction of the carboxymethylglucans (CMC and CMS) to the hydroxyethylglucans (HCMC and HCMS) was carried out by the method used by Taylor and co-workers[9,10] for the reduction of the carboxyl group of uronic acid residues in polysaccharides. The carboxymethylglucans were reacted with 1-ethyl-3-(3-dimethyl-

TABLE I

GLC AND GLC–MASS SPECTROMETRY OF SUGAR DERIVATIVES FROM HYDROLYSATES OF REDUCED CARBOXYMETHYLGLUCAN

GLC–mass spectrometry was carried out as described previously[8].

Peak No.	*Relative retention time*[a,b]	*Sugar derivatives*[c] *(as acetate)*	*Prominent fragments (m/z)*	*Percentage from peak area*[a,b]		
				HCMC-1	*HCMC-2*	*HCMS*
1	0.62(0.58)	1,2-O-etn-α-D-Gf	43 73 127 170 187 212 273	2.98	3.41	5.41
2	0.77(0.59)	1,2-O-etn-α-D-Gp	43 73 86 157 170 199 230 259 272	5.39	5.95	9.24
3	1.00(1.00)	G	43 73 145 217 289 361 375	39.94	18.50	61.79
4	1.64(1.32)	1,2-O-etn-β-D-Gp	43 73 86 157 170 199 230 259 272	2.11	1.52	3.96
5	1.91(1.54)	1,2-O-etn-6-O-he-α-D-Gf	43 73 87 127 187	1.82	2.88	0.53
6	2.54(1.70)	1,2-O-etn-6-O-he-α-D-Gp	43 73 86 87 157 199 274 316	4.46(2.99)	7.23(5.31)	1.76
	(1.95)	1,2-O-etn-3-O-he-α-D-Gf	43 73 87 127 170 212 272	(1.47)	(1.92)	
7	2.92(2.21)	6-O-he-G	43 87 115 117 375	14.43	13.52	1.69
8	3.34(2.43)	2-O-he-G	43 73 87 115 189 375 405	17.67(9.41)	21.12(12.39)	15.72(10.18)
	(2.53)	3-O-he-G	43 87 115 261 333 375	(8.26)	(8.73)	(5.54)
9	3.88(2.73)	1,2-O-etn-3-O-he-D-Gp	43 73 86 87 157 170 243	2.63	3.62	
10	4.99(2.97)	1,2-O-etn-6-O-he-β-D-Gp	43 73 86 87 157 199 274 316	1.90	2.83	0.77
11	10.15(3.95)	2,3-O-dihe-G	43 73 87 189 305 375 449	6.67	20.22	0.11

[a] Relative to hexa-O-acetyl-D-glucitol.

[b] Values in parentheses were obtained with a capillary column (CP-Sil 88).

[c] Glucitol (G) derivatives except for 1,2-O-ethyleneglucose (Gf and Gp) derivatives.

aminopropyl)carbodiimide in aqueous media and the resulting carbodiimide-activated carboxymethylglucans were reduced with $NaBH_4$ to yield the hydroxyethylglucans. From the results of carbon-13 nuclear magnetic resonance spectroscopy of the reduced carboxymethylglucans (hydroxyethylglucans) in 2 *M* NaO^2H, the complete reduction of carboxymethyl groups were confirmed by there being no signal in the carbonyl region of the spectrum. These reduced carboxymethylglucans were hydrolysed with formic acid and then TFA. In the acidic hydrolysis, the resulting 2-O-hydroxyethylglucose derivatives were partially converted into 1,2-O-ethyleneglucose derivatives[8]. The hydrolysates thus obtained were reduced with $NaBH_4$ and acetylated with acetic anhydride in pyridine.

The sugar derivatives from the acid hydrolysates of reduced CMC (DS = 0.6–0.8) (HCMC-1) were separated with a 2% EGSS-X glass column. By reference to the retention time of authentic standards and mass spectral analysis[11], the individual peaks in Table I were identified with increasing retention time as follows: 1,2-O-ethylene-α-D-glucofuranose (1,2-O-etn-α-D-Gf), 1,2-O-ethylene-α-D-glucopyranose (1,2-O-etn-α-D-Gp), glucitol (G), 1,2-O-etn-β-D-Gp, 1,2-O-ethylene-6-O-hydroxyethyl-α-D-glucofuranose (1,2-O-etn-6-O-he-α-D-Gf), 1,2-O-ethylene-6-O-hydroxyethyl-α-D-glucopyranose (1,2-O-etn-6-O-he-α-D-Gp), 1,2-O-etn-3-O-he-α-D-Gf, 6-O-hydroxyethylglucitol (6-O-he-G), 2-O-he-G, 3-O-he-G, 1,2-O-etn-3-O-he-D-Gp, 1,2-O-etn-6-O-he-β-D-Gp, 2,3-di-O-hydroxyethylglucitol (2,3-O-dihe-G). 2-O-He-G and 3-O-he-G could not be separated satisfactorily with this 2% EGSS-X glass column, so they were also analysed with a CP-Sil 88 capillary column. The assignment of 2-O-he-G for peak 8 reported previously[8] was corrected to overlap of 2-O-he-G and 3-O-he-G, and the assignment of 3-O-he-G for peak 9 was corrected to 1,2-O-etn-3-O-he-D-Gp from the present study with a capillary column. Also, the previous peak 6 was separated into 1,2-O-etn-6-O-he-α-D-Gp and 1,2-O-etn-3-O-he-α-D-Gf by the capillary column. As reported previously[8], the GLC analysis of hydroxyethylcellulose and hydroxyethylstarch synthesized by the reaction of ethylene oxide with cellulose and starch gave 2-O-(2′-hydroxyethoxy)ethylglucitol and its derivatives. However, with the hydroxyethylglucans (HCMC and HCMS) prepared by the reduction of CMC and CMS, no such compounds are afforded. CMC (DS = 1.0–1.5) and CMS (DS = 0.3–0.5) were reduced under the same conditions to give HCMC-2 and HCMS, and analysed by the same GLC method as HCMC-1. The sugar derivatives of each sample are summarized in Table I. The distribution patterns of carboxymethyl groups in each glucan are also shown in Table I. The carboxymethyl groups were located mainly at O-2 and O-2,3 of the glucosyl residue in CMC, and at O-2 of the glucosyl residue in CMS. The proportion of 6-O-carboxymethylglucosyl residue in CMC was greater than that in CMS. The DS values of these samples measured by this method are similar to those listed in commercial products (see Table II).

In conclusion, complete reduction of carboxymethyl groups to hydroxyethyl groups was carried out by the reaction of carboxymethylglucan with carbodiimide and sodium borohydride. The hydrolysates of the resulting hydroxyethylglucans were analysed by a GLC method as the acetates of alditol and 1,2-O-ethyleneglucose derivatives. As the substituted sugars in these carboxymethylglucans can be accurately determined, the DS and the distribution of carboxymethyl substituent can be determined satisfactorily. This method simplifies the determination of the degree and pattern of carboxymethyl substitution of CMC and CMS.

TABLE II

PATTERNS OF CARBOXYMETHYL SUBSTITUTION ON GLUCOSE UNIT IN CMC AND CMS

Compound	*Percentage of total*						
	Glc	*2-cmG*[a]	*3-cmG*	*6-cmG*	*2,3-dicmG*[b]	*2,6-dicmG*[c]	*DS*[d]
HCMC-1 [CMC (DS 0.6–0.8)]	39.94	19.89	8.26	14.43	13.76	3.72	0.78
HCMC-2 [CMC (DS 1.0–1.5)]	18.50	23.27	8.73	13.52	31.07	5.71	1.19
HCMS [CMS (DS 0.3–0.5)]	61.79	28.79	5.54	1.69	0.87	1.30	0.40

[a] Total of 2-he-G: 1,2-O-etn-α-D-Gf, 1,2-O-etn-α-D-Gp, 1,2-etn-β-D-Gp, 2-O-he-G.
[b] Total of 2,3-dihe-G: 1,2-O-etn-3-O-he-α-D-Gf, 1,2-O-etn-3-O-he--D-Gp, 2,3-O-dihe-G.
[c] Total of 2,6-dihe-G: 1,2-O-etn-6-O-he-α-D-Gf, 1,2-O-etn-6-O-he-α-D-Gp, 1,2-etn-6-O-he-β-D-Gp.
[d] Degree of substitution.

REFERENCES

1 R. W. Eyler, E. D. Klug and F. Diephuis, *Anal. Chem.*, 19 (1947) 24.
2 I. Sakurada, *J. Soc. Chem. Jpn.*, 31 (1938) 19.
3 A. Z. Conner and R. W. Eyler, *Anal. Chem.*, 22 (1950) 1129.
4 C. V. Francis, *Anal. Chem.*, 25 (1953) 941.
5 S. Mukhopadhyay, B. Ch. Mitra and S. R. Palit, *Anal. Chem.*, 45 (1973) 1775.
6 H. C. Black, Jr., *Anal. Chem.*, 23 (1951) 1792.
7 F. F.-L. Ho and D. W. Klosiewicz, *Anal. Chem.*, 52 (1980) 913.
8 S. Ukai, A. Honda, K. Nagai, T. Kiho and T. Tsuchiya, *J. Chromatogr.*, 435 (1988) 374.
9 R. L. Taylor and H. E. Conrad, *Biochemistry*, 11 (1972) 1383.
10 R. L. Taylor, J. E. Shively and H. E. Conrad, *Methods Carbohydr. Chem.*, 6 (1976) 149.
11 K. Nagai, A. Honda, T. Kiho and S. Ukai, *Carbohydr. Res.*, 190 (1989) 165.

Journal of Chromatography, 513 (1990) 344–348
Elsevier Science Publishers B.V., Amsterdam

CHROM. 22 461

Note

Identification of very long polyenoic acids as picolinyl esters by Ag^+ ion-exchange high-performance liquid chromatography, reversed-phase high-performance liquid chromatography and gas chromatography–mass spectrometry

TOMÁŠ ŘEZANKA
Institute of Microbiology, Czechoslovak Academy of Sciences, 142 20 Prague 4 (Czechoslovakia)
(First received February 16th, 1990; revised manuscript received March 19th, 1990)

Very long-chain fatty acids, *i.e.*, acids with 22 carbon atoms and longer, have recently been investigated[1,2], but they were mostly saturated fatty acids. In very long-chain polyunsaturated fatty acids (VLCPUFA) the situation is much more complicated and few systematic studies of their isolation and identification have been reported. So far, their occurrence has been demonstrated primarily in animal tissues (*e.g.*, the retina and in various brain diseases such as Zellweger syndrome)[3,4] and in marine species such as the herring (*Clupea harengus*)[5] and sponges[6].

The main problem in the identification of these compounds in natural materials is their low concentrations, which usually do not exceed, with a few exceptions (*e.g.*, certain sponges), tenths of a percent. Their identification is also complicated by their sensitivity to heat and aerial oxygen. In previous methods natural fatty acid mixtures were enriched with VLCPUFA and analyses were based mainly on chromatographic methods[4]. The detection of eluted components is complicated as fatty acids hardly absorb in the UV region. Therefore, it is necessary to use either terminal absorption of the carboxylic bond or of double bond(s) or to derivatize the carboxylic group. Picolinyl esters are the only derivatives that can later be used also for gas chromatographic–mass spectrometric (GC–MS) identification. Unlike the use of pyrrolidides, which show only terminal absorption in the UV spectrum, Ag^+ ion-exchange high-performance liquid chromatography (HPLC) and reversed-phase (RP) HPLC, the former method separating compounds according to the number of double bonds and the latter according to the equivalent chain number, appear to be the most promising. Ion-exchange HPLC has only been applied to methyl esters[7], whereas by means of RP-HPLC picolinyl esters could also be separated[8]. In this work the advantages of both methods were combined, followed by identification of the eluted components by GC–MS with the aim of preparing standards that are not available commercially.

0021-9673/90/$03.50

EXPERIMENTAL

Materials

Free fatty acids were obtained by basic hydrolysis of total lipids obtained by extraction of fish meat with chloroform–methanol[9]. Picolinyl esters were prepared from free fatty acids by reaction with thionyl chloride followed by 3-pyridyl carbinol as described by Harvey[10]. The reaction mixture was diluted with water, extracted with hexane and evaporated to dryness. The residue was dissolved in diethyl ether and purified on Supelclean solid-phase extraction tubes containing LC-NH_2 (Supelco, Gland, Switzerland). The eluate was evaporated to dryness, dissolved in acetonitrile–hexane and stored at −25°C. Aerial oxygen was removed from the solvents used for HPLC by bubbling with helium; 70 mg/l of butylated hydroxytoluene (Sigma, St. Louis, MO, U.S.A.) were added to other solvents. All the vessels and the rotary evaporator were flushed with nitrogen before use.

HPLC

Preparative HPLC was performed in a Gradient LC System G-I (Shimadzu, Kyoto, Japan) with two LC-6A pumps (4 ml/min), an SCL-6A system controller, an SPD ultraviolet detector (266 nm), a SIL-1A sample injector and a C-R3A data processor. Semi-preparative columns, 30 cm × 7.9 mm I.D. packed with a strongly acidic cation exchanger (SO_3H groups, SCR-101 H, 10-μm spherical particles; Shimadzu) impregnated according Christie *et al.*[7], and 25 cm × 21.1 mm I.D. packed with ODS(5-μm particles; Shimadzu) were employed.

Silver ion exchange

After injection of 10 mg of picolinyl esters, elution was carried out with a gradient from hexane–dioxane–isopropanol (40:10:50) to dioxane–isopropanol (50:50) in 20 min and then to pure isopropanol in a further 25 min.

In the reversed-phase mode, 5 mg were injected and elution was carried out with a gradient from water–acetic acid–triethylamine–methanol–isopropanol (291:3:6:690:10) to the same mixture in the proportions 9.7:0.1:0.2:700:290 in 28 min and then isocratically for 15 min.

Individual classes of picolinyl esters and individual picolinyl esters after HPLC were collected and evaporated.

GC–MS

The fraction containing both 28:7 isomers was separated and identified using a Finnigan MAT (San Jose, CA, U.S.A.) 1020 B instrument. The injector temperature was 100°C and an HP-1 cross-linked methylsilicone (Hewlett-Packard, Palo Alto, CA, U.S.A.) fused-silica capillary column (25 × 0.2 mm I.D. film thicknes 0.11 μm) was used. The temperature programme was 100°C (1 min), then increased at 20°C/min to 230°C and at 4°C/min to 339°C. The carrier gas was hydrogen at a flow-rate of 75 cm/s. The ionization energy was 70 eV and mass spectra were scanned in the range m/z 150–550.

Infrared spectroscopy

For scanning infrared spectroscopy of the fraction 28:7$n-6$ and 28:7$n-3$ (in

carbon tetrachloride), a Perkin-Elmer Model 1310 infrared spectrophotometer was used.

RESULTS AND DISCUSSION

As described previously[9], herring is a suitable source of VLCPUFA, even if only of $n-3$ isomers. In that work, two 28:7 positional isomers, *i.e.*, $n-3$ and $n-6$, were identified in preliminary tests. In the present work, attention was therefore focused on a conclusive demonstration of the previously proposed structure. Combination of HPLC–GC of picolinyl esters having satisfactory chromatographic properties, either in HPLC or GC, *i.e.*, with an aromatic ring showing intensive UV absorption and not too high an elution temperature, can accelerate both qualitative and quantitative analyses. Separation of picolinyl esters by means of Ag^+ ion-exchange HPLC has not previously been described. It was necessary to solve two problems, *viz.*, detection of the eluted compounds and the question of whether the contribution of the double bond is sufficient for separation as the picolinyl ester already contains an aromatic system. Picolinyl esters fulfil very well the first condition, absorbing at 266 nm ($\varepsilon = 10^4$). When solving the latter problem we utilized literature data[11] on the chromatography on benzoyl derivatives of non-hydroxy fatty acid ceramides. Although the molecule of ceramides after derivatization contained a benzene ring, it was not difficult to separate compounds with 0–3 double bonds.

On the chromatogram obtained by means of Ag^+ ion-exchange HPLC (Fig. 1a), seven distinctly separated peaks can be seen. Unfortunately, the peak 6+7 contains compounds with six and seven double bonds. RP-HPLC as described by Christie and Stefanov[8] was used for an additional semi-preparative separation. However, it was found that the separation of picolinyl esters without a buffer, *i.e.*, in pyridine–acetic acid, is poor and therefore a mass detector had to be used instead of a UV detector. The problem can be solved by replacing pyridine with triethylamine as the elution mixture

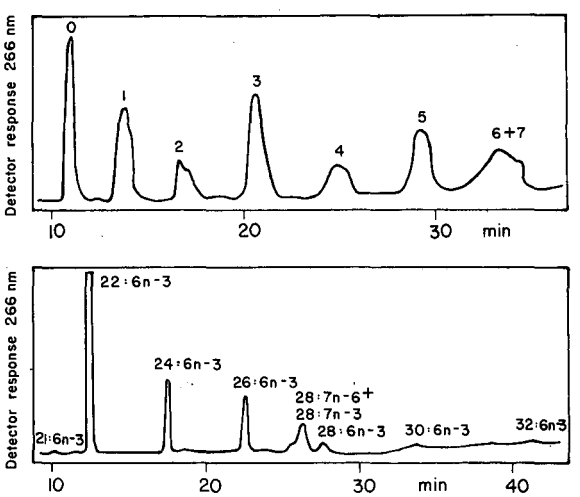

Fig. 1. Preparative chromatography of picolinyl esters from herring. For conditions, see text. Top: preparative Ag^+ ion-exchange HPLC. Bottom: preparative RP-HPLC.

no longer absorbs above 230 nm. By applying RP-HPLC, individual esters could be separated to the baseline, except for 28:7 positional isomers.

Common methods for the determination of configurations of double bond(s) include infrared spectroscopy. Some peaks at 967 cm^{-1}, *i.e.*, the characteristic absorbance for *trans* isomers, were not identified. From the above argument is to be expected that double bonds are *cis*.

Separation of $n-3$ and $n-6$ methyl esters and of free PUFA is in general difficult. Aveldano *et al.*[4] separated 22:5$n-3$ from 22:5$n-6$, whereas Narce *et al.*[12] could not separate 18:3$n-3$ and 18:3$n-6$. With picolinyl esters, none of the positional isomers, *e.g.*, 18:3$n-3$ and $n-6$, 20:3$n-3$ and $n-6$ and 20:4$n-3$ and $n-6$) could be separated[8]. It follows from Fig. 1b that both 28:7 isomers are partially separated, but the separation is not sufficient for further identification. GC of VLCPUFA on capillary columns has been reported only a few times[13,14] and only using non-polar columns. In previous work[9] both 28:7 isomers were separated as methyl esters on a polar capillary column for the first time. However, picolinyl esters of 28:7 isomers were not eluted from the same column. Christie *et al.*[15] also found that it is necessary to increase the elution temperature of picolinyl esters by 50°C above that for methyl esters. Therefore, in the case of peaks 6+7, it was necessary to use a non-polar phase. The elution order $n-9$, $n-6$, $n-3$ (22:3$n-9$, 22:3$n-6$ or 35:6$n-6$, 36:6$n-3$) was found for methyl esters[14] and the same order was also observed for picolinyl esters (22:5$n-6$, 22:5$n-3$)[15].

GC–MS of the mixed peak 28:7 obtained after RP-HPLC confirmed the assumptions concerning the elution order, i.e., 28:7$n-6$ was followed by 28:7$n-3$, which was demonstrated by the mass spectra (see Fig. 2). Interpretation of the mass spectra of picolinyl esters has been described[10,15,16]. In polyenoic acids containing methylene-interrupted double bonds, gaps of 26 u for any double bond were found. However, Christie[16] showed that it is easier to detect gaps of 40 u between the terminal

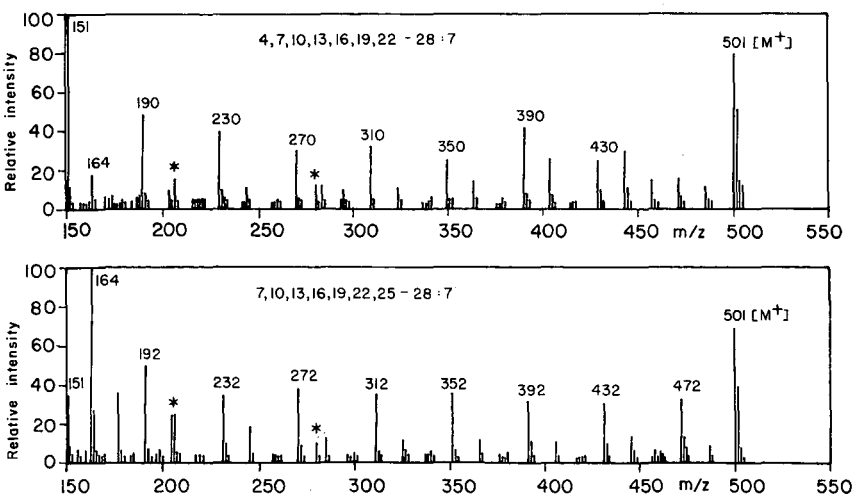

Fig. 2. Mass spectra of picolinyl esters of octacosaheptaenoic acids. Top: mass spectrum of 28:7$n-6$ picolinyl esters. Bottom: mass spectrum of 28:7$n-3$ picolinyl esters. Asterisks indicate peaks of polysiloxanes (stationary phase).

end of any of the double bonds and the methylene group on the carboxyl end. This fact was confirmed also with the two 28:7 isomers. It follows from Fig. 2 (top) that the molecular ion (*m/z* 501) was present and that degradation products (M − 15, M − 15 − 14, etc.) could be found. The first double bond from the CH_3 end is in position *n* − 6, as also reflected by an ion of *m/z* 430. Gaps of 26 u are not so pronounced as 40 u and, hence, are much more suitable for identification. A certain problem arose with the identification of the Δ^4 double bond, where a gap of only 26 u could be demonstrated. With the second isomer (Fig. 2, bottom) the situation is almost identical, values of diagnostically significant ions differing by only 2 u, being shifted towards higher values. The ratio of ions of *m/z* 151 and 164 is another auxiliary criterion for the position of the double bond. When this bond is not in the Δ^4 position the abundance of the ion of *m/z* 164 is higher than that of the ion of *m/z* 151 (see Fig. 2 and the literature[10,16]). In the presence of the Δ^4 double bond the opposite occurs (Fig. 2). As the abundance of ions above *m/z* 150 is low with these polyenes, as also described by Harvey[10], we scanned the mass spectra beginning with *m/z* 150. Ions having lower *m/z* values are diagnostically not very significant. The chromatographic behaviour of both 28:7 isomers is in agreement with the data obtained so far, *i.e.*, the order is *n* − 6–*n* − 3. The mass spectra of both isomers of picolinyl esters are clearly different and ions with gaps of 40 u are much more intense and hence more significant for identification than ions with gaps of 26 u. Both isomers therefore yield sufficiently characteristic spectra that can be used for their identification and determination of their structure.

It can be concluded that the above combination of three separation methods, *i.e.*, ion-exchange HPLC, RP-HPLC and GC–MS of picolinyl esters, yields conclusive data even in the identification of unusual VLCPUFA. The use of characteristic gaps of 40 u during the degradation of polyene picolinyl esters can also contribute to their easier identification. Naturally, the combination of the above methods is not limited only to VLCPUFA from fish but can also be used with any biological material containing these rare acids.

REFERENCES

1 T.Řezanka, *Prog. Lipid. Res.*, 28 (1989) 147.
2 J. M. Tiffany, *Adv. Lipid Res.*, 22 (1987) 1.
3 A. Poulos, *Prog. Lipid Res.*, 28 (1989) 35.
4 M. I. Aveldano, M. Van Rollins and L. A. Horrocks, *J. Lipid Res.*, 24 (1983) 83.
5 R. R. Linko and H. Karinkanta, *J. Am. Oil Chem. Soc.*, 47 (1970) 42.
6 M. P. Lawson, P. R. Berquist, A. Lawis and R. C. Cambie, *Biochem. Syst. Ecol.*, 12 (1984) 63.
7 W. W. Christie, E. Y. Brechany and K. Stefanov, *Chem. Phys. Lipids*, 46 (1988) 127.
8 W. W. Christie and K. Stefanov, *J. Chromatogr.*, 392 (1987) 259.
9 T. Řezanka, *LC · GC*, 8 (1990) in press.
10 D. J. Harvey, *Biomed. Mass Spectrom.*, 11 (1984) 340.
11 M. Smith, P. Monchamp and F. B. Jungalwala, *J. Lipid. Res.*, 22 (1981) 714.
12 M. Narce, J. Gresti and J. Bezard, *J. Chromatogr.*, 448 (1988) 249.
13 W. M. Grogan, *Lipids*, 19 (1984) 341.
14 A. Poulos, P. Sharp, D. Johnson and C. Easton, *Biochem. J.*,253 (1988) 645.
15 W. W. Christie, E. Y. Brechany, S. B. Johnson and R. T. Holman, *Lipids*, 21 (1986) 657.
16 W. W. Christie, *Gas Chromatography and Lipids*, Oily Press, Ayr, 1989.

Journal of Chromatography, 513 (1990) 349–353
Elsevier Science Publishers B.V., Amsterdam

CHROM. 22 473

Note

Information theory of column chromatography on the basis of the information measure FUMI

YUZURU HAYASHI* and RIEKO MATSUDA
National Institute of Hygienic Sciences, 18–1, Kamiyoga 1-Chome, Setagaya-ku, Tokyo 158 (Japan)
(First received December 8th, 1988; revised manuscript received January 23rd, 1990)

Precision and accuracy are of the greatest importance in all aspects of the theory and practice in analytical chemistry[1]. The information measure FUMI (FUnction of Mutual Information) quantitatively describes the precision of measurements in chromatography[2–4] and the concept involved is known in information theory as mutual information[5]. The optimum condition can be clearly defined as one which can provide the maximum amount of mutual information FUMI.

The aim of this paper is to consider the amount of information obtained from peaks in some chromatographic circumstances from the viewpoint of information theory based on FUMI. The treatment of the optimum peak separation has disparate views in the so-far developed optimization methods using the resolution R_s[6–9]. The optimum separation can be deduced as a theoretical consequence from the maximum amount of FUMI.

UNDERLYING CONCEPT

The optimum peak separation under a particular operating condition can be derived from FUMI[10]. If the leading peak ($j = 1$) is fixed at a retention time τ_1, then the optimum retention time $\hat{\tau}_2$ ($>\tau_1$) for the second peak is expressed as

$$\hat{\tau}_2 = \frac{N^{1/2} + \gamma}{N^{1/2} - \gamma} \cdot \tau_1 \tag{1}$$

where N denotes the plate number of the column and γ is a constant ($= 2.07$). Using the well known approximation[11,12] $(1 + x/2)/(1 - x/2) \approx 1 + x$, we obtain the least capacity factor $\hat{k}_2$ corresponding to $\hat{\tau}_2$:

$$\hat{k}_2 = \left(1 + \frac{2\gamma}{N^{1/2}}\right) k_1 + \frac{2\gamma}{N^{1/2}} \tag{2}$$

In the above, the peak areas A_j are assumed to be the same. The optimum peak

0021-9673/90/$03.50

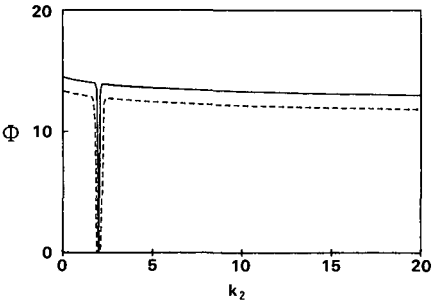

Fig. 1. Effect of the degree of peak overlap on FUMI for a two-peak system. The capacity factor k_1 is fixed (= 2); k_2 is varied. A_j = 5000 (j = 1, 2); N = 10 000 (solid line) or 1000 (dashed line); the hold-up time τ_0 = 200; $\tilde{a}$ = 1; γ = 2.07. Filtering-off points: $\kappa_f(1) = \tau_2 - \beta\sigma_2$; $\kappa_f'(2) = 2\tau_2 - (\tau_1 + \beta\sigma_1)$, where $\beta = 2\gamma - \pi^{1/2}/2^{10}$.

separation was derived under the condition that the optimum suffers no strong peak overlap, *i.e.*, the information loss $\delta\Phi = 0$.

CHROMATOGRAPHIC POWERS

Fig. 1 shows the influence of peak overlap and separation on the mutual information Φ. It is assumed that one peak is fixed at a position τ_1 and the other moves; the other variables, N, A_j, etc., are invariant. There exists a deep trough, which stems from strong peak overlap. In addition to the trough, the FUMI Φ gradually decreases with increasing capacity factor k_2 of the moving peak because of the peak-widening effect[3].

The maximum of FUMI at the right-hand side of the trough shown in Fig. 1 indicates the optimum separation for peaks in a column of plate number N. The maximum information can be obtained from the optimally separated peaks and can be derived from eqn. 2 and FUMI[3,4]:

$$\Phi = \psi_1^* + \psi_2^* - \frac{1}{2}\log\left[(k_1 + 1)^2\left(1 + \frac{2\gamma}{N^{1/2}}\right)\right] \tag{3}$$

where

$$\psi_j^* \equiv \frac{1}{2}\log\left(\frac{A_j^2 N^{1/2}}{2\pi^{1/2}\tau_0\tilde{a}}\right) \tag{4}$$

τ_0 is the hold-up time and $\tilde{a}$ denotes the power spectrum intensity of white noise[4]. The function $N/(1 + 2\gamma/N^{1/2})$ involved in Φ increases monotonously with respect to N and then the plate number effect varies accordingly. If N = 1000 and k_1 = 2.00, then $\hat{k}_2$ = 2.39 and Φ = 12.76. If N is improved, FUMI selects sharper but closer peaks of higher precision as the optimum. If N = 10 000 and k_1 = 2.00, then $\hat{k}_2$ = 2.14 and Φ = 13.95.

The information Φ can vary, even if the relative retention α (= k_2/k_1) is kept

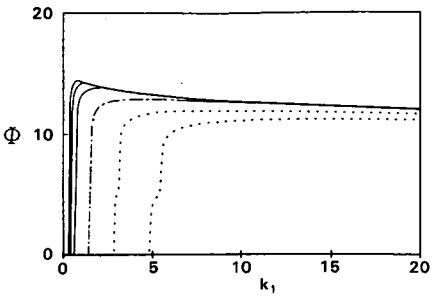

Fig. 2. Effect of capacity factor k_1 on FUMI for various values of the relative retention α. $A_j = 5000$; $\tilde{a} = 1$; $\gamma = 2.07$; $N = 10\,000$; $\tau_0 = 200$. $\hat{\alpha} = 1.041$ (theoretical). From top to bottom, $\alpha = 1.100$ [the maximum of $\Phi = 14.48$ ($\delta\Phi = 0$) at $k_1 = 0.78$ from simulation (0.73 from eqn. 5)]; 1.080 [$\Phi_{max} = 14.28$ (0.005) at $k_1 = 1.16$ (1.12)]; 1.060 [$\Phi_{max} = 13.88$ (0.025) at $k_1 = 2.16$ (2.38)]; 1.040 [$\Phi_{max} = 12.89$ (0.509) at $k_1 = 4.28$]; 1.030 [$\Phi_{max} = 11.92$ (0.956) at $k_1 = 7.92$]; 1.025 [$\Phi_{max} = 11.18$ (1.181) at $k_1 = 13.88$].

constant. As the capacity factors k_1 and k_2 of the peaks increase, the mutual information increases abruptly, reaches a maximum and gradually decreases [see Fig. 2 (solid lines)]. The small amounts of information at both sides of the Φ maximum can be attributed to too strong peak overlap and excessive widening of peaks. The maximum information in Fig. 2 is given approximately by substituting in FUMI the optimum capacity factors of the constant α:

$$\hat{k}_1 \approx \frac{2\gamma}{N^{1/2}(\alpha - 1) - \gamma(\alpha + 1)} \tag{5}$$

(and $\hat{k}_2 = \alpha\hat{k}_1$ when eqn. 1 is used).

A column of plate number N has a definite lower limit $\hat{\alpha}$ and any peaks characterized by α ($<\hat{\alpha}$) cannot be quantified with the required precision in the column:

$$\hat{\alpha} = 1 + \frac{2\gamma}{N^{1/2}} \tag{6}$$

This can be obtained from the restriction that the denominator in eqn. 5 should be positive. The behaviour of the information Φ towards α is shown in Fig. 2 (N = constant). If α is larger than the lower limit, then the mutual information Φ takes a high peak (solid lines). A drastic change in Φ occurs at the lower limit as a boundary (dot-dashed line). Below the limit $\hat{\alpha}$, FUMI can no longer reach the information obtained above $\hat{\alpha}$ and the peaks fail to provide the precision in any k_1 or k_2 examined (dotted lines). This degraded information is attributed to the unavoidable information loss $\delta\Phi$ arising from strong peak overlap.

Eqn. 6 also indicates that sufficiently separated peaks ($\alpha \geqslant \hat{\alpha}$) can be quantified with satisfactory precision even if a column of lower N [but $N^{1/2} \geqslant 2\gamma/(\alpha - 1)$] is used. It involves at least two cases: (i) a column of the same size but lower N; (ii) a short column of the same plate height. In case (i), the information decreases according to the

equation of FUMI. In contrast, shortening of the column leads to an increase in the information of the sufficiently separated peaks ($\alpha \geqslant \hat{\alpha}$).

A change in the column length L affects the retention time τ_j and plate number N. If the length of the colunn L is changed to xL, FUMI is described by

$$\Phi = \psi_1^* + \psi_2^* - \frac{1}{2} \log [(k_1 + 1)(k_2 + 1)] - \log (x^{1/2}) \tag{7}$$

By replacing N in eqn. 2 with $\hat{x}N$, we can obtain the optimum column length $\hat{x}L$ for the peaks:

$$\hat{x}^{1/2} = \frac{2\gamma}{N^{1/2}} \cdot \frac{k_1 + 1}{k^2 - k_1} \tag{8}$$

Eqns. 3–8 will be useful for determining the amount of information that can be obtained from peaks with the optimum separation in various situations.

Plots of R_s under the same conditions as shown in Figs. 1 and 2 will display no similarity to the plots of FUMI. R_s plots are monotonously increasing functions of k_2 at a fixed k_1 and of k_1 at a fixed α[6]. The plot of R_s against N will be similar in shape to that of FUMI, but there is a difference: $R_s \propto N^{1/2}$; $\Phi = \log N^{1/2} + \text{constant}$. The above results reflect a clear distinction between information and separation.

A two-peak system has been treated here for simplicity. The theory of FUMI can easily be applied to optimization of multi-peak systems without any other conditions because of its additivity: $\Phi = \sum_{j=1}^{q} \varphi_j$ (φ_j denotes the individual peak information). The calculation of FUMI is also very easy: for Gaussian peaks, it requires only peak area, peak width, retention time and noise level.

FUMI contains an arbitrary constant γ which can be determined according to the conformity with linearity of the chromatograph and peak-resolving power of the data processing sytem. In this paper, γ is set at 2.07 for mathematical peak resolution by Kalman filter. FUMI, however, holds for other data processing such as the perpendicular dropping if γ takes another appropriate value. For the optimum peak resolution, γ is closely related to R_s[10]. If the least acceptable separation (*e.g.*, $R_s = 1.5$ or 3.0) is specified, then FUMI can select the optimum conditions according to the corresponding γ. The optima from FUMI and R_s-based criteria will not always be the same because of the difference in the basic concepts.

Analytical applications of FUMI are now under development. Its merits and limitation should be elucidated by further study of the optimization of many chromatographic variables.

REFERENCES

1 D. L. Massart, B. G. M. Vandeginste, S. N. Deming, Y. Michotte and L. Kaufman, *Chemometrics: a Textbook*, Elsevier, Amsterdam, 1988.
2 Y. Hayashi, S. Yoshioka and Y. Takeda, *Anal. Sci.*, 5 (1989) 329.
3 Y. Hayashi and R. Matsuda, *Anal. Chim. Acta*, 222 (1989) 313.

4 Y. Hayashi, *Anal. Sci.*, 6 (1990) 15.
5 S. Arimoto, *Johou Riron (Information Theory)*, Kyoritsu Shuppan, Tokyo, 1976.
6 P. J. Schoenmakers, *Optimization of Chromatographic Selectivity*, Elsevier, Tokyo, 1986.
7 H. J. G. Debets, B. L. Bajema and D. A. Doornbos, *Anal. Chim. Acta*, 151 (1983) 131.
8 C. E. Goewie, *J. Liq. Chromatogr.*, 9 (1985) 1431.
9 J. C. Berridge, *Anal. Chim. Acta*, 191 (1986) 243.
10 Y. Hayashi, *Anal. Sci.*, 6 (1990) 257.
11 J. M. Gidding, *Anal. Chem.*, 39 (1967) 1027.
12 Japan Society of Analytical Chemistry, Kanto Region Branch, *Kosoku Ekitai Kuromatogurafu Bunseki (High-Performance Liquid Chromatographic Analysis)*, Sangyo Tosho, Tokyo, 1982.

Journal of Chromatography, 513 (1990) 354–359
Elsevier Science Publishers B.V., Amsterdam

CHROM. 22 485

Note

Optimization of high-performance liquid chromatographic analysis with UV detection: light-scattering detection to establish the coelution of UV- and non-UV-absorbing constituents

C. ELFAKIR, M. LAFOSSE and M. DREUX*

Laboratoire de Chimie Bioorganique et Analytique (LCBA), URA 499, UFR Sciences, Université d'Orléans, B.P. 6759, F-45067 Orléans Cedex 2 (France)

(First received December 5th, 1989; revised manuscript received April 3rd, 1990)

The high-performance liquid chromatographic (HPLC) analysis of complex mixtures with UV detection can sometimes be difficult to achieve, *e.g.*, with a mixture of trace amounts of a UV-absorbing solute in the presence of large amounts of non-UV-absorbing compounds. However, the choice of UV detection is valuable owing to the specificity and sensitivity of this method in the routine analysis of UV-absorbing solutes at trace levels.

However, quantitative UV measurements can be altered by coelution of non-UV-absorbing and UV-absorbing products, ghost peaks linked to the injection solvent which differs from the mobile phase composition, peaks resulting from the residual solvent in the sample studied, etc. A wavelength change sometimes gives information about other compounds that do not absorb at the wavelength of the solute determination. In spite of this, UV detection does not always permit the optimization of the analytical parameters (repeatability, sensitivity, etc.) in order to obtain a validation method. Hence non-detection of the major products does not enable one to ascertain that the elution of the UV-absorbing product traces and that of the major compounds are not concomitant. Connection of a universal detector to the specific UV detector provides a solution to the problem.

The determination of trace amounts of cetylpyridinium chloride (CPC) in an alcoholic solution illustrates this problem, as large amounts of surfactant are included in cosmetic or pharmaceutical samples, either as an emollients or as lubricants. Several chromatographic methods have been reported for the determination of CPC using various chromatographic systems[1–4], including a rapid and specific HPLC procedure directly applied to CPC in mouthwash[1]. The variability of the results we obtained with this procedure made it necessary to optimize the proposed determination.

For this study, refractive index detection is limited owing to the very long equilibration time required for the detection limit and because it is impossible to use gradient elution for the analysis of complex mixtures. Light-scattering detection

0021-9673/90/$03.50

(LSD), which is more sensitive than refractive index detection, is easy to use and compatible with gradient elution[5,6]. Scattered light produced by microparticles permits a universal detection method for non-volatile solutes. The development of LSD has been described in several papers and many applications have been published in both HPLC[7,8] and supercritical fluid chromatography (SFC)[9–11]. This paper describes for the first time the compatibility of LSD with selected salted eluents. It also gives an explanation for the variability of the determination of CPC in mouthwash using the HPLC conditions described by Meyer and Takahashi[1] and presents a specific and rapid new procedure.

EXPERIMENTAL

Chemicals

The mobile phase solvents used were reversed-phase HPLC-grade methanol (Prolabo, Paris, France), HPLC-grade acetonitrile (Fisons, Loughborough, U.K.) and distilled water (Cooperation Pharmaceutique Française, Melun, France). Other reagents were of analytical-reagent grade.

Apparatus

Chromatography was carried out using a Knauer (Berlin, F.R.G.) Model 64 pump, a Rheodyne (Cotati, CA, U.S.A.) Model 7125 valve, and a Shimadzu (Touzart et Matignon, Vitry-sur-Seine, France) CR 3A integrator.

Three different detectors were used: a Model SF 769 UV spectrophotometer (Kratos, Ramsey, NJ, U.S.A.) set at 258 nm, a differential refractometer (LDC, Riviera Beach, FL, U.S.A.) and a Model Sedex 45 light scattering detector, (Sedere Vitry-Sur-Seine, France). LSD uses the following principle: the effluent is nebulized by an inert gas (nitrogen) and the solvent is vaporized in a warm tube. The non-volatile solutes give a mist of small particles which scatter the light. Scattered light is measured at 120° to the collimated light source[6,8,12].

Columns

The columns used were 10-μm μBondapak CN (150 × 3.9 mm I.D.) purchased from Waters Assoc. (Milford, MA, U.S.A.) and 7-μm Zorbax CN (150 × 4.6 mm I.D.) purchased from DuPont (Wilmington, DE, U.S.A.).

Mobile phases

Solution S was a 3.6 g l^{-1} aqueous solution of tetramethylammonium hydroxide pentahydrate (Aldrich, Strasbourg, France) adjusted to pH 4.2 with acetic acid. Solution T was a 10^{-3} mol l^{-1} aqueous solution of triethylamine (Aldrich) adjusted to pH 4.2 with trifluoroacetic acid. The eluents were as follows: A, mixture of 700 ml of methanol and 300 ml of solution S; B, mixture of 700 ml of acetonitrile and 300 ml of solution S; C, mixture of 700 ml of methanol and 300 ml of solution T; and D, mixture of 700 ml of acetonitrile and 300 ml of solution T.

Samples

Solution M_1 was prepared by dissolving cetylpyridinium chloride (CPC) at 500 ppm (0.05%) in 95% ethanol. Solution M_2 was a 50 ppm (0.005%) solution of CPC

obtained by diluting solution M_1 10-fold with 95% ethanol. Solution M_3 was a 40 000 ppm solution of hydrogenated polyoxyethylenated castor oil (HPCO) in 95% ethanol.

A standard mixture M_4 was prepared by mixing 10 ml of M_1 and 20 ml of M_3 with 70 ml of distilled water in a 100-ml flask.

The analyte was a commercial mouthwash used as received.

RESULTS AND DISCUSSION

The CPC analysis performed with a μBondapak CN column, with a methanol–water mobile phase containing tetramethylammonium (eluent A) as defined by Meyer and Takahashi[1] led to the chromatograms in Fig. 1 and to the quantitative results in Table I.

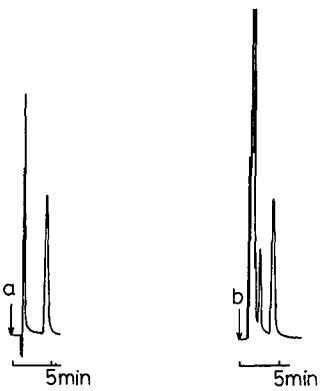

Fig. 1. Typical chromatograms of CPC on μBondapak CN (150 × 4.6 mm I.D.) with a UV detector. Eluent A, methanol–aqueous buffer; flow-rate, 1.5 ml min^{-1}; pressure, 134 bar; injection loop, 20 μl; detection, UV at 258 nm. (a) Standard solution M_2 of CPC; (b) commercial mouthwash.

The method is rapid and simple and the CPC peak is easily identified as the lasted peak elutes. However, the repeatability determined from eight replicate injections was unsatisfactory both for the standard mixture and for the mouthwash [relative standard deviation (R.S.D.) 8.6% and 6.1%, respectively].

No difference in the CPC UV peak is observed in the chromatogram of standard M_2 (Fig. 1a) and mouthwash (Fig. 1b). Standard M_4 and mouthwash solution differ from standard M_2 owing to the large amount of hydrogenated polyoxyethylenated castor oil (HPCO). This seems to be the cause of the above high R.S.D.s for standard M_4 and the mouthwash compared with that of standard M_2 (2.9%). The cause of the variability should be established by using another detection mode. Therefore, we first attempted to carry out a chloroform extraction of CPC prior to its determination in the standard M_4 or mouthwash solution; the extraction selectivity and extraction yield were poor and did not improve the repeatability. Next, we connected the light-scattering detector to the specific UV detector, and then all the non-volatile compounds including UV-absorbing solutes and non-UV-absorbing solutes were detected. This form of detection requires readily evaporated eluent in order to obtain a low enough background noise. Therefore, tetramethylam-

TABLE I

REPEATABILITY FOR STANDARD SOLUTION M_2, STANDARD MIXTURE M_4 AND THE COMMERCIAL MOUTHWASH

Column, μBondapak CN (150 × 3.9 mm I.D.); eluent A, methanol–aqueous buffer; detection, UV at 258 nm.

Peak-area units

Standard solution M_2 (CPC 50 ppm)	*Standard mixture M_4 (CPC 50 ppm, castor oil 8000 ppm)*	*Commercial mouthwash*
709 091	642 874	714 576
717 410	779 244	679 613
730 641	725 461	627 895
753 395	801 945	616 727
774 929	749 800	601 250
750 376	769 679	610 277
766 105	757 587	610 791
748 382	613 207	604 006
Mean: 743 791	729 974	633 142
R.S.D.: 2.9%	8.6%	6.1%

monium acetate salt in eluent A must be replaced with a more volatile salt, triethylammonium trifluoroacetate, which constitutes eluent C.

This is the first time we have demonstrated the application of LSD in eluents containing salts. Using an organic–aqueous mobile phase containing a 10^{-3} mol l^{-1} concentration of salt, the evaporation temperature in the diffusion tube remains below 50°C; this possibility is only afforded by the Sedex 45 detector. Other applications using various salts will be presented later[13]. Such a modification of the mobile phase does not produce a difference in the CPC retention. Indeed, UV detection gives for the standard solution M_4 or the mouthwash the same pattern as Fig. 1. Fig. 2 displays the same analysis as Fig. 1 but with LSD.

LSD proved conclusively that the elution of HPCO was quicker than that of CPC. However, the high concentration of HPCO in relation to the concentration of CPC in mouthwash and elution spreading produced by the diverse components present in the HPCO mixture led to partial co-elution of CPC with castor oil. This co-elution cannot be revealed using the UV detection mode as HPCO is a non-UV-absorbing mixture. It was co-elution in Meyer and Takahashi's UV method[1] that caused the variability in our results.

The UV signal consists of two contributions: a direct UV CPC signal and a UV signal given by the change in the refractive index of the effluent at the elution time of CPC in standard solution M_2 and the refractive index of the effluent containing castor oil at the elution time of CPC in standard solution M_4 (or mouthwash). The latter contribution was not constant and resulted in variability in the determination of CPC. Changes in the chromatographic elution conditions, discriminating without greatly modifying the procedure, should allow CPC and HPCO elutions to be carried out.

First, replacement of methanol with acetonitrile permitted a more rapid elution

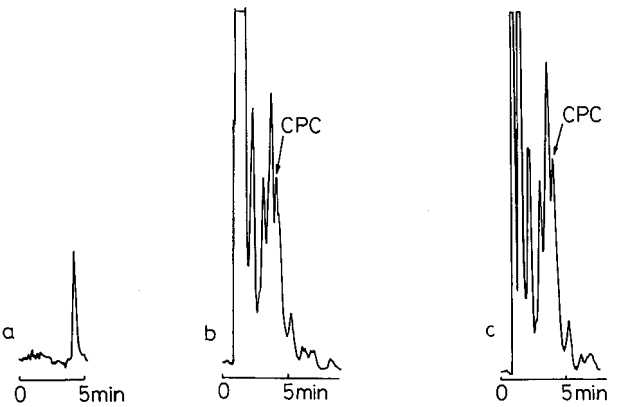

Fig. 2. Chromatograms of CPC on μBondapak CN (150 × 4.6 mm I.D.) with a light-scattering detector. Eluent C, methanol–aqueous buffer; flow-rate, 1.5 ml min^{-1}; pressure, 134 bar; injection loop, 20 μl. LSD conditions: evaporation temperature, 40°C; nebulizer gas, 2.5 bar. (a) Standard solution M_2 of CPC (50 ppm); (b) commercial mouthwash; (c) standard mixture M_4 of CPC (50 ppm) and HPCO (8000 ppm).

of the compounds apart from CPC. Second, replacement of μBondapak CN with Zorbax CN increased the separation of HPCO and CPC. Under these conditions an acceptable chromatogram was obtained with rapid elution. The choice of Zorbax CN rather than μBondapak CN resulted from comparisons made by Goldberg[14] which showed that the stationary phases are different in terms of classification of polar and non-polar phases. Our previous similar work[15,16] demonstrated the great difference between Zorbax and μBondapak the hydrophobic contribution to retention being greater with Zorbax.

Typical chromatograms of the commercial mouthwash solution obtained using the three different detection modes are presented in Fig. 3. When considering the universal detection modes, clearly LSD (Fig. 3b) afforded greater more sensitivity

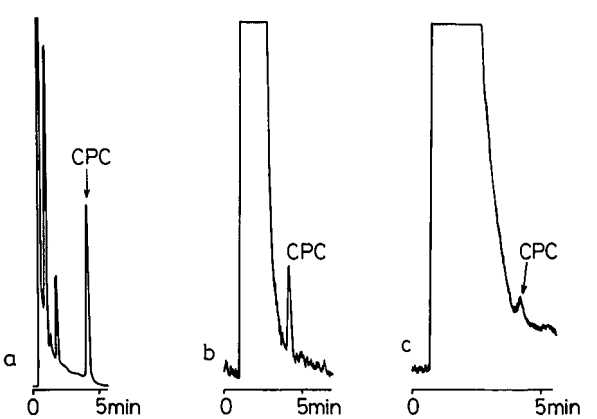

Fig. 3. Typical chromatograms of commercial mouthwash on Zorbax CN (150 × 4.6 mm I.D.) with three different detection modes. Flow-rate, 1.5 ml min^{-1}; pressure, 41 bar; injection loop, 20 μl. (a) UV detection at 258 nm. Eluent B = acetonitrile–aqueous buffer. (b) Light-scattering detection. Nebulizer gas, 2.5 bar; evaporation temperature, 40°C. Eluent D = acetonitrile–aqueous buffer. (c) Differential refractometric detection. Eluent B = acetonitrile–aqueous buffer.

than refractive index detection (Fig. 3c), despite the unfavourable elution conditions (addition of salt to the mobile phase). Moreover, the variation of the refractive index of the effluents was very large and the CPC peak was partially masked by lack of resolution; ethanol in the mouthwash preparation was the major cause of the large refractive index change or disturbance.

With the new chromatographic conditions and UV detection, a calibration graph for CPC determination was established with seven reconstituted solutions of increasing CPC concentration from 5 to 75 ppm containing a constant concentration of HPCO (8000 ppm). The graph was linear with an acceptable regression value (R = 0.9997) and passed very close to the origin. Now, using the new chromatographic conditions, the repeatability established using six injections of a commercial mouthwash was better; the R.S.D. obtained (2.8%) compared favourably with that for the standard CPC solution under the same conditions.

It appears that the effects of HPCO on the determination of CPC using the new chromatographic conditions were negligible; the chromatographic procedure is satisfactory and capable of achieving excellent separations.

CONCLUSION

Variability in the UV determination of low CPC concentrations in a mouthwash by HPLC was caused by the co-elution of UV-absorbing and non-UV-absorbing compounds. Universal detection connected with UV detection afforded information enabling the variability problem to be solved. The LSD mode was superior to the refractive index mode for two reasons: a higher detection limit and the injection solvent, being of a different nature from that of the eluent, does not produce a disturbance in the chromatogram. Using LSD new elution conditions were established and the routine UV determination of CPC in mouthwash became an accurate and rapid analysis.

REFERENCES

1 R. C. Meyer and L. T. Takahashi, *J. Chromatogr.*, 280 (1983) 159.
2 B. Wyhowski de Bukanski, *Int. J. Cosmet. Sci.*, 9 (1987) 193.
3 V. T. Wee and J. M. Kennedy, *Anal. Chem.*, 54 (1982) 1631.
4 S. Kawase, K. Hirose and S. Ukai, *J. Chromatogr.*, 213 (1981) 265.
5 J. M. Charlesworth, *Anal. Chem.*, 50 (1978) 1414.
6 A. Stolyhwo, H. Colin and G. Guiochon, *J. Chromatogr.*, 265 (1983) 1.
7 M. Lafosse, M. Dreux, L. Morin-Allory and J. M. Colin, *J. High Resolut. Chromatogr. Chromatogr. Commun.*, 8 (1985) 39.
8 M. Lafosse, M. Dreux and L. Morin-Allory, *J. Chromatogr.*, 404 (1987) 95.
9 P. Carraud, D. Thiebaut, M. Caude, R. Rosset, M. Lafosse and M. Dreux, *J. Chromatogr. Sci.*, 25 (1987) 395.
10 M. Lafosse, L. Morin-Allory, B. Herbreteau, C. Elfakir, M. Dreux, J.-C. Battard and C. Chauvette, in M. Perrut (Editor), *Proceedings of the 1st International Symposium on Supercritical Fluids, Nice, October 1988*, Vol. 1, Institut National Polytechnique de Lorraine, Nancy, 1988, p. 517.
11 D. Nizery, D. Thiebaut, M. Caude, R. Rosset, M. Lafosse and M. Dreux, *J. Chromatogr.*, 467 (1989) 49.
12 R. Macrae, *Int. Analyst*, 1 (1987) 14.
13 M. Dreux, in preparation.
14 A. P. Goldberg, *Anal. Chem.*, 54 (1982) 342.
15 J. R. Chrétien, B. Walczak, L. Morin-Allory, M. Dreux and M. Lafosse, *J. Chromatogr.*, 371 (1986) 253.
16 B. Walczak, L. Morin-Allory, M. Lafosse, M. Dreux and J. R. Chrétien, *J. Chromatogr.*, 395 (1987) 183.

Journal of Chromatography, 513 (1990) 360–366
Elsevier Science Publishers B.V., Amsterdam

CHROM. 22 455

Note

Optimization of the isocratic high-performance liquid chromatographic separation of selected phthalates using the overlapping resolution mapping technique

MIRIAM REHANA KHAN, CHYE PENG ONG, SAM F. Y. LI and HIAN KEE LEE*
Department of Chemistry, National University of Singapore, Kent Ridge, Singapore 0511 (Singapore)
(First received February 15th, 1990; revised manuscript received March 16th, 1990)

The use of a systematic experimental design to optimize the separation conditions in high-performance liquid chromatography (HPLC) serves to minimize, if not eliminate, the laborious trial-and-error attempts to achieve desired separation conditions generally associated with the latter technique. One of these systematic approaches makes use of mixture designs followed by overlapping resolution mapping[1]. This method requires only seven preliminary experiments based on the solvent selectivity triangle[2–4] to predict the mobile phase compositions for optimum separation. The selection of the criteria desired for a particular analysis is made at this stage; these criteria include a reasonable analysis time (which forms the basis on which the solvent strength of the eluent mixture may be calculated) and a certain required resolution between adjacent component peaks in the chromatogram.

The overlapping resolution mapping technique has previously been applied with success to the analysis of eleven priority substituted phenols[5]. In this paper, the use of five plasticizers (dimethyl, diethyl, dibutyl, diallyl and benzyl-*n*-butyl phthalate) as model systems to test the isocratic overlapping resolution mapping scheme is described. Although the biological effects of plasticizers present in the environment have not been fully evaluated, the facts that these compounds are very widely used, and are therefore ubiquitous in the environment and that they may possess undesirable biological effects, justify the need to analyse for them. Indeed, four of the five phthalates mentioned above (the exception being diallyl phthalate), plus a sixth, bis(2-ethylhexyl) phthalate (not considered in this present work, for reasons given below), are on the priority pollutant list of the United States Environmental Protection Agency (USEPA).

EXPERIMENTAL

Chemicals and reagents

Dimethyl, diethyl, dibutyl, diallyl and benzyl-*n*-butyl phthalate (of at least 97% purity) were obtained from Fluka (Switzerland). Standard solutions of the individual

0021-9673/90/$03.50

phthalates and mixtures (in the concentration range 160–260 ppm for each component) were prepared using methanol. The methanol (J. T. Baker, U.S.A.) and acetonitrile (Ajax, Australia) used were of HPLC grade and the 2-propanol and dimethylformamide (Ajax) were of analytical-reagent grade. Mobile phases were prepared according to the A + B (*quantum sufficit*) addition procedure recommended by Runser[6]. In this method, the modifier amounts are measured, and then the volume is brought to the desired value with water, the final component in the mixture. All solutions and solvents were filtered and degassed by sonication before use.

Instrumentation

The HPLC system consisted of a Shimadzu (Kyoto, Japan) LC-6A pump, a Shimadzu SPD-6A variable-wavelength UV spectrophotometric detector and a Chromatopac CR-3A data processor. The reversed-phase column used for the evaluation of the optimization scheme was a Shimadzu Shimpack CLC-ODS (15 cm × 6 mm I.D.; 5 μm particle size). Once the optimum mobile phase had been determined, a Whatman Partisil-5 ODS-3 column (10 cm × 4.6 mm I.D.; 5 μm particle size) was used to separate the phthalates. The detection wavelength was 224 nm. The flow-rate used was 1.0 ml min^{-1}, except for 2-propanol–water (0.6 ml min^{-1}); the lower flow-rate was used because of the excessively high column pressure obtained with 2-propanol–water as mobile phase.

A Rheodyne 7125 injection valve with a 20-μl loop was used for sample injections. All chromatographic runs were duplicated with a reproducibility between runs of 2% or better. The void volume was obtained for all mobile phases by using methanol as the unretained component.

RESULTS AND DISCUSSION

Preliminary experiments

In defining the first vertex of the solvent selectivity triangle using methanol–water[2] as the binary mixture, the first selection criterion to be specified was the desired analysis time. With three randomly selected methanol–water compositions (60:40, 70:30 and 72.4:27.6), it was determined that the shortest retention time for the last-eluting component in the standard phthalate mixture was a reasonable 22 min for the composition 72.4:27.6. The solvent strength (ST) of the eluent mixture of this composition was then calculated from the equation[2]

$$ST = s_a\varphi_a + s_b\varphi_b + \ldots \quad (1)$$

where s_i = the individual solvent strengths and φ_i = the volume fractions of each component i.

The solvent compositions of the other binary mixtures (acetonitrile–water and 2-propanol–water, which define the other two vertices of the triangle) having the same solvent strength were then determined using eqn. 1.

To effect changes in selectivity, solvents from different selectivity groups[4] should be chosen to establish the solvent selectivity triangle. As methanol and acetonitrile are the most common reversed-phase HPLC solvents, and they are in different solvent groups, they were picked (as binary mixtures with water) to be the two corners of the

TABLE I

ELUENT MIXTURES USED IN PRELIMINARY EXPERIMENTS

Solvent compositions are given as percetages of binary mixtures in the mobile phase.

Eluent mixture	*Methanol–water*	*Acetonitrile–water*	*2-Propanol–water*
1	100	0	0
2	0	100	0
3	0	0	100
4	50	50	0
5	50	0	50
6	0	50	50
7	33.3	33.3	33.3

triangle. For the third corner, 2-propanol (+ water) was selected instead of the customary tetrahydrofuran (THF) for work of this nature mainly because of the added expense of obtaining antioxidant-free THF. The other solvents in the same group as THF, methoxyethanol and dimethylformamide, were ruled out because of their toxic and irritant properties. Moreover, 2-propanol is in the same group as methanol which, in our view, is an added advantage because of its good solvating power.

The solvent selectivity triangle having been established, the next step was to conduct experiments using the other six eluent mixtures representing the acetonitrile–water and 2-propanol–water vertices, the three mid-points of the vertices and the centre of the triangle[1]. The seven eluent mixtures used for these preliminary experiments are shown in Table I. Table II shows each of these eluent mixtures as a percentage of the pure solvents in the mobile phase.

It is worth mentioning that during the setting up of the solvent compositions representing the second and third vertices of the solvent selectivity triangle, it is usual to make small adjustments to the amounts of the organic modifier in order to obtain equivalent k' values[2]. If this were done, however, the solvent strength would no longer be constant. A change in solvent strength is not useful for improving the resolution

TABLE II

ELUENT MIXTURES USED IN PRELIMINARY EXPERIMENTS

Solvent compositions are given as percentages of pure solvents in the mobile phase.

Eluent mixture	*Void time, t_0 (min)*	*Methanol*	*Acetonitrile*	*2-Propanol*	*Water*
1	2.662	72.40	0.00	0.00	27.60
2	2.683	0.00	70.00	0.00	30.00
3	4.037	0.00	0.00	51.70	48.30
4	2.760	36.20	35.00	0.00	28.80
5	2.532	36.20	0.00	25.85	37.95
6	2.325	0.00	35.00	25.85	39.15
7	2.600	24.13	23.33	17.23	35.31

TABLE III

CAPACITY FACTORS (k') OF PHTHALATES CHROMATOGRAPHED USING THE ELUENT MIXTURES LISTED IN TABLE II

DMP = Dimethyl phthalate; DEP = diethyl phthalate; DAP = diallyl phthalate; BBP = benzyl-*n*-butyl phthalate; DBP = dibutyl phthalate.

Eluent mixture	*DMP*	*DEP*	*DAP*	*BBP*	*DBP*
1	0.381	0.991	1.538	6.848	7.211
2	0.371	0.838	1.133	3.517	4.145
3	0.288	0.618	0.958	2.733	2.776
4	0.407	1.022	1.485	5.670	6.385
5	0.337	0.810	1.296	5.057	5.377
6	0.449	0.996	1.373	4.311	5.220
7	0.363	0.904	1.337	5.027	5.935

between peaks[7]. Therefore, in this work, no adjustments to the composition of the mobile phase were made.

From the results of the seven preliminary runs, the resolutions, R_s, between every pair of peaks in the chromatogram were obtained for each eluent mixture using the equation[8]

$$R_s = \frac{1}{4}(\alpha - 1)N^{0.5}\left(\frac{k'}{1 + k'}\right) \tag{2}$$

where k' is the average capacity factor for the two peaks, α the relative retention ratio and N the number of theoretical plates. The calculated R_s values were then fitted into a second-order polynomial equation[2]:

$$R_s = a_1x_1 + a_2x_2 + a_3x_3 + a_{12}x_1x_2 + a_{13}x_1x_3 + a_{23}x_2x_3 + a_{123}x_1x_2x_3 \tag{3}$$

TABLE IV

RESOLUTION (R_s) BETWEEN ADJACENT PEAKS CALCULATED FOR PHTHALATES CHROMATOGRAPHED USING THE ELUENT MIXTURES LISTED IN TABLE II

Eluent mixture	R_s			
	Peak pair[a]			
	DMP–DEP	*DEP–DBP*	*DBP–DAP*	*DAP–BBP*
1	5.428	2.569	23.233	0.387
2	3.955	1.456	12.260	1.183
3	2.977	2.020	10.015	0.183
4	5.249	2.100	18.353	0.901
5	3.492	2.564	18.393	0.441
6	3.818	1.713	13.191	1.453
7	4.817	2.109	17.499	1.276

[a] Abbreviations of phthalates as in Table III.

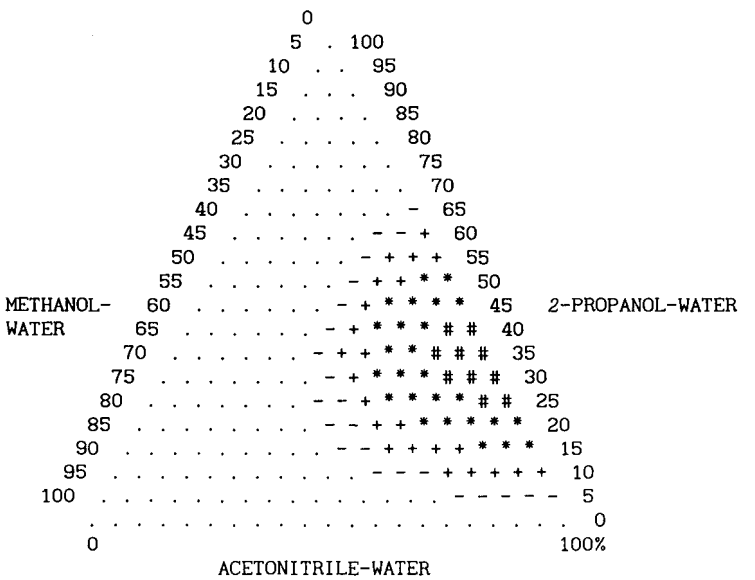

Fig. 1. Overlapping resolution mapping plot for all four phthalate peak pairs. · = $R_s \leqslant 1.2$; − = $1.2 \leqslant R_s \leqslant 1.3$; + = $1.3 \leqslant R_s \leqslant 1.4$; * = $1.4 \leqslant R_s \leqslant 1.5$; # = $R_s \geqslant 1.5$.

where a_i = coefficients and x_i = volume fractions of the three binary mixtures, methanol–water, acetonitrile–water and 2-propanol–water. The values of a_i for each pair of peaks were determined using a BASIC program[2] slightly modified for our purposes. Subsequently, using eqn. 3, R_s values within the solvent selectivity triangle were calculated. Table III shows the capacity factors of the five phthalates chromatographed using the seven eluent mixtures. The calculated R_s values for adjacent peaks in each of the eluent mixtures are given in Table IV [note that with eluent mixture 6, the minimum resolution is close to that specified (1.5) for our optimization scheme (see below)].

Overlapping resolution mapping: optimization of solvent composition

From the calculated R_s values, Venn diagrams[1] were generated[2] for each pair of components in the chromatogram at a specified resolution of 1.5 between each adjacent pair of peaks. By superimposing (overlapping) all seven Venn diagrams, areas corresponding to solvent compositions giving the desired resolution amongst all the peaks in a phthalate mixture were established. Such an overlapping resolution mapping diagram for the five phthalates considered in this work is depicted in Fig. 1. The area described by the symbol # represents all possible mobile phase compositions using which the optimum separation (*i.e.*, where $R_s \geqslant 1.5$) of all the phthalates may be achieved. The other symbols indicate various mobile phase compositions which are not optimized to achieve a complete separation between each peak pair for all the components in the mixture.

To evaluate the optimization scheme, a point within the region encompassed by the symbol # on the overlapping resolution mapping diagram was taken; this

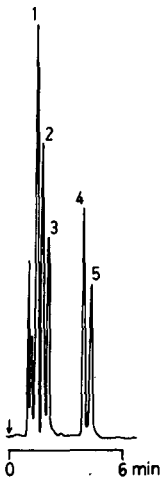

Fig. 2. Chromatogram of phthalates obtained using optimum eluent mixture (methanol–acetonitrile–2-propanol–water, 3.6:42.0:18.1:36.3) derived from overlapping resolution mapping diagram in Fig. 1. Peaks: 1 = dimethyl phthalate; 2 = diethyl phthalate; 3 = diallyl phthalate; 4 = benzyl-*n*-butyl phthalate, 5 = dibutyl phthalate. The Whatman Partisil 5 ODS-3 column was used to generate this chromatogram. Other conditions are as given in the text. The void time for this column was 1.1 min.

corresponds to a mobile phase composition of methanol–acetonitrile–2-propanol–water (3.6:42.0:18.1:36.3). Using this mobile phase, a different C_{18} column and under isocratic elution, a chromatogram of the five phthalates was generated, as shown in Fig. 2. As can be seen, satisfactory separation was achieved. Note that the analysis time was less than 6 min. The value of the overlapping resolution mapping technique has thus been clearly illustrated. In spite of the fact that not all of the adjacent peaks could be separated in each of the seven preliminary experiments, after the overlapping resolution mapping scheme had been established an optimized mobile phase composition could be identified by the simple expedient of selecting a point (and consequently a solvent composition) within the region of the overlapping resolution mapping diagram where $R_s \geqslant 1.5$ (or any other required resolution). Although, as mentioned above, with eluent mixture 6 it was possible to obtain a minimum resolution of 1.45 (for diallyl phthalate and benzyl-*n*-butyl phthalate), which is close to the specified R_s value, an even better resolution (*i.e.*, 1.5 or greater, symbolized by # in Fig. 1) could be achieved for this pair when the optimum mobile phase, derived from the optimization scheme, was used. This systematic approach therefore reduces to a minimum the time spent in method development and is also economical in terms of amounts of solvents used. Another point worth emphasizing is that the chromatogram in Fig. 2 was obtained using a different reversed-phase column from that used to establish the optimum mobile phase composition in the optimization exercise. This further illustrates the flexibility and versatility of the overlapping resolution mapping scheme; for a particular application, subsequent routine analyses may be carried out without resort to the original column used for method development.

Limitations of the present approach

As indicated by the results, the present isocratic technique has been found to be highly satisfactory for the separation of five priority phthalates. However, with the addition of a sixth plasticizer, bis(2-ethylhexyl) phthalate, possibly because its retention behaviour is different from that of the other five under the conditions employed here, it was not possible to generate an overlapping resolution map from which an optimized solvent composition (with specified $R_s \geqslant 1.5$) could be selected for the complete separation of all six components. Obviously, a different approach needs to be considered in this situation. Work is currently being conducted to overcome this difficulty.

ACKNOWLEDGEMENTS

The authors gratefully acknowledge the financial support of the National University of Singapore and the technical assistance of Ms. Tan Geok Kheng and Ms. Frances Lim.

REFERENCES

1 J. L. Glajch, J. J. Kirkland, K. M. Squire and J. M. Minor, *J. Chromatogr.*, 199 (1980) 57.
2 J. C. Berridge, *Techniques for the Automated Optimization of HPLC Separations,* Wiley, Chichester, 1985, Ch. 4.
3 L. R. Snyder, *J. Chromatogr.*, 92 (1974) 223.
4 L. R. Snyder, *J. Chromatogr. Sci.*, 19 (1983) 223.
5 C. P. Ong, H. K. Lee and S. F. Y. Li, *J. Chromatogr.*, 464 (1989) 405.
6 D. J. Runser, *Maintaining and Troubleshooting HPLC Systems, User's Guide,* Wiley, New York, 1981, p. 19.
7 L. R. Snyder, M. A. Quarry and J. L. Glajch, *Chromatographia*, 24 (1987) 33.
8 L. R. Snyder and J. J. Kirkland, *Introduction to Modern Liquid Chromatography,* Wiley, New York, 2nd ed., 1979, Ch. 2.

Journal of Chromatography, 513 (1990) 367–369
Elsevier Science Publishers B.V., Amsterdam

CHROM. 22 426

Note

Effect of type and concentration of coupling buffer on coupling yield in the coupling of proteins to a tresyl-activated support for affinity chromatography

KOJI NAKAMURA, TSUTOMU HASHIMOTO and YOSHIO KATO*
Central Research Laboratory, TOSOH Corporation, Tonda, Shinnanyo, Yamaguchi 746 (Japan)
and
KIYOHITO SHIMURA and KEN-ICHI KASAI
Faculty of Pharmaceutical Sciences, Teikyo University, Sagamiko, Kanagawa 199-01 (Japan)
(First received November 23rd, 1989; revised manuscript received February 27th, 1990)

Affinity chromatography is a very powerful technique for separating biological substances such as proteins, owing to its selectivity. However, a different support coupled with a ligand that is complementary to the sample to be separated must be prepared for a different kind of sample. To simplify this, it is desirable to have good activated supports to which many ligands can be coupled easily under mild conditions. Various activation methods were examined in the past, and a method with tresyl chloride[1] was found to be useful. Subsequently some tresyl-activated supports based on agarose or silica became commercially available but they had unsatisfactory mechanical or chemical stability of the base material. However, new tresyl-activated supports based on synthetic hydrophilic resin have become commercially available recently under the trade-names TSKgel Tresyl-Toyopearl 650M (ref. 2) and Tresyl-5PW (ref. 3). We have been evaluating these supports for the coupling of proteins and have reported results of the study of coupling conditions, pH of the coupling buffer, temperature, reaction time and amount of reacted ligand[2]. We have now examined the effects of the type and concentration of the coupling buffer on the coupling yield and the results are reported here.

EXPERIMENTAL

Proteins were dissolved in 4 ml of coupling buffer and mixed with 0.4 g of dried Tresyl-Toyopearl 650M powder, which gives a volume of 2.0 ml in the swollen state. After the mixture had been left to stand with gentle shaking at a constant temperature for a certain period of time, 36 ml of distilled water were added and the diluted mixture was filtered with a sintered-glass funnel (this dilution was necessary to prevent adsorption of proteins on the support without covalent bonding in some instances). The protein coupling yield was calculated from the UV absorption at 280 nm of protein solutions before and after the coupling reaction. The coupling buffers

0021-9673/90/$03.50

examined were 0.1–1 *M* carbonate buffers (pH 8.0), 0.1–1 *M* N-(2-hydroxyethyl)piperazine-N'-2-ethanesulphonic acid (HEPES) buffers (pH 8.0), 0.1–1 *M* phosphate buffers (pH 8.0) and 0.1 *M* carbonate buffer (pH 8.0) containing 0.5–2.0 *M* sodium chloride. The proteins employed were purchased from Sigma (St. Louis, MO, U.S.A.).

RESULTS AND DISCUSSION

The coupling yields observed for bovine serum albumin in the various buffers are summarized in Table I. When the buffer concentration increased from 0.1 to 1 *M*, the coupling yield remained almost unchanged with carbonate buffer, but it increased with HEPES and phosphate buffers. It also increased with increase in the sodium chloride concentration in 0.1 *M* carbonate buffer. In particular, it increased to a great extent when the concentration of phosphate buffer was raised to 1 *M*. We postulate that this great increase in coupling yield occurred because the bovine serum albumin was forced to approach near the surface of the support owing to the salting-out effect of 1 *M* phosphate buffer and the coupling reaction between bovine serum albumin and tresyl groups then became easier. We also examined if 1 *M* phosphate buffer is effective for the coupling of other proteins. Some proteins were coupled in 1 *M* phosphate buffer (pH 8.0) and in 0.1 *M* carbonate buffer (pH 8.0) containing 0.5 *M* sodium chloride. Proteins for which low coupling yields were observed in carbonate buffer were selectively used in this experiment. The results are summarized in Table II. Much higher coupling yields were obtained in 1 *M* phosphate buffer than in carbonate buffer for all the proteins examined except cytochrome C. In particular, almost quantitative coupling yields were achieved for α-1-antitrypsin, bovine serum albumin, myoglobin and α-chymotrypsin, although the coupling reaction was performed at 4°C for 4 h. The coupling yield did not change for cytochrome *c* with the two buffers, probably because phosphate buffer of 1 *M* is not concentrated enough to salt-out cytochrome *c* as the latter is very hydrophilic. The coupling yield may be increased by further increasing the phosphate buffer concentration, *e.g.*, up to 1.5 *M*.

It is concluded that 1 *M* phosphate buffer is very effective in general for the coupling of protein ligands to Tresyl-Toyopearl 650M. It is better than buffers which have been commonly employed in the coupling of ligands to various types of activated

TABLE I

EFFECTS OF TYPE AND CONCENTRATION OF COUPLING BUFFER ON COUPLING YIELD

Bovine serum albumin (30 mg) was reacted with TSKgel Tresyl-Toyopearl 650M (0.4 g) in 4 ml of various buffers (pH 8.0) at 25°C for 5 h.

Coupling buffer	*Coupling yield (%)*	*Coupling buffer*	*Coupling yield (%)*
0.1 *M* carbonate buffer	16	0.1 *M* phosphate buffer	17
0.5 *M* carbonate buffer	15	0.5 *M* phosphate buffer	41
1.0 *M* carbonate buffer	12	1.0 *M* phosphate buffer	88
0.1 *M* HEPES buffer	16	0.1 *M* carbonate buffer containing 0.5 *M* NaCl	28
0.5 *M* HEPES buffer	35	0.1 *M* carbonate buffer containing 1.0 *M* NaCl	29
1.0 *M* HEPES buffer	32	0.1 *M* carbonate buffer containing 2.0 *M* NaCl	36

TABLE II

COUPLING OF VARIOUS PROTEINS TO TSKgel Tresyl-Toyopearl 650M

Proteins (20 mg) were reacted with Tresyl-Toyopearl 650M (0.4 g) in 4 ml of (A) 0.1 *M* carbonate buffer (pH 8.0) containing 0.5 *M* NaCl and (B) 1 *M* phosphate buffer (pH 8.0) at 4°C for 4 h.

Protein	*pI*	*Coupling yield (%)*	
		A	B
α_1-Acid glycoprotein	1.8–2.8	2	58
α-1-Antitrypsin	4.0	25	98
Bovine serum albumin	4.9	31	99
Myoglobin	6.8–7.8	55	99
α-Chymotrypsin	9.1	70	100
Cytochrome *c*	10.1	43	46

supports, such as 0.1 *M* carbonate buffer (pH 8.0) containing 0.5 *M* sodium chloride. When 1 *M* phosphate buffer is not effective in achieving a high coupling yield, higher concentrations, *e.g.*, 1.5–2 *M*, may be useful for increasing the coupling yield. It is considered that other buffers having similar salting-out effects to 1 *M* or more concentrated phosphate buffer would also be effective.

REFERENCES

1 K. Nilsson and K. Mosbach, *Biochem. Biophys. Res. Commun.*, 102 (1981) 449.
2 K. Nakamura, K. Toyoda, Y. Kato, K. Shimura and K. Kasai, *J. Chromatogr.*, 478 (1989) 159.
3 K. Nakamura, T. Hashimoto, Y. Kato, K. Shimura and K. Kasai, *J. Chromatogr.*, 510 (1990) 101.

Journal of Chromatography, 513 (1990) 370–374
Elsevier Science Publishers B.V., Amsterdam

CHROM. 22 493

Note

Separation of enantiomers using polymeric copper–amine–cellulose columns

S. MURALIDHARAN* and H. FREISER
Strategic Metals Recovery Research Facility, Department of Chemistry, University of Arizona, Tucson, AZ 85721 (U.S.A.)
(First received July 24th, 1989; revised manuscript received April 10th, 1990)

Though always intellectually challenging, with the current high interest in biotechnology, the problem of separating and analyzing enantiomeric mixtures is one of high importance. Liquid chromatography (LC) has been investigated extensively for the convenient and rapid separation of enantiomers. Several LC methods have been applied for the separation of enantiomers, namely, the use of chiral mobile phase additives, the use of chiral stationary phases (Pirkle columns), ligand exchange, charge transfer complex formation and inclusion complex formation with cyclodextrins[1–3]. It has been demonstrated that ligand-exchange chromatography (LEC) is very effective for the separation of optical isomers without prior derivatization[4]. LEC involves the use of a chiral ligand and copper(II) in the stationary phase or mobile phase and the optical isomers are separated primarily by the difference in the stabilities of the copper(II)–chiral ligand–enantiomer complexes. The major problems with the existing LEC columns are, (1) they are difficult to prepare and consequently expensive and (2) the separated analytes are contaminated with Cu^{II} either due to the addition of Cu^{II} to the mobile phase or the leaching of Cu^{II} from the stationary phase. We have addressed these problems in the current work.

We have developed in our laboratory several polymeric Cu^{II}–amine–cellulose complexes, where amine is diamine like 1,3-diaminopropane and cellulose is unmodified or modified cellulose[5]. Cu^{II} on the average is complexed to one glucose unit of cellulose and one amine molecule in these complexes. Cellulose provides the chiral environment necessary for the separation of optical isomers, which in combination with Cu^{II} becomes an excellent choice as column material. These compounds are easy to prepare, inexpensive and can be coated with ease in various amounts to obtain different loadings of Cu^{II} on a variety of substrates like silica and polystyrene. Columns for both analytical- and preparative-scale separations can be thus readily made. Further, as described in the Experimental section, these columns are stable under a variety of conditions exhibiting insignificant leaching of Cu^{II}. Cellulose and its derivatives as well as other polysaccharides like Sephadex have been used as chiral stationary phases for the separation of optical isomers[6,7]. However, these separations were not achieved by LEC and were not very efficient. We have achieved excellent

separation of D- and L-alanines from a racemic mixture using copper^{II}–1,3-diaminopropane–cellulose coated on silica by LEC. The experimental procedure and results are described here.

EXPERIMENTAL

Reagents

The alanines (D, L and the racemic mixture), $CuSO_4 \cdot 5H_2O$ and 1,3-diaminopropane were obtained from Aldrich and were >99% purity. High-purity cellulose of average particle size 10 μm without any binder, suitable for thin-layer chromatography (manufactured by Machery, Nagel & Co., F.R.G., and distributed by Brinkman Instruments, New York, U.S.A.) was used to prepare the Cu^{II}–1,3-diaminopropane–cellulose complexes. Silica gel (70–150 μm) was from Analtech. All the solvents used were HPLC grade and were purchased from Mallinckrodt. Deionized water for the HPLC experiments was distilled twice over permanganate.

Apparatus

The separation of D- and L-alanines were performed on a Perkin-Elmer Series 4 liquid chromatograph with Rheodyne 7125 injector containing a 20-μl loop, a Perkin-Elmer LC 95 UV–visible spectrophotometric detector and Alltech Linear 1200 strip-chart recorder. The leaching of Cu^{II} under the various experimental conditions used for the separation of the racemic alanine was checked using the Perkin-Elmer 6500 inductively coupled plasma–atomic emission spectrometry (ICP–AES) system at the 224.7 nm emission wavelength (detection limit: 0.2 ppm).

Procedure

The Cu^{II}–1,3-diaminopropane–cellulose complex was prepared as previously reported[5]. The proposed structure for this complex is shown in Fig. 1. Silica gel, 15.5 g, was washed three times with deionized water, three times with methanol and finally with deionized water. It was stirred with 50 ml of Cu^{II}–1,3-diaminopropane–cellulose complex containing $8.8 \cdot 10^{-3}$ mol of Cu^{II} for 1 h and allowed to settle. A blue colored

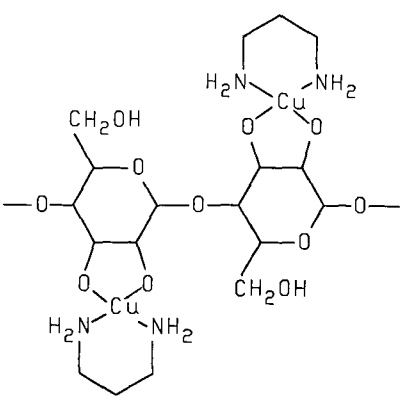

Fig. 1. Proposed structure for copper(II)–1,3-diaminopropane–cellulose.

gel and a clear aqueous layer were obtained, indicating that the silica gel has been coated with the complex. The gel was filtered on a medium frit funnel, washed several times with distilled water and dried in vacuum at room temperature for 12 h. The blue colored silica gel, 1.2 g (Cu^{II} = 5.6 · 10^{-4} mol/g of silica), was slurried with methanol and packed into a stainless-steel high-performance LC column of 28 cm × 0.3 cm I.D. at a flow-rate of 1 ml/min at room temperature. No significant amount of Cu^{II} was found to leach from the column with water (pH 3–9), 0.1 *M* NH_3, methanol and acetonitrile as eluents. This was determined by analyzing the eluent for Cu^{II} using ICP–AES. Water solutions were directly analyzed while organic solvents were evaporated and the container washed with an appropriate volume of water for analysis by ICP–AES. Several eluent compositions were tried to obtain the best separation for a solution containing 10^{-3} *M* (89 μg/ml) racemic DL-alanine in water at pH 7

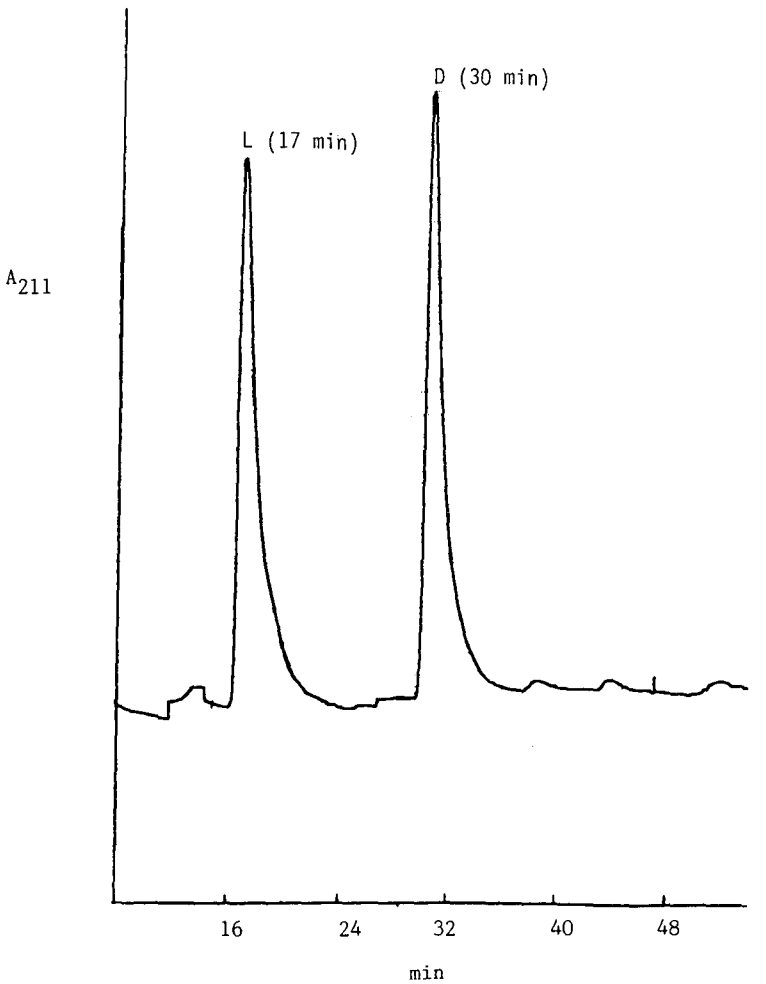

Fig. 2. Separation of DL-alanine using copper(II)–1,3-diaminopropane–cellulose coated on silica.

(phosphate buffer). An eluent composition of methanol–water–acetonitrile (80:10:10) at a flow-rate of 1 ml/min afforded the best separation of the D and L forms. The detection wavelength was 211 nm. The individual components were identified by injecting separately D- and L-alanine of the same concentration as the mixture. The retention time for the non-adsorbing analyte acetone under these conditions was 1.7 min.

RESULTS AND DISCUSSION

Excellent baseline separation of the D- and L-alanines from the racemic mixture was obtained under the experimental conditions as shown in Fig. 2. The retention times are 17 and 30 min for L- and D-alanines, respectively. The corresponding capacity factors using the retention time for the non-adsorbing analyte acetone for L- and D-alanines are 9.0 and 16.7, respectively. These results yield a separation factor α of 1.85. The separation factors for the separation of racemic DL-alanine using some other columns reported in the literature are collected in Table I. As may be seen from this table, the separation factors obtained using the Cu^{II}–1,3-diaminopropane–cellulose coated on silica are comparable or superior to these other columns. The most significant advantage to the column we have developed is the simplicity of its preparation. Application of this column for the separation of several other racemic compounds are currently under investigation.

We may also notice from Fig. 2 that the peaks for L- and D-alanines have about the same width, *i.e.*, the number of theoretical plates calculated from the peak widths using the equation for asymmetric peaks are markedly different (373 for the L isomer and 1162 for the D isomer)[13]. This difference could be rationalized using the Knox equation for reduced plate height h[14]. Stout *et al.*[15] have shown that the B and C terms of the Knox equation which account for the diffusion and mass transfer of the analyte

TABLE I

LITERATURE VALUES FOR SEPARATION FACTOR (α) OF D- AND L-ALANINES

Column material	α	*Ref.*
Polystyrene derivatized with (*R*)-N′,N′-dibenzyl 1,2-propanediamine	1.43	8
Silica gel derivatized with (*R*)-N-[11-(triethoxysilyl)undecanoyl]-α-(6,7-dimethyl-1-napthyl)isobutylamine	1.28 (as the N-3,5-dinitrobenzoyl derivatives)	9
Silica gel derivatized with N-ω-(dimethylsiloxy)undecanoyl-L-valine	2.34 (as the 5-dimethylaminonapthalene-1-sulphonyl derivatives)	10
Polystryene derivatized with L-methionine-*l*-sulphoxide	1.19	11
Lichrosorb RP-18 with Cu^{II} and N,N-dimethyl-L-phenylalanine in the eluent	1.75	12
Silica gel derivatized with β-cyclodextrin	1.20	2

depend on its capacity factor, B increasing and C decreasing with the capacity factor. The magnitude of the change in C can be much higher than B if the diffusion of the analyte within the intraparticle region is impeded by steric effects and/or pore size of the solid support. The three-point interaction that is generally believed to be responsible for chiral recognition by ligand exchange indicates that the most likely contributing factor for our columns is steric effect[16]. As a result the h value for the more retained D-alanine is smaller and hence its plate number larger compared to the less retained L-alanine. This aspect is under further investigation.

REFERENCES

1 G. Wulff and M. Minarik, in M. Zief and L. J. Crane (Editors), *Chromatographic Chiral Separations*, Marcel Dekker, New York, 1988, p. 40.
2 D. W. Armstrong and W. Demond, *J. Chromatogr. Sci.*, 22 (1984) 411.
3 W. H. Pirkle and T. C. Pochapsky, *Adv. Chromatogr.*, 27 (1987) 73.
4 V. A. Davankov, A. Kurganov and A. S. Bochkov. *Adv. Chromatogr.*, 22 (1983) 71.
5 S. Muralidharan and H. Freiser, *J. Mol. Catal.*, 50 (1989) 181.
6 A. Mannschreck, H. Koller and R. Wenicke, *Kontakte (Darmstadt)*, (1985) 41.
7 S. Yuasa, M. Itoh and A. Shimada, *J. Chromatogr. Sci.*, 22 (1984) 288.
8 V. A. Davankov and A. A. Kurganov, *Chromatographia*, 13 (1980) 339.
9 W. H. Pirkle and M. H. Hyunn, *J. Org. Chem.*, 49 (1984) 3043.
10 B. Feibush, M. J. Cohen and B. L. Karger, *J. Chromatogr.*, 282 (1983) 3.
11 B. B. Berezin, I. A. Yamskov and V. A. Davankov, *J. Chromatogr.*, 261 (1983) 301.
12 R. Wernicke, *J. Chromatogr. Sci.*, 23 (1985) 39.
13 J. P. Foley and J. G. Dorsey, *Anal. Chem.*, 55 (1983) 730.
14 J. H. Knox and H. P. Scott, *J. Chromatogr.*, 282 (1983) 297.
15 R. W. Stout, J. J. DeStefano and L. R. Snyder, *J. Chromatogr.*, 282 (1983) 263.
16 C. E. Dalgleish, *J. Chem. Soc.*, (1952) 3940.

Journal of Chromatography, 513 (1990) 375–378
Elsevier Science Publishers B.V., Amsterdam

CHROM. 22 459

Note

Optical resolution of dihydropyridine enantiomers by high-performance liquid chromatography using phenylcarbamates of polysaccharides as a chiral stationary phase

YOSHIO OKAMOTO*, RYO ABURATANI and KOICHI HATADA
Department of Chemistry, Faculty of Engineering Science, Osaka University, Toyonaka, Osaka 560 (Japan)
and
MIKIKO HONDA, NOBUO INOTSUME and MASAHIRO NAKANO
Department of Pharmaceutical Service, Kumamoto University Hospital, 1–1–1 Honjo, Kumamoto 860 (Japan)
(First received October 12th, 1989; revised manuscript received March 20th, 1990)

Chiral dihydropyridines such as nilvadipine and nicardipine have been attracting much attention as potent calcium antagonists. Although these dihydropyridines exhibit different pharmacological effects between enantiomers[1], racemic mixtures have been used mainly because of difficulties in obtaining optical isomers in pure form and determining their optical purity in plasma. Therefore, high-performance liquid chromatographic (HPLC) separation of optical isomers of dihydropyridines is expected to be beneficial in solving these problems.

Recently, the successful chromatographic resolution of a dihydropyridine, nilvadipine, was achieved with optically active (+)-poly(triphenylmethyl methacrylate) (Chiralpak OT)[2]. It has also been reported that a stationary phase composing of α_1-acid glycoprotein is able to separate a series of dihydropyridine enantiomers using buffers[3]. We reported that optical resolution of nicardipine was possible on HPLC columns packed with xylan bis(3,5-dichlorophenylcarbamate)[4] and cellulose tris(4-*tert.*-butylphenylcarbamate)[5].

In this study, we examined the optical resolution of six dihydropyridines, nimodipine, nilvadipine, benidipine, nitrendipine, isradipine and nicardipine, on phenylcarbamate derivatives of cellulose, amylose and xylan using organic eluents.

EXPERIMENTAL

Polysaccharide phenylcarbamates and chiral stationary phases for HPLC were prepared as reported previously[6]. The stationary phases were packed manually in HPLC columns (25 × 0.46 cm I.D.). The theoretical plate numbers of the columns for benzene were 2800–3700.

Optical resolution was performed on a Jasco Trirotar-II chromatograph equipped with UV (254 nm, Jasco Uvidec 100-III) and polarimetric detectors (435 nm,

0021-9673/90/$03.50

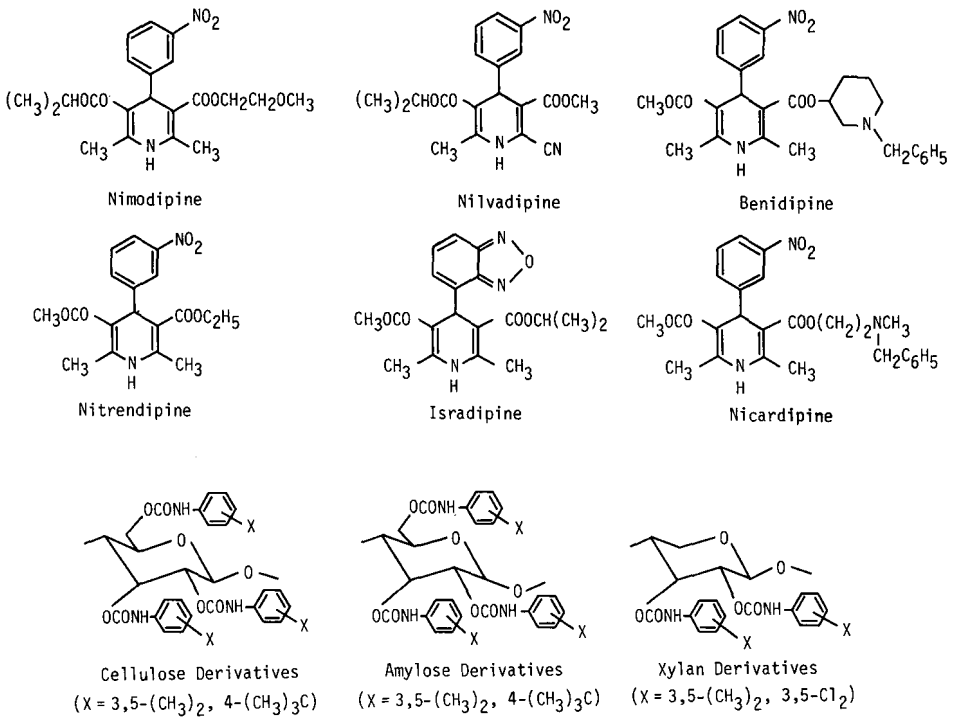

Jasco DIP-181C). The elution time of 1,3,5-tri-*tert.*-butylbenzene was used as the dead time (t_0).

Nimodipine (Bayer Yakuhin), nilvadipine (Fujisawa Pharmaceutical), benidipine (Kyowa Hakko Kogyo), nitrendipine (Sigma), isradipine (Sandoz Pharmaceuticals) and nicardipine (Sigma) were used as analytes without purification.

RESULTS

Fig. 1 shows the optical resolution of nimodipine, nilvadipine and benidipine on xylan bis(3,5-dichlorophenylcarbamate), which showed an effective chiral recognition ability for nicardipine[4]. Although nilvadipine was not completely resolved, nimodipine and benidipine were completely resolved.

Isradipine and nitrendipine were more effectively resolved on cellulose 4-*tert.*-butylphenylcarbamate. The resolution of israpidine, nitrendipine and nicardipine was examined in more detail with four chiral columns and the results are summarized in Table I. Cellulose tris(3,5-dimethylphenylcarbamate), which shows high optical resolving abilities for many racemates[7–9], showed no separation of three dihydropyridines. However, cellulose 4-*tert.*-butylphenylcarbamate resolved the three compounds. Amylose tris(3,5-dimethylphenylcarbamate) showed a more effective chiral recognition ability for isradipine (Fig. 2). Although nicardipine was almost completely resolved on cellulose tris(4-*tert.*-butylphenylcarbamate) and xylan bis(3,5-dichlorophenylcarbamate) using hexane–2-propanol (90:10), the elution time was long[4,5].

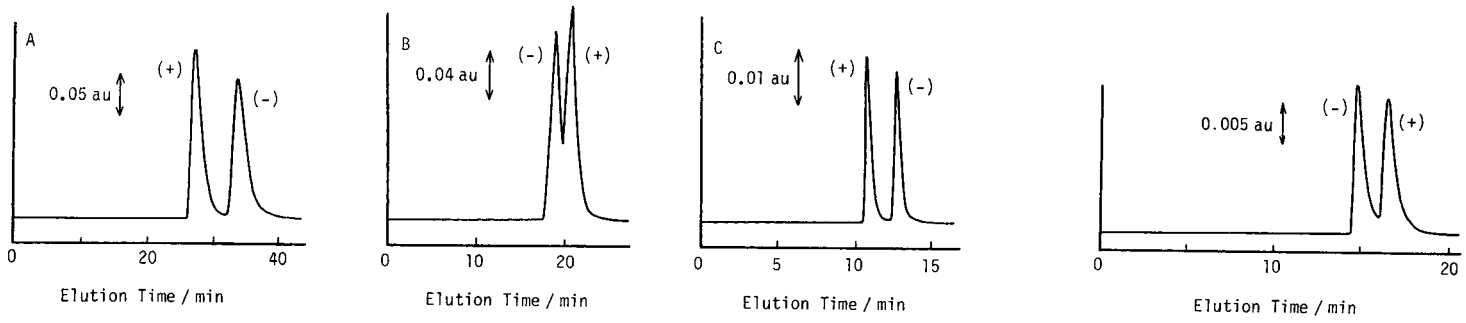

Fig. 1. Chromatographic resolution of dihydropyridine derivatives on xylan bis(3,5-dichlorophenylcarbamate). (A) Nimodipine; (B) nilvadipine; (C) benidipine. Eluent: A and B, hexane–2-propanol–diethylamine (85:15:0.1), 0.5 ml/min; C, hexane–2-propanol–diethylamine (80:20:0.1), 0.5 ml/min.

Fig. 2. Optical resolution of isradipine on amylose tris(3,5-dimethylphenylcarbamate). Eluent: hexane–2-propanol (90:10), 0.5 ml/min.

TABLE I

OPTICAL RESOLUTION OF NITRENDIPINE, ISRADIPINE AND NICARDIPINE ON PHENYLCARBAMATE DERIVATIVES OF POLYSACCHARIDES

Eluent: hexane–2-propanol (90:10).

Polysaccharide	*X*	*Nitrendipine*			*Isradipine*			*Nicardipine*		
		k'_1	α	R_s	k'_1	α	R_s	k'_1	α	R_s
Cellulose	3,5-$(CH_3)_2$	2.22	1.00		1.58	1.00		~1		
Cellulose	4-*tert.*-$(CH_3)_3C$	1.45(+)	1.27	2.14	0.98(−)	1.11	0.77	8.05(−)	1.21	1.29
Amylose	3,5-$(CH_3)_2$	1.78(+)	1.07		1.49(−)	1.19	1.35	5.5	1.00	
Amylose	4-*tert.*-$(CH_3)_3C$	2.72(−)	1.13	0.66	1.82	1.00		3.19	1.00	

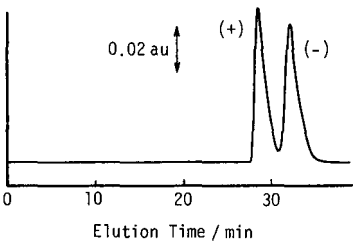

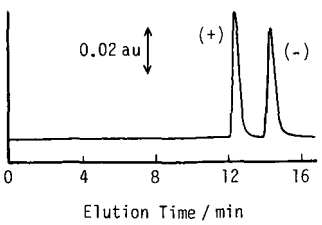

Fig. 3. Enantiomeric resolution of nicardipine on xylan bis(3,5-dimethylphenylcarbamate). Eluent: hexane–2-propanol (90:10), 0.5 ml/min.

Fig. 4. Enantiomeric resolution of nitrendipine on cellulose tris(4-*tert.*-butylphenylcarbamate). Eluent: hexane–2-propanol–chloroform (85:10:5), 0.5 ml/min.

However, as shown in Fig. 3, a more expeditious separation was attained on xylan bis(3,5-dimethylphenylcarbamate) using the same eluent.

The influence of the elution system on the chiral recognition abilities was investigated by adding 5% of chloroform to hexane–2-propanol (90:10). For instance, nitrendipine was better resolved with a small capacity factor ($k'_1 = 0.99$) and a larger separation factor ($\alpha = 1.32$) on cellulose tris(4-*tert.*-butylphenylcarbamate) (Fig. 4). The resolution factor ($R_s = 2.67$) was also larger than those (1.22 and 1.81) on EnantioPac and Chiral-AGP columns, respectively[3]. In contrast, isradipine was less efficiently resolved by adding 5% of chloroform to the eluent with amylose tris(3,5-dimethylphenylcarbamate), giving an α value of 1.10.

The possibility of preparative separation was examined with nitrendipine. About 0.5 mg of the sample was injected in one dose onto the cellulose tris(4-*tert.*-butylphenylcarbamate) column with hexane–2-propanol–chloroform (85:10:5) as the eluent and was almost completely separated into two peaks with an R_s value of 0.97. This suggests that preparative separations will be possible with a larger column.

REFERENCES

1 K. Tamazawa, H. Arima, T. Kojima, Y.Isomura, M. Okada, S. Fujita, T. Furuya, T. Takenaka, O. Inagaki and M. Terai, *J. Med. Chem.*, 29 (1986) 2504–2511.
2 Y. Tokuma,T. Fujiwara and H. Noguchi, *J. Pharm. Sci.*, 76 (1987) 310–311.
3 E. Delee, I. Jullien and L. Le Garrec, *J. Chromatogr.*, 450 (1988) 191–197.
4 Y. Okamoto, R. Aburatani, K. Hatano and K. Hatada, *J. Liq. Chromatogr.*, 11 (1988) 2147–2163.
5 Y. Okamoto, K. Hatano, R. Aburatani and K. Hatada, *Chem. Lett.*, (1989) 715–718.
6 Y. Okamoto, M. Kawashima and K. Hatada, *J. Chromatogr.*, 363 (1986) 173–186.
7 Y. Okamoto, M. Kawashima, R. Aburatani, K. Hatada, T. Nishiyama and M. Masuda, *Chem. Lett.*, (1986) 1237–1240.
8 Y. Okamoto, R. Aburatani, Y. Kaida, K. Hatada, N. Inotsume and M. Nakano, *Chirality*, 1 (1989) 239–242.
9 Y. Okamoto, K. Hatada, T.Senoh and H. Nakane, *Chirality*, 1 (1989) 216–222.

Journal of Chromatography, 513 (1990) 379–383
Elsevier Science Publishers B.V., Amsterdam

CHROM. 22 431

Note

Analytical and preparative separation of glucosylceramide and galactosylceramide by borate-impregnated silica gel chromatography

YOSHIHIRO SAGA, SHINSEI GASA* and AKIRA MAKITA
Biochemistry Laboratory, Cancer Institute, Hokkaido University School of Medicine, Sapporo 060 (Japan)
and
KIYOSHI OIKAWA
Department of Pediatric Dentistry, School of Dentistry, Hokkaido University, Sapporo 060 (Japan)
(First received December 28th, 1989; revised manuscript received March 7th, 1990)

Monohexosylceramides (MHCs), galactosylceramide (GalCer) and glucosylceramide (GlcCer) are the simplest glycolipids and the biosynthetic precursors common to elongation of the carbohydrate chains in all glycolipid series. GalCer can be extended enzymatically to glycolipids belonging to galaseries and to GalCer sulphate. GlcCer can be elongated to all other glycolipid series via lactosylceramide[1]. The relative distributions of GalCer and GlcCer appear to be characteristic for tissues, cell types and animal species (for a review, see ref. 2). For instance, MHCs of adult mammalian brain and Gaucher's spleen consist almost exclusively of GalCer and GlcCer, respectively, whereas in many other tissues the two classes coexist.

In order to separate GlcCer and GalCer, chromatography on a borate-impregnated thin-layer plate[3], prepared from a silica gel slurry in a borax solution, has been employed. More recently, high-performance liquid chromatography (HPLC) of perbenzoylated MHC derivatives was adopted for the separation[4]. These procedures are suitable for analytical purposes rather than preparative separations. However, the necessity for preparative separation of MHCs in tissues is often encountered, such as for the composition analysis of the lipid moieties in each MHC class.

This paper describes an improved thin-layer chromatographic (TLC) and a preparative separation method for GlcCer and GalCer. With the use of these procedures, relative amounts of the two classes in MHCs in various tissues were determined.

EXPERIMENTAL

Materials

Precoated TLC plates (silica gel 60, 20 × 20 cm) and silicic acid (Iatrobeads 6RS-8060) were obtained from Merck (Darmstadt, F.R.G.) and Iatron (Tokyo,

0021-9673/90/$03.50

Japan), respectively. Other reagents were of analytical-reagent grade. Human renal cell carcinoma tissues were obtained at operation and dissected into tumour and uninvolved portions. From the cancer tissues or from the other tissues (see Results and Discussion), an MHC fraction was obtained as described previously[5]. MHC from bovine milk was kindly donated by Snow Brand Milk Products (Tokyo, Japan). Standard glycolipids were prepared in this laboratory. Tritium labeling of GlcCer and GalCer was carried out as described by Schwarzmann[6].

Modified thin-layer chromatography

Proportions of components of solvent mixtures are expressed by volume. In place of a laboratory-made borate-impregnated silica gel plate[3], a precoated silica gel plate was employed. The plate was sprayed with 1% (w/v) aqueous borax (sodium tetraborate), air dried and activated at 110°C in an oven before use. The plate was developed with chloroform–methanol–water–15 *M* ammonia solution (280:70:6:1) (solvent A)[3] or chloroform–methanol–pyridine (60:40:2) (solvent B). Glycolipids were revealed with orcinol–sulphuric acid reagent.

Borate-impregnated silica gel column chromatography

Iatrobeads were suspended in three volumes of 3% (w/v) aqueous borax with vigorous stirring, filtered and dried at 110°C in an oven. A slurry of the silica gel in chloroform–methanol–pyridine–water (70:30:2:1, solvent C) saturated with borax was packed under normal pressure into a glass tube to make a column of 41 × 1.0 cm I.D. Approximately 50 mg of an MHC mixture dissolved in the minimum volume of the same solvent were applied to the column. The column was eluted in a stepwise manner with five column volumes each of solvent C and chloroform–methanol–water (50:50:5, solvent D). The eluates were collected (2 ml per fraction), each concentrated *in vacuo* and monitored by TLC as described above using solvent B for separation of GalCer and GlcCer. The separated MHC was combined, evaporated for the solvent and subjected to Folch's partition[7] to remove the salt.

Analytical methods

The compositions of monosaccharide, fatty acid and long-chain base were determined as described previously[8] using a Shimadzu GC-8A gas chromatograph equipped with a capillary column (25 m × 0.3 mm I.D.) coated with HR-1. The ratio of GalCer and GlcCer in the mixture was also measured by densitometry of the glycolipid spots on the TLC plate with a Shimadzu GS-910 chromatogram scanner as described previously[9].

RESULTS AND DISCUSSION

Improved thin-layer chromatography

When MHCs were developed with two solvent systems containing ammonia solution (solvent A, Fig. 1A) or pyridine (solvent B, Fig. 1B) on the borate-impregnated plates, much better resolution of GlcCer and GalCer with their subcomponents was achieved with the latter solvent. MHC fractions from the same tissue of different animal species and different tissues of the same species were examined by TLC (Fig. 1C). Pig spleen contained only GlcCer, whereas equine spleen contained a small

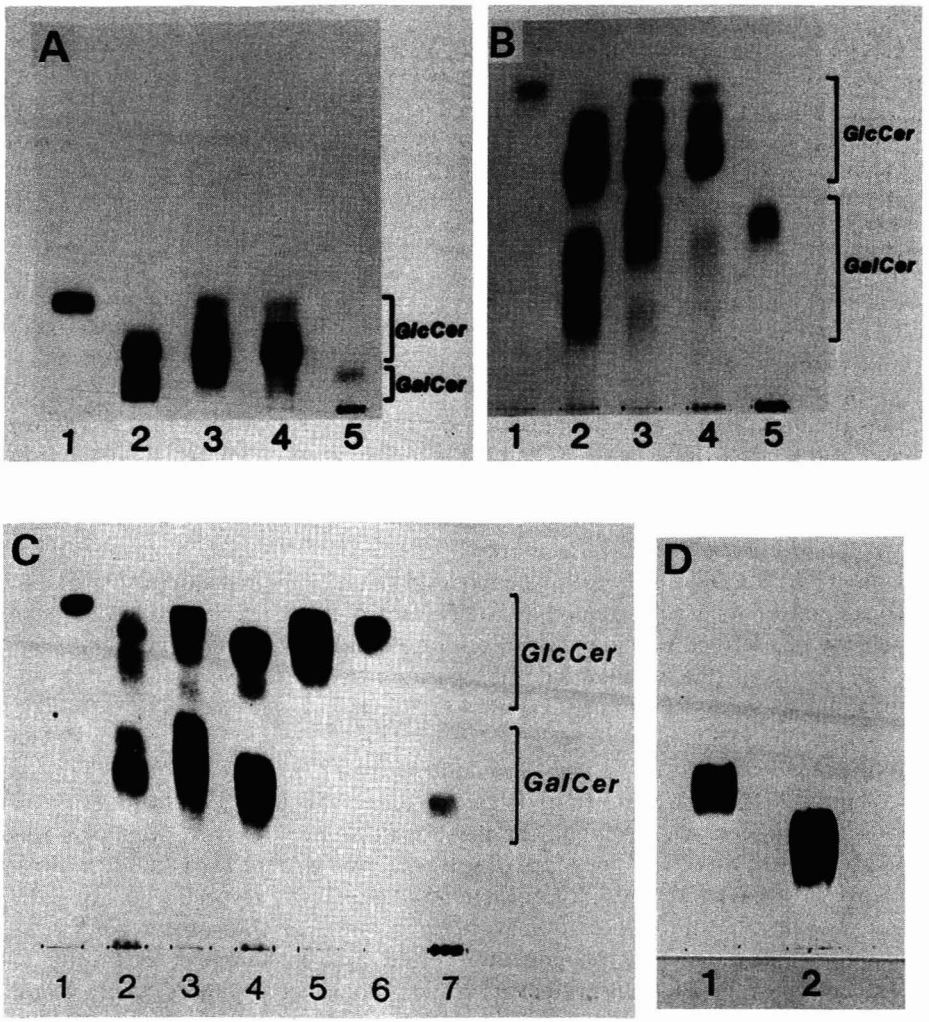

Fig. 1. Borate-impregnated TLC of various MHC with previous and present solvents. A, solvent A[3]; B, C and D, solvent B. Plates A and B: 1 = pig spleen; 2 = equine kidney; 3 = rat kidney; 4 = dog kidney; 5 = cat brain. Plate C: 1 = pig spleen; 2 = pig erythrocyte; 3 = pig serum; 4 = pig intestine; 5 = equine spleen; 6 = bovine milk; 7 = cat brain. Plate D: 1 = upper band of equine kidney GalCer separated by borate-impregnated silica column chromatography; 2 = lower band of the GalCer.

amount of GalCer in addition to GlcCer. For kidney, MHCs from the horse and rat consisted of the two glycolipid classes with a higher content of GlcCer (Fig. 1B), whereas dog contained largely GlcCer (Table I). These results were consistent with observations on rat[10] and dog[11] kidney obtained by carbohydrate analysis of the MHC fractions. An MHC pattern characteristic of tissues was observed in pig (Fig. 1C, Table I). Pig erythrocytes, serum and intestine afforded similar compositions of GlcCer and GalCer, whereas the spleen MHC was exclusively GlcCer. MHC from adult cat brain was composed of exclusively GalCer (Fig. 1), like brain MHC from many other animal species.

TABLE I

RELATIVE CONTENTS OF GlcCer AND GalCer IN VARIOUS TISSUES

Relative contents were determined by densitometric analysis of glycolipid spots on the TLC plate.

Tissue	*GlcCer (%)*	*GalCer (%)*	*Tissue*	*GlcCer (%)*	*GalCer (%)*
Equine kidney	68	32	Pig intestine	66	34
Rat kidney	66	34	Pig spleen	100	0
Dog kidney	90	10	Equine spleen	94	6
Pig erythrocytes	61	39	Bovine milk	100	0
Pig serum	57	43	Cat brain	0	100

On the other hand, when human kidney tumour was measured for the relative contents of the two MHC classes, GlcCer was increased in comparison with that in uninvolved tissue (Table II). In the GlcCer fraction a faster moving component composed mainly of lignoceric and behenic acids (71% of total acids) and sphingenine (95% of total long-chain bases) was markedly increased (Table III). As a significant elevation of PAPS: GalCer sulphotransferase level brought about a marked increase in GalCer sulphate in renal cell carcinoma[5], a decrease in GalCer relative to GlcCer in the tumour may be ascribed to enhanced utilization of GalCer for sulphatide synthesis.

The improved TLC method did not separate two dihexosylceramides, lactosylceramide and galabiosylceramide (Gal-α1–4-GalCer).

Borate-impregnated silica gel column chromatography

When an MHC mixture (50 mg) of equine kidney was subjected to separation on a borate-impregnated silica column, the best separation of the two glycolipids was attained by elution with 5 volumes each of solvent C and solvent D (data not shown). The recoveries of GlcCer and GalCer were 95% and 85%, respectively, using the tritiated glycolipids. Although elution with ten volumes of chloroform–methanol–pyridine (85:15:2) containing no aqueous borate gave a complete separation of GlcCer, the recovery of GalCer thereafter was poor. In instances where slight

TABLE II

MONOHEXOSYLCERAMIDE COMPOSITION IN HUMAN RENAL CELL CARCINOMA

Case[a]	*GlcCer (%)*[b]	*GalCer (%)*
1 U	56(20)	44
1 T	93(86)	7
2 U	89(44)	11
2 T	92(74)	8
3 U	82(29)	18
3 T	93(74)	7

[a] U = Uninvolved tissue; T = tumour tissue.

[b] Values in parentheses indicate percentages of faster moving GlcCer in total GlcCer.

TABLE III

LONG-CHAIN BASE COMPOSITION OF GlcCer AND GalCer FROM EQUINE AND RAT KIDNEY

Kidney	*Glycolipid*	*Composition (%)*[a]			
		d18:1	*d18:0*	*t18:0*	*t20:0*
Equine	GlcCer	1	11	25	63
	GalCer (whole)	38	19	10	33
	GalCer (upper)	86	10	2	2
	GalCer (lower)	3	1	39	57
Rat	GlcCer	8	43	36	13
	GalCer	85	19	5	N.D.

[a] The composition was determined by gas chromatography. d = Dihydroxy base; t = trihydroxy base. N.D. = Not detected.

coelution of two glycolipids (less than 10% of GlcCer with major GalCer) occurs, this overlapping could be prevented by increasing the elution volume of the first solvent mixture, or rechromatography of the overlapped fractions was sufficient for complete separation. As GalCer of equine kidney gave two subfractions with upper and lower bands, the lipid compositions of the subfractions were analysed. The lower components contained fairly large amounts of trihydroxy long-chain bases compared with those in the upper components (Table III), while the fatty acid composition in rat MHC was similar in the two glycolipid classes which could not be separated into subfractions by the column; GalCer contained more dihydroxy bases and 2-hydroxy acids than GlcCer. Thus, in addition to the interaction between borate ion and the galactose moiety of the MHC mixture, the lipid moiety containing *cis*-diol groups also interacts with borate ion, as was observed previously[12].

In conclusion, the improved borate-treated silical gel chromatography on a precoated plate and a column gave a clearer and simpler separation of GlcCer and GalCer for subsequent determination and preparation, respectively.

REFERENCES

1 A. Makita and N. Taniguchi, in H. Wiegandt (Editor), *New Comprehensive Biochemistry*, Vol. 10, Elsevier, Amsterdam, 1985, p. 1.
2 C. C. Sweeley and B. Siddiqui, in M. I. Horowitz and W. Pigman (Editors), *The Glycoconjugates*, Vol. 10, Academic Press, New York, 1977, p. 459.
3 E. L. Kean, *J. Lipid Res.*, 7 (1966) 449.
4 R. H. McCluer, M. A. Williams, S. K. Gross and M. H. Meisler, *J. Biol. Chem.*, 256 (1981) 13112.
5 N. Sakakibara, S. Gasa, K. Kamio, A. Makita and T. Koyanagi, *Cancer Res.*, 49 (1989) 335.
6 G. Schwarzmann, *Biochim. Biophys. Acta*, 529 (1978) 106.
7 J. Folch, M. Lees and G. H. Sloan-Stanley, *J. Biol. Chem.*, 226 (1957) 497.
8 F. Sako, S. Gasa and A. Makita, *Int. J. Biochem.*, 19 (1987) 923.
9 S. Ando, N. C. Chang and R. K. Yu, *Anal. Biochem.*, 89 (1978) 437.
10 J. Kawanami, *J. Biochem.*, 64 (1968) 625.
11 S. J. Sung, W. J. Esselman and C. C. Sweeley, *J. Biol. Chem.*, 248 (1977) 6528.
12 A. Hara and T. Taketomi, *J. Biochem.*, 78 (1975) 923.

Journal of Chromatography, 513 (1990) 384–388
Elsevier Science Publishers B.V., Amsterdam

CHROM. 22 436

Note

High-performance ion-exchange chromatography of peptides on a pellicular ion exchanger

YOSHIO KATO*, SHIGERU NAKATANI, TAKASHI KITAMURA, AKANE ONAKA and TSUTOMU HASHIMOTO

Central Research Laboratory, TOSOH Corporation, Tonda, Shinnanyo, Yamaguchi 746 (Japan)

(First received December 6th, 1989; revised manuscript received February 27th, 1990)

Totally porous supports have commonly been employed in high-performance liquid chromatography (HPLC). On the other hand, pellicular supports, which were once explored in the early stages of HPLC but did not come into general use, have been drawing attention during the last few years particularly in the separation of biopolymers. After Unger and co-workers had shown that pellicular supports of small particle diameter (1.5 μm) are very useful for rapid separations of proteins[1–3], various types of pellicular supports were prepared and some of them have become commercially available. TSKgel DEAE-NPR and TSKgel SP-NPR are such supports for ion-exchange chromatography[4]. They were prepared by introducing diethylaminoethyl or sulphopropyl groups into non-porous spherical hydrophilic resins of 2.5 μm in diameter. We recently demonstrated that proteins[4], oligonucleotides[5] and DNA restriction fragments[6] could be separated rapidly with high resolution on these supports. We have now investigated the separation of peptides on SP-NPR and the results are presented here.

EXPERIMENTAL

Chromatographic measurements were performed at 25°C on a 35 mm × 4.6 mm I.D. stainless-steel column with a system consisting of a Model CCPM double-plunger pump and a Model UV-8000 variable-wavelength UV detector operated at 215 nm (TOSOH, Tokyo, Japan). All peptides were purchased from the Peptide Institute (Osaka, Japan), except insulin, which was obtained from Sigma (St. Louis, MO, U.S.A.).

RESULTS AND DISCUSSION

Fig. 1 shows the separation of a peptide mixture. As exemplified here, peptides of relatively high molecular weights could be separated rapidly with high resolution. However, small peptides of molecular weight below about 1000 were usually eluted as broad tailing peaks (see Table I). The reason is probably that SP-NPR is resin-based

0021-9673/90/$03.50

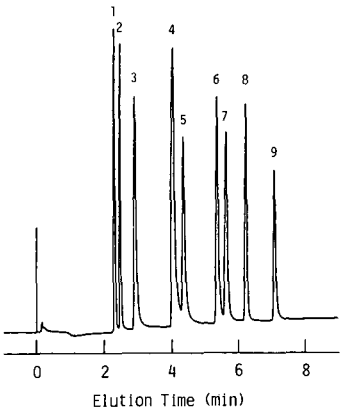

Fig. 1. Separation of a peptide mixture on TSKgel SP-NPR. A mixture of γ-endorphin (1), bombesin (2), luteinizing hormone-releasing hormone (3), somatostatin (4), α-melanophore-stimulating hormone (5), substance P (6), glucagon (7), insulin (8) and β-endorphin (9) was separated with a 30-min linear gradient of sodium sulphate from 0 to 0.25 *M* in a mixture of 20 m*M* acetate buffer (pH 3.5) and acetonitrile (60:40, v/v) at a flow-rate of 1.5 ml/min. Sample loads were 0.25 μg for components 2, 3 and 5 and 0.5 μg for others. The 20 m*M* acetate buffer (pH 3.5) was prepared by adding 20 m*M* sodium acetate to 20 m*M* acetic acid until the pH became 3.5.

TABLE I

PEAK WIDTHS OF PEPTIDES OBSERVED ON SP-NPR

Conditions as in Fig. 1. Peak widths were measured at half-height and multiplied by 1.70.

Peptide	*Molecular weight*	*Peak width (ml)*	*Elution volume (ml)*
TRH[a]	369	0.22	2.13
Leu-enkephalin	556	0.82	1.79
Met-enkephalin	574	0.84	1.49
Angiotensin III	931	0.75	8.75
Oxytocin	1007	0.15	1.07
Angiotensin II	1046	0.43	6.00
Bradykinin	1060	0.42	7.91
LH-RH[b]	1182	0.17	4.48
Angiotensin I	1297	0.47	8.70
Substance P	1348	0.19	8.23
Mastoparan	1480	0.41	11.85
Bombesin	1620	0.13	3.80
Somatostatin	1638	0.24	6.27
α-MSH[c]	1665	0.19	6.63
α-Endorphin	1746	0.15	3.70
γ-Endorphin	1859	0.15	3.49
Motilin	2700	0.18	9.60
VIP[d]	3326	0.27	16.73
β-Endorphin	3465	0.19	11.15
Glucagon	3483	0.16	8.66
Insulin	5808	0.17	9.53

[a] Thyrotropin-releasing hormone.
[b] Luteinizing hormone-releasing hormone.
[c] α-Melanophore-stimulating hormone.
[d] Vasoactive intestinal polypeptide.

and is assumed to have very small pores, although it is said to be non-porous. If small molecules enter such small pores, the diffusion rate there should be slow, which must result in broad and tailing peaks. Some peptides with higher molecular weights were also eluted as slightly broad peaks.

Elution conditions for obtaining good peptide separations were examined. When peptides were separated with eluents that did not contain organic solvents, some were eluted late as broad peaks, probably owing to hydrophobic interactions between the peptides and the support. We then examined the effect of addition of acetonitrile to the eluent. Peptides were separated with 30-min linear gradients of sodium sulphate from 0 to 0.25 *M* in mixtures of 20 m*M* acetate buffer (pH 3.5) and acetonitrile (100:0 to 50:50, v/v) at a flow-rate of 1.5 ml/min. All peptides tested were eluted without significant retardation on addition of more than 20% of acetonitrile to the buffer. The addition of less than 20% of acetonitrile was not sufficient to eliminate the abnormal elution behaviour of some peptides. At acetonitrile concentrations above 20% the peak widths were almost uanchanged, although the selectivity changed to some extent with the content of acetonitrile.

The effect of salt concentration gradient was examined by separating a mixture of insulin and β-endorphin with linear gradients of sodium sulphate from 0 to 0.25 *M* in a mixture of 20 m*M* acetate buffer (pH 3.5) and acetonitrile (60:40, v/v) at a flow-rate of 1.5 ml/min. The gradient time was varied between 5 and 60 min. The resolution for the separation of insulin and β-endorphin is plotted against gradient time in Fig. 2. The resolution increased with increasing gradient time up to 30 min, then became constant. If we consider the separation time and dilution of the sample, which increase as the gradient time becomes longer, gradient times of *ca.* 30 min corresponding to a gradient of about 8 m*M*/min sodium sulphate appear to be a good compromise. Sodium sulphate was employed because it is not corrosive to stainless steel even at low pH and its UV absorption at low wavelengths, *e.g.*, 215 nm, is low. These properties of the salt are important in the separation of peptides on cation exchangers because peptides are usually separated at low pH and detected at low

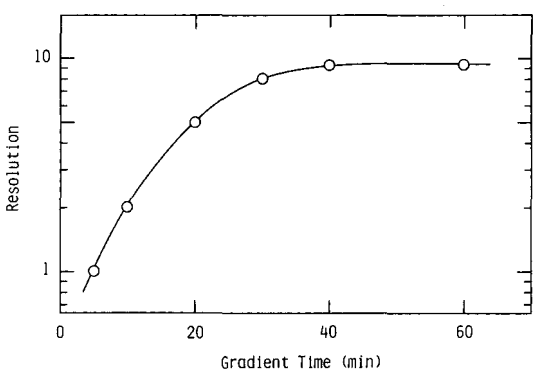

Fig. 2. Dependence of resolution on gradient time in the separation of peptides on TSKgel SP-NPR. A mixture of insulin and β-endorphin was separated under the conditions in Fig. 1 except that the gradient time was varied between 5 and 60 min. The resolution was calculated from the peak widths and elution volumes of the two peptides.

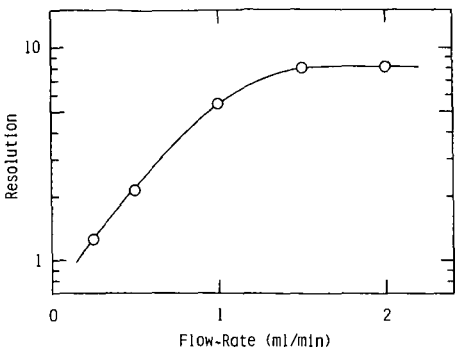

Fig. 3. Dependence of resolution on flow-rate in the separation of peptides on TSKgel SP-NPR. A mixture of insulin and β-endorphin was separated under the conditions in Fig. 1 except that the flow-rate was varied between 0.25 and 2.0 ml/min. Resolutions calculated as in Fig. 2.

wavelength. Some other salts such as sodium perchlorate may be used also in place of sodium sulphate.

The effect of flow-rate was examined by separating a mixture of insulin and β-endorphin with a 30-min linear gradient of sodium sulphate from 0 to 0.25 *M* in a mixture of 20 m*M* acetate buffer (pH 3.5) and acetonitrile (60:40, v/v) at flow-rates of 0.25–2.0 ml/min. The resolution for the separation of insulin and β-endorphin is plotted against flow-rate in Fig. 3. The resolution increased with increasing flow-rate up to 1.5 ml/min, then became constant at higher flow-rates. Although the separation time becomes slightly shorter as the flow-rate increases, the samples are more diluted and the pressure drop becomes higher almost proportionally with the increase in flow-rate. Therefore, flow-rates of *ca.* 1.5 ml/min appear to be a good compromise.

The loading capacity was evaluated by separating some peptides individually with various sample loads. The peak widths remained constant at sample loads up to about 2 μg, then increased with further increase in sample load. Accordingly, the maximum sample load in order to obtain the highest resolution is only about 2 μg for pure samples, although it is expected to be much larger for crude samples as in the separation of proteins[4]. This low loading capacity must be due to the small surface area of SP-NPR and is the greatest disadvantage of pellicular supports.

As demonstrated above, peptides with molecular weights above about 1000 can be separated rapidly with high resolution on the pellicular cation exchanger SP-NPR, whereas small peptides with molecular weights below about 1000 are eluted as broad tailing peaks. The elution with a 30-min linear gradient of sodium sulphate from 0 to 0.25 *M* in a mixture of 20 m*M* acetate buffer (pH 3.5) and acetonitrile (60:40, v/v) at a flow-rate of 1.5 ml/min is generally a good compromise with respect to resolution, separation time and dilution of sample, although shorter gradient times, *e.g.*, 10 min, are recommended when very rapid separations are required.

REFERENCES

1 B. Anspach, K. K. Unger, H. Giesche and M. T. W. Hearn, presented at the *4th International Symposium on HPLC of Proteins, Peptides and Polynucleotides, Baltimore, MD, December 1984*, paper 103.

2 K. K. Unger, G. Jilge, J. N. Kinkel and M. T. W. Hearn, *J. Chromatogr.*, 359 (1986) 61.
3 K. K. Unger, G. Jilge, R. Janzen, H. Giesche and J. N. Kinkel, *Chromatographia*, 22 (1986) 379.
4 Y. Kato, T. Kitamura, A. Mitsui and T. Hashimoto, *J. Chromatogr.*, 398 (1987) 327.
5 Y. Kato, T. Kitamura, A. Mitsui, Y. Yamasaki and T. Hashimoto, *J. Chromatogr.*, 447 (1988) 212.
6 Y. Kato, Y. Yamasaki, A. Onaka, T. Kitamura and T. Hashimoto, *J. Chromatogr.*, 478 (1989) 264.

Journal of Chromatography, 513 (1990) 389–391
Elsevier Science Publishers B.V., Amsterdam

CHROM. 22 439

Note

Simple method for the isolation of azadirachtin by preparative high-performance liquid chromatography

T. R. GOVINDACHARI*, G. SANDHYA and S. P. GANESHRAJ
Agrochemical Research Laboratory, SPIC Science Foundation, 110 Mount Road, Guindy, Madras 600 032 (India)
(First received October 24th, 1989; revised manuscript received January 5th, 1990)

Azadirachtin, first isolated by Butterworth and Morgan[1] from neem (*Azadirachta indica* A. Juss.) kernels, has been studied intensively during the past 15 years by organic chemists probing and finally solving[2–5] its intricate molecular architecture and by entomologists on account of its powerful antifeedant and hormonal activity towards many species of insects[6]. Although azadirachtin is present to the extent of 0.2–0.6% in neem kernels, its isolation[1,3,7–12] in a pure state is tedious and time consuming, involving repeated partitioning between solvents and elaborate chromatography under a variety of conditions. It is neither necessary nor practical to use azadirachtin as such for insect control. Only small amounts are required for biological studies and as an analytical standard.

In the course of numerous high-performance liquid chromatographic (HPLC) determinations of the azadirachtin content of ethonolic extracts of neem kernels, it was observed that azadirachtin could always be obtained as a peak distinct from those of most other components. This suggested the possibility of developing a simple procedure for the isolation of azadirachtin by direct preparative HPLC, using an ODS column and methanol–water (60:40) as eluent. The azadirachtin obtained by the direct preparative HPLC method was identical in all respects with a sample prepared by the procedure of Schroeder and Nakanishi[12], which was modified after the vacuum liquid chromatographic stage as we did not succeed in improving the azadirachtin content by carbon tetrachloride crystallisation. The azadirachtin-rich fraction from vacuum liquid chromatography was further purified by medium-pressure liquid chromatography on silica gel with a final purification by preparative HPLC on an ODS column. The specific rotation and ^1H and ^{13}C NMR data were in excellent agreement with data reported by Kraus *et al.*[5] and Butterworth *et al.*[7].

EXPERIMENTAL AND RESULTS

HPLC studies were carried out on a Shimadzu Model LC-8A system linked to a C-R4A data processor. The peaks were detected with a Shimadzu SPD-6AV detector at 215 nm. A Shimpack analytical ODS column (15 cm × 4.6 mm I.D.) was used for

0021-9673/90/$03.50

analytical studies and a Shimpack preparative ODS column (25 cm × 20 mm I.D.) for preparative work.

Neem kernel powder (15 g) was defatted with hexane in a Soxhlet apparatus for 2 h. The dry, defatted powder was extracted with four 15-ml portions of boiling 95% ethanol on a hot water-bath for 10 min, each time decanting the extract through a filter-paper and diluting to 100 ml with 95% ethanol.

A 20-μl portion was removed for determination of the azadirachtin content by analytical HPLC with methanol–water (60:40) as eluent. Valley-to-valley integration of the azadirachtin peak and calculation of the azadirachtin content from a calibration graph of peak area (ordinate) *versus* azadiractin content in nanograms (abscissa) showed a total content of 0.4%.

The alcohol was removed *in vacuo* at 45°C and the residue was dried to constant weight (1.5 g). A weighed portion of the residue was also analysed for azadirachtin content and the result was in agreement with the earlier analysis.

The hexane extract was repeatedly shaken with 90% methanol. The hexane layer on evaporation yielded an oil (5.1 g). The residue from the methanol layer (0.5 g) contained a detectable amount of azadirachtin as shown by HPLC. Apparently, the oil carries with it a small amount of azadirachtin and other compounds. Similar fractions from a number of runs can be pooled and processed for recovery of azadirachtin. It is essential, however, to defat the kernels with hexane, as they contain 30% of oil and the azadirachtin content is *ca.* 0.3%. It is not desirable to load the reversed-phase column with an excess of non-polar material.

Isolation of pure azadirachtin by preparative HPLC

A 500-mg amount of the ethanol extract residue was dissolved in 1 ml of methanol, centrifuged at 15 500 *g* to remove insoluble matter, filtered through a Millipore filter (0.25 μm) and then injected into the preparative column and eluted with methanol–water (60:40). The flow-rate was adjusted at 10 ml/min. for the first 25 min. Under these conditions, components of high polarity were eluted in the first 10 min, followed by a small peak. The azadirachtin peak appeared next and was centred at 14.4 min during the preparative run. As the left-hand segment of the peak ascended from the baseline, the eluent was collected until the peak had attained two thirds of the maximum height (fraction A). Collection of the azadirachtin fraction was begun when this two thirds of peak height had been reached and was ended when the peak descended to the baseline again (fraction B). Fraction A contained, in approximately equal amounts, azadirachtin with a retention time of 5.3 min on an analytical ODS column and a compound with a slightly shorter retention time of 5.1 min. Fraction B yielded azadirachtin, identical with an authentic sample as shown by HPLC. At 18.5 min, another peak was detected which was also collected for further investigation. After 25 min, the flow-rate was increased to 50 ml/min. to remove all of the less polar components from the column, this process taking about 45 min. At least six distinct peaks were collected for further investigation. The less polar compounds could be removed better by eluting the column with pure methanol for 20 min at a flow-rate of 25 ml/min. Restabilization of the column with methanol–water (60:40) for another 20 min at a flow-rate of 25 ml/min renders it ready for the next run.

Preparation of the standard sample

Neem kernels (1 kg) were extracted with three 1-l portions of methanol over a period of 3 days. The methanol was removed *in vacuo* at 45°C and the residue partitioned between aqueous methanol–hexane and aqueous methanol–ethyl acetate as reported by Schroeder and Nakanishi[12]. The residue of the ethyl acetate extract (34.5 g) was subjected to vacuum liquid chromatography on silica gel (Acme, 250–400 mesh, 500 g) using hexane–ethyl acetate (25:75). The azadirachtin-containing fraction yielded a residue (11.4 g) which was subjected to medium-pressure liquid chromatography on a Büchi column (450 mm × 49 mm I.D.) loaded with silica gel (Acme, 250–400 mesh, 500 g). The column was eluted with hexane–ethyl acetate (25:75) and fifteen 250-ml fractions were collected. The azadirachtin-enriched residue of fraction 9 (2.8 g) was subjected to preparative HPLC in portions with methanol–water (60:40). From 500 mg of this enriched fraction 170 mg of azadirachtin were isolated. It had a retention time of 5.3 min when analysed on an analytical ODS column eluted with methanol–water (60:40) at a flow-rate of 0.8 ml/min. $[\alpha]_D^{28}$ − 53°. ^1H and ^{13}C NMR data were in excellent agreement with earlier data[5,7].

DISCUSSION

Using an ODS column of I.D. 20 mm, the optimum batch size was 500 mg of the residue from the ethanolic extract (the total residue from 15 g of kernels was 1.5 g). Using the procedure described under Experimental and Results, each run could be completed in about 1 h, yielding 10–15 mg of azadirachtin and several runs can be effected in succession. Using larger preparative columns (I.D. 50 mm and above), which are commercially available, the batch size can be increased to 5 g.

ACKNOWLEDGEMENTS

We are grateful to Professors Rembold and Nakanishi for samples of azadirachtin, Dr. N. Chandrakumar (CLRI, India) for ^1H NMR spectra and Dr. R. Balasubramanian (University of Madras, India) for ^{13}C NMR spectra.

REFERENCES

1 J. H. Butterworth and E. D. Morgan, *J. Insect Physiol.*, 17 (1971) 969.
2 D. A. H. Taylor, *Tetrahedron*, 43 (1987) 2779.
3 C. J. Turner, M. S. Tempesta, R. B. Taylor, M. G. Zagorski, J. S. Termini, D. R. Schroeder and K. Nakanishi, *Tetrahedron*, 43 (1987) 2789.
4 J. N. Bilton, H. B. Broughton, P. S. Jones, S. V. Ley, Z. Lidert, E. D. Morgan, H. S. Rzepa, R. N. Sheppard, A. M. Z. Slawin and D. J. Williams, *Tetrahedron*, 43 (1987) 2805.
5 W. Kraus, M. Bokel, A. Bruhn, R. Cramer, I. Klaiber, A. Klenk, G. Nagl, H. Pohnl, H. Sadlo and B. Vogler, *Tetrahedron*, 43 (1987) 2817.
6 H. Rembold, in H. Wagner and R. Norman (Editors), *Economic and Medicinal Plant Research*, Vol. 3, Academic Press, New York, 1989, p. 57.
7 J. H. Butterworth, E. D. Morgan and G. R. Percy, *J. Chem. Soc., Perk Trans. 1*, (1972) 2445.
8 P. R. Zanno, I. Miura, K. Nakanishi and D. L. Elder, *J. Am. Chem. Soc.*, 97 (1975) 1975.
9 K. Nakanishi, in V. C. Runeckles (Editor), *Recent Advances in Phytochemistry*, Vol. 9, Plenum Press, New York, 1975; and references cited therein.
10 E. C. Uebel, J. D. Warthen, Jr. and M. Jacobson, *J. Liq. Chromatogr.*, 2 (1979) 875.
11 R. B. Yamasaki, J. A. Klocke, S. M. Lee, G. A. Stone and M. V. Darlington, *J. Chromatogr.*, 356 (1986) 220.
12 D. R. Schroeder and K. Nakanishi, *J. Nat. Prod.*, 50 (1987) 241.

Journal of Chromatography, 513 (1990) 392–396
Elsevier Science Publishers B.V., Amsterdam

CHROM. 22 515

Note

High-performance liquid chromatographic analysis of trimethoprim in the presence of its degradation products

J. J. BERGH* and J. C. BREYTENBACH
Department of Pharmaceutical Chemistry, Potchefstroom University for Christian Higher Education, Private Bag X6001, Potchefstroom 2520 (South Africa)
and
J. L. DU PREEZ
Institute for Industrial Pharmacy, Potchefstroom University for Christian Higher Education, Potchefstroom 2520 (South Africa)
(First received September 25th, 1989; revised manuscript received April 23rd, 1990)

Various analytical methods have been used to determine trimethoprim in pharmaceuticals and biological fluids, including colorimetric analysis[1], first-derivative spectrophotometry[2], potentiometric analysis[3], polarography[4,5], gas–liquid chromatography[6,7], high-performance liquid chromatography (HPLC)[8–12] and thin-layer chromatography[13–17]. The last method[17] is claimed to be free from interferences by related and degradation products. Although with some of these procedures trimethoprim could be separated from its metabolites[5,10,13–15] with only one HPLC method trimethoprim was determined in the presence of two of its degradates[8].

We have succeeded in isolating five trimethoprim degradation products[18] and have published an HPLC analysis of trimethoprim in pharmaceuticals, using a Zorbax TMS column[19]. This method was free from interferences by the degradation products but when such a column was used during a kinetic study on samples containing trimethoprim in various buffer solutions, distortion of the trimethoprim peak occurred.

A trouble-free method, using a Partisil 10 ODS-3 column was then developed. The method was subsequently evaluated in the analyses of tablets and suspensions. This assay, which is described here, was found to be stability indicating and reliable.

EXPERIMENTAL

Degradation of trimethoprim

The degradation of trimethoprim and the isolation of degradation products (Fig. 1) were achieved as described previously[18].

0021-9673/90/$03.50

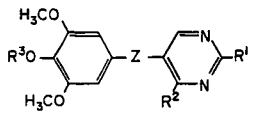

	R^1	R^2	R^3	Z
1	NH_2	NH_2	CH_3	$-CH_2-$
2	NH_2	NH_2	CH_3	$-\overset{O}{\overset{\|}{C}}-$
3	OH	OH	CH_3	$-CH_2-$
4	OH	NH_2	CH_3	$-CH_2-$
5	NH_2	OH	CH_3	$-CH_2-$
6	NH_2	OH	H	$-CH_2-$

Fig. 1. Structures of trimethoprim (1) and its degradation products.

Materials

Ammonium acetate (analytical grade) and acetonitrile (HPLC grade) both from Merck, South Africa, were used. Trimethoprim was supplied by Wellcome, South Africa.

Instrumentation

An M-45 dual-piston pump and a Model 441 fixed-wavelength detector at 254 nm, both from Waters Assoc. (Milford, MA, U.S.A.) were used. Sample injection was accomplished by means of a Rheodyne loop injector, Type 7012 equipped with a 20-μl loop. Peaks were integrated with a Waters 740 data module. Degassed mobile phase, consisting of acetonitrile (25%) and ammonium acetate (1%) in water at a flow-rate of 1 ml/min was used. A stainless-steel column (250 × 4.6 mm I.D.) packed with Partisil 10 ODS-3 (Whatman, Clifton, NJ, U.S.A.) was used.

Preparation of chromatographic solutions

Standard solutions containing 200–300 μg of trimethoprim per ml of methanol were prepared to obtain calibration graphs.

Sample solutions, to test the reproducibility of the method, were prepared using commercial tablets and a suspension (a single brand of each). Twenty tablets (100 mg of trimethoprim per tablet) were weighed, powdered and an amount of powder equivalent to 100 mg of trimethoprim was suspended in methanol, sonicated for 2 min, filtered and diluted with methanol to a concentration of about 250 μg of trimethoprim/ml. The suspension samples (50 mg of trimethoprim/5 ml) were diluted with methanol to the same concentration as above, sonicated and filtered.

Unfortified and fortified samples were prepared to evaluate the accuracy of the procedure. The unfortified tablet and suspension samples contained about 125 μg of trimethoprim/ml and were prepared in a similar manner as the sample solutions above.

Fortified sample solutions were prepared by spiking the unfortified samples with 60–120% of trimethoprim.

Analytical procedure

The analysis was performed in two separate stages. The first stage included all the tablet samples and the second stage the suspension samples. Six calibration samples (200–300 μg of trimethoprim/ml) were included in both the stages. All of the first stage solutions were chromatographed in sequence, followed by a second and third run after which the procedure was repeated with the suspension stage. The average of the three areas under the curves thus obtained was used in the calculations. *n*-Propyl *p*-hydroxybenzoate, present in the suspension and having a retention time of more than 50 min, can be eluted by flushing the column with acetonitrile for 6 min.

RESULTS AND DISCUSSION

A number of stationary phases were evaluated during the development of this method. Initially a Zorbax TMS column (DuPont, Wilmington, DE, U.S.A.) was used as it gave reproducible results with tablets and suspensions[19]. However, when this type of column was used during a kinetic study, distortion of the trimethoprim peak was evident in all samples containing buffer components (phosphates, sodium borate, potassium chloride, hydrochloric acid and sodium hydroxide). At lower buffer concentrations peaks tended to be flattened and broadened while higher buffer concentrations yielded completely distorted peaks. The reason for this distortion is not clear. It may possibly be attributed to the adsorption of inorganic ions to free silanol groups on the support which could then change the kinetics of molecular exchange. It was also found that the trimethoprim peaks obtained from suspension samples were flatter and slightly broader than those obtained from tablet samples. This phenomenon is probably due to various excipients in the suspension causing the same problem as mentioned above.

No peak distortion or change in theoretical plate count were observed when reverting back to trimethoprim solutions free of inorganic substances. These findings seem to indicate that peak distortion on the TMS column is the result of the composition of the sample rather than that of the mobile phase. Thus, although the mechanism which causes peak distortion is not known, it is clear that the process is reversible with no permanent damage to the column. These problems ruled out the TMS column for samples containing buffer components during a kinetic study.

A trouble-free method using a Partisil 10 ODS-3 column was subsequently developed. Baseline separation of trimethoprim in the presence of its degradates was achieved (Fig. 2a), which indicates that the method is stability-indicating. Identification of the five degradation products is possible in a single run. When this method was applied to various sample solutions during a kinetic study it was found that buffer components (hydrochloric acid, sodium hydroxide, sodium tetraborate, sodium acetate, citric acid, potassium dihydrogen phosphate, potassium chloride and trishydroxymethylaminomethane) caused no interference or peak distortion. The analysis was also carried out on trimethoprim–sulphamethoxazole combinations and it was found that sulphamethoxazole (retention time 3.9 min) presented no problem during the procedure. Chromatograms of the tablet and suspension samples are shown in Fig. 2b and c.

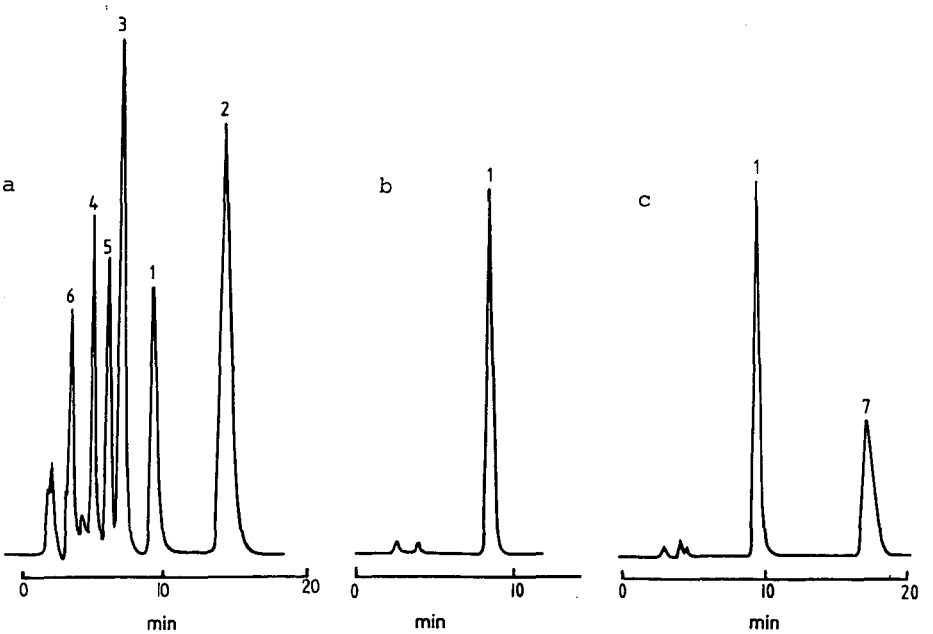

Fig. 2. (a) Chromatogram of trimethoprim (50 μg/ml) in the presence of its degradation products. Peak Nos. 1–6 refer to Fig. 1. (b and c) Chromatograms of trimethoprim in tablets (b) and suspension (c). Peak 7 = methyl *p*-hydroxybenzoate.

A Nucleosil C_{18} column (Machery-Nagel, Düren, F.R.G.) gave results similar to the Partisil ODS, the only exception being an incomplete separation between methyl *p*-hydroxybenzoate (present in the suspension) and compound 2 on the former column. This phenomenon however, did not influence the analysis of trimethoprim.

The pH of the mobile phase, which was adjusted to 6.90 ± 0.1 by ammonium acetate, is important for proper separation. While a pH value of 6.5 still rendered satisfactory results, baseline separation between trimethoprim and compound 5 (50 μg/ml of each) could not be achieved at pH values $\leqslant 6$.

Although a mobile phase containing 25% acetonitrile was used, the speed of analysis can be optimized by using the highest concentration of acetonitrile that will still effect baseline separation between trimethoprim and its degradates.

Calibration and calculation

A linear response was obtained for peak area *versus* concentration of the trimethoprim standard solutions between 200 and 300 μg/ml. The equations of the calibration graphs for six solutions were $y = 8.980x - 37.96$ ($r^2 = 0.9997$) and $y = 9.002x - 30.50$ ($r^2 = 0.9998$) for the tablet and suspension stages, respectively, where x is the concentration of trimethoprim and y the corresponding peak area.

The quantity of trimethoprim in the samples was calculated using the external standard method by substituting the peak area (y) in the appropriate equation above.

Range of linearity and detection limits

The detector response was found to be linear between 1.0–500 μg/ml (r^2 = 0.9999) while the limit of detection (signal-to-noise ratio 3:1) was 0.2 μg/ml.

Reproducibility

The coefficients of variation (C.V.) were 0.98 and 0.56%, respectively, for six tablet and six suspension samples. The average C.V. for three injections, calculated for all the chromatographed solutions, was 0.45%.

Accuracy

The average recovery, calculated from six fortified and six unfortified tablet samples was 99.4% (C.V. = 0.87%). The result for the same number of suspension samples was 99.1% (C.V. = 0.80%).

CONCLUSION

The method described for the quantification of trimethoprim in tablets and suspensions is simple, accurate and reproducible. Buffer components, sulphamethoxazole, methyl *p*-hydroxybenzoate and *n*-propyl *p*-hydroxybenzoate caused no interference during the analyses.

REFERENCES

1 A. K. Sanyal and D. Laha, *J. Assoc. Off. Anal. Chem.*, 66 (1983) 1447.
2 M. A. Korany, A. M. Wahbi, M. A. Elsayed and S. Nandour, *Anal. Lett.*, 17 (1984) 1373.
3 S.-Z. Yao, J. Shiao and L.-H. Nie, *Talanta*, 34 (1987) 983.
4 L. G. Chatten, B. S. Pons and P. McLeod, *Analyst (London)*, 107 (1982) 1026.
5 M. A. Brooks, J. A. F. de Silva and L. D'Arconte, *J. Pharm. Sci.*, 62 (1973) 1395.
6 E. Röder and W. Stuthe, *Dtsch. Apoth.-Ztg.*, 115 (1975) 1461.
7 A. P. Lötter and A. P. Goossens, *S. Afr. Pharm. J.*, 44 (1977) 282.
8 R. O. Singletary, Jr. and F. D. Sancilio, *J. Pharm. Sci.*, 69 (1980) 144.
9 O. Spreux-Varoquaux, J. P. Chapalain, P. Cordonnier, C. Advenier, M. Pays and L. Lamine, *J. Chromatogr.*, 274 (1983) 187.
10 L. Nordholm and L. Dalgaard, *J. Chromatogr.*, 305 (1984) 391.
11 *The United States Pharmacopeia*, Mack Printing Co., Easton, PA, 22nd rev., 1990, p. 1292–1294.
12 K. van der Steuijt and P. Sonneveld, *J. Chromatogr.*, 422 (1987) 328.
13 D. E. Schwartz, W. Vetter and G. Englert, *Arzneim.-Forsch.*, 20 (1970) 1867.
14 C. W. Sigel and M. E. Grace, *J. Chromatogr.*, 80 (1973) 111.
15 C. W. Sigel, M. E. Grace, C. A. Nichol and G. H. Hitchings, *J. Pharm. Sci.*, 63 (1974) 1203.
16 H. Tomankova, M. Vasatova and J. Zyka, *Anal. Lett.*, 21 (1988) 227.
17 K. Datta and S. K. Das, *J. Liq. Chromatogr.*, 11 (1988) 3079.
18 J. J. Bergh, J. C. Breytenbach and P. L. Wessels, *J. Pharm. Sci.*, 78 (1989) 348.
19 J. J. Bergh and J. C. Breytenbach, *J. Chromatogr.*, 387 (1987) 528.

Journal of Chromatography, 513 (1990) 397–400
Elsevier Science Publishers B.V., Amsterdam

CHROM. 22 457

Note

Determination of isoflavones from *Ononis spinosa* L. extracts by high-performance liquid chromatography with ultraviolet diode-array detection

PIERGIORGIO PIETTA* and PIERLUIGI MAURI
Dipartimento di Scienze e Tecnologie Biomediche, Sezione di Chimica Organica, Università di Milano, Via G. Celoria 2, 20133 Milan (Italy)
and
ENRICO MANERA and PIERLUIGI CEVA
S.I.T., Via Cavour 70, 27035 Mede (Italy)
(First received November 8th, 1989; revised manuscript received March 1st, 1990)

The root extracts of *Ononis spinosa* L. are known[1] to be diuretically active. In a previous paper[2] we reported the high-performance liquid chromatographic (HPLC) determination of flavonoids from *Ononis spinosa* L. roots. Isolation of these components was carried out by extraction of the tissue with 50% ethanol at 70°C. Chromatographic separation was then performed on a μBondapak C_{18} column by gradient elution with acetonitrile–water (pH 2.6). However, isocratic conditions are preferred for quantitative analysis because of the greater reproducibility, especially when routine determinations are required.

In this respect, it has been recently been shown that eluents containing C_3 alcohols and ethers have great potential for the isocratic HPLC determination of flavonoids in different extracts, such as *Passiflora incarnata L.*[3], *Crataegus monogyna*[3], *Matricaria chamomilla*[4], *Ginkgo biloba*[5] and *Betulae folium*[6]. This paper describes a similar approach for the determination of genistein, formononetin and biochanin A in *Ononis spinosa* L. extracts.

Isolation of the isoflavones is carried out by percolation of the extract through a Sep-Pak C_{18} cartridge, washing with water followed by water–acetonitrile (75:25) and selective elution of the retained isoflavones with methanol. Determination of the isolated isoflavones is carried out by HPLC on a C_8 Aquapore RP 300 column and UV diode-array detection (DAD). Elution is isocratic using 2-propanol–tetrahydrofuran–water (28:2:70).

EXPERIMENTAL

Materials

Authentic samples of genistein (ICN Pharmaceuticals, Plainview, NY, U.S.A.), formononetin (Extrasynthese, Genay, France) and biochanin A (Aldrich Europe,

0021-9673/90/$03.50

Beerse, Belgium) were purchased as standards. *Ononis spinosa* root extracts were obtained from different commercial sources.

2-Propanol and tetrahydrofuran were of HPLC grade (Baker, Deventer, The Netherlands). Sep-Pak C_{18} cartridges (Waters Assoc., Milford, MA, U.S.A.) were used for sample preparation.

Apparatus

The HPLC analysis was carried out on a Waters Assoc. liquid chromatograph equipped with a Model U6K universal injector and a Model 510 pump connected to a Model HP 1040A photodiode-array detector (Hewlett-Packard, Waldbronn, F.R.G.). The column used was a C_8 Aquapore RP 300 (7 μm spherical) (250 × 4.6 mm I.D.) (Brownlee Labs., Santa Clara, CA, U.S.A.). The mobile phase was 2-propanol–tetrahydrofuran–water (28:2:70, v/v/v) at a flow-rate of 1 ml/min.

The signals were acquired (all with 4 nm band width) at 254, 280 and 310 nm. The acquisition of UV spectra was automatic at the apex, both inflection points and the base of all peaks (200–400 nm, 2-nm steps).

Purity assay of the chromatographic peaks

The UV spectra acquired for each peak, after subtraction of the corresponding UV base spectrum, were computer normalized and the plots were superimposed. Peaks were considered as chromatographically pure when there was exact coincidence among their corresponding UV spectra.

Sample preparation

A Sep-Pak C_{18} cartridge was activated by passing 3 ml of methanol followed by 5 ml of water. An 1-ml volume of *Ononis spinosa* L. hydro–alcoholic extract was diluted with 1 ml of water, percolated through the cartridge and washed with 3 ml of water and 5 ml of water–acetonitrile (3:1). The isoflavones were then eluted with methanol (4 ml). The solvent was evaporated to dryness and the residue was dissolved in methanol (1 ml).

Calibration graphs

Genistein, formononetin and biochanin A were dissolved in methanol at concentrations of 1 mg/ml. These stock solutions were diluted with the eluent to obtain reference solutions containing 0.01–0.2 μg in 10 μl.

RESULTS AND DISCUSSION

The chromatogram in Fig. 1 shows a typical run with a standard mixture of genistein, formononetin and biochanin A. As indicated in Fig. 2, adequate separation of the isoflavones in *Ononis spinosa* L. extracts can be achieved in less than 18 min.

The UV spectra of genistein (G), formononetin (F) and biochanin A (B) are presented in Fig. 3. When the acquired UV spectra were computer normalized, plotted and superimposed, exact coincidence curves were obtained (match factor >990). Consequently, the peaks were assumed to be pure. The first chromatographic runs were carried out using 2-propanol–water (30:70) as eluent, and sharp peaks were obtained. However, from the DAD analysis it was clear that the formononetin peak

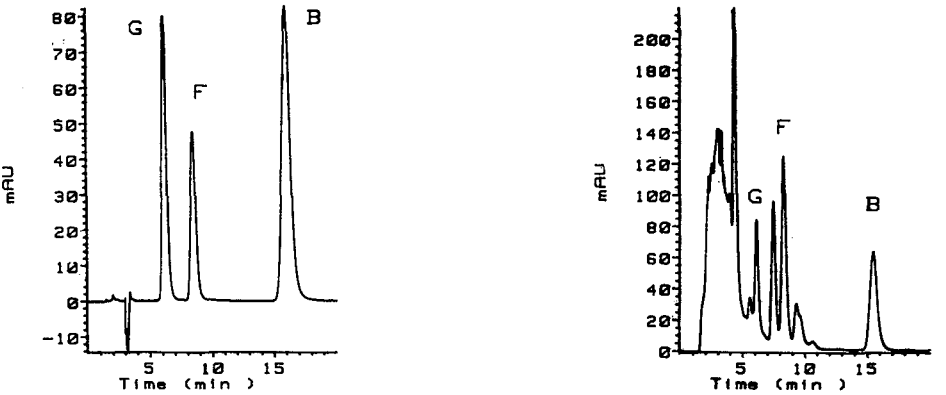

Fig. 1. Chromatogram of genistein (G, 60 ng), formononetin (F, 30 ng) and biochanin A (B, 80 ng) standards. Chromatographic conditions: column, C_8 Aquapore RP 300; eluent, 2-propanol–tetrahydrofuran–water (28:2:70); flow-rate, 1.0 ml/min; UV detection at 254 nm.

Fig. 2. Typical chromatogram of an *Ononis spinosa* L. extract. Chromatographic conditions as in Fig. 1.

was not pure. Addition of 2% of tetrahydrofuran to the 2-propanol phase allowed formononetin to be separated from later eluting components (the broad peak at 9.5 min). Further exact coincidence between the UV spectra of the peaks and those of their corresponding isoflavone standards was found, thus confirming their previous identification through the retention times.

Rectilinear responses between peak area and amounts injected were obtained from three replicate injection of genistein, formononetin and biochanin A standard solutions in the range 10–200 ng, as indicated by the following equations:

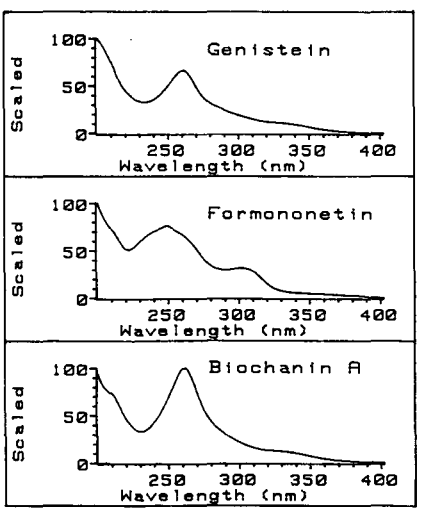

Fig. 3. UV spectra of genistein (G), formononetin (F) and biochanin A (B).

TABLE I

CONTENTS OF GENISTEIN, FORMONONETIN AND BIOCHANIN A IN THREE COMMERCIAL *ONONIS SPINOSA* EXTRACTS

Extract	*Compound (mg per 100 g)*		
	Genistein	*Formononetin*	*Biochanin A*
I	1.7	3.2	0.08
II	2.1	4.7	0.21
III	3.8	5.9	0.30

$y = 10.4x + 0.53$ $r = 0.998$ (genistein)
$y = 26.4x + 2.31$ $r = 0.996$ (formononetin)
$y = 12.1x + 1.03$ $r = 1.000$ (biochanin A),

where y represents the peak area and x the amount injected (ng).

Tests on standards gave recoveries of 98 $\pm$ 1.5% and, with a certain amount of standard added to the extract, 96.4 $\pm$ 4.2%. Intra-day relative standard deviations were determined by assaying the samples four times on the same days and were 2.9%, 3.0% and 3.4% for genistein, formononetin and biochanin A, respectively. Inter-day relative standard deviations were obtained by analysing the samples daily for a week and were 2.6%, 2.9% and 3.2% for genistein, formononetin and biochanin A, respectively.

Analysis of commercial extracts was performed by external standardization, with a good relative standard deviation of 3.2% ($n = 5$), and the results are reported in Table I.

REFERENCES

1 E. Steinegger and R. Hansel, *Lehrbuch der Pharmakognosie*, Springer, Berlin, 1972, p. 148.
2 P. G. Pietta, A. Calatroni and C. Zio, *J. Chromatogr.*, 280 (1983) 172.
3 P. G. Pietta, E. Manera and P. L. Ceva, *J. Chromatogr.*, 357 (1986) 233.
4 P. G. Pietta, E. Manera and P. L. Ceva, *J. Chromatogr.*, 404 (1987) 279.
5 P. G. Pietta, P. L. Mauri and A. Rava, *J. Chromatogr.*, 437 (1988) 453.
6 P. G. Pietta, P. L. Mauri, E. Manera and P. L. Ceva, *Chromatographia*, 28 (1989) 311.

Journal of Chromatography, 513 (1990) 401–404
Elsevier Science Publishers B.V., Amsterdam

CHROM. 22 451

Note

Use of thin-layer chromatography for the testing of avermectins produced by *Streptomyces avermitilis* strains

M. MALANÍKOVÁ and V. MALANÍK
Research Institute for Feed Supplements and Veterinary Drugs, 281 61 Kouřim (Czechoslovakia)
and
M. MAREK*
Biotechnology Centre, Department of Biochemistry and Microbiology, Institute of Chemical Technology, 166 28 Prague (Czechoslovakia)
(First received November 7th, 1989; revised manuscript received February 27th, 1990)

Avermectins are macrocyclic disaccharide antiparasitic agents having anthelmintic and insecticidal properties and are produced[1] by fermentation of *Streptomyces avermitilis*. Their structure was described[2] as sixteen-membered lactones containing an α-L-oleandrosyl-α-L-oleandrosyl disaccharide attached to the lactone ring through the allylic C_{13} hydroxy group. The complex contains four closely related major components, A_1a, A_2a, B_1a and B_2a, in varying proportions and four minor components, A_1b, A_2b, B_1b and B_2b, each of which is a lower homologue of the corresponding major component.

Avermectins do not show any antibiotic activity and therefore instead of microbiological methods for their determination a biological test based on the movement paralysis of the free-living nematode *Caenorhabditis elegans* is commonly used[3,4]. The test is simple, but for a higher accuracy of determination of individual major components in an avermectin complex it is desirable to combine it with a chromatographic assay. The avermectin complex produced by investigated microorganism strains can be tested by means of thin-layer chromatography (TLC) of extracts of the cultivating medium. The advantages of this technique are its simplicity and rapidity and the possibility of simultaneously determining a larger number of samples.

However, the separation of the major compounds under the TLC conditions described so far[1,2,5–7] is not sufficient to make a densitometric determination possible. The purpose of this investigation was to achieve an effective TLC separation of the major components A_1a, A_2a, B_1a and B_2a of avermectins, permitting their densitometric determination.

EXPERIMENTAL

Preparation of samples

The samples for TLC were prepared by extracting (5 min) the homogeneous

0021-9673/90/$03.50

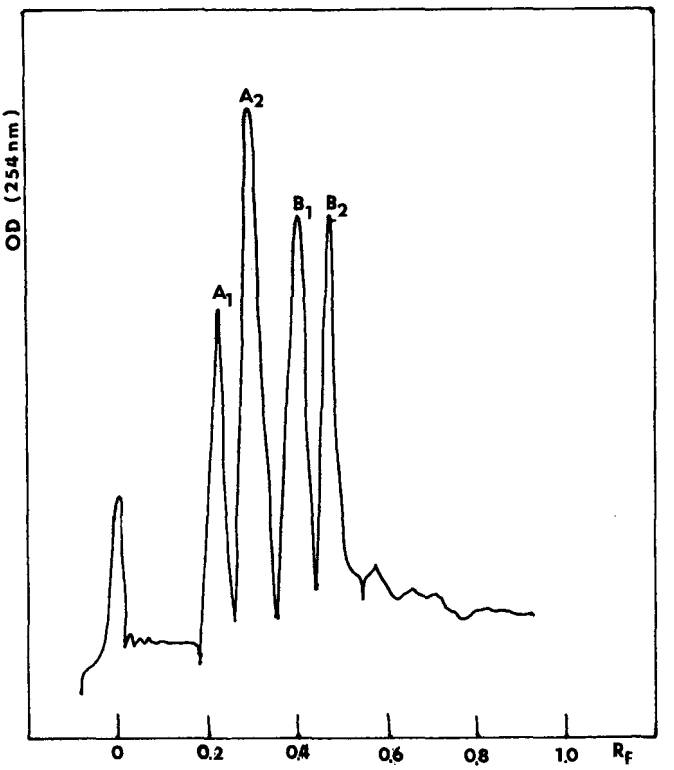

Fig. 1. TLC of an extract from the cultivation medium of *Streptomyces avermitilis* producing avermectins. Solvent system: hexane–acetone–methanol (14:6:0.05). R_F values of avermectins: A_1 = 0.41; A_2 = 0.36; B_1 = 0.26; B_2 = 0.20. Detection at 254 nm.

cultivation medium (5 ml) with a volume of chloroform so as to give a final avermectin concentration in the organic layer of *ca.* 1 mg/ml. The chloroform layer was separated by centrifugation (10 min, 5000 *g*).

Thin-layer chromatography

The samples (5–10 μl of organic layer) were applied to TLC plates (LK6F, 20 × 20 cm; Whatman, Maidstone, U.K.) with a Linomat III instrument (Camag, Muttenz, Switzerland). The plates were developed for 30–40 min with different solvent systems. The best results were obtained with hexane–acetone–methanol (14:6:0.05) or hexane–isopropyl alcohol–methanol (14:4:0.05). For quantitative evaluation, the plates were measured at 254 nm by means of a TLC Scanner II densitometer (Camag) with Hewlett-Packard HP 3390 A integrator. Typical chromatograms are shown in Figs. 1 and 2. The concentrations of individual types of avermectin were determined from a calibration graph (Fig. 3). Ivermectin [22,23-dihydrogen avermectins (Merk, St. Louis, MO, U.S.A.) (modified B_1a and B_1b avermectins giving one peak only on TLC plates), similarly to a main component A_1 which is a mixture of A_1a and A_1b compounds; see below] was used as a standard.

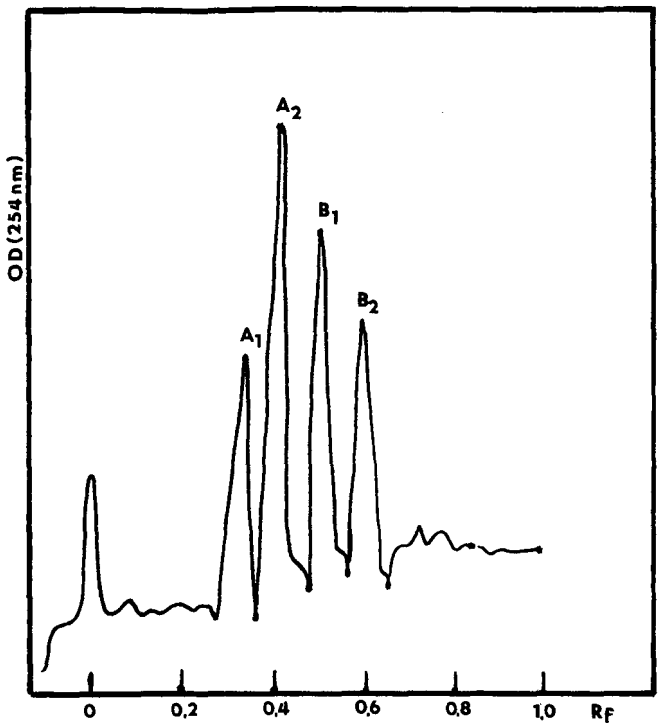

Fig. 2. TLC of an extract from the cultivation medium of *Streptomyces avermitilis* producing avermectins. Solvent system: hexane–isopropyl alcohol–methanol (14:4:0.05). R_F values of avermectins: A_1 = 0.53; A_2 = 0.45; B_1 = 0.38; B_2 = 0.30. Detection at 254 nm.

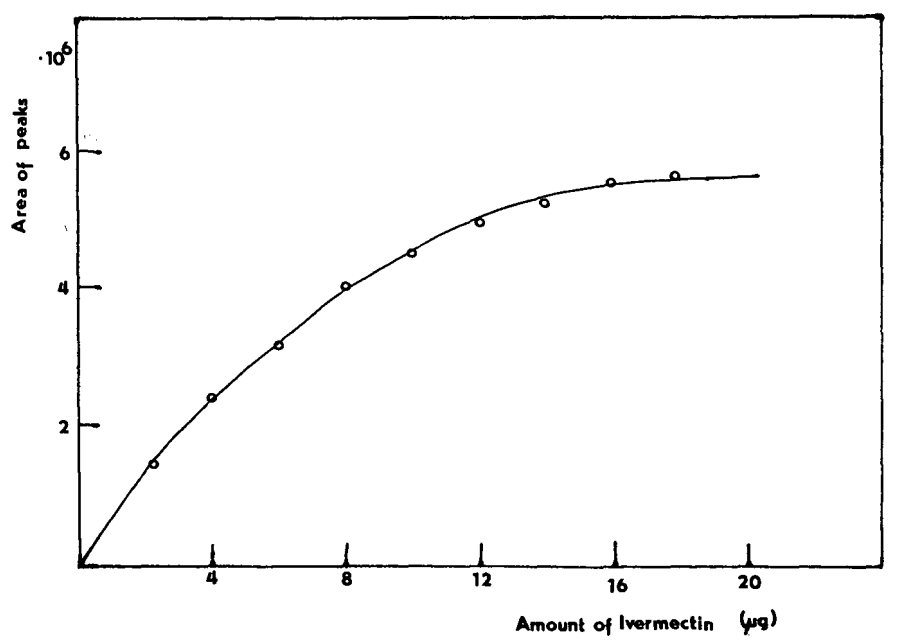

Fig. 3. Dependence of the peak area (measured densitometrically on TLC plates) on the amount of ivermectin.

RESULTS

Different solvent systems were tested for the determination of individual avermectins in cultivation media by TLC: chloroform–ethyl acetate–methanol–methylene chloride (9:9:1:2) (according to ref. 1), ethyl acetate–ethanol (95:5), methylene chloride–methanol (95:5 and 98:2), diethyl ether–light petroleum (30:70 and 180:20), hexane–ethyl acetate (85:5) (according to ref. 6), hexane–ethyl acetate (2:1), methylene chloride–tetrahydrofuran–ethanol (90:9.7:0.3 and 89.7:10:0.3) (according to ref. 7), and some other combinations of these solvents. The best results were obtained with the systems hexane–acetone–methanol (14:6:0.05) and hexane–isopropyl alcohol–methanol (14:4:0.05). Under these conditions, the mixture of avermectins was separated into four main components, A_1, A_2, B_1 and B_2, each containing both the major and the minor parts (*e.g.*, component A_1 included compounds designated A_1a and A_1b). From a comparison of Figs. 1 and 2 it is evident that the second solvent system gives a better separation of the components, with higher R_F values. The determination of individual avermectins in the cultivation medium based on measurement of corresponding peak areas using the calibration graph (Fig. 3) showed an inter-assay deviation of ± 10% under standard conditions. The shapes of the peaks of the individual avermectins and the ivermectin standard were very similar over the whole sample concentration range applied (the percentage deviation may be affected by possible differences in the molar absorptivities for the individual avermectins and ivermectin).

The TLC technique described here permits an effective screening of *Streptomyces avermitilis* strains from the viewpoint of the qualitative and quantitative composition of the avermectins produced.

REFERENCES

1 R. W. Burg, B. M. Miller, E. E. Baker, J. Birnbaum, S. A. Currie, R. Hartman, Y.-L. Kong, R. L. Monaghan, G. Olson, J. Putter, J. B. Tunac, H. Wallick, E. O. Stapley, R. Óiva and S. Ómura, *Antimicrob. Agents Chemother.*, 15 (1979) 361–367.
2 G. Alberts-Schönberg, B. H. Arison, J. C. Chabala, A. W. Douglas, P. Eskola, M. H. Fischer, A. Lusi, H. Mrozik, J. L. Smith and R. L. Tolman, *J. Am. Chem. Soc.*, 103 (1981) 4216–4221.
3 S. Brenner, *Genetics*, 77 (1974) 71–94.
4 J. M. Schaeffer and H. W. Haines, *Biochem. Pharmacol.*, 38 (1989) 2329–2338.
5 M. H. Fisher, A. Lusi and R. L. Tolman, *U.S. Pat.*, 4 200 581 (1980).
6 H. Mrozik, B. O. Linn, P. Escola, A. Lusi, A. Matzuk, F. A. Preiser, D. A. Ostlind, J. M. Schaeffer and M. H. Fisher, *J. Med. Chem.*, 32 (1982) 375–384.
7 H. Mrozik, P. Eskola, B. H. Arison, G. A. Schönberg and M. H. Fisher, *J. Org. Chem.*, 47 (1982) 489–492.

Journal of Chromatography, 513 (1990) 405–407
Elsevier Science Publishers B.V., Amsterdam

CHROM. 22 456

Letter to the Editor

Preparation of pyrrolidides from fatty acids via trimethylsilyl esters for gas chromatographic–mass spectrometric analysis

Sir,

Pyrrolidides have been recognized as useful derivatives of fatty acids for their characterisation by gas chromatography–mass spectrometry (GC–MS) with electron impact ionization[1–4]. This functional group directs the fragmentation of a carbon chain in such a way that structural features such as the location of branchings or of one or two double bonds can be recognized much more readily than with the acid itself or its esters[2].

Later, other derivatives, such as β-picolines[5], dimethyloxazolines[6] and triazolopyridines[7], were found which show the same type of fragmentation even more strongly and now even the double bonds in polyunsaturated acids can be located. The formation of the derivatives requires activation of the acid in a first step, either to the acid chloride[5], to an activated ester[6,7] or at least to a methyl ester in the case of the pyrrolidide[1].

However, from an experimental point of view, all these derivatives suffer from the serious shortcoming that, in contrast to esterification with diazomethane or trimethylsilylation with a commercial reagent, their preparation from the acids is not sufficiently simple for everyday use in the laboratory. It therefore appeared worthwhile to study the preparation of such fragmentation-directing derivatives on a microscale with the aim of developing a procedure comparable in simplicity to esterification or silylation and preferably also without the need for work-up before GC–MS analysis.

Considering the nucleophilic power of pyrrolidine, which is sufficient to convert various esters into pyrrolidides under mild conditions, we reasoned that trimethylsilyl (TMS) esters would be converted analogously. This would allow a simple experimental set-up because the preparation of the TMS ester and subsequent conversion to the amide could be carried out in one procedure. The technique would resemble very closely that of the commonly used silylation procedure, except that the tertiary base pyridine would be replaced with pyrrolidine.

Fig. 1 shows the results of a kinetic study on the reaction of stearic acid with three commercially available silylating reagents and pyrrolidine. It turned out that the best reagent is trimethylsilylimidazole (TSIM), which produces a quantitative yield of the pyrrolidide in less than 6 h at room temperature. As is common practice in silylation derivatization for GC–MS analysis, the liquid reagent is employed in large excess and serves as the solvent of the reaction mixture. With regard to the amount of

0021-9673/90/$03.50

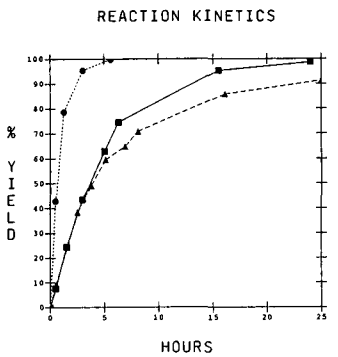

Fig. 1. Yield of stearylpyrrolidide from stearic acid. Experimental conditions: 1 mg of stearic acid, 100 μl of pyrrolidine, 100 μl of trimethylsilyl reagent. ○ = Trimethylsilylimidazole; □ = hexamethyldisilazane; ▲ = bistrimethylsilyltrifluoroacetamide. All experiments at room temperature.

pyrrolidine, it is essential to use an excess over the silylating reagent because the latter reacts with the acid and also with the pyrrolidine, but only *free* pyrrolidine appears to be able to attack the TMS ester under mild conditions. We usually employ TSIM and pyrrolidine in 1:1 volume ratio, which corresponds to a 1:2 molar ratio. The total volume is usually 200 μl. The reaction mixture is used directly for GC–MS analysis.

If alcohol groups are present in the sample, it is found that they are silylated under the conditions employed, but silylation often appears incomplete in GC–MS analysis. This is presumably due to desilylation in the injector of the gas chromatograph by the free pyrrolidine present in the reaction mixture. In such instances an additional silylation step has to be performed after the completion of the pyrrolidide formation. In this step sufficient reagent, now preferably bistrimethylsilylacetamide is added to convert the free pyrrolidine into its TMS derivative.

Ester groups present in the sample are split by the TSIM–pyrrolidine reagent under the conditions employed, resulting in a pyrrolidide and a TMS ether as expected. This reaction proceeds more slowly and heating is usually required to complete it in a practicable time. Studies are under way to find the optimum conditions for this reaction which may be analytically useful in itself.

Unfortunately, a comparatively simple procedure has not been found for the conversion of acids to the other derivatives mentioned above[5–7]. The nucleophilicity of these reagents appears to be too weak for an attack on TMS esters under mild conditions.

ACKNOWLEDGEMENTS

We are indebted to Messrs. A. Rippstein, P. Samirant and G. Färber for their valuable help in these experiments, and to Dr. R. Barner for fruitful discussions.

F. Hoffmann-La Roche Ltd.,
Department ZFE/Phy,
CH-4002 Basle (Switzerland)

WALTER VETTER
WILLI WALTHER

1 W.Vetter, M. Vecchi and W. Walther, *Helv. Chim. Acta*, 54 (1971) 1599.
2 B. A. Andersson and R. T. Holman, *Lipids*, 9 (1974) 185.

3 B. A. Andersson, *Prog. Chem. Fats Lipids*, 16 (1978) 279.
4 W. W. Christie, in *Gas Chromatography and Lipids*, Oily Press, Ayr, 1989, p. 166.
5 D. J. Harvey, *Biomed. Mass Spectrom.*, 9 (1982) 33.
6 Q. T. Yu, B. N. Liu, Y. J. Zhang and Z. H. Huang, *Lipids*, 23 (1988) 804.
7 W. Vetter, W. Meister and G. Oesterhelt, *Org. Mass Spectrom.*, 23 (1988) 566.

(First received January 10th, 1990; revised manuscript received March 13th, 1990)

Author Index

Instructions to Authors

JOURNAL OF CHROMATOGRAPHY

JOURNAL OF CHROMATOGRAPHY, BIOMEDICAL APPLICATIONS

JOURNAL OF CHROMATOGRAPHY, SYMPOSIUM VOLUMES

Elsevier Science Publishers
Desk-Editorial Office Journal of Chromatography:
Sara Burgerhartstraat 25, 1055 KV Amsterdam, The Netherlands
P.O. Box 330, 1000 AH Amsterdam, The Netherlands
Tel. 31-20-5862793
FAX 31-20-5862304
Telex 10704 espom

ELSEVIER
AMSTERDAM – OXFORD – NEW YORK – TOKYO

General

The JOURNAL OF CHROMATOGRAPHY publishers papers on all aspects of **chromatography, electrophoresis** and related methods. Contributions consist mainly of research papers dealing with chromatographic theory, instrumental development and their applications.

BIOMEDICAL APPLICATIONS. This section, which is under separate editorship, deals with the following aspects: developments in and applications of chromatographic and electrophoretic techniques related to clinical diagnosis or alterations during medical treatment; screening and profiling of body fluids or tissues with special reference to metabolic disorders; results from basic medical research with direct consequences in clinical practice; drug level monitoring and pharmacokinetic studies; clinical toxicology; analytical studies in occupational medicine.

SYMPOSIUM VOLUMES. This publication, which is under separate editorship, publishes proceedings of symposia on chromatography, electrophoresis and related methods.

Types of contributions

The following types of papers are published in the JOURNAL OF CHROMATOGRAPHY and the section on BIOMEDICAL APPLICATIONS: Regular research papers (full-length papers), Notes, Review articles and Letters to the Editor. Notes are usually descriptions of short investigations and reflect the same quality of research as full-length papers, but should preferably not exceed six printed pages. Letters to the Editor can comment on (parts of) previously published articles, or they can report minor technical improvements of previously published procedures; they should preferably not exceed two printed pages. Review articles are invited or proposed in writing to the Editors. An outline of the proposed review should first be forwarded to the Editors for preliminary discussion prior to preparation.

Submission of an article is understood to imply that the article is original and unpublished and is not being considered for publication elsewhere.

Upon acceptance of an article by the journal, the author(s) will be asked to transfer the copyright of the article to the publisher. This transfer will ensure the widest possible dissemination of information.

Submission of papers

Manuscripts (***four*** copies are required), in English, should be submitted to:

for the JOURNAL OF CHROMATOGRAPHY:

Editorial office
JOURNAL OF CHROMATOGRAPHY
P.O. Box 681
1000 AR Amsterdam, The Netherlands

for the BIOMEDICAL APPLICATIONS section:

Dr. K. Macek
The Editor of
JOURNAL OF CHROMATOGRAPHY,
BIOMEDICAL APPLICATIONS
P.O. Box 681
1000 AR Amsterdam, The Netherlands

Manuscripts for the SYMPOSIUM VOLUMES section (*three* copies are required) should be sent by *regular airmail (NOT by registered, special delivery of private mail services)* to:

Dr. E. Heftmann
The Editor of
JOURNAL OF CHROMATOGRAPHY,
SYMPOSIUM VOLUMES
P.O. Box 928
ORINDA, CA 94563-0818, U.S.A.

Every paper must be accompanied by a letter from the senior author, stating that he/she is submitting the paper for publication in the *Journal of Chromatography*.

Manuscripts

Manuscripts should be typed in ***double spacing*** on consecutively numbered paper of uniform size. The manuscript should be preceded by a sheet of manuscript paper carrying the title of the paper and the name and full postal address of the person to whom the proofs are to be sent. As a rule, papers should be divided into sections, headed by a caption (*e.g.* Abstract, Introduction, Experimental, Results, Discussion). All illustrations, photographs, tables, etc. should be on separate sheets. **Four** copies of the complete manuscript should be submitted.

Title

The title of the paper should be concise and informative. Since titles ares widely used in information retrieval systems, care should be taken to include the key words. The title should be followed by the authors' full names, academic or professional affiliations, and the address of the laboratory where the work was carried out. If the present address of an author is different from that mentioned, it should be given in a footnote. Acknowledgements of financial support are not to be made in a footnote to the title or name of the author, but should be included in the Acknowledgements at the end of the paper.

Introduction

Every paper must have a concise introduction mentioning what has been done before on the topic described, and stating clearly what is new in the paper now submitted.

Abstract

Full-length papers and Review articles should have an abstract of 50–100 words which clearly and briefly indicates what is new, different and significant.

Illustrations

The figures should be submitted in a form suitable for reproduction, either drawn in Indian ink on drawing or tracing paper, or as sharp glossy prints. Axes of a graph should be clearly labelled. Please note that any lettering should also be in a form suitable for reproduction. Lettering (which should be kept to a minimum) and spacing on axes of graphs should be such that numbers, etc., remain legible after reduction. One original and three photocopies are required. The figures should preferably be of such a size that the same degree of reduction can be applied to all of them. Standard symbols should be used in line drawings, the following are available to the printers and can also be used in the legends:

○ ● □ ■ △ ▲ ◇ ◆

Photographs should have good contrast and intensity. Sharp, glossy photographs are required to obtain good halftones. References to the illustrations should be included in appropriate places in the text using Arabic numerals and the approximate position of the illustration should be indicated in the margin of the manuscript. Each illustration should have a legend, all the *legends* being typed (with double spacing) together on a *separate sheet*.

If structures are given in the text, the original drawings should be provided.

Coloured illustrations are reproduced at the author's expense, the cost being determined by the number of pages and by the number of colours needed.

The written permission of the author and publisher must be obtained for the use of any figure already published. Its source must be indicated in the legend.

Tables

The tables should be typed (in double spacing) on separate pages, and numbered in Roman numerals according to their sequence in the text. A brief descriptive heading should be given above each table. Below the heading the experimental conditions should be described. The layout of the tables should be given serious thought, so that the reader can grasp quickly the significance of the results.

Nomenclature, symbols and abbreviations

Widely accepted symbols, abbreviations and units (SI) should be used. If there is any doubt about a particular symbol or abbreviation, the full expression followed by the abbreviation should be given the first time it appears in the text. Abbreviations used in tables and figures should be explained in the legends. In general, the recommendations of the International Union of Pure and Applied Cemistry (I.U.P.A.C.) should be followed.

References

References should be numbered in the order in which they are cited in the text, and listed in numerical sequence on a separate sheet at the end of the article. The numbers should appear in the text at the appropriate places in square brackets. In the reference list, periodicals [1], books [2], multi-author books [3], and proceedings [4] should be cited in accordance with the following examples:

1 A.T. James and A.J.P. Martin, *Biochem. J.*, 50 (1952) 679.
2 L.R. Snyder, *Principles of Adsorption Chromatography*, Marcel Dekker, New York, 1968, p. 201.
3 R.D. Marshall and A. Neuberger, in A. Gottschalk (Editor), *Glycoproteins*, Part A, Elsevier, Amsterdam, 2nd ed., 1972, Ch. 3, p. 251.
4 R.H. Doremus, B.W. Roberts and D. Turnbull (Editors), *Growth and Preparation of Crystals, Proc. Int. Conf. Crystal Growth, Coopertown, NY, August 27–29, 1958*, Wiley, New York, 1958.

Abbreviations for the titles of journals should follow the system used by *Chemical Abstracts*. Articles not yet published should be given as "in press" (journal should be specified), "submitted for publication" (journal should be specified), "in preparation" or "personal communication". The JOURNAL OF CHROMATOGRAPHY; JOURNAL OF CHROMATOGRAPHY, BIOMEDICAL APPLICATIONS and JOURNAL OF CHROMATOGRAPHY, SYMPOSIUM VOLUMES should be cited as *J. Chromatogr.*

Dispatch

Before dispatch of the manuscript please check that the envelope contains four copies of the paper complete with references, legends and figures. One of the sets of figures must be the originals suitable for direct reproduction. Please also ensure that permission to publish has been obtained from your institute.

Proofs

One set of proofs will be sent to the author to be carefully checked for printer's errors. Corrections must be restricted to instances in which the proof is at variance with the manuscript. We shall be obliged to make a charge for all "extra corrections" at a rate in accordance with their cost to us.

To ensure fastest possible publication, proofs are sent to authors by *airmail* and must be returned to the publisher also by *airmail*. If this is not done, the article will be passed for publication with house correction only. Proofs may also be returned by FAX; the FAX number of *Journal of Chromatography* is: 31 (The Netherlands) -20 (Amsterdam) -5862304.

Reprints

Fifty reprints of Full-length papers, Notes and Letters to the Editor will be supplied free of charge. Additional reprints can be ordered by the authors. The order form containing price quotations will be sent to the authors together with the proofs of their article.

Subscription orders

Subscription orders should be sent to Elsevier Science Publishers B.V., P.O. Box 211, 1000 AE Amsterdam, The Netherlands. The JOURNAL OF CHROMATOGRAPHY and the BIOMEDICAL APPLICATIONS section can be subscribed to separately. Cumulative Author and Subject Indexes can also be ordered separately. Write to the Marketing Manager, Chemistry, at the above address for more details.

Vol. 513

journal of chromatography news section

AWARDS

M.J.E. GOLAY AWARD

At the 10th International Symposium on Capillary Chromatography which was held last year, at Riva del Garda, Italy, the first M.J.E. Golay Awards, named after the inventor of the open-tubular columns, were presented to Dr. R. Kaiser, Dr. R. Dandeneau and Mr. E. Zerenner for their pioneering work in the development of capillary chromatography.

Following the death of Professor Golay, the Perkin-Elmer Corporation, in cooperation with the Permanent Organization Committee of the International Symposia on Capillary Chromatography agreed to take over the sponsorship of the M.J.E. Golay Award. This Award, which consists of a medal, a scroll and an endowment, is to be presented at the yearly Symposia to a scientist or scientists who made significant contributions to the evolution of capillary chromatography.

The award winner is to be selected from those who are nominated by the Chromatographic Community. The nomination is open to everybody, except members of the Award Committee and the Chairman of the Permanent Organization Committee of the Symposia (who does not serve on the Award Committee). For the administration of the Award and the evaluation of the nominations an Award Committee consisting of scientists from various countries has been organized. The chairman of the Award Committee is Prof. Dr. C.A. Cramers.

The M.J.E. Golay Award in Capillary Chromatography, sponsored by the Perkin-Elmer Corporation has been presented at the 11th International Symposium on Capillary Chromatography (Monterey, California, May 14–17, 1990) and will be presented at the forthcoming 12th International Symposium on Capillary Chromatography (Kobe, Japan, September 11–14, 1990).

The Award Committee is soliciting nominations for the Award to be presented at the 13th International Symposium on Capillary Chromatography to be held May 13–16, 1991, in Riva del Garda, Italy. Deadline for the nomination is *October 1, 1990.* They sould be sent in five copies and include a discussion of the nominee's activities with particular emphasis to the specific achievement for which the presentation of the award is proposed.

The nominations should be sent to the Chairman of the Award Committee: Prof. Dr. C.A. Cramers, Eindhoven University of Technology, Lab. Instrumental Analysis, P.O. Box 513, 5600 MB Eindhoven, The Netherlands. Tel.: (31) 40.479.111; Fax: (31) 40.442.576.

THE MARTIN AWARD

The Martin Award was presented at the 14th International Symposium on Column Liquid Chromatography to William Howard Pirkle — born in Shreveport, Louisiana on May 2, 1934, and raised in California in a small town on the edge of the Sierra Nevada mountains. His interest in chemistry developed after he began studies at the University of California at Berkeley, where he supported his

studies through work in the chemistry department storerooms and alkaloid isolation for Professor Henry Rapoport. His Ph. D research was conducted on morphine chemistry under the direction of Professor Marshall Gates at the University of Rochester, NY, after a Postdoctoral Fellowship with Professor E.J. Corey at Harvard University. Pirkle joined the faculty at the University of Illinois in Champaign-Urbana in the fall of 1964. Here he has remained and is now a Full Professor with appointments in both Analytical and Organic Chemistry, his co-workers coming from both areas.

It is just this combination of interests that has enabled Professor Pirkle's research group to make the contributions to stereochemical analysis and stereoisomer separation which are so widely recognized. Pirkle's work in these fields was initiated by the discovery that the addition of certain chiral solvating agents to NMR samples of mixed enantiomers caused the chemical shifts of these enantiomers to differ. Thus, enantiomeric purity could be directly determined by NMR methods. Mechanistic studies in this area, coupled with the development of chromatographic methods for obtaining the chiral solvating agents in enantiomerically pure form, led to the design of chiral compounds having different affinities for enantiomers. These chiral selectors were immobilized on silica to afford chiral stationary phases of rather broad scope. Intentionally not patented, these chiral phases were quickly commercialized by several companies. "Pirkle columns" are now available worldwide. Using one chiral phase to aid in the design of others, Pirkle's group has generated a large number of chiral phases and attained levels of enantioselectivity which transcend the needs of even preparative chromatography. While still deeply interested in attaining an understanding of basic chiral recognition mechanisms, Pirkle's work is now advancing into the realm of enantioselective membranes, materials which have considerable potential for industrial scale separations of stereoisomers.

ANNOUNCEMENTS OF MEETINGS

CONFERENCE ON CAPILLARY ELECTROPHORESIS, FREDERICK, MD, U.S.A., OCTOBER 15–16, 1990

The Conference on Capillary Electrophoresis will be held at the NCI-Frederick Cancer Research and Development Center in Frederick, MD, U.S.A., October 15–16, 1990.

The focus of this meeting is the scientific exchange and dissemination of the technical aspects of capillary electrophoresis (CE). We invite discussions of established methodologies as well as creative and innovative new approaches and techniques. The format will include workshops, oral and poster presentations by individual conference participants, and optional enrollment in a definitive CE course. Invited speakers will provide expert overviews of the basic aspects and applications of CE including, but not limited to, instrument and column design, detection, the role of the buffer and factors that influence mobility, selectivity, resolution and optimization. Also, the application of CE to the separation of small ions as well as large biomolecules will be presented and discussed.

There is no registration fee; however, registration is mandatory to ensure participation. A nominal fee of US$50.00 will be charged for participation in the CE course. State-of-the-art equipment displays and literature will be made available to participants by the leading manufacturers of CE instrumentation.

For further information on registration, abstract submittal, and course participation, please contact: Margaret L. Fanning, Conference Coordinator, PRI, NCI-FCRDC, P.O. Box B, Frederick, MD 21701, U.S.A. Tel.: (301) 698-1089; Fax: (301) 698-5866.

10th INTERNATIONAL SYMPOSIUM ON HIGH-PERFORMANCE LIQUID CHROMATOGRAPHY OF PROTEINS, PEPTIDES AND POLYNUCLEOTIDES, WIESBADEN, F.R.G., OCTOBER 29–31, 1990

The 10th International Symposium on HPLC of Proteins, Peptides, and Polynucleotides will be held in Wiesbaden, F.R.G. from October 29th to October 31st, 1990.

New developments and applications in the area of HPLC and other high resolution techniques is

the major theme of this symposium series. Scientists from academia and industry can meet and discuss in an informal way recent advances in the development of new stationary phases, the growth of complementary techniques such as electrophoresis and the suitability of these for the isolation and analysis of biopolymers.

A special scientific and social program is being planned in order to highlight the anniversary of ISPP and 10 years of achievements in research in high-performance liquid chromatography.

The three-day scientific programme consists of oral presentations, poster sessions and discussions. Recognized authorities will review current trends and future perspectives in various topics, including: column technology and support materials, protein–surface interaction, isolation and purification techniques, regulatory issues and QC, detection and amplification, electrophoresis, polynucleotides, membrane proteins, separation and protein engineering, membrane technology and special topics.

Registration fee is DM 720, which covers all scientific and social events, including a copy of the proceedings. Students will be eligible for a reduced rate of DM 360 (a copy of the proceedings is not included).

For further details, contact: Secretariat, 10th ISPP, P.O. Box 28, S-751 03 Uppsala, Sweden.

SHORT COURSE ON CHROMATOGRAPHIC CHIRAL SEPARATIONS, EDISON, NJ, U.S.A., NOVEMBER 9–11, 1990

The Short Course on Chromatographic Chiral Separations will be held at the Holiday Inn at Raritan Center, Edison NJ, U.S.A., November 9–11, 1990.

This short course is designed for researchers faced with the separation or analysis of optically active compounds. These include drugs, natural and synthetic products and metabolites.

The course covers HPLC, GC, TLC and several preparative separation methods.

Prospective participants should have a basic knowledge of chromatography and have previous experience with routine HPLC. Two laboratory demonstrations and work sessions are included.

The main topics are: chiral separations; examination of LC methods; gas chromatography, selecting the proper columns for an analysis; special problems; basic chiral recognition theory. The course instructors are: Daniel W. Armstrong, Irving W. Wainer, Thomas E. Beesley, Apryll M. Stalcup and Willie L. Hinze.

The registration fee of $895.00 covers registration, class materials and banquet.

For further information contact: Ms. Mary Jo Richards, Chromatographic Separation of Enantiomers, Department of Chemistry, University of Missouri-Rolla, Rolla, MO 65401-0249, U.S.A. Tel.: (314) 341-4429.

INTERNATIONAL SYMPOSIUM ON CHROMATOGRAPHY, ALIGARH, INDIA, DECEMBER 10–12, 1990

The International Conference on Chromatography, will be held at the Aligarh Muslim University, Aligarh, India, December 10–12, 1990

The scope of the conference is to provide a forum for discussion on recent developments in chromatography. The following topics will be covered: fundamentals, synthesis of new materials, planar/column/ion exchange/ligand exchange/gas chromatography, recent developments, instrumentation, separation science and technology, and application to the environment.

The conference consists of invited lectures, oral and poster presentations in the relevant fields of chromatography. English will be the official language of the conference.

The registration fee will be Rupees 250.00 for domestic participants; US$ 150.00 for overseas participants.

All correspondence should be addressed to: Dr. K.G. Varshney, Organizing Secretary, ICC 90, Department of Applied Chemistry, Faculty of Engineering and Technology, Aligarh Muslim University, Aligarh-202 002, India.

2nd INTERNATIONAL SYMPOSIUM ON FIELD-FLOW FRACTIONATION (FFF'91) AND FFF WORKSHOP III, SALT LAKE CITY, UT, U.S.A., FEBRUARY 2–6, 1991

The symposium will be held for three days, February 4–6, 1991. The FFF workshop will occupy the Saturday preceding the symposium, February 2, 1991. (There is another FFF workshop scheduled for June 11, 1991).

The symposium will have presentations covering all aspects of FFF, ranging from recent theoretical developments to applications in industry, biochemistry, and environmental studies. Invited lectures along with contributed papers and posters will be scheduled.

The FFF Workshop is intended for those desiring a working knowledge of field-flow fractionation. Topics will include basic theory, principles of operation and optimization, and instrumental systems and characteristics. A hands on experience will be provided. Enrollment will be limited to maintain an informal learning environment.

Titles of proposed oral and poster presentations are invited. Posters are particularly encouraged. Final titles will be selected by a scientific committee. The due date for abstracts will be September 17, 1990.

For further details contact: Julie Westwood, FFF Research Center, Department of Chemistry, University of Utah, Salt Lake City, UT 84112, U.S.A., Tel.: (801) 581-5419.

42nd PITTSBURGH CONFERENCE AND EXPOSITION ON ANALYTICAL CHEMISTRY AND APPLIED SPECTROSCOPY, CHICAGO, IL, U.S.A., MARCH 4–8, 1991

The Pittsburgh Conference and Exposition is the premiere event in analytical chemistry and applied spectroscopy. The technical program is committed to educational goals that will expand to the limits of our scientific range. A program that features both the emerging science on the cutting edge as well as the state-of-the-art techniques for established operations in the field is planned. To reach goals that extend across the range, the committee is planning a diverse selection of symposia, contributed papers, courses and plenary sessions followed by round table discussion seminars. These will be arranged and presented by outstanding scientists from a wide variety of scientific disciplines. Each Conferee will have the opportunity to gain the maximum benefit from each encounter.

The special week-long educational program features short courses. UMIX symposia, hands-on workshops, and informal round table discussions. Special tours of major scientific installations in the region;*i.e.* Fermilab, Bell Labs, Argonne National Laboratory, etc., may be offered.

Original, unpublished papers may be contributed in all areas of analytical chemistry, spectroscopy and related scientific areas. August 3, 1990 is the deadline for receipt of abstracts. One copy of a 250-word abstract must be submitted for review. All abstracts will be carefully evaluated. The abstract should clearly state: the objective of the work, the research plan, equipment and procedures used, sufficient experimental evidence to indicate success of the research plan, and results and/or conclusions. Abstracts must include sufficient content and organization for adequate evaluation by the Conference Program Committee. The Pittsburgh Conference Program Committee reserves the right to accept, place on a waiting list, or reject any paper. In November 1990 the designated speaker will be informed of the paper's status: accepted, on the waiting list, or rejected. Specific references to vendor products in the titles of papers are not permitted and will be automatically deleted. Conference Proceedings of contributed papers will not be published. Authors may publish their papers after the Conference. If the paper is accepted, a second abstract will be required for reproduction in book form for distribution to the conferees. Forms and instructions concerning this second abstract will be sent to the designated speaker with the notification of acceptance of the paper. The abstract for publication will be due December 7, 1990. The title of the paper and the author information originally submitted cannot be changed for the second abstract, be sure to have the desired title and author information on the original abstracts. The Pittsburgh Conference does not provide financial support to authors of contributed papers.

Authors wishing to present papers at the 1991 Pittsburgh Conference and Exposition Technical Program should submit, one copy of a 250-word abstract on or before August 3, 1990 to: Mrs. Alma Johnson, Program Secretary, The Pittsburgh Conference, 300 Penn Center Blvd., suite 332, Pitts-

burgh, PA 15235, U.S.A. A self-addressed envelope should be enclosed which will be returned to indicate receipt of abstract. This receipt will not indicate acceptance of the abstract for the 1991 Pittsburgh Conference Program.

INTERNATIONAL ELECTROPHORESIS SOCIETY MEETING, WASHINGTON, DC, U.S.A., MARCH 19–21, 1991

The International Electrophoresis Society Meeting, which will be held at the Sheraton Washington Hotel, in Washington, DC, U.S.A., March 19–21, 1991, will bring together experts from the areas of 2D electrophoresis, analytical electrophoresis, capillary zone electrophoresis, clinical medicine, clinical pathology, computerized image analysis, genomic sequencing, molecular biology, and preparative electrophoresis to examine aspects of the development and application of electrophoretic techniques in molecular biology.

The three-day program will include lecture and poster presentations, discussion sessions, workshops, and exhibits. Invited lecturers have included Robert Allen, Norman Anderson, Bruce Budowle, Charles Cantor, Gilbert Chu, Ronald Davis, Denis Hochstrasser, Leroy Hood, Donald Hunt, Robert Kelly, Eric Lai, James Neel, David Patterson, Bruce Roe, Steven Smith, Edwin Southern and Allan Wilson.

Papers, describing original research, in the following areas are invited: biotechnology, capillary zone electrophoresis, detection and imaging methods, forensic DNA methods, gel electrophoresis, genetic testing, genome project, high resolution 2D electrophoresis, polymerase chain reaction, risk assessment, and sequencing.

The Scientific Committee welcomes your suggestions for additional topics to be covered in the Symposium. The Deadline for submission of abstracts is September 1, 1990. Abstracts received after September 1 will be considered for poster presentation.

For abstract forms, program and registration information, contact: Mrs. Janet Cunningham, IES Symposium Manager, Barr Enterprises, P.O. Box 279, Walkersville, MD 21793, U.S.A. Tel.: (301) 898-3772; Fax: (301) 898-5596.

4th SYMPOSIUM ON FAST PROTEIN LIQUID CHROMATOGRAPHY, MAARSSEN, THE NETHERLANDS, MARCH 26, 1991

Fast protein liquid chromatography (FPLC) of biomolecules is an important technique in the high performance field. This symposium offers participants the opportunity to get acquainted with and discuss the high-performance liquid chromatography of biomolecules.

The scientific programme will consist of poster presentations and discussion sessions dealing with the following applications of FPLC and BioPilot™: protein purification and characterization; peptide structure elucidation; biologically active molecules; monoclonal antibodies; membrane proteins; preparative chromatography; quality control; affinity chromatography; poly- and oligonucleotides; column selection and maintenance.

Lectures or posters on these topics are invited. For instructions for lectures, abstracts or poster presentations contact Marianne Wobma, before October 1, 1990, at the address given below. The deadline for submission of Abstracts is December 29, 1990. Manuscripts and Abstracts will be published in the proceedings of the symposium. The proceedings will be available at no extra cost for speakers at the symposium.

Most lectures will be held in Dutch, however, a small number will be given in English

The registration fee will be Dfl. 150.00

For further details, contact: Marianne Wobma, Pharmacia Nederlands BV, Houttuinlaan 4, 3447 GM Woerden, The Netherlands. Tel.: (03480) 77631.

3rd INTERNATIONAL SYMPOSIUM ON PHARMACEUTICAL AND BIOMEDICAL ANALYSIS, BOSTON, MA, U.S.A., APRIL 28–MAY 1, 1991

The 3rd International Symposium on Pharmaceutical and Biomedical Analysis (PBA '91) will be held at the Boston Park Plaza Hotel, Boston, MA, U.S.A., April 28–May 1, 1991.

The three-day program will feature invited plenary, keynote, and submitted research lectures, parallel discussion sessions, and poster presentations covering a wide range of topics in pharmaceutical and biomedical analysis. The following topics will be included: advances in detection methodologies — UV, FL, FT-IR, CL, NMR and MS; advances in immuno-diagnostics — recombinant DNA technologies and clinical applications of monoclonal antibodies; analytical considerations of biotechnology; applications in industrial and clinical analysis; automated sample preparation; biosensors; capillary electrophoresis and CE–MS; chiral separations in GC, LC, TLC and SFC; computer-aided methods of analysis; derivatization techniques in LC, GC and RIA; drug metabolism and pharmacokinetics; electrochemical methods of analysis; frontiers in therapeutic drug monitoring, clinical and forensic toxicology; microcolumn separations; multidimensional/multimodal chromatography; planar chromatography; preparative separations; substance abuse testing and sports medicine; supercritical fluid chromatography and extraction.

Abstracts of original research in any of the previously mentioned topics are invited. All papers presented will be published after refereeing in a special Symposium issue of the *Journal of Pharmaceutical and Biomedical Analysis*. Completed manuscripts will be due at the time of the symposium.

For further details contact: Ms. Shirley E. Schlessinger, Symposium Manager of PBA '91, 400 East Randolph Drive, Suite 1015, Chicago, IL 60601, U.S.A. Tel.: (312) 527-2011.

8th INTERNATIONAL SYMPOSIUM ON PREPARATIVE CHROMATOGRAPHY, PREP-91, ARLINGTON, VA, U.S.A., MAY 13–15, 1991

The 8th International Symposium on Preparative Chromatography (Prep '91) will be held at the Key Bridge Marriott Hotel in Arlington, VA, U.S.A., May 13–15, 1991. The three-day program will include invited and contributed lectures, poster presentations, and discussion sessions.

Papers describing original research are invited in areas of preparative chromatography and especially: theory of non-linear chromatography, overloaded elution and displacement chromatography; kinetics of mass transfers at high concentrations in chromatographic columns; stationary phases; applications to recombinant and natural proteins, to peptides, other biopolymers, chiral separations, etc.; optimization of experimental conditions; economics of preparative chromatography; instrumentation.

The deadline for submission of abstracts is November 15, 1990. Abstracts received after November 15 will be considered for poster presentation.

For further details, contact: Janet E. Cunningham, Barr Enterprises, P.O. Box 279, Walkersville, MD 21793, U.S.A. Tel.: (301) 898-3772; Fax: (301) 898-5596.

5th SYMPOSIUM ON HANDLING OF ENVIRONMENTAL AND BIOLOGICAL SAMPLES IN CHROMATOGRAPHY, BADEN BADEN, F.R.G., SEPTEMBER 26–27, 1991

The 5th Symposium on Handling of Environmental and Biological Samples in Chromatography will be held in Baden Baden, F.R.G., September 26–27, 1991. A Short Course on Sample Handling in Liquid Chromatography will precede the symposium (September 24–25, 1991).

The Symposium will be the 5th in a series of very successful meetings initiated by the late Professor Roland Frei under the auspices of the International Association of Environmental Analytical Chemistry. It is the intention of the organizers to continue the work of Roland Frei and to follow the ideas and objectives he has laid down for carrying out these symposia: main goal is to bring together experts and practicing analytical chemists who can give a good account of both the state-of-the-art in their respective speciality and first-hand experiences in practical sample handling.

Robotics, continuous flow techniques, column switching methodologies to accomplish operations such as extraction, derivatisation, enrichment or dialysis for the handling of complex samples are among the topics which will be treated and discussed. Special emphasis will be placed on techniques with automation potential and procedures suitable for the automated handling of larger series of samples. Most of these methodologies and strategies can be applied to all kind of analysis and matrices. It is however the intention to focus on samples which are either of biological (blood, urine, tissue, plant material) or environmental (water, waste water, sediments, air) origin. Consequently drugs (pharmaceuticals) and priority pollutants respectively are the analytes of major interest.

For further details contact: Workshop Office IAEAC, M. Frei-Häusler, Postfach 46, CH-4123 Allschwil 2, Switzerland, Tel. (004161) 632789 and (004161) 732950.

11th INTERNATIONAL SYMPOSIUM ON HIGH-PERFORMANCE LIQUID CHROMATOGRAPHY OF PROTEINS, PEPTIDES AND POLYNUCLEOTIDES, WASHINGTON, DC, U.S.A., OCTOBER 20–23, 1991.

The 11th International Symposium on HPLC of Proteins, Peptides and Polynucleotides will be held in Washington, DC, U.S.A., October 20–23, 1991.

The program will include invited and contributed lectures, poster presentations, and discussion sessions organized into different sessions. Recognized authorities will review current trends and future prospectives in various topics, including: electrokinetic separations; column technology and support materials; protein conformation and chromatographic behaviour; polypeptide structural studies; protein purity and QC of recombinant proteins; polynucleotides; polysaccharides; membrane proteins; affinity chromatography; analytical applications; sample preparation; preparative chromatography of biopolymers; high resolution electrophoresis; integrated purification systems; biospecific detectors; process monitoring; recovery of recombinant proteins.

The deadline for submission of abstracts is June 3, 1991.

For further details contact: Janet E. Cunningham, Barr Enterprises, P.O. Box 279, Walkersville, MD 21793, U.S.A. Tel.: (301) 898-3772; Fax: (301) 898-5596.

1992 WINTER CONFERENCE ON PLASMA SPECTROCHEMISTRY, CALIFORNIA, U.S.A., JANUARY 6–11, 1992

The 1992 Winter Conference on Plasma Spectrochemistry will be held Monday, January 6 through Saturday, January 11, 1992 in Southern California. Short courses highlighting special topics will be offered Saturday, January 4 and January 11 and Sunday, January 5. A three-day exhibition of spectroscopic instrumentation and accessories will also be included.

Program features and symposia will include: automation, expert systems, and robotics with plasma spectroscopy; chemometric applications in plasma spectrochemistry; chromatography with plasma source detection; flow injection plasma spectrometry; glow discharge and low pressure plasma atomic and mass spectrometry; laser assisted plasma spectrochemistry; mechanisms and process in plasma sources; modern sample preparation and calibration techniques; new instrumentation for plasma spectrochemistry; plasma source mass spectrometry; process control, remote, and on-line plasma analysis; sample introduction techniques and phenomena; spectrochemical applications of plasma sources; and transform spectroscopy, interferometry for plasma sources.

Titles and 50-word abstracts for submitted lecture or poster papers are sollicited by July 1, 1991. Extended conference abstracts are requested by October 7, 1991.

For further information contact: 1992 Winter Conference on Plasma Spectrochemistry, Attn. Dr. R. Barnes, c/o ICP Information Newsletter, Department of Chemistry, GRC Towers, University of Massachusetts, Amherst, MA 01003-0035, U.S.A. Tel. (413) 545-2294, Fax: (413) 545-4490; BITNET: RBARNES@UMASS.

PUBLICATION SCHEDULE FOR 1990

Journal of Chromatography and Journal of Chromatography, Biomedical Applications

MONTH	J	F	M	A	M	J	J	A	S
Journal of Chromatography	498/1 498/2 499	500 502/1	502/2 503/1 503/2 504/1	504/2 505/1	505/2 506 507 508/1	508/2 509/1 509/2 510	511 512 513	514/1 514/2 515	The publication schedule for further issues will be published later
Cumulative Indexes, Vols. 451–500		501							
Bibliography Section		524/1		524/2		524/3		524/4	
Biomedical Applications	525/1	525/2	526/1	526/2 527/1	527/2	528/1 528/2	529/1	529/2 530/1	530/2

INFORMATION FOR AUTHORS

(Detailed *Instructions to Authors* were published in Vol. 513, pp. 413–416. A free reprint can be obtained by application to the publisher, Elsevier Science Publishers B.V., P.O. Box 330, 1000 AH Amsterdam, The Netherlands.)

Types of Contributions. The following types of papers are published in the *Journal of Chromatography* and the section on *Biomedical Applications:* Regular research papers (Full-length papers), Notes, Review articles and Letters to the Editor. Notes are usually descriptions of short investigations and reflect the same quality of research as Full-length papers, but should preferably not exceed six printed pages. Letters to the Editor can comment on (parts of) previously published articles, or they can report minor technical improvements of previously published procedures; they should preferably not exceed two printed pages. For review articles, see inside front cover under Submission of Papers.

Submission. Every paper must be accompanied by a letter from the senior author, stating that he is submitting the paper for publication in the *Journal of Chromatography*. Please do not send a letter signed by the director of the institute or the professor unless he is one of the authors.

Manuscripts. Manuscripts should be typed in double spacing on consecutively numbered pages of uniform size. The manuscript should be preceded by a sheet of manuscript paper carrying the title of the paper and the name and full postal address of the person to whom the proofs are to be sent. Authors of papers in French or German are requested to supply an English translation of the title of the paper. As a rule, papers should be divided into sections, headed by a caption (*e.g.*, Summary, Introduction, Experimental, Results, Discussion, etc.). All illustrations, photographs, tables, etc., should be on separate sheets.

Introduction. Every paper must have a concise introduction mentioning what has been done before on the topic described, and stating clearly what is new in the paper now submitted.

Summary. Full-length papers and Review articles should have a summary of 50–100 words which clearly and briefly indicates what is new, different and significant. In the case of French or German articles an additional summary in English, headed by an English translation of the title, should also be provided. (Notes and Letters to the Editor are published without a summary.)

Illustrations. The figures should be submitted in a form suitable for reproduction, drawn in Indian ink on drawing or tracing paper. Each illustration should have a legend, all the *legends* being typed (with double spacing) together on a *separate sheet*. If structures are given in the text, the original drawings should be supplied. Coloured illustrations are reproduced at the author's expense, the cost being determined by the number of pages and by the number of colours needed. The written permission of the author and publisher must be obtained for the use of any figure already published. Its source must be indicated in the legend.

References. References should be numbered in the order in which they are cited in the text, and listed in numerical sequence on a separate sheet at the end of the article. Please check a recent issue for the layout of the reference list. Abbreviations for the titles of journals should follow the system used by *Chemical Abstracts*. Articles not yet published should be given as "in press" (journal should be specified), "submitted for publication" (journal should be specified), "in preparation" or "personal communication".

Dispatch. Before sending the manuscript to the Editor please check that the envelope contains three copies of the paper complete with references, legends and figures. One of the sets of figures must be the originals suitable for direct reproduction. Please also ensure that permission to publish has been obtained from your institute.

Proofs. One set of proofs will be sent to the author to be carefully checked for printer's errors. Corrections must be restricted to instances in which the proof is at variance with the manuscript. "Extra corrections" will be inserted at the author's expense.

Reprints. Fifty reprints of Full-length papers, Notes and Letters to the Editor will be supplied free of charge. Additional reprints can be ordered by the authors. An order form containing price quotations will be sent to the authors together with the proofs of their article.

Advertisements. Advertisement rates are available from the publisher on request. The Editors of the journal accept no responsibility for the contents of the advertisements.

Announcing a new journal.....

PROCESS CONTROL AND QUALITY

The science and technology of process quality measurement systems.

An international journal

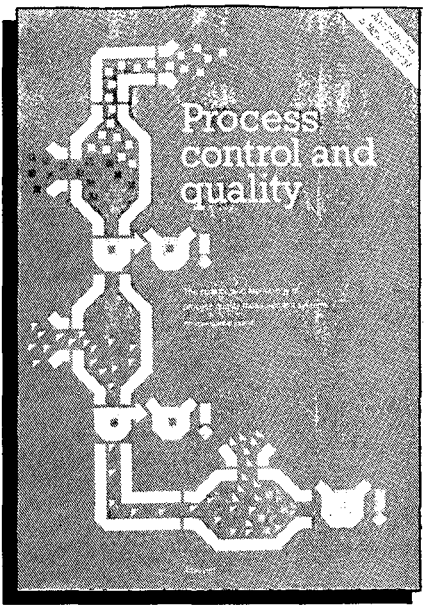

In-process analytical instrumentation is becoming increasingly important for process control and product quality measurement in a production environment in many industries, including the following: petroleum, petrochemical, chemical, pharmaceutical, food and biotechnology. The journal is intended to provide a multidisciplinary forum for scientists and engineers involved in research, plant design, process quality control and environmental monitoring. Chemists, chemical/mechanical/electrical and instrument engineers, computer scientists, quality assurance engineers, instrument manufacturers and consultants will form the primary audience.

Topics covered will include: sampling, sample handling, instrumentation measurement techniques, automation, (real-time) expert systems, control theory, system validation, data management and statistical process control. The emphasis will be on the practical aspects of these topics. In addition to original research papers, the journal will publish tutorial papers, reviews, case studies, applications and short communications, and will have a section in which product descriptions, meeting reports and critical reviews of relevant products are included.

Frequency: Publication will be quarterly with Vol. 1, No. 1 appearing in summer 1990

Editor-in-Chief: **K.J. Clevett,** Clevett Associates Inc., Watchung, NJ 07060, USA

Editors: **E.H. Baughman, K.G. Carr-Brion, J.E. Doss, E.L. Johnson**

Subscription Information:
1990/91: Volume 1 (4 issues)
Price: US$ 197.50 / Dfl. 395.00
including postage
ISSN 0924-3089

The Dutch Guilder (Dfl.) price is definitive.
US $ price is subject to exchange rate fluctuations.

PROCESS QUALITY AND CONTROL

- ☐ Please send me a free sample copy
- ☐ Please enter my subscription for 1990/91 and send me an invoice
- ☐ Please send me Instructions for Authors
- ☐ Please send Advertising Rates

Name: _____

Address: _____

_____

_____

Send this coupon (or a photocopy) to:
Elsevier Science Publishers
P.O. Box 330, 1000 AH Amsterdam
The Netherlands

In the USA and Canada:
Elsevier Science Publishers
Attn: Journal Information Center
655 Avenue of the Americas
New York, NY 10010, USA